FINAL REPORT

Abiotic and Biotic Mechanisms Controlling In Situ Remediation of NDMA

SERDP Project ER-1421

MAY 2009

James E. Szecsody
Jim P. McKinley
Andrew T. Breshears
Brooks J. Devary
Pacific Northwest National Laboratory

Fiona Crocker
Herbert L. Fredrickson
Karen Thompson
USA ERDC

DoD EPA DOE SERDP
Strategic Environmental Research and Development Program

Report Documentation Page

Form Approved
OMB No. 0704-0188

1. REPORT DATE	2. REPORT TYPE	3. DATES COVERED
MAY 2009		**00-00-2009 to 00-00-2009**

4. TITLE AND SUBTITLE	5a. CONTRACT NUMBER
Abiotic and Biotic Mechanisms Controlling In Situ Remediation of NDMA	5b. GRANT NUMBER
	5c. PROGRAM ELEMENT NUMBER
6. AUTHOR(S)	5d. PROJECT NUMBER
	5e. TASK NUMBER
	5f. WORK UNIT NUMBER
7. PERFORMING ORGANIZATION NAME(S) AND ADDRESS(ES) **Pacific Northwest National Laboratory,902 Battelle Boulevard,Richland,WA,99354**	8. PERFORMING ORGANIZATION REPORT NUMBER
9. SPONSORING/MONITORING AGENCY NAME(S) AND ADDRESS(ES)	10. SPONSOR/MONITOR'S ACRONYM(S)
	11. SPONSOR/MONITOR'S REPORT NUMBER(S)

12. DISTRIBUTION/AVAILABILITY STATEMENT
Approved for public release; distribution unlimited

13. SUPPLEMENTARY NOTES

14. ABSTRACT

15. SUBJECT TERMS

16. SECURITY CLASSIFICATION OF:			17. LIMITATION OF ABSTRACT	18. NUMBER OF PAGES	19a. NAME OF RESPONSIBLE PERSON
a. REPORT	b. ABSTRACT	c. THIS PAGE			
unclassified	**unclassified**	**unclassified**	**Same as Report (SAR)**	**260**	

Executive Summary

This project was initiated to investigate whether *in situ* coupled abiotic/biotic degradation of N-nitrosodimethylamine (NDMA, an emerging contaminant) could be used as a permeable reactive barrier for remediation at the Aerojet, California site, where groundwater contains up to 36-ppb NDMA. The sediment mainly used in experiments is from the Aerojet groundwater aquifer (260-ft depth), with additional sediments from other groundwater aquifers (i.e., not shallow soils, Ft. Lewis, Washington, 60-ft depth, Puchack, New Jersey, 273-ft depth). Different *in situ* remediation processes were compared in this study: a) biostimulation (oxic, anaerobic, iron-reducing, sulfate-reducing), b) abiotic iron-reducing environment (by dithionite reduction of sediment or zero valent iron addition), c) coupled abiotic/biotic remediation (iron-reducing environment), and d) sequential iron-reducing, then oxic, biostimulation. The overall goal was to understand and optimize the combined effects of abiotic and biotic processes to degrade NDMA to nontoxic products. Iron-reducing conditions were created by chemical reduction of a sediment using sodium dithionite, and in a few cases, a natural reduced aquifer sediment or sediment with zero valent iron addition.

When subsurface sediments are chemically or naturally reduced, abiotic surface phase(s) rapidly degraded NDMA (8-hour half-life for high reduction, slower for low reduction) to nontoxic dimethylamine (DMA). Experiments showed up to 80% conversion of NDMA to DMA, with further degradation to nitrate (up to 40% molar conversion), formate (trace concentration) and carbon dioxide (up to 82% molar conversion). Methylamine and formaldehyde (likely intermediates) were not detected. Experiments with 100 and 10 ng/L NDMA starting concentration had a rapid degradation half-life (4.7 hours), and NDMA was degraded to <3 ng/L (detection limit). Although degradation to DMA is sufficient for remediation (DMA is not toxic at <5 mg/L), because NDMA mass was degraded further to more toxic intermediates, NDMA mineralization (i.e., to CO_2) was considered the lowest risk product, and was the main focus of this study. NDMA degradation was most rapid with high sediment reduction. These sediments had a higher mass of ferrous surface phases (ferrous oxides, carbonates, sulfides, adsorbed ferrous iron, green rust) and a more alkaline pH (pH increased from 9.1 to 10.5). The NDMA reactivity of these different iron phases showed that adsorbed ferrous iron was the dominant reactive phase that promoted NDMA reduction. Alkaline hydrolysis by itself (no sediment, pH 11) did not degrade NDMA, nor did alkaline hydrolysis with anaerobic sediment (a potential catalyst). Iron sulfides, while present in the reduced sediment, did not change the NDMA degradation rate. Iron(II) carbonate (siderite) also showed little reactivity with NDMA, as its removal did not influence NDMA degradation. Although magnetite itself (with no sediment) did not promote NDMA degradation, magnetite removal from the reduced sediment decreased the NDMA degradation rate to some extent (3 times). This effect was caused by adsorbed ferrous iron on the magnetite. Removal of adsorbed Fe(II) substantially decreased NDMA degradation (15 times). Removal of amorphous and/or crystalline Fe(II/III) surface phases also greatly decreased reactivity with NDMA, also due to adsorbed ferrous iron. Ferrous iron itself (aqueous) did not promote NDMA degradation; an iron oxide or 2:1 clay was needed for electron transfer.

NDMA degradation to DMA under iron-reducing conditions is an abiotic process, as the presence of a bactericide did not alter the observed rate. In contrast, NDMA mineralization in

oxic sediment is predominantly a biotic process, as the NDMA was being degraded by a co-metabolic monooxygenase enzyme process. Under iron-reducing conditions, NDMA was also mineralized, but apparently predominantly by abiotic processes. These are the first reported experiments of abiotic NDMA mineralization. Both the Aerojet dithionite-reduced aquifer sediment and the Puchack natural reduced aquifer sediment showed NDMA mineralization (16% to 23%) with a bactericide present. The NDMA mineralization rate and extent in oxic systems was oxygen dependent, which was indicative of the microbial monooxygenase enzyme pathway promoting mineralization. Propane addition with prestimulation in oxic sediments did promote more rapid NDMA mineralization (i.e., propane monooxygenase enzymes mineralizing NDMA), but methane and toluene additions did not. Acetylene addition also did not block mineralization. Yeast, humic acid, and trace nutrient addition in oxic systems had little influence on NDMA mineralization. NDMA mineralization by 2000 hours in oxic Aerojet sediment averaged (n = 10) 51.0% mineralization with 17.8% species remaining aqueous (<0.1% NDMA), 2.0% sorbed to sediment, 0.7% sorbed to microbes, and 5.7% NDMA carbon mass incorporated into microbes (total mass balance 80.0%). NDMA oxic mineralization was as high as 82% in the Ft. Lewis sediment. This high carbon mass balance in the oxic systems is indicative of significant microbial control. For anoxic and reduced sediment, carbon additions normally associated with increasing monooxygenase pathways (propane, methane, toluene) had no influence on NDMA mineralization, as expected, indicating this pathway was not mineralizing NDMA. Other carbon additions (humic acid, yeast extract, trace nutrients) did not increase mineralization, indicating that reduced system mineralization likely has significant abiotically control, which was confirmed by the bactericide addition with little change in NDMA mineralization. Reduced Aerojet sediment carbon mass balance at 2000 hours (n = 7) showed 40.2% aqueous, 9.9% mineralized, 0.35% sorbed to sediment and microbes, and 0.18% incorporated into microbes. NDMA mineralization in reduced sediments was as high as 26%.

Although NDMA mineralization in *batch* oxic sediment systems showed that higher mineralization rates and extent than reduced systems, large 1-D column systems (high sediment/water ratio of aquifers) showed much more rapid NDMA mineralization in reduced sediment systems. NDMA mineralization in reduced Aerojet sediment columns (half-life 410 ± 147 hours) were 5.6 times more rapid than in oxic, biostimulated sediment columns (half-life 2293 ± 1866 hours) and in sequential reduced/oxic biostimulated sediment columns (half-life 3180 ± 1094 hours). Oxic columns had NDMA-laden water and air/propane injection to promote NDMA co-metabolic degradation. These results are not surprising as column systems exhibit significantly less mixing than in batch systems, so much of the microbial population may be nutrient limited. In fact, oxic biomineralization rates in columns were 150 times slower than predicted from batch experiments. In contrast, NDMA mineralization in the reduced sediment columns were only 4 times slower than predicted from batch studies, indicating abiotic process scale up is much more efficient (not influenced by the need for aqueous nutrients at surface sites). It is possible that more efficient methods to inject and mix nutrients *in situ* can increase the biomineralization rate in oxic systems. NDMA mineralization rates in sequential reduced-oxic sediment columns indicate the process is inefficient, as NDMA degradation intermediates from the upgradient reduced column are not being biodegraded as easily as NDMA itself. This may indicate that the abiotic, reduced sediment NDMA mineralization pathway is different from the oxic biomineralization pathway.

Results of this study demonstrate that dithionite- or natural-reduced aquifer sediments under iron-reducing conditions degrade NDMA rapidly (32.1-hour half-life) and also mineralize NDMA slowly (410-hour half-life). This reactivity was maintained for 84 pore volumes, when experiments ended. It is expected that the reactivity would last longer (estimated 150 to 200 pore volumes for the Aerojet sediment). These promising laboratory-scale results for NDMA mineralization should be evaluated at field scale. Other methods to create a subsurface iron-reducing environment may also yield similar results (i.e., zero valent iron injection or biostimulation). Although numerous experiments evaluating additions to stimulate *in situ* microbial activity were largely ineffective in this study, *ex situ* bioreactors utilizing appropriate monooxygenase isolates have been shown successful in other studies. Therefore, future studies of NDMA remediation should focus on the comparison of *in situ* abiotic NDMA mineralization (iron-reducing environments) to *ex situ* biomineralization.

Acknowledgments

We would like to acknowledge support from Dr. Andrea Leeson at the SERDP Office for funding and involvement. Within this project, geochemical, coupled abiotic/biotic process, and reactive transport work was mainly conducted at Pacific Northwest National Laboratory by Dr. Jim Szecsody, Dr. Jim McKinley, Brooks Devary, Andrew Breshears, Dr. Don Girvin, Jerry Phillips, and Tom Resch. Microbial isolate work was conducted at the U.S. Army Engineer Research and Development Center by Dr. Fiona Crocker, Karen Thompson, and Dr. Herb Fredrickson.

Acronyms and Abbreviations

DCB	dithionite-citrate-bicarbonate soil extraction for ferric oxides
di/Fe	molar ratio of sodium dithionite to reducible ferrous iron in sediment; dithionite is used to chemically reduce ferric iron surface phases
dithionite	sodium dithionite or hydrosulfite, CAS 7775-14-6, an aqueous reductant used for *in situ* reduction with potassium carbonate (pH buffer) to dissolve and reduce some ferrous oxides in aquifer sediments (Szecsody et al. 2004)
DMA	1,1-dimethylamine, abiotic degradation product of NDMA under some alkaline, reducing conditions, CAS 124-40-3
DNFB	2,4-dinitroflorobenzene, used to derivatize DMA for HPLC analysis
DOD	U.S. Department of Defense
DOE	U.S. Department of Energy
EPA	U.S. Environmental Protection Agency
EPPS	N-2-hydroxyethylpiperazine propane sulfonic acid, pH buffer
ERDC	U.S Army Environmental Research and Development Center, Waterways Experiment Station, Vicksburg, MS
GC	gas chromatography
Fe/NDMA	molar ratio of redox reactive ferrous iron to NDMA
FTIR	Fourier transform infrared (spectrometry)
HEPES	4-(2-hydroxyethyl)-1-piperazine ethane sulfonic acid, pH buffer
HMN	hydroxymethylnitrosamine, biotic degradation product of NDMA
HMX	octahydro-1,3,5,7-tetranitro-1,3,5,7-tetrazocine
HPLC-UV	high performance liquid chromatography with ultraviolet detection
ID	inside diameter
ISRM	*in situ* redox manipulation
K_d	distribution coefficient describing solute mass sorbed/aqueous
KOH	potassium hydroxide
LC/MS	liquid chromatography/mass spectrometry
MSM	mineral salt media used for microbial experiments
N_2O	nitrous oxide, abiotic degradation product of NDMA
NDMA	n-nitrosodimethylamine, CAS 62-75-9 – other names: dimethylnitrosamine (DMN, DMNA)
NH_4	ammonia, abiotic degradation product of NDMA
NO	nitrogen monoxide, abiotic degradation product of NDMA

NOM	natural organic matter
PIPES	1,4-piperazinediethanesulfonic acid, pH buffer
PLFA	phospholipids fatty acids
PNNL	Pacific Northwest National Laboratory
ppb	parts per billion (µg/L)
ppm	parts per million (mg/L)
ppt	parts per trillion (ng/L)
PRB	permeable reactive barrier
pv	pore volumes
R_f	retardation factor; multiplier describing the relative groundwater velocity of a solute to an unretarded tracer
RDX	hexahydro-1,3,5-trinitro-1,3,5-triazine, royal demolition explosive, CAS 121-8-24
SERDP	Strategic Environmental Research and Development Program
TCE	trichloroethylene
TNT	1,3,5-trinitrotoluene, CAS 118-96-7
UDMH	unsymmetrical dimethylhydrazine, abiotic degradation product of NDMA under some acidic reducing conditions, CAS 57-14-7
UV	ultraviolet
WES	Waterways Experiment Station (U.S Army ERDC, Vicksburg, MS)
ZVI	zero valent iron

Contents

Figures

Tables

1.0 Introduction

This is the final report for Strategic Environmental Research and Development Program (SERDP) project 1421 entitled "Abiotic and Biotic Mechanisms Controlling *In Situ* Remediation of NDMA" for the period March 2005 to December 2008. Funding delays resulted in the laboratory studies being extended for a year. This laboratory study of the fate of n-nitrosodimethylamine (NDMA) in contaminated subsurface environments involves research at Pacific Northwest National Laboratory (PNNL; Dr. Jim McKinley, Dr. Jim Szecsody, Dr. Don Girvin, and others) and at the U.S. Army Engineer Research & Development Center, Waterways Experiment Station (Dr. Herb Fredrickson, Dr. Fiona Crocker, and Karen Thompson).

The general objective of the project is to stimulate NDMA degradation/mineralization through combined biotic and abiotic processes in natural, contaminated aquifer sediments. We hypothesize that an initial degradative (iron reducing) environment can be readily induced in the subsurface through the injection of sodium dithionite. The reduction in the sediment of structural iron in sediment minerals will produce a porous reactive barrier that can degrade NDMA. We further hypothesize that the complete mineralization of NDMA will require or be facilitated by the *in situ* microbial community, if it is appropriately stimulated by the addition of an electron donor in the reducing environment or downgradient oxic environment. This addition will further sustain reducing conditions in the subsurface and prolong the useful life of the reactive barrier. Preliminary results from experiments initiated before this project suggested that degradation could occur through biotic or abiotic processes, although the nature of the processes were not well understood.

2.0 Background

2.1 Technical Objective

The objective of this study was to investigate abiotic and coupled abiotic/biotic processes that led to NDMA degradation in chemically reduced natural sediment by measurement of potential degradation products. These degradation products are believed to differ according to pathway. In previous studies, NDMA degradation in reduced sediment was demonstrated, although the mechanism was not well understood. In this study, the ability of microbial consortia to degrade NDMA in sediments and as isolates will also be investigated. It is hypothesized that that bioremediation may supplement abiotic degradation if an appropriate electron donor is supplied along with dithionite during soil reduction. Other studies show that a significant fraction of *in situ* populations survive dithionite treatment and may be able to bioremediate organic compounds (although whether appropriate isolates that degrade NDMA survive dithionite treatment is not known). The ultimate objective of this research is to conduct a field trial of an abiotic/biotic methodology for the remediation of aquifer-born NDMA.

Our research followed an upscaling toward field implementation:

- Task 1 – Abiotic reduction experiments to identify reduction pathways relevant to natural systems
- Task 2 – Incorporation of a biotic component in coupled biotic/abiotic experiments to provide needed information about the role and effectiveness of microbially mediated reduction
- Task 3 – Coupled abiotic/biotic experiments for NDMA degradation/mineralization
- Task 4 – Large laboratory-scale 1-D column studies with sequential reducing, then oxic environments to evaluate NDMA degradation and mineralization under field-scale geochemical conditions in Aerojet aquifer sediment.

Our research team is an interdisciplinary group of scientists with appropriate experience, located at PNNL, and at U.S. Department of Defense (DOD) Waterways Experiment Station (WES, Vicksburg, MS). Our collaborator at WES provided expertise in microbiology and access to known microbial degraders of a variety of organic and nitramine explosive contaminants.

2.2 *In Situ* Reactive Zone Concept

In situ redox manipulation (ISRM) of sediment by the chemical amendment and injection of groundwater has been shown to be effective in the remediation of a variety of redox sensitive inorganic contaminants (Fruchter et al. 2000; Vermeul et al. 2002) and organic contaminants that can be degraded through a reductive pathway (Szecsody 2007; Szecsody et al. 2004, 2008a). The remediation strategy is to induce a permeable reactive zone (abiotic, biotic, or coupled) in the subsurface that will persist and effect the removal of the contaminant of interest as it moves through the barrier by advection. Reactive barriers are successful when contaminant residence times are sufficient to allow complete mineralization, or to produce intermediates that can be rapidly degraded in aerobic zones downgradient. Enhanced bioremediation of energetics and

other nitroaromatic compounds in the subsurface is often successful in removing parent compounds, but mineralization (i.e., complete destruction) rates are not necessarily faster than natural biodegradation, and often too slow or nonexistent. For example, Boopathy et al. (1994) observed enhanced 1,2,5-trinitrotoluene (TNT) biotransformation by seven different carbon sources but mineralization was not observed. Preliminary laboratory studies (discussed below) indicated that NDMA was readily and rapidly degraded by dithionite-reduced Aerojet sediments, suggesting that ISRM might be successful at that site. However, a number of uncertainties need to be evaluated to allow the design and completion of a field test. The design, implementation, and assessment of a field remediation test would require knowledge of NDMA degradation mechanisms, and the ability to quantitate its degradation products. The potential role of microbial bioremediation in NDMA degradation, particularly at the low levels found at the Aerojet site, must be determined. ISRM with biostimulation may improve degradation efficiency and the longevity of the reactive barrier. When the combined effects of chemical and biological degradation are known, an optimized and efficient could be developed through intensive experimentation. Field testing based on a hypothetically robust and efficient design would have the greatest chance of success.

2.3 The Aerojet Site

The Aerojet site is in Rancho Cordoba, California, ~15 miles east of Sacramento. The facility is a Superfund site, and has been operated by Aerojet since 1953. Operations at the site included manufacture of liquid and solid propellants for rocket engines, and the formulation of pesticides, pharmaceuticals, and industrial chemicals. Some wastes were disposed on the site in surface impoundments, landfills, deep injection wells, leachate field, and open burn areas. The prevalent contaminants in groundwater are trichloroethene, perchlorate, and NDMA, occurring in plumes that extend across the site boundaries into the surrounding community. A number of community water supply wells have been lost to production due to contamination. The aquifer at the site is divided into five vertical zones, or layers, A – D, with distinct contaminant profiles. In general, the maximum concentrations of NDMA, perchlorate, and trichloroethylene (TCE) are 1.3, 11,000, and 9,400 $\mu g\ L^{-1}$, respectively. The ISRM method is known to be effective for TCE degradation, and appears to be effective for NDMA in laboratory-scale experiments.

The *in situ* geochemical reduction technology used in this project is based on previous experience with the immobilization of chromate by a permeable reactive barrier containing reduced sediment. The geochemical reduction of chromate (CrVI) to Cr(III) occurs by reaction with ferrous iron within the barrier. This reduced zone of sediment – sediment in which a significant fraction of sedimentary Fe(III) is converted to reactive Fe(II) – is created by the injection of an aqueous reductant (sodium dithionite) through a standard groundwater well. The longevity of the reduced zone depends upon the oxidation of the ferrous iron by chromate and other electron acceptors, such as dissolved oxygen, during the natural advection of groundwater through the treatment zone. *In situ* microbial respiration will also have an effect.

2.4 NDMA Degradation Mechanism

Some experimentation on NDMA reduction pathways has been published, suggesting several potential mechanisms (summarized below). The determination of the effective pathway or pathways in the subsurface environment after ISRM treatment would be a necessary preliminary

step in designing and implementing a field remediation project. This information would be necessary to optimize the treatment strategy, chemistry, and design. Published and preliminary studies to date included NDMA in the presence of metallic iron and nickel-iron mixtures, and ferrous iron in reduced sediments (Gui et al. 2000).

For zero valent iron and Ni/Fe mixed metal, three possible mechanisms for NDMA degradation have been proposed: 1) direct electron transfer from zero valent iron, 2) electron transfer from adsorbed Fe^{2+}, and 3) catalyzed hydrogenolysis by H_2 produced from iron corrosion. While degradation of many compounds appears to occur via the first or second mechanism, recent evidence suggests that the third mechanism was most likely (Odziemkowski et al. 2000), based on several lines of evidence. First, the direct reduction of NDMA by zero valent iron was judged to be unlikely, based on electrochemical potentials of the two species. The redox potential for NDMA, -1.3 volts in the pH range 7 to 12, is larger than the potential for zero valent iron, ca. -0.6 volts. (For comparison, our results indicate that reduced sediment has a potential of about -0.2 volts and an aqueous 0.1 mol/L dithionite solution has a potential of -0.56 volts.) Chemical evidence also supported the conclusion that surface hydrogenation degraded NDMA. The direct electrochemical reduction of NDMA produces dimethylamine (DMA) and nitrous oxide (i.e., proposed degradation products for mechanism #1), but the batch and column experiments conducted by Odziemkowski et al. (2000) with zero-valent and Ni/Fe-mixed metals produced the products of hydrogenation: DMA and ammonia. The hydrogenation mechanism is illustrated in Figure 2.1. Electron transfer from zero valent iron hydrolyzes water to yield hydrogen. This hydrogen adsorbs to the iron surface and reacts with NDMA via catalytic hydrogenation. In addition, because most of the zero valent metals are coated with a magnetite (Fe_3O_4) film (Odziemkowski et al. 2000), the proposed mechanism involves magnetite (Figure 2.1).

The degradation pathway of NDMA in contact with reduced sediments is largely unknown. As described earlier, "reduced sediment" refers to one or more ferrous iron species present, which for several sediments (Szecsody et al. 2004) are predominantly adsorbed ferrous iron and siderite, but may also include reduced structural iron in clays. Current literature describes only portions of a hypothesized royal demolition explosive (RDX) degradation pathway, which includes NDMA and in which some rearrangement of NDMA can form three other molecules, some of which follow a further chemical pathway. However, since NDMA is along the pathway of RDX mineralization, the mineralization of RDX necessitates the degradation of NDMA (Jalal Hawari, personal communication). Because the complete mineralization of RDX cannot occur entirely abiotically (i.e., microbes are involved in final steps to produce carbon dioxide), the complete mineralization of NDMA in reduced sediment, if it occurs, also likely requires both abiotic and biotic steps. Also, the aqueous or surface reducing conditions created by reduced sediment are not as electronegative as zero valent iron. For comparison, reduced sediment is about -0.2 volts and aqueous 0.1 mol/L dithionite is -0.56 volts, relative to the -0.6 volts for zero valent iron. It is therefore unlikely that water is hydrolyzing at the reduced sediment surface, so zero valent iron pathway is unlikely to occur for reduced

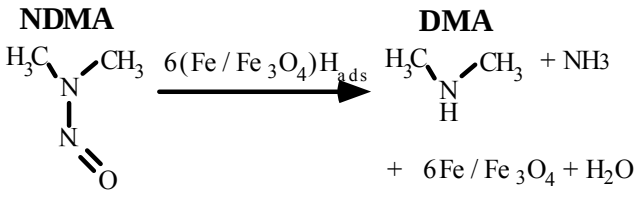

Figure 2.1. NDMA degradation pathway for Fe^0 and Ni^o/Fe^o.

sediment. The identification of the reaction intermediates of NDMA degradation for reduced sediments is needed to determine its reduction pathway in that system. Because all three proposed mechanisms for zero valent iron produce DMA, it is a likely degradation product for reduced sediment also. In addition, the production of 1,1-dimethylhydrazine, nitrous oxide, or methane would indicate the first mechanism, whereas production of ammonia would indicate the third mechanism.

2.5 Abiotic NDMA Degradation in Sediments

In a preliminary study (Szecsody et al. 2001), a series of batch (i.e., no flow) and small 1-D column experiments (i.e., simulates idealized groundwater flow) with chemically reduced aquifer sediments were conducted by us to determine the NDMA degradation rate (Table 2.1). Two different sediments were used: a) Ft. Lewis (WA) 60-ft depth sediment, and b) Aerojet (CA) 260-ft depth sediment. NDMA was reduced in these sediments. There was a dependence of the NDMA reduction rate on the molar ratio of the reductant (ferrous iron in reduced sediment or dithionite) to NDMA concentration (Table 2.1). Some experiments showed moderate NDMA degradation rates, and the appearance of a possible degradation product, while other experiments showed little or no NDMA degradation. In general, the Ft. Lewis sediment degraded NDMA at a rate sufficient to be useful for subsurface remediation (<100-hour half-life), but the Aerojet sediment degraded NDMA slowly. In addition, NDMA was rapidly degraded directly by dithionite.

Table 2.1. NDMA degradation in sediment.

		molar	pseudo f.o. rate		intrinsic rate
NDMA	Fe2+	ratio	half-life	kf'	kf
(mg/L)	(mol)	Fe/NDMA	(h)	(1/h)	(1/h)
Ft Lewis Sediment:					
25.0	1.88E-04	18.6	8090	8.57E-05	4.49E+04
25.0	1.47E-03	135	2700	2.60E-04	1.63E+04
0.72	1.58E-04	544	none		
0.72	1.52E-03	4920	203	0.00341	7.24E+06
25	3.04E-04	493	2000	0.00035	1.87E+06
2.5	2.42E-04	3200	380	0.00182	9.97E+07
0.25	2.44E-04	31400	66	0.0105	5.53E+09
Aerojet Sediment:					
5.34	1.42E-02	3360	447	0.00155	2.58E+04
5.34	1.42E-02	3360	none		
0.036	5.22E-02	490000	(14)*	0.0496	8.90E+06
0.036	5.22E-02	490000	(45.1)*	0.0154	2.76E+06
0.036	5.22E-02	490000	(117)*	0.0059	1.06E+06
0.036	5.22E-02	490000	(338)*	0.0021	3.77E+05
5.00	1.47E-02	4120	264	0.00262	5.01E+04
5.00	1.47E-02	4120	none		
4.74	5.18E-04	4710	173	0.00401	7.03E+07
0.036	1.41E-02	432000	15.8	0.044	9.54E+07
0.036	1.41E-02	432000	10.7	0.065	1.41E+08
dith.	dithionite	dith/NDMA			
5.27	5.40E-03	1260	2.51	0.276	1.20E+07

d(NDMA)/dt = kf (Fe2+)(NDMA), kf = intrinsic first order rate coefficient

d(NDMA)/dt = kf' (pseudo first-order approximation from data)

*sediment column was partially reduced and may contain dithionite

We began our preliminary experiments by using sediment for which properties were well known, derived a rate expression from the initial results, and then investigated interaction with less well-known Aerojet sediment. The NDMA degradation experiments were initiated with a geochemically well-characterized sediment from the unconfined aquifer at Ft. Lewis, Washington (Tacoma, WA). The <4 mm fraction, used in experimentation, of this glacial till sediment (silty, sandy gravel) contained a wide variety of ferric iron-containing minerals including 8.5% 2:1 smectite clays, 13% biotite, and 0.8% iron oxides. The total reducible iron was 159 μmol/g, roughly twice that of the Aerojet sediment (74.1 μmol/g reducible iron). The relatively high clay content in the Ft. Lewis sediment rather than the difference in reducible iron may have been responsible for the high NDMA reactivity.

NDMA was observed to be systematically degraded in reduced Ft. Lewis sediment (Szecsody et al. 2000). A total of seven batch

experiments were conducted at different soil/water and NDMA concentrations to achieve a wide range of electron donor (ferrous iron) to electron acceptor (NDMA) ratios. Three experiments (Figure 2.2) showed that with a higher ferrous iron/NDMA ratio, the resulting degradation rate increased from a 2000-hour half-life (25-mg/L NDMA) to a 66-hour half-life (0.25-mg/L NDMA; also minor differences in the soil/water ratio). The results could be scaled to a field application. The soil/water ratios in batch studies (0.666 g/cm^3) are 4.8 times smaller than is achieved in the aquifer or packed soil columns (3.2 g/cm^3), so a 14-hour half-life for NDMA degradation is predicted in a packed column of reduced Ft. Lewis sediment. Theoretically, a total of 6 electrons are needed to degrade NDMA to carbon dioxide, although the actual pathway is largely unknown. Considering only the NDMA loss rate with Fe^{2+} as the reductant (reaction 2.1), rate expression can be written to describe the intrinsic degradation rate (expression 2.2):

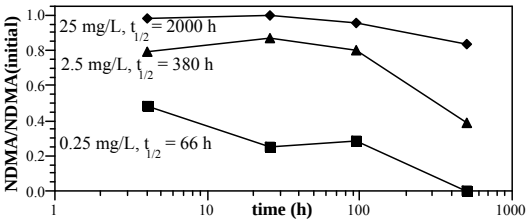

Figure 2.2. NDMA degradation in reduced Ft. Lewis sediment.

$$NDMA + Fe^{2+} \Longleftrightarrow \text{intermediate \#1} + Fe^{3+} + OH^- \quad (2.1)$$

$$d(NDMA)/dt = k_f (Fe^{2+}) (NDMA) \quad (2.2)$$

can be used to calculate the intrinsic rate coefficient (k_f) from the different experiments to remove the differences in iron and NDMA concentrations. The intrinsic rate coefficient for the dithionite/NDMA reaction was calculated at 1.2 x 10^7 h^{-1} (Table 2.1), whereas the log-average intrinsic rate for the Ft. Lewis sediment/NDMA reaction was 5.2 x 10^7 h^{-1}, and Aerojet sediment/ NDMA reaction was 1.1 x 10^8 h^{-1} (i.e., the rates were nearly all the same). This result indicated that the surface-promoted redox reaction was essentially the same as the aqueous reaction, suggesting that the surface did not act as a catalyst, but only as an electron donor; i.e., it acted similarly to dithionite. In addition, differences in sediment mineralogy between the Aerojet and Ft. Lewis sediments were insignificant, so the reducible iron content should predict NDMA degradation behavior.

NDMA degradation experiments were conducted in reduced Aerojet sediment columns to determine rates that could be achieved at field-scale soil/water ratios. A total of 11 column experiments were conducted with Aerojet sediment. In experiments where the Fe/NDMA was ca. 4000 (Table 2.1), the observed NDMA degradation of NDMA included no degradation and half-lives of 178 to 264 hours. These NDMA degradation rates were relatively slow, and surprising compared with the results using the Ft. Lewis sediments.

Two column experiments were conducted with 100% reduced Aerojet sediment and Aerojet groundwater in which the Fe/NDMA was ca. 43,000 (Table 2.1; 36-ppb NDMA; Figure 2.3); these experiments showed the predicted rate of ~14 hours (see previous section), based on the high reductant/NDMA ratio that would be present in the Aerojet aquifer. Although there are only a few points on each breakthrough curve shown in Figure 2.3, the two column experiments exhibited significant NDMA degradation. In the experiment with a 28-hour residence time in the

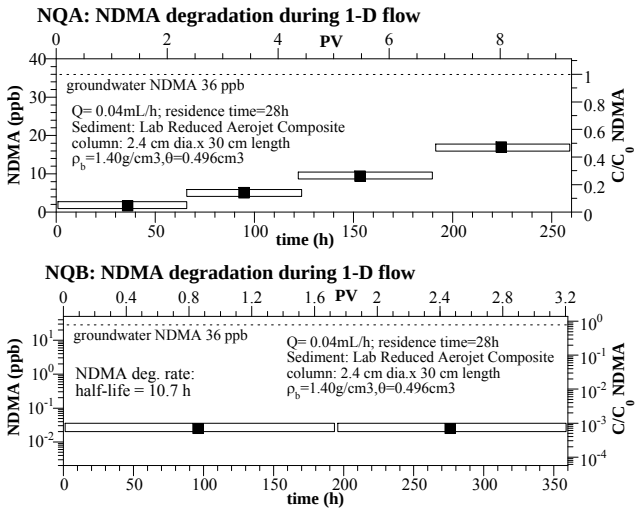

Figure 2.3. NDMA degradation in reduced Ft. Lewis sediment columns at 36 ppb.

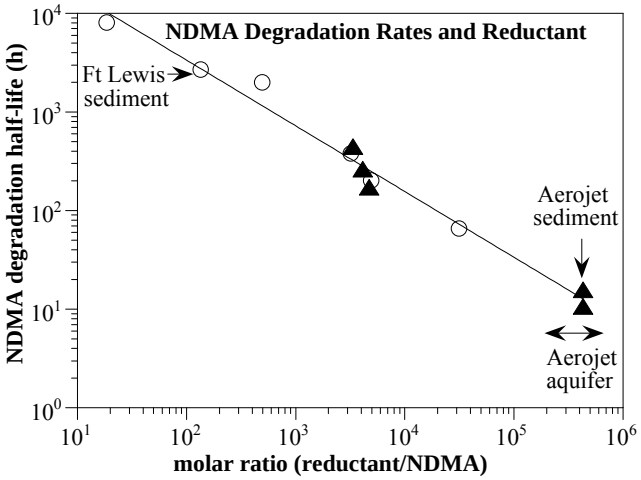

Figure 2.4. NDMA degradation in reduced sediments (open circles and triangles) and with aqueous dithionite (diamond).

column, the average effluent concentration was 10.5 ppb (after 2 pore volumes), which produced an NDMA degradation half-life of 15.8 hours. In the second experiment with a 112-hour residence time in the column, the average effluent concentration was 0.025 ppb, which indicated the average NDMA degradation half-life was 10.7 hours. The wide bars on the graph signify the actual size of the sample (i.e., the 100 mL collected was ~ 1.5 pore volumes).

Sorption of NDMA was additionally calculated from NDMA breakthrough in oxic column experiments. The K_d value of 0.15 cm^3/g is sufficiently small that it can be ignored during transport considerations.

NDMA degradation rates achieved in reduced Aerojet sediments in Aerojet groundwater (36-ppb NDMA, degradation rates 14.8- and 10.7-hour half-life) are ideal for construction of a permeable reactive barrier. A plot of the NDMA degradation rates versus the ratio of reductant to initial NDMA concentration (Figure 2.4) illustrates the key conclusions of this preliminary study. First, direct reduction of NDMA by aqueous dithionite is 2 to 3 orders of magnitude more efficient than reduced sediment. This is not useful in a subsurface aquifer because dithionite disproportionates with a 27-hour half-life (discussed above); it is no longer present in effective concentrations after a 1-week residence in the subsurface. It is unknown whether this aqueous NDMA degradation is caused by dithionite or possibly hydrolysis of NDMA at high pH (which occurs with explosives).

The results using different sediments are consistent. By fitting a straight line to the six open circles (degradation rates achieved at much lower molar ratios of reductant to NDMA) and examining its position in the "Aerojet aquifer" region of the plot, the reduction rate predicted for the Aerojet sediment can be compared to the observed rate. The reduction rate in the Aerojet aquifer, in which there is a 100,000 to 500,000 greater mass of reducible iron relative to the *in situ* 36-ppb NDMA (molar ratio basis), is predicted by Ft. Lewis results to agree with the

observed rate of 14 hours. There is apparently no meaningful difference in iron mineralogy between the two sediments, in terms of NDMA reactivity (i.e., total mass of reducible iron sufficiently predicts NDMA behavior).

The correlation of the high Fe/NDMA molar ratio and the NDMA degradation rate may be caused by a ferrous iron phase (or other phase) present in very small concentrations relative to the total redox capacity of the sediment. Additional information is needed to determine the mechanism on reduced natural sediments, including identification of reaction products.

2.6 Biotic NDMA Degradation

Early studies showed that NDMA can be degraded by aerobic environmental consortia (Kaplan and Kaplan 1985; Mitch et al. 2003) and soil microcosms (Mallik and Testai 1981). These results were confirmed in our laboratory (WES) using ^{14}C-NDMA (Figure 2.5). Gunnison et al. (2000) has shown that NDMA was mineralized by subsurface soil microbial communities native to the Rocky Mountain Arsenal. Thirty to 60% of ^{14}C-NDMA (50 – 500 μg/L) added to soil slurries was mineralized to $^{14}CO_2$ within 30 days. No $^{14}CO_2$ was produced from soil slurries poisoned with mercuric chloride. Equivalent rates of mineralization were achieved when the microcosms were incubated under aerobic and anaerobic conditions. The contaminated Rocky Flats aquifer is microaerophilic and pH is ~7. These conditions are conducive to NDMA degradation and were suggested to be the reason that NDMA has not migrated off the Rocky Flats site. The microorganisms mediating NDMA biodegradation, NDMA biodegradation products, and biochemical pathways have not been identified. It is also not known if these biodegradation mechanisms will be operable on the products resulting from abiological reduction of NDMA.

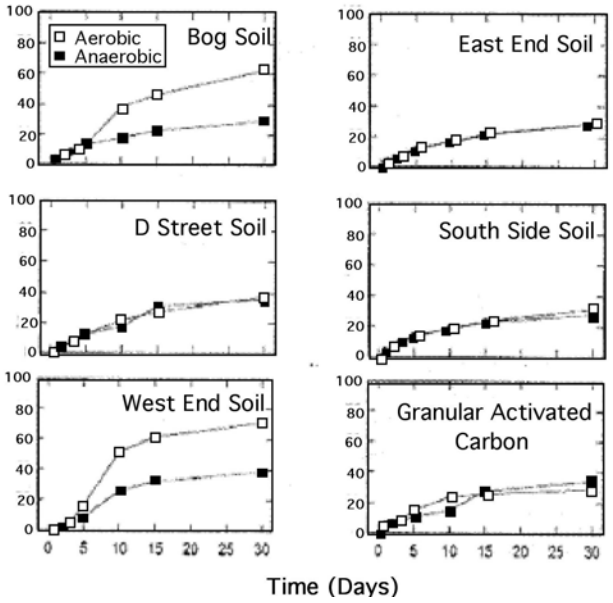

Figure 2.5. ^{14}C-NDMA mineralization in slurries of materials collected from the Northern Boundary Containment System from the Rocky Flats Arsenal (Gunnison et al. 2000).

The proposed NDMA degradation pathway (catalytic hydrogenation) with Ni/Fe metals (Odziemkowski et al. 2000) appears to include magnetite at the metal surface. Magnetite is present in Aerojet sediments (36 vol. %) and could act as a catalytic surface in the presence of hydrogen. Chemically reduced sediment is unlikely to provide hydrogen in this system by hydrolysis, but microbial hydrogen could be significant. Biostimulation could cause rapid metabolic activity, producing H_2 at concentrations several orders of magnitude greater than NDMA.

2.7 Abiotic Sediment Reduction Technology

The ISRM technology utilizes existing iron in aquifer sediment that is chemically treated with a reductant (sodium dithionite buffered at high pH) by injection or a short time into the contaminated sediment (typically 24 to 60 hours), to reduce mineral Fe(III)-oxides. The product Fe(II) may reside in reduced phases or may be solubilized and reside as adsorbed species on mineral surfaces. The reduction process results in chemically reducing groundwater conditions and the resultant disappearance of dissolved oxygen.

The chemically produced reduced iron phases in sediment behave similarly to zero-valent permeable iron walls for some reactions such as TCE dechlorination (Szecsody et al. 2004) and chromate reduction (Fruchter et al. 2000). The similarity of reduced sediment to zero-valent barriers is due to their operational equivalence. Zero-valent barriers rely not on the oxidation of metallic Fe(0), but rather on the oxidation of Fe(0) to Fe(II). Ferrous iron is the reactive compound that is oxidized to ferric iron, either from adsorbed Fe(II) or from Fe(II) minerals such as green rust (Genin et al. 1998), to reductively remediate chlorinated aliphatic contaminants (Balko and Tratnyek 1998; Johnson et al. 1998) or reduction of metals such as chromate (Blowes et al. 1997; Buerge and Hug 1997). While aqueous Fe(II) can reduce chromate (Eary and Rai 1988), Fe(II) either as a structural mineral component or adsorbed to an Fe(III)-oxide, clay surface, or zero valent iron surface is necessary for dechlorination reactions. The role of the surface in this reaction is not clearly understood.

The dithionite chemical treatment dissolves and reduces amorphous and some crystalline Fe(III) oxides. Although adsorbed Fe(II) appears to be the dominant Fe(II) component, there may be other Fe(II) mineral phases produced, including Fe(II)-carbonate (siderite), FeS (iron sulfite), and others. Although more than one Fe(III) phase is likely reduced in a natural sediment, a simple a chemical model can generally describe experimental and field observations. The reaction that describes a single phase of iron that is reduced by sodium dithionite:

$$S_2O_4^{-2} + 2 >Fe^{3+} + 2H_2O <==> 2 >Fe^{2+} + 2SO_3^{-2} + 4H^+ \quad (2.3)$$

shows that the forward rate is a function of the dithionite concentration and the square of the reducible iron concentration (rate is overall a third-order function of concentration). Modeling reaction progress in this system may require a relatively simple modification to accommodate sediment heterogeneity. Experimental evidence from previous studies with Hanford sediments has shown that at least two parallel reduction reactions are needed to describe iron reduction data (i.e., a fraction of sites are quickly reduced and a fraction more slowly reduced). This may be the result of the reduction of two or more major Fe(III) phases. If the number of slowly reducing sites is small and the mass of iron is far in excess of the dithionite, reaction 1 can be reduced to a first-order reaction in which Fe^{3+} remains constant.

While available Fe(III) is a primary consideration, the implementation of ISRM at a field site must also account for the effective neutralization of dithionite during injection and for the reaction of dithionite with other system components. A reaction other than that described in (2.1) occurs spontaneously in the sedimentary system to consume dithionite: the disproportionation of dithionite

$$2S_2O_4^{-2} + H_2O \;<==>\; S_2O_3^{-2} + 2HSO_3^- \qquad (2.4)$$

accounts for dithionite that cannot be used for iron reduction. While the rate of this reaction is system-dependent, previous studies have shown that this reaction has a half-life on the order of ~27 hours (basaltic sediments). The consequence of this reaction is to limit how slowly dithionite can be reacted with (i.e., injected into) sediment in the field. If dithionite is injected too slowly, a significant amount of the mass is lost to disproportionation.

2.8 Abiotic/Biotic Reduced Zone Longevity

Once the sediment is reduced, subsequent oxidation of adsorbed and structural ferrous iron in the sediments of the permeable redox barrier occurs naturally by the inflow of dissolved oxygen through the barrier, and additionally by contaminants (e.g., NDMA) and other electron acceptors present. In most subsurface systems, dissolved oxygen in water is the dominant oxidant of reduced iron species, as contaminants are generally present at lower molar concentrations relative to dissolved oxygen. Under oxygen-saturated conditions (8.4-mg L^{-1} O_2, 1 atm, 25ºC), 1.05-mmol L^{-1} Fe(II) is consumed. Experimental evidence indicates that the oxygenation of Fe(II) in solutions (pH >5) is generally found to be first order with respect to Fe(II) and O_2 concentration and second-order with respect to OH^-. Although the rate of oxidation of aqueous Fe^{2+} by oxygen at pH 8, as a half-life, is a few minutes (Eary and Rai 1988; Buerge and Hug 1997), the oxidation rate observed in natural was found to be 0.3 to 1.1 hour (Szecsody et al. 2000).

A measure of the total reductive capacity of reduced sediment is achieved by oxidization of sediment (Figure 2.6), in this case by O_2 saturated water, yielding 0.4% ferrous iron species, which corresponds to 270 pore volumes of oxygen-saturated water. This redox capacity can be related to the specific field system by knowing the average aquifer concentrations of dissolved oxygen and other electron acceptors, as detailed in the following calculation.

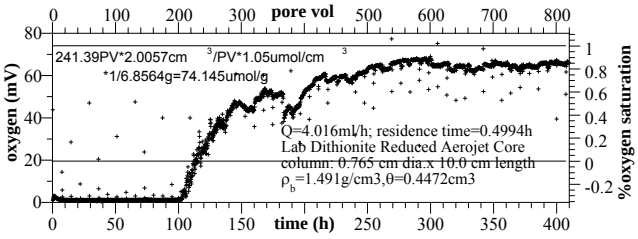

Figure 2.6. Reductive capacity of chemically reduced sediment.

Barrier Longevity (reductive capacity) Calculation: For a candidate (Aerojet, CA, 250-ft depth), the average mass of reducible iron that was dithionite reduced was estimated to be 74.1 µmol/g (0.41% reducible iron). The longevity of this barrier (i.e., reductive capacity of the ferrous iron and other reduced transition metals) can be calculated per unit volume of water (i.e., pore space) in packed porous media:

Electron donor: moles of electrons per cm^3 liquid from the Fe(II):

74.1 µmol Fe^{2+}/g x 1 µmol e-/µmol Fe^{2+} x 1.49 g sed/cm^3 tot x cm^3tot/0.447 cm^3 liq x mol/10^6 µmol

= 1.06 x 10^{-3} mol e-/cm^3 liquid #1 (with field bulk density and porosity)
= 2.47 x 10^{-4} mol e-/cm^3 liquid #2 (with laboratory bulk density and porosity)

Electron acceptors: moles of electrons per cm^3 liquid from dissolved oxygen and others (NDMA, etc.):

- 8.4-mg/L O_2 (field average) x g/1000 mg x mol O_2/32 g x L/1000 mL x 4 mol e-/molO_2 = 1.05 x 10^{-6} mol e-/cm^3
- 0.036-mg/L NDMA (field average) x g/1000 mg x mol NDMA/74 g x L/1000 mL x 1 mol e-/mol NDMA = 4.9 x 10^{-10} mol e-/cm^3 (i.e., NDMA has little influence on oxidizing the barrier)

Longevity in dimensionless pore volumes (electron donors/acceptors):

total electron donors/acceptors: 1.06 x 10^{-3} /[1.05 x 10^{-6}]
= 1009 pore volumes (scenario #1, with estimated field porosity and bulk density)
= 235 pore volumes (scenario #2, with laboratory porosity and bulk density)

An estimated longevity in years, based on an estimated groundwater flow rate (1.0 ft/day) and an average reduced sediment barrier diameter of 30 ft (site-specific values).

Longevity in years:

30 ft x day/1.0 ft x 1009 pore vol x year/365.25 days = 83 years (scenario #1)
30 ft x day/1.0 ft x 235 pore vol x year/365.25 days = 19 years (scenario #2).

2.9 Description of Tasks

NDMA abiotic and coupled degradation mechanisms will be investigated over four tasks in increasingly complex systems from mechanisms in purely abiotic systems (Task 1), biotic systems (Task 2), coupled abiotic and biotic processes (Task 3), and upscaling to sequential reduced then oxic environment during advective flow in 1-D columns (Task 4).

Task 1 – Abiotic Degradation of NDMA. In this task, the NDMA degradation mechanism in chemically reduced natural sediments will be investigated by measurement of degradation products. Preliminary studies (earlier section) show that NDMA is degraded in dithionite-reduced natural aquifer sediments, although the mechanism and pathway were not determined. We hypothesize that NDMA is degraded by sediment minerals containing Fe^{2+}. Because NDMA was not degraded by the same oxic sediments, the chemical reduction likely reduced some mineral ferric iron. Sodium dithionite is known to reduce ferric iron in 2:1 smectite clays (Stucki et al. 1984). There may be a small amount of H_2 production at magnetite surfaces in the reduced sediment, which could catalyze NDMA degradation rate through reaction with H_2. Our previous research has shown that limited quantities of H_2 can be produced in the natural subsurface abiotically by release from mafic minerals (Stevens and McKinley 2000).

Experiments in this task are designed to identify the reactive phase that is degrading NDMA in natural sediments, as well as identify the degradation pathway (i.e., NDMA reaction products). In the first subtask (Task 1.1), degradation products will be measured in systems containing chemically reduced aquifer sediments (i.e., focus is on the NDMA portion of the redox reaction). In the second subtask (Task 1.2), ferric and ferrous iron minerals in natural sediments will be

physically and chemically separated in order to identify the reactive phase. In addition, the third subtask (Task 1.3) will address the role of H_2 in NDMA degradation. Finally, the longevity of this abiotic NDMA reduction process will be quantified. Analysis of NDMA and its byproducts at low concentrations is a key and difficult part of this task. We will begin by consulting Charles Luce at Aerojet, who has long experience with NDMA analysis. PNNL will adapt Aerojet methodology for analysis of NDMA and byproduct for which analytical protocols are known, and will additionally develop methods as needed.

Task 1.1 – Measurement of NDMA Degradation Products. We hypothesize that NDMA is being degraded by sediment minerals containing Fe^{2+}. NDMA is known to be degraded by Fe and Fe/Ni metals, and is thought to reductively degrade in the presence of Fe through several potential pathways (Gui et al. 2000). These include 1) catalytic hydrogenation to form DMA and ammonia, 2) two-electron transfer to form DMA and N_2O without production of ammonia, and 3) initial reduction across the N=O bond to form unsymmetrical dimethylhydrazine (UDMH) followed by DMA and ammonia. We hypothesize that the third pathway could occur with ferrous iron-containing minerals such as 2:1 smectite clays or H_2 produced from mafic minerals, so UDMH, DMA, and ammonia are the most likely degradation products.

Degradation products that will be measured in batch studies will include DMA by derivatization, then ultraviolet (UV) absorption, nitrous oxide by gas chromatography, methane by gas chromatography, ammonia by colorometric or ion chromatography, and NDMA and UDMH by liquid chromatography. NDMA has been previously measured in aqueous solution by high performance liquid chromatography (HPLC). In this HPLC method, 50 µL of the sample were injected into an aqueous stream of 60% water and 40% methanol at a flow rate of 0.8 mL/min into a C-18 phase bonded silica column (ThermoHypersil 255-901, 250 x 4.6 mm). NDMA detection was by UV absorption at 235 nm with retention times of 4.1 minutes (418.4 mAU/mg/L). Additionally, NDMA and its degradation products will be determined using HPLC - Electrospray ionization triple quadrapole mass spectrometry (ABI/Sciex Q Trap). Analytical conditions similar to those used by Hawari et al. (2002) will be used. This analysis will enable the effects of the remediation system on co-contaminants (e.g., perchlorate) to also be determined.

Geochemically characterized Aerojet sediments (200- to 255-ft depth composite) or other aquifer sediments will be used to conduct the time-course NDMA degradation pathway and rate studies in batch systems. The batch experiments consist of a series of steps: a) sediment reduction by sodium dithionite for 120 hours; b) addition of reduced sediment and NDMA-laden water to glass, septa-top vials under anaerobic conditions; and c) measurement of NDMA and degradation products of the aqueous solution at specified times. A range of NDMA concentrations will be used in batch experiments (0.25- to 5.4-mg/L NDMA), so that degradation products at sufficient concentrations can be analyzed.

Task 1.2 – Redox-Reactive Minerals in Reduced Sediments. Given the successful completion of Task 1.1 (i.e., NDMA degradation products are identified, which indicates a pathway), then a more clear hypothesis of the electron donor (i.e., ferrous iron minerals in the sediment or H_2 generated from minerals) will be established. Since we hypothesize that a potential electron donor is ferrous iron-containing 2:1 smectite clays, we will use mechanical size separation to separate out clay minerals from the sediment. If the redox-reactive phase(s) were evenly distributed on surfaces and there was no influence of clays, then the NDMA dechlorination rate

per unit surface area would be constant. This was not the case for a study of TCE degradation; the normalized TCE dechlorination rate was greater for smaller particles, implying that clays were be more reactive per unit surface area.

In addition, sequential chemical extractions will be used to strip off different iron oxides or iron-containing phases, leaving clays to determine whether adsorbed or structural ferrous iron controls NDMA reactivity. At each step of the way, the remaining NDMA reactivity will be measured with a relatively simple batch experiment.

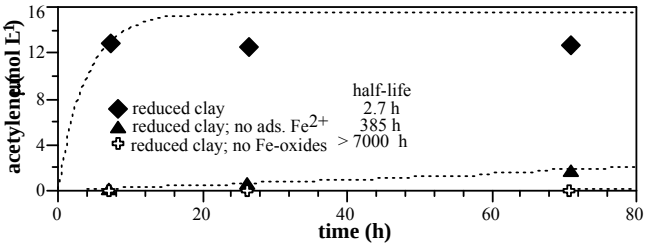

Figure 2.7. TCE degradation to acetylene in the 82% clay (<30 micron) fraction of reduced sediment (Szecsody et al. 2004).

In an example with TCE, the reduced <30-m fraction of a natural sediment (no extractions) quickly reduced TCE (half-life 2.67 hours; Figure 2.7, diamonds). TCE was dechlorinated 14 times slower when adsorbed Fe^{2+} was removed (triangles), again indicating adsorbed Fe^{2+} was the main electron donor, but some reactivity remained. Because Fe^{2+} may be adsorbed to iron oxides or clays, additional extractions were used to sequentially remove most of the amorphous and crystalline iron oxides, leaving predominantly clay. These additional sequential extractions (NH_2OH*HCl, DCB) all resulted in reduction of all TCE reactivity (no acetylene observed). These results imply that the any reduced structural iron in the 7% clays present in this sediment had little reactivity. The role of the 2:1 smectite clays may be significantly different for NDMA degradation, since there is no direct link between NDMA degradation and adsorbed ferrous iron (which there is for TCE). In a similar study, reduction of nitroaromatics was caused both by adsorbed iron on edge surfaces of clays as well as structural iron in the 2:1 smectite clays (Hofstetter et al. 1999, 2003).

Iron extractions will be conducted on untreated and dithionite-treated sediments in an anerobic chamber consisting of: a) 1 M $CaCl_2$ (Fe^{II} ion exchangeable) (Heron et al. 1994); b) 0.5 M HCl; c) NH_2OH, HCl (Chao et al. 1983); d) ammonium oxalate; e) Ti-EDTA; f) dithionite-citrate-bicarbonate (DCB); and g) 5 M HCl. Aqueous Fe^{II} and Fe_{total} from extractions were quantified by ferrozine (Gibbs 1976), where Fe_{total} (Fe^{II}+Fe^{III}) samples reduced aqueous Fe^{III} to Fe^{II} by 0.025 M NH_2OH, HCl. Extracted Fe^{III} was the difference between Fe_{total} and Fe^{II}. The $Fe^{II}CO_3$ + FeS ferrous phase was defined by the 0.5 M HCl minus the 1 M $CaCl_2$ extraction. Amorphous and poorly crystalline Fe^{III} oxides were defined by the ammonium oxalate and NH_2OH, HCl extractions, and crystalline Fe^{III} oxides were defined by the DCB minus the NH_2OH, HCl extraction. Total Fe^{II} and Fe^{III} oxides and carbonates were defined by the 5M HCl extraction.

Task 1.3 – Controlled H_2 Experiments for NDMA Degradation. There may be a small amount of H_2 production at magnetite surfaces in the reduced sediment, which could catalyze NDMA degradation rate through reaction with H_2. Our previous research has shown that limited quantities of H_2 can be produced in the natural subsurface abiotically by release from mafic minerals (Stevens and McKinley 2000). Dithionite-reduced sediment can achieve a moderate reducing environment (-230 mv), and the Eh can be adjusted between 0 and -230 mv by the

amount of reduction. Previous laboratory experiments with a mixture of zero valent iron and natural sediment showed that only a moderate reducing environment (-50 mV) was necessary for mineralization and that more highly reduced conditions did not increase the mineralization rate (Singh et al. 1999). Because one hypothesis that is causing NDMA degradation is H_2 generated by mafic minerals, we will determine the relationship between the H_2 present in a system and the NDMA degradation rate with a bench-scale Eh-pH stat system (Petrie et al. 1998).

Task 1.4 – Long-Term Performance of NDMA Abiotic Degradation by Reduced Sediments. For this abiotic (or coupled abiotic/biotic) process to be a viable technology at the field scale, NDMA needs to be degraded for hundreds of pore volumes in the reduced sediment barrier. For any chemically reduced sediment, the sediment reductive capacity is measured by oxidizing the sediment with air-saturated water, as previously described in the background section (Figure 2.6). Most sediments range from 200 to 1000 pore volumes of reductive capacity. In this subtask, the NDMA degradation rate will be measured as reduced sediment is oxidized over hundreds to thousands of pore volumes. This will be accomplished by collecting NDMA degradation rate data at 0, 50, 100, 200, and 300 pore volumes (given that it takes 300 pore volumes to fully oxidize the sediment). A specific sediment-NDMA contact time is needed to achieve degradation (e.g., 100 hours), so instead of conducting a 3000-hour experiment, the experiment was accomplished efficiently by: a) 100-hour residence time for 5 pore volumes to collect NDMA samples, b) followed by 0.5-hour residence time for 45 pore volumes of oxygen-saturated water to oxidize the sediment, and c) repeating the cycle. An example of this type of experiment is illustrated in Figure 2.8 with TCE dechlorination to acetylene, then ethylene by chemically reduced sediment. As the sediment is oxidized over 250 pore volumes, the mass of degradation products decreased (i.e., rate of TCE degradation decreased). The conclusion was that although the sediment ferrous iron will consume oxygen for 250 pore volumes, it will degrade TCE for only about half that number of pore volumes, likely because sufficient reducing conditions to catalyze TCE no longer occur.

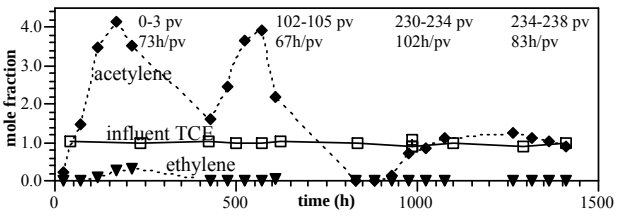

Figure 2.8. TCE long-term dechlorination in reduced sediment, as shown by acetylene and ethylene degradation products (Szecsody et al. 2000, 2004).

The column experimental system for these proposed NDMA degradation studies is designed to minimize mass losses to volatilization and diffusion, because some degradation products had moderate to high vapor pressures. The column influent, consisting of groundwater containing NDMA will be contained in a 5-L metalized bag. Influent and effluent will be monitored over experiments ranging from 200 to 1400 hours shown. Effluent will be collected in 154-mL anaerobic vials with 10-mm-thick septa tops (no exposure to air, Figure 2.9). The flow rate will be measured from the sample volume and elapsed time. An automated switching valve was used to collect the samples over 24- or 48-hour intervals. Materials used in the column system were stainless steel or PEEK, both of which have extremely low permeabilities to organic compounds. Dissolved oxygen was monitored during this experiment with in-line electrodes, as described earlier. NDMA and degradation products measured in the inlet and effluent samples will be measured by methods determined in Task 1.1.

Figure 2.9. Collection of column effluent in anaerobic vials.

Task 2 – Microbial Degradation of NDMA. Native soil microorganisms may affect NDMA in at least three ways. First, as discussed above, microorganisms can directly attack and mineralize NDMA. Second, microorganisms may mineralize the products of NDMA that results from its chemical reduction. Third, the general respiration of the subsurface microbial community on all the substrates available to them will help poise the redox conditions in the soil environment. In this context, the biological production of H_2 and its effect on NDMA reduction (see Task 1.3) and long-term sustainment of the reduced semi-permeable barrier are important practical issues.

Task 2.1 – NDMA Biodegradation in a Microbe/Sediment System. NDMA biodegradation will be studied in soil slurry microcosms using an experimental design that enabled direct measurements of mineralization potential, rates of lose of NDMA, and identification of some degradation products. These slurry experiments will be conducted with and without prior chemical reduction. A modified version of the method developed by Fulthorpe et al. (1996) and detailed in Ringelberg et al. (2001) will be used to assess microbial NDMA potentials. Two grams (wet weight) of slurry material, from each respective soil, will be placed into 15-ml Teflon-lined screw cap test tubes to which will be added 2.7 mL of a modified Stanier's Basal media (or groundwater) and a tracer amount of the ^{14}C-NDMA. These slurry microcosms will be run in triplicate and spiked with 20,000 dpm of ^{14}C-NDMA (N-[methyl-^{14}C]; >95% radiochemical purity; Sigma Chemical Co, St. Louis, MO) at a specific activity of 56.0 mCi/mmole. Glass fiber filters (Whatman, Maidstone, UK), 10-mm diameter, saturated in 1-M barium hydroxide will be used to trap evolved $^{14}CO_2$. Test tubes will be incubated at 20ºC on a tube roller inclined at 45 degrees and rotated at 10 rpm. The BaOH saturated filters will be collected daily over a 30-day period and placed into 1.5 ml of scintillation cocktail (Ultima Gold, Packard Instruments Co., Downers Grove, IL) before counting on a top count microplate scintillation counter (Packard Instrument Co., Downers Grove, IL). Filters will be counted twice, and counts will be corrected for background and counting efficiency using the external standard method described by the manufacturer.

Replicate soil slurry microcosms were collected and analyzed on days 1, 3, 7, 10, 14, 18, 21, 25, and 30. Test tubes will be centrifuged to pellet the soils. Samples of the water will be taken for NDMA HPLC analysis as described above. Samples of the water and sediment will be taken and analyzed by liquid scintillation counting for constructing ^{14}C mass balances. This entire experimental setup will also be place in a Coy glove bag under an atmosphere of oxygen-free carbon dioxide/nitrogen to determine the effects of anoxia on NDMA biodegradation.

Task 2.2 – NDMA Biodegradation by Microbial Isolates. Microbial communities in soil slurry microcosms showing the best rates of ^{14}C-NDMA mineralization will be selectively enriched using two different approaches. In the first approach, samples of the actively ^{14}C-NDMA mineralizing soil slurries will be transferred into modified Stanier's basal salts solutions containing ^{14}C-NDMA as either the sole nitrogen (added acetate and glucose) of sole carbon

source. Turbidity and $^{14}CO_2$ will be used as makers for NDMA degradation activity. Tubes showing NDMA degradation activity will be repeated transferred to fresh media until a stable consortia of pure cultures are obtained. The second approach to enriching and isolating NDMA degrading microorganisms is the same as the first except that the actively NDMA degrading slurry is first serially diluted before enrichment with NDMA as the sole carbon or nitrogen source. This enrichment scheme favors NDMA degraders that may be a minority in the original slurry.

In both Tasks 2.1 and 2.2, the microbial community biomass and community composition will be determined using polar membrane lipid fatty acids. Briefly, a 2 g (wet weight) aliquot from 5 g total (per reactor) of slurry material will be extracted for 3 hours at room temperature in 6 ml of a mixture of dichloromethane:methanol:water (1:2:0.8, v:v:v). Amino-propyl solid phase extraction columns (Supelco, Bellefonte, PA) will be used to separate the total lipid into neutral, glyco- and polar lipid fractions. Phospholipid fatty acid methyl esters (from the polar lipid fraction) will be prepared for gas chromatography/mass spectrometry (GC/MS) by mild alkaline methanolic transesterification. The resulting phospholipid fatty acid methyl esters will be dissolved in hexane containing methyl nonadecanoate (50 pmol μL^{-1}) as an internal standard and analyzed using a gas chromatograph equipped with a 50-m x 0.25-mm (inside diameter [ID]) DB-1 capillary column (0.1-µm film thickness, J&W Scientific, Folsom, CA) and a flame ionization detector. Peak identities will be confirmed using a gas chromatograph-mass selective detector (Hewlett Packard GC6890-5973 MSD) with electron impact ionization at 70eV. Areas under the peaks will be converted to concentrations, summed and then normalized to the gram weight extracted for biomass determinations. For community comparisons, the percent contribution of each peak will be calculated and then normalized using an arcsine square root transformation.

Task 3 – Coupled Abiotic/Biotic Degradation of NDMA. The details of activities under this task are contingent on results of the abiotic and biotic degradation investigations (i.e., go/no decisions of Tasks 1 and 2 affect this task). Preliminary results, however, are sufficient to pose a hypothetical set of activities for experimental evaluation of mixed biotic and abiotic NDMA degradation. We hypothesize that the chemical reduction of sediments creates a "preconditioned" reduced zone and the microbial population within or downgradient can be stimulated to:

- utilize SO_4 produced from dithionite reacting with iron oxides as an electron acceptor
- utilize NDMA as a cosubstrate rather than the primary electron donor (i.e., addition of a specific electron donor with a similar reductase as NDMA)
- drive the reducing conditions sufficiently negative to generate significant H_2.

The preliminary results of abiotic experimentation (Task 1) indicated that NDMA was degraded by ISRM treated sediments in the subsurface. In field trials, it has been shown that a single injection of dithionite delivers 13,000 mole equivalents of reducing capacity, resulting in a total reducing capacity in the *in situ* sediment of ~6,500 mole equivalents; the injection is 50% efficient (Vermeul et al. 2002). The distribution of reducing capacity may be manipulated by varying the concentration of dithionite and the injection rate of the reducing solution into the subsurface (Chilakapati et al. 2000). In Task 1, we will have determined the abiotic degradation pathway and optimized the degradation process in the laboratory. In addition, within a funded SERDP project (Enhancement of In Situ Bioremediation of Energetic Compounds by Coupled

Abiotic/Biotic Processes, CU-1376, FY04 - FY06), the coupled abiotic/biotic degradation of energetics will be investigated by some of the scientists in this proposed project, specifically by modifying the dithionite injection strategy to enhance microbial survival. Results of that project (differing chemical composition or injection strategy to maximize microbial survival, where the microbes are capable of energetic degradation) will be applied to this coupled NDMA degradation task.

We may assume also that NDMA, at the trace concentrations present in Aerojet groundwater, will be degraded with some efficiency by indigenous bacteria, if the bacteria are stimulated by the introduction of the appropriate electron donor (Task 2). These bacteria would not be expected to degrade NDMA specifically, but if they are presented with NDMA as a component of a nutrient-rich mixture, it is likely to be incidentally degraded along with the abundant electron donor. The efficiency of this process will have been investigated and optimized under laboratory conditions in Task 2.

There is some laboratory- and field-scale evidence that the dithionite treatment of sediments kills some of the microbial population, but that the surviving fraction can function and biodegrade compounds including energetics. The introduction of large quantities of dithionite at a pH of 10 to 11, itself degrading to form several reactive intermediates while reducing sedimentary Fe(III), could sterilize the impacted sedimentary environment. This does not seem to be the case. Field experiments suggest that the microbial community survives, and microbial degradation of the explosive RDX has been shown to occur after injection. At Ft. Lewis, Washington, for example, the injection of dithionite to reduce the aquifer system resulted in the reduction of *in situ* bacteria from 2 x 10^6 cfu ml^{-1} of groundwater to 6 x 10^5 cfu ml^{-1} of groundwater; i.e., 30% of the indigenous population survived. There is parallel laboratory-scale evidence that indicates that dithionite-reduced sediments can still biodegrade energetics. Although RDX is known to be degraded abiotically in sediments after dithionite injection, the mineralization of RDX to CO_2 is not possible via an abiotic pathway. In sediments injected with dithionite, after a lag for microbial recovery, RDX was observed to undergo mineralization (Figure 2.10). It is not known at present from these experiments what the potential viability of the surviving population is for degrading NDMA. However, these results suggest that a biotic/abiotic field process could significantly remove NDMA from contaminated aquifer systems.

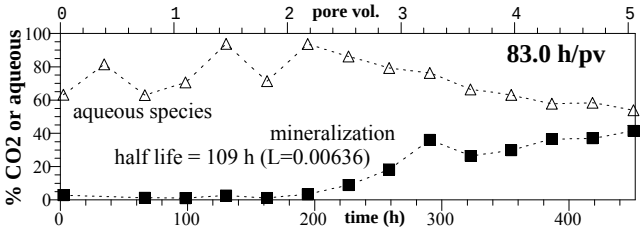

Figure 2.10. Initial abiotic degradation of RDX followed by biodegradation of intermediates.

The conceptual approach to implementing a coupled biotic/abiotic remediation of NDMA is straightforward. The appropriate concentrations of dithionite and ethanol would be injected to form a permeable redox barrier in the subsurface. Abiotic reduction of NDMA would occur as it was advected into the barrier, and biotic reduction would follow after a lag for microbial community recovery from the injection. What is not known is the relative significance of the two processes. The abiotic pathway may be the most significant. In that case, the expected life of the barrier would be affected by the function of microbiota in removing potentially oxidizing species such as nitrate or oxygen. Alternatively, the biotic pathway may be more significant

over time than the abiotic one. In that case, the injection of dithionite might act to 'prime' the subsurface ecosystem by inducing an anaerobic environment. The reduced sediment zone would act as a buffer for the anaerobes, and utilization of the co-injected ethanol would drive the reduction of NDMA. Ethanol could be renewed by repeated injections either into the barrier directly or by supplement to the contaminated groundwater upgradient of the barrier. The barrier capacity will be 200 to 1000 pore volumes, and the activity of an anaerobic community could prolong its temporal lifetime by limiting the impact of dissolved oxygen.

Laboratory experiments under this task would be conducted to evaluate and optimize the combined impact of biotic and abiotic treatments of NDMA in the subsurface. The experimental protocols would be similar to those used in Tasks 1 and 2, but they would be conducted simultaneously and in combination. The goal of this experimentation would be final conceptualization and design for Task 4.

Task 4 – Large 1-D Laboratory-Scale Demonstration of NDMA Degradation and Mineralization. Given the success in laboratory-scale abiotic (Task 1) or coupled (Tasks 2 and 3) NDMA degradation experiments, then a small field-scale demonstration of the abiotic only (i.e., sodium dithionite injection) or coupled abiotic/biotic technology was originally proposed. Although abiotic degradation of NDMA to DMA (Task 1) was rapid, the lack of control of the degradation intermediates (DMA is not toxic, but other intermediates are) lead to the conclusion that *mineralization* of NDMA is the lowest risk of a remediation technology. Therefore, Task 4 was rescoped to coupled abiotic/biotic experiments conducted in Task 3 were upscaled to large 1-D columns with an upgradient reduced sediment column and a downgradient oxic sediment column. The NDMA degradation and mineralization rate and longevity was investigated in these sequential reduced/oxic systems (series of 15 separate column systems).

3.0 Experimental Methods

3.1 Task 1 – Abiotic Degradation of NDMA

3.1.1 Measure Degradation Products NDMA analysis by HPLC

NDMA at concentrations of 50- to 0.1-mg L^{-1} concentrations were measured using HPLC methods. NDMA and possible degradation products were measured in aqueous solution by liquid chromatography by an HPLC method (modification of U.S. Environmental Protection Agency [EPA] Method 8330, HPLC Analysis of Explosives) and by liquid chromatography/mass spectrometry (LC-MS)/MS. With this HPLC system, compounds that are more polar or of lower molecular weight will elude sooner than NDMA. Detection was by UV absorption at 235 nm with retention times of 2.7 minutes (unknown 1), 2.8 minutes (unknown 2), 3.0 minutes (unknown 3), and 5.60 minutes for NDMA. The specific conditions of the HPLC system include:

- Keystone NA C-18 column, 250 mm x 4.6 mm
- 40% methanol, 60% water (isocratic), degassed with continuous helium
- flow rate 0.8 mL/min, 2200 psi, HP1050 series HPLC pump
- samples in 1.5-mL HDPE vials, 50-µL injection volume
- UV detection at 230 nm, HP1050 series multiple wavelength detector.

Calibration of NDMA from 0.1 to 100 mg/L was linear to 50 mg/L (Figure 3.1), and most experiments were conducted with an initial NDMA concentration of 5 mg/L. Calibration at higher concentration (to 100 mg/L) was nonlinear, but could be accomplished with a power function fit. Additional calibration of NDMA (3 to 0.06 mg/L, Figure 3.2) was essentially the same, and showed the lower reliable detection limit of 0.07 mg/L, with an average standard deviation of 1.0% (placed on graphs with NDMA analysis).

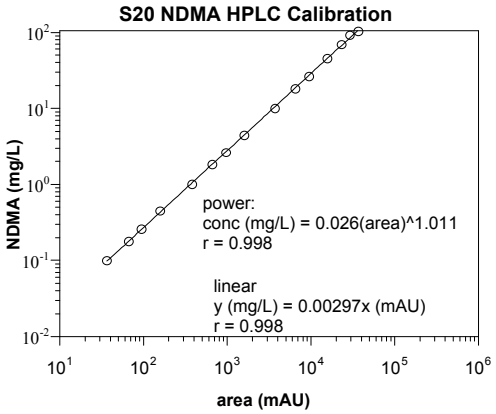

Figure 3.1. NDMA calibration by HPLC-UV detection to 100 mg/L.

3.1.1.1 NDMA by Scintillation Counting

A total of 5 mCi of ^{14}C-labeled NDMA was purchased for experiments at PNNL and WES. Due to the high specific activity of this labeled compound (56 mCi/mmol, thanks to Perkin Elmer/ New England Nuclear), concentrations down to 0.3 ppt could be analyzed. Experiment samples were analyzed for: a) total aqueous ^{14}C (aqueous NDMA and aqueous degradation products), b) aqueous NDMA (method described below), c) gas phase CO_2 generated during degradation, d) adsorbed NDMA and adsorbed aqueous degradation products (methanol/water extraction; described below), and e) ^{14}C incorporated into microbes (NaOH extraction; described below). ^{14}C-labeled samples were analyzed from experiments at times ranging from 30 seconds to

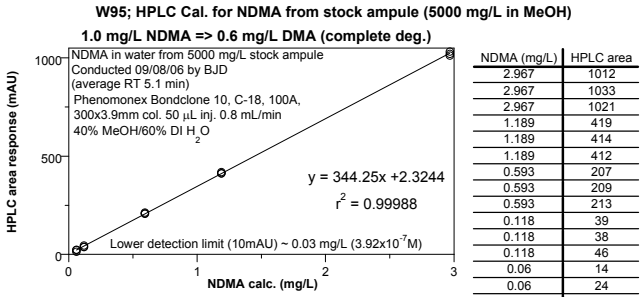

Figure 3.2. NDMA calibration by HPLC-UV detection to 3 mg/L.

1000 hours. Total aqueous ^{14}C involved removing an ~0.5-mL sample of the aqueous experiment solution, filtering, and analyzing by scintillation counting. In many experiments, multiple samples were taken from the same experiment, so sampling reduced the volume of the experiment (to some extent), and the mass of liquid and ^{14}C removed was accounted for in subsequent samples. Carbon dioxide (gas phase) generated from mineralization of NDMA and intermediates was analyzed by the use of a CO_2 trap in the experimental vial. These traps contained 0.25 mL of 1.0 mol/L NaOH. At specified times, the NaOH was extracted from the trap without uncapping the vial (with a needle through the septa) and counted for ^{14}C-labeled carbon dioxide. The purpose of maintaining the vial seal was to keep gas-phase reaction products in the system. In this case, the aqueous volume of the system is unchanged by sampling, but there is ^{14}C mass removal, so the cumulative amount of ^{14}C extracted over time was accounted for.

NDMA (^{14}C-labeled) was measured by removing a 1.5-mL sample at specified times from the system and injecting it into a preparatory-scale HPLC system, which contained a C18 column (as described above for HPLC analysis of NDMA) with a 12% methanol/88% water mobile phase. While the HPLC system used a 4.6-mm diameter by 250-mm length column (4.1 cm^3 total volume), the preparatory-scale HPLC system used a 11-mm diameter by 476-mm length (41.1 cm^3 total volume) column that was 10 times the volume. This enabled injection of a 1.0-mL sample (compared to 50 to 100 µL sample for the HPLC), with clear separation of NDMA from other aqueous degradation products and collection of a 13-mL sample. This 13-mL sample was then counted in a scintillation counter. Two different scintillation counters will be used to achieve the parts per trillion NDMA levels. The current scintillation counter (used for most experiments) has a background level of 13 counts per minute (background radiation), so 2.5-ppt NDMA is near the lower detection limits, even when counting for 3 hours. The second scintillation counter is a specialized low-level counter with extensive shielding to lower the background radiation considerably. This counter is likely to achieve <1-ppt NDMA levels of counting. Separation of NDMA is shown in Figure 3.3, with nonradioactive NDMA injection and a flow through UV detector (i.e., y-axis represents relative UV absorbance, offset between injections for clarity). The NDMA peak (4 to 7 minutes or a 13 g collection after 39 g) is collected separately for analysis by scintillation counting. Dimethylamine (NDMA degradation product) was eluting at ~2.5 minutes.

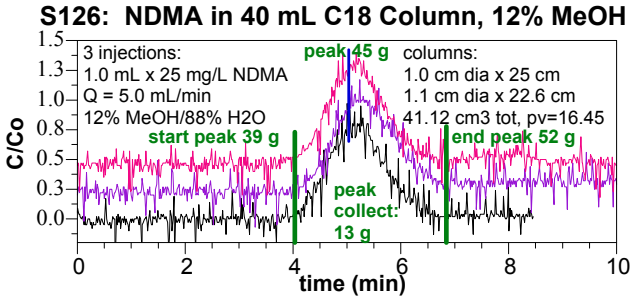

Figure 3.3. NDMA (^{14}C labeled) separation on a preparatory-scale HPLC NDMA analysis to parts per trillion levels.

For mineralization experiments in the 2.5- to 0.25-ppm range, cold NDMA stock was added to the ^{14}C-labeled NDMA. For 25-ppb to 2.5-ppt experiments, the NDMA concentration from only the ^{14}C-labeled compound was used. Standard mineralization experiments were used for 2.5-ppm to 250-ppt experiments, with 6 mL of solution (with 400- to 5000-dpm/mL ^{14}C activity from NDMA) and 1.0 g of sediment. For 25- and 2.5-ppt experiments, significantly more solution was added (100 mL) containing 42 dpm/mL (25 ppt) or 4.2 dpm/mL (2.5 ppt) with 16.5 g of sediment to have sufficient ^{14}C activity above background for meaningful experiments. The 0.25-mL CO_2 traps essentially concentrate the ^{14}C activity significantly, so the total ^{14}C activity in each bottle, if 100% mineralized would be in the CO_2 trap. For the 25-ppt experiment, the total counts in the experiment was 4200, and for the 2.5-ppt experiment, 420 counts. If the minimum mineralization precision is 1% (i.e., 1% of the 420 counts), then the 4.2 dpm/mL is still possible to separate from the 13-dpm/mL background (to a statistical confidence interval of 0.2%).

Four NDMA degradation batch experiments were conducted with ^{14}C-labeled NDMA with reduced Aerojet sediment. The starting concentration of these experiment were 2.5 ppm, 36 ppb (maximum observed concentration in groundwater at the Aerojet, CA site), 100 ppt, and 10 ppt. In each experiment, the total aqueous ^{14}C, NDMA, and mineralization was measured at specified times ranging from 24 to 2000 hours. At the end of the experiment (2000 hours), extractions were then conducted of the sediment to measure the amount of NDMA sorbed onto the sediment surface (considered very minimal, based on earlier K_d measurements on the same sediment) and on the microbial surface, and to measure the amount of carbon (^{14}C-labeled) incorporated into microbes. These extractions were described earlier, and consisted of a methanol/water mixture for sorbed phase extraction (1-hour mix, then filtering before analysis), and a 2-M NaOH extraction (to dissolve microbes), with filtering before analysis.

3.1.1.2 DMA and UDMH Analysis

Two different DMA derivatization methods were considered:

- DMA and 9-fluorenymethylchloroformate: Lopez et al. (1996)
- DMA and 2,4-dinitroflorobenzene (DNFB) or Stanger's reagent: Gui et al. (2000).

Due to simplicity, the derivatization method with DNFB was used. The method was modified from this original reference to be able to get to lower detection limits. The original method uses the DMA sample and 50:1 molar ratio excess of DNFB, and some additional reagents (acetonitrile and NaOH). While this method worked fine for high DMA concentrations, the size of the DNFB peak was large relative to the DMA peak, so limited DMA low concentration analysis. It was determined that lowering the DNFB/DMA molar ratio from 50/1 to 20/1 solved this problem. As shown in Figure 3.4a, DMA analysis (derivatized the DNFB) produced the same area counts with DNFB/DMA molar ratios ranging from 10 to 60. However, with molar ratios of >50, the size of the DNFB peak was 5 times larger than the DMA peak (Figure 3.4b, at 0.3-mg/L DMA), but using a lower 25/1 DNFB/DMA ratio resulted in similar areas (on HPLC analysis), so that a lower DMA area could be measured.

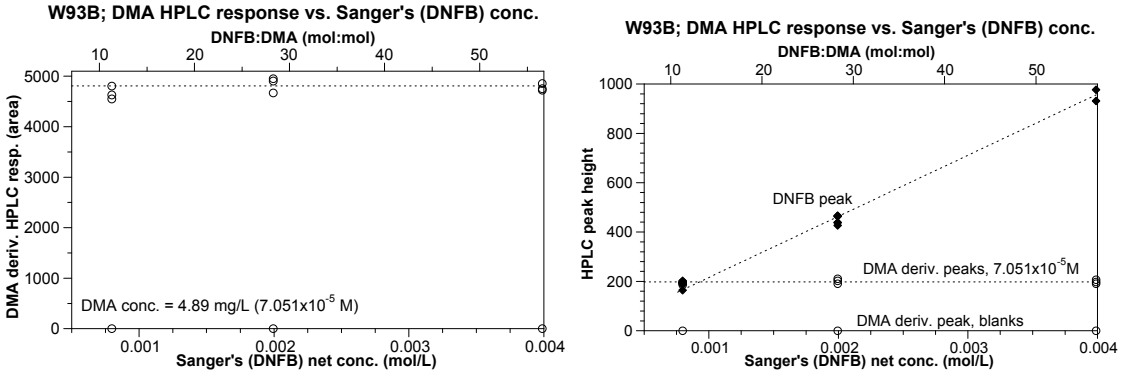

Figure 3.4. Dimethylamine (DMA) response with differing DNFB concentration at: a) high 5-mg/L DMA concentration and b) 0.3-mg/L DMA.

The DMA HPLC calibration curve with the modified DNFB reagents (Figure 3.5) shows linear response from 3- to 0.06-mg/L DMA (detection limit ~0.01-mg/L DMA). The same derivatization agent (DNFB) can be used for UDMH, and some work was done to develop this method. This was abandoned as it was decided that UDMH appearance was highly unlikely (only shown as a degradation products under acidic conditions).

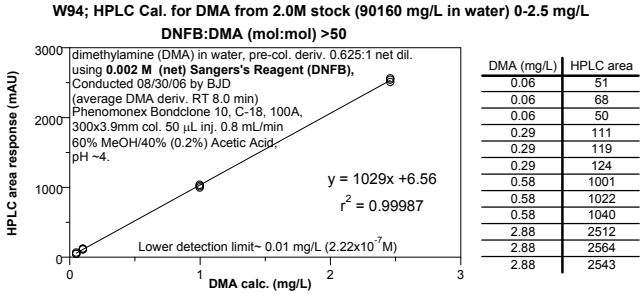

DMA (mg/L)	HPLC area
0.06	51
0.06	68
0.06	50
0.29	111
0.29	119
0.29	124
0.58	1001
0.58	1022
0.58	1040
2.88	2512
2.88	2564
2.88	2543

Figure 3.5. Dimethylamine (DMA) calibration, derivitized with DNFB.

3.1.2 Investigation of Redox-Reactive Minerals in Reduced Sediments

Aerojet sediment from well 30053, composited from depths 200 to 255 ft were reduced by dithionite in three different experiments to achieve a differing amount of sediment reduction. In previous years experiments, the sediment was reduced in a column, then pH-equilibrated. This consisted of about 130 cm^3 of sediment packed into a stainless steel column and sodium dithionite/potassium carbonate injected into the column with a 5-hour residence time for 120 hours with a differing concentration of dithionite. The maximum reductive capacity of the Aerojet composite sediment is 71.5 µmol/g, and molar ratio of dithionite injected into the sediment equaled: a) 26.8 times dithionite/ferrous iron (experiment W21), b) 2.83 times dithionite/ferrous iron (experiment W22), and c) 0.54 times dithionite/ferrous iron (experiment W23). The residence time was the approximate half-life of the sediment reduction reaction. The total time of injection (120 hours) allowed for nearly complete sediment reduction. In 2007, several batches of the Aerojet composite sediment were reduced in batch experiments. This consisted of 100 g of sediment plus 500 mL of solution containing specific dithionite/carbonate concentration to achieve the desired dithionite/iron ratio (25, 3, 1.1). The sediment/water system (with no dithionite) was flushed with helium for an hour inside an anaerobic chamber before adding dithionite to insure gas phase and dissolved oxygen was not consuming dithionite. The reaction was allowed to continue for 120 hours (same as the

column reduced dithionite), but the difference was reduced sediment was then not pH equilibrated. The pH of the final sediment was ~10 (described in Section 4.0).

3.2 Task 2 – Microbial Degradation of NDMA

3.2.1 Biodegradation in Reduced Sediment Systems

The experiments with dithionite-treated sediment were set up to determine the effect of dithionite exposure on the soil microbial community's ability to mineralize NDMA. Batch soil slurries were prepared in a Coy anaerobic glove bag using 1 g of a soil from Ft. Lewis and 3 ml of a sodium dithionite/K_2CO_3 solution. The water in each tube was bubbled with ultra-pure nitrogen for 30 minutes before the appropriate amount of potassium carbonate and sodium dithionite were added. There were three treatments in this experiment that consisted of different donor/acceptor ratios where dithionite was the donor and no acceptor was supplied. The ratios used were 29.68, 1.48, and 0.29, and dithionite and carbonate were kept at a ratio of 1:4. Controls contained soil and water without the addition of dithionite or carbonate. All treatments were incubated for 5 days under these conditions and were then washed twice with anaerobic pH 7 buffered water to remove residuals. A mineralization study was carried out anaerobically by resuspending the washed soil in 6 ml of buffered water containing ^{14}C-NDMA. The concentration of NDMA in the solution was 10 mg/L and contained 5000 dpm/ml of radioactivity. To measure mineralization, filter disks were dipped in a 1-M barium hydroxide solution and inserted into the top of each test tube cap so that $^{14}CO_2$ would be absorbed. At appropriate time points, the disks were removed and placed in 15 ml of scintillation cocktail to be counted. Fresh disks with barium hydroxide were then placed in each cap. This mineralization study was carried out for 60 days and all experiments were performed in duplicate.

3.2.2 Biodegradation by Microbial Isolates

Gordonia sp. KTR9 and *Williamsia* sp. KTR4 were previously isolated from surface soils associated with an explosive manufacturing and testing facility at China Lake, CA (Thompson et al. 2005). *Gordonia* sp. KTC13 was isolated from the same soil by similar procedures except that the nitrogen source for growth was the explosive hexanitrohexaazaisowurtzitane (CL-20, HNIW) (unpublished data). Additional bacterial cultures were obtained from the Deutsche Sammlung von Mikroorganismen und Zellkulturen Gmb H (DSMZ) (Table 3.1) and were maintained on Trypticase soy agar plates at 4ºC. Bacteria were initially grown in a mineral salts medium (K_2HPO_4 0.38 g; $MgSO_4.7H_2O$ 0.2 g; $FeCl_3.6H_2O$ 0.05 g; H_2O 1L, pH 7.0) containing 4 mM KNO_3, 10 mM glycerol, 5 mM glucose, and 5 mM succinate. After several days of growth, the cultures were used to inoculate fresh mineral salts medium containing [^{14}C]-NDMA and non-radiolabelled NDMA to provide a final concentration of 5000 dpm/mL and 10 mg/L. Nitrogen (KNO_3, 4 mM) or carbon amendments (glycerol, 10 mM; glucose, 5 mM; and succinate, 5 mM) were added when applicable. Cultures were set up in 125-mL serum bottles containing 30 mL of the medium and an inner vial containing 1 mL of 1 N potassium hydroxide (KOH) to absorb $^{14}CO_2$. The serum bottles were inoculated with a 1/10 volume of bacterial culture and then sealed with Teflon-coated butyl stoppers and aluminum crimp seals. The bottles

were incubated in the dark at 30°C with constant shaking at 150 rpm. The KOH was periodically sampled and added to 15 ml of Ultima Gold scintillation cocktail followed by counting on a scintillation counter. Each time the KOH was sampled, it was replaced by a fresh volume of KOH.

Table 3.1. Bacterial strains used in this study.

Strain	Source	Carbon or Nitrogen Added		
Gordonia alkanivorans	DSMZ 44369^T	GGS[a]	KNO_3	None
Gordonia amarae	DSMZ 43392^T	GGS	KNO_3	None
Gordonia desulfuricans	DSMZ 44462^T	GGS	KNO_3	None
Gordonia nitida	DSMZ 44499^T	GGS	KNO_3	None
Gordonia polyisoprenivorans	DSMZ 44302^T	GGS	KNO_3	None
Gordonia rhizosphera	DSMZ 44383^T	GGS	KNO_3	
Gordonia rubripertincta	DSMZ 43197^T	GGS	KNO_3	None
Gordonia terrae	DSMZ 43249^T	GGS		
Gordonia sp. KTR9	Thompson et al. 2005	GGS	KNO_3	None
Gordonia sp. KTC13	Thompson et al. unpublished	GGS		
Williamsia maris	DSMZ 44693^T			None
Williamsia sp. KTR4	Thompson et al. 2005	GGS	KNO_3	None

T: type strain for species; a: GGS: glucose, glycerol and succinate

Anaerobic NDMA Mineralization

Anaerobic mineralization of [^{14}C]-NDMA was studied in screw cap test tubes. One gram of Aerojet soil or 1 mL of Rocky Mountain Arsenal groundwater was added to each sterile test tube along with 5 mL of mineral salts medium. Nitrogen gas had been bubbled through the medium for at least 30 minutes to reduce the oxygen content. NDMA was added at 10 mg/L and 5000 dpm/mL. To capture the $^{14}CO_2$ produced, 1-N BaOH saturated filter paper disks were used as liners in the screw caps. Microcosms were prepared and incubated in an anaerobic Coy™ glove box at 25°C and with an anaerobic atmosphere of 4% H_2 and 96% N_2 gas. The BaOH saturated filter disks were sampled periodically by scintillation counting and replaced with freshly saturated disks.

3.3 Task 3 – Coupled Abiotic/Biotic Degradation of NDMA

NDMA mineralization experiments were conducted with Aerojet sediments to measure both oxic and anaerobic/reducing system mineralization without and with additional nutrients or co-metabolites. A total of 108 mineralization experiments were conducted. This included oxic

and reduced system mineralization in Aerojet sediment at 2.5 ppm, 250 ppb, 1.8 ppb, 102 ppt, and 10.2 ppt starting concentration. Another series of experiments included oxic, anaerobic (not reduced) sediment, and reduced system mineralization with a single concentration of methane or propane or toluene or acetylene all at 250-ppb NDMA. Another series of experiments included different carbon additions in reduced Aerojet sediment (yeast extract, humic acid, or TCE addition). Because a biotic NDMA degradation pathway is with a propane- or methane- or toluene-monooxygenase pathway, these compounds were added to see if that enzyme pathway was stimulated. Acetylene is also known to inhibit most (not all) monooxygenase pathways. Reduced sediment degrades TCE by a pathway that produces chloroacetylene, then acetylene, then ethylene, then ethane. Therefore, TCE addition would degrade to some acetylene, which could inhibit the monooxygenase pathway for NDMA degradation. Because there was little response to the carbon additions (yeast, humic acid), additional experiments were conducted with differing concentrations and 1600 hours of prestimulation (i.e., contact with the carbon source and NDMA before ^{14}C-NDMA was added). These experiments included oxic and reduced Aerojet mineralization with addition of yeast (three differing concentrations) and humic acid (three differing concentrations), all with the prestimulation time of 1632 hours. Because the propane addition showed some response, additional propane experiments were conducted at three differing concentrations (of propane) and 1600 hours of prestimulation.

Sequential reduced system, then oxic system NDMA mineralization studies were conducted by either: a) oxidizing existing reduced sediment, b) removing aqueous solution and placing it with oxic sediment, and c) adding oxic sediment to the system. A total of 16 sequential reduced/oxic experiments were conducted (1600 hours of prestimulation, 2200 hours of reduced system degradation, then 1000 hours of oxic system degradation). Additional oxygen (all experiments), propane, humic acid, or yeast was added to experiments. An additional seven experiments were conducted in which oxic system NDMA mineralization was additionally stimulated at 2000 hours with additional humic acid, oxygen, and/or propane to determine if microbes were still alive but there was a nutrient limitation in the system. Experiments at 25 and 2.5 ppt (initial concentration) used only the ^{14}C-labeled NDMA, which had a specific activity of 56 mCi/mmol. For higher NDMA concentration experiments, 1 g of sediment was mixed with 6 mL of liquid, and lower NDMA concentration experiments 16.5 g of sediment was mixed with 100 mL of water. The ^{14}C activity in each vial is explained in Section 3.1.1.

Sediments

Three sediment samples were obtained from Scott Neville at Aerojet, which were from boring/ monitoring well 30053 (next to extraction well 4450). The three samples were within a depth interval of 200 to 255 ft, so are in a sand/gravel aquifer unit, which is at a depth of 194 to 264 ft at this location (based on the 30053 well log). These three samples were mixed with equal mass proportions to obtain a sufficient volume for experiments. This unit is described as a medium to very coarse-grained sand/gravel with 2- to 4-ft-thick interbeds of sand and gravel and 0.5- to 1-ft-thick interbeds of sandy clay. The Aerojet sediment samples obtained were not fully characterized mineralogically, but did contain unusually high magnetite (36.4% by weight), and trace amounts of biotite (< 2%).

3.4 Task 4 – Upscaled Demonstration of NDMA Degradation in Sequential Reduced, then Oxic Systems

NDMA mineralization experiments were conducted in large-scale laboratory columns to evaluate whether NDMA degradation in reduced sediment followed by downgradient mineralization of NDMA (or intermediates) was more efficient than NDMA mineralization in oxic systems. This was proposed because numerous experiments have demonstrated that NDMA degradation in reduced sediment is very rapid (hours to tens of hours). The original scope for Task 4 was to evaluate NDMA degradation in a field-scale experiment at the Aerojet site. While NDMA could rapidly be degraded to DMA, which is not toxic, because DMA is degraded further to more toxic intermediates, it was concluded that the objective of this task should be rescoped to optimizing NDMA mineralization. At a field setting, sequential reduced then oxic systems have been investigated and implemented at field scale for biotic and abiotic processes (Bell et al. 2003; Morkin et al. 2000). In this study, a reduced zone is created by sodium dithionite treatment of aquifer sediment, which dissolves/reduces some of the ferric oxides to various ferrous oxides and sulfides. Various redox-sensitive aqueous solutes advecting into this zone may be reduced (metals, nitrate, chlorinated solvents, and dissolved oxygen), which results in a plume of anoxic water (and degradation intermediates) downgradient. A downgradient oxic zone is naturally created at some distance due to advective mixing of oxic water that did not pass through the permeable reduced zone. However, the most efficient means of creating an oxic zone downgradient of a reduced zone is to inject air.

In this study, the configuration of the sequential reduced sediment with downgradient oxic sediment columns consists of a 1-D reduced sediment column (8.8 to 60 cm in length) with downgradient mixing "T" into which a mixture of air and propane is injected (20% by volume relative to the water flow). The groundwater injected into these systems consisted of a 0.01-mol/L $CaCO_3$ solution with 250-ppb NDMA (radiolabeled). The water/air/propane then flows into a downgradient oxic sediment column (30 to 60 cm in length). Effluent water/air/propane from the oxic sediment column is collected in sealed septa-top vials (200-mL volume), which collects the water and gas (collection time, 3 days to 2 weeks). These liquid/gas effluent samples are analyzed for: a) total aqueous ^{14}C (NDMA and other aqueous degradation intermediates), b) NDMA (by preparatory-scale HPLC, scintillation counting), c) CO_2 (headspace CO_2 trap), and d) volatile organic compounds (by headspace activated carbon trap).

A total of nine sequential reduced/oxic column systems were conducted with residence times ranging from 69 hours (total residence time in reduced plus oxic columns) to 1323 hours. In addition, to compare these results, three reduced column only and three oxic column only experiments were conducted (Table 3.2). Each column system was run for a total time ranging from 18 days (432 hours) to 35 days (840 hours).

The calculated NDMA degradation rate, aqueous removal rate, and mineralization rate were calculated from aqueous (or gas phase) concentrations and residence times. While the residence time of a single type of system (i.e., reduced or oxic) is clear, the residence time of a coupled system (when it is unclear whether the degradation reaction is occurring in the reduced column, oxic column, or both) results in some ambiguity for calculated rates, as described in further detail in Section 4.0. Due to the fairly rapid NDMA degradation to DMA, reduced sediment columns were small, so had correspondingly small residence times of ~9 to 150 hours. Degradation of

NDMA or intermediates to CO_2 took hundreds to thousands of hours (based on previous batch experiments), so oxic system residence times ranged from 60 to 1200 hours.

It should be noted that previous batch mineralization experiments are conducted as significantly lower sediment/water ratios (typically 0.167 g/mL, although these can range up to 1 g/mL). Higher sediment/water ratios are not possible in batch systems, as there needs to be some free liquid above the sediment in order to sample the system. These column systems had a sediment/water ratio of 4.6 to 5.2 g/mL, or ~30 times higher than batch systems. Abiotic degradation of NDMA is caused by one or more surface iron phases, so these column systems exhibited correspondingly higher NDMA degradation rates (to DMA) than batch systems. Biotic degradation processes (demonstrated to produce CO_2) are caused by the specific microbial isolates on the sediment surface, so again, these higher sediment/ water ratio column systems exhibited faster NDMA mineralization rates than observed in previous batch studies.

Table 3.2. Residence times of sequential reduced/oxic systems.

	residence time (h)		total
#	reduced column	oxic column*	residence time (h)
sequential reduced/oxic columns			
X160	8.91	60.1	69.0
X161	9.00	266.2	275.1
X162	8.08	104.2	112.3
X180	32.0	216.1	248.1
X181	10.7	317.3	328.0
X182	28.3	364.5	392.8
X190	148.3	1000.3	1148.6
X191	29.94	885.8	915.8
X192	95.25	1227.7	1323.0
reduced column only			
X164	8.16	--	8.16
X184	27.64	--	27.64
X194	118.08	--	118.08
oxic column only			
X163	--	62.16	62.16
X183	--	216.77	216.77
X193	--	1625.7	1625.7

*aqueous component only

The water injection flow rate in each column system was controlled by an Hitachi L6200 HPLC pump, although the flow rates (and residence times) were calculated from the actual effluent volume and elapsed time. Delivery of the air/propane gas mixture in between the outlet of the upgradient reduced sediment column and down gradient oxic sediment column was accomplished with Kloehn digital syringe pump with 48,000 step motor. To achieve the fairly low flow rates, a 100-µL syringe was used on the syringe pump, and the air/propane gas mixture source was in a 5-L metallized gas sampling bag. Five coupled column systems were conducted simultaneously in a radiation zone (^{14}C-NDMA was used).

4.0 Results

The overall objective of this project is to develop an *in situ* remediation technology for NDMA, which may occur by abiotic, biotic, or both processes. Abiotic processes in aqueous solution, in oxic and reduced sediment, and in mineral phases isolated from sediment are described in Task 1. Biodegradation of NDMA in sediments and in sediment isolated is described in Task 2 results. Sediment/water systems that are reduced and also biostimulated (simultaneous abiotic/ biotic processes) and sequential reduced system followed by oxic sediment systems at later times are described in Task 3 results. Finally, sequential reduced/oxic degradation and mineralization of NDMA is investigated in large-scale 1-D column systems that have close to the same sediment/ water ratio as field systems (Task 4). Portions of the experimental data are presented in this section, with all experimental data in Appendixes A.1 to A.14.

4.1 Task 1 – Abiotic Degradation of NDMA

4.1.1 Aqueous Stability

Aqueous solutions of NDMA at a concentration of 2.3 mg L^{-1} were held for periods of 2 to 700 hours at pH 2 to 14 (Figure 4.1a). At low pH (i.e., pH 2.5), NDMA degraded minimally after 27 hours; at other pH, within the error of measurement, NDMA was not degraded after 700 hours. There was some interference in HPLC analysis of NDMA for samples < pH 2 (data not shown), so it appears that NDMA is stable over a wide pH range (4 to 14), but may degrade in highly acidic waters. The NDMA degradation rate at pH 2 showed a 2540-hour half-life. The experiments were repeated again (Figure 4.1b) under only alkaline conditions, as these are the conditions of the reduced sediment. NDMA was stable to 1000 hours, with <2% degradation.

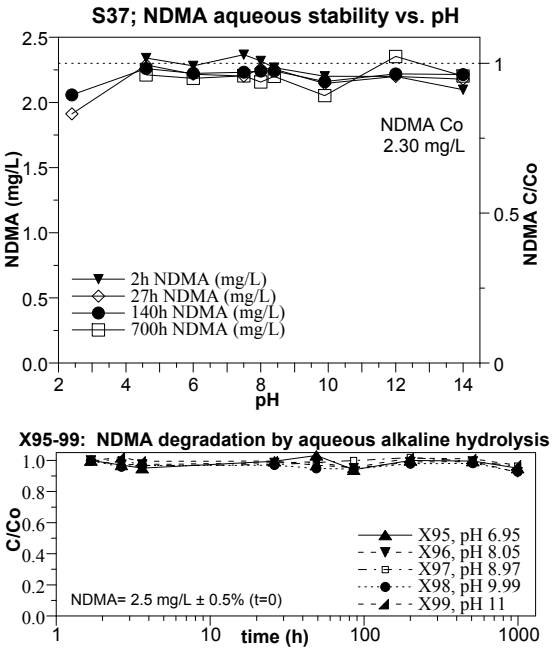

Figure 4.1. NDMA aqueous stability with pH.

In other solutions, NDMA was held at varying Eh (i.e., -597, -310, -230, and +100 mV), for varying periods up to 700 hours (Figure 4.2a). At the most negative Eh, ca. -600 mV fixed by 0.1 M dithionite, results were equivocal. NDMA concentrations were variable over the time course of experiments at that Eh, suggesting that some degradation occurred, but the results were not consistent with increasing degradation with time: no degradation was indicated after 700 hours, but ~40% of the NDMA was degraded after 125 hours. Since the degradation could not have spontaneously reversed itself, the apparent differences in concentration were due to poor precision of measurement under those experimental conditions.

Under less reducing conditions, NDMA was not degraded after 700 hours of reaction. The rate of NDMA degradation by the dithionite solution was as great as a 230-hour half-life (Figure 4.2b).

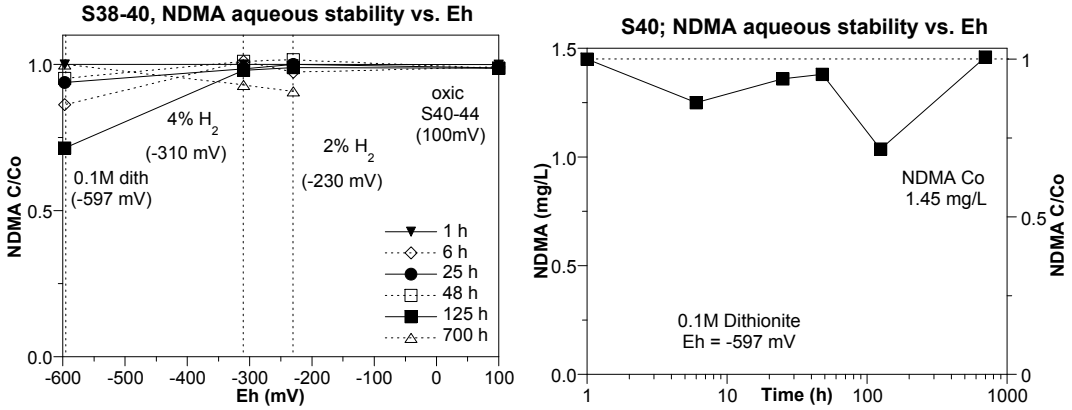

Figure 4.2. NDMA stability over time in aqueous reducing conditions.

NDMA photodegradation in fluorescent light was tested to ensure mass stability in batch and column experiments. There was no photodegradation with both foil-wrapped amber glass vials and clear glass vials over 150 hours (Figure 4.3a). In this experiment, 25-mg/L NDMA was used in the septa-top glass vials that were used in subsequent batch studies described in the following section. Photodegradation was examined further (Figure 4.3b), where it was shown that there was 3% degradation in 800 hours in laboratory fluorescent light (18,000-hour half-life), which would have no influence on experiments. NDMA could be photodegraded in high intensity UV light designed to kill microbes, as shown (Figure 4.3b), with a half-life of 360 hours. This light source was located about 30 cm from the experiment vial. More rapid UV degradation is typically accomplished by a higher energy UV lights at closer proximity (i.e., water traveling in a tube surrounded by UV light). Because reduced sediment was at pH 10, additional alkaline hydrolysis experiments were conducted in 2007. These experiments demonstrated that from pH 7 to 11, NDMA was not degraded within 1000 hours (Figure 4.3b), so alkaline hydrolysis (to pH 11) was not degrading NDMA. A current experiment in progress tests whether alkaline conditions can degrade NDMA in presence of anoxic sediment (i.e., the potential for the sediment acting as a catalyst. Results to 100 hours show no NDMA degradation at pH 11 with anoxic sediment (Figure 4.4). The decrease in NDMA concentration at

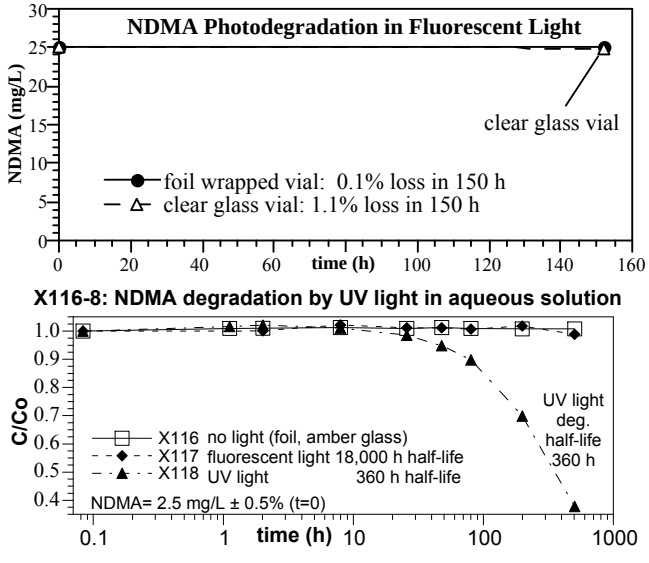

Figure 4.3. NDMA photodegradation in (a) fluorescent light and (b) UV light.

<1 hour was caused by NDMA sorption to the sediment, and not degradation, as demonstrated by the lack of further change in the aqueous NDMA concentration from 1 to 100 hours. The hypothesis of whether alkaline hydrolysis with the (oxic) sediment acting as a surface catalyst was the purpose of this experiment.

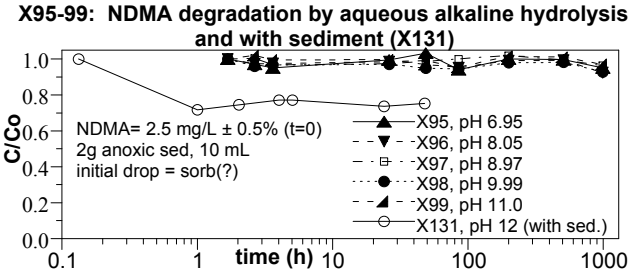

Figure 4.4. NDMA degradation in reduced Ft. Lewis sediment.

4.1.2 NDMA Degradation Pathways

NDMA is a small compound that is relatively stable in aqueous solution and sorbs minimally (sorption K_d in the Aerojet sediment is 0.12 L/kg). NDMA will degrade abiotically by zero valent iron or magnetite under alkaline pH conditions to DMA or UDMH under acidic conditions. It will biotically degrade by a separate pathway (Figure 4.5). The most rapid mineralization of NDMA may involve initial abiotic degradation of NDMA under reducing conditions followed by biodegradation of DMA or other intermediates under different environmental conditions (i.e., oxic). NDMA degradation in abiotic reducing conditions (zero valent iron, reduced sediment, minerals) was investigated in this project to determine the most rapid abiotic degradation pathway that would be compatible with biodegradation of intermediates. Purely biodegradation of NDMA was also considered (Task 2), and coupled abiotic/biotic mineralization (Task 3).

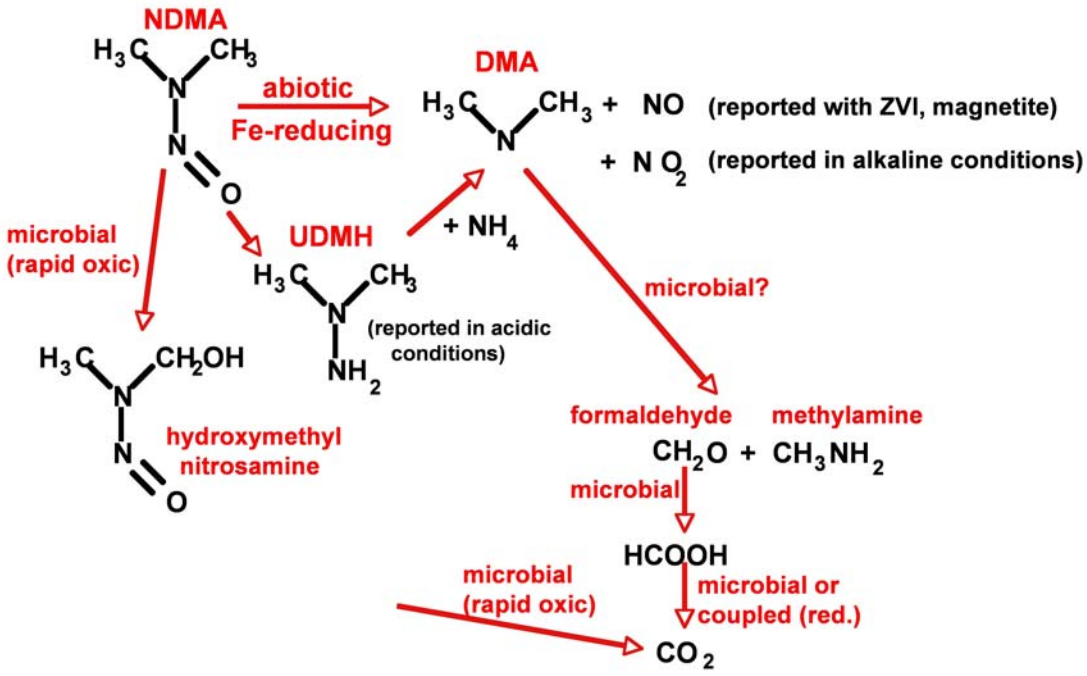

Figure 4.5. NDMA degradation pathways (Odziemkowski et al. 2000).

4.1.3 NDMA Degradation Rate and Mechanism in Sediment

Previous studies have shown that NDMA degrades in dithionite reduced sediment at rates varying from 10 to 300 hours (McKinley et al. 2005, 2007). This variability was examined in greater detail to determine the cause. Although the method to reduce the Aerojet sediment with sodium dithionite (and potassium carbonate buffered to pH 10.5) was the same, the post-reduction treatment has changed over time to include additional pH equilibration (to pH 8). The natural pH of the Aerojet sediment is 9.2.

Dithionite reduction of Aerojet sediment with no post-reduction pH equilibration showed a direct relationship between the amount of dithionite used and the resulting rate of NDMA degradation (Figure 4.6). Sediment treated with great excess dithionite (dithionite/reducible iron ratio = 25) showed a 6-hour half-life to degrade NDMA, whereas use of somewhat less dithionite (di/Fe = 3) had a 13-hour half-life, and use of even less dithionite (di/Fe = 1.1) had a 2000+-hour half-life for NDMA degradation. NDMA degradation in reduced sediment was an abiotic process, as shown by the lack of change in the degradation rate when a bactericide was added (Figure 4.6c). These results indicate that either different surface mineral phases were greated at higher dithionite concentration (such as iron sulfides), which has a lower redox potential during the reduction process, or the pH is influencing NDMA degradation. The pH could result in direct homogeneous NDMA degradation (i.e., alkaline hydrolysis), indirect or heterogeneous NDMA degradation (i.e., surface catalyzed NDMA degradation), or the pH could result in different surface speciation. Alkaline hydrolysis (homogeneous) is not degrading NDMA, as shown in Figure 4.4. Light is also not affecting the rate of NDMA degradation (Figure 4.3), as laboratory fluorescent light does not degrade NDMA (Figure 4.4a) and the rate at which the UV light degrades NDMA (Figure 4.4b) is much slower (i.e., 360 hours half-life) than observed rates with reduced sediment of 10- to 20- hour half-life. Subsequent experiments were, nonetheless, conducted in light free vials.

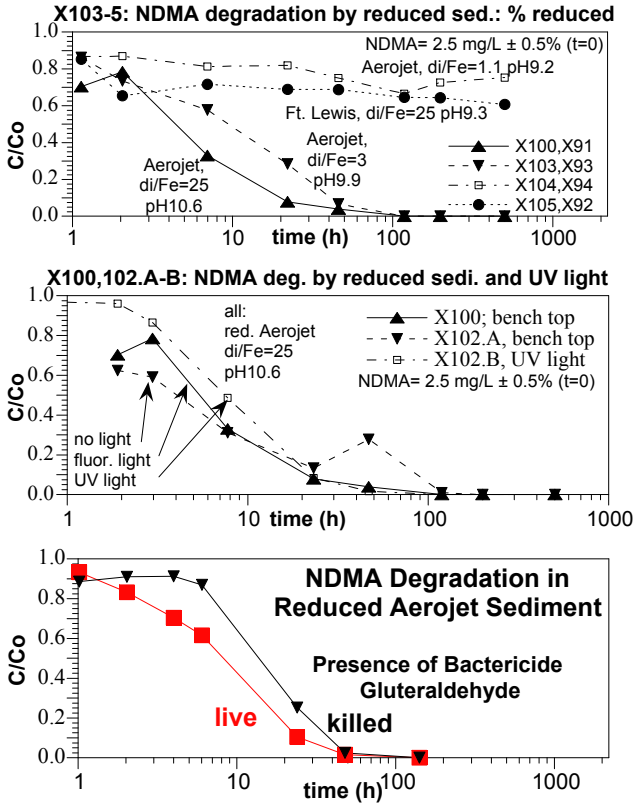

Figure 4.6. NDMA degradation in dithionite-reduced sediments.

To test the influence of pH on the NDMA degradation rate, sediment was uniformly reduced with dithionite at pH 10.6, then subsamples were pH equilibrated to pH 7, 8, 9, and 10. Results showed that the NDMA degradation rate was highly dependent on the final pH during the NDMA degradation experiment (Figure 4.7). High pH (10.6) degraded NDMA most rapidly,

with progressively slower degradation with lower pH. The hypothesis that the sediment surface is acting as a catalyst to alkaline hydrolysis (i.e., surface is not involved in electron transfer) was addressed earlier (Figure 4.4). Alkaline hydrolysis without sediment or with sediment is not the cause of the rapid NDMA degradation observed in reduced sediment.

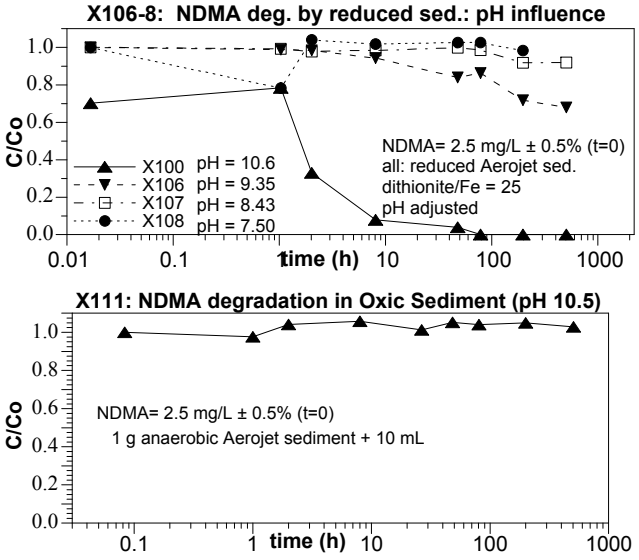

Figure 4.7. NDMA degradation for: a) sediment reduced at pH 10.6, then pH equilibrated to different pH, and b) oxic sediment at pH 10.5.

Although some different mineral phases are present upon sediment reduction (adsorbed Fe^{2+}, $FeCO_3$, FeS_2, magnetite, silica, 1:1 clay kaolinite, 2:1 clays biotite, illite, montmorillonite, nontronite, hectorite), oxic sediment pH equilibrated to pH 10.5 did not degrade NDMA (Figure 4.7b), which partially indicates that alkaline hydrolysis with the surface acting as a catalyst is unlikely. As described in Section 4.1.6, adsorbed ferrous iron is the most likely cause of NDMA degradation to DMA.

4.1.4 Influence of Iron Sulfide

The addition of high purity iron sulfide to anaerobic (but not reduced) Aerojet sediment did not result in any NDMA degradation, which indicates this surface phase (which is produced with dithionite reduction of the sediment) appears to not be involved in NDMA degradation (Figure 4.8a). The iron sulfide was carefully ground to expose fresh surfaces in an anerobic chamber before adding to the anaerobic sediment. This experiment was repeated again (Figure 4.8b, open squares) with iron sulfite that was just ground added to reduced sediment (in this case). There was actually slightly slower NDMA degradation compared to the sediment that was reduced (no phases removed or added), which again clearly indicates that the iron sulfide added had no influence on NDMA degradation.

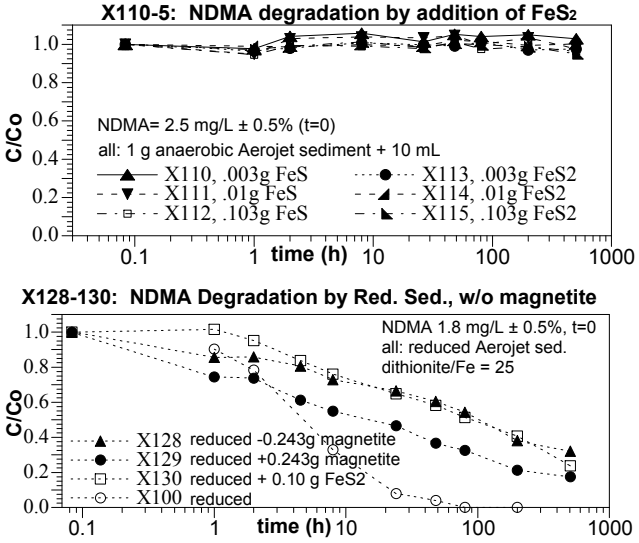

Figure 4.8. NDMA degradation for: a) sediment with addition of FeS_2 and b) addition or removal of magnetite.

4.1.5 Influence of Magnetite

The removal of magnetite in the reduced Aerojet sediment had a significant effect on the NDMA degradation rate (Figure 4.8b). The NDMA degradation rate with reduced sediment had a 7-hour half-life (open circles), whereas magnetite removal (triangles) had an 85-hour NDMA degradation rate. In these experiments, magnetite was removed with a magnet (all in an anaerobic chamber), ground to separate magnetite associated with other mineral phases, which is common in natural sediment, added back to the original sediment, then magnetite removed a second time with a magnet. Interestingly, our previous (2005) results show no influence of freshly ground magnetite on degrading NDMA (Figure 4.9a). One hypothesis that could explain the observed data (Figure 4.8b) is that adsorbed ferrous iron on magnetite is responsible for the NDMA degradation, and not the magnetite itself. A subsequent experiment (X136 in Figure 4.9b) tested this hypothesis by removal of the magnetite prior to reduction of the sediment. The results showed more influence of magnetite removal after reduction, which is consistent with the hypothesis that adsorbed ferrous iron on magnetite is contributing to NDMA degradation.

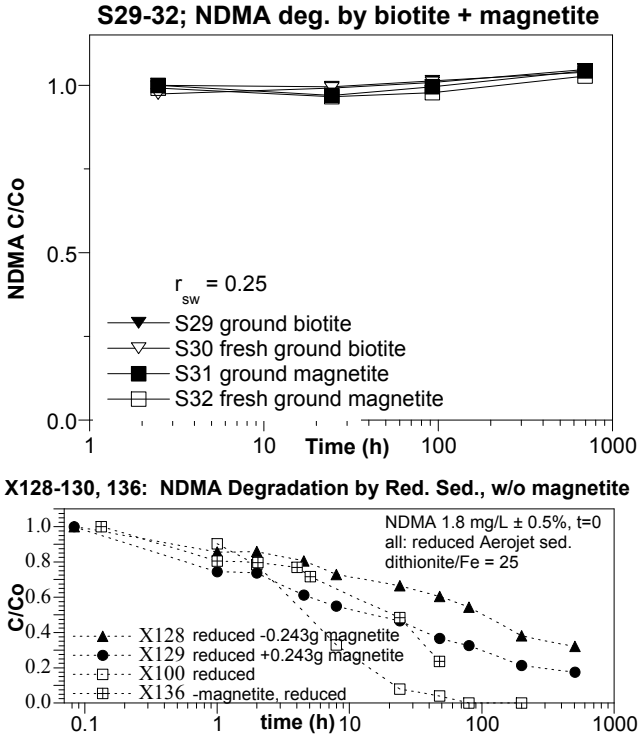

Figure 4.9. NDMA degradation half-life in freshly ground pure mineral phases.

Magnetite was removed from the sediment after reduction (12.0% by weight, Figure 4.9b, triangles), then the NDMA degradation rate experiment was conducted. Results showed that the NDMA degradation rate was slower with the magnetite removed (~30-hour half-life compared to ~8-hour half-life with reduced sediment that includes magnetite), indicating some loss in reductive capacity, but there was apparently still sufficient reduced surface phases present to degrade NDMA to DMA. This appears to indicate that adsorbed Fe^{2+} *on magnetite* is not the primary reduced phase that degrades NDMA.

When the reactive magnetite was added to a separate experiment containing reduced Aerojet sediment (dark circles, Figure 4.9b), the NDMA degradation rate was more rapid than the system in which the magnetite was removed. This indicates that the phase (presumed to be ferrous iron adsorbed onto magnetite) is somewhat reactive with the NDMA. One should note, however, that NDMA is still being degraded in the system with magnetite removed, so there may still be adsorbed ferrous iron on other surfaces.

4.1.6 Influence of Adsorbed Ferrous Iron

If NDMA is being degraded by adsorbed ferrous iron (or $FeOH^-$ species), it is more reactive under alkaline conditions. A change in the pH to a more neutral pH, then increase back to 10.5 should, therefore, not affect the reactivity of this species (i.e., it would be in equilibrium). Several experiments were conducted in which the same reduced sediment was pH equilibrated to pH 9.4, 8.5, and 7.8 for 24 hours, then the pH was pH equilibrated back to 10.5. The redox potential of the final solution was monitored. These experiments were conducted in an anaerobic chamber with additional helium bubbling in the solution (and in the acid used), so there was little chance of introduction of dissolved oxygen (although the possibility exists). In all experiments, a pH shift down resulted in a large decrease in the NDMA degradation rate (Figure 4.10a). In addition, the final redox potential of the samples was less negative the lower the pH was changed to. For example, the Eh of the unaltered reduced sediment was -732 mV, whereas the sediment that was adjusted to pH 9.4 (then back to 10.5) had an Eh of -654 mV, and the sediment that was adjusted to pH 7.8 (then back to pH 10.5) had a final Eh of -455 mV. The redox potential indicates the same geochemical conditions no longer exist, either surface mineral phases have changed or there is less adsorbed ferrous iron (i.e., may indicate adsorbed ferrous iron is not the redox reactive phase with NDMA), but a ferrous phase.

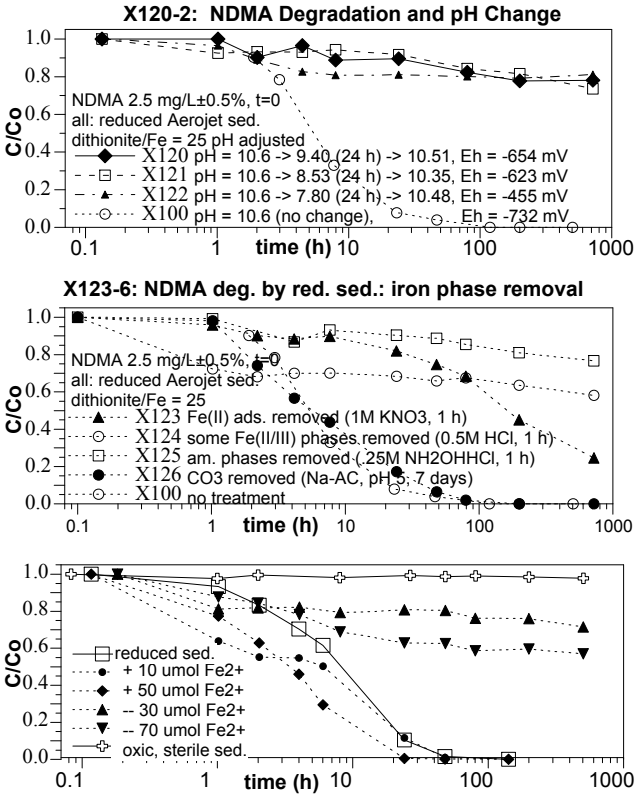

Figure 4.10. NDMA degradation in reduced Aerojet sediment with: a) a pH shift from 10.5 to lower pH, then back to 10.5, b) various Fe surface phases removed with chemical extraction, and c) addition or removal of Fe^{2+} to oxic sediment.

In separate experiments, chemical treatments were used to sequentially strip off one or more iron surface phases. A 1-M solution of KNO_3 was used to remove adsorbed ferrous iron (i.e., by ion exchange, Figure 4.10b). These results (untreated = open circles, adsorbed Fe^{2+} removed = triangles) indicate a substantial decrease in the NDMA degradation rate with adsorbed ferrous iron removed.

Finally, in separate experiments, the addition or removal of Fe^{2+} (Figure 4.10c) clearly had a significant influence on the NDMA degradation rate. Removal of a significant (nearly all) of the adsorbed ferrous iron (70 µmol/g) resulted in a very slow NDMA degradation rate (triangles, Figure 4.10c), although this still retained some ability to degrade NDMA compared to oxic

sediment (crosses). Addition of increasing amounts of ferrous iron (diamonds) to reduced sediment increased the NDMA degradation.

Therefore, adsorbed ferrous iron does appear to be a primary electron donor to degrade NDMA. It should be noted that, in some cases, ferrous iron requires a surface as a catalyst in order to be redox reactive. For example, carbon tetrachloride (Johnson et al. 2000) and TCE (Szecsody et al. 2004) do not degrade in the presence of just aqueous ferrous iron or even ferrous iron adsorbed to silica and other inert surfaces, but will degrade in systems with ferrous iron adsorbed to specific iron oxides or 2:1 clays. The mechanisms may involve these surfaces acting as either a catalyst or a semiconductor for electron transfer. To address this hypothesis, separate mineral phases in sediment (with and without adsorbed ferrous iron and/or structural ferrous iron were investigated, as described in the following sections.

4.1.7 Influence of Iron (II) Carbonate (Siderite)

Removal of some carbonate from the reduced sediment was accomplished by sodium acetate (pH 5) for 7 days. This actually had no influence on the NDMA degradation rate, which may indicate siderite ($Fe(II)CO_3$) is not redox reactive with NDMA. Two other chemical treatments were also conducted in which amorphous iron oxides were removed (0.25 M NH2OH-HCl, Figure 4.10b) or some amorphous and crystalline iron oxides were removed (0.5 M HCl). In both of these cases, the result was less NDMA degradation (even slower than with the adsorbed Fe^{2+} removed), although the pH of these treatments were also influencing the results (not just the iron phase partially removed).

Overall, these batch studies are indicative of primarily adsorbed ferrous iron present at pH 10 in the dithionite-reduced Aerojet sediment is reacting rapidly to degrade NDMA. A major reactive phase appears to be adsorbed ferrous iron, and it appears to be adsorbed onto magnetite (among other surface phases).

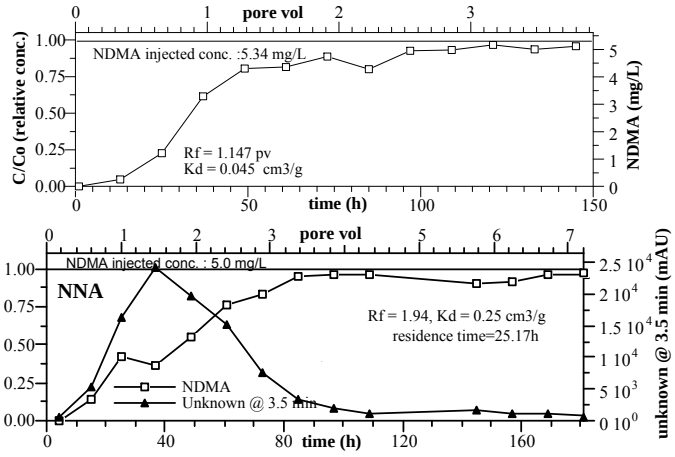

Figure 4.11. NDMA sorption and degradation in reduced Aerojet columns (Szecsody et al. 2003).

4.1.8 Influence of Unaltered Minerals

NDMA in contact with mineral phases that did not contain structural iron generally did not degrade. Sorption of NDMA is typically very small, which results in NDMA far-field migration in subsurface sediments. In a previous study, the sorption of NDMA at 20-ppb concentration was determined in column experiments (Figure 4.11). Data from that study was used to calculate the adsorption of NDMA. The initial breakthrough of NDMA in these two columns was at 1.147 and 1.94 pore volumes, whereas a tracer, by

definition, breaks through at 1.0 pore volume. This "retardation factor" (R_f) defines both the relative solute velocity to tracer velocity and also the distribution coefficient (K_d), which defines sorption with the following equation:

$$R_f = 1 + \rho_b K_d/\theta \quad (4.1)$$

where K_d is the ratio of NDMA mass on the sediment surfaces (mg NDMA/g soil) to NDMA mass in solution (mg NDMA/cm^3 liquid), ρ_b is the dry bulk density of the sediment (g/cm^3), and θ is the porosity. The K_d values for these two experiments were 0.17 and 0.026 cm^3/g. The K_d values of are sufficiently small that it can be ignored during experiments with this sediment.

In this study, high surface area silica (600 m^2/g) exhibited NDMA loss from solution, which was constant for 700 hours, and attributed to sorption (Figure 4.12a, diamonds). Contact with biotite, magnetite particles (oxidized), and aluminum oxide (also Figure 4.12b) showed no degradation of NDMA over 700 hours, as expected.

NDMA contact with preparations of freshly ground magnetite, Fe_3O_4, and the aluminosilicate mica biotite, $K(Fe,Mg)_3AlSi_3O_{10}(F, OH)_2$ did not degrade NDMA, even when these minerals were freshly ground before experimentation. We hypothesized that minerals with ferrous structural iron might degrade NDMA. Ferrous iron from dissolution of biotite is reported to reduce pertechnetate and chromate, so is redox reactive to some extent. The importance of grinding the magnetite and biotite is to expose fresh surfaces. This grinding process was accomplished in an anaerobic chamber as to not oxidize the exposed surfaces to oxygen.

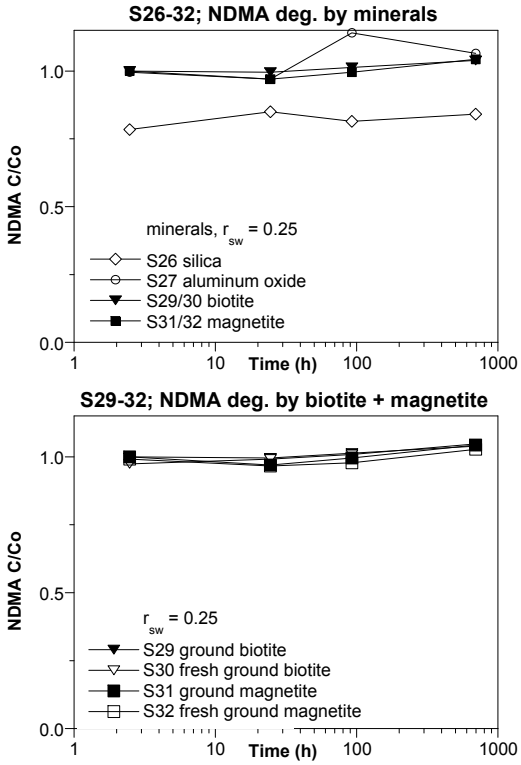

Figure 4.12. a) NDMA reactions with minerals with no structural or adsorbed Fe(II) and b) biotite and magnetite (largely unavailable structural Fe^{2+}).

We hypothesized that minerals with available (or redox reactive) ferrous structural iron might degrade NDMA. A series of 1:1 and 2:1 phylosilicates were reacted with NDMA that included kaolinite (1:1 clay), illite (2:1 clay), hectorite (2:1 smectite clay, 0.0% iron), montmorillonite (2:1 smectite clay 2% iron), and nontronite (2:1 smectite clay 22% iron). Hectorite and nontronite represent end members of 2:1 smectite clay [K $(Fe, Mg)_3$ $AlSi_3$ O_{10} $(F, OH)_2$.], with montmorillonite being the most common. We did not attempt to determine the valence of the structural iron before experimentation, and for the fine clay minerals, whose structures could be readily accessed by pore solutions, we expected the iron to be Fe(III). NDMA degradation did not occur (Figure 4.13) with acid washed clays (at the low soil/water ratio used in these experiments), suggesting that the presence of structural ferrous iron, at natural concentrations, was not sufficient to cause

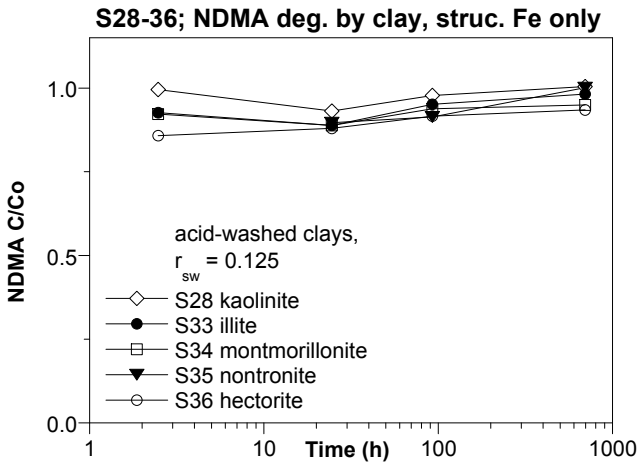

Figure 4.13. NDMA reactions with acid washed clays.

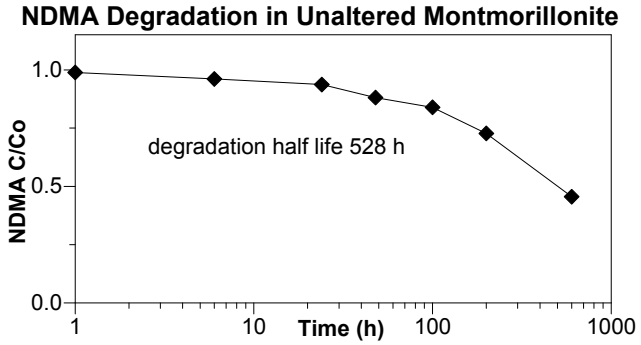

Figure 4.14. NDMA degradation in natural (unaltered) montmorillonite.

degradation. The 2:1 clays (montmorillonite, nontronite) that contain some structural ferrous iron can partially be reduced with a strong aqueous reductant such as sodium dithionite (Stucki et al. 1984), although these acid washed clays were oxic. The acid washing also removes iron and manganese oxide coatings on the clay surface, which is naturally present.

Degradation of NDMA by 2:1 smectite montmorillonite (not acid washed) was observed (Figure 4.14), which may indicate the importance of either adsorbed metals on the clay surface or iron oxides on the clay surface. The rate of NDMA degradation on the unaltered montmorillonite was relatively slow (528-hour half-life).

4.1.9 Degradation by Dithionite-Reduced Smectite Clays

We hypothesized that reduced structural iron in smectite clay fractions could be responsible for NDMA degradation. This was a logical result of experimentation with reduced sediment and unreduced minerals. Since unreduced minerals containing ferrous iron did not degrade NDMA, and reduced sediment did degrade NDMA, even in the absence of adsorbed Fe^{2+}, we concluded that Fe(II) containing minerals with high accessible surface areas were likely to contribute electrons to the aqueous NDMA. We reduced a pure mineral separate, montmorillonite, containing 2.2 wt.% iron, using dithionite, then extracted potentially adsorbed Fe^{2+} using 1-M KNO_3, and, in separate experiments additionally treated the clay with 0.5 M for 1 hour (to remove some iron oxides from the clay surface and other metals) and 1.0-M HCl for 200 hours to remove all iron oxides and dissolve edges of some of the clays. The various treated clays were then reacted with NDMA and any change in degradation rate observed over 1000 hours. Interestingly, dithionite reduction of the montmorillonite had essentially no influence on the rate of NDMA degradation (Figure 4.15a), compared with the unaltered montmorillonite. Because dithionite reduction of 2:1 smectite clays does reduce some structural iron in the clays, this data suggests that either structural ferrous iron in clay is not redox reactive with NDMA, or there is little electron transfer with this ferrous iron.

Dithionite treatment of montmorillonite followed by 24 hours of 1-M KNO_3 (to remove adsorbed Fe(II)) also showed essentially the same degradation rate, indicating that the adsorbed ferrous iron appeared to not be involved in NDMA degradation (also in Figure 4.15a).

However, additional treatments of 0.5-M HCl (1 hour) or 1.0-M HCl (200 hours) after dithionite reduction of montmorillonite showed a considerable increase in the NDMA degradation rate (Figure 4.15b), which was gone by 600 hours. The 0.5-M HCl treatment for 1 hour will dissolve some iron oxides (if present on the surface of clays). The 1-M HCl treatment for 200 hours is considered a "total iron oxide" removal (Heron et al. 1994; Szecsody et al. 2005a) for sediments, although effect on clays are not discussed in that paper. It is likely that the acid treatment will dissolve some broken edge bonds on the montmorillonite, so might provide additional access to the structural ferrous iron.

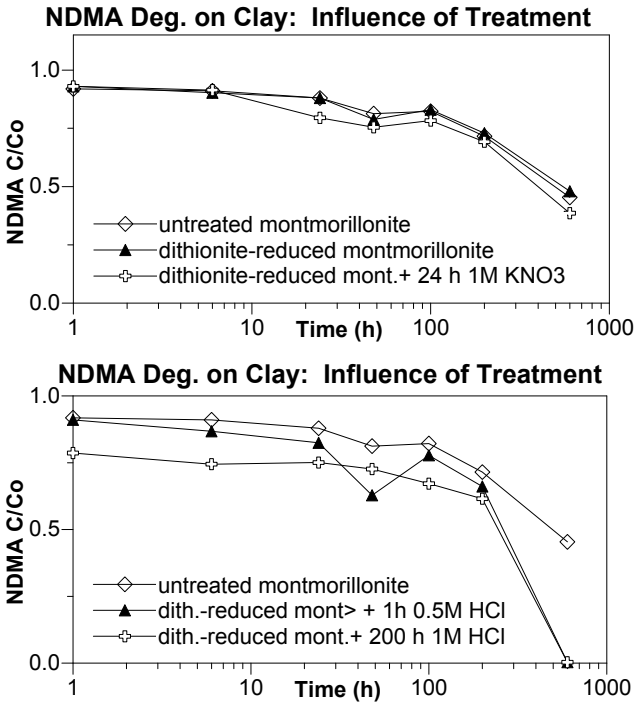

Figure 4.15. a) NDMA degradation by reduced montmorillonite with/without adsorbed Fe(II) and b) with additional Fe-oxide phases removed.

4.1.10 NDMA Degradation by Zero Valent Iron and Zero Valent Iron/Sediment

An alternate method to create a subsurface reduced zone in an aquifer is to inject zero valent iron by high pressure air/water or water. Zero valent iron will create some adsorbed ferrous iron which will desorb onto surrounding sediment, so there are geochemical changes that occur within the sediment as a result of the zero valent iron (i.e., the reduced zone is not limited to a small area associated just with the zero valent iron grains. In this study, NDMA experiments with zero valent iron only were conducted as well as zero valent iron mixed with sediment. Initially, NDMA was reacted with an aqueous solution containing differing amounts of two different zero valent iron samples. These were Aldrich zero valent iron (40-micron diameter), and a 5-micron diameter injectable zero valent iron (ARS Technologies H-200). The purpose of these zero valent iron studies is to have a comparison of NDMA degradation products in a pure system (zero valent iron) to reduced sediments and minerals.

NDMA appears to degrade slowly with the 5-micron zero valent iron (Figure 4.16), where only a few percent degradation (2.5 mg/L) is observed at four different iron/water ratios. The area of an unknown degradation product (likely DMA, identification not confirmed), however, does increase over time, and is proportional to the amount of zero valent iron (Figure 4.16b). Based on these preliminary results, studies were conducted with the Aldrich zero valent iron at a higher NDMA concentration (22 mg/L, Figure 4.17a). The same results were observed; a slow NDMA degradation, and production of a degradation compound.

In contrast, the 40-micron Aldrich zero valent iron (possibly with greater surface area) is much more reactive with NDMA. In a previous study, it was found that mixed metals (Fe, Ni) degraded NDMA more rapidly than zero valent iron alone, and all commercially available zero

valent iron particles have some trace metals. NDMA degradation was a direct function of the iron/NDMA ratio (Figure 4.17b), with a more rapid NDMA degradation rate at a higher molar ration of Fe/NDMA.

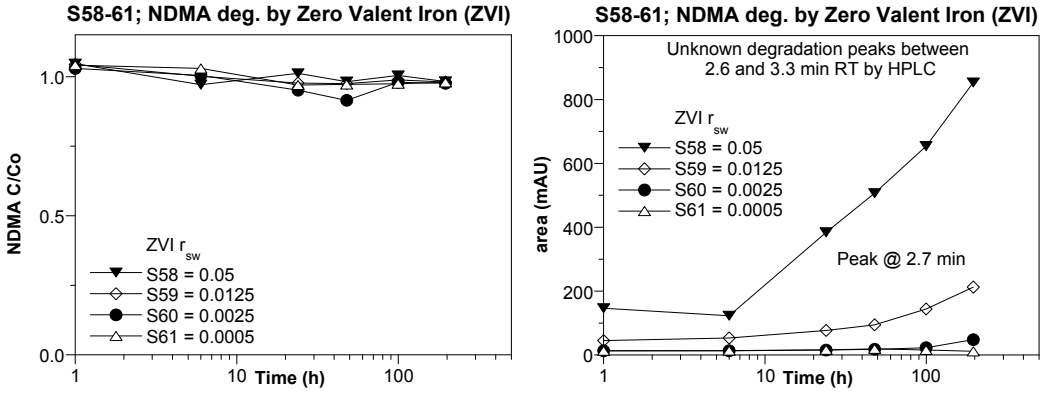

Figure 4.16. 2.5-mg/L NDMA degradation with 5-micron zero valent iron.

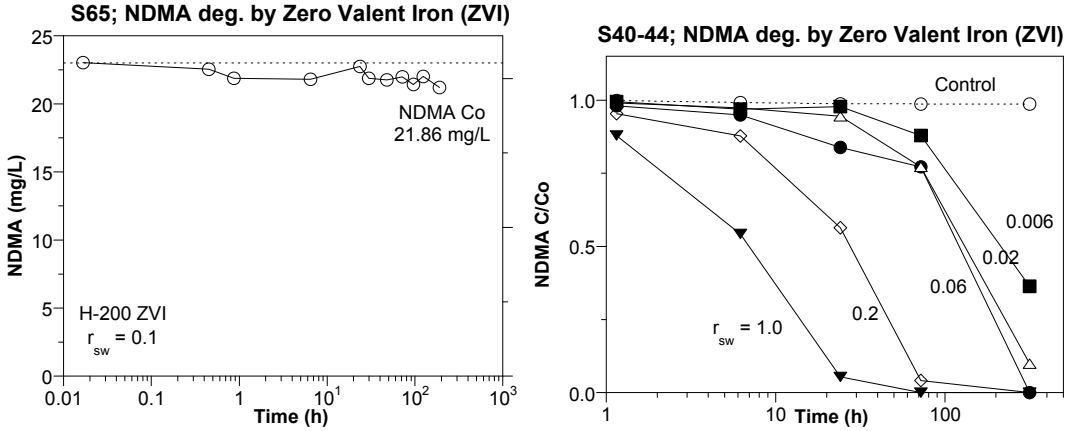

Figure 4.17. 22-mg/L NDMA degradation with: a) 5-micron and b) 40-micron zero valent iron.

Anaerobic sediment with zero valent iron takes a few 100 hours to develop reducing conditions (Figure 4.18). Alternatively, although the chemically reduced sediment is initially under more reducing conditions, it is not as reducing conditions as the zero valent iron-sediment system. However, biotic processes (in the presence of an appropriate carbon source) result in further reduction over hundreds of hours (Figure 4.18), which eventually produces the about the same reducing conditions as the zero valent iron-sediment system. In order to compare these rates with those in reduced sediments, a molar ratio of iron (zero valent in this case) to NDMA was plotted against the NDMA degradation half-life (in hours, Figure 4.19). Compared to reduced Aerojet and Ft. Lewis sediment (molar ratio of ferrous iron to NDMA), the 40-micron zero valent iron is 1 to 3 orders of magnitude more rapid, or only a small quantity of zero valent iron in sediment is needed to degrade NDMA at the same rate as reduced sediment.

In general, a reactive zone created at the field scale can be a few feet in flow path length (i.e., pure zero valent iron wall) or 30 to 40 ft (dithionite reduction of sediment). A new technology for injecting 5-micron size zero valent iron particles into an aquifer using shear-thinning fluid can place a small concentration of zero valent iron particles directly in the aquifer through a well. Large grain size zero valent iron has been previously used for coupled abiotic/biotic remediation in soils (i.e., were sediments can be mixed with zero valent iron) and to some extent in shallow aquifers where it has been determined to be some microbial activity near zero valent iron walls. However, zero valent iron walls are typically limited in depth to <50 to 100 ft by trench installation. Deeper zero valent iron walls can be installed by shear plane injection with wells spaced 15 ft apart (i.e., process developed by GeoSierra). In addition, 5-micron zero valent iron particles can be injected into aquifers in a low concentration (<2%) using a shear thinning fluid to achieve a relatively uniform spatial distribution of particles (Dr. Mart Oostrom, PNNL). The shear thinning fluid is necessary to keep the very dense iron particles in suspension.

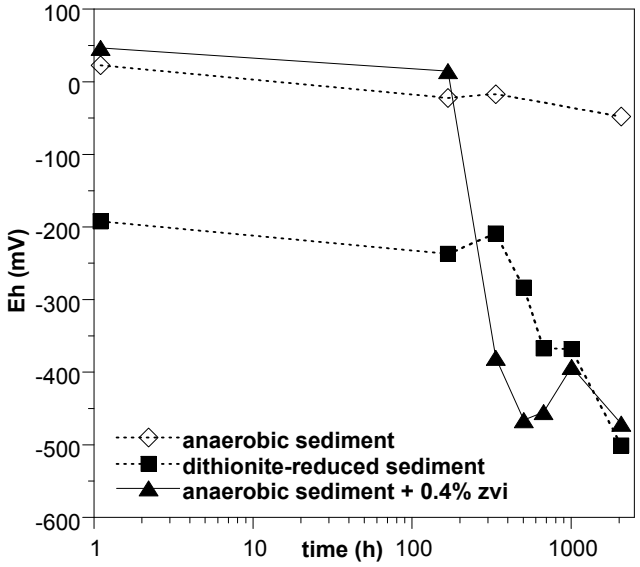

Figure 4.18. Change in redox conditions over time.

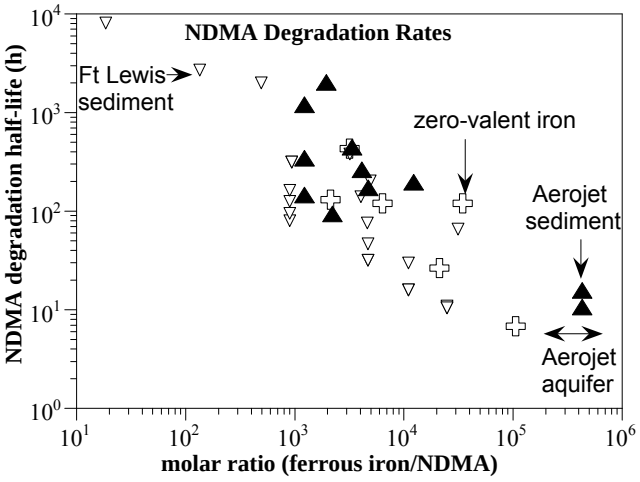

Figure 4.19. Comparison of NDMA degradation rates in reduced sediments to 40-micron zero valent iron.

With the various technologies available to introduce zero valent iron or reduced sediment in the subsurface, the residence time of a contaminant such as NDMA can be relatively short (hours to tens of hours) for thin zero valent iron walls, or 1000 hours for a 40-ft thick reduced sediment zone. As such, rates that are relevant at the field scale are typically <300 hours (half-life) for viable field-scale remediation (Figure 4.19). At this scale, if the 40-micron zero valent iron could be placed in aquifer sediments, only a few percent zero valent iron would be needed. The 5-micron zero valent iron is injectable, but experiments (Figures 4.16 and 4.17) show much slower NDMA degradation rates compared with the 40-micron zero valent iron.

Additional experiments were conducted with the 5- and 40-micron zero valent iron (Figure 4.20) at different zero valent iron/NDMA ratios. These results showed progressively more rapid degradation with increasing zero valent iron concentration. As before, the degradation rate was

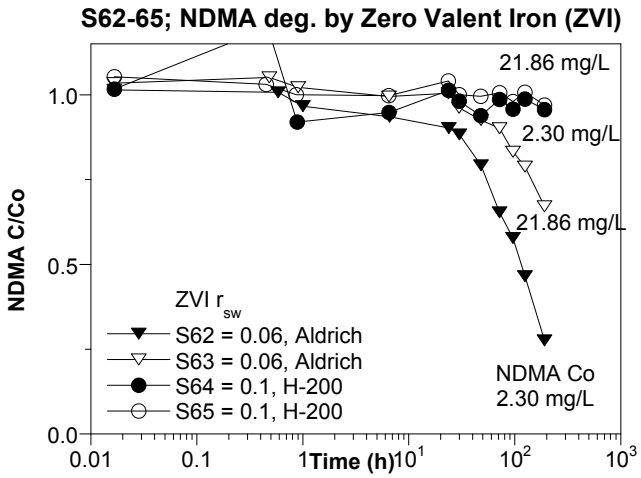

Figure 4.20. NDMA degradation by 40-micron zero valent iron at different iron/NDMA ratios.

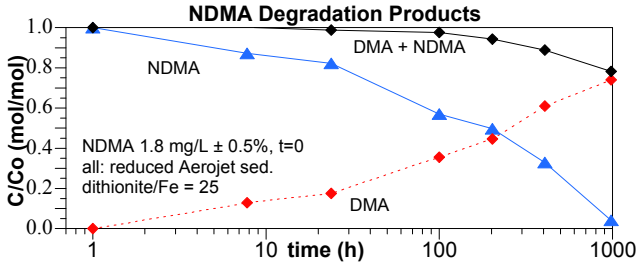

Figure 4.21. NDMA degradation to DMA in reduced Aerojet sediment at pH 10.5.

inversely proportional to the concentration of NDMA. The effectiveness of degradation with zero valent iron suggests that this could act as an injectible reductant in aquifer systems.

4.1.11 NDMA Degradation Products

In most experiments described above, the concentration of any NDMA degradation products were not measured. A common degradation intermediate, dimethalamine or DMA (Gui et al. 2000), can be measured on an HPLC using a fluorescent tag, as described in Section 3.0. This method was modified somewhat from literature in order to measure lower DMA concentrations. An experiment was conducted in which the reduced Aerojet sediment at pH 10.5 was used, and NDMA and DMA were measured. Results of this experiment (Figure 4.21) show that NDMA is degrading more slowly (half-life 191 hours) than previously shown at pH 10.5 (Figures 4.6 and 4.10; half-life as fast as 8 hours) due to a smaller sediment/water ratio used in the experiment. By 1000 hours, the initial 1.8-mg/L NDMA had degraded to 4% of the injection concentration (0.075 mg/L), which is essentially the lower reliable detection limit. Separate samples taken were derivatized and analyzed for DMA (red points, Figure 4.21), which showed that DMA is the major degradation product for the first 1000 hours (likely along with N_2O (reported under alkaline conditions, Figure 4.5) or NO (reported with zero valent iron or magnetite). Mass balance of just NDMA + DMA (black diamonds, Figure 4.21) decreased after 100 hours, and was at 78% by 1000 hours, indicating DMA was being degraded to a further, unknown product. Additional column experiment results show DMA concentrations in 1-D column experiment effluent ranging from 0% to 40% of the mass of NDMA degraded, so this current mass balance experiment is much greater (Figure 4.22, Table 4.1). DMA also appears to be unstable in some aqueous conditions, although this has not been fully investigated. DMA was degrading in oxic water at a half-life of 120 hours (pH 7). Because DMA in this experiment (pH 10.5, reducing conditions) appears to be much more stable, it could be the pH that results in the DMA stability. The derivitization method uses NaOH (pH 12), and DMA is reported stable for a few hours as a complex. The most likely reason for the alkaline conditions is to ionize the derivitization agent (DNFB, dinitrofluorobenzene), as DMA is ionized (pKa = 10.73). DMA is highly soluble (354 g/100 mL), but is known to degrade under weak acid conditions.

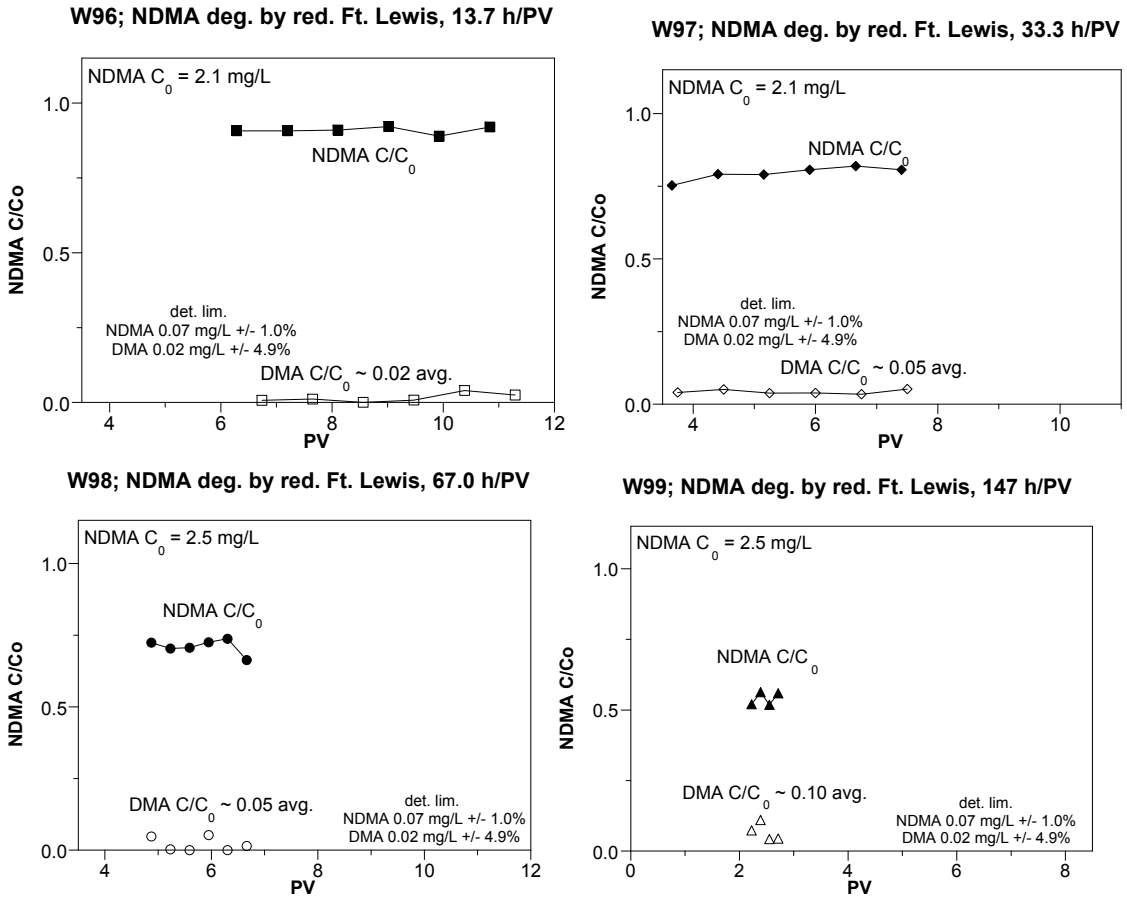

Figure 4.22. NDMA degradation to DMA in reduced Ft. Lewis sediment in 1-D columns with differing residence times: a) 13.7 hours, b) 33.3 hours, c) 67 hours, and d) 147 hours.

Table 4.1. NDMA degradation rates in Ft. Lewis and Aerojet sediment columns.

exp.	description	influent NDMA (mg/L)	effluent NDMA (C/Co)	residence time (h)	NDMA half-life (h)	NDMA lost (C/Co)	effluent DMA (C/Co)	DMA/ NDMA (mol/mol)	pv elapsed
W96	1-D, red. Fe Lewis sed (di/Fe = 4)	2.5	0.888	13.7	79.9	0.112	0.043	0.384	0-12
W97	1-D, red. Fe Lewis sed (di/Fe = 4)	2.5	0.784	33.3	94.8	0.216	0.049	0.227	12-19
W98	1-D, red. Fe Lewis sed (di/Fe = 4)	2.5	0.692	67.0	126.1	0.308	0.054	0.175	19-26
W99	1-D, red. Fe Lewis sed (di/Fe = 4)	2.5	0.535	147	162.4	0.466	0.1036	0.222	26-29
W100	1-D, red. Ft Lewis sed.(di/Fe=12)	2.44	0.872	15.0	75.9	0.128	0.006	0.047	0 - 7
W101	1-D, red. Ft Lewis sed.(di/Fe=12)	2.78	0.719	66.8	140.3	0.281	0 - 0.403	--	0 - 5
W102	1-D, red. Aerojet sed.(di/Fe=27)	2.5	0.975	12.6	345	0.025	0.000	0.000	0 - 11
W103	1-D, red. Aerojet sed.(di/Fe=27)	2.5	0.959	72.6	1202	0.041	0 - 0.125	--	11 - 18
W104	1-D, red. Aerojet sed.(di/Fe=2.8)	2.5	0.888	25.0	146	0.112	0.016	0.143	0 - 6
W105	1-D, red. Aerojet sed.(di/Fe=2.8)	2.5	0.954	134	1972	0.046	0.000	0.000	6 - 8
W106	1-D, red. Aerojet sed.(di/Fe=0.54)	2.44	0.901	14.1	93.7	0.099	0.000	0.000	0 - 9
W107	1-D, red. Aerojet sed.(di/Fe=0.54)	2.78	0.975	73.9	2023	0.025	0.000	0.000	9 - 16

These results and NDMA mineralization results presented in Task 2 and Task 3 results show that DMA is degraded to further, unidentified products. Carbon mass balance (with ^{14}C-labeled NDMA) conducted at 3000 hours in oxic and reduced systems (described under Task 2) revealed some interesting results. In oxic systems, which are known to be dominated by a monooxygenase pathway (likely propane monooxygenase) shows 80.0% average total mass balance. In contrast, carbon mass balance in reduced systems shows only 51% mass balance. Some NDMA is mineralized in reduced systems by unknown abiotic/biotic pathways, and there appears to be significantly less biomass in reduced systems (implying degradation may be in part abiotically controlled). Carbon mass balance accounted for NDMA, all aqueous ^{14}C-containing species, CO_2 (mineralized), NDMA adsorbed to sediment and microbes, and carbon mass incorporated in microbes.

In reduced systems, one phase that was not well accounted for in reduced systems was low molecular weight species that may be volatile (i.e., in the headspace in the vials). Possible DMA degradation pathway (Figure 4.5) could produce formaldehyde, methylamine, and formate, all of which are somewhat volatile. In a few final experiments of this project, samples taken after 1000 and 2000 hours of NDMA reaction with dithionite-reduced sediment were analyzed for low molecular weight compounds. The initial NDMA concentration was 2.5 mg/L (34 μM). At both 1000 and 2000 hours, the NDMA concentration was below detection limits (0.05 mg/L) and 1.1-mg/L (17.7-μM) nitrate was detected (1100 hours), and 0.4-mg/L nitrate at 2000 hours. It should be noted that nitrous oxide is suspected to form under these alkaline conditions (Figure 4.5), but this was not analyzed for. In addition, methylamine and formaldehyde was not detected, although trace concentrations of formate were detected.

A series of 12-column experiments have been conducted with dithionite-reduced sediment (Ft. Lewis and Aerojet) with measurement of DMA (dimethylamine, Szecsody et al. 2008a, b). The initial NDMA concentration in all of these columns was 2.1 to 2.8 mg/L, so the NDMA degradation rate will be rather slow. Long sediment-NDMA contact times where chosen for the column studies in order to have some NDMA degradation occur. DMA was analyzed by derivatization with DNFB and HPLC analysis, as described in the experimental section. While some issues of the DNFB peak interfering with the DMA peak were resolved, the problem persisted at low DMA concentrations and resulted in poor DMA concentration accuracy at low DMA concentration. Column experiments (Figure 4.22) typically showed very consistent NDMA concentration lower than influent concentration, indicating a steady-state rate of degradation. Sorption of NDMA was minimal ($K_d < 0.1$ cm^3/g), so would influence lag in NDMA concentration at <2 pore volumes.

The NDMA effluent concentration relative to influent concentration was used to calculate an NDMA degradation rate (Table 4.1). NDMA degradation half-lives for the Ft. Lewis sediment ranged from 76 to 162 hours in six different column experiments, and appeared to have a trend of slower degradation rate with each successive column. These rates were similar to other columns (Table 4.2, described in a following section).

The DMA concentration in the effluent was small, ranging from 0.0% to 40% of the influent NDMA molar concentration (comparison on a molar basis). The average DMA effluent concentration accounted for 25% ± 9% of the NDMA mass loss, with a range from 5% to 38%. DMA aqueous stability has not been fully investigated, but some experiments (Figure 4.23) show that

it is not stable in aqueous solution at pH 7 in a dark container. This experiment was run for 125 hours at 5°C, and showed 56% degradation (degradation half-life 104 hours at 5°C, DMA concentration 39 mg/L). Because column studies are run at time scales form tens to hundreds of hours, significant DMA degradation of effluent samples (underivatized) is likely occurring, so effluent vials contain derivatization chemicals (DNFB, NaOH, acetonitrile). This can minimize DMA degradation once the aqueous solution leaves the column, but there may be degradation in the water in the column over the long time scales of the column experiment. Because DMA is unstable in aqueous solution, then it would be difficult to achieve NDMA to DMA mass balance in experiments. UDMH (or other degradation products indicated in Figure 4.5) may also be produced during NDMA contact with reduced sediment that current analytical methods are not detecting.

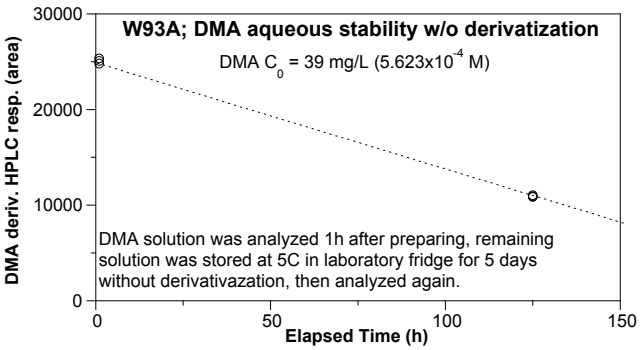

Figure 4.23. DMA aqueous stability at 5°C.

A series of six column experiments were conducted with reduced Aerojet sediment at three different amounts of sediment reduction, as defined by the molar ratio of dithionite to reducible iron in the sediment (dithionite/ferrous iron = 27, 2.8, and 0.54, Table 4.1). The NDMA degradation half-lives in these experiments varied widely from 94 to 2023 hours, indicating an inconsistent dithionite reduction of sediment. Additional Aerojet sediment is currently being reduced to repeat these studies. With very slow NDMA degradation rates, most of these Aerojet sediment experiments showed no DMA in the effluent, although two experiments showed small concentrations of DMA.

4.1.12 Upscaling to Field Conditions: High Sediment/Water Ratio

As shown in previous sections, the observed NDMA degradation rate is proportional to the amount of adsorbed Fe^{2+} and surface phases, so a higher sediment/water ratio results in a higher observed NDMA degradation rate (Figure 4.19), assuming all other conditions are the same. In a groundwater aquifer, the sediment/water ratio is quite high (5 to 10 g/mL), but there is little mixing of the solution with the surface, that occurs in batch experiments. A series of 32 stop-flow 1-D column experiments were conducted to quantify the NDMA degradation rate that occurs at a high sediment/water ratio of an aquifer. Residence times ranged from 1 to 400 hours. Single "points" in Figure 4.24 represent an average concentration of four analyzed effluent samples. Batch experiments have demonstrated that the amount of sediment reduction has a significant influence on NDMA degradation (Figure 4.6a). Even with high sediment reduction, there was additional influence of the pH on the NDMA degradation rate (Figure 4.7a). Four different sediment conditions were addressed ranging from more ideal conditions for NDMA degradation to conditions that have been shown to exhibit slower NDMA degradation: a) fully reduced Aerojet sediment (pH 10.5) injecting pH 10.5 NDMA-laden water, b) weakly (10%) reduced Aerojet sediment (pH 10.5), c) fully reduced Aerojet sediment with pH 7 unbuffered water, and d) fully reduced Aerojet sediment (pH 10.5) at pH 7 buffered water (Figure 4.24).

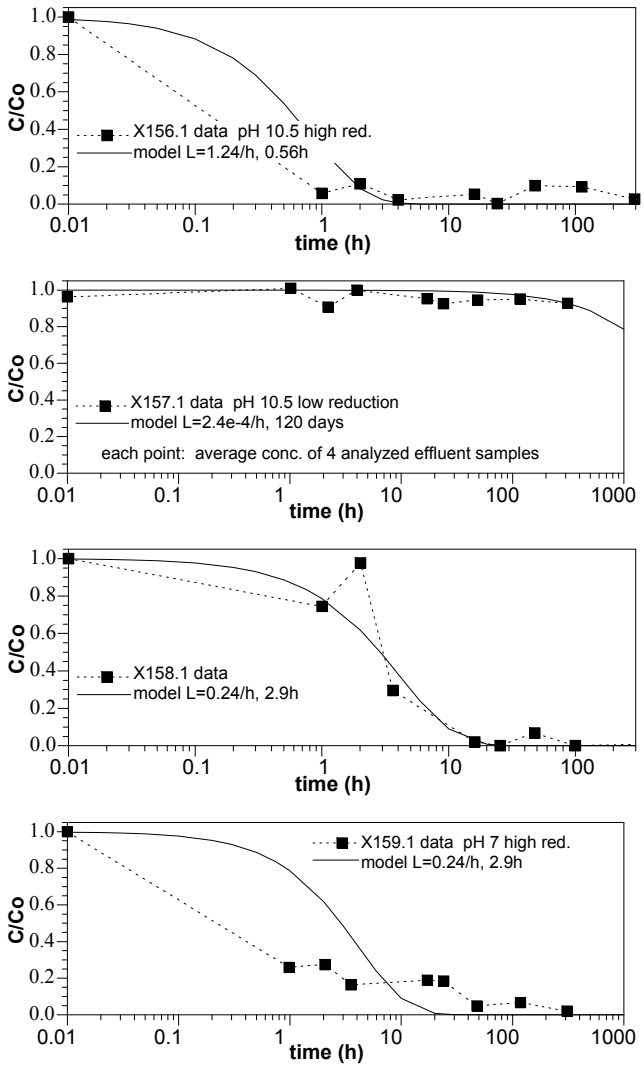

Figure 4.24. NDMA degradation in stop-flow columns (sediment/water ratio = 5.6 g/mL).

Under the most ideal conditions of fully reduced Aerojet sediment at pH 10.5 (the Aerojet aquifer is at pH 9.3, but the carbonate buffered solution used to reduce sediment is at pH 10.5), NDMA was quickly degraded. A series of eight stop-flow columns (four data points collected for NDMA concentration on each) at residence times ranging from 1 to 200 hours showed an NDMA degradation rate greater than 0.56 hour (Figure 4.24a, sediment/ water ratio averaged 5.6 g/mL). However, packing columns with 10% highly reduced sediment and 90% anoxic sediment, this NDMA degradation rate decreases to 120 days, or 1000 times slower (Figure 4.24b). This method to create "partially" reduced sediment (or very small pockets of highly reduced sediment in anoxic sediment) would not produce the same results as shown earlier where anoxic sediment is reduced with lower concentrations of dithionite. Under conditions where the highly reduced Aerojet sediment (at pH 10.5) was subjected to the NDMA-laden influent water at pH 7 (unbuffered, Figure 4.24c), the pH should slowly decrease, thus slowing NDMA degradation (comparable batch experiment in Figure 4.7a). The observed NDMA degradation rate for eight stop-flow columns was (half-life, 2.9 hours, Figure 4.24c) was five times slower than under the most ideal conditions (Figure 4.24a, influent water pH 10.5). When pH 7 buffered (10 mM PIPES buffer) NDMA-laden water was injected into columns, the NDMA degradation rate was about the same (Figure 4.24d) with a half-life of 2.9 hours. It is expected that while these experiments only subjected the columns to about 52 pore volumes of water (and the reductive capacity is expected to last about 250 pore volumes of O_2-saturated water), over time, the reductive capacity will decrease, and the NDMA degradation rate will slow considerably. Longevity of the barrier is addressed in Task 3.

An additional 10 stop-flow columns were conducted with reduced Aerojet sediment that was pre-equilibrated at pH 7.5 (50 pore volumes over a week) to ensure pH 7.5 was achieved throughout the sediment in the columns (Figure 4.25). As shown in an earlier batch experiment (Figure 4.7a), NDMA degradation is weak, and there was no DMA measured in any of the columns, with residence times ranging from 50 to 800 hours (likely due to the combination of low DMA concentration produced and aqueous degradation of DMA). As the sediment pH is changed from

10.5 to 7.5 adsorbed ferrous iron is not as redox reactive, as well as the process of manipulating the conditions in the sediment (anoxic water) washes out much of the adsorbed ferrous iron, so these results are not surprising. These results would be not be representative of field conditions at Aerojet, which the aquifer pH is 9.2.

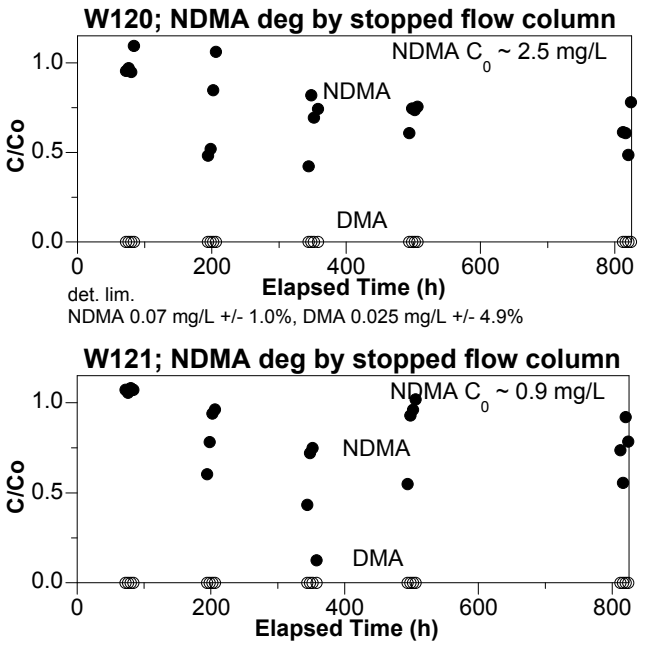

Figure 4.25. NDMA degradation in stop-flow columns at pH 7.5 (buffered) water with DMA analysis.

4.1.13 Upscaling to Field Conditions: Advective Flow and Temperature

Field-scale conditions of a high soil/water ratio for reduced sediment with advective flow can be achieved in 1-D sediment columns. Groundwater temperature can also be easily achieved in laboratory experiments. Aerojet groundwater geochemistry can also be achieved. A series of twenty-four 1-D column experiments was conducted at varying temperature (each experiment shown separately in Appendix A.8), NDMA concentration, and sediment reduction to determine NDMA degradation rates that would occur under field-scale conditions (Figure 4.26). NDMA degradation rates were determined from each experiment (Table 4.2). Each plot shows NDMA degrading in four different column experiments at different amounts of sediment reduction. In Figure 4.26a (22°C), the least reduced sediment shows NDMA breakthrough at 75% to 90% of the injection value. The flow rate in this experiment was very slow (75 h/pore volume). Sediments with greater reduction (other three experiments plotted in Figure 4.26a) showed much greater degradation (which calculates to a faster NDMA degradation rate, Table 4.2). Higher temperature studies (Figure 4.26c through 4.26e) show less degradation, as (apparently) NDMA abiotic degradation is an exothermic reaction.

These temperature studies showed that NDMA degraded more slowly at higher temperature (i.e., it is an exothermic reaction), which is different from CL-20, RDX, and octahydro-1,3,5,7-tetranitro-1,3,5,7-tetrazocine (HMX) degradation by reduced sediment. The NDMA degradation half-lives were rapid for highly reduced sediment (9 to 10 hours) and 315 hours for partially reduced sediment (at 22°C).

Based on NDMA degradation experiments conducted in columns at different temperature, the NDMA degradation reaction appeared to be exothermic, with an activation energy of 58 kJ/mol (Figure 4.27), indicating the reaction is chemically controlled. The sediment at low reduction may have been oxidized due to limited capacity, so the rate data is suspect.

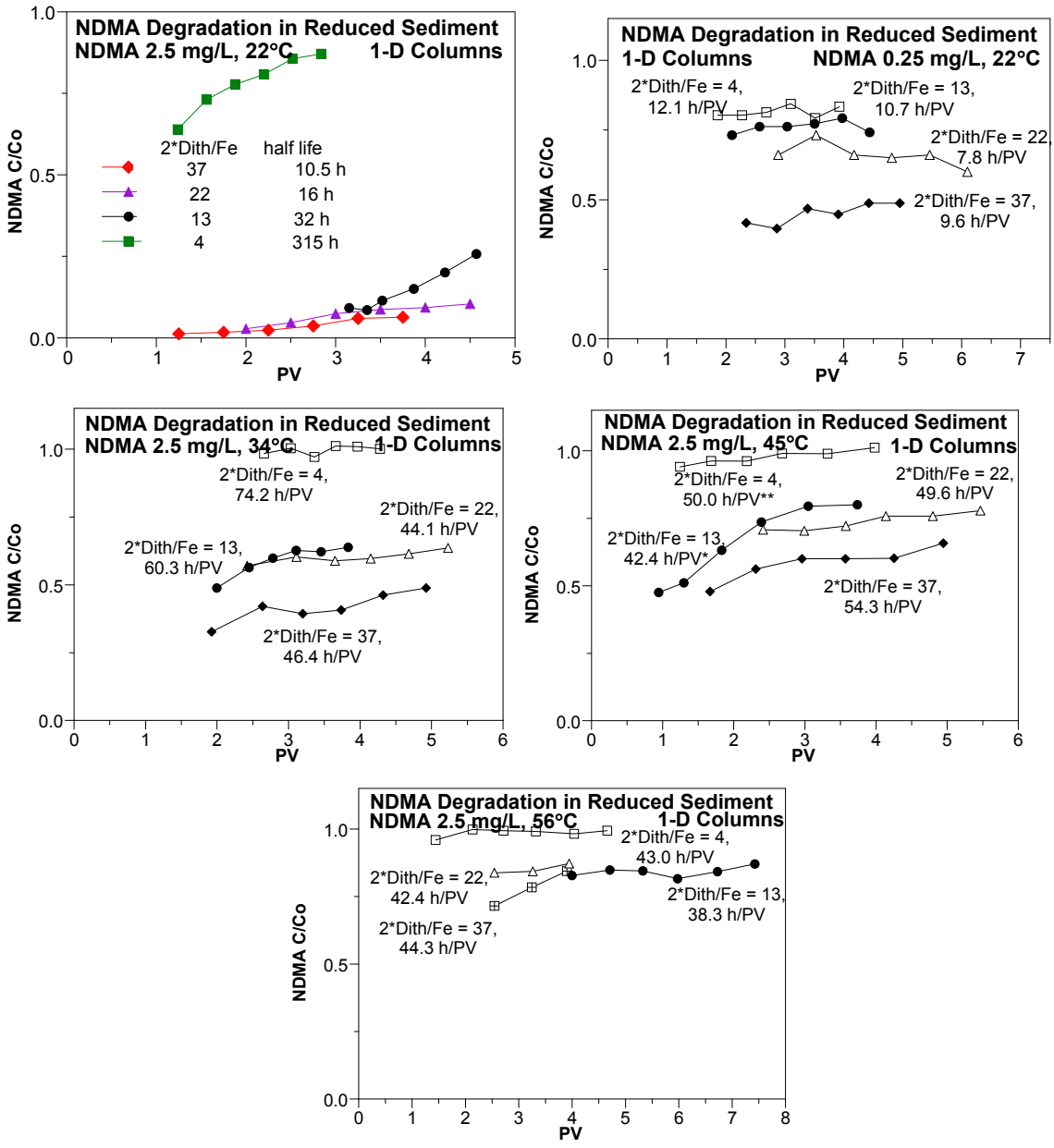

Figure 4.26. NDMA degradation in 1-D columns at four different reductions at: a) 22°C, 2.5-mg/L NDMA; b) 22°C, 0.25-mg/L NDMA; c) 34°C, 2.5-mg/L NDMA; d) 45°C, 2.5-mg/L NDMA; and e) 56°C, 2.5-mg/L NDMA.

Groundwater conditions expected in the 5-layer Aerojet aquifer include:

- temperature from 16°C to 21°C (depending on depth)
- NDMA concentration from extremely low part per trillion levels to 36 ppb
- unknown dissolved oxygen concentration.

Table 4.2. NDMA degradation rates in dithionite-reduced sediments in 1-D column studies at different temperature.

	NDMA intrinsic degradation rate (mol/h) and half-life [h]			
T (°C)	high reduction (di/Fe = 37)	(di/Fe = 22)	(di/Fe = 13)	low reduction (di/Fe = 4)
22	1.56E-8 [10.5]	1.03E-8 [15.9]	5.15E-9 [31.8]	5.20E-10 [315]
22*	1.78E-9 [9.2]	1.50E-9 [12.8]	5.49E-10 [30]	3.49E-10 [45]
34	4.62E-9 [35.4]	2.79E-9 [58.7]	1.80E-9 [91.1]	2.56E-11 [6300]
45	2.23E-9 [73.6]	1.36E-9 [121]	1.27E-9 [129]	2.84E-11 [5800]
56	1.31E-9 [125]	9.05E-10 [181]	1.03E-9 [159]	1.65E-11 [9900]

* at 0.25 mg/L NDMA, all other studies at 2.5 mg/L NDMA

The NDMA degradation rate at aquifer temperature can be extrapolated from the temperature studies (Table 4.2) and the change in rate between laboratory and field (36 ppb) concentration can be extrapolated from the relationship in Figure 4.19.

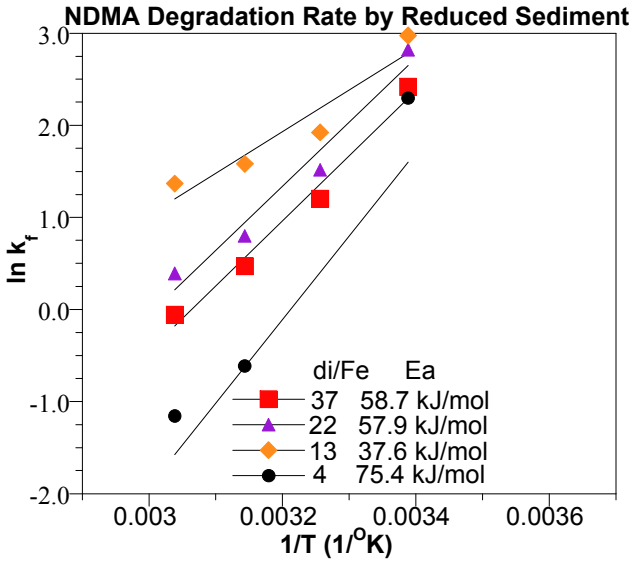

Figure 4.27. NDMA activation energy in reduced sediment.

The temperature studies indicate NDMA will be degraded with a half-life of 8.8 hours (16°C) to 10.2 hours (21°C), given the average rate change of 0.28 hour (half-life) per degree Celsius. The NDMA degradation rate increases 19.3 times for every order of magnitude decrease in NDMA concentration (line plotted in Figure 4.19, log-log fit), so assuming the field experiment is conducted at 36-ppb NDMA concentration (laboratory studies at 2.5 mg/L), there should be a 35.5-time increase in the NDMA degradation rate. Therefore, the estimated NDMA degradation half-life in highly reduced sediment at 16°C and 36-ppb NDMA is 0.24 and 0.29 hour at 21°C. These represent the fastest rates that would be observed, as this is the most reduced sediments. Partially reduced sediments will degrade NDMA more slowly. In sediments with low reduction, the NDMA degradation rate is about 30 times slower or a 7.2-hour half-life at 16°C and 36-ppb NDMA.

4.1.14 Calculated NDMA Degradation Rate under Aerojet Aquifer Conditions

Assuming a dithionite-reduced zone is created in a single well in a single aquifer unit, the relative NDMA concentration decrease in groundwater flowing through the reduced zone can be calculated.

These calculations (Table 4.3) use the laboratory-derived degradation half-lives of 0.26 hour (highly reduced sediment) and 7.2 hours (partially reduced sediment), as previously described, with a range of field conditions: a) 10- and 30-ft diameter reduced zone, b) groundwater flow rates from 0.01 to 1.0 ft/day (natural in the 0.01 to 0.1 ft/day, 1 ft/day would be rate near a pumping well), and c) 36-ppb NDMA (highest recorded at Aerojet; lower concentrations would degrade more rapidly). Given the action limit of 0.7 ppt, the NDMA concentration calculated in Table 4.3 (in ppb) needs to be <7.00E-04. With a zone of high reduction, ("high reduction" column in Table 4.3), even a 5-ft radius injection of dithionite would be effective. However, if only low reduction is achieved at the field scale, then a larger 15-ft radius reduced zone is still not effective at a very high groundwater flow rate (1.0 ft/day).

Table 4.3. NDMA estimated concentration down gradient of a reduced sediment zone.

barrier width (ft)	groundwater flow (ft/day)	residence time in zone (days)	high reduction: NDMA degraded (ppb)*	low reduction: NDMA degraded (ppb)**
10	0.01	1000	0.00E+00	5.42E-41
10	0.10	100	1.08E-114	2.37E-03
10	1.0	10	1.01E-10	1.37E+01
30	0.01	3000	0.00E+00	1.23E-124
30	0.10	300	0.00E+00	1.02E-11
30	1	30	7.94E-34	2.00E+00

* C/Co = exp[-2.66/h * residence time]*36

*2.66/h = rate for 0.26 h half-life

**0.0963/h = rate for 7.2 h half-life

The parameters that define the greatest difference in NDMA degradation are: a) amount of sediment reduction, b) groundwater flow rate, and c) NDMA concentration. These results show that the field test should not be conducted near a pumping well (with high effective groundwater flow rates and subsequently very low residence times in the reduced zone). In addition, a small, highly reduced zone is more effective than a larger zone with low reduction. The injection strategy can easily be designed to create a small, highly reduced zone. Overall, these results show that in all possible cases, it is possible to determine whether NDMA is degraded (i.e., worst case of low reduction, small reduced zone, and high flow, there is still a NDMA concentration decrease), but a viable remediation scheme to degrade NDMA to action limits requires a highly reduced zone and sufficient residence time in the zone to degrade to parts per trillion levels. NDMA degradation to parts per trillion levels is measured (described in Section 4.3).

4.1.15 Reduced Zone Longevity for Aerojet Sediment

A reduced zone created in the Aerojet aquifer will reduce all electron acceptors passing through the zone, which includes NDMA and dissolved oxygen. Over time, the barrier will oxidize, and the NDMA degradation rate will decrease, as shown in separate experiments with sediments with

differing amounts of reduction. The Aerojet aquifer has considerable capacity (Figure 4.28), so longevity as defined by oxygen consumption (i.e., total ferrous iron consumption), the longevity is about 23 years:

$$(30\ \text{ft})(\text{day}/1.0\ \text{ft})(277\ \text{pore volume})(\text{year}/365.25\ \text{days}) = 23\ \text{years} \quad (4.2)$$

for 8.4-mg/L O_2,

The longevity of the reduced zone for degrading NDMA to 0.7 ppt is less than this value. While separate 1-D column experiments with fully and partially reduced sediments have been conducted (Figure 4.26), the decrease in the NDMA degradation rate as sediment is oxidized over a long period of time is shown in Task 3 results. This type of experiment is shown in Figure 4.29 for chromate (separate project), in which the chromate reduction half-life increases considerably at about 150 pore volumes (total ferrous iron, as defined by dissolved oxygen consumption was 250 pore volumes; Szecsody et al. 2004, 2005b).

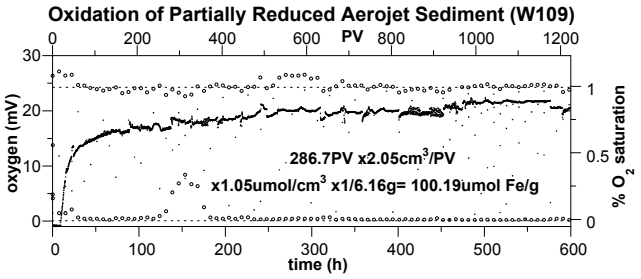

Figure 4.28. Oxidation of reduced Aerojet sediment with oxygen-saturated water.

A question to address with a proposed treatment process is does the degradation product have considerably lower toxicity than NDMA. In other words, is degradation to dimethylamine (DMA) sufficient, or is mineralization required. Results in this study indicate that DMA is produced with reaction of NDMA with reduced sediment, as defined by HPLC analysis of degradation products and DMA standard. However, since DMA is degraded further (Figure 4.21), NDMA mineralization needs to be considered, as described in Tasks 2, 3, and 4 results (following sections).

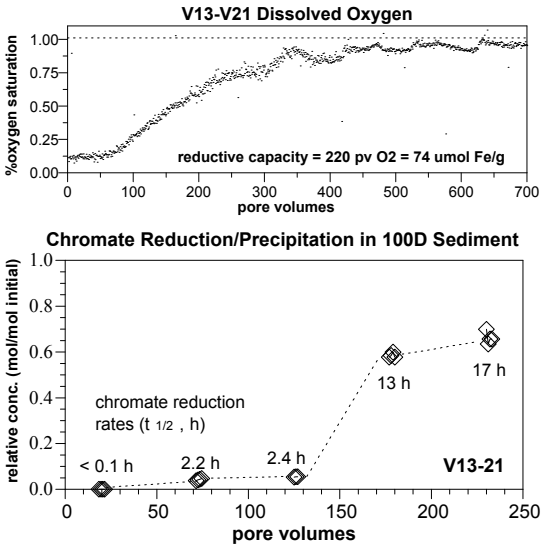

Figure 4.29. Long-term oxidation column experiment with a reduced sediment column in which 2-mg/L chromate, 8.4-mg/L O_2, and 60-mg/L nitrate was injected. Effluent concentration of dissolved oxygen (a), and chromate (b) are shown.

The toxicity of DMA was considered. It appears to be toxic at very high concentrations, so would not be toxic at <36 ppb in the Aerojet aquifer, assuming 100% of the NDMA was degraded to DMA. In aqueous solution, DMA has a threshold limit value of 5 ppm and short-term exposure limit of 15 ppm, so is not classifiable as a human carcinogen. In a long-term toxicity study of rates, DMA at 0, 10, 50, or 175 ppm for 6 hours/day, 5 days/week for 12 months through inhalation showed less weight gain and had olfactory sensor cell lesions for the 175-ppm case (Buckley et al. 1985).

4.2 Task 2 – Microbial Degradation of NDMA

Mineralization studies with sediments have been conducted under natural oxic, anoxic, and reducing conditions. A comparison of NDMA mineralization results are shown in the following sections. Most of the results presented in Task 2 reflect oxic and anoxic conditions, where there is essentially no abiotic NDMA degradation. NDMA mineralization results in chemically reduced sediment are presented in Section 4.3, as both abiotic and biotic processes are contributing to the observed degradation.

4.2.1 Overview of NDMA Mineralization in Sediments

Mineralization experiments conducted in the same sediment under oxic and reducing conditions for two different aquifer sediments (Figure 4.30) all show some mineralization, but: a) mineralization in oxic systems was ~10 times faster and ~5 times greater extent compared to reduced systems, b) NDMA mineralization rate decreased with decreasing concentration, c) NDMA mineralization extent decreased with increasing NDMA concentration, and d) trace nutrient addition did not increase the NDMA mineralization rate or extent (described in the following sections).

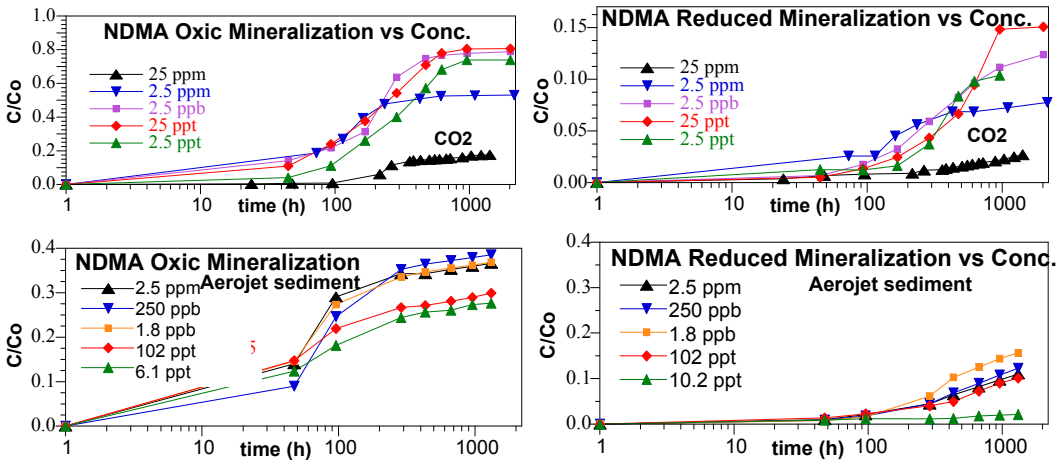

Figure 4.30. NDMA mineralization over a range in concentration from 25 ppm to 2.5 ppt in a) oxic Ft. Lewis sediment, b) reduced Ft. Lewis sediment, c) oxic Aerojet sediment, and d) oxic Aerojet sediment.

NDMA mineralization in oxic systems was as high as 78% (Figure 4.30a) for NDMA concentrations <2.5 ppb, but 50% for 2.5 ppm and 22% for 25 ppm, which is hypothesized to be caused by a sediment nutrient limitation. The same observation of more limited NDMA mineralization extent with increasing NDMA concentration occurred in reduced sediment systems (Figure 4.30b), although the extends were ~5 times less than in the comparable oxic systems. The calculated NDMA mineralization rate in these oxic and reduced systems (mol NDMA/h, Figure 4.31) decreased with decreasing NDMA concentration, for both the Ft. Lewis sediment and Aerojet sediment.

Under purely oxic conditions, NDMA mineralization (25 ppm) was evaluated for three sediments. More than 25.6% of the total NDMA was degraded by *in situ* microbial communities in contaminated sediment and water in NDMA-contaminated Aerojet sediment and 31.2% in NDMA-contaminated Rocky Mountain Arsenal water, but 17.7% in Ft. Lewis sediment with no prior exposure to NDMA.

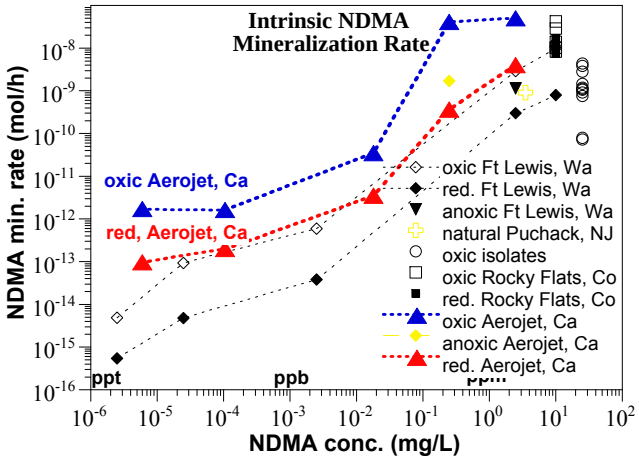

Figure 4.31. NDMA mineralization rates (mol NDMA degraded per hour) as a function of NDMA concentration in oxic and reduced systems.

The ability of the soil microbial community to mineralize NDMA was investigated in under varying redox conditions (Figure 4.32b). NDMA mineralization was greatest (17.4%) with no dithionite exposure, which may indicate that NDMA biodegradation in anaerobic water may be more rapid than in dithionite-reduced sediments, although too few experiments have been conducted to date. In these experiments, NDMA was supplied as the sole electron donor in anaerobic systems; the effects of stimulation by nutrient addition using, e.g., ethanol yet to be evaluated. The following sections investigate NDMA mineralization under oxic conditions with various additions.

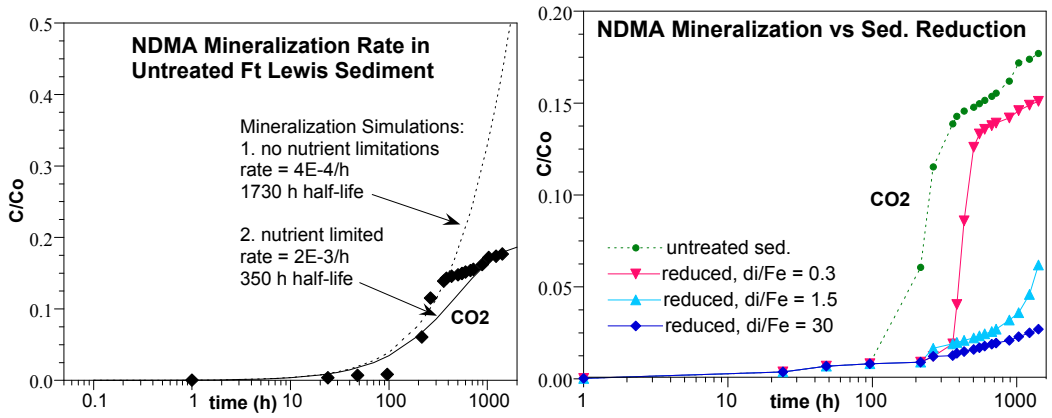

Figure 4.32. NDMA mineralization rate in an oxic environment (a) and under varying redox conditions (b) for 25-ppm NDMA in Ft. Lewis aquifer sediment.

The rate of NDMA mineralization in the oxic, untreated Ft. Lewis sediment was simulated (lines, Figure 4.32a), which showed that the microbial exponential growth phase was limited. A simulation with a nutrient limitation (i.e., ending mineralization at 20%) could approximate the observed data with slow rate (1700 hours). These preliminary results indicate that nutrient additions are needed to increase both the extent of biomineralization and rate of mineralization.

4.2.2 Carbon Additions in Oxic and Reduced Systems

Because NDMA can be mineralized in oxic systems by a monooxygenase enzyme pathway (Sharp et al. 2005, 2007), methane-, propane-, and toluene-monooxygenase pathways were investigated in oxic, anaerobic, and reduced sediment to investigate the relative contribution of this biotic mineralization (generally in oxic systems by the monooxygenase pathways) and potential abiotic contributions. In these experiments, quantities of methane or propane gas (or aqueous toluene) were added to the respective oxic, anaerobic, or reduced sediment system (contains headspace) at the same time the ^{14}C-labeled NDMA was added (i.e., no preconditioning time). In addition, acetylene is known to block some monooxygenase enzyme pathways, so was additionally added in some systems. In the oxic systems (Figure 4.33a), monooxygenase enzyme pathways should be enhanced by the addition of methane or propane or toluene (separate monooxgyenase enzyme pathways), although some amount of acclimation time (weeks) is needed to build up the microbial population. In these experiments with no acclimation time, the effect of methane, propane, or toluene addition to oxic sediment was actually a decreased the NDMA mineralization rate. Addition of acetylene also decreased the NDMA mineralization rate.

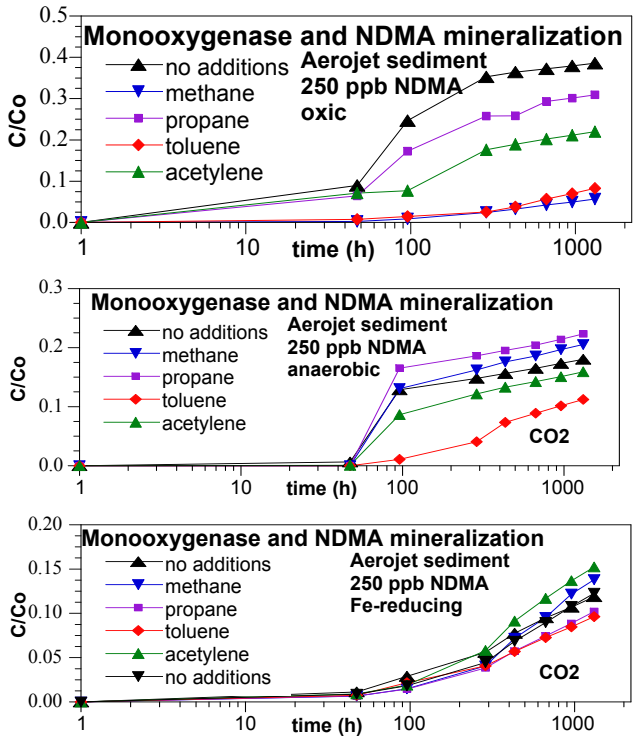

Figure 4.33. NDMA mineralization in oxic (a), anaerobic (b), and reduced (c) sediment systems with promotion of enzyme pathways (but no prestimulation time).

In anaerobic- and iron-reducing (i.e., dithionite-reduced sediment creating ~80 µmol Fe^{2+}/g) conditions, the addition of methane, propane, toluene, and acetylene would have a similar effect as the oxic system only if the same monooxygenase enzyme pathway was occurring. It is possible in the anaerobic sediment to have small isolated zones of oxic sediment, but highly unlikely in the reduced sediment, as there is a large redox capacity to reduce any available oxygen. These results (Figure 4.33b and c) indeed seem to support this hypothesis, as the anaerobic sediment system showed a similar significant decrease with the additions, whereas the iron-reducing system showed essentially no change in the NDMA mineralization rate and extent with these additions. The fact that 8% to 15% of NDMA is still mineralized under iron-reducing systems (Figure 4.33c) indicates that it is accomplished by a different enzyme pathway. The significance of oxygen (and the monooxygenase pathways) is clearly shown by experiments conducted at the same NDMA concentration, but differing amounts of oxygen and under differing iron-reducing conditions (Figure 4.34).

The question as to whether NDMA is being mineralized biotically and/or abiotically in aquifer sediments was addressed in experiments without and with the addition of a bactericide (gluteraldehyde, Figure 4.35). While mineralization is clearly biotic in the presence of only microbial isolates (described in following sections), both abiotic and biotic processes could be occurring in sediments. A bactericide (2% gluteraldehyde) placed in the sediment/water system for 48 hours before the ^{14}C-NDMA was added may kill most of the microbial population and (hopefully) not influence abiotic degradation/mineralization of NDMA. NDMA degradation (not mineralization) in reduced sediment was abiotic (Figure 4.6c). In oxic sediment, NDMA mineralization in unaltered sediment could be biotic and/or abiotic, but assuming the bactericide kills the majority of the microbial population, the change in mineralization rate between "live" (unaltered) and "killed" (bactericide added) sediment systems generally reflects the biotic contribution of NDMA mineralization.

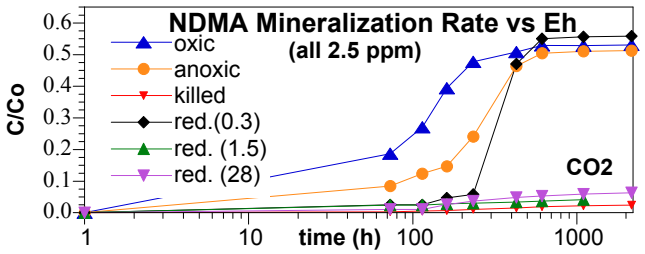

Figure 4.34. Importance of oxygen for NDMA mineralization.

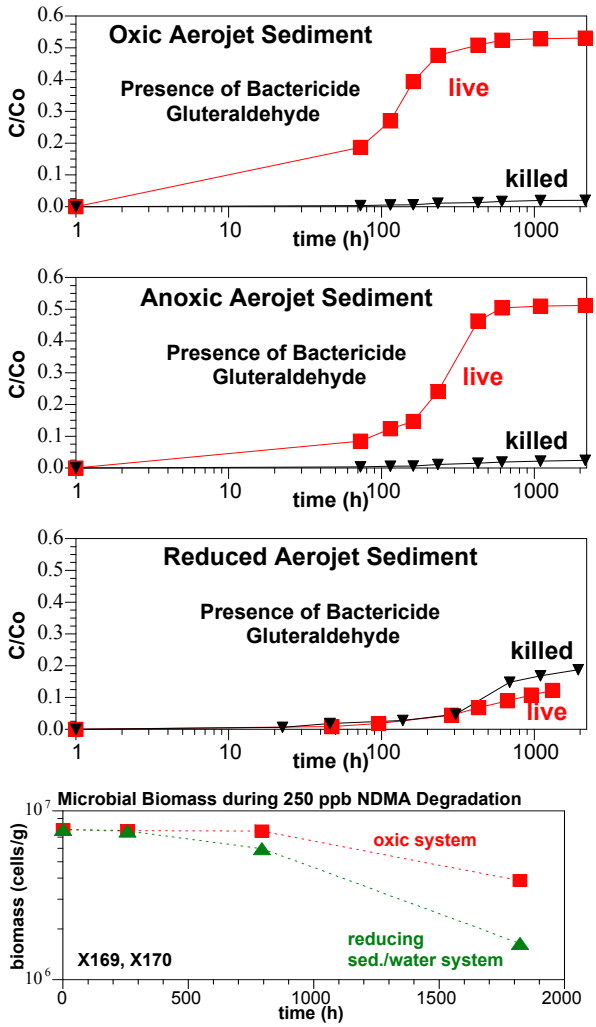

Figure 4.35. Relative contribution of biotic and abiotic mineralization of NDMA.

NDMA mineralization in *oxic* sediment/water systems (Figure 4.35a) was nearly all (>98%) biotic, as expected, and likely by a monooxygenase pathway. The NDMA mineralization rate in the killed system (>50,000-hour half-life, <2% after 2000 hours) was very slow. Described in Section 4.2.5 (NDMA degradation with microbial isolates), NDMA is being utilized as a co-substrate, so it was not expected to grow in systems with no other carbon source. Measure microbial biomass in an oxic system over 1800 hours (Figure 4.35d, red line) shows a slow decrease in biomass, consistent with this hypothesis. As hypothesized earlier, NDMA mineralization in anoxic sediment/water systems (Figure 4.35b) appeared also to be nearly (>98%) all biotic. This may indicate that there is some oxygen remaining in the anoxic system (trapped in sediment microfractures, for example. In contrast, NDMA mineralization in *reduced* sediment/water systems (Figure 4.35c) was primarily abiotic, as the presence of the bactericide did not alter the slow rate of NDMA mineralization. As shown earlier (Figure 4.30),

NDMA mineralization in oxic systems was as great as 80%, with an average half-life of 342 ± 36 hours (Aerojet sediment) in contrast to only 17% (by 2000 hours) with an average half-life of 3475 ± 504 hours. Therefore, oxic (biotic) NDMA mineralization was 10 times more rapid (and mineralization extent 4.7 times greater) than the abiotic mineralization under iron-reducing conditions. As described in Section 4.3, additional reduced systems were investigated (naturally reduced clay from a New Jersey aquifer), which showed mineralization as great as 23%. So, abiotic NDMA mineralization does occur, but the rate is generally not very viable for field-scale remediation (thousands of hours half-life), as groundwater advection of NDMA would move the NDMA through the reduced zone before there would be time to fully mineralize it.

At each NDMA concentration, the rate of NDMA mineralization in oxic and reduced sediment was compared (Figure 4.36). These results show little trend in the ratio of mineralization rate or extent difference between oxic and reduced systems at different NDMA concentration.

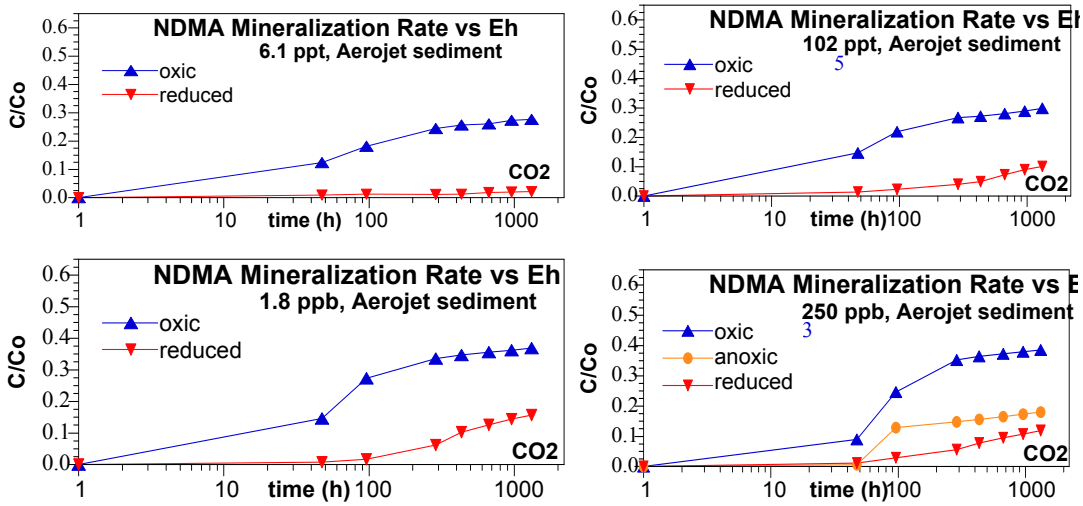

Figure 4.36. NDMA mineralization comparison in oxic and reduced systems at differing NDMA concentration.

4.2.3 Monooxygenase Enzymes and NDMA Mineralization in Oxic Systems

NDMA oxic mineralization was studied with propane addition to the Aerojet sediment at differing propane/oxygen ratios (in the headspace above the liquid), and with 1632 hours of prestimulation time before the ^{14}C NDMA was added. Results (Figure 4.37a) show a definite increase in the NDMA mineralization with a propane/oxygen ratio of 0.4, but essentially no increase in oxic system mineralization for lower (0.04) and higher (3.8) propane/oxygen ratios. However, it can be concluded that propane monooxygenase enzymes can be stimulated in the Aerojet subsurface sediment (from 250-ft depth) to promote more rapid NDMA mineralization (although this by itself is not very efficient). Additional propane addition experiments were tried to promote further NDMA mineralization. In the initial experiments were conducted to 1000 hours (6 weeks), after which further additions were made to the systems: a) oxic sediment was added (Figure 4.37b, black triangles) and b) oxic sediment, oxygen, and propane was added (blue triangles). When additional oxic sediment was added, there was some additional NDMA

mineralization (<5%) over 1000 hours, which is significantly less than the previous 1000 hours in which 45% to 60% NDMA mineralization was observed. It appears that nearly all the NDMA that can be mineralized was completed by 1000 hours and roughly the other half of the carbon from NDMA was likely converted into methane. The amount of carbon incorporated into microbes was also characterized, as described in the following section.

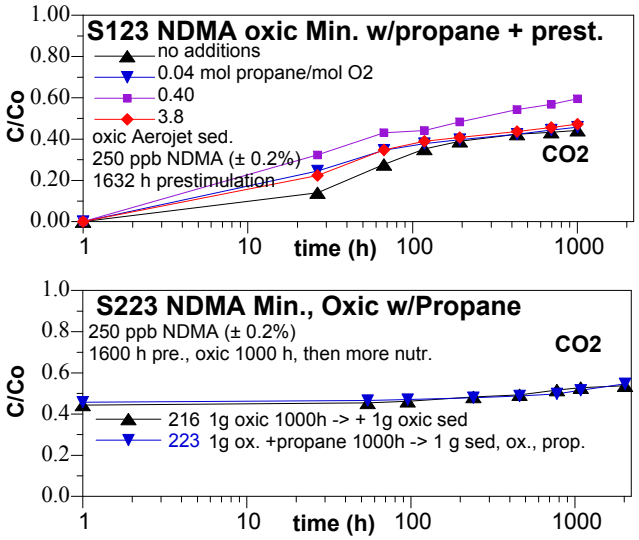

Figure 4.37. Oxic NDMA mineralization in sediment with propane addition (a) and additional sediment/ |oxygen/propane addition after 1000 hours (b).

Addition of other carbon nutrients in oxic systems were investigated including yeast and humic acid addition. For 250-ppb NDMA concentration, the addition of higher concentrations of yeast increased the NDMA degradation rate and extent slightly (Figure 4.38a), whereas the low concentration addition showed a significant decrease in NDMA mineralization. The addition of humic acid at three differing concentrations (Figure 4.38b) had no influence on NDMA mineralization. In both of these studies, 1632 hours of prestimulation (10 weeks) or contact time was used between the carbon addition and the sediment before ^{14}C NDMA was added.

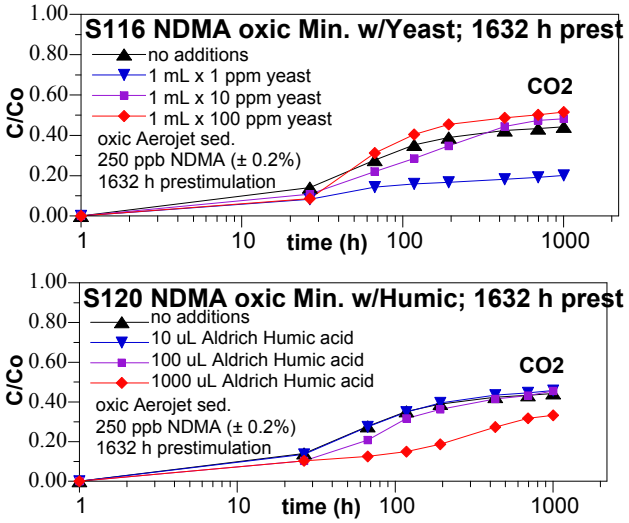

Figure 4.38. NDMA mineralization in oxic Aerojet sediment with yeast or humic acid addition.

In these oxic systems, addition of propane (Figure 4.37a) and yeast (Figure 4.38a) showed some increase in the NDMA mineralization rate, whereas addition of humic acid (Figure 4.38b) showed no influence. To test the validity of the humic acid and yeast addition results, these carbon sources were added again to the oxic sediment systems after 1000 hours. As a baseline, an oxic sediment system (1 g of sediment initially in system) with no additions (black triangles in Figure 4.38a) received an additional 1 g of sediment and oxygen, but no other additions (Figure 4.39a and b, black triangles) after 1000 hours. This showed an additional 6% NDMA mineralization for the next 2000 hours on top of the 46% mineralization in the first 1000 hours. Again, this appears to indicate that ~50% of the NDMA carbon was converted into CO_2 (and measured in the traps) with essentially no additional mineralization with the addition of sediment (containing additional microbes). Because the additional 6% NDMA that was mineralized between 2000 and 3000 hours was very

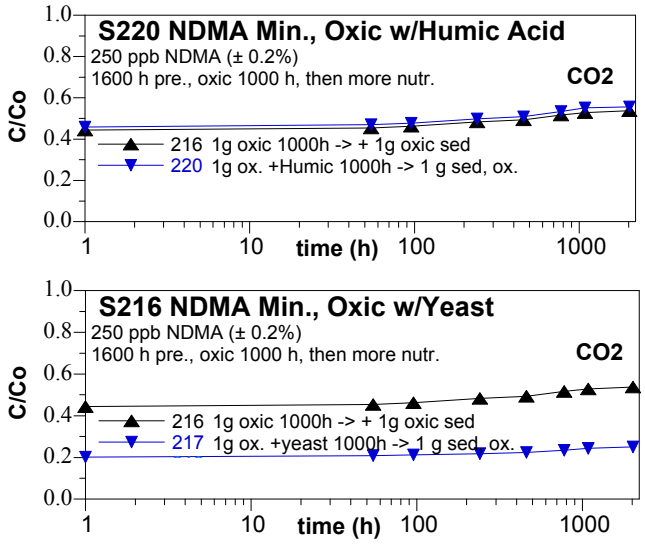

Figure 4.39. NDMA mineralization with additional sediment, oxygen, and humic acid or yeast addition after 1000 hours of oxic mineralization.

slow (not characteristic of exponential growth phase of microbes), it is hypothesized that it is simply NDMA carbon mass associated with microbes that are degraded.

4.2.4 Carbon Mass Balance in Oxic Systems

At the end of all of these oxic system (and other reduced system and sequential reduced/oxic system) studies, the amount of carbon mass sorbed onto microbes was quantified and the amount incorporated into microbes was also quantified. A methanol/water mixture for 1 hour was used to desorb any NDMA on the microbial surface. After this extraction was completed, 10-M NaOH was then used for 24 hours to dissolve the microbial biomass in order to count the total ^{14}C from NDMA associated with microbes. For 10 oxic systems in which the ^{14}C mass balance for NDMA mineralization (at 3000 hours) was conducted, the average mineralization was 51.0% ± 11.5% and average aqueous concentration of 17.8% ±12.4%. Based on the previously defined NDMA sorption parameter (K_d) of 0.12 mL/g, there should be 2.0% of the NDMA mass sorbed on the sediment surface at the sediment/water ratio used in these experiments (1 g to 6 mL). The total *measured* sorption (i.e., sorbed to sediment and microbes, extracted with methanol) in these oxic systems was 2.7% ± 4.5%, indicating maybe 0.7% of the NDMA mass was likely sorbed to the microbial surface. An average of 5.7% ± 1.3% of the NDMA carbon mass was measured as *incorporated* into the microbes (subtracting out the sorbed mass). Overall, these oxic systems had a total carbon mass balance of 80.0% ± 15.6%. This was relatively high compared to the reduced systems described in the following section. This high association of NDMA with the microbial biomass implies a significant contribution of microbes to NDMA mineralization, which has already been demonstrated to be true (Figure 4.35a, system with killed microbes does not mineralize NDMA).

4.2.5 NDMA Degradation by Bacterial Isolates

Initial experiments conducted with bacterial isolates found a number of bacteria that mineralize 25-ppm NDMA in an oxic aqueous environment when using this compound as a source of carbon and nitrogen for growth. The extents of NDMA mineralized by these strains when used as a carbon and nitrogen source are listed in Table 4.4. These mineralization extent values were measured after 600 hours. These results indicate that NDMA is susceptible to biological degradation by pure bacterial cultures, using NDMA as the sole electron source. Subsequent experiments involved carbon, nitrogen, and trace nutrient additions in aerobic and anaerobic conditions.

NDMA degradation by microbial isolates was further investigated. Experiments were set up to determine whether various bacteria could degrade and utilize NDMA as a source of nitrogen, or carbon and nitrogen for growth.

Gordonia sp. KTR9 and *Gordonia desulfuricans* did not appear to grow on NDMA as a nitrogen source or a nitrogen and carbon source (Figure 4.40). Under these conditions, degradation of NDMA by both strains occurred. *G. desulfuricans* degraded 14% and 31% of the NDMA while strain KTR9 degraded 45% and 50% of the NDMA when it was added as the nitrogen source or when it was added as the nitrogen plus carbon source, respectively (Figure 4.40). These values are consistent with the mineralization data for these two strains which indicated that *G. desulfuricans* and strain KTR9 mineralized NDMA to ~24% and 55% carbon dioxide, respectively, when NDMA was supplied as the nitrogen and carbon source for growth (Table 4.4). However, the results between these two experiments are not directly comparable since the cultures for the mineralization assay had not been treated to remove traces of the culture medium. The mineralization assay was repeated with washed cells of strain KTR9 to remove traces of medium. In this case, mineralization of NDMA to ~20% carbon dioxide was only observed when NDMA was added as the sole nitrogen source (Figure 4.41). It is not clear why NDMA was not mineralized when added as a carbon or carbon plus nitrogen source. The absence of growth in the degradation experiments appears to support the co-metabolic transformation and mineralization of NDMA by both strains. Degradation of NDMA by a co-metabolic process was recently shown to occur in *Pseudomonas mendocina* KR1 (Fournier et al. 2006; Yang et al. 2005). In strain KR1 a toluene-4-monooxygenase enzyme was shown to transform NDMA, but it is unknown whether this enzyme is present in either *Gordonia* strain. Also, it appears that the *Gordonia* species that we have examined are able to transform NDMA to a metabolite(s) that can be further mineralized to a high percentage of carbon dioxide (FY 2005 annual report), while *P. mendocina* KR1 only poorly mineralized NDMA (Fournier et al. 2006). Additional experiments are underway to

Table 4.4. Oxic mineralization extent of 25-ppm NDMA by bacterial isolates with NDMA as nitrogen, carbon source (600 hours).

Bacterial Isolate	Extent of NDMA Mineralized (%)
Gordonia desulfuicans	23.89 ± 3.47
Gordonia rubripertincta	35.06 ± 4.53
Gordonia nitida	29.77 ± 2.70
Gordonia polyisoprenivorans	72.72 ± 1.17
Gordonia alkanivorans	68.13 ± 1.29
Gordonia amarae	27.06 ± 0.51
Gordonia sp. KTR9	56.72 ± 2.56
Williamsia sp. KTR4	28.06 ± 2.85

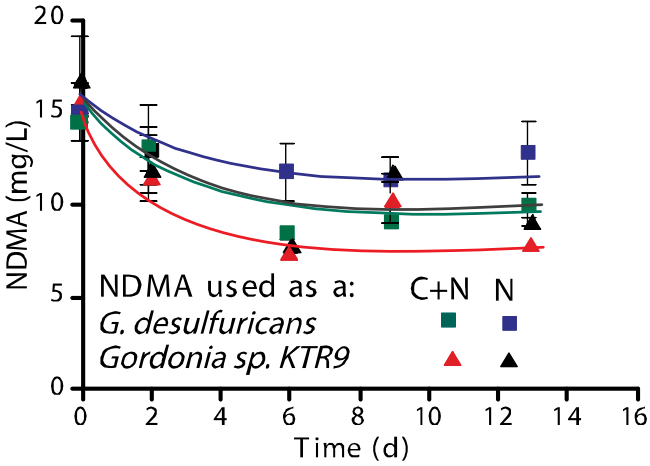

Figure 4.40. Degradation of NDMA added as a nitrogen source (closed symbols) or as a nitrogen and carbon source (open symbols) by *G. desulfuricans* (squares) and *Gordonia* sp. KTR9 (triangles).

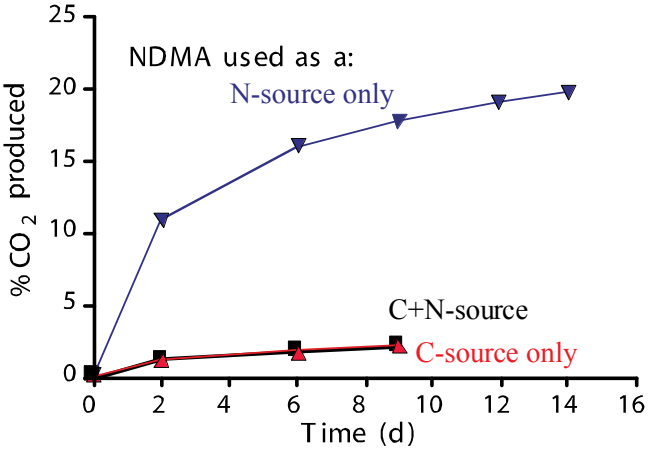

Figure 4.41. Mineralization of NDMA by washed cells of *Gordonia* sp. KTR9.

confirm the co-metabolic transformation and mineralization of NDMA by *G. desulfuricans*, strain KTR9 and the *Gordonia* strains that were previously used to determine the mineralization potential of NDMA.

In a second mineralization assay (Table 4.5), 10-ppm NDMA was mineralized in an oxic, aqueous environment by several *Gordonia* and *Williamsia* bacterial species that had been grown on glucose, glycerol, and succinate as carbon sources and nitrate as the nitrogen source (details in Figures 4.42 and 4.43). The maximum amount of NDMA mineralized ranged from about 3.3% to 72.5% depending on the species and type of nutrient amendment. In general, the presence of an added carbon source stimulated the mineralization of NDMA.

Table 4.5. Oxic mineralization extent of 10-ppm NDMA by bacterial isolates with NDMA as nitrogen, carbon source (720 hours).

	Extent of $^{14}CO_2$ produced (%) with amendment[a]		
Strain	Carbon	Nitrogen	None
Gordonia alkanivorans	66.10 (1.55)	18.98 (4.1)	3.31 (1.7)
Gordonia amarae	58.49 (1.48)	11.35 (4.74)	17.46 (12.5)
Gordonia desulfuricans	30.04 (0.96)	9.51 (0.1)	6.72 (0.73)
Gordonia nitida	32.62 (0.57)	21.57 (0.55)	5.00 (3.36)
Gordonia polyisoprenivorans	69.43 (0.88)	72.5 (2.25)	74.29 (3.08)
Gordonia rhizosphera	26.16 (2.66)	25.7 (9.56)	
Gordonia rubripertincta	69.63 (0.87)	47.63 (1.10)	38.68 (0.9)
Gordonia terrae	64.88 (2.23)		
Gordonia sp. KTR9	69.55 (0.42)	70.26 (1.48)	60.4 (2.17)
Gordonia sp. KTC13	25.92 (0.58)		
Williamsia maris			15.77 (1.64)
Williamsia sp. KTR4	67.48 (1.32)	53.20 (1.75)	54.91 (1.91)

a. Standard error in parentheses.

In comparison, the presence of an added nitrogen source inhibited the extent of mineralization and the rate of mineralization for *G. amarae*, *G. alkanivorans*, *G. desulfuricans*, *G. nitida*, *G. rubripertincta*, and KTR4. The smallest extents of mineralization were observed for *G. alkanivorans*, *G. desulfuricans*, and *G. nitida* in the absence of any nutrient amendment. These results indicate that *Gordonia* and *Williamsia* strains can constitutively degrade NDMA and that the degradation is probably co-metabolic. The constitutive degradation of NDMA has also been observed for *Rhodococcus jostii* RHA1 when RHA1 has been grown on non-specific carbon sources (Sharp et al. 2007). In these experiments with *Gordonia* and *Williamsia* species, neither the inoculum density nor the growth of the strains was followed and so it is not known whether the species in Table 4.5 can utilize NDMA as a carbon or nitrogen source for growth. While it has been shown that wastewater treatment systems and soils can degrade or mineralize NDMA (Arienzo et al. 2006; Bradley et al. 2005; Gunnison et al. 2000; Yang et al. 2005), studies with pure bacterial cultures have not shown a direct metabolic role for NDMA

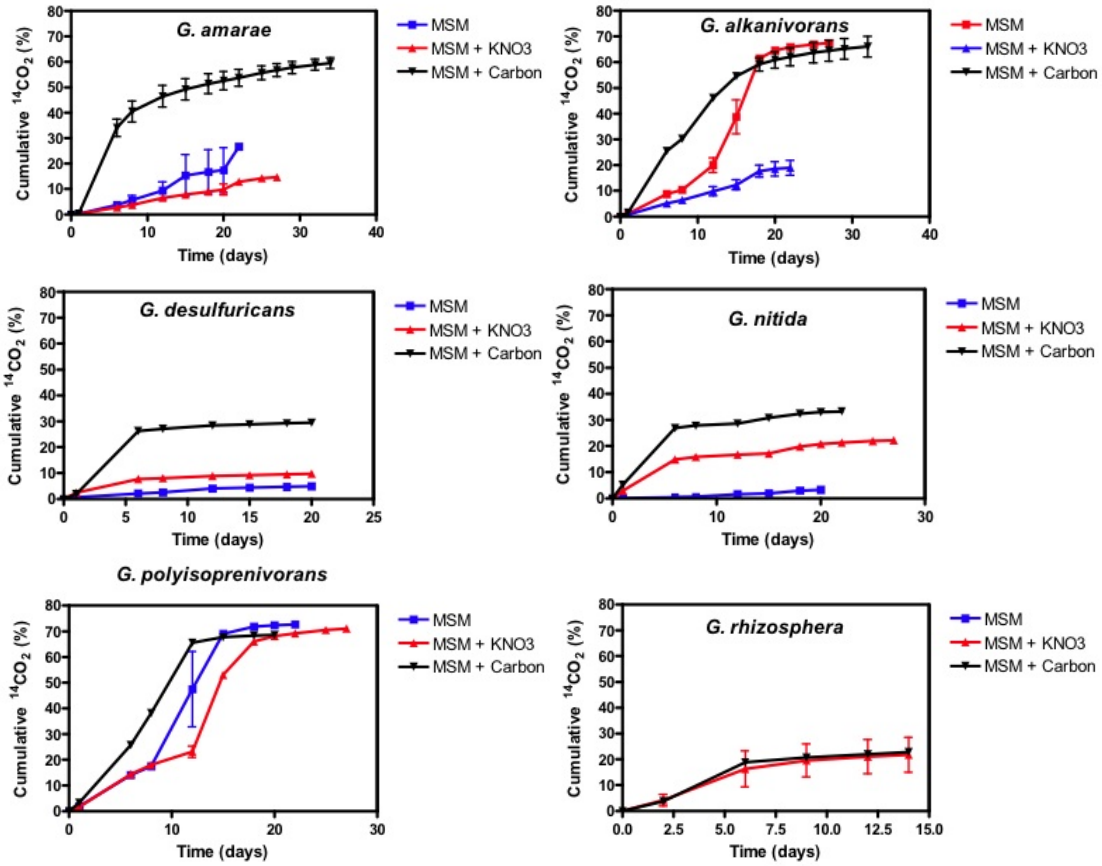

Figure 4.42. Oxic mineralization of [^{14}C]-NDMA to $^{14}CO_2$ by pure bacterial species in the absence (MSM ■) or presence of a nitrogen (MSM + KNO_3 ▲) or carbon amendment (MSM + Carbon ▼).

(Fournier et al. 2006; Sharp et al. 2005, 2007). Thus, co-metabolism appears to be the primary mechanism for the biotic removal of NDMA.

Mixed microbial populations indigenous to groundwater from Rocky Mountain Arsenal and soil from the Aerojet facility mineralized NDMA under similar conditions as used with the bacterial cultures. With these materials the maximum amount of NDMA mineralized was ~20% under either aerobic (Figure 4.44) or anaerobic conditions (Figure 4.45). The addition of a nitrogen amendment tended to decrease the extent and rate of mineralization, while the carbon amendment had either no effect or stimulated the extent of mineralization. The inhibition of NDMA mineralization by nitrate in soil was previously suggested by Bradley et al. (2005) as an indication that NDMA could function as a terminal electron acceptor or nitrogen source for growth by soil microbial populations.

These experiments also indicated that NDMA biotransformation by microorganisms was possible without stimulation of monooxygenase enzymes using substrates such as methane, propane, or toluene. This implies that NDMA mineralization under aerobic and anaerobic conditions is proceeding by an unidentified microbial pathway. However, the rate of degradation of NDMA following propane or toluene stimulation in strains *Rhodococcus jostii* RHA1 and

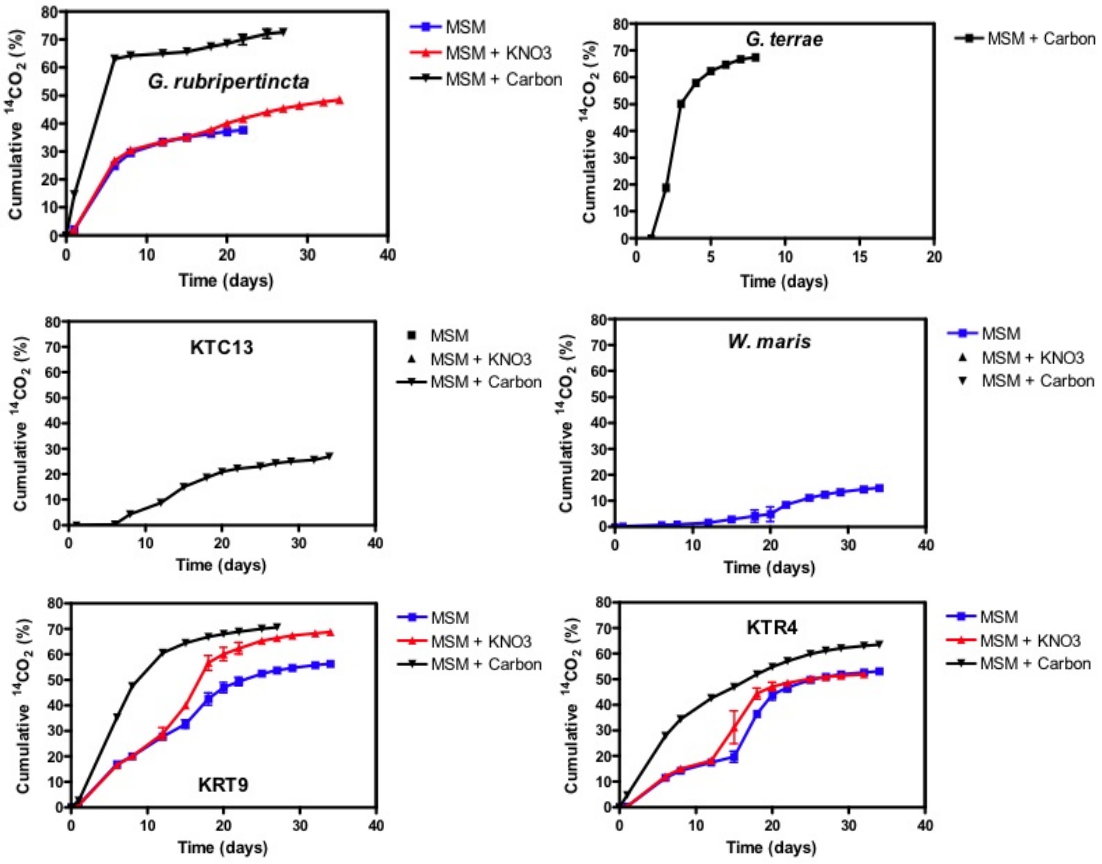

Figure 4.43. Oxic mineralization of [^{14}C]-NDMA to $^{14}CO_2$ by pure bacterial species in the absence (MSM ■) or presence of a nitrogen (MSM + KNO_3 ▲) or carbon amendment (MSM + Carbon ▼).

Pseudomonas mendocina RK1 was considerably faster (Fournier et al. 2006; Sharp et al. 2007) than the constitutive rate observed in this study.

In comparison to microbial isolate studies in this section, soil microbial communities were less able to mineralize NDMA after chemical reduction (i.e., in an iron-reducing environment) of Ft. Lewis soil with dithionite (Figure 4.32b). The extent of NDMA mineralization in the absence of dithionite treatment was 17.4% and the extent of mineralization decreased with increasing ratios of dithionite to iron. A slight decrease in the extent of mineralization occurred at a donor/acceptor ratio (2*di/Fe) of 0.29. In addition, the length of the lag phase prior to NDMA mineralization was significantly longer with this treatment. At this ratio of dithionite to iron, the indigenous microbial populations recovered slowly from the chemical reduction treatment. However, at dithionite to Fe ratios above 1.48 there was a significant decrease in the rate and extent of NDMA mineralization. At donor/acceptor ratios of 1.48 and 29.68, the mineralization values dropped to 6.4% and 2.6%, respectively. Under these conditions, the activity of the indigenous microbial population is significantly reduced and the populations may not be able to recover from the chemical treatment. Similarly, measurements of total microscopic counts (acridine orange staining) and ^{14}C-acetate mineralization rates have shown an order of magnitude lower cell counts and a 10-time reduction in acetate mineralization rates as a result of a 2*di/Fe ratios (Szecsody et al. 2007a). In contrast to NDMA, the dithionite treatment stimulated the

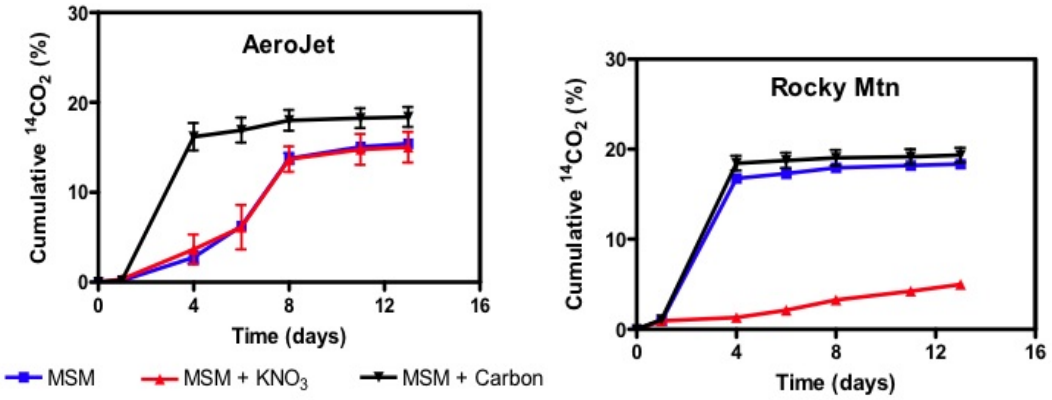

Figure 4.44. Anaerobic mineralization of [^{14}C]-NDMA to $^{14}CO_2$ by Aerojet soil and Rocky Mountain Arsenal groundwater in the absence (MSM ■) or presence of a nitrogen (MSM + KNO_3 ▲) or carbon amendment (MSM + Carbon ▼).

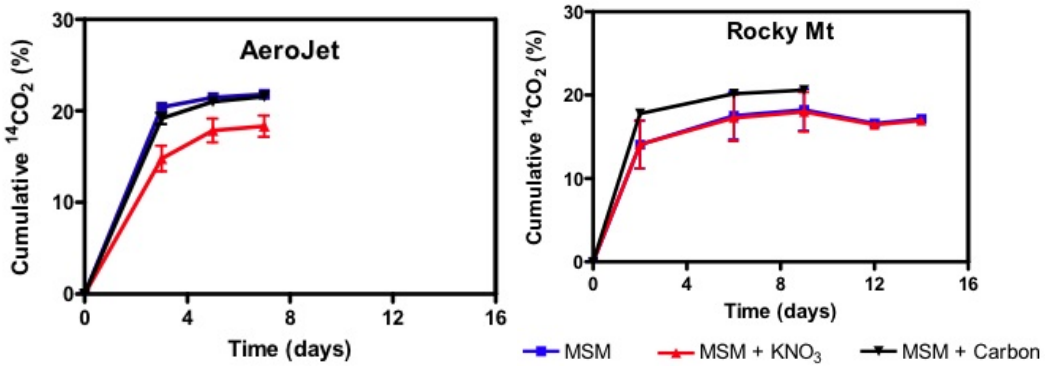

Figure 4.45. Aerobic mineralization of [^{14}C]-NDMA to $^{14}CO_2$ by Aerojet soil and Rocky Mountain Arsenal groundwater in the absence (MSM ■) or presence of a nitrogen (MSM + KNO_3 ▲) or carbon amendment (MSM + Carbon ▼).

mineralization of hexahydro-1,3,5-trinitro-1,3,5-triazine (RDX) and octahydro-1,3,5,7-tetranitro-1,3,5,7-tetrazocine (HMX) by the microbial populations as a result of a combined abiotic/biotic transformation of the energetics (Szecsody et al. 2007a).

In summary, NDMA was biotransformed by various bacterial species both in pure culture studies and in soil and groundwater microcosms. NDMA was biotransformed to carbon dioxide and the extent of transformation could be quite extensive (up to 70% converted to carbon dioxide). In general carbon amendments stimulated the rate and extent of mineralization to carbon dioxide, indicating a co-metabolic route for biotic transformation of NDMA. The role of NDMA as a carbon or nitrogen source for bacterial growth was not proven by the experiments conducted in this study. Degradation intermediates were also not identified in these studies and so the route for biotransformation is not known. In contrast to RDX and HMX, dithionite reduction of Ft. Lewis soil led to an inhibition of the rate and extent of NDMA mineralization by the indigenous microorganisms.

4.3 Task 3 – Coupled Abiotic/Biotic Degradation of NDMA

In this section, NDMA mineralization in reduced sediment, then in sequential reduced, then oxic sediment are described. Aerojet sediment that has been chemically reduced with dithionite treatment to create 80 µmol ferrous iron/g of sediment exhibit slow NDMA mineralization (Figure 4.30), which ranges from 8% to 15% by 1000 hours. These reduced systems do not contain dissolved oxygen that can be used as an electron acceptor, so the microbial monooxygenase enzyme pathway that appears to promote NDMA degradation in oxic systems is not the mechanism responsible in these reduced systems. As demonstrated earlier (Figure 4.6), NDMA is rapidly (under ideal conditions, half-life ~10 hours) abiotically degraded to DMA. While DMA is not toxic and this could work as a field-scale technique, DMA is not the final end product, so mineralization is still of greater interest for field-scale remediation. In this section, different carbon sources are added in an attempt to increase NDMA mineralization in reducing sediment systems. In addition, sequential reduced abiotic degradation, then oxic sediment systems (for primarily biodegradation) were investigated, which would parallel a reduced zone in the field, with degradation products flowing into down-gradient oxic sediment.

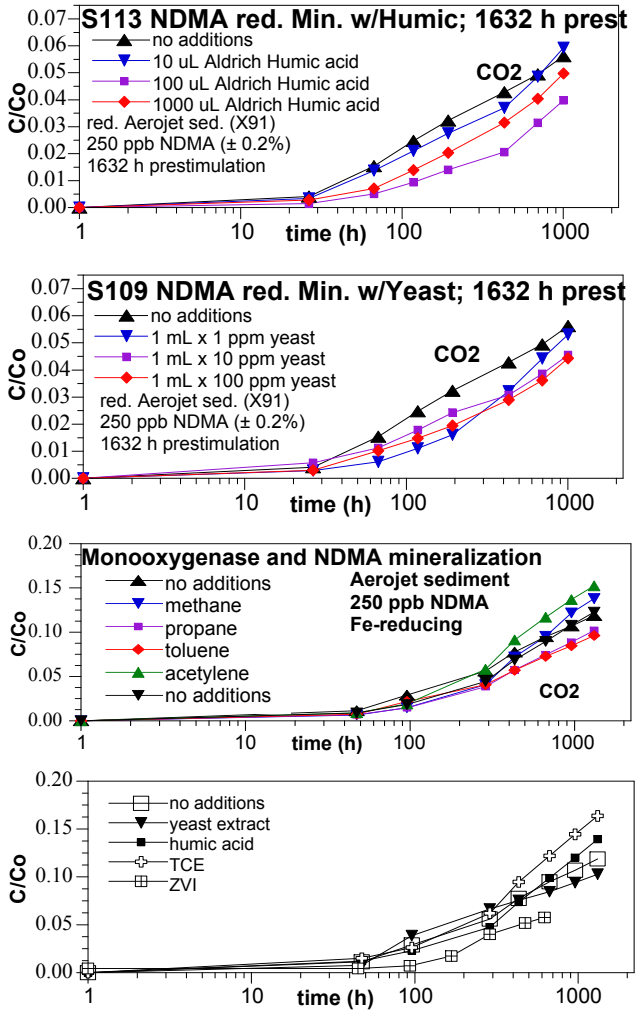

Figure 4.46. NDMA mineralization in reduced sediment with additions of: a) humic acid, b) yeast extract, c) gasses, and d) TCE or zero valent iron.

4.3.1 Abiotic and Biotic Mechanisms of NDMA Mineralization in Reduced Sediment

In reduced systems, NDMA is mineralized more slowly and to a more limited extent, which suggests a nutrient limitation. The subsurface Aerojet sediment (250- to 260-ft depth) has little organic matter, and with no additions, results in 7% to 15% NDMA mineralization (2.5 ppm to 6 ppt, Figure 4.30), with essentially no influence of monooxygenase enzyme carbon addition (i.e., propane, methane, toluene; Figure 4.46c). This appears to indicate microbial mineralization in reduced systems is small. Other carbon additions (humic acid, yeast, TCE; Figure 4.46) also showed no influence in the NDMA mineralization rate or extent. Although these data sets indirectly indicate a weak microbial component of NDMA mineralization in *reduced* systems, the addition of a bactericide to reduced sediment did not

change the NDMA mineralization (Figure 4.35c) is direct evidence that most NDMA mineralization under iron-reducing conditions in subsurface sediment appears to be abiotically controlled. The initial step of NDMA degradation to DMA also appears to be abiotic (Figure 4.6c).

The monooxygenase pathway cannot utilize nitrate as the electron acceptor, so if this were the only enzyme pathway to mineralize NDMA (biotically), nitrate additions would not increase mineralization. However, if there were other enzyme pathways that could utilize nitrate as the terminal electron acceptor (and could co-metabolically mineralize NDMA), then nitrate additions would increase NDMA mineralization. With the addition of only 30 mM nitrate (excess) to reduced Aerojet sediment, NDMA mineralization actually decreased from 12.2% (no nitrate, Figure 4.47a) to 8.2%. Clearly, any enzyme pathway to utilize nitrate was not biomineralizing NDMA. Addition of both nitrate and glucose (to stimulate microbial growth) did not increase NDMA mineralization (Figure 4.47b). Carbon mass balance showed that by 2000 hours, 75% of the aqueous intermediates (including NDMA) were gone (only 25% aqueous ^{14}C remaining). Of the 250 ppb starting concentration, 1.0 to 2.2 ppb remained at 2000 hours. Volatile carbon (by an activated carbon trap in the headspace) was 6.3% to 9.4%. Therefore, total carbon mass balance for the nitrate only system was 39.2% (8.2% + 24.7% + 6.3%). Because aqueous ^{14}C and gas trap CO_2 are highly accurate, it is likely that the balance of the ^{14}C are small, volatile compounds that are not captured on the activated carbon trap. For the nitrate and glucose system, the total carbon balance was 47.0%. Overall, this set of experiments is consistent with NDMA mineralization being predominantly an abiotic process.

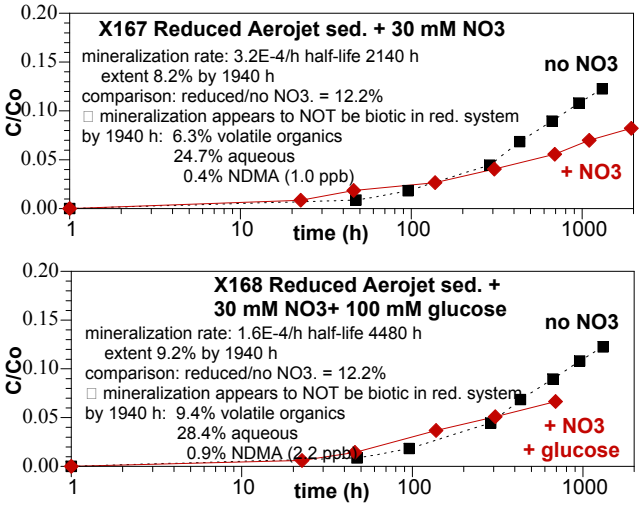

Figure 4.47. NDMA mineralization in reduced sediment with additions of nitrate and glucose.

This abiotic control of NDMA mineralization in reduced systems was investigated further in a natural reduced aquifer sediment from Puchack, New Jersey (273-ft depth) with 2.5% natural organic matter and reduced clay. NDMA mineralization of the Aerojet sediment with and without a bactericide was the same (Figures 4.35c and 4.48a), indicating mineralization was most likely abiotic. NDMA mineralization of the Puchack aquifer sediment without a bactericide (28.3%) and with a bactericide (19.5%) likely also indicates mineralization was most likely abiotic (Figure 4.48b). This sediment sample contains 30% 2:1 smectite clay, which is reduced and also contains 2.25% organic carbon and 0.04% inorganic carbon. Previous analysis of the organic matter (Vermeul et al. 2006) was conducted on a separate project. The Fourier transform infrared (FTIR) spectrum of the organic matter present in the filtrate resulting from the base/heat treatment of the sediment was used to identify the organic phases removed. Though it is difficult to identify discrete compounds from a complex mix such as natural organic matter (NOM), it is possible to identify the chemical nature of some of the components present

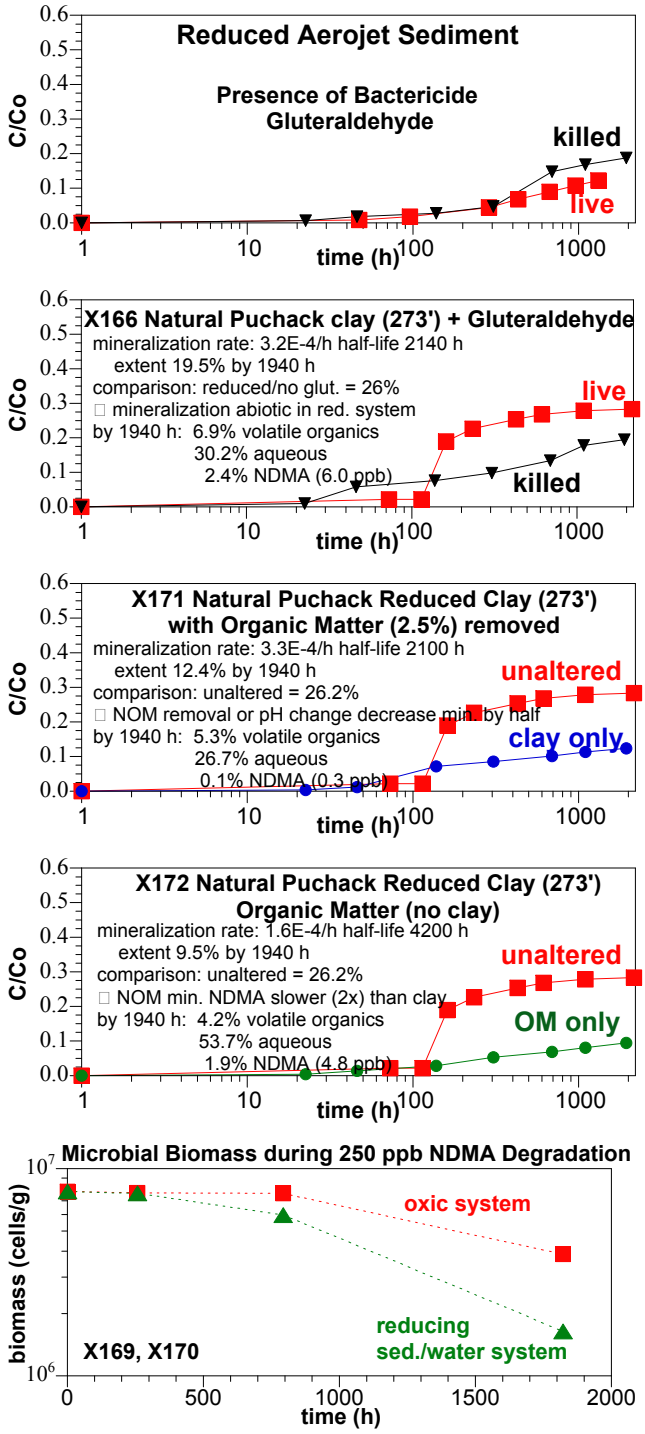

Figure 4.48. NDMA abiotic mineralization in (a) Aerojet sediment, (b-d) Puchack sediment, and (e) biomass change in oxic and reduced systems.

in the NOM. The spectrum obtained is consistent with organic compounds such as humic substances (Nardi et al. 2005) and lignites (Burns et al. 2005). The characteristic broad bands of the O-H stretching vibrations of carboxylic acid functional groups can be seen around 2810 cm^{-1} and aromatic ring stretching band (C=C) at 1567 cm^{-1}. The presence of other oxygen containing functional groups also found in NOM such as alcohols and ethers are indicated with the presence of the strong C-O stretches at 1105 and 1000 cm^{-1} with the O-H stretch from the alcohols incorporated in the broad peak centered around 2810 cm^{-1} of the carboxylic acids along with any C-H stretch bands from alkanes, alkyls, and alkenes, all of which are found either to the left or right of 3000 cm^{-1}.

Removal of most of the organic matter from the sediment with a NaOH resulted in a loss of half of the ability of the sediment to mineralize NDMA (Figure 4.48c), with 12.4% mineralization after 2000 hours compared to 28.3% for unaltered sediment. This could indicate that the organic matter was responsible for part of the NDMA mineralization, and/or the reductive capacity of the clay has been altered to some extent by the base treatment. An additional NDMA mineralization experiment with the organic matter removed from the Puchack sediment (which also contained some clay; Figure 4.48d, green) showed 9.5% mineralization after 2000 hours, which appears to indicate that both the clay and natural organic matter were responsible for mineralizing NDMA. Carbon mass balance (shown on the graphs; Figure 4.48) showed that the unaltered Puchack sediment had 30% aqueous ^{14}C remaining at 2000 hours, the clay by itself had 26.7% aqueous ^{14}C remaining, but the organic matter/some clay had 53.7% aqueous ^{14}C remaining. This roughly indicates that the clay may be responsible for most of the NDMA reactivity, although the influence of organic matter cannot be dismissed. Microbial biomass

decreased fourfold in reduced systems over 1800 hours (Figure 4.48e), as NDMA is not providing much of a carbon or nitrogen source, and no other nutrients were added to this system.

4.3.2 Carbon Mass Balance in Reduced Systems

Carbon mass balance conducted on seven reduced Aerojet aquifer sediment systems showed that the average mineralization at 3000 hours was 9.9% ± 1.6% (other reduced sediment systems showed mineralization as high as 17%). The average aqueous (i.e., NDMA plus other aqueous species) carbon mass was 40.2%. The calculated NDMA sorption to sediment (in these systems with 1 g of sediment and 6 mL of water) was 2.0% of the mass. The measured NDMA sorption to sediment and microbes in these reduced systems was 0.35% ± 2.6% (range 0.0% to 4.1%), in contrast to the 2.7% ± 4.5% (range 0% to 12%) in comparable oxic systems. Less NDMA sorption in reduced sediment systems has been noted previously, but this also suggests limited sorption to microbial biomass in reduced sediment systems. Although the biomass has not been measured, this may simply reflect much greater biomass in oxic systems. The total percent carbon (from NDMA) incorporated into microbes was 0.18% ± 2.2%, in contrast to 5.7% ± 1.3% in oxic systems. Again, this could represent more limited biomass in reduced systems. The chemical reduction of sediment reduces the biomass about tenfold from ~10^7 to 10^6 cfu/g, and while microbes are know to be involved in NDMA oxic mineralization (Figure 4.48e) and respond a small amount to propane and yeast additions in oxic systems, there is essentially no influence of any carbon additions on NDMA mineralization in reduced systems, which suggests the microbial role is small (mineralization is also slow). The likely hypothesis for the much lower NDMA carbon mass incorporation into microbes in reduced systems is just lower microbial biomass (which can be measured). The total carbon mass balance in reduced systems was 50.6% ± 27.6% in contrast to 80.0% ± 15.6% (i.e., accounted for aqueous, mineralized, sorbed to sediment and microbes, and incorporated into microbes). Clearly, reduced system NDMA degradation pathway is significantly different from the oxic system. If the carbon mass is not in aqueous solution (i.e., the aqueous measurement accounts for all aqueous species, additional chromatograph separation is needed to measure ^{14}C-NDMA, as described in Section 4.0), it could be present in the headspace as volatile compounds that are not sequestered in the CO_2 trap (i.e., 1-M NaOH). A carbon trap (i.e., activated carbon) in the headspace can be used to trap any of these volatile organic compounds, as was previously reported for RDX mineralization (Szecsody et al. 2007a).

Four ^{14}C-NDMA labeled experiments were conducted in which ^{14}C-NDMA was measured over time down to parts per trillion concentration. This technique used a large (44-cm^3 volume) preparatory-scale HPLC column (described in Section 3.0) to separate NDMA from smaller molecular weight compounds. Then, the separated NDMA was counted on a scintillation counter. At a starting NDMA concentration of 2.5 ppm, the NDMA degradation half-life was 102 hours (Figure 4.49a). At a starting NDMA concentration of 36 ppb (highest level recorded in the Aerojet aquifer), the NDMA degradation half-life was 109 hours (Figure 4.49). At starting concentrations of 100 and 10 ppt (Figures 4.49c and d), NDMA had degraded below detection limits (3 ppt) by the first sample (24 hours). This is a half-life of 4.7 hours or faster.

4.3.3 NDMA Mineralization in Sequential Reduced then Oxic Sediment Systems

Since NDMA can be rapidly degraded to DMA in reduced sediment, mineralization experiments were conducted in order to determine if sequential reduced sediment, then oxic sediment could be used to mineralize NDMA *in situ*. If a successful system can be optimized, the field-scale application would be a chemically reduced zone with downgradient oxic biostimulation zone. Three different additions were added to the initial reduced systems: a) varying amounts of carbon as yeast extract (Figure 4.50a), b) varying amounts of humic acid (Figure 4.51a), and c) varying amounts of propane. As previously discussed, these additions did not increase NDMA mineralization in the reduced sediment (as most of the mineralization appears to be abiotic), but it does acclimate the microbial population with the additions.

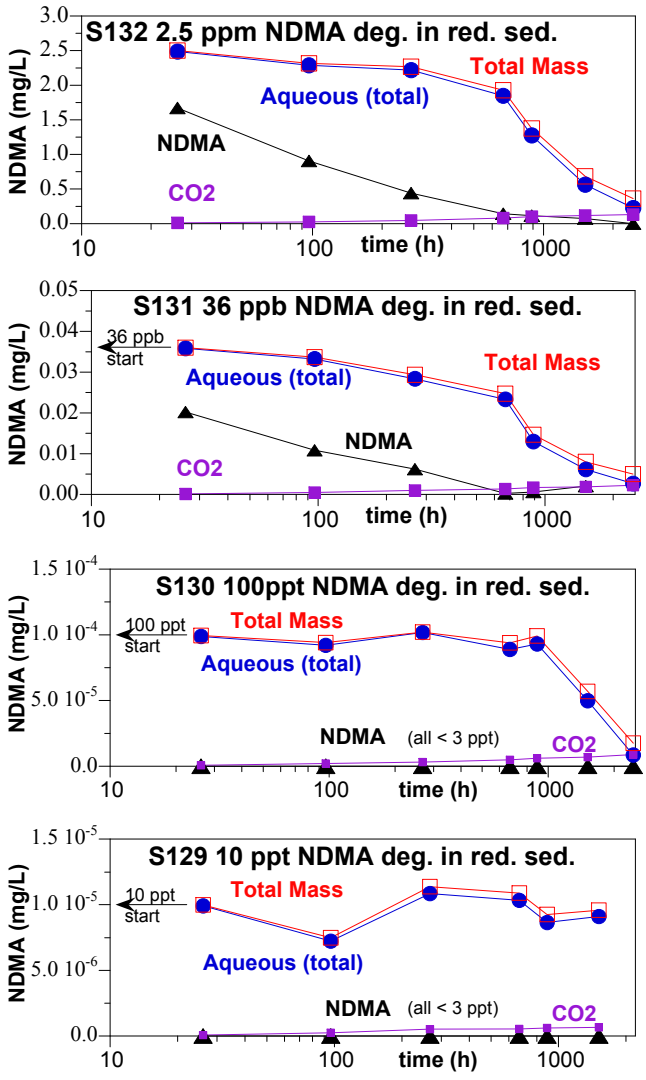

Figure 4.49. NDMA degradation and carbon mass balance in reduced Aerojet sediment with ^{14}C NDMA.

These systems were also initially pre-acclimated with NDMA for 1632 hours before the start of the experiments. In all cases, NDMA mineralization was 4% to 6% in the reduced sediment. At 1000 hours, all of the systems were oxidized and carbon additions were made (Figures 4.50b, 4.51b, 4.52b).

At the field scale, a reduced sediment zone created by chemical reduction of 30 to 40 ft in width would remove dissolved

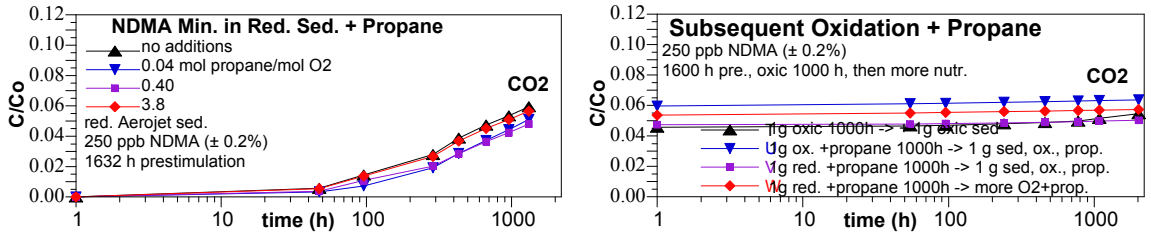

Figure 4.50. NDMA mineralization in sequential reduced, then oxic systems with propane addition.

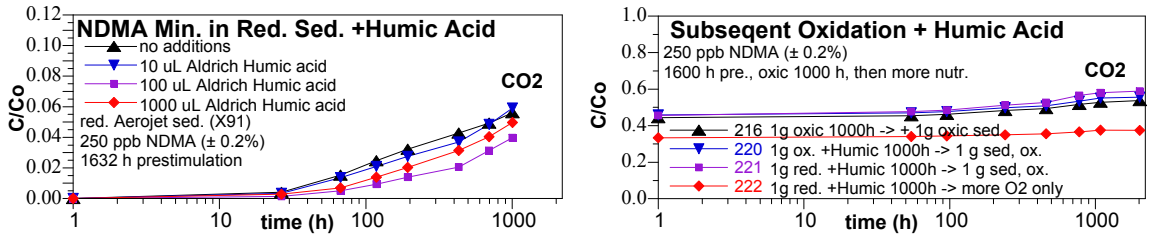

Figure 4.51. NDMA mineralization in sequential reduced, then oxic systems with humic acid addition.

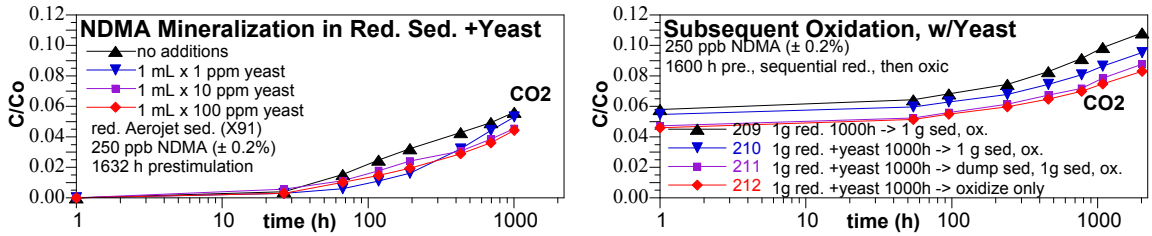

Figure 4.52. NDMA mineralization in sequential reduced, then oxic systems with yeast addition.

oxygen, so downgradient groundwater would be anaerobic. A sequential system would have to sparge air into the aquifer downgradient of the reduced zone. This type of sequential treatment has been previously implemented (Bell et al. 2003; Morkin et al. 2000). Three different types of reduction, then oxidation treatments were conducted in these systems.

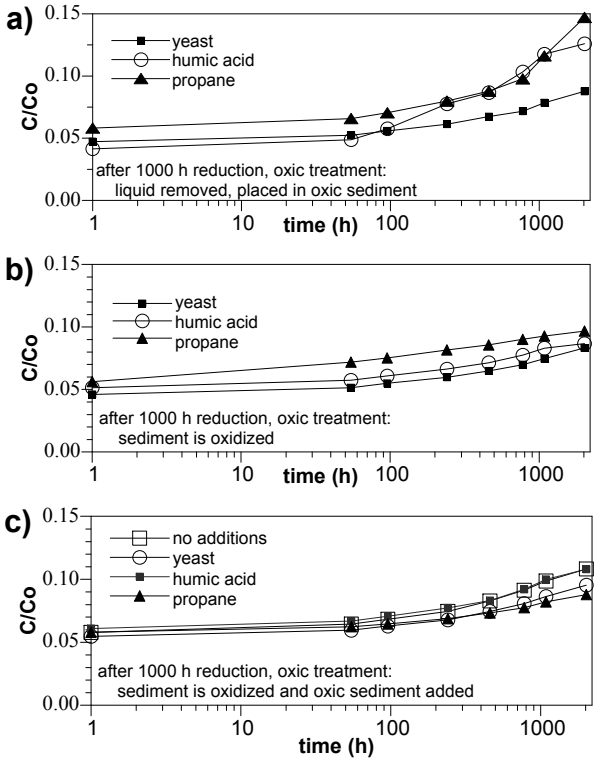

Figure 4.53. NDMA mineralization in sequentially reduced, then oxic systems (oxic system shown). The 0.25-mg/L NDMA is reduced for 1000 hours, then subjected to different oxidation treatments: a) liquid removed from reduced sediment, added to oxic sediment, b) reduced sediment was oxidized, and c) reduced sediment was oxidized and oxic sediment was added.

An approximation of sequential reduction, then downgradient oxidation in batch systems was accomplished by NDMA mineralization for 1000 hours in reduced Aerojet sediment, removal of the aqueous solution, and placing it in oxic sediment (Figure 4.53a). The initial reduction step resulted in 5% to 6% NDMA mineralization. The subsequent oxidation for 2100 hours resulted in 14.5% total mineralization (propane addition), 12.4% mineralization (humic acid addition), and 7.6% mineralization (yeast addition). Although the subsequent oxidation (with additions) did promote additional NDMA mineralization, the rate and extent was still significantly less than or equal to that for purely oxic systems (Figure 4.33).

NDMA mineralization was also measured in two other sequential reduced, then oxidation treatment systems. Mineralization in the reduced sediment (4.8% to 5.5%), then oxidation of the reduced sediment resulted in a total mineralization of 7.2% to 9.8% after 2200 hours (Figure 4.53b). Since this was less efficient than mineralization in oxic sediment (Figure 4.33), this may indicate that microbes in the reduced zone are not easily adapted to the subsequent oxic environment. At field scale, this means oxidation of a reduced zone does not contain as viable a microbial community as a zone that had remained oxic. Although microbial attachment is generally high, microbes do migrate with groundwater. To approximate oxic microbial invasion into a reduced sediment zone, the reduced sediment was oxidized and oxic sediment was also added. The resulting NDMA mineralization extent during mineralization was only 8.3% to 11.1% (Figure 4.53c), or still less than purely oxic sediment.

An additional set of sequential reduced, then oxic sediment systems were conducted at differing initial NDMA concentration from 2.5 ppm, 36 ppb, 100 ppt, and 10 ppt (Figure 4.54). NDMA degradation in the 3000 hours in reduced sediment is previously described (Figure 4.49), with NDMA concentration to <3 ppt by a few hundred hours. NDMA mineralization by 2000 hours in the reduced sediment was 9.2% (10 ppt and 100 ppt; Figure 4.54a and c), 8.9% (36-ppb initial NDMA concentration; Figure 4.54e), and 5.5% (2.5-ppb initial NDMA concentration; Figure 4.54g). The subsequent oxidation of the reduced sediment increased NDMA mineralization slightly over the next 8900 hours (371 days) to 12.8%, 9.7%, 9.0%, and 5.6%, respectively (Figure 4.54b, d, f, and h).

In conclusion, NDMA mineralization occurs biotically in oxic sediment if specific monooxygenase enzymes are present in some of the population, and in contrast NDMA mineralization in reduced sediment appears to be primarily abiotic. Although NDMA degradation is very rapid (10-hour half-life, ideal conditions) in reduced sediment, NDMA mineralization is 10 times slower in reduced systems (3480-hour half-life) relative to oxic Aerojet sediment (342-hour half-life). The mineralization extent in reduced systems is also significantly less, at 5% to 17% compared to 30% to 60% in oxic sediment. For the reduced Aerojet sediment, carbon addition normally associated with increasing monooxygenase pathways (propane, methane, and toluene) had no influence on NDMA mineralization. Other carbon additions (humic acid, yeast extract, trace nutrients) also did not increase mineralization. NDMA mineralization in these sequential reduced sediment followed by oxic sediment treatment did result in slightly more rapid mineralization and a greater mineralization extent relative to reduced systems. However, these increases were minor, so aerobic NDMA mineralization with oxygen and propane addition are the most viable NDMA mineralization strategy. However, rates and extent could not be well controlled for the three aquifer sediments (Aerojet, Ft. Lewis, Puchack) by various additions, which suggested other, unidentified nutrients were limiting.

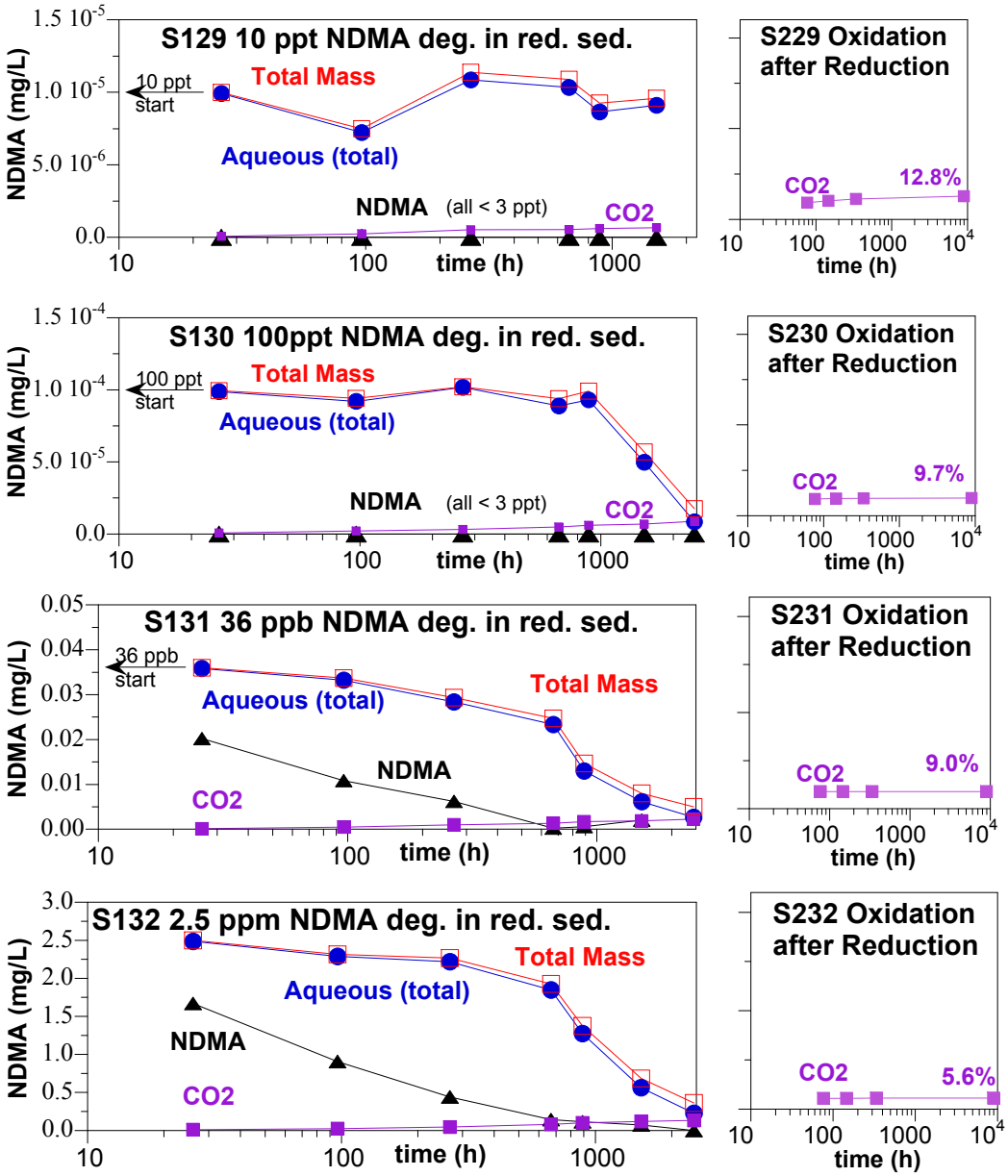

Figure 4.54. NDMA mineralization in sequential reduced then oxic systems at differing NDMA initial concentration.

4.4 Task 4 – Large-Scale NDMA Mineralization under Aquifer Conditions

NDMA degradation in reduced sediment occurs primarily by adsorbed ferrous iron on iron oxide and/or clay surfaces, and the rate is relatively well defined by numerous experiments. In contrast, NDMA mineralization does occur in oxic, reduced, and sequential reduced/oxic sediment systems, but there is a poor ability to increase the rate by various additions. Measurement of the rates that would occur at field scale require a high sediment/water ratio of the aquifer (or packed column) and advection of NDMA. Due to the need to characterize NDMA degra–dation and mineralization rates under field-like conditions, Task 4 was rescoped from a small field demonstration to large laboratory 1-D column systems with: a) reduced sediment only, b) oxic sediment only, and c) reduced sediment followed by oxic sediment (with air/propane injection before the oxic column). These systems were injected with ^{14}C-labeled NDMA for 2500 hours at varying flow rates to characterize the mass balance of NDMA degradation. Higher sediment/water ratios in these 1-D columns mean proportionally higher ferrous iron and microbial population are present per mole of aqueous NDMA, so observed rates (expressed as a half-life) are more rapid.

Advection of NDMA (and oxygen/propane for the oxic column) will be less efficient in these 1-D column systems, compared to previously described batch systems. In other words, dissolved oxygen and propane may not advect to all of the microbes in these columns, whereas in batch systems, there is parallel access to all of the microbial population on the sediment. This generally leads to lower degradation rates in 1-D column systems relative to batch systems.

The main purpose of these experiments is to quantify relevant rates of NDMA degradation and mineralization in reduced sediment, oxic sediment, and sequential reduced-oxic sediment under field relevant conditions of high sediment/water ratio and advective flow. Specific questions to address include:

- Is NDMA degradation most rapid in reduced versus oxic sediment (and sequential reduced/oxic sediment system is predominantly driven by the reduced system)?
- Which system most rapidly mineralizes NDMA: oxic, biotic system or reduced, abiotic system or sequential reduced-oxic system (abiotic/biotic)?
- Is NDMA mineralization in reduced system abiotic?
- Does the sequential reduced-oxic system demonstrate more rapid NDMA mineralization than either reduced or oxic systems?
- Is the biotic NDMA mineralization in oxic systems less efficient compared to previously reported batch systems?
- Is the abiotic NDMA mineralization in reduced systems the same as previously reported batch systems?
- Can the NDMA degradation and mineralization behavior be sustained?

These questions were addressed in a series of 15 long-term (3-month) column studies with reduced sediment only or oxic sediment only (with NDMA-laden water, propane, and air injection) or sequential reduced, then oxic sediment columns (described in detail in Section 3.0). The general configuration of experiments (Figure 4.55) shows NDMA-laden water injection into reduced or oxic sediment columns, or a more complex configuration for sequential reduced-oxic sediment columns of NDMA-laden water injection into the reduced sediment column, and propane/air (4:1 ratio) injection in between the reduced and oxic columns (gas was 20% of the water volume). Because NDMA degradation to DMA in reduced sediment was fairly rapid (10-hour half-life or more rapid, as reported earlier in batch and 1-D columns), the residence time in reduced columns was relatively small (ranging from 8 to 150 hours; Table 4.6). In contrast, the biotic NDMA degradation/mineralization was relatively slow (hundreds to thousands of hours half-life), so the residence time in oxic columns was large (ranging from 60 to 1230 hours). The residence time in each column was controlled by a combination of the volume of the column and flow rate. Results from all experiments are described in the following sections.

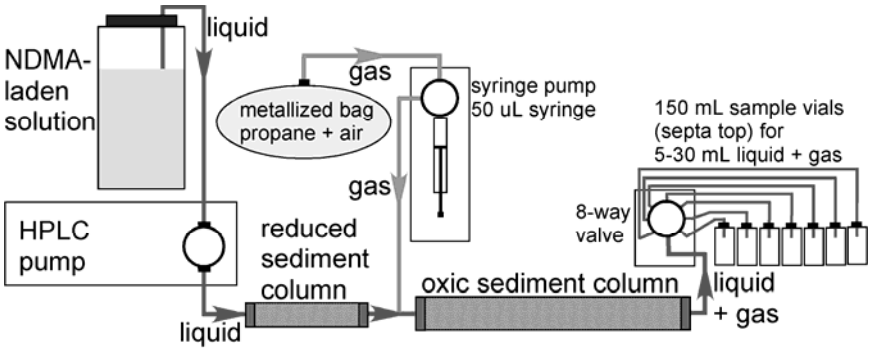

Figure 4.55. System used for sequential reduced/oxic sediment degradation and mineralization of NDMA.

Table 4.6. Results of sequential reduced, oxic sediment column mineralization of NDMA.

	column residence time (h)			pore volumes		final concentrations						
#	reduced	oxic	both	start	end	NDMA (C/Co)	aqueous (C/Co)	CO_2 (C/Co)	volatile C (C/Co)	NDMA deg. half-life (h)*	NDMA min. half-life (h)*	NDMA min. half-life (h)**
sequential reduced/oxic columns												
X160	8.91	60.1	69.0	0	6.4	0.482	0.525	0.044	--	10.3	224.7	2124
X161	9.00	266.2	275.1	0	1.7	0.155	0.182	0.121	--	5.41	153.5	4694
X162	8.08	104.2	112.3	0	3.8	0.121	0.488	0.048	--	7.04	274.0	3805
X180	32.0	216.1	248.1	6.4	9.1	0.456	0.464	0.104	0.001	33.2	231.2	1790
X181	10.7	317.3	328.0	1.7	3.5	0.258	0.359	0.135	0.001	7.16	66.4	2030
X182	28.3	364.5	392.8	3.8	5.6	0.372	0.455	0.101	0.003	22.5	187.1	2598
X190	148.3	1000.3	1148.6	9.1	9.9	0.096	0.439	0.161	0.003	46.3	410.0	3177
X191	29.94	885.8	915.8	3.5	4.6	0.010	0.340	0.225	0.012	4.50	130.5	3992
X192	95.25	1227.7	1323.0	5.6	6.3	0.028	0.343	0.257	0.004	18.9	317.8	4411
	mean ± standard deviation:									**17.2±14.5**	**222±104**	**3180±1094**
reduced column only												
X164	8.16	--	8.16	0	50	0.717	0.765	0.022	--	28.6	368.6	
X184	27.64	--	27.64	50	80	0.550	0.537	0.062	0.003	36.8	287.7	
X194	118.08	--	118.08	80	87	0.070	0.507	0.168	0.004	31.0	573.5	
	mean ± standard deviation:									**32.1±4.2**	**410±147**	
oxic column only												
X163	--	62.16	62.16	0	7.1	0.616	0.684	0.047	--	150.4		838.9
X183	--	216.77	216.77	7.1	10.2	0.605	0.636	0.062	0.007	299.1		1642
X193	--	1625.7	1625.7	10.2	10.9	0.082	0.391	0.252	0.013	478.3		4398
	mean ± standard deviation:									**309±164**		**2293±1866**

* using the residence time in the reduced column only

□□ using the total residence time (reduced and oxic columns)

4.4.1 NDMA Mass Balance in Reduced 1-D Column Systems

The NDMA degradation rate has been quantified in ~50 1-D columns previously reported, although these experiments additionally quantify the mineralization rate. Three 1-D columns (Figure 4.56) showed an average NDMA degradation half-life of 32.1 hours (± 4.3 hours; Table 4.6), based on the residence time in the column (8.2 to 118 hours) and steady-state effluent NDMA concentration (7.0% to 72% of the influent 250-ppb NDMA). This was slower than expected (predicting 2.0- to 10.0-hour half-life), although there may have been some loss in the reductive capacity of this sediment. NDMA degradation in the reduced sediment is primarily abiotic, as described in previous experiments (Figure 4.36). NDMA mineralization was surprisingly fast, with an average half-life of 410 ± 147 hours (Table 4.6). Mineralization in batch experiments averaged 3475 ± 504 hours half-life with a sediment/water ratio of 1 g/6 mL. These column studies had an averaged sediment/water ratio of 4.68 g/mL (based on the averaged dry bulk density of 1.78 g/cm^3/ porosity of 0.38), or 28 times greater sediment (and reduced iron) to NDMA in the aqueous phase. Based on batch experimental results, the NDMA mineralization rate is predicted at a 124-hour half-life. The observed NDMA mineralization half-life of 410 hours (3.3 times slower than predicted) for this presumed abiotic process is likely caused by the lack of mixing in 1-D columns (between the NDMA in solution and surface phases) relative to much greater mixing in batch systems. The NDMA mineralization half-life of 410 hours (range 288 to 573 hours, Table 4.6) is somewhat slow for field application. Generally a reaction half-life of <100 hours is needed in order to have sufficient residence time in a 20- to 30-ft diameter reduced zone to degrade the contaminant of interest. Although DMA and other intermediates were not measured, the total aqueous intermediates (from measuring total aqueous ^{14}C) ranged from 51% to 77% compared to 7.0% to 72% NDMA. Volatile carbon compounds averaged 0.35% and total carbon mass balance averaged 68.9% ± 9.3%, and 30% lost must be volatile low molecular weight compounds that are not adsorbed onto activated carbon.

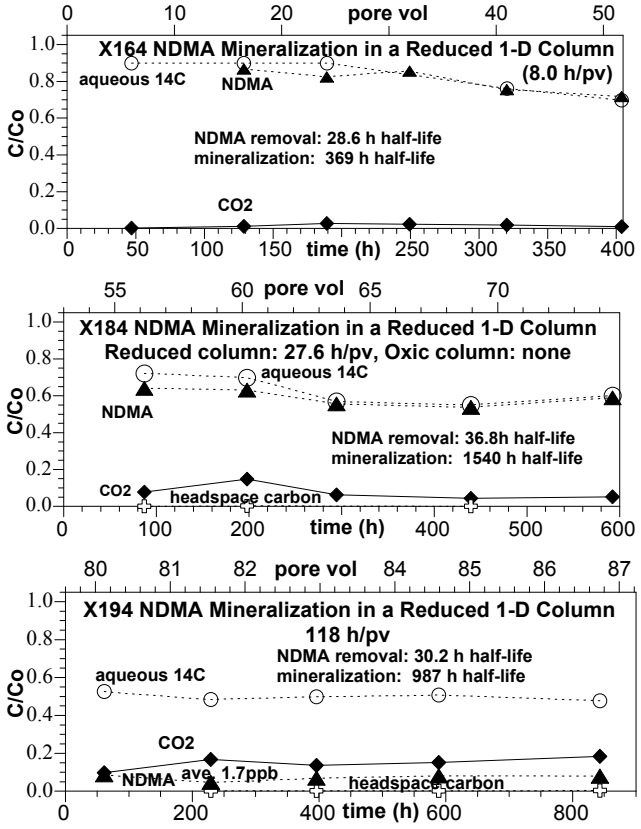

Figure 4.56. NDMA degradation and mineralization in large 1-D reduced sediment columns.

4.4.2 NDMA Mass Balance in Oxic 1-D Column Systems

The NDMA degradation rate in oxic sediment in previous batch studies was extremely slow, but NDMA was biotically mineralized with an average half-life of 342 ± 36 hours (sediment/water ratio of 1 g/6 mL). With the 28 times greater sediment/water ratio in columns, these data show a predicted biotic, oxic system mineralization half-life in the large columns of 12.2 hours. It should be noted that bioremediation in column systems are typically significantly slower than predicted from batch results (orders of magnitude) due to the lack of mixing of prime electron donor/acceptor as well as trace nutrients. For example, biodegradation may occur rapidly near the inlet using up all of a specific nutrient, which leads to no microbial activity in the remainder of the column. The apparent biodegradation rate is based on the total residence time in the column system, so the rates look artificially low.

In these large 1-D columns, three experiments (shown in Figure 4.57, results in Table 4.6) with residence times ranging from 62 to 1625 hours, the NDMA effluent ranged from 62% to 8.2% of influent concentration, total aqueous ^{14}C ranged from 68% to 39%, and mineralization ranged from 4.7% to 25.2%. In addition, the volatile carbon ranged from 0.7% to 1.3%. Due to the very large residence times, the observed NDMA degradation half-life of 309 ± 164 hours and mineralization half-life of 2293 ± 1866 hours (Figure 4.57, Table 4.6). This oxic, biotic mineralization rate in the 1-D columns (2293-hour half-life average) was 188 times slower than predicted from batch biodegradation studies. There was a trend of slower residence time produced a slower NDMA mineralization rate (62-hour residence time had a 839-hour mineralization rate, 1625-hour residence time had a 4400-hour residence time), which may indicate a nutrient limitation at the slow flow rates (such as dissolved oxygen). Only these three oxic columns were conducted, although it is possible that a much greater gas to liquid injection into the oxic column (Figure 4.55) would be more efficient.

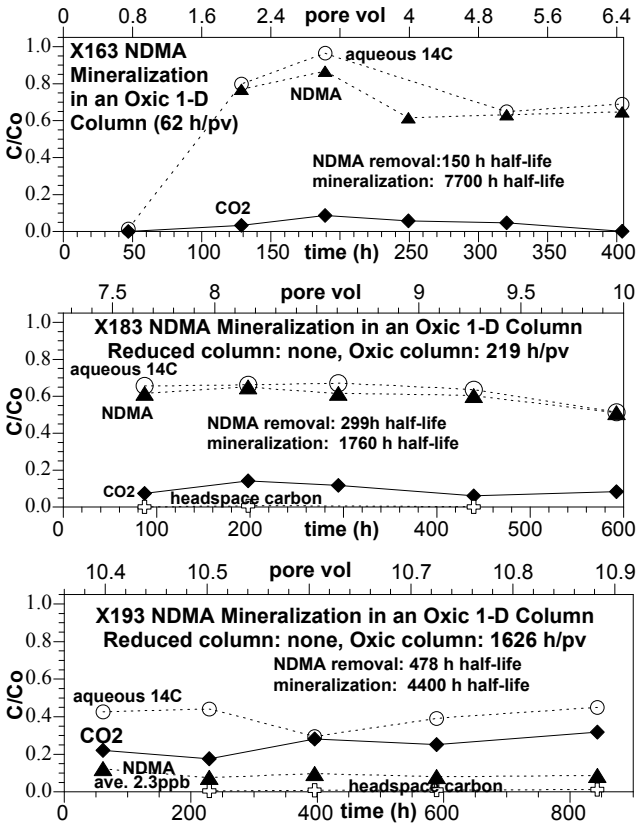

Figure 4.57. NDMA degradation and mineralization in large 1-D oxic sediment columns.

4.4.3 NDMA Mass Balance in Reduced then Oxic 1-D Column Systems

NDMA degradation and mineralization in sequential reduced/oxic column systems was characterized in nine experiments with a range of residence times and a range of differences in

residence time between the reduced and oxic sediment columns (Figure 4.58). The NDMA effluent concentration was 12% to 48% for short-residence time systems, and 2.8% to 10% for longer residence times, which corresponded to a relatively constant NDMA degradation rate. The NDMA degradation (average half-life 17.2 ± 14.5 hours, Table 4.6) was a slight function of residence time, with longer residence times exhibiting slower apparent rates (black squares, Figure 4.59), but no trend indicated for the three reduced sediment columns (green triangles).

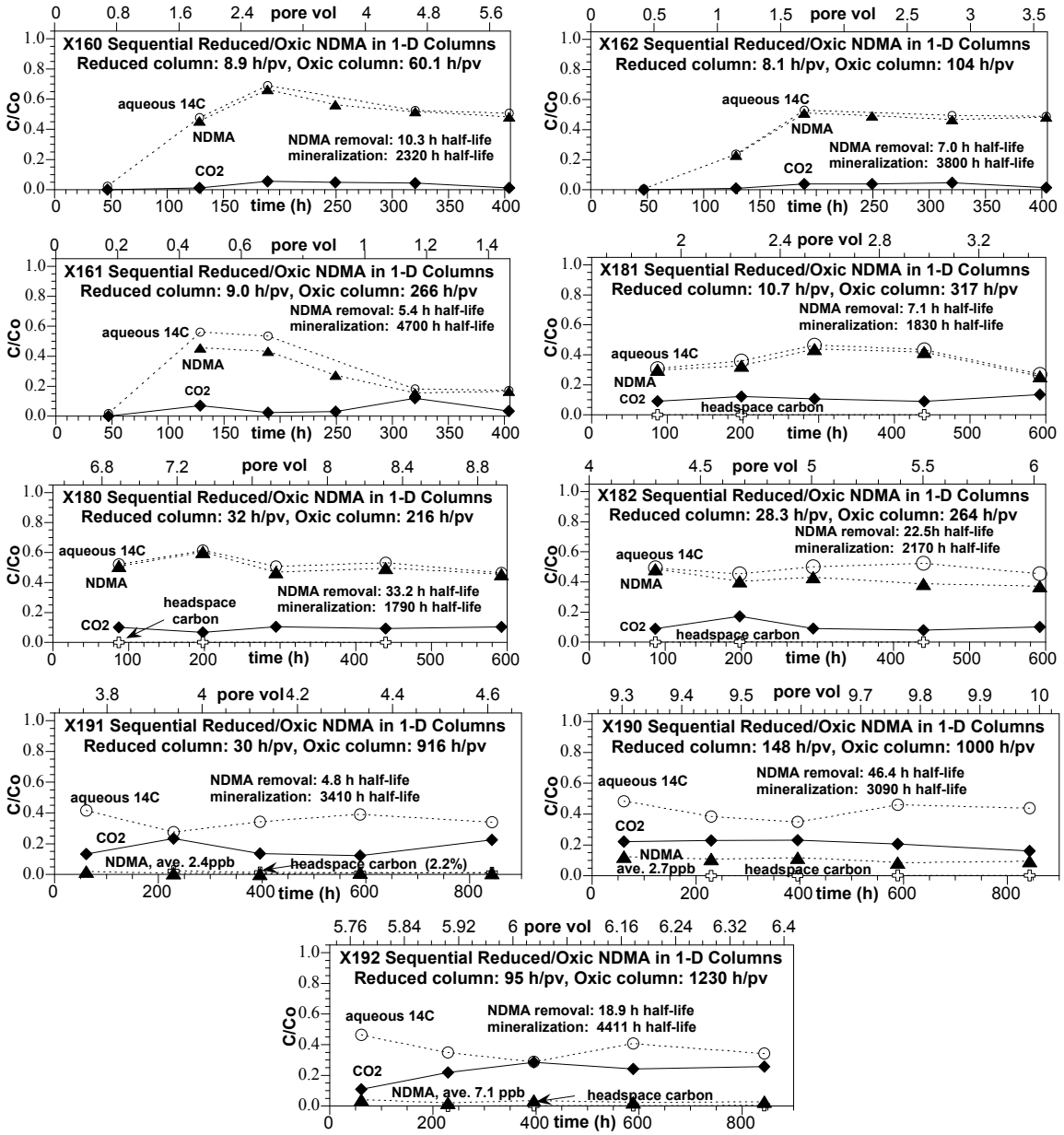

Figure 4.58. NDMA degradation and mineralization in large sequential reduced/oxic sediment columns.

Many of the interpretation questions are focused on the relative reactivity of the sequential system versus the reduced or oxic column systems. Data interpretation is somewhat ambiguous for the sequential column system, as there are two different residence times (reduced column and oxic column). As previous experiments have clearly demonstrated, NDMA degradation occurs 3 to 4 orders of magnitude more rapidly in reduced sediment and is abiotic. Therefore, NDMA degradation rates are calculated in the sequential systems using the residence time for the reduced column only. Comparison of the NDMA degradation half-life obtained in these sequential columns (17.2 ± 14.5 hours) to reduced columns (32.1 ± 4.2 hours) and oxic columns (309 ± 164 hours) shows similar results for the sequential and reduced only columns, so NDMA degradation in the sequential systems is likely dominated by reactivity in the reduced sediment portion of the system. It should be noted that the average NDMA degradation half-life in the sequential system indicated twice the reaction rate compared to the average in the reduced columns alone. This may be indicative of some additional degradation of NDMA in the oxic column portion of the sequential systems. Clearly, oxic sediment by itself (with supplied propane/air) was only degrading NDMA slowly, with an average 309-hour half-life. Therefore, these data are consistent with previous batch and 1-D column studies that indicate NDMA degradation is 10 to 20 times more rapid in reduced sediment (abiotic mechanism) than in oxic, biostimulated sediment. The NDMA degradation rate in the coupled reduced-oxic columns was calculated based on the average NDMA degradation rate in the reduced sediment columns alone (32.1-hour half-life, rate 0.0216/hour) and oxic sediment columns alone (309-hour half-life, rate 0.00224/hour). The average calculated sequential system half-life was 13.5 ± 4.8 hours, which was surprisingly close to the observed rate of 17.2 ± 14.5 hours half-life calculated assuming most of the degradation was in the reduced sediment column. For the calculated rate, the contribution of the reduced sediment accounted for 60.5% of NDMA degradation (oxic columns had 12 times the residence time of the reduced sediment columns).

As described in the previous two sections, NDMA mineralization in the reduced sediment columns showed an average half-life of 410 hours, and the oxic sediment columns had an average half-life of 2293 hours. There was considerably more variability in the oxic sediment columns, which may also be indicative of a biotic process. Interpretation of NDMA mineralization in the sequential reduced/oxic columns is problematic, as both the reduced and oxic sediment columns can contribute to NDMA mineralization.

Assuming NDMA mineralization is nearly all occurring in the reduced sediment, NDMA degradation half-life calculated in the sequential systems using the residence time of NDMA in the reduced column only result in an average of 222 ± 104 hours, or twice as fast as the half-life for the separate reduced sediment columns alone (410 ± 147 hours, Table 4.6). If true, this implies most of the NDMA mineralization occurring in the reduced sediment, with some slight additional mineralization in the downgradient oxic column (to account for the increased mineralization rate for the sequential columns compared to just the reduced sediment columns). Similar to the NDMA degradation half-life (Figure 4.59), there is a trend observed with residence time for the oxic biomineralization of NDMA (Figure 4.60a, red circles), but nearly no trend with the abiotic reduced sediment mineralization or sequential systems.

Alternatively, assuming NDMA mineralization is occurring in both the reduced and oxic columns, the half-life calculated assuming this total residence time is considerably greater (compared to just the reduced sediment column residence time), so the average half-life is 3180 ± 1094 hours.

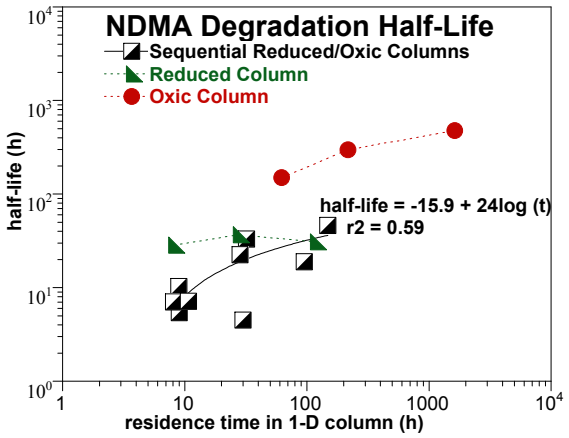

Figure 4.59. Comparison of NDMA degradation half-life in reduced, oxic, and sequential systems.

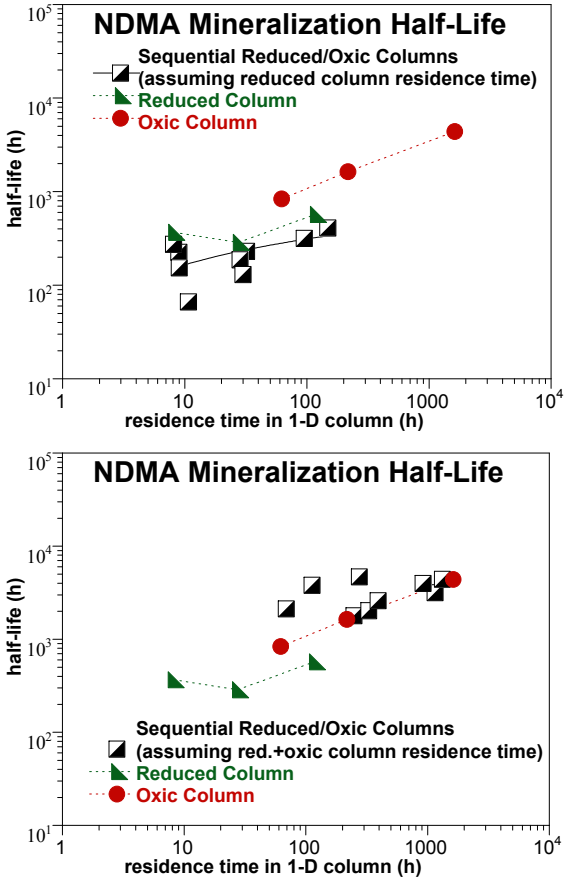

Figure 4.60. Comparison of NDMA mineralization half-life in reduced, oxic, and sequential systems calculated assuming residence time of: a) reduced column only and b) reduced and oxic columns.

This is slower than either the oxic sediment alone (half-life 2293 ±1866 hours) or reduced sediment alone (half-life 410 ± 147 hours). In addition, NDMA mineralization half-life for the sequential systems is not statistically separate from the oxic column systems (residence time trend shown in Figure 4.60b). Therefore, an alternate hypothesis is that NDMA mineralization in these sequential reduced/oxic systems are slower than the oxic system alone due to degradation of NDMA to DMA and other intermediates in the reduced sediment is harder to biodegrade than NDMA itself. Calculation of the NDMA mineralization in the sequential reduced-oxic systems based on the average rates for the separate reduced sediment (half-life 410 hours, rate 0.0017/hour), and oxic sediment (half-life 2293 hours, rate 0.000302/hour) had an average half-life of 1719 ± 240 hours. This calculated NDMA mineralization rate in the sequential reduced-oxic systems was much more rapid than the observed half-life of 3180 ± 1094 hours, which may indicate the oxic sediment portion of the system was not working efficiently (i.e., insufficient nutrient delivery, for example).

Another method to address trends in data was considered to address the role of the reduced and oxic columns for NDMA mineralization in the sequential systems. Reduced sediment columns with all the same residence time, but increasing residence times of the oxic sediment column (downgradient) would show increasing degradation as a result of and reactivity in the oxic sediment, or would show no change in degradation/ mineralization if there is very little reactivity in the oxic sediment. There were five sequential column systems with nearly the same residence time in the reduced sediment (8 to 10 hours), but the residence time in the downgradient oxic column varied from 60 to 317 hours. A second set of three sequential experiments had a reduced sediment residence time of 28 hours, but the residence time in the downgradient oxic column varied from 264 to 885 hours. In all cases, the NDMA degradation rate and NDMA mineralization rate was more rapid with

increasing residence time in the downgradient oxic column (Figure 4.61). This clearly indicates the oxic sediment did influence the reactivity in the system for both NDMA degradation as well as NDMA mineralization (i.e., the observed reactivity was not purely a function of purely abiotic reactivity in the reduced sediment).

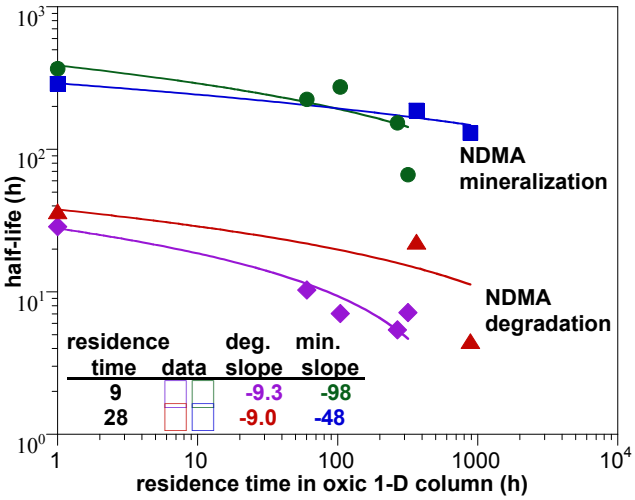

Figure 4.61. Sequential system: change in NDMA degradation and mineralization with increasing reaction time in downgradient oxic column.

The slope of the relationship between residence time in the oxic sediment column compared to the resulting NDMA degradation or mineralization half-life [half-life = (slope) log (t)] provides a rough indication of the significance of (in this case) biodegradation processes. For NDMA biodegradation at 9- and 28-hour residence times, the slope was -9.0 to -9.3 (Figure 4.61), whereas for NDMA mineralization the slope was -48 to -98. This was consistent with the hypothesis that NDMA degradation is primarily an abiotic process, but NDMA mineralization can be an abiotic or biotic process (biotic processes are much more significant).

To quantify the importance of the reactions that take place in the upgradient reduced sediment column, trends were plotted using the sequential systems with the same residence time in the oxic column, but varying residence time in the reduced sediment column. The presence of up gradient reduced sediment column (compared to oxic sediment column alone) increased the NDMA degradation rate 2 orders of magnitude (Figure 4.62), clearly indicating the significance of reactivity in the reduced sediment. In contrast, presence of the reduced sediment had little influence on NDMA mineralization, where two data sets showed an increase in mineralization and one data set showed a decrease in mineralization in the presence of the reduced sediment.

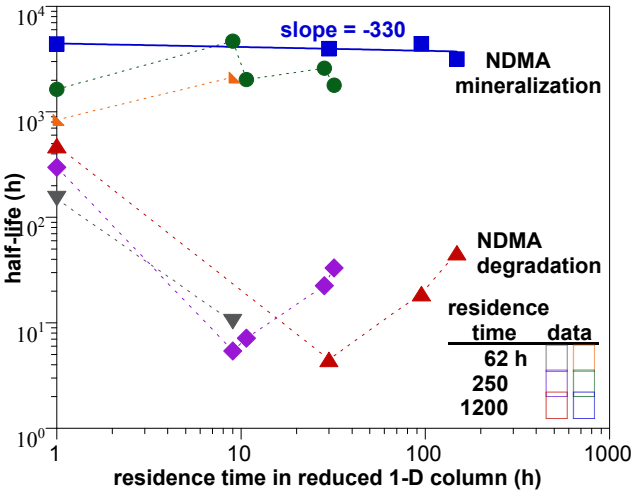

Figure 4.62. Sequential system: change in NDMA degradation and mineralization with increasing reaction time in upgradient reduced sediment column.

Finally, to address the question of longevity of the reactivity observed in the reduced, oxic, and sequential column systems, NDMA degradation and mineralization half-lives are plotted against the number of pore volumes of water injected into the systems (Figure 4.63). The reduced sediment system with a reductive capacity of 100 µmol Fe(II)/g has a high longevity of 277 pore

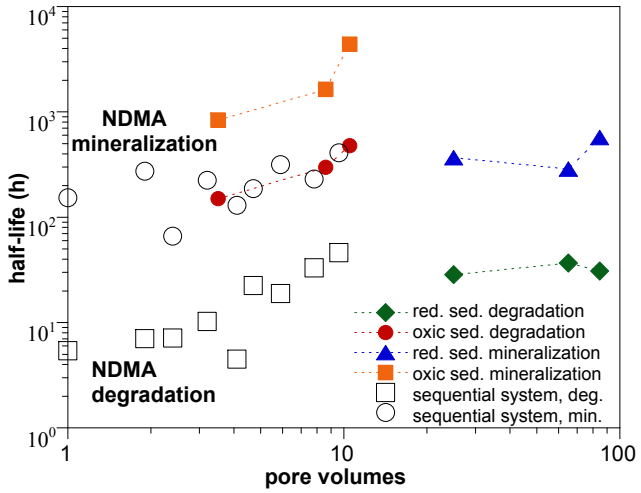

Figure 4.63. Longevity of reactivity in column systems.

volumes of oxygen-saturate water (Figure 4.38). It is expected that the ability of the adsorbed ferrous iron to degrade NDMA will decrease more rapidly than this reductive capacity. Large 1-D column studies show that between 20 and 84 pore volumes, there was no decrease in the reported NDMA degradation half-life (Figure 4.63, green diamonds). In addition, the NDMA mineralization half-life in the reduced sediment columns (presumed to be abiotic) showed a slight increase in half-life (Figure 4.63, blue triangles). In contrast, longevity of the biotic processes was limited, which is not surprising considering few nutrients are added to the systems. In the oxic (only) sediment columns, the NDMA degradation half-life (red circles, Figure 4.63) and NDMA mineralization half-life (orange squares, Figure 4.63) showed a significant decrease in rate with increasing pore volumes (from 1 to 10 pore volumes). Based on the trends observed in these single-process columns, trends observed in the sequential reduced-oxic columns are likely caused by the decreased biotic reactivity with increasing pore volumes in the oxic sediment columns.

In summary, this series of large-scale 1-D reduced sediment, oxic sediment, and sequential reduced-oxic sediment column systems at the high sediment/water ratio of field aquifers and advective flow over thousands of hours provided significant insight into the relative reactivity of reduced and oxic systems for degrading and mineralizing NDMA. More specifically, the following conclusions were reached:

- NDMA degradation is ~10 times or more rapid in reduced sediment columns (averaging 32.1 ± 4.2-hour half-life) relative to oxic sediment columns with propane/air injection (averaging 309 ± 164-hour half-life). These results are consistent with all previous reduced sediment results, but do show increased biotic reactivity in the oxic sediment columns, likely due to the injection of propane and air.
- NDMA mineralization is most rapid in the reduced sediment (half-life 410 ± 147 hours), followed by the oxic sediment with propane/air addition (half-life 2293 ±1866 hours), then the coupled reduced-oxic columns (half-life 3180 ± 1094 hours). Batch studies for two sediments with and without a bactericide clearly showed NDMA mineralization in reduced sediment was predominantly abiotic. The comparison of oxic to reduced system mineralization was in contrast to previous batch studies, which showed ~10 times more rapid NDMA mineralization in oxic sediment was 188 times slower in these column systems than predicted from batch studies. These results are not surprising, as column systems exhibit significantly less mixing than in batch systems, so much of the microbial population may be nutrient limited. NDMA mineralization in the reduced sediment was 4 times slower in these column systems than predicted from batch studies, which is reasonable due to the slight additional mixing limitations for an abiotic reaction in the column system.

- NDMA degradation in the sequential reduced-oxic sediment systems was slightly (2 times) more rapid (17.2 ± 14.5-hour half-life) than reduced sediment alone (32.1 ± 4.2 hours), as caused by the (inefficient and slow) downgradient biodegradation in the oxic sediment column. NDMA mineralization rates in the sequential reduced-oxic sediment systems (3180 ± 1094 hours) were slightly (40%) slower than in the oxic columns (2293 ± 1866 hours). Both these data sets indicate sequential degradation was inefficient, caused either by NDMA degradation intermediates from the upgradient reduced column not being biodegraded as easily as NDMA itself and/or removal of dissolved oxygen from the water that is injected into the down gradient oxic column (with air/propane) was not efficiently maintaining an oxic environment.
- The abiotic NDMA degradation and mineralization in the reduced sediment column maintained the same reaction rate for 84 pore volumes (expected reductive capacity of this sediment was ~275 pore volumes). These results are not surprising considering the predominant electron donor was adsorbed ferrous iron on iron oxide and clay surfaces.

These results demonstrate the importance of scaling up batch results to field relevant systems. Abiotic reactivity scales relatively well as the sediment/water ratio increases, as the ability to degrade and mineralize NDMA increases as the ferrous iron/NDMA ratio (sediment/water ratio) increases. Scaling up oxic biodegradation of NDMA in from small batch systems to large 1-D columns was significantly less efficient and most likely reflects the lack of ability to deliver major and/or trace nutrients to microbes throughout the column. Reactivity in the coupled reduced-oxic sediment columns was mixed. Degradation of NDMA calculated from rates in separate reduced and oxic sediment columns (13.5-hour half-life) was close to the observed half-life (17.2 hours). Since most of the NDMA degradation occurred in the reduced sediment, this up gradient column performed nearly the same as in separate experiments. However, the NDMA mineralization rate was actually slower in the coupled system (half-life 3180 hours) compared to either the reduced sediment (410-hour half-life) or oxic sediment (2293-hour half-life). The NDMA mineralization half-life calculated in the coupled system based on rates in reduced and oxic columns (1718-hour half-life) was considerably slower than the observed half-life in the coupled systems, indicating a significant decrease in mineralization efficiency, most likely for the biotic (oxic) column.

Results in this study demonstrate that dithionite-reduced aquifer sediment degrades NDMA rapidly (half-life 32.1 hours in a column system) and also mineralizes NDMA slowly (half-life 410 hours in a column system). This reactivity was maintained for 84 pore volumes, when experiments ended. It is expected that the reactivity would last longer, but at some point, the ability of the reduced sediment to degrade/mineralize NDMA would decrease. Dithionite-reduced sediment results in the dissolution of ferric oxides and the creation of predominantly adsorbed ferrous iron on oxide/clay surfaces. For the Aerojet sediment (natural pH 9.1), the resulting pH of the dithionite/carbonate treatment was 10.5). There may be other, more efficient methods to create an iron-reducing environment in the subsurface that have this or greater reactivity, which should be investigated in future studies. Mixtures of zero valent iron with sediment did not show significant reactivity with NDMA (Section 4.1.10) nor did it enhance NDMA mineralization (Figure 4.46d), although the development of a reduced zone in sediment/ zero valent iron mixtures can take hundreds of hours. Biostimulation is commonly used at field

scale to create an iron- or sulfate-reducing environment, which may be and efficient method to create a zone to abiotically mineralize NDMA. Additions of ferrous nitrate or some other means to inject ferrous iron may also be used to create a subsurface zone containing sufficient reductive capacity and appropriate electron transfer surfaces to mineralize NDMA. Although NDMA mineralization in batch systems was of a moderate rate in batch systems (342-hour half-life), biomineralization of NDMA in column systems tested was inefficient (half-life 2293 hours) likely due to nutrient limitations. Numerous experiments evaluating additions to stimulate *in situ* microbial activity were largely ineffective. However, *ex situ* bioreactors utilizing appropriate monooxygenase isolates is very successful. Therefore, field-scale remediation of NDMA may focus on a comparison of *in situ* abiotic NDMA mineralization to *ex situ* biotic NDMA mineralization.

5.0 Summary

The purpose of this laboratory-scale project was to investigate the *in situ* abiotic/biotic degradation of NDMA as a viable remediation alternative to pump-and-treat methods currently in use (i.e., *ex situ* treatments; UV degradation, oxic bioremediation, Mitch et al. 2003). The research was focused specifically for the Aerojet, California site, which has NDMA groundwater abiotic contamination (to 36 ppb), so most experiments used Aerojet aquifer sediment (260-ft depth), although other aquifer sediments used included Ft. Lewis Logistics Center (60-ft depth, Tacoma, WA) and Puchack Superfund site (273-ft depth, Camden, NJ). An overall economic reason for choosing *in situ* treatment over *ex situ* treatment is the cost of pumping water from the subsurface and need to treat the contaminant of interest as well as other constituents in water before reinjecting. However, it should also be said that *in situ* treatments are much more difficult to control due to limited access for biogeochemical manipulations and physical mixing.

In this laboratory-scale project, *in situ* degradation of NDMA is investigated in abiotic, biotic (i.e., microbial isolates from sediment), and in coupled (parallel and sequential) abiotic/biotic sediment systems (oxic, anoxic, Fe-reducing, SO_4-reducing conditions) to develop a viable remediation technology process (or combination of processes). Initially, it was hypothesized that NDMA degradation to DMA (dimethylamine, relatively nontoxic) would be sufficient for remediation (this can be accomplished rapidly by abiotic processes). However, because DMA degrades to further, more toxic intermediates, it was decided that NDMA mineralization was the goal. Before initiation of this project, *in situ* NDMA mineralization was thought to occur only by microbial processes (abiotic NDMA mineralization was demonstrated in this project). It was then hypothesized that sequential abiotic NDMA degradation to intermediates followed by oxic mineralization (of intermediates) may be more rapid than oxic biomineralization, as the initial abiotic NDMA mineralization (in Fe-reducing conditions) was very rapid. Ultimately, the comparison of single *in situ* processes in sediment/water systems (i.e., oxic biomineralization, Fe-reducing conditions with abiotic mineralization) to sequential process systems (sequential Fe-reducing, then oxic conditions) were used to evaluate the NDMA mineralization efficiency of the different systems.

5.1 NDMA Degradation Processes and Pathways

5.1.1 Aqueous Stability

In aqueous solutions (no sediment), NDMA (2.5 mg/L) was stable for 700 hours at a pH of 3.5 to 14 (Figure 4.1a). Some NDMA degradation was observed at pH 2.5. Aqueous solutions of NDMA at different redox conditions induced by H_2 bubbling in water (Eh = -597, -310, -230, and +100 mV) was also stable for hundreds of hours (McKinley et al. 2007; Figure 4.2). NDMA did, however, slowly degrade in 0.1 mol/L sodium dithionite solution (chemical reductant, Eh = -560 mV) with a half-life of 230 hours. Ferrous iron in aqueous solution (no sediment) also did not degrade NDMA. Although there was no photodegradation of NDMA in fluorescent light, experiments were conducted in amber glass vials or PEEK columns. NDMA does photodegrade in UV light (Figure 4.3).

5.1.2 Degradation Mechanism with Reduced Sediment and Minerals

NDMA (2.5 mg/L) is stable and exhibits negligible degradation by 1200 hours in oxic, sterile Aerojet sediment at pH 7.0 to 11 (Figure 4.1b; Figure 5.1a, crosses). In dithionite-reduced Aerojet sediment (reductive capacity 80 µmol/g, Eh = -200 mV, pH = 10.2) NDMA degraded rapidly (11-hour half-life, Figure 5.1a, open squares). This degradation reaction was abiotic (Szecsody et al. 2006), as the addition of a bactericide (gluteraldehyde) did not change the NDMA degradation rate (Figure 5.1b). The initial degradation product is DMA, which was degraded to other products after hundreds of hours (described in the following section; Szecsody et al. 2008a). The reduced sediment contains multiple ferrous iron phases, including adsorbed ferrous iron, ferrous oxides, carbonates, and sulfides. Dithionite reduction also results in the reduction of some structural Fe(III) in 2:1 smectite clays (Stucki et al. 1984).

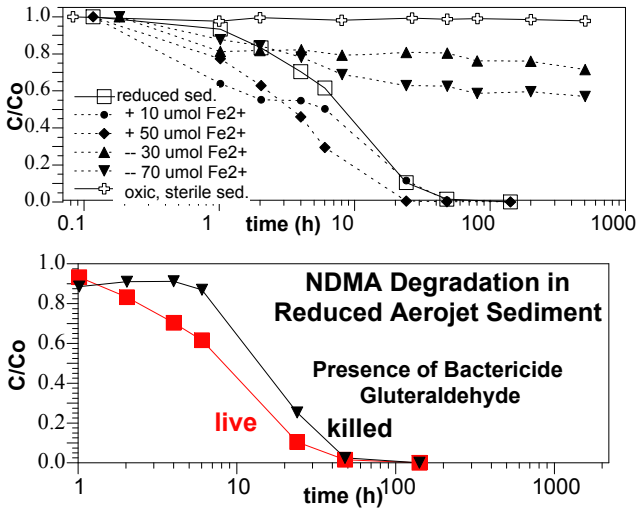

Figure 5.1. NDMA degradation in oxic and reduced sediment with adsorbed ferrous iron manipulation.

Evidence for the strong role of adsorbed ferrous iron for NDMA degradation was shown by removal of adsorbed ferrous iron from the sediment (by ion exchange with Ca^{2+}), which slowed the NDMA degradation rate considerably. With 30 and 70 µmol of adsorbed ferrous iron removal from the batch system, the NDMA degradation half-life increased to 122 and 310 hours, respectively (triangles, Figure 5.1a). Additions of ferrous iron increased the NDMA degradation rate (diamonds and circles, Figure 5.1a), but not to the extent that ferrous iron removal influenced the rate.

Although adsorbed ferrous iron appears to be the primary reductant for NDMA, the influence of crystalline ferrous phases was also investigated. Alkaline hydrolysis with the oxic or anaerobic sediment (as a catalyst) did not degrade NDMA (i.e., a reactive phase in the reduced sediment appears to be involved in electron transfer, Figure 4.4). Iron sulfides, while present in the reduced sediment, did not promote significant NDMA degradation, as additions did not change the NDMA degradation rate (Figure 4.8). Iron(II) carbonate (siderite) removal did not change the NDMA degradation rate (Figure 4.10b). Magnetite removal or addition to reduced sediment did exhibit some influence on NDMA degradation, although the effect appears to be adsorbed Fe^{2+} on magnetite. There is no NDMA degradation (to 1000 hours) in freshly ground magnetite (no sediment, Figure 4.9a), although magnetite removal from the Aerojet aquifer sediment after reduction shows a significant influence (Figure 4.9b). The NDMA degradation rate with reduced sediment had a 7-hour half-life (open circles), whereas magnetite removal (triangles) had an 85-hour NDMA degradation rate. When the reactive magnetite was added to a separate experiment containing reduced Aerojet sediment (dark circles, Figure 4.9b), the NDMA degradation rate was more rapid than the system in which the magnetite was removed. Finally, in a system in

which the magnetite was removed from the sediment prior to dithionite reduction, NDMA degradation was slighly slower (Figure 4.9b, X136 data), which is consistent with the hypothesis that adsorbed ferrous iron on magnetite was contributing to NDMA degradation (i.e., magnetite removal after reduction has some surface adsorbed ferrous iron).

NDMA did slowly degrade in unaltered 2:1 smectite clay (montmorillonite; Figure 4.14), although this contained adsorbed cations and also surface iron oxides, which may have contributed to the degradation. Removal of the adsorbed cations did not change the NDMA degradation rate (half-life 528 hours), indicating there was insufficient adsorbed Fe^{2+} (or Mn^{2+}) to degrade NDMA. Acid treatment of the clay to remove some iron oxides (0.5 M HCl, 1 hour) or most of the iron oxides (1.0 M HCl, 200 hours) also did not change the NDMA degradation rate (Figure 4.15b). Dithionite treatment of the montmorillonite can reduce the 2.2% structural iron in the clay (Stucki et al. 1984). Dithionite treatment followed by removal of adsorbed Fe^{2+} resulted in the same degradation rate as unaltered clay, indicating (apparently) any additional structural Fe(II) was not reactive with the NDMA.

The NDMA degradation rate was highly dependent on the final pH (Figure 5.2b). Alkaline conditions (pH 10.6) promoted the most rapid NDMA degradation, but pH adjustment of the reduced sediment at pH 10.6 to pH 9.3, 8.4, or 7.5) systematically decreased the NDMA degradation rate. The most likely explanation is the $FeOH^-$ phase present under alkaline conditions promotes rapid NDMA degradation. The alkaline sediment by itself does not promote NDMA degradation (Figure 4.4), so it is not acting as a catalyst.

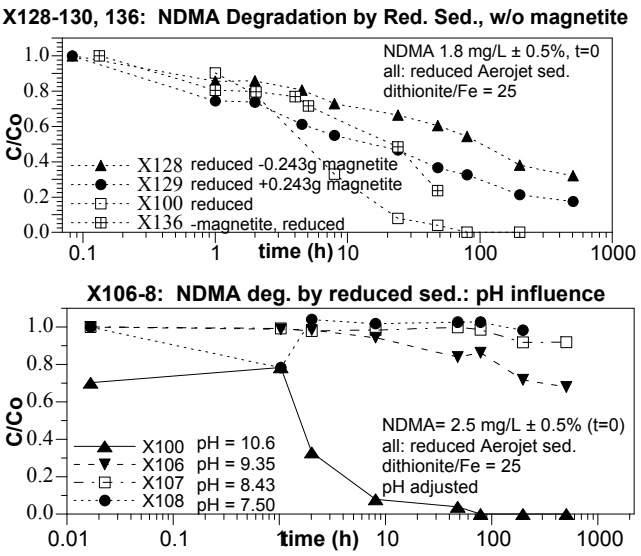

Figure 5.2. NDMA degradation in sediment/water systems with: a) magnetite removal or addition and b) pH equilibration after reduction.

An alternate method to create a subsurface reduced zone in an aquifer is to inject zero valent iron by high-pressure air/water or water. Zero valent iron will create some adsorbed ferrous iron which will desorb onto surrounding sediment, so there are geochemical changes that occur within the sediment as a result of the zero valent iron (i.e., the reduced zone is not limited to a small area associated just with the zero valent iron grains. NDMA appears to degrade slowly with the 5-micron zero valent iron (Figure 4.16), where only a few percent degradation (2.5 mg/L) is observed at four different iron/water ratios. In contrast, the 40-micron Aldrich zero valent iron (possibly with greater surface area) is much more reactive with NDMA. Anaerobic sediment with zero valent iron takes a few hundred hours to develop reducing conditions (Figure 4.18). Alternatively, although the chemically reduced sediment is initially under more reducing conditions, it is not as reducing conditions as the zero valent iron-sediment system. Compared to reduced Aerojet and Ft. Lewis sediment (molar ratio of ferrous iron to NDMA), the 40-micron zero valent iron showed roughly the same or slightly more rapid degradation rate, with zero

valent iron substitution for the 60 µmol/g ferrous iron (0.34% ferrous iron per gram of sediment). The effectiveness of degradation with zero valent iron suggests that this could act as an injectible reductant in aquifer systems.

5.1.3 Abiotic and Biotic NDMA Degradation Pathways

NDMA is a small compound that is relatively stable in aqueous solution and sorbs minimally (sorption K_d in the Aerojet sediment is 0.12 L/kg). NDMA will degrade abiotically by zero valent iron or magnetite under alkaline pH conditions to DMA or UDMH under acidic conditions (Odziemkowski et al. 2000). It will biotically degrade by a separate pathway (Figure 5.3). As described in the previous section, NDMA is rapidly abiotically degraded in reduced sediment to DMA (Figure 5.4). NDMA mineralization was also investigated in this project under oxic, anoxic, and reducing conditions with microbial isolates, microbes in sediment, and purely abiotic sediment conditions (i.e., addition of a bactericide). Sequential NDMA degradation was investigated with initial abiotic degradation of NDMA under reducing conditions followed by biodegradation of DMA or other intermediates under oxic environmental conditions with the addition of various microbial nutrients.

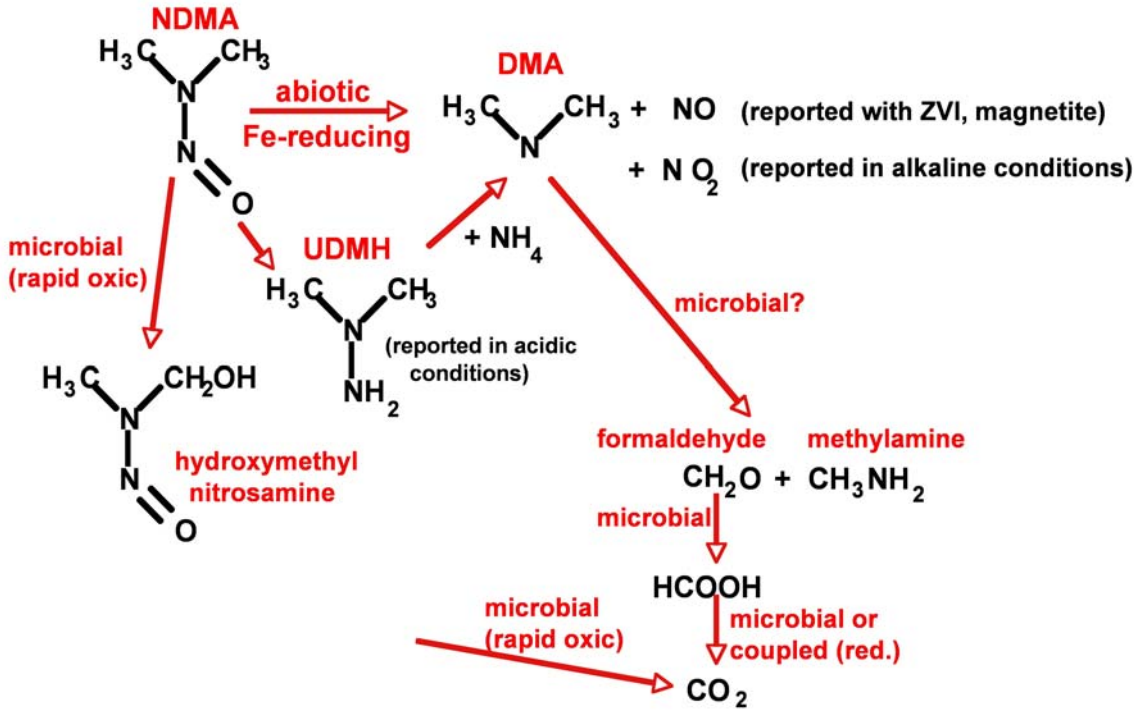

Figure 5.3. NDMA degradation pathways.

5.1.4 Degradation/Mineralization in Reduced Sediment

In this study under iron-reducing conditions created by dithionite reduction of sediment (Eh ~-200 mV, pH 10.5), NDMA is rapidly degraded to DMA (Figure 5.4). This reaction occurs rapidly (Figure 5.1b), with a half-life of 10 hours to hundreds of hours, depending on the ferrous

iron/NDMA molar ratio (more rapid with greater ferrous iron. Rates quantified in different sediment/water systems are described in Section 5.2). At both 1000 and 2000 hours, the NDMA concentration was below detection limits (0.05 mg/L) and 1.1-mg/L (17.7 µM) nitrate was detected (1100 hours), and 0.4-mg/L nitrate at 2000 hours (Figure 5.4b). It should be noted that nitrous oxide is suspected to form under these alkaline conditions (Figure 4.5), but this was not analyzed for. In addition, methylamine and formaldehyde was not detected, although trace concentrations of formate were detected.

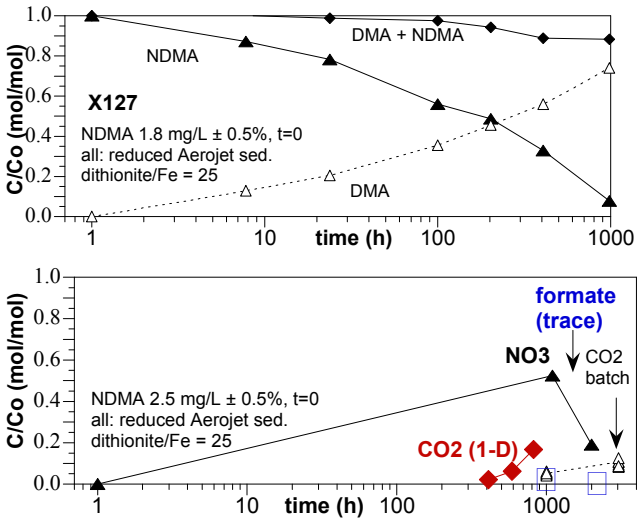

Figure 5.4. NDMA degradation products identified in reduced sediment: a) dimethylamine and b) various compounds (composite of multiple experiments).

This NDMA degradation to DMA by sediment under iron-reducing conditions is abiotic (Figure 5.1b), as the presence of a bactericide does not alter the observed rate. NDMA degradation experiments conducted in reduced sediment at different temperature were used to quantify the activation energy of the reaction (59 kJ/mol for highly reduced sediment, decreasing to 38 kJ/mol for partially reduced sediment (Figure 4.27). The NDMA degradation in reduced sediment was an exothermic reaction, as the rate was more rapid at colder temperature. The NDMA degradation rate increased 26.8% for every 10ºC decrease in temperature. The degradation rate also increased 19.3 times for every order of magnitude decrease in NDMA concentration.

Mineralization of NDMA under iron-reducing conditions also appears to be an abiotic reaction (Figure 5.5). The rate at which NDMA is mineralized in the reduced Aerojet and Ft. Lewis sediment is a function of the ratio of ferrous iron to NDMA, so in most batch experiments (low sediment/water ratio) showed a relatively slow CO_2 (5% to 13% by 1000 to 3000 hours). However, NDMA mineralization in reduced sediment in 1-D columns at higher sediment/water ratios was more rapid (2.2% at 410 hours, 6.2% at 590 hours, 16.8% at 822 hours, Figure 5.3b; see Section 4.4.1). This reactivity was maintained for 84 pore volumes, when experiments ended. It is expected that the reactivity would last longer, but at some point, the ability of the reduced sediment to degrade/mineralize NDMA would decrease.

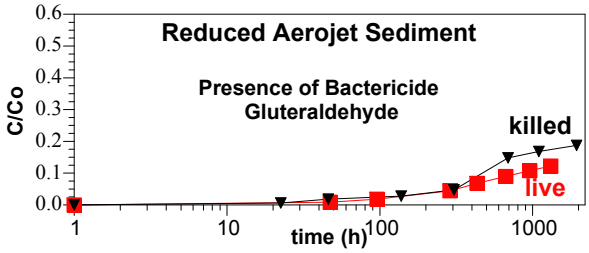

Figure 5.5. NDMA mineralization in reduced Aerojet sediment with and without a bactericide.

Numerous attempts were made to simulate microbes in the reduced sediment (Figures 4.46 and 4.47) with additions of humic acid, yeast, methane, propane, toluene, acetylene, TCE, nitrate, and glucose. None of the additions showed any influence on the NDMA mineralization rate

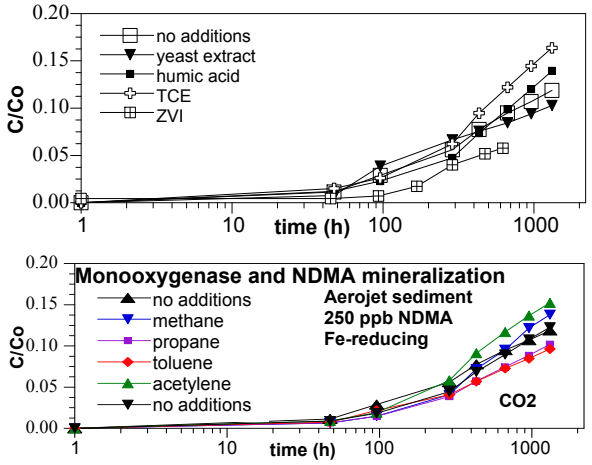

Figure 5.6. NDMA mineralization in the presence of various carbon additions.

(summary in Figure 5.6a). Monooxygenase enzyme carbon additions (i.e., propane, methane, toluene, Figure 5.6b) were not expected to show any influence, as oxygen is also needed (monooxygenase pathway cannot utilize nitrate as the electron acceptor). The microbial biomass actually decreased in the reduced sediment over 1900 hours (Figure 4.48d).

The NDMA mineralization rate in the reduced sediment was not a function of NDMA concentration (Figure 5.7), but mineralization extent was related to NDMA concentration. Higher NDMA concentrations showed lower mineralization extent (Figure 5.7b), which may simply be a function of insufficient adsorbed ferrous iron to degrade the NDMA (as this reaction is presumed to be abiotic). In one case (Aerojet sediment, 10-ppt data, Figure 5.7a), a very low NDMA concentration was degraded more slowly than higher NDMA concentrations.

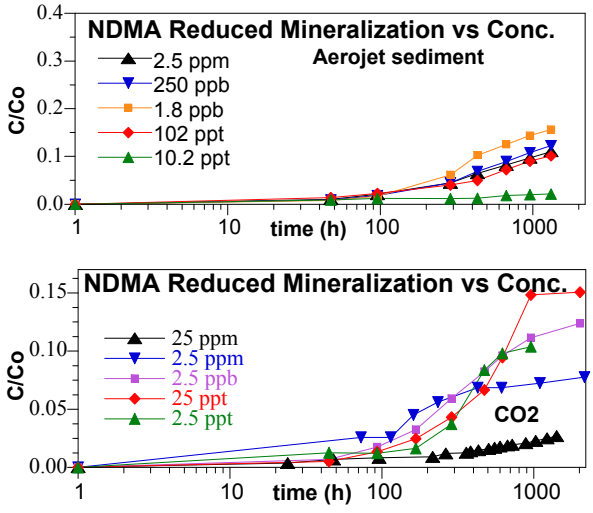

Figure 5.7. NDMA mineralization over a range of NDMA concentration in reduced Aerojet sediment (a) and reduced Ft. Lewis sediment (b).

Carbon mass balance conducted on seven reduced Aerojet aquifer sediment systems showed that the average mineralization at 3000 hours was 9.9% ± 1.6% (other reduced sediment systems showed mineralization as high as 17%). The average aqueous (i.e., NDMA plus other aqueous species) carbon mass was 40.2%. The calculated NDMA sorption to sediment (in these systems with 1 g of sediment and 6 mL of water) was 2.0% of the mass. The measured NDMA sorption to sediment and microbes in these reduced systems was 0.35% ± 2.6% (range 0.0% to 4.1%), in contrast to the 2.7% ± 4.5% (range 0% to 12%) in comparable oxic systems. The total percent carbon (from NDMA) incorporated into microbes was 0.18% ± 2.2%, in contrast to 5.7% ± 1.3% in oxic systems. Again, this could represent more limited biomass in reduced systems. The total carbon mass balance in reduced systems was 50.6% ± 27.6% in contrast to 80.0% ± 15.6% (i.e., accounted for aqueous, mineralized, sorbed to sediment and microbes and incorporated into microbes). Clearly, reduced system NDMA degradation pathway is significantly different from the oxic system.

Because the NDMA mineralization is presumed to be an abiotic reaction in reduced sediment, NDMA degradation should continue until it is all consumed (as opposed to a microbial reaction may exhibit a low concentration at which a nutrient is no longer utilized). To test this hypothesis, four ^{14}C-NDMA labeled experiments were conducted in which ^{14}C-NDMA was measured over time down to parts per trillion concentration (Figure 4.49). At a starting NDMA concentration of 2.5 ppm, the NDMA degradation half-life was 102 hours. At a starting NDMA concentration of 36 ppb (highest level recorded in the Aerojet aquifer), the NDMA degradation half-life was 109 hours. At starting concentrations of 100 and 10 ppt, NDMA had degraded below detection limits (3 ppt) by the first sample (24 hours). This is a half-life of 4.7 hours or faster.

5.1.5 Degradation/Mineralization in Oxic Sediment

NDMA mineralization in oxic sediment is primarily a biotic process, as demonstrated by the addition of a bactericide stopping nearly all of the mineralization (Figure 5.8a). The NDMA mineralization rate in the killed system (>50,000-hour half-life, <2% after 2000 hours) was very slow. The presence of oxygen clearly increased NDMA mineralization (Figure 5.8c).

NDMA mineralization in oxic systems was presumably by a monooxygenase enzyme pathway, methane-, propane-, and toluene-monooxygenase enzymes, and propane addition at specific oxygen/propane ratios (Figure 5.8b) did increase the mineralization rate and extent a small amount. Additions of methane, toluene, and acetylene had no influence on NDMA mineralization (Figure 4.33). Other carbon additions (yeast, humic acid, glucose; Figures 4.38 and 4.39) also did not influence NDMA mineralization.

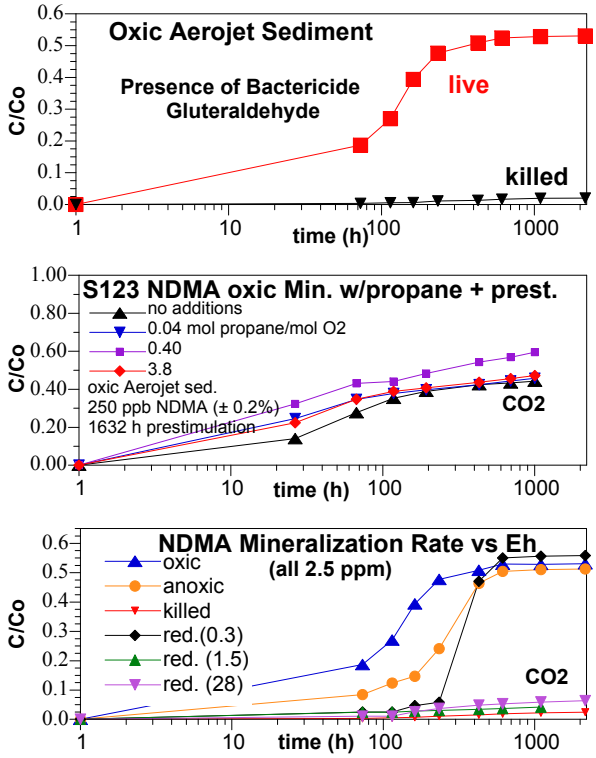

Figure 5.8. NDMA mineralization in oxic Aerojet sediment with various additions.

Because NDMA is mineralized co-metabolically via the monooxygenase enzyme pathway, it is not a necessary nutrient, and (in general) NDMA can be biotically mineralized to very low concentrations. In contrast, if NDMA were biotically mineralized as a primary substrate, there would likely be a slower degradation rate at a low concentration. In this study, NDMA was biotically mineralized in oxic Aerojet and Ft. Lewis sediment at concentrations ranging from 25 ppm to 2.5 ppt starting concentration (Figure 5.9a, b). The microbial biomass decreased slightly over 1900 hours in these systems (Figure 5.9c). There was generally not a relationship between the NDMA oxic, biomineralization rate and NDMA concentration, although the highest concentration (25 mg/L)

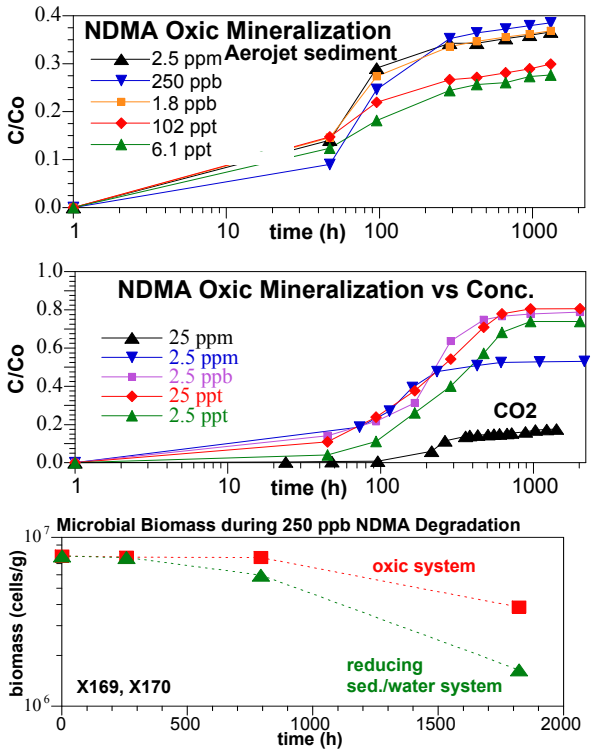

Figure 5.9. Relative contribution of biotic and abiotic mineralization of NDMA.

did show a slower mineralization rate and lower extent, which could possibly be caused by a toxic effect (although this was not investigated).

Although there was reasonably good success mineralizing NDMA in these oxic batch systems, *in situ* bioremediation relies upon efficient delivery of nutrients to microbes distributed throughout the sediment. This is significantly more difficult in packed porous media (1-D columns, aquifer) than in batch systems. In 1-D columns with oxygen and propane addition, the measured NDMA mineralization rate was relatively slow (half-life 2293 ±1866 hours), or 188 times slower than previously quantified in batch systems (Section 4.4.2). This may be indicative of poor delivery of nutrients. In fact, NDMA degradation is ~10 times or more rapid in reduced sediment columns (averaging 32.1 ± 4.2-hour half-life) relative to oxic sediment columns with propane/air injection (averaging 309 ± 164-hour half-life), and NDMA mineralization is most rapid in the reduced sediment (half-life 410 ± 147 hours), compared to oxic sediment with propane/air addition (half-life 2293 ± 1866 hours).

For 10 oxic systems in which the ^{14}C mass balance for NDMA mineralization (at 3000 hours) was conducted, the average mineralization was 51.0% ± 11.5% and average aqueous concentration of 17.8% ±12.4%. Based on the previously defined NDMA sorption parameter (K_d) of 0.12 mL/g, there should be 2.0% of the NDMA mass sorbed on the sediment surface at the sediment/water ratio used in these experiments (1 g to 6 mL). The total *measured* sorption (i.e., sorbed to sediment and microbes, extracted with methanol) in these oxic systems was 2.7% ± 4.5%, indicating maybe 0.7% of the NDMA mass was likely sorbed to the microbial surface. An average of 5.7% ± 1.3% of the NDMA carbon mass was measured as *incorporated* into the microbes (subtracting out the sorbed mass). Overall, these oxic systems had a total carbon mass balance of 80.0% ± 15.6%.

5.1.6 Degradation/Mineralization by Sediment Microbial Isolates

Initial experiments conducted with bacterial isolates found a number of bacteria that mineralize 25-ppm NDMA in an oxic aqueous environment when using this compound as a source of carbon and nitrogen for growth. Further investigation demonstrated that *Gordonia* sp. KTR9 and *Gordonia desulfuricans* did not appear to grow on NDMA as a nitrogen source or a nitrogen and carbon source (Figure 4.40). However, both microbes mineralized NDMA to ~24% and 55% carbon dioxide, respectively, when NDMA was supplied as the nitrogen and carbon source for growth (Table 4.4). It should be noted that these microbial isolates had not been treated to

remove traces of the culture medium. Experiments repeated with washed cells to more traces of the medium showed mineralization of NDMA to ~20% carbon dioxide was only observed when NDMA was added as the sole nitrogen source (Figure 4.41). It is not clear why NDMA was not mineralized when added as a carbon or carbon plus nitrogen source. The absence of growth in the degradation experiments appears to support the co-metabolic transformation and mineralization of NDMA by both strains. Degradation of NDMA by a co-metabolic process was recently shown to occur in *Pseudomonas mendocina* KR1 (Fournier et al. 2006).

In a second mineralization assay (Table 4.5), 10-ppm NDM was mineralized in an oxic, aqueous environment by several *Gordonia* and *Williamsia* bacterial species that had been grown on glucose, glycerol, and succinate as carbon sources and nitrate as the nitrogen source (details in Figures 4.42 and 4.43). The maximum amount of NDMA mineralized ranged from about 3.3% to 72.5% depending on the species and type of nutrient amendment. In general, the presence of an added carbon source stimulated the mineralization of NDMA. In comparison, the presence of an added nitrogen source inhibited the extent of mineralization and the rate of mineralization for *G. amarae*, *G. alkanivorans*, *G. desulfuricans*, *G. nitida*, *G. rubripertincta*, and KTR4 (Figures 4.42 and 4.43).

Mixed microbial populations indigenous to groundwater from Rocky Mountain Arsenal and soil from the Aerojet facility mineralized NDMA under similar conditions as used with the bacterial cultures. With these materials the maximum amount of NDMA mineralized was ~20% under either aerobic (Figure 5.10) or anaerobic conditions (Figure 4.45). The addition of a nitrogen amendment tended to decrease the extent and rate of mineralization, while the carbon amendment had either no effect or stimulated the extent of mineralization. These experiments also indicated that NDMA biotransformation by microorganisms was possible without stimulation of monooxygenase enzymes using substrates such as methane, propane, or toluene. This implies that NDMA mineralization under aerobic and anaerobic conditions is proceeding by an unidentified microbial pathway. However, the rate of degradation of NDMA following propane or toluene stimulation in strains *Rhodococcus jostii* RHA1 and *Pseudomonas mendocina* RK1 was considerably faster (Fournier et al. 2006; Sharp et al. 2007) than the constitutive rate observed in this study.

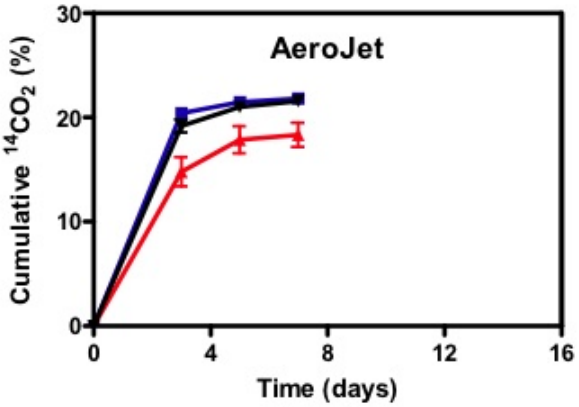

Figure 5.10. Aerobic mineralization of [^{14}C]-NDMA to $^{14}CO_2$ by Aerojet sediment in the absence (MSM ■) or presence of a nitrogen (MSM + KNO_3 ▲) or carbon amendment (MSM + Carbon ▼).

5.1.7 Degradation/Mineralization in Sequential Reduced, then Oxic Sediment

It was initially hypothesized that because NDMA can be rapidly degraded to intermediates (half-life 2 to 10 hours) in reduced sediment (abiotic process), a sequential treatment system of a reducing environment followed by a downgradient oxic, biostimulation zone may be the most rapid treatment process. An approximation of sequential reduction, then downgradient oxidation

in batch systems was accomplished by NDMA mineralization for 1,000 hours in reduced Aerojet sediment, removal of the aqueous solution, and placing it in oxic sediment. The subsequent oxidation for 2100 hours resulted in some additional mineralization for propane addition (Figure 4.53a), but little influence of additions of yeast and humic acid. In addition, the mineralization rate and extent was actually slower and less than in purely oxic systems.

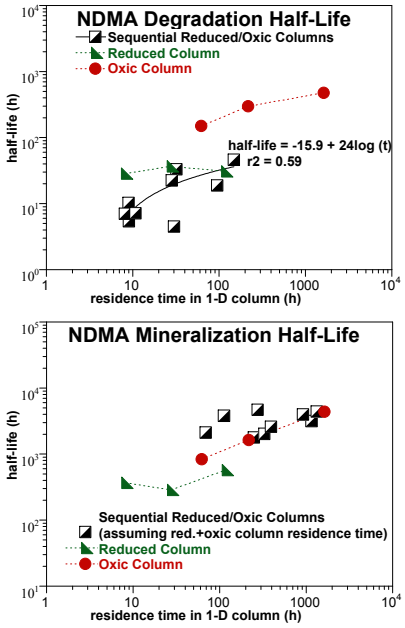

Figure 5.11. NDMA degradation and mineralization rates in reduced, oxic, and sequential 1-D columns.

More field-realistic sequential reduced-oxic systems were conducted in 1-D columns, with addition of propane/air between the upgradient reduced column and downgradient oxic sediment column (Figure 4.55). NDMA degradation and mineralization in sequential reduced/oxic column systems was characterized in nine experiments with a range of residence times and a range of differences in residence time between the reduced and oxic sediment columns.

NDMA degradation in the sequential reduced-oxic sediment systems (Figure 5.11a) was slightly (2 times) more rapid (17.2 ± 14.5-hour half-life) than reduced sediment alone (32.1 ± 4.2 hours), as caused by the (inefficient and slow) downgradient biodegradation in the oxic sediment column (Szecsody et al. 2008a). NDMA mineralization rates in the sequential reduced-oxic sediment systems (3180 ± 1094 hours) were slightly (40%) slower than in the oxic columns (2293 ± 1866 hours; Figure 5.11b). Both these data sets indicate sequential degradation was inefficient, caused either by NDMA degradation intermediates from the upgradient reduced column not being biodegraded as easily as NDMA itself and/or removal of dissolved oxygen from the water that is injected into the down gradient oxic column (with air/propane) was not efficiently maintaining an oxic environment.

5.2 NDMA Degradation/Mineralization Rates

NDMA degradation rates quantified in experiments are listed in Table 5.1. NDMA can be degraded rapidly in reduced sediment (as rapid as a 3-hour half-life). NDMA degradation increased with the ratio of ferrous iron to NDMA in various sediment/water systems, and the rate of NDMA degradation was predictable from the intrinsic NDMA degradation half-life and this ferrous iron/NDMA ratio (Figure 5.12a). NDMA degradation rates observed in batch experimental systems were slow (hundreds to thousands of hours), but more rapid in column systems (tens of hours) because of a higher ferrous iron/NDMA ratio in columns. Rates observed in columns (Table 5.1) that are <200 hours are viable for field-scale remediation. NDMA at 100 and 10 ppt (Figure 4.49), were rapidly degraded (<4.7-hour half-life), NDMA degraded so fast, it could not be accurately measured.

The NDMA removal rate was most rapid in reduced Aerojet sediment (Figure 5.12b, batch = solid green squares, 1-D columns = open green squares). Rates in oxic sediment were 2 to 3 orders of magnitude slower. Rates in zero valent iron/sediment mixtures varied with the zero

valent iron type, but were almost as rapid as the reduced sediment. Rates in 2:1 smectite clays were measurable, but 2 to 3 orders of magnitude slower than reduced sediment, indicating adsorbed ferrous iron on iron oxides/clays at pH 10 (some $FeOH^-$ present) was very efficient at degrading NDMA.

Table 5.1. NDMA degradation rates observed in experiments.

								----- NDMA degradation -----			----- NDMA mass removal rates		
								pseudo f.o. rate		intrinsic ra	mass	mass	mass flux 3
exp.		NDMA	H_2O	NDMA	sed.	Fe2+	molar ratio	half-life	kf'	kf	flux 1	flux 2	mol ndma/
name	system	(mg/L)	(g)	(mol)	(g)	(mol)	Fe/NDMA	(h)	(1/h)	(1/h mol^2)	mol NDMA/h	mol/g/day	mol Fe/d
	aqueous												
	pH 7, fluorescent light	2.5						no degradation - stable					
X118	pH 8.1, UV light (30w UVC, 30 cm)	2.5	10	3.37E-07				361	1.92E-03				
	0.1M dithionite	5.27	60	4.27E-06				2.51	0.276				
	0.1M dithionite	2.30	10	3.1E-07				230	3.01E-03				
	reducing (0 to - 0.2 v)	2.60						no degradation - stable					
	acidic (pH = 2.0)	2.30	6	1.86E-07				2540	2.73E-04				
X95-9	basic (pH 7.0,8.1, 9.0, 10.0, 11.0)	2.60						no degradation to 1000 h - stable					
	pH (4 to 12)	2.30						no degradation - stable					
	bacterial isolates/water					CFU/mL				(1/h mol cfu)			
	Gordonia sp. KTR9 (C + N addition)	25.0	6.0	2.02E-06		5.0E+08		52.8	1.31E-02	1.30E-05	2.66E-08		
	Gordonia sp. KTR9 (N addition)	25.0	6.0	2.02E-06		5.0E+08		65.3	1.06E-02	1.05E-05	2.15E-08		
	Williamsia sp. KTR4 (C+N addition)	25.0	6.0	2.02E-06		5.0E+08		67.5	1.03E-02	1.01E-05	2.08E-08		
	Williamsia sp. KTR4 (N addition)	25.0	6.0	2.02E-06		5.0E+08		79.2	8.75E-03	8.64E-06	1.77E-08		
	mineral/water systems												
	silica, Al2O3	2.5						no degradation - stable					
	magnetite (ground)	2.5						no degradation - stable					
	biotite (ground)	2.5						no degradation - stable					
	kaolinite (acid washed)	2.5						no degradation - stable					
	illite (acid washed)	2.5						no degradation - stable					
	nontronite (acid washed)	2.5						no degradation - stable					
	hectorite (acid washed)	2.5						no degradation - stable					
	montmorillinite (a. w.)	2.5						no degradation - stable					
	montmorillonite	2.5	5.0	1.69E-07	0.25	8.95E-05	5.31E+02	528	1.31E-03	8.69E+07	2.22E-10	2.13E-08	5.94E-05
	reduced montmorillonite	2.5	5.0	1.69E-07	0.25	8.95E-05	5.31E+02	528	1.31E-03	8.69E+07	2.22E-10	2.13E-08	5.94E-05
	red. mont., no ads Fe(II)	2.5	5.0	1.69E-07	0.25	8.95E-05	5.31E+02	480	1.44E-03	9.56E+07	2.44E-10	2.34E-08	6.53E-05
	red. mont.+ 1 h HCl	2.5	5.0	1.69E-07	0.25	8.95E-05	5.31E+02	340	2.04E-03	1.35E+08	3.44E-10	3.30E-08	9.22E-05
	red. mont.+ 200 h HCl	2.5	5.0	1.69E-07	0.25	8.95E-05	5.31E+02	278	2.49E-03	1.65E+08	4.21E-10	4.04E-08	1.13E-04
	zero valent/water												
	H-200, 5-micron	2.5	5.0	1.52E-06	0.1	1.79E-02	1.18E+04	1700	4.08E-04	1.50E+04	6.19E-10	1.49E-07	8.30E-07
	H-200, 5-micron	2.3	5.0	1.24E-06	0.1	7.16E-02	5.77E+04	4500	1.54E-04	1.73E+03	1.91E-10	4.59E-08	6.41E-08
	H-200, 5-micron	25	5.0	1.35E-05		7.16E-02	5.31E+03	none					
	Aldrich, 40-micron	2.5	5.0	1.69E-07	1.0	1.79E-02	1.06E+05	6.82	1.02E-01	3.36E+07	1.71E-08	4.12E-07	2.30E-05
	Aldrich, 40-micron	2.5	5.0	1.69E-07	0.2	3.58E-03	2.12E+04	26.57	2.61E-02	4.32E+07	4.40E-09	5.28E-07	2.95E-05
	Aldrich, 40-micron	2.5	5.0	1.69E-07	0.06	1.07E-03	6.37E+03	120.4	5.76E-03	3.18E+07	9.72E-10	3.89E-07	2.17E-05
	Aldrich, 40-micron	2.5	5.0	1.69E-07	0.02	3.58E-04	2.12E+03	131	5.29E-03	8.76E+07	8.93E-10	1.07E-06	5.98E-05
	Aldrich, 40-micron	2.3	5.0	1.24E-06	0.01	4.30E-02	3.46E+04	120	5.78E-03	1.08E+05	7.17E-09	2.87E-05	4.01E-06
	Aldrich, 40-micron	25	5.0	1.35E-05	0.06	4.30E-02	3.18E+03	432	1.60E-03	2.77E+03	2.17E-08	8.66E-06	1.21E-05
	sediment/water, batch, 22C												
	reduced Ft Lewis sed.	25.0	30	1.01E-05	1.18	1.88E-04	1.86E+01	8090	8.57E-05	4.49E+04	8.69E-10	1.76E-08	1.11E-04
	reduced Ft Lewis sed.	25.0	32	1.09E-05	9.22	1.47E-03	1.35E+02	2700	2.57E-04	1.61E+04	2.80E-09	7.28E-09	4.58E-05
	reduced Ft Lewis sed.	0.72	30	2.9E-07	0.99	1.58E-04	5.44E+02	none					
	reduced Ft Lewis sed.	0.72	32	3.09E-07	9.57	1.52E-03	4.92E+03	203	0.00341	7.24E+06	1.05E-09	2.64E-09	1.66E-05
	reduced Ft Lewis sed.	25	1.8	6.16E-07	1.91	3.04E-04	4.93E+02	2000	0.00035	1.87E+06	2.16E-10	2.71E-09	1.70E-05
	reduced Ft Lewis sed.	2.5	2.2	7.55E-08	1.52	2.42E-04	3.20E+03	380	0.00182	9.97E+07	1.37E-10	2.17E-09	1.37E-05
	reduced Ft Lewis sed.	0.25	2.3	7.78E-09	1.54	2.44E-04	3.14E+04	66	0.0105	5.53E+09	8.16E-11	1.28E-09	8.03E-06
	reduced Ft Lewis sed.	2.5	10	3.37E-07	1.52	6.68E-04	1.98E+03	830	8.35E-04	3.71E+06	2.82E-10	4.45E-09	1.01E-05
	red.Ft Lewis, no ads. Fe(II)	2.5	10	3.37E-07	1.52	6.68E-04	1.98E+03	830	8.35E-04	3.71E+06	2.82E-10	4.45E-09	1.01E-05
	red.Ft Lewis + 1 h HCl	2.5	10	3.37E-07	1.52	6.68E-04	1.98E+03	540	1.28E-03	5.70E+06	4.33E-10	6.84E-09	1.56E-05
	red.Ft Lewis + 200 h HCl	2.5	10	3.37E-07	1.52	6.68E-04	1.98E+03	2020	3.43E-04	1.52E+06	1.16E-10	1.83E-09	4.16E-06
	reduced Aerojet sed.	5.34	59	4.23E-06	192	7.67E-03	1.81E+03	447	1.55E-03	2.58E+04	6.56E-09	8.21E-10	2.05E-05
	reduced Aerojet sed.	5.34	59	4.23E-06	192	7.67E-03	1.81E+03	none					
	reduced Aerojet sed.	0.036	220	1.07E-07	705	7.05E-03	6.61E+04	(14)*	0.0496	8.90E+06	5.29E-09	1.80E-10	1.80E-05
	reduced Aerojet sed.	0.036	220	1.07E-07	705	7.05E-03	6.61E+04	(45.1)*	0.0154	2.76E+06	1.64E-09	5.59E-11	5.59E-06
	reduced Aerojet sed.	0.036	220	1.07E-07	705	7.05E-03	6.61E+04	(117)*	0.0059	1.06E+06	6.29E-10	2.14E-11	2.14E-06
	reduced Aerojet sed.	0.036	220	1.07E-07	705	7.05E-03	6.61E+04	(338)*	0.0021	3.77E+05	2.24E-10	7.63E-12	7.63E-07
	reduced Aerojet sed.	5.00	53	3.57E-06	198	7.92E-03	2.22E+03	264	0.00262	5.01E+04	9.34E-09	1.13E-09	2.83E-05
	reduced Aerojet sed.	5.00	53	3.57E-06	198	7.92E-03	2.22E+03	none					
	reduced Aerojet sed.	4.74	1.7	1.1E-07	6.99	2.80E-04	2.54E+03	173	0.00401	7.03E+07	4.41E-10	1.52E-09	3.79E-05
	reduced Aerojet sed.	0.036	67	3.27E-08	190	3.03E-02	9.27E+05	15.8	0.044	9.54E+07	1.44E-09	1.81E-10	1.14E-06
	reduced Aerojet sed.	0.036	67	3.27E-08	190	3.03E-02	9.27E+05	10.7	0.065	1.41E+08	2.12E-09	2.68E-10	1.68E-06
W120	red. Aerojet s.(di/Fe=26,W21)stop flow	2.5	5.0	1.69E-07	33	2.22E-04	1.32E+03	1273	5.45E-04	1.45E+07	9.19E-11	6.68E-11	9.93E-06
W121	red. Aerojet s.(di/Fe=26,W21)stop flow	0.91	5.0	6.14E-08	33	2.22E-04	3.61E+03	2122	3.27E-04	2.40E+07	2.01E-11	1.46E-11	2.17E-06
S129	red. Aerojet s.(di/Fe=26,pH 10.5, X91)	0.000010	10	1.35E-12	5.0	2.00E-04	1.48E+08	4.7	1.47E-01	5.46E+14	1.99E-13	9.56E-13	2.39E-08
S130	red. Aerojet s.(di/Fe=26,pH 10.5, X91)	0.00010	10	1.35E-11	5.0	2.00E-04	1.48E+07	4.7	1.47E-01	5.46E+13	1.99E-12	9.56E-12	2.39E-07
S131	red. Aerojet s.(di/Fe=26,pH 10.5, X91)	0.036	10	4.86E-09	5.0	2.00E-04	4.12E+04	109	6.36E-03	6.54E+09	3.09E-11	1.48E-10	3.71E-06
S132	red. Aerojet s.(di/Fe=26,pH 10.5, X91)	2.51	10	3.39E-07	5.0	2.00E-04	5.90E+02	102	6.80E-03	1.00E+08	2.30E-09	1.11E-08	2.76E-04

Table 5.1. (contd)

								----- NDMA degradation -----			----- NDMA mass removal rates		
								pseudo f.o. rate	intrinsic ra		mass	mass	mass flux 3
exp.		NDMA	H2O	NDMA	sed.	Fe2+	molar ratio	half-life	kf'	kf	flux 1	flux 2	mol ndma/
name	system	(mg/L)	(g)	(mol)	(g)	(mol)	Fe/NDMA	(h)	(1/h)	(1/h mol^{-1})	mol NDMA/h	mol/g/day	mol Fe/d
	chemically modified sediment/water, batch, 22C												
X100	red. Aerojet s.(di/Fe=26,pH 10.5, X91)	2.5	10	3.37E-07	5.0	2.00E-04	5.93E+02	7.1	9.76E-02	1.45E+09	3.29E-08	1.58E-07	3.95E-03
X101	red. Aerojet s.(di/Fe=26,pH 7.5, w21)	2.5	10	3.37E-07	5.0	2.00E-04	5.93E+02	320	2.17E-03	3.21E+07	7.31E-10	3.51E-09	8.77E-05
X102	red. Aerojet s.(di/Fe=26,pH 10.5), no light	2.5	10	3.37E-07	5.0	2.00E-04	5.93E+02	6.6	1.05E-01	1.56E+09	3.54E-08	1.70E-07	4.25E-03
X102b	red. Aerojet s.(di/Fe=26,pH 10.5), UV light	2.5	10	3.37E-07	5.0	2.00E-04	5.93E+02	7.6	9.12E-02	1.35E+09	3.08E-08	1.48E-07	3.69E-03
X103	red. Aerojet s.(di/Fe=3,pH 9.9, X93)	2.5	10	3.37E-07	5.0	2.00E-04	5.93E+02	14.8	4.68E-02	6.94E+08	1.58E-08	7.59E-08	1.90E-03
X104	red. Aerojet s.(di/Fe=1,pH 9.2, X94)	2.5	10	3.37E-07	5.0	2.00E-04	5.93E+02	265	2.62E-03	3.88E+07	8.83E-10	4.24E-09	1.06E-04
X105	red. Ft Lewis s.(di/Fe=1,pH 9.3, X92)	2.5	10	3.37E-07	5.0	2.00E-04	5.93E+02	594	1.17E-03	1.73E+07	3.94E-10	1.89E-09	4.73E-05
X106	red. Aerojet s.(di/Fe=26, X91) pH to 9.35	2.5	10	3.37E-07	5.0	2.00E-04	5.93E+02	378	1.83E-03	2.72E+07	6.19E-10	2.97E-09	7.43E-05
X107	red. Aerojet s.(di/Fe=26, X91) pH to 8.43	2.5	10	3.37E-07	5.0	2.00E-04	5.93E+02	3920	1.77E-04	2.62E+06	5.97E-11	2.86E-10	7.16E-06
X108	red. Aerojet s.(di/Fe=26, X91) pH to 7.50	2.5	10	3.37E-07	5.0	2.00E-04	5.93E+02	12000	5.78E-05	8.56E+05	1.95E-11	9.36E-11	2.34E-06
X109	anaer. Aerojet sed.(1g)+0.001FeS,pH 8.5	2.5	10	3.37E-07	1.005	4.02E-05	1.19E+02	none (to 900 h)					
X110	anaer. Aerojet sed.(1g)+0.01FeS,pH 8.5	2.5	10	3.37E-07	1.05	4.20E-05	1.24E+02	none (to 900 h)					
X111	anaer. Aerojet sed.(1g)+0.1FeS,pH 8.5	2.5	10	3.37E-07	1.1	4.40E-05	1.30E+02	none (to 900 h)					
X112	anaer. Aerojet sed.(1g)+0.001FeS2,pH 8.5	2.5	10	3.37E-07	1.005	4.02E-05	1.19E+02	none (to 900 h)					
X113	anaer. Aerojet sed.(1g)+0.01FeS2,pH 8.5	2.5	10	3.37E-07	1.05	4.20E-05	1.24E+02	none (to 900 h)					
X114	anaer. Aerojet sed.(1g)+0.1FeS2,pH 8.5	2.5	10	3.37E-07	1.1	4.40E-05	1.30E+02	none (to 900 h)					
X120	red. Aero. s.(di/Fe=26)pH 10.5->9.4->10.5	2.5	10	3.37E-07	5.0	2.00E-04	5.93E+02	558	1.24E-03	1.84E+07	4.19E-10	2.01E-09	5.03E-05
X121	red. Aero. s.(di/Fe=26)pH 10.5->8.5->10.5	2.5	10	3.37E-07	5.0	2.00E-04	5.93E+02	698	9.93E-04	1.47E+07	3.35E-10	1.61E-09	4.02E-05
X122	red. Aero. s.(di/Fe=26)pH 10.5->7.8->10.5	2.5	10	3.37E-07	5.0	2.00E-04	5.93E+02	2100	3.30E-04	4.89E+06	1.11E-10	5.35E-10	1.34E-05
X123	red. Aero. s.(di/Fe=26)pH 10.5, Fe2+ gone	2.5	10	3.37E-07	5.0	2.00E-04	5.93E+02	117	5.92E-03	8.78E+07	2.00E-09	9.60E-09	2.40E-04
X124	red. Aero. s.(di/Fe=26)pH10.5, Fe(II/III)rem.	2.5	10	3.37E-07	5.0	2.00E-04	5.93E+02	1085	6.39E-04	9.47E+06	2.16E-10	1.03E-09	2.59E-05
X125	red. Aero. s.(di/Fe=26)pH 10.5, am.FeIIIrem.	2.5	10	3.37E-07	5.0	2.00E-04	5.93E+02	1900	3.65E-04	5.41E+06	1.23E-10	5.91E-10	1.48E-05
X126	red. Aero. s.(di/Fe=26)pH 10.5, CO3 gone	2.5	10	3.37E-07	5.0	2.00E-04	5.93E+02	11	6.30E-02	9.34E+08	2.13E-08	1.02E-07	2.55E-03
X127	red. Aero. s.(di/Fe=26)pH 10.5, DMA anal.	2.5	10	3.37E-07	1.0	4.00E-05	1.19E+02	190	3.65E-03	2.70E+08	1.23E-09	2.95E-08	7.39E-04
X128	red. Aero.(di/Fe=26)pH 10.5, magnetite rem.	2.5	10	3.37E-07	4.75	1.90E-04	5.63E+02	105	6.60E-03	1.03E+08	2.23E-09	1.13E-08	2.81E-04
X129	red. Aero.(di/Fe=26)pH 10.5,+ magnetite	2.5	10	3.37E-07	5.25	2.10E-04	6.22E+02	25	2.77E-02	3.91E+08	9.36E-09	4.28E-08	1.07E-03
X130	red. Aero. s.(di/Fe=26)pH 10.5 + 0.1g FeS2	2.5	10	3.37E-07	5.1	2.04E-04	6.04E+02	120	5.78E-03	8.39E+07	1.95E-09	9.17E-09	2.29E-04
X131	anaer. Aerojet sed.(1g), pH 12	2.5	10	3.37E-07	1.1	4.40E-05	1.30E+02	none (to 900 h)					
X132	anaer. Aerojet sed.(1g), pH 11.7, + FeCl2	2.5	10	3.37E-07	1.1	4.40E-05	1.30E+02	none (to 900 h)					
X133	red. Aero. s.(di/Fe=26)pH 10.5	2.5	10	3.37E-07	1.0	4.00E-05	1.19E+02	216	3.21E-03	2.38E+08	1.08E-09	2.60E-08	6.50E-04
X134	red. Aero. s.(di/Fe=26)pH 9.43, Fe2+ gone	2.5	10	3.37E-07	1.0	4.00E-05	1.19E+02	81	8.56E-03	6.34E+08	2.89E-09	6.93E-08	1.73E-03
X136	Aero sed - mag., red (di/Fe=2, pH 10.5)	2.5	10	3.37E-07	2.5	1.00E-04	2.96E+02	30.1	2.30E-02	6.82E+08	7.77E-09	7.46E-08	1.87E-03
X148	red. Aero.(di/Fe=26)pH 10.5,Fe2+ 10.04 uMol	2.5	10	3.37E-07	1.0	4.40E-05	1.30E+02	6.03	1.15E-01	7.74E+09	3.88E-08	9.31E-07	2.12E-02
X149	red. Aero.(di/Fe=26)pH 10.5,Fe2+ 25.14 uMol	2.5	10	3.37E-07	1.0	5.00E-05	1.48E+02	4.00	1.73E-01	1.03E+10	5.85E-08	1.40E-06	2.81E-02
X150	red. Aero.(di/Fe=26)pH 10.5,Fe2+ 50.25 uMol	2.5	10	3.37E-07	1.0	6.00E-05	1.78E+02	3.02	2.30E-01	1.13E+10	7.75E-08	1.86E-06	3.10E-02
X151	red. Aero.(di/Fe=26)pH 10.5,Fe2+ 100.08 uMol	2.5	10	3.37E-07	1.0	8.00E-05	2.37E+02	16.03	4.32E-02	1.60E+09	1.46E-08	3.50E-07	4.38E-03
X152	red. Aero.(di/Fe=26)pH 10.5,Fe2+ - < 10 uMol	2.5	10	3.37E-07	1.0	3.60E-05	1.07E+02	1971	3.52E-04	2.90E+07	1.19E-10	2.85E-09	7.91E-05
X153	red. Aero.(di/Fe=26)pH 10.5,Fe2+ - 30 uMol	2.5	10	3.37E-07	1.0	2.80E-05	8.30E+01	1341	5.17E-04	5.47E+07	1.74E-10	4.19E-09	1.50E-04
X154	red. Aero.(di/Fe=26)pH 10.5,Fe2+ - 30 uMol	2.5	10	3.37E-07	1.0	2.80E-05	8.30E+01	745	9.30E-04	9.85E+07	3.14E-10	7.54E-09	2.69E-04
X155	red. Aero. (di/Fe=26)pH 10.5,Fe2+ - 70 uMol	2.5	10	3.37E-07	1.0	1.20E-05	3.56E+01	2886	2.40E-04	5.93E+07	8.11E-11	1.95E-09	1.62E-04
	sediment/water, 1-D column (high sediment/water ratio), variables: fraction reduction, temperature, flow rate (residence time)												
W96	1-D, red. Fe Lewis sed (di/Fe = 4)	2.5	6.3	2.13E-07	34.6	2.22E-04	1.04E+03	79.9	8.68E-03	1.84E+08	1.84E-09	1.28E-09	1.99E-04
W97	1-D, red. Fe Lewis sed (di/Fe = 4)	2.5	13	4.25E-07	55.4	2.22E-04	5.22E+02	94.8	7.31E-03	7.75E+07	3.11E-09	1.35E-09	3.36E-04
W98	1-D, red. Fe Lewis sed (di/Fe = 4)	2.5	6.3	2.13E-07	34.6	2.22E-04	1.04E+03	126.1	5.50E-03	1.16E+08	1.17E-09	8.10E-10	1.26E-04
W99	1-D, red. Fe Lewis sed (di/Fe = 4)	2.5	13	4.25E-07	55.4	2.22E-04	5.22E+02	162.4	4.27E-03	4.52E+07	1.81E-09	7.87E-10	1.96E-04
W100	1-D, red. Ft Lewis sed (di/Fe=12)	2.44	6.3	2.08E-07	30.3	1.11E-03	5.35E+03	75.9	9.13E-03	3.96E+07	1.90E-09	1.50E-09	4.10E-05
W101	1-D, red. Ft Lewis sed.(di/Fe=12)	2.78	6.3	2.36E-07	30.3	1.11E-03	4.70E+03	140.3	4.94E-03	1.66E+07	1.17E-09	9.26E-10	2.53E-05
W1	red. Ft Lewis sed. (di/Fe=37) 22C	2.5	7.0	2.36E-07	37.0	5.88E-03	2.49E+04	10.5	6.60E-02	4.75E+07	1.56E-08	1.01E-08	6.36E-05
W2	red. Ft Lewis sed. (di/Fe=22) 22C	2.5	7.0	2.36E-07	37.0	2.59E-03	1.10E+04	15.9	4.36E-02	7.13E+07	1.03E-08	6.68E-09	9.54E-05
W3	red. Ft Lewis sed. (di/Fe=13) 22C	2.5	7.0	2.36E-07	37.0	1.11E-03	4.70E+03	31.8	2.18E-02	8.31E+07	5.15E-09	3.34E-09	1.11E-04
W4	red. Ft Lewis sed. (di/Fe=4) 22C	2.5	7.0	2.36E-07	37.0	2.22E-04	9.40E+02	315	2.20E-03	4.20E+07	5.20E-10	3.37E-10	5.62E-05
W5	red. Ft Lewis sed. (di/Fe=37) 22C	0.25	7.0	2.36E-08	37.0	5.88E-03	2.49E+04	9.2	7.53E-02	5.42E+07	1.78E-09	1.15E-09	7.26E-06
W6	red. Ft Lewis sed. (di/Fe=22) 22C	0.25	7.0	2.36E-08	37.0	2.59E-03	1.10E+04	10.9	6.36E-02	1.04E+08	1.50E-09	9.74E-10	1.39E-05
W7	red. Ft Lewis sed. (di/Fe=13) 22C	0.25	7.0	2.36E-08	37.0	1.11E-03	4.70E+03	29.8	2.33E-02	8.87E+07	5.49E-10	3.56E-10	1.19E-05
W8	red. Ft Lewis sed. (di/Fe=4) 22C	0.25	7.0	2.36E-08	37.0	2.22E-04	9.40E+02	46.9	1.48E-02	2.82E+08	3.49E-10	2.26E-10	3.77E-05
W9	red. Ft Lewis sed. (di/Fe=37) 34C	2.5	7.0	2.36E-07	37.0	5.88E-03	2.49E+04	35.42	1.96E-02	1.41E+07	4.62E-09	3.00E-09	1.89E-05
w10	red. Ft Lewis sed. (di/Fe=22) 34C	2.5	7.0	2.36E-07	37.0	2.59E-03	1.10E+04	58.7	1.18E-02	1.93E+07	2.79E-09	1.81E-09	2.58E-05
w11	red. Ft Lewis sed. (di/Fe=13) 34C	2.5	7.0	2.36E-07	37.0	1.11E-03	4.70E+03	91.15	7.60E-03	2.90E+07	1.80E-09	1.17E-09	3.88E-05
w12	red. Ft Lewis sed. (di/Fe=4) 34C	2.5	7.0	2.36E-07	37.0	2.22E-04	9.40E+02	6403	1.08E-04	2.06E+06	2.56E-11	1.66E-11	2.76E-06
w13	red. Ft Lewis sed. (di/Fe=37) 45C	2.5	7.0	2.36E-07	37.0	5.88E-03	2.49E+04	73.56	9.42E-03	6.78E+06	2.23E-09	1.44E-09	9.08E-06
w14	red. Ft Lewis sed. (di/Fe=22) 45C	2.5	7.0	2.36E-07	37.0	2.59E-03	1.10E+04	120.7	5.74E-03	9.39E+06	1.36E-09	8.80E-10	1.26E-05
w15	red. Ft Lewis sed. (di/Fe=13) 45C	2.5	7.0	2.36E-07	37.0	1.11E-03	4.70E+03	128.6	5.39E-03	2.06E+07	1.27E-09	8.26E-10	2.75E-05
w16	red. Ft Lewis sed. (di/Fe=4) 45C	2.5	7.0	2.36E-07	37.0	2.22E-04	9.40E+02	5759	1.20E-04	2.30E+06	2.84E-11	1.84E-11	3.07E-06
w17	red. Ft Lewis sed. (di/Fe=37) 56C	2.5	7.0	2.36E-07	37.0	5.88E-03	2.49E+04	124.9	5.55E-03	3.99E+06	1.31E-09	8.50E-10	5.35E-06
w18	red. Ft Lewis sed. (di/Fe=22) 56C	2.5	7.0	2.36E-07	37.0	2.59E-03	1.10E+04	180.8	3.83E-03	6.26E+06	9.05E-10	5.87E-10	8.39E-06
w19	red. Ft Lewis sed. (di/Fe=13) 56C	2.5	7.0	2.36E-07	37.0	1.11E-03	4.70E+03	158.7	4.37E-03	1.67E+07	1.03E-09	6.69E-10	2.23E-05
w20	red. Ft Lewis sed. (di/Fe=4) 56C	2.5	7.0	2.36E-07	37.0	2.22E-04	9.40E+02	9920	6.99E-05	1.33E+06	1.65E-11	1.07E-11	1.78E-06
W102	1-D, red. Aerojet sed.(di/Fe=27)	2.5	7.5	2.54E-07	36.7	3.03E-02	1.19E+05	345	2.01E-03	2.61E+05	5.11E-10	3.34E-10	4.05E-07
W103	1-D, red. Aerojet sed.(di/Fe=27)	2.5	7.5	2.54E-07	36.7	3.03E-02	1.19E+05	1202	5.77E-04	7.48E+04	1.47E-10	9.60E-11	1.16E-07
W104	1-D, red. Aerojet sed.(di/Fe=2.8)	2.5	7.0	2.35E-07	36.7	3.03E-03	1.29E+04	146	4.75E-03	6.68E+06	1.11E-09	7.28E-10	8.82E-06
W105	1-D, red. Aerojet sed.(di/Fe=2.8)	2.5	7.0	2.35E-07	36.7	3.03E-03	1.29E+04	1972	3.51E-04	4.95E+05	8.24E-11	5.39E-11	6.53E-07
W106	1-D, red. Aerojet sed.(di/Fe=0.54)	2.44	7.0	2.29E-07	36.7	5.30E-04	2.32E+03	93.7	7.40E-03	6.09E+07	1.69E-09	1.11E-09	7.66E-05
W107	1-D, red. Aerojet sed.(di/Fe=0.54)	2.78	7.0	2.61E-07	36.7	5.30E-04	2.03E+03	2023	3.43E-04	2.48E+06	8.94E-11	5.85E-11	4.04E-06
W112	1-D, red. Aerojet sed.(di/Fe=28,W110)	2.58	5.0	1.74E-07	33.0	3.03E-03	1.74E+04	38.6	1.80E-02	3.41E+07	3.12E-09	2.27E-09	2.47E-05
W113	1-D, red. Aerojet sed.(di/Fe=26,W21)	2.58	5.0	1.74E-07	33.0	3.03E-03	1.74E+04	98.1	7.07E-03	1.34E+07	1.23E-09	8.93E-10	9.73E-06
W114	1-D, red. Aerojet sed.(di/Fe=28,W110)	0.25	5.0	1.68E-08	33.0	5.30E-04	3.15E+04	234	2.96E-03	3.32E+08	4.99E-11	3.63E-11	2.26E-06
W115	1-D, red. Aerojet sed.(di/Fe=26,W21)	0.25	5.0	1.68E-08	33.0	5.30E-04	3.15E+04	9.56	7.25E-02	8.12E+09	1.22E-09	8.88E-10	5.53E-05
W116	1-D, red. Aerojet sed.(di/Fe=28,W110)	0.227	5.0	1.53E-08	33.0	3.03E-03	1.98E+05	14.3	4.85E-02	1.05E+09	7.41E-10	5.39E-10	5.87E-06
W117	1-D, red. Aerojet sed.(di/Fe=26,W21)	0.227	5.0	1.53E-08	33.0	3.03E-03	1.98E+05	19.4	3.57E-02	7.71E+08	5.46E-10	3.97E-10	4.33E-06
W118	1-D, red. Aerojet sed.(di/Fe=28,W110)	0.259	5.0	1.74E-08	33.0	5.30E-04	3.04E+04	75.4	9.19E-03	9.94E+08	1.60E-10	1.17E-10	7.26E-06
W119	1-D, red. Aerojet sed.(di/Fe=26,W21)	0.259	5.0	1.74E-08	33.0	5.30E-04	3.04E+04	29.1	2.38E-02	2.57E+09	4.16E-10	3.02E-10	1.88E-05

Table 5.1. (contd)

								----- NDMA degradation -----			----- NDMA mass removal rates		
								pseudo f.o. rate		intrinsic ra	mass	mass	mass flux 3
exp.		NDMA	H_2O	NDMA	sed.	Fe2+	molar ratio	half-life	kf'	kf	flux 1	flux 2	mol ndma/
name	system	(mg/L)	(g)	(mol)	(g)	(mol)	Fe/NDMA	(h)	(1/h)	(1/h mol²)	mol NDMA/h	mol/g/day	mol Fe/d
	sediment/water, 1-D column (high sediment/water ratio), variables: fraction reduction, temperature, flow rate (residence time)												
X156A	1-D, red. Aero. Sed(di/Fe=26, X139), 1.0 h/pv	2.86	1.65	6.37E-08	11.21	4.48E-04	7.04E+03	0.243	2.85E+00	9.99E+10	1.82E-07	3.89E-07	9.73E-03
X156B	1-D, red. Aero. Sed(di/Fe=26, X139), 2.0 h/pore vol.	2.86	1.65	6.37E-08	11.21	4.48E-04	7.04E+03	0.628	1.10E+00	3.86E+10	7.03E-08	1.51E-07	3.76E-03
X156C	1-D, red. Aero. Sed(di/Fe=26, X139), 4.1 h/pv	2.86	1.65	6.37E-08	11.21	4.48E-04	7.04E+03	0.738	9.39E-01	3.29E+10	5.98E-08	1.28E-07	3.20E-03
X156D	1-D, red. Aero. Sed(di/Fe=26, X139), 16.1 h/pv	2.86	1.65	6.37E-08	11.21	4.48E-04	7.04E+03	3.378	2.05E-01	7.18E+09	1.31E-08	2.80E-08	7.00E-04
X156E	1-D, red. Aero. Sed(di/Fe=26, X139), 24.1 h/pv	2.86	1.65	6.37E-08	11.21	4.48E-04	7.04E+03	2.884	2.40E-01	8.41E+09	1.53E-08	3.28E-08	8.19E-04
X156F	1-D, red. Aero. Sed(di/Fe=26, X139), 48.1 h/pv	2.86	1.65	6.37E-08	11.21	4.48E-04	7.04E+03	14.41	4.81E-02	1.68E+09	3.06E-09	6.56E-09	1.64E-04
X156G	1-D, red. Aero. Sed(di/Fe=26, X139), 112.3 h/pv	2.86	1.65	6.37E-08	11.21	4.48E-04	7.04E+03	32.7	2.12E-02	7.42E+08	1.35E-09	2.89E-09	7.23E-05
X156H	1-D, red. Aero. Sed(di/Fe=26, X139), 294.4 h/pv	2.86	1.65	6.37E-08	11.21	4.48E-04	7.04E+03	56.75	1.22E-02	4.28E+08	7.78E-10	1.67E-09	4.16E-05
X157A	1-D, red. Aero. Sed(di/Fe=26, X139), 1.0 h/pv	2.86	1.69	6.52E-08	1.045	4.18E-05	6.41E+02	22.3	3.11E-02	1.14E+10	2.03E-09	4.66E-08	1.16E-03
X157B	1-D, red. Aero. Sed(di/Fe=26, X139), 2.0 h/pv	2.86	1.69	6.52E-08	1.045	4.18E-05	6.41E+02	15.81	4.38E-02	1.61E+10	2.86E-09	6.57E-08	1.64E-03
X157C	1-D, red. Aero. Sed(di/Fe=26, X139), 4.1 h/pv	2.86	1.69	6.52E-08	1.045	4.18E-05	6.41E+02	271.2	2.56E-03	9.37E+08	1.67E-10	3.83E-09	9.57E-05
X157D	1-D, red. Aero. Sed(di/Fe=26, X139), 17.1 h/pv	2.86	1.69	6.52E-08	1.045	4.18E-05	6.41E+02	248.2	2.79E-03	1.02E+09	1.82E-10	4.18E-09	1.05E-04
X157E	1-D, red. Aero. Sed(di/Fe=26, X139), 24.1 h/pv	2.86	1.69	6.52E-08	1.045	4.18E-05	6.41E+02	217.1	3.19E-03	1.17E+09	2.08E-10	4.78E-09	1.20E-04
X157F	1-D, red. Aero. Sed(di/Fe=26, X139), 48.6 h/pv	2.86	1.69	6.52E-08	1.045	4.18E-05	6.41E+02	612.9	1.13E-03	4.15E+08	7.38E-11	1.69E-09	4.24E-05
X157G	1-D, red. Aero. Sed(di/Fe=26, X139), 117.2 h/pv	2.86	1.69	6.52E-08	1.045	4.18E-05	6.41E+02	1665	4.16E-04	1.53E+08	2.72E-11	6.24E-10	1.56E-05
X157H	1-D, red. Aero. Sed(di/Fe=26, X139), 312.6 h/pv	2.86	1.69	6.52E-08	1.045	4.18E-05	6.41E+02	2915	2.38E-04	8.72E+07	1.55E-11	3.56E-10	8.91E-06
X158A	1-D, red. Aero. Sed(di/Fe=26), 1.0 h/pv, inj. pH 7.0	2.86	1.71	6.6E-08	11.34	4.54E-04	6.87E+03	2.354	2.94E-01	9.83E+09	1.94E-08	4.11E-08	1.03E-03
X158B	1-D, red. Aero. Sed(di/Fe=26), 2.0 h/pv, inj. pH 7.0	2.86	1.71	6.6E-08	11.34	4.54E-04	6.87E+03	59.79	1.16E-02	3.87E+08	7.65E-10	1.62E-09	4.05E-05
X158C	1-D, red. Aero. Sed(di/Fe=26), 3.6 h/pv, inj. pH 7.0	2.86	1.71	6.6E-08	11.34	4.54E-04	6.87E+03	2.071	3.35E-01	1.12E+10	2.21E-08	4.68E-08	1.17E-03
X158D	1-D, red. Aero. Sed(di/Fe=26), 16.1 h/pv, inj. pH 7.0	2.86	1.71	6.6E-08	11.34	4.54E-04	6.87E+03	2.879	2.41E-01	8.04E+09	1.59E-08	3.36E-08	8.41E-04
X158E	1-D, red. Aero. Sed(di/Fe=26), 25.5 h/pv, inj. pH 7.0	2.86	1.71	6.6E-08	11.34	4.54E-04	6.87E+03	3.654	1.90E-01	6.33E+09	1.25E-08	2.65E-08	6.63E-04
X158F	1-D, red. Aero. Sed(di/Fe=26), 48.1 h/pv, inj. pH 7.0	2.86	1.71	6.6E-08	11.34	4.54E-04	6.87E+03	12.41	5.59E-02	1.87E+09	3.69E-09	7.80E-09	1.95E-04
X158G	1-D, red. Aero. Sed(di/Fe=26), 100.1 h/pv, inj. pH 7.0	2.86	1.71	6.6E-08	11.34	4.54E-04	6.87E+03	23.57	2.94E-02	9.82E+08	1.94E-09	4.11E-09	1.03E-04
X158H	1-D, red. Aero. Sed(di/Fe=26), 305.2 h/pv, inj. pH 7.0	2.86	1.71	6.6E-08	11.34	4.54E-04	6.87E+03	44.78	1.55E-02	5.17E+08	1.02E-09	2.16E-09	5.41E-05
X159A	1-D, red. Aero. (di/Fe=26), 1.0 h/pv, inj. pH 7.0buff	2.86	1.66	6.41E-08	11.28	4.51E-04	7.04E+03	0.505	1.37E+00	4.75E+10	8.80E-08	1.87E-07	4.68E-03
X159B	1-D, red. Aero. (di/Fe=26), 2.1 h/pv, inj. pH 7.0buff	2.86	1.66	6.41E-08	11.28	4.51E-04	7.04E+03	1.11	6.24E-01	2.16E+10	4.00E-08	8.51E-08	2.13E-03
X159C	1-D, red. Aero. (di/Fe=26), 3.5 h/pv, inj. pH 7.0 buff.	2.86	1.66	6.41E-08	11.28	4.51E-04	7.04E+03	1.36	5.10E-01	1.76E+10	3.27E-08	6.95E-08	1.74E-03
X159D	1-D, red. Aero. (di/Fe=26), 17.2 h/pv, inj. pH 7.0 buff.	2.86	1.66	6.41E-08	11.28	4.51E-04	7.04E+03	7.16	9.68E-02	3.35E+09	6.20E-09	1.32E-08	3.30E-04
X159E	1-D, red. Aero. (di/Fe=26), 24.1 h/pvj. pH 7.0 buff.	2.86	1.66	6.41E-08	11.28	4.51E-04	7.04E+03	9.86	7.03E-02	2.43E+09	4.51E-09	9.59E-09	2.40E-04
X159F	1-D, red. Aero. (di/Fe=26), 48.1 h/pv, inj. pH 7.0 buff.	2.86	1.66	6.41E-08	11.28	4.51E-04	7.04E+03	11.01	6.30E-02	2.18E+09	4.03E-09	8.58E-09	2.15E-04
X159G	1-D, red. Aero. (di/Fe=26), 118 h/pv, inj. pH 7.0 buff.	2.86	1.66	6.41E-08	11.28	4.51E-04	7.04E+03	30.34	2.28E-02	7.90E+08	1.46E-09	3.12E-09	7.79E-05
X159H	1-D, red. Aero. (di/Fe=26), 310 h/pv, inj. pH 7.0 buff.	2.86	1.66	6.41E-08	11.28	4.51E-04	7.04E+03	54.93	1.26E-02	4.36E+08	8.09E-10	1.72E-09	4.30E-05
X160	Seq. red./oxic 1-D (red 8.9 h/pv, oxic 60.1 h/pv)	0.25	54.2	2.02E-08	260.2	2.19E-04	1.08E+04	10.3	6.73E-02	1.52E+10	1.36E-09	1.26E-10	1.50E-04
X161	Seq. red./oxic 1-D (red 9.0 h/pv, oxic 266 h/pv)	0.25	48.8	2.02E-08	235.7	1.98E-04	9.78E+03	5.41	1.28E-01	3.20E+10	2.59E-09	2.64E-10	3.14E-04
X162	Seq. red./oxic 1-D (red 8.1 h/pv, oxic 104 h/pv)	0.25	82.1	2.02E-08	396.4	3.33E-04	1.64E+04	7.0	9.85E-02	1.46E+10	1.99E-09	1.21E-10	1.44E-04
X180	Seq. red./oxic 1-D (red 32.0 h/pv, oxic 216.1 h/pv)	0.25	54.2	1.83E-07	260.2	2.19E-04	1.19E+03	33.2	2.09E-02	5.22E+08	3.82E-09	3.52E-10	4.19E-04
X181	Seq. red./oxic 1-D (red 10.7 h/pv, oxic 317.3 h/pv)	0.25	48.8	1.65E-07	235.7	1.98E-04	1.20E+03	7.16	9.68E-02	2.97E+09	1.59E-08	1.62E-09	1.93E-03
X182	Seq. red./oxic 1-D (red 28.3 h/pv, oxic 364.5 h/pv)	0.25	82.1	2.77E-07	396.4	3.33E-04	1.20E+03	22.5	3.08E-02	3.34E+08	8.54E-09	5.17E-10	6.15E-04
X190	Seq. red./oxic 1-D (red 148.3 h/pv, oxic 1000 h/pv)	0.25	54.2	1.83E-07	260.2	2.19E-04	1.19E+03	46.3	1.50E-02	3.74E+08	2.74E-09	2.53E-10	3.01E-04
X191	Seq. red./oxic 1-D (red 29.9 h/pv, oxic 885.8 h/pv)	0.25	48.8	1.65E-07	235.7	1.98E-04	1.20E+03	4.5	1.54E-01	4.72E+09	2.54E-08	2.58E-09	3.08E-03
X192	Seq. red./oxic 1-D (red 95.2 h/pv, oxic 1228 h/pv)	0.25	82.1	2.77E-07	396.4	3.33E-04	1.20E+03	18.9	3.67E-02	3.98E+08	1.02E-08	6.15E-10	7.32E-04
X164	1-D red. Aerojet sed. (di/Fe=26; 8.16 h/pv)	0.25	6.0	2.02E-08	27.5	1.10E-03	5.43E+04	28.6	2.42E-02	1.09E+09	4.91E-10	4.28E-10	1.07E-05
X184	1-D red. Aerojet sed. (di/Fe=26; 27.6 h/pv)	0.25	6.0	2.03E-08	27.5	1.10E-03	5.42E+04	36.8	1.88E-02	8.44E+08	3.82E-10	3.33E-10	8.34E-06
X194	1-D red. Aerojet sed. (di/Fe=26; 118.1 h/pv)	0.25	6.0	2.03E-08	27.5	1.10E-03	5.43E+04	31.0	2.24E-02	1.00E+09	4.54E-10	3.96E-10	9.89E-06
X163	Oxic Aerojet sed. in 1-D column (62.2 h/pv)	0.25	47.8	2.02E-08	217.4	4.00E-06	1.98E+02	150.4	4.61E-03	5.69E+10	9.33E-11	1.03E-11	5.60E-04
X183	Oxic Aerojet sed. in 1-D column (216.7 h/pv)	0.25	47.8	1.61E-07	217.4	4.00E-06	2.48E+01	299.1	2.32E-03	3.59E+09	3.74E-10	4.13E-11	2.24E-03
X193	Oxic Aerojet sed. in 1-D column (1626 h/pv)	0.25	47.8	1.61E-07	217.4	4.00E-06	2.48E+01	478.3	1.45E-03	2.25E+09	2.34E-10	2.58E-11	1.40E-03

Because NDMA degradation was an abiotic reaction, rates were not a function of NDMA concentration (Figure 5.12c). Partially reduced sediment had less ferrous iron than fully reduced sediment, so the Fe/NDMA ratio was smaller (and NDMA degradation rates slower (Figure 5.12b).

The rate of NDMA degradation in sequential reduced-oxic systems (purple diamonds, Figure 5.12b) was essentially the same as the reduced sediment columns, as it appears the addition of the downgradient oxic sediment column did not add any additional reactivity. As described in detail in Section 4.4.3, both NDMA degradation and NDMA mineralization in the sequential reduced-oxic sediment columns was inefficient. It is hypothesized that NDMA biomineralization in oxic systems proceeds along a different pathway than the abiotic NDMA mineralization in reduced systems, so DMA and other intermediates formed in the reduced sediment column are not readily degraded in the downgradient oxic columns.

NDMA mineralization rates were also quantified in oxic, anaerobic, and reduced sediment systems and portions of subsurface systems (i.e., just aqueous solution, mineral phases,

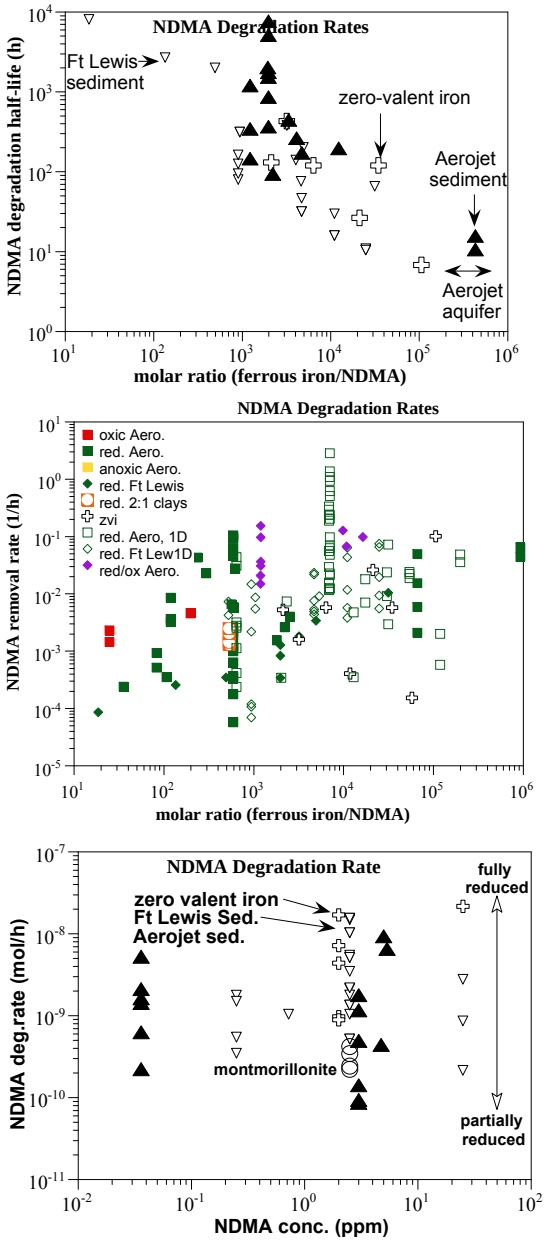

Figure 5.12. NDMA degradation rate as a function of (a) Fe/NDMA ratio and b) NDMA concentration.

Table 5.2). The molar ratio of ferrous iron to NDMA in these sediment systems was important for NDMA mineralization in reduced sediments (Figure 5.13, green squares), as additional ferrous iron promotes additional NDMA degradation.

In contrast, NDMA mineralization in oxic sediments was not related to the ferrous iron/NDMA ratio (i.e., yellow and red squares all plot at a low ratio). In batch systems, microbial isolates (Figure 5.13, crosses plotted on Y-axis) had NDMA mineralization rates that were comparable to oxic sediment-water systems (i.e., biomineralization), but reduced sediment systems (i.e., abiotic mineralization) were slower by one or more orders of magnitude. This suggests that *ex situ* treatment of biomineralization (as is already being done) would be effective. In contrast, in 1-D column systems, the NDMA mineralization was fastest in the reduced sediment columns (circled green squares in Figure 5.13), with mineralization in the oxic columns 55 times slower (circled red squares in Figure 5.13). The sequential reduced-oxic sediment columns showed rates in between these two systems (light green circles), although further analysis showed that nearly all of the reactivity was occurring in the reduced sediment columns.

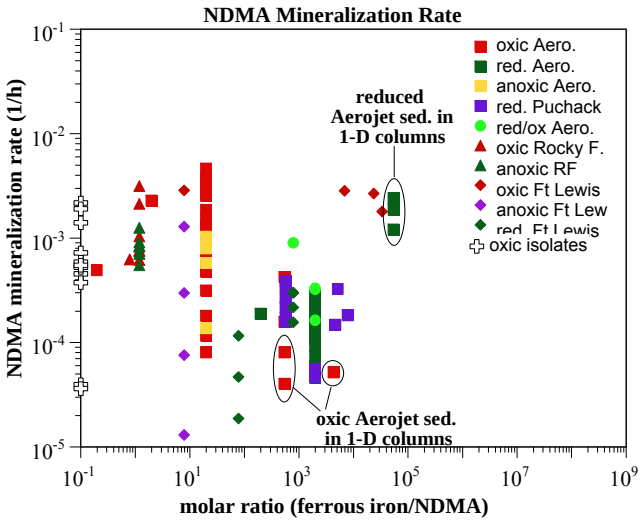

Figure 5.13. NDMA mineralization and ferrous iron/NDMA ratio.

Table 5.2. NDMA mineralization rate and extent.

								---- NDMA mineralization rate ----				mineralization extent		
exp.	description	NDMA (mg/L)	H2O (g)	NDMA (mol)	sed. (g)	Fe2+ (mol)	ratio Fe/NDMA	half-life (h)	first-order rate (1/h)	intrinsic re (1/h mol2)	mass flux1 mol NDMA/h	(% CO2)	at t (h)	mass flux 2 mol/g/day
	Batch Systems with Aerojet, CA subsurface sediment (255' depth)/water system (all: oxic, anaerobic, reduced, sequential reduced/oxic)													
wes5	oxic Aerojet sediment, pH 9.1	25.0	6	2.02E-06	1.0	4.00E-07	1.98E-01	1406	4.93E-04	6.09E+08	9.98E-10	25.6	600	1.97E-02
S82	oxic Aerojet sediment, pH 9.1	2.5	6.0	2.02E-07	1.0	4.00E-07	1.98E+00	301.1	2.30E-03	2.84E+10	4.66E-10	36.5	1963	4.22E-04
S83	oxic Aerojet sediment, pH 9.1	0.25	6.0	2.02E-08	1.0	4.00E-07	1.98E+01	309.7	1.07E-03	2.31E+11	3.80E-11	36.5	1963	5.16E-05
S84	oxic Aerojet sediment, pH 9.1	0.0025	6.0	2.02E-10	1.0	4.00E-07	1.98E+03	305.7	2.27E-03	2.80E+13	4.59E-13	36.9	1963	4.29E-07
S85	oxic Aerojet sediment, pH 9.1	0.00010	6.0	8.1E-12	1.0	4.00E-07	4.94E+04	378.3	1.83E-03	5.66E+14	1.48E-14	28.1	1963	2.12E-08
S86	oxic Aerojet sediment, pH 9.1	0.000010	6.0	8.1E-13	1.0	4.00E-07	4.94E+05	355.6	1.95E-03	6.02E+15	1.58E-15	25.9	1963	1.99E-09
S87	red. Aerojet sed.(di/Fe=26,W21, pH8.5)	2.5	6.0	2.02E-07	1.0	4.00E-05	1.98E+02	3672	1.89E-04	2.33E+07	3.82E-11	11.1	1316	5.15E-03
S88	red. Aerojet sed.(di/Fe=26,W21, pH8.5)	0.25	6.0	2.02E-08	1.0	4.00E-05	1.98E+03	4098	1.69E-04	2.09E+08	3.42E-12	12.3	1316	5.75E-04
S89	red. Aerojet sed.(di/Fe=26,W21, pH8.5)	0.0025	6.0	2.02E-10	1.0	4.00E-05	1.98E+05	3083	2.25E-04	2.78E+10	4.55E-14	15.6	1316	4.32E-06
S90	red. Aerojet sed.(di/Fe=26,W21, pH8.5)	0.00010	6.0	8.1E-12	1.0	4.00E-05	4.94E+06	3048	2.27E-04	7.02E+11	1.84E-15	10.1	1316	1.71E-07
S91	red. Aerojet sed.(di/Fe=26,W21, pH8.5)	0.000010	6.0	8.1E-13	1.0	4.00E-05	4.94E+07	10500	6.60E-05	2.04E+12	5.35E-17	2.1	1316	5.89E-08
S92	oxic Aerojet sed.+ 1 mL methane	0.25	6.0	2.02E-08	1.0	4.00E-07	1.98E+01	8633	8.03E-05	9.91E+09	1.63E-12	5.7	1317	1.21E-03
S93	oxic Aerojet sed.+ 1 mL propane	0.25	6.0	2.02E-08	1.0	4.00E-07	1.98E+01	471	1.47E-03	1.82E+11	2.98E-11	30.9	1317	6.60E-05
S94	oxic Aerojet sed.+ 50 uL toluene	0.25	6.0	2.02E-08	1.0	4.00E-07	1.98E+01	5906	1.17E-04	1.45E+10	2.38E-12	8.2	1317	8.28E-04
S95	oxic Aerojet sed.+ 1 mL acetylene	0.25	6.0	2.02E-08	1.0	4.00E-07	1.98E+01	778	8.91E-04	1.10E+11	1.80E-11	22.0	1317	1.09E-04
S96	anaerobic Aerojet sed.	0.25	6.0	2.02E-08	1.0	4.00E-07	1.98E+01	672	7.95E-04	9.81E+10	1.61E-11	18.0	1317	1.22E-04
S97	anaerobic Aerojet sed.+ 1 mL methane	0.25	6.0	2.02E-08	1.0	4.00E-07	1.98E+01	824	8.41E-04	1.04E+11	1.70E-11	20.5	1317	1.16E-04
S98	anaerobic Aerojet sed.+ 1 mL propane	0.25	6.0	2.02E-08	1.0	4.00E-07	1.98E+01	670	1.03E-03	1.28E+11	2.09E-11	22.3	1317	9.39E-05
S99	anaerobic Aerojet sed.+ 50 uL toluene	0.25	6.0	2.02E-08	1.0	4.00E-07	1.98E+01	5045	1.37E-04	1.70E+10	2.78E-12	11.1	1317	7.07E-04
S100	anaerobic Aerojet sed.+ 1 mL acetylene	0.25	6.0	2.02E-08	1.0	4.00E-07	1.98E+01	1204	5.76E-04	7.11E+10	1.17E-11	15.9	1317	1.69E-04
S101	red. Aerojet sed.(di/Fe=26)	0.25	6.0	2.02E-08	1.0	4.00E-05	1.98E+03	2957	2.34E-04	2.89E+08	4.75E-12	11.9	1317	4.15E-04
S102	red. Aerojet (di/Fe=26)+ 1 mL methane	0.25	6.0	2.02E-08	1.0	4.00E-05	1.98E+03	4531	1.53E-04	1.89E+08	3.10E-12	13.8	1317	6.35E-04
S103	red. Aerojet (di/Fe=26)+ 1 mL propane	0.25	6.0	2.02E-08	1.0	4.00E-05	1.98E+03	4860	1.43E-04	1.76E+08	2.89E-12	10.2	1317	6.81E-04
S104	red. Aerojet (di/Fe=26)+ 50 uL toluene	0.25	6.0	2.02E-08	1.0	4.00E-05	1.98E+03	4135	1.68E-04	2.07E+08	3.39E-12	9.6	1317	5.80E-04
S105	red. Aerojet (di/Fe=26)+ 1 mL acetylene	0.25	6.0	2.02E-08	1.0	4.00E-05	1.98E+03	3420	2.03E-04	2.50E+08	4.10E-12	15.2	1317	4.80E-04
S106	red. Aerojet (di/Fe=26)+ 100uL yeast	0.25	6.0	2.02E-08	1.0	4.00E-05	1.98E+03	2497	2.78E-04	3.43E+08	5.62E-12	10.3	1317	3.50E-04
S107	red. Aerojet (di/Fe=26)+ 100uL humic acid	0.25	6.0	2.02E-08	1.0	4.00E-05	1.98E+03	3257	2.13E-04	2.63E+08	4.31E-12	13.9	1317	4.57E-04
S108	red. Aerojet (di/Fe=26)+ 1 uL TCE	0.25	6.0	2.02E-08	1.0	4.00E-05	1.98E+03	2629	2.64E-04	3.26E+08	5.34E-12	16.4	1317	3.69E-04
X165	Red. Aerojet sed., + gluteraldehyde (bactericide)	0.25	6.0	2.02E-08	1.0	4.00E-05	1.98E+03	3617	1.92E-04	2.37E+08	3.88E-12	19.5	1940	5.07E-04
X167	Reduced Aerojet sediment + 30 mM nitrate	0.25	6.0	2.02E-08	1.0	4.00E-05	1.98E+03	5777	1.20E-04	1.48E+08	2.43E-12	8.2	1940	8.10E-04
X168	Red Aerojet + 30 mM nitrate + 100 mM glucose	0.25	6.0	2.02E-08	1.0	4.00E-05	1.98E+03	4478	1.55E-04	1.91E+08	3.13E-12	9.2	1940	6.28E-04
S109	red. Aerojet sed.(di/Fe=26), 68 day prest.	0.25	6.0	2.02E-08	1.0	4.00E-05	1.98E+03	3756	1.85E-04	2.28E+08	3.74E-12	5.8	1002	5.27E-04
S110	red. Aerojet +1 ppm yeast. 68 day prest.	0.25	6.0	2.02E-08	1.0	4.00E-05	1.98E+03	7531	9.20E-05	1.14E+08	1.86E-12	5.5	1002	1.06E-03
S111	red. Aerojet+10 ppm yeast, 68 day prest.	0.25	6.0	2.02E-08	1.0	4.00E-05	1.98E+03	5097	1.36E-04	1.68E+08	2.75E-12	4.7	1002	7.15E-04
S112	red. Aerojet +100 ppm yeast, 68 day prest.	0.25	6.0	2.02E-08	1.0	4.00E-05	1.98E+03	5880	1.18E-04	1.46E+08	2.39E-12	4.6	1002	8.24E-04
S113	red. Aerojet+1.6 ppm humic acid, 68d prest.	0.25	6.0	2.02E-08	1.0	4.00E-05	1.98E+03	4320	1.60E-04	1.98E+08	3.25E-12	6.1	1002	6.06E-04
S114	red. Aerojet+16 ppm humic acid, 68d prest.	0.25	6.0	2.02E-08	1.0	4.00E-05	1.98E+03	9220	7.52E-05	9.28E+07	1.52E-12	4.2	1002	1.29E-03
S115	red. Aerojet+160 ppm humic acid, 68d prest	0.25	6.0	2.02E-08	1.0	4.00E-05	1.98E+03	6486	1.07E-04	1.32E+08	2.16E-12	5.2	1002	9.09E-04
S116	oxic Aerojet sediment, 68 day prestimulation	0.25	6.0	2.02E-08	1.0	4.00E-07	1.98E+01	224.2	3.09E-03	3.82E+11	6.26E-11	44.4	1002	3.14E-05
S117	oxic Aerojet sed.+1 ppm yeast, 68d prest.	0.25	6.0	2.02E-08	1.0	4.00E-07	1.98E+01	533	1.30E-03	1.61E+11	2.63E-11	20.2	1002	7.47E-05
S118	oxic Aerojet sed.+10 ppm yeast, 68d prest.	0.25	6.0	2.02E-08	1.0	4.00E-07	1.98E+01	273	2.54E-03	3.13E+11	5.14E-11	48.3	1002	3.83E-05
S119	oxic Aerojet sed.+100 ppm yeast, 68d prest.	0.25	6.0	2.02E-08	1.0	4.00E-07	1.98E+01	189.2	3.66E-03	4.52E+11	7.42E-11	51.6	1002	2.65E-05
S120	oxic Aerojet+1.6 ppm humic acid, 68d prest	0.25	6.0	2.02E-08	1.0	4.00E-07	1.98E+01	224.2	3.09E-03	3.82E+11	6.26E-11	45.9	1002	3.14E-05
S121	oxic Aerojet+16 ppm humic acid, 68d prest	0.25	6.0	2.02E-08	1.0	4.00E-07	1.98E+01	269.3	2.57E-03	3.18E+11	5.21E-11	45.6	1002	3.78E-05
S122	oxic Aerojet+160 ppm humic acid, 68d prest	0.25	6.0	2.02E-08	1.0	4.00E-07	1.98E+01	532	1.30E-03	1.61E+11	2.64E-11	33.4	1002	7.46E-05
S123	oxic Aerojet+prop.(prop/ox=0.04), 68d pre	0.25	6.0	2.02E-08	1.0	4.00E-07	1.98E+01	194	3.57E-03	4.41E+11	7.23E-11	45.8	1002	2.72E-05
S124	oxic Aerojet+prop.(prop/ox=0.4), 68d pre	0.25	6.0	2.02E-08	1.0	4.00E-07	1.98E+01	149	4.65E-03	5.74E+11	9.42E-11	59.6	1002	2.09E-05
S125	oxic Aerojet+prop.(prop/ox=4), 68d prest.	0.25	6.0	2.02E-08	1.0	4.00E-07	1.98E+01	190	3.65E-03	4.50E+11	7.39E-11	47.4	1002	2.66E-05
S209	red. Aerojet (1000h),then ox. Aero. sed.	0.25	6.0	2.02E-08	1.0	4.00E-05	1.98E+03	12500	5.55E-05	6.85E+07	1.12E-12	10.8	3044	1.75E-03
S210	red. Aerojet+yeast (1000h),ox. Aero. sed.	0.25	6.0	2.02E-08	1.0	4.00E-05	1.98E+03	13070	5.30E-05	6.55E+07	1.07E-12	9.5	3044	1.83E-03
S211	S111aq(1000h) placed w/oxic Aero. sed.	0.25	6.0	2.02E-08	1.0	4.00E-05	1.98E+03	14620	4.74E-05	5.85E+07	9.60E-13	8.8	3044	2.05E-03
S212	red. Aerojet (1000h)+yeast; oxidized	0.25	6.0	2.02E-08	1.0	4.00E-05	1.98E+03	15060	4.60E-05	5.68E+07	9.32E-13	8.3	3044	2.11E-03
S213	red. Aerojet (1000h)+1.6 ppm humic acid	0.25	6.0	2.02E-08	1.0	4.00E-05	1.98E+03	11510	6.02E-05	7.44E+07	1.22E-12	10.8	3044	1.61E-03
S214	red. Aerojet (di/Fe=26)+16 ppm humic acid	0.25	6.0	2.02E-08	1.0	4.00E-05	1.98E+03	11640	5.95E-05	7.35E+07	1.21E-12	12.6	3044	1.63E-03
S215	red. Aerojet (di/Fe=26)+160 ppm humic acid	0.25	6.0	2.02E-08	1.0	4.00E-05	1.98E+03	13550	5.12E-05	6.32E+07	1.04E-12	8.7	3044	1.90E-03
S216	oxic Aerojet sed.(1000h), then oxic sed.	0.25	6.0	2.02E-08	1.0	4.00E-07	1.98E+01	1436	4.83E-04	5.96E+08	9.77E-12	53.7	3044	2.01E-04
S217	oxic Aerojet + yeast (1000h), then oxic sed.	0.25	6.0	2.02E-08	1.0	4.00E-07	1.98E+01	3827	1.81E-04	2.24E+08	3.67E-12	25.0	3044	5.37E-04
S218	oxic Aerojet + yeast (10ppm), then oxic sed.	0.25	6.0	2.02E-08	1.0	4.00E-07	1.98E+01	1373	5.05E-04	6.23E+08	1.02E-11	52.2	3044	1.93E-04
S219	oxic Aerojet+100 ppm yeast. O2 at 1000h	0.25	6.0	2.02E-08	1.0	4.00E-07	1.98E+01	1195	5.80E-04	7.16E+08	1.17E-11	58.6	3044	1.68E-04
S220	oxic Aerojet+1.6 ppm HA , ox.sed. at 1000h	0.25	6.0	2.02E-08	1.0	4.00E-07	1.98E+01	1371	5.06E-04	6.24E+08	1.02E-11	55.6	3044	1.92E-04
S221	oxic Aerojet+16 ppm HA, ox. sed. at 1000h	0.25	6.0	2.02E-08	1.0	4.00E-07	1.98E+01	1306	5.31E-04	6.55E+08	1.07E-11	58.9	3044	1.83E-04
S222	oxic Aerojet+160 ppm HA, O2 at 1000h	0.25	6.0	2.02E-08	1.0	4.00E-07	1.98E+01	2193	3.16E-04	3.90E+08	6.40E-12	37.5	3044	3.07E-04
S223	oxic Aerojet +propane, ox. sed. at 1000 h	0.25	6.0	2.02E-08	1.0	4.00E-07	1.98E+01	1449	4.78E-04	5.91E+08	9.69E-12	54.7	3044	2.03E-04
S224	oxic Aerojet +propane, ox. sed. at 1000 h	0.25	6.0	2.02E-08	1.0	4.00E-07	1.98E+01	980	7.07E-04	8.73E+08	1.43E-11	63.7	3044	1.37E-04
S225	oxic Aerojet sed.+prop., O2+prop at 1000h	0.25	6.0	2.02E-08	1.0	4.00E-07	1.98E+01	1433	4.84E-04	5.97E+08	9.79E-12	50.4	3044	2.01E-04

In the reduced sediment, mineralization rates of the different sediments show significant differences. Although NDMA mineralization is mainly controlled by the adsorbed ferrous iron on mineral phases, accounting for just this ferrous iron (reductive capacity) for the Aerojet sediment (100 µmol/g) and Ft. Lewis sediment (160 µmol/g) did not show the same mineralization rate (corrected for the difference in reductive capacity. The Aerojet sediment had higher mineralization rates than the Ft. Lewis sediment. Although some of the minor mineral phases are characterized in both sediments, there is no explanation for the difference in reactivity. Characterization of the Aerojet reduced mineral phases before and after reactions with NDMA

by Mossbauer was unsuccessful due to the low fraction of iron phases in the sediment, although may have revealed some additional information of which phases ferrous iron was adsorbed to was controlling NDMA degradation.

Table 5.2. (contd)

								---- NDMA mineralization rate ----				mineralization extent		
		NDMA	H2O	NDMA	sed.	Fe2+	ratio	half-life	first-order	intrinsic ra	mass flux1			mass flux 2
exp.	description	(mg/L)	(g)	(mol)	(g)	(mol)	Fe/NDMA	(h)	rate (1/h)	(1/h mol2)	mol NDMA/h	(% CO2)	at t (h)	mol/g/day
	1-D Columns with Aerojet, CA subsurface sediment (255' depth)/water system (all: oxic, anaerobic, reduced, sequential reduced/oxic)													
X160	Seq. red./oxic 1-D (red 8.0 h/pv, oxic 60.1 h/pv)	0.25	54.2	2.02E-08	260.2	1.04E-04	5.14E+03	2124	3.26E-04	2.24E+08	3.67E-12	4.4	410	2.98E-04
X161	Seq. red./oxic 1-D (red 9.0 h/pv, oxic 266 h/pv)	0.25	48.8	2.02E-08	235.7	9.43E-05	4.66E+03	4694	1.48E-04	2.24E+08	3.67E-12	12.1	410	6.58E-04
X162	Seq. red./oxic 1-D (red 8.1 h/pv, oxic 104 h/pv)	0.25	82.1	2.02E-08	396.4	1.59E-04	7.83E+03	3805	1.82E-04	2.24E+08	3.67E-12	4.8	410	5.34E-04
X180	Seq. red./oxic 1-D (red 32.0 h/pv, oxic 216.1 h/pv)	0.25	54.2	1.83E-07	260.2	1.04E-04	5.69E+02	1790	3.87E-04	2.24E+08	3.67E-12	10.4	590	2.27E-03
X181	Seq. red./oxic 1-D (red 10.7 h/pv, oxic 317.3 h/pv)	0.25	48.8	1.65E-07	235.7	9.43E-05	5.72E+02	2030	3.41E-04	2.24E+08	3.67E-12	13.5	590	2.32E-03
X182	Seq. red./oxic 1-D (red 28.3 h/pv, oxic 364.5 h/pv)	0.25	82.1	2.77E-07	396.4	1.59E-04	5.72E+02	2598	2.67E-04	2.24E+08	3.67E-12	10.1	590	4.98E-03
X190	Seq. red./oxic 1-D (red 148.3 h/pv, oxic 1000 h/pv)	0.25	54.2	1.83E-07	260.2	1.04E-04	5.69E+02	3177	2.18E-04	2.24E+08	3.67E-12	16.1	822	4.02E-03
X191	Seq. red./oxic 1-D (red 29.9 h/pv, oxic 885.8 h/pv)	0.25	48.8	1.65E-07	235.7	9.43E-05	5.72E+02	3992	1.74E-04	2.24E+08	3.67E-12	22.5	822	4.55E-03
X192	Seq. red./oxic 1-D (red 95.2 h/pv, oxic 1220 h/pv)	0.25	82.1	2.77E-07	396.4	1.59E-04	5.72E+02	4411	1.57E-04	2.24E+08	3.67E-12	25.7	822	8.46E-03
X164	1-D red. Aerojet sed. (di/Fe=26; 8.16 h/pv)	0.25	6.0	2.02E-08	27.5	1.10E-03	5.43E+04	368.6	1.88E-03	8.44E+07	3.81E-11	2.2	410	5.17E-05
X184	1-D red. Aerojet sed. (di/Fe=26; 27.6 h/pv)	0.25	6.0	2.03E-08	27.5	1.10E-03	5.42E+04	287.7	2.41E-03	1.08E+08	4.89E-11	6.2	590	4.04E-05
X194	1-D red. Aerojet sed. (di/Fe=26; 118.1 h/pv)	0.25	6.0	2.03E-08	27.5	1.10E-03	5.43E+04	573.5	1.21E-03	5.42E+07	2.45E-11	16.8	822	8.05E-05
X163	Oxic Aerojet sed. in 1-D column (62.2 h/pv)	0.25	47.8	2.02E-08	217.4	8.70E-05	4.29E+03	838.9	8.26E-04	4.69E+08	1.67E-11	4.7	410	1.18E-04
X183	Oxic Aerojet sed. in 1-D column (216.7 h/pv)	0.25	47.8	1.61E-07	217.4	8.70E-05	5.39E+02	1642	4.22E-04	3.01E+07	6.81E-11	6.2	590	1.83E-03
X193	Oxic Aerojet sed. in 1-D column (1626 h/pv)	0.25	47.8	1.61E-07	217.4	8.70E-05	5.39E+02	4398	1.58E-04	1.12E+07	2.54E-11	25.2	822	4.91E-03
	Puchack subsurface sediment (273' depth)/water system (naturally reduced clay with NOM)													
S71	natural reduced Puchack, NJ sediment	2.5	30	1.01E-06	5.0	7.95E-04	7.85E+02	769	9.01E-04	1.12E+06	9.13E-10	28.4	2155	5.39E-03
X166	natural reduced Puchack, NJ sed. + gluteraldehy	0.25	6.0	2.02E-08	1.0	4.00E-05	1.98E+03	2136	3.25E-04	4.01E+08	6.57E-12	19.5	1940	3.00E-04
X171	natural reduced Puchack, NJ sed., 2.5% organic	0.25	6.0	2.02E-08	1.0	4.00E-05	1.98E+03	2103	3.30E-04	4.07E+08	6.67E-12	12.4	1940	2.95E-04
X172	natural reduced Puchack, NJ sed. organic matte	0.25	6.0	2.02E-08	1.0	4.00E-05	1.98E+03	4228	1.64E-04	2.02E+08	3.32E-12	9.5	1940	5.93E-04
	Batch systems with Ft Lewis, WA subsurface sediment (60' depth)/water system (oxic, anaerobic, reduced)													
S66	ox.Ft Lewis sediment	2.5	30	1.01E-06	5.0	7.95E-06	7.85E+00	241.8	2.87E-03	3.56E+08	2.90E-09	53.1	2155	1.70E-03
S67	anox.FtLew sed,S67	2.5	30	1.01E-06	5.0	7.95E-06	7.85E+00	611.1	1.13E-03	1.41E+08	1.15E-09	51.2	2155	4.28E-03
S68	anox.FtLew sed+bact.,S68	2.5	30	1.01E-06	5.0	7.95E-06	7.85E+00	53485	1.30E-05	1.61E+06	1.31E-11	2.48	2155	3.75E-01
S69	anox.FtLew sed + gluc,S69	2.5	30	1.01E-06	5.0	7.95E-06	7.85E+00	538.6	1.29E-03	1.60E+08	1.30E-09	45.4	2155	3.78E-03
S70	anox.FtLew sed+zvi, S70	2.5	30	1.01E-06	5.0	7.95E-06	7.85E+00	9138	7.59E-05	9.42E+06	7.68E-11	6.26	2155	6.41E-02
S72	red.FtLew (d/Fe=28),S72	2.5	30	1.01E-06	5.0	7.95E-04	7.85E+02	2330	2.98E-04	3.70E+05	3.01E-10	7.76	2155	1.63E-02
S73	red.FtLew (d/Fe=1.6),S73	2.5	30	1.01E-06	5.0	7.95E-04	7.85E+02	4431	1.56E-04	1.94E+05	1.58E-10	6.33	2155	3.11E-02
S74	red.FtLewd/Fe1.6+trnut,S74	2.5	30	1.01E-06	5.0	7.95E-04	7.85E+02	3190	2.17E-04	2.70E+05	2.20E-10	4.15	1097	2.24E-02
S75	red.FtLew sed,di/Fe0.3,S75	2.5	30	1.01E-06	5.0	7.95E-04	7.85E+02	2295	3.02E-04	3.75E+05	3.06E-10	55.8	2014	1.61E-02
S76	ox.Ft Lewis sediment	0.0025	6	2.02E-10	1.0	1.59E-06	7.85E+03	244.2	2.84E-03	8.82E+12	5.75E-13	78.9	2014	3.42E-07
S77	ox.Ft Lewis sediment	2.50E-05	100	3.37E-11	5.0	7.95E-06	2.36E+05	258.8	2.68E-03	9.98E+12	9.04E-14	80.6	2014	6.05E-08
S78	ox.Ft Lewis sediment	2.50E-06	100	3.37E-12	5.0	7.95E-06	2.36E+06	384.2	1.80E-03	6.72E+13	6.09E-15	73.9	2014	8.98E-09
S79	reduced Ft Lewis sed. (d/Fe=28)	0.0025	6	2.02E-10	1.0	1.59E-04	7.85E+05	3667	1.89E-04	5.87E+09	3.83E-14	12.4	2014	5.14E-06
S80	reduced Ft Lewis sed. (d/Fe=28)	2.50E-05	100	3.37E-11	5.0	7.95E-04	2.36E+07	4517	1.53E-04	5.72E+09	5.18E-15	15.1	2014	1.06E-06
S81	reduced Ft Lewis sed. (d/Fe=28)	2.50E-06	100	3.37E-12	5.0	7.95E-04	2.36E+08	4861	1.43E-04	5.31E+10	4.81E-16	10.4	2014	1.14E-07
wes1	reduced Ft Lewis sed (di/Fe = 30)	25.0	6	2.02E-06	1.0	1.59E-04	7.85E+01	37000	1.87E-05	5.82E+04	3.79E-11	2.7	1416	5.19E-01
wes2	reduced Ft Lewis sed (di/Fe = 1.5)	25.0	6	2.02E-06	1.0	1.59E-04	7.85E+01	14800	4.68E-05	1.45E+05	9.48E-11	6.2	1416	2.08E-01
wes3	reduced Ft Lewis sed (di/Fe = 0.3)	25.0	6	2.02E-06	1.0	1.59E-04	7.85E+01	6000	1.16E-04	3.59E+05	2.34E-10	15.1	1416	8.41E-02
wes4	oxic Ft Lewis sed.	25.0	6	2.02E-06	1.0	1.59E-06	7.85E-01	1730	4.01E-04	1.24E+08	8.11E-10	17.7	1416	2.43E-02
	Batch systems with Rocky Flats, CO soil (0-6' depth)/water system (oxic, anaerobic)													
wesA	oxic Rocky Flats Arsenal sed.	25.0	6	2.02E-06	1.0	1.59E-06	7.85E-01	1112	6.23E-04	1.94E+08	1.26E-09	31.2	600	1.56E-02
	oxic Rocky Flats Arsenal, bog sed.*	10.0	100	1.35E-05	10.0	1.59E-05	1.18E+00	325	2.13E-03	9.94E+06	2.88E-08	61.0	720	3.04E-02
	anoxic Rocky Flats Arsenal, bog sed.*	10.0	100	1.35E-05	10.0	1.59E-05	1.18E+00	838	8.27E-04	3.85E+06	1.12E-08	32.0	720	7.83E-02
	oxic Rocky Flats Arsenal, E.end sed.*	10.0	100	1.35E-05	10.0	1.59E-05	1.18E+00	920	7.53E-04	3.51E+06	1.02E-08	31.0	720	8.60E-02
	anoxic Rocky Flats Arsenal, E.end sed.	10.0	100	1.35E-05	10.0	1.59E-05	1.18E+00	902	7.06E-04	3.29E+06	9.53E-09	29.0	720	9.10E-02
	oxic Rocky Flats Arsenal, D.Street sed.*	10.0	100	1.35E-05	10.0	1.59E-05	1.18E+00	909	7.63E-04	3.55E+06	1.03E-08	38.5	720	8.50E-02
	anoxic Rocky Flats Arsenal, D.Street sed.	10.0	100	1.35E-05	10.0	1.59E-05	1.18E+00	823	8.42E-04	3.92E+06	1.14E-08	37.0	720	7.69E-02
	oxic Rocky Flats Arsenal, S.end sed.*	10.0	100	1.35E-05	10.0	1.59E-05	1.18E+00	1120	6.19E-04	2.88E+06	8.35E-09	31.5	720	1.05E-01
	anoxic Rocky Flats Arsenal, S.end sed.	10.0	100	1.35E-05	10.0	1.59E-05	1.18E+00	1260	5.50E-04	2.56E+06	7.43E-09	29.4	720	1.18E-01
	oxic Rocky Flats Arsenal, W.end sed.*	10.0	100	1.35E-05	10.0	1.59E-05	1.18E+00	220	3.15E-03	1.47E+07	4.25E-08	71.0	720	2.06E-02
	anoxic Rocky Flats Arsenal, W.end sed.	10.0	100	1.35E-05	10.0	1.59E-05	1.18E+00	552	1.26E-03	5.85E+06	1.70E-08	39.0	720	5.16E-02
	oxic Rocky Flats Arsenal, GAC*	10.0	100	1.35E-05	10.0	1.59E-05	1.18E+00	669	1.04E-03	4.83E+06	1.40E-08	30.2	720	6.25E-02
	anoxic Rocky Flats Arsenal, GAC*	10.0	100	1.35E-05	10.0	1.59E-05	1.18E+00	760	9.12E-04	4.25E+06	1.23E-08	37.0	720	7.10E-02
	Batch systems with bacterial isolates (all oxic)					**cells/mL**				**(1/h mol cfu)**				
wesB	*Gordonia dulfuicans* (tr. nutr, no C, N)	25.0	6	2.02E-06	--	5.0E+08		1523	4.55E-04	4.50E-07	9.22E-10	23.9	600	2.14E-02
wesC	*Gordonia rubripertincta* (tr. nutr, no C, N)	25.0	6	2.02E-06	--	5.0E+08		962	7.21E-04	7.12E-07	1.46E-09	35.1	600	1.35E-02
wesD	*Gordonia nitida* (tr. nutr, no C, N)	25.0	6	2.02E-06	--	5.0E+08		1175	5.90E-04	5.82E-07	1.19E-09	29.8	600	1.65E-02
wesE	*Gordonia polyisoprenivorans* (no C, N)	25.0	6	2.02E-06	--	5.0E+08		320	2.17E-03	2.14E-06	4.38E-09	72.7	600	4.49E-03
wesF	*Gordonia alkanivorans* (tr. nutr, no C, N)	25.0	6	2.02E-06	--	5.0E+08		364	1.91E-03	1.88E-06	3.86E-09	68.1	600	5.10E-03
wesG	*Gordonia amarae* (tr. nutr, no C, N)	25.0	6	2.02E-06	--	5.0E+08		1318	5.26E-04	5.19E-07	1.06E-09	27.1	600	1.85E-02
wesH	*Gordonia sp. KTR9* (tr. nutr, no C, N)	25.0	6	2.02E-06	--	5.0E+08		497	1.40E-03	1.38E-06	2.83E-09	56.7	600	6.96E-03
wesI	*Gordonia sp. KTR9* (C + N addition)	25.0	6	2.02E-06	--	5.0E+08		17641	3.93E-05	3.88E-08	7.96E-11	2.33	600	2.47E-01
wesJ	*Gordonia sp. KTR9* (C addition)	25.0	6	2.02E-06	--	5.0E+08		19135	3.62E-05	3.58E-08	7.33E-11	2.15	600	2.68E-01
wesK	*Gordonia sp. KTR9* (N addition)	25.0	6	2.02E-06	--	5.0E+08		1853	3.74E-04	3.69E-07	7.57E-10	20.1	600	2.60E-02
wesL	*Williamsia sp. KTR4* (tr. nutr. no C. N)	25.0	6	2.02E-06	--	5.0E+08		1263	5.49E-04	5.42E-07	1.11E-09	28.1	600	1.77E-02
	*data from Gunnison et al., 2000. Fe2+ content estimated													

The comparison of NDMA degradation rate to NDMA mineralization rate should show a correlation in reduced sediment, if mineralization occurred on the same surface sites that NDMA was initially degraded to DMA on. Reduced sediment with greater ferrous iron degraded NDMA more quickly (x-axis, Figure 5.14), but there was essentially no correlation with the mineralization rate, which appeared to proceed at about the same rate in all reduced sediment. Nearly all of the data points were from batch experiments. Because there is a good correlation between ferrous iron and the NDMA degradation rate (Figure 5.12a), but not with abiotic NDMA mineralization, this suggests a rate limiting step for mineralization that is not a function of the ferrous iron concentration.

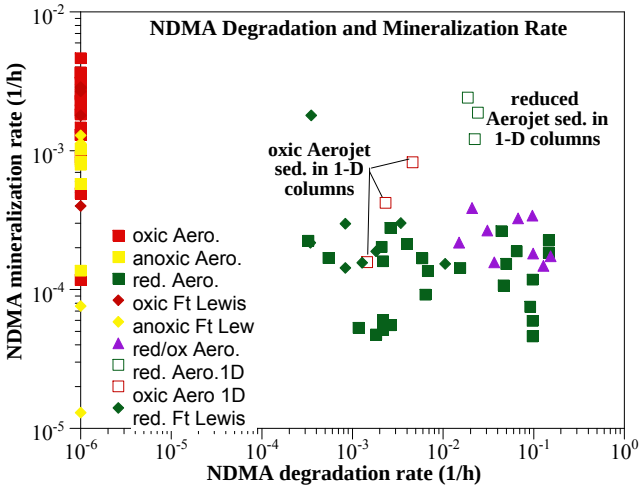

Figure 5.14. Correlation of NDMA degradation and mineralization in reduced and oxic sediments.

The only exceptions were the 1-D column experiments (open green squares, Figure 5.14), which did show a higher NDMA mineralization rate. Overall, this comparison shows that the most rapid NDMA mineralization rates were observed in: a) batch systems with oxic sediment, and b) 1-D column systems with reduced sediment, which points to either *ex situ* oxic bioreactor or an *in situ* reduced sediment zone (and not *in situ* bioremediation).

A comparison of NDMA mineralization rate (as a half-life) to mineralization extent shows a general correlation (Figure 5.15) that indicates oxic bioreactors are the most efficient systems. Certainly, the highest mineralization extents (70% to 80%) were in oxic sediments. However, in 1-D columns (noted in Figure 5.15) showed that the NDMA mineralization rate observed in reduced sediment columns were as fast as any batch bioreactor (and 55 times faster than 1-D columns with oxic, biostimulated sediment). The mineralization extent in the reduced sediment columns was low to moderate (2.2%, 6.2%, and 16.8%; higher than any reduced batch system), but these were limited by the flow rate in the columns (i.e., experiments were not exhaustive to conduct longer residence times that should result in higher mineralization extents. In comparison, the mineralization extents for comparable batch systems were for 800 to 3200 hours. Mineralization rate and extent for microbial isolates (crosses) followed the same trend observed in sediment systems.

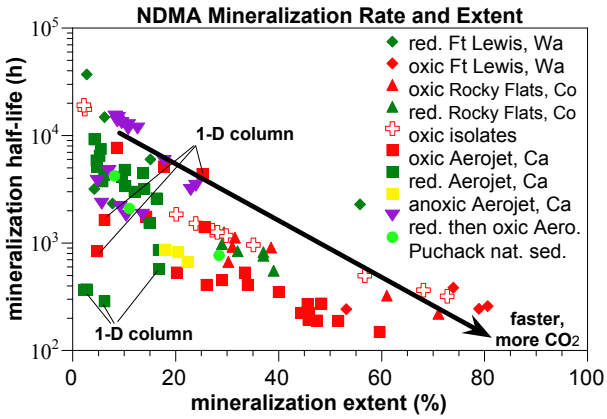

Figure 5.15. NDMA mineralization extent and rate.

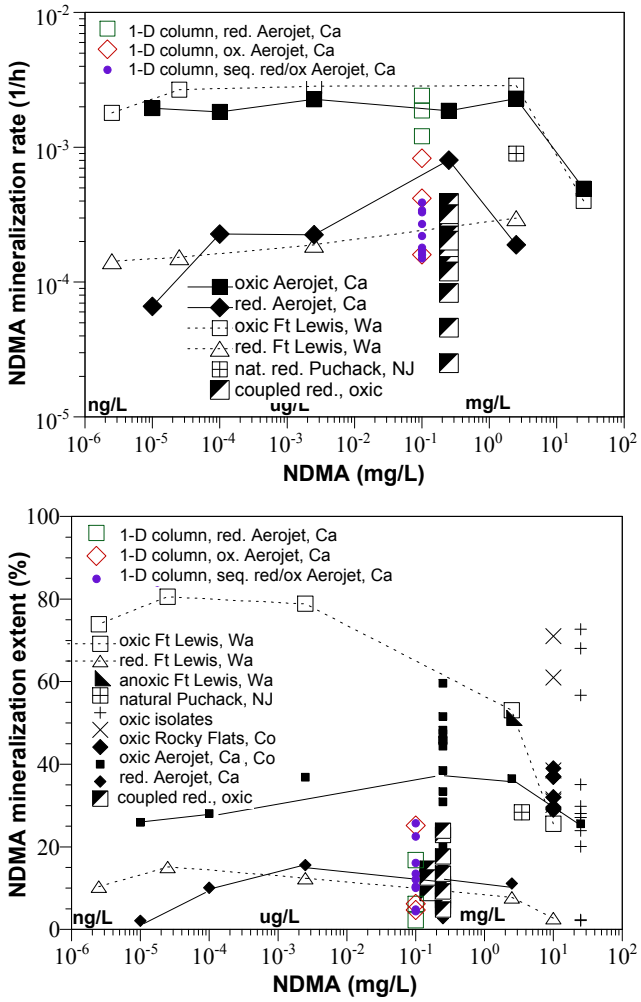

Figure 5.16. NDMA concentration and resulting mineralization rate (a) and mineralization extent (b).

Finally, because NDMA needs to be remediated to parts per trillion levels, sufficient experiments were conducted to characterize NDMA mineralization rate and extent as a function of the NDMA concentration (Figure 5.16). The NDMA mineralization rate did not change with NDMA concentration in oxic sediments (Aerojet and Ft. Lewis, Figure 5.16a, squares), which is presumably due to the co-metabolic degradation of NDMA does not control the metabolic process (i.e., a primary substrate would generally show a decrease in reaction rate with lower concentration. The NDMA mineralization rate for reduced sediment (Aerojet and Ft. Lewis, Figure 5.16a, diamonds and triangles) also did not change with NDMA concentration. Since reduced systems are controlled by abiotic NDMA by adsorbed ferrous iron, as the NDMA concentration decreases, the ferrous iron/ NDMA ratio increases and it is expected that the observed mineralization rate would increase. The NDMA mineralization rate in sequential reduced/oxic systems showed slower rates than either oxic or reduced sediment systems. Mineralization rates in large laboratory 1-D columns showed more rapid rates in reduced sediment systems (green open squares) than oxic/ biostimulated systems (open red diamonds).

The NDMA mineralization extent did not vary with NDMA concentration in reduced sediment (Figure 5.16b), but did increase with lower NDMA concentration for the oxic Ft. Lewis sediment (but not the oxic Aerojet sediment). Mineralization extent in these batch systems is somewhat a function of the total time of the experiment (varied from 800 to 3200 hours), but in most cases, mineralization ceased, as other microbial nutrients were limiting (i.e., microbial biomass in Figure 5.9c). In general, batch systems containing only microbial isolates were better able to utilize the NDMA, and produced a higher mineralization extent.

5.3 Viability of Processes for Field-Scale *In Situ* Remediation

The specific questions needed to justify upscaling the laboratory-scale results to a single well proof-of-principle are: a) is NDMA degraded at a sufficiently rapid rate under field conditions, b) is NDMA degraded to a nontoxic product, c) can the treatment process be implemented at field scale, and d) can the field site be monitored to prove the treatment worked? It was

originally hypothesized in the proposal of this project that NDMA mineralization was needed in order to remediate NDMA at the field scale. Recent evidence shows that NDMA is degraded in reduced sediments to DMA, which is nontoxic. This reduction of risk may be sufficient for remediation, even though the intermediates are not mineralized. However, DMA is further degraded in both oxic and reduced sediment-water systems to other intermediates that are more toxic.

At the highest recorded NDMA concentration in the Aerojet aquifer (36 ppb), the NDMA is estimated to degrade with a 0.26-hour half-life (highly reduced sediment) to 7.2-hour half-life (partially reduced sediment). NDMA needs to be degraded to the action limit of 0.7 ppt in order to be a viable remediation strategy. Laboratory results show that NDMA can be degraded to <3 ppt, which is the detection limit for the ^{14}C-NDMA method (Figure 4.54). Given a range of groundwater flow velocity (0.01 to 0.1 ft/day) and barrier width (10- to 30-ft diameter), NDMA will be degraded to below the action limit in all cases except those at very high velocity near pumping wells (1.0 ft/day). In addition, experimental results show that a small, highly reduced zone would be more effective than a larger zone with low reduction, so a field injection strategy should be designed as such (Szecsody et al. 2007b). Highly reduced sediment degrade NDMA rapidly in 1-D sediment columns (Figure 5.17a); ~10 to 55 times more rapid than oxic (biotic) reactions in biostimulated 1-D columns.

Therefore, although NDMA is degraded to nontoxic DMA, because it degraded further, mineralization of NDMA should be the focus of field-scale remediate, as it represents the lowest risk. Numerous batch experiments were conducted in this study to characterize NDMA mineralization in oxic, anaerobic, and reduced sediment-water systems. In the final year of the project, a series of large-scale 1-D columns were conducted with reduced sediment, oxic sediment, and sequential reduced, then oxic sediment, at the high sediment/water ratio of field aquifers with advective flow over thousands of hours to provide insight into the relative reactivity of the systems. The results are significant, and demonstrate the importance of scaling up batch results to field relevant systems.

In batch systems, NDMA mineralization was generally 10 times more rapid in the oxic, biostimulated sediment systems compared to the same sediment under iron-reducing conditions. Mineralization rates were an order of magnitude slower under iron-reducing conditions for the same sediment (mineralization half-life in oxic Aerojet sediment = 342 ± 36 hours, reduced Aerojet sediment = 3475 ± 504 hours; oxic Ft. Lewis sediment = 282 hours, anaerobic Ft. Lewis sediment = 611 hours, reduced Ft. Lewis sediment = 2330 hours). However, in the large-scale 1-D columns, NDMA mineralization is most rapid in the reduced sediment (half-life 410 ± 147 hours, Figure 5.17b), followed by the oxic sediment with propane/air addition (half-life 2293 ± 1866 hours), then the coupled reduced-oxic columns (half-life 3180 ± 1094 hours). Batch studies for two sediments

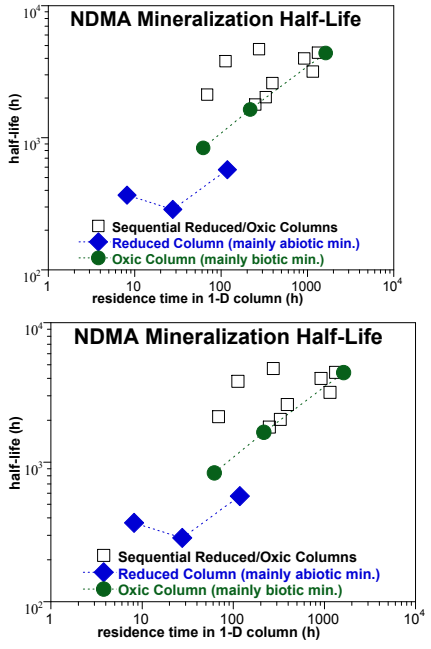

Figure 5.17. NDMA degradation and mineralization rates in reduced, oxic, and sequential 1-D columns.

with and without a bactericide clearly showed NDMA mineralization in reduced sediment was predominantly abiotic. The comparison of oxic to reduced system mineralization was in contrast to previous batch studies, which showed ~10 times more rapid NDMA mineralization in oxic sediment was 188 times slower in these column systems than predicted from batch studies. These results are not surprising, as column systems exhibit significantly less mixing than in batch systems, so much of the microbial population may be nutrient limited. NDMA mineralization in the reduced sediment was 4 times slower in these column systems than predicted from batch studies, which is reasonable due to the slight additional mixing limitations for an abiotic reaction in the column system.

Abiotic reactivity scales relatively well as the sediment/water ratio increases, as the ability to degrade and mineralize NDMA increases as the ferrous iron/NDMA ratio (sediment/water ratio) increases. Scaling up oxic biodegradation of NDMA in from small batch systems to large 1-D columns was significantly less efficient and most likely reflects the lack of ability to deliver major and/or trace nutrients to microbes throughout the column. NDMA degradation in the sequential reduced-oxic sediment systems was slightly (2 times) more rapid (17.2 ± 14.5-hour half-life) than reduced sediment alone (32.1 ± 4.2 hours; Figure 5.17a), as caused by the (inefficient and slow) downgradient biodegradation in the oxic sediment column. NDMA mineralization rates in the sequential reduced-oxic sediment systems (3180 ± 1094 hours) were slightly (40%) slower than in the oxic columns (2293 ± 1866 hours). Both these data sets indicate sequential degradation was inefficient, caused either by NDMA degradation intermediates from the upgradient reduced column not being biodegraded as easily as NDMA itself and/or removal of dissolved oxygen from the water that is injected into the down gradient oxic column (with air/propane) was not efficiently maintaining an oxic environment.

Results in this study demonstrate that dithionite-reduced aquifer sediment degrades NDMA rapidly (half-life 32.1 hours in a column system) and also mineralizes NDMA slowly (half-life 410 hours in a column system). This reactivity was maintained for 84 pore volumes, when experiments ended (Figure 5.18). It is expected that the reactivity would last longer, but at some point, the ability of the reduced sediment to degrade/mineralize NDMA would decrease. Dithionite-reduced sediment results in the dissolution of ferric oxides and the creation of predominantly adsorbed ferrous iron on oxide/clay surfaces. For the Aerojet sediment (natural pH 9.1), the resulting pH of the dithionite/carbonate treatment was 10.5). There may be other, more efficient methods to create an iron-reducing environment in the subsurface that have this or greater reactivity, which should be investigated in future studies. Mixtures of zero valent iron with sediment did not show significant reactivity with NDMA (Section 4.1.10) nor did it enhance NDMA mineralization (Figure 4.46d), although the development of a reduced zone in

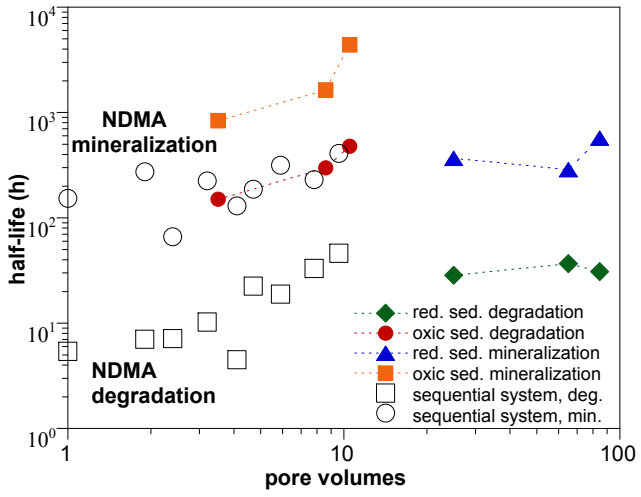

Figure 5.18. Longevity of reactivity in column systems.

sedment/zero valent iron mixtures can take hundreds of hours. Biostimulation is commonly used at field scale to create an iron- or sulfate-reducing environment, which may be and efficient method to create a zone to abiotically mineralize NDMA. Additions of ferrous nitrate or some other means to inject ferrous iron may also be used to create a subsurface zone containing sufficient reductive capacity and appropriate electron transfer surfaces to mineralize NDMA. Although NDMA mineralization in batch systems was of a moderate rate in batch systems (342-hour half-life), biomineralization of NDMA in column systems tested was inefficient (half-life 2293 hours) likely due to nutrient limitations. Numerous experiments evaluating additions to stimulate *in situ* microbial activity were largely ineffective. However, *ex situ* bioreactors utilizing appropriate monooxygenase isolates is very successful. Therefore, based on the results of this study field-scale remediation of NDMA should likely focus on a comparison of *in situ* abiotic NDMA mineralization (iron-reducing environments) to *ex situ* biomineralization.

6.0 References

Arienzo M, J Gan, F Ernst, S Qin, S Bondarenko, and D Sedlak. 2006. "Loss Pathways of *N*-Nitrosodimethylamine (NDMA) in Turfgrass Soils." *Journal of Environmental Quality* 35:285–292.

Balko BA and PG Tratnyek. 1998. "Photoeffects on the Reduction of Carbon Tetrachloride by Zero-Valent Iron." *The Journal of Physical Chemistry B* 102(8):1459–1465.

Bell L, J Devlin, R Gillham, and P Benning. 2003. "A Sequential Zero Valent Iron and Aerobic Biodegradation Treatment System for Nitrobenzene." *Journal of Contaminant Hydrology* 66(3–4):201-217.

Blowes DW, CJ Ptacek, and JL Jambor. 1997. "In-Situ Remediation of Cr(VI)-Contaminated Ground Water Using Permeable Reactive Walls: Laboratory Studies." *Environmental Science and Technology* 31(12):3348-3357.

Boopathy R, CF Kulpa, J Manning, and CD Montemagno. 1994. "Biotransformation of 2,4,6-Trinitrotoluene (TNT) by Co-Metabolism with Various Co-Substrates: A Laboratory-Scale Study." *Bioresource Tech*. 47:205–208.

Bradley PM, SA Carr, RB Baird, and FH Chapelle. 2005. "Biodegradation of N-nitrosodimethylamine in Soil from a Water Reclamation Facility." *Bioremediation Journal* 9:115-120.

Buckley L, K Morgan, J Swenberg, and R James. 1985. "Toxicity of Dimethylamine in F-344 Rates and B6C3F1 Mice Following a 1-Year Inhalation Exposure. *Fundam. Appl. Toxicol.* 5(2):341–352.

Buerge IJ and SJ Hug. 1997. "Kinetics and pH Dependence of Chromium (VI) Reduction by Iron (III)." *Environmental Science and Technology* 31:1426–1432.

Burns CA, J-F Boily, RJ Crawford, and IH Harding. 2005. "Cd(II) Sorption onto Chemically Modified Australian Coals." *Fuel* 84:1653–1660.

Chao TT and L Zhou. 1983. "Extraction Techniques for Selective Dissolution of Amorphous Iron Oxides from Soils and Sediments." *Soil Science Society of America Journal* 47:225–232.

Chilakapati A, M Williams, S Yabusaki, and C Cole. 2000. Optimal Design of an In Situ Fe(II) Barrier: Transport Limited Reoxidation. *Environmental Science and Technology* 34(24):5215–5221.

Eary LE and D Rai. 1988. Chromate Removal from Aqueous Wastes by Reduction with Ferrous Ion. *Environmental Science and Technology* 22(8):972–977.

Fournier D, J Hawari, SH Streger, K McClay, and PB Hatzinger. 2006. "Biotransformation of *N*-Nitrosodimethylamine by *Pseudomonas mendocina* KR1." *Applied and Environmental Microbiology* 72:6693–6698.

Fruchter J, C Cole, M Williams, V Vermeul, J Amonette, J Szecsody, J Istok, and M Humphrey. 2000. "Creation of a Subsurface Permeable Treatment Barrier Using In Situ Redox Manipulation." *Ground Water Monitoring Review* 66–77.

Fulthorpe R, A Rhodes, and J Tiedge. 1996. "Pristine Soils Mineralize 3-Chlorobenzoate and 2,4-Dichlorophenoxyacetate via Different Microbial Populations." *Applied and Environmental Microbiology* 62(4):1159–1166.

Genin J, G Bourrie, and F Trolard. 1998. Thermodynamic Euilibriua in Aqueous Suspensions of Synthetic and Natural Green Rusts: Occurrences of the Mineral in Hydromorphic Soils." *Environmental Science and Technology* 32(8):1058–1068.

Gibbs CR. 1976. "Characterization and Application of Ferrozine Iron Reagent as a Ferrous Iron Indicator." *Analytical Chemistry* 48(8):1197–1200.

Gui L, R Gillham, and M Odziemkowski. 2000. "Reduction of N-Nitrosodimethylamine with Granular Iron and Nickel-Enhanced Iron. 1. Pathways and Kinetics." *Environmental Science and Technology* 34(16):3489–3494.

Gunnison D, ME Zappi, C Teeter, JC Pennington, and R Bajpai. 2000. "Attenuation Mechanisms of *N*-Nitrosodimethylamine at an Operating Intercept and Treat Groundwater Remediation System." *Journal of Hazardous Materials* B73:179–197.

Hawari J, A Halasz, C Groom, S Deschamps, L Paquet, C Beaulieu, and A Corriveau. 2002. "Photodegradation of RDX in Aqueous Solution: A Mechanistic Probe for Biodegradation with *Rhodococcus* sp." *Environmental Science and Technology* 36(23):5117–5123.

Heron G, C Crouzet, AC Bourg, and TH Christensen. 1994. "Speciation of Fe(II) and Fe(III) in Contaminated Aquifer Sediments using Chemical Extraction Techniques. *Environmental Science and Technology* 28:1698–1705.

Hofstetter TB, CG Heijman, SB Halderlein, C Holliger, and RP Schwarzenbach. 1999. "Complete Reduction of TNT and Other Polynitroaromatic Compounds under Iron-Reducing Subsurface Conditions." *Environmental Science and Technology* 33(9):1479–1487.

Hofstetter TB, RP Schwarzenbach, and SP Halderlein. 2003. "Reactivity of Fe(II) Species Associated with Clay Minerals." *Environmental Science and Technology* 37(3):519–528.

Johnson TL, W Fish, YA Gorby, and PG Tratnyek. 1998. "Degradation of Carbon Tetrachloride by Iron Metal: Complexation Effects on the Oxide Surface." *Journal of Contaminant Hydrology* 29(4):379–398.

Kaplan DL and AM Kaplan. 1985. "Biodegradation of *N*-Nitrosodimethylamine in Aqueous and Soil Systems." *Applied and Environmental Microbiology* 50:1077–1086.

Lopez M, M Alvarez, A Miranda, and P Blanco. 1996. "Determination of Dimethylamine in Groundwater by Liquid Chromatography and Precolumn Derivatization with 9-Fluorenylmethylchloroformate." *Journal of Chromatography* 721(2):231–239.

Mallik MA and K Testai. 1981. "Transformation of Nitrosamines in Soil and In Vitro by Soil Microorganisms." *Bulletin of Environmental Contamination and Toxicology* 27(1):115–121.

McKinley J, J Szecsody, A Breshears, R Kukkadapu, and B Devary. 2007. *Abiotic Degradation and Microbial Mineralization of NDMA in Subsurface Sediments*. SERDP Annual Conference, December 2007, Washington, D.C.

McKinley J, J Szecsody, T Resch, A Fischer, K Thompson, H Fredrickson, C Luce, and S Neville. 2005. *Abiotic and Biotic Processes Controlling Remediation of NDMA in Sediments*. SERDP Annual Meeting, December 2005, Washington, D.C.

Mitch WA, JO Sharp, RR Trussell, RL Valentine, L Alvarez-Cohen, and DL Sedlak. 2003. "*N*-Nitrosodimethylamine (NDMA) as a Drinking Water Contaminant: A Review." *Environmental Engineering Science* 20:389–404.

Morkin M, J Devlin, J Barker, and B Butler. 2000. "In Situ Sequential Treatment of a Mixed Contaminant Plume." *Journal of Contaminant Hydrology* 45 (3–4):283–302.

Nardi S, M Tosoni, D Pizzeghello, MR Provenzano, A Cilenti, A Sturaro, A Rella, and A Vianello. 2005. "Chemical Characteristics and Biological Activity of Organic Substances Extracted from Soils by Root Exudates." *Soil Science Society of America Journal* 69:2012–2019.

Odziemkowski M, L Gui, and R Gillham. 2000. "Reduction of N-Nitrosodimethylamine with Granular Iron and Nickel-Enhanced Iron. 2. Mechanistic Studies. *Environmental Science and Technology* 34(16):3495–3500.

Petrie RA, PR Grossl, and RC Sims. 1998. "A Controlled Environment Potentiostat to Study Solid/Aqueous Systems." *Soil Science Society of America Journal* 62:379–382.

Ringelberg D, J Talley, E Perkins, and H Fredrickson. 2001. "Succession of Phenotypic, Genotypic, and Metabolic Community Characteristics during In Vitro Bilslurry Treatment of Polycyclic Aromatic Hydrocarbon-Contaminated Sediments." *Applied and Environmental Microbiology* 65(4):1543–1550.

Sharp JO, TK Wood, and L Alvarez-Cohen. 2005. "Aerobic Biodegradation of *N*-Nitrosodimethylamine (NDMA) by Axenic Bacterial Strains." *Biotechnology and Bioengineering* 89:608–618.

Sharp JO, CM Sales, JC LeBlanc, J Liu, TK Wood, LD Eltis, WW Mohn, and L Alvarez-Cohen. 2007. "An Inducible Propane Monoxygenase is Responsible for *N*-Nitrosodimethylamine Degradation by *Rhodococcus* sp. Strain RHA1." *Applied and Environmental Microbiology* 73:6930–6938.

Singh J, SD Comfort, and PJ Shea. 1999. "Iron-Mediated Remediation of RDX-Contaminated Water and Soil under Controlled Eh/pH." *Environmental Science and Technology* 33(9):1488–1494.

Stevens TO and JP McKinley. 2000. "Abiotic Controls on H_2 Production from Basalt-Water Reactions and Implications for Aquifer Biogeochemistry." *Environmental Science Technology* 34:826–831.

Stucki JW, DC Golden, and CB Roth. 1984. "Preparation and Handling of Dithionite-Reduced Smectite Suspensions." *Clays and Clay Minerals* 32(3):191–197.

Szecsody J. 2007. "In Situ Chemical Reduction and Resulting Abiotic/Biotic Reactivity." *In Situ Chemical Reduction for Source Zones*, University Consortium for Field-Focused Groundwater Contamination Research, Denver, Colorado.

Szecsody JE, JS Fruchter, DS Sklarew, and JC Evans. 2000. *In Situ Redox Manipulation of Subsurface Sediments from Fort Lewis, Washington: Iron Reduction and TCE Dechlorination Mechanisms*. PNNL-13178, Pacific Northwest National Laboratories, Richland, Washington.

Szecsody J, J Fruchter, M McKinley, and T Gilmore. 2001. *Feasibility of In Situ Redox Manipulation for RDX Remediation in Pantex Sediments*. PNNL-13746, Pacific Northwest National Laboratory, Richland, Washington.

Szecsody J, J Fruchter, J Campbell, and B Devary. 2003. *Feasibility of the Use of In Situ Redox Manipulation for Groundwater Remediation of N-Nitrosodimethylamine (NDMA) and Perchlorate at the Aerojet Facility, California: Laboratory-Scale Tests*. Letter report, Pacific Northwest National Laboratory, Richland, Washington.

Szecsody J, M Williams, J Fruchter, V Vermeul, and D Sklarew. 2004. "In Situ Reduction of Aquifer Sediments: Enhancement of Reactive Iron Phases and TCE Dechlorination." *Environmental Science and Technology* 38:4656–4663.

Szecsody J, J Fruchter, VR Vermeul, M Williams, and B Devary. 2005a. "In Situ Reduction of Aquifer Sediments to Create a Permeable Reactive Barrier to Remediate Chromate: Bench-Scale Tests to Determine Barrier Longevity." Chapter 9, in J Jacobs, ed., *Groundwater Remediation of Chromate*, CRC Press.

Szecsody JE, JL Phillips, VR Vermeul, JS Fruchter, and MD Williams. 2005b. *Influence of Nitrate on the Hanford 100D Area In Situ Redox Manipulation Barrier Longevity*. PNNL-15262, Pacific Northwest National Laboratory, Richland, Washington.

Szecsody J, J McKinley, J Fruchter, M Williams, V Vermeul, H Fredrickson, and K Thompson. 2006. "In Situ Chemical Reduction of Sediments for TCE, Energetics, and NDMA Remediation. *Remediation of Chlorinated and Recalcitrant Compounds*, Monterey, California.

Szecsody JE, S Comfort, HL Fredrickson, HK Boparai, BJ Devary, KT Thompson, JL Phillips, F Crocker, DC Girvin, CT Resch, P Shea, A Fischer, and L Durkin. 2007a. *SERDP ER-1376 Enhancement of In Situ Bioremediation of Energetic Compounds by Coupled Abiotic/Biotic Processes: Final Report for 2004-2006*. PNNL-16754, Pacific Northwest National Laboratory, Richland, Washington.

Szecsody J, J McKinley, A Breshears, and F Crocker. 2008a. "Abiotic/Biotic Degradation and Mineralization of N-Nitrosodimethylamine in Aquifer Sediments." *Remediation* 19(1):109–123.

Szecsody J, J McKinley, A Breshears, R Kukkadapu, and C Burns. 2008b. "Coupled Abiotic/Biotic Degradation of N-Nitrosodimethylamine in Subsurface Sediments." *Remediation of Chlorinated and Recalcitrant Compounds*, Sixth International Conference, Monterey, California.

Thompson KT, FH Crocker, and HL Fredrickson. 2005. "Mineralization of the Cyclic Nitramine Explosive Hexahydro-1,3,5-Trinitro-1,3,5-Triazine by *Gordonia* and *Williamsia* spp." *Applied and Environmental Microbiology* 71:8265–8272.

Vermeul VR, MD Williams, JE Szecsody, JS Fruchter, CR Cole, and JE Amonette. 2002. "Creation of a Subsurface." In *Groundwater Remediation of Trace Metals, Radionuclides, and Nutrients, with Permeable Reactive Barriers*, Academic Press.

Vermeul VR, JE Szecsody, MJ Truex, CA Burns, DC Girvin, JL Phillips, BD Devary, AE Fischer, and SMW Li. 2006. *Treatability Study of In Situ Technologies for Remediation of Hexavalent Chromium in Groundwater at the Puchack Well Field Superfund Site, New Jersey*. PNNL-16194, Pacific Northwest National Laboratory, Richland, Washington.

Yang WC, J Gan, WP Liu, and R Green. 2005. "Degradation of *N*-Nitrosodimethylamine (NDMA) in Landscape Soils." *Journal of Environmental Quality* 34:336–341.

7.0 List of Project Publications

Journal Publications

Boparai H, S Comfort, J Szecsody, and P Shea. 2008. "Degradation of RDX, TNT, and HMX by Dithionite-Treated Aquifer Sediment and Surface Soil." *Chemosphere* 71:933–941 (partially funded by this ER-1421, partially by ER-1376).

Campbell J, J Szecsody, B Devary, and B Valenzuela. 2007. "Electrospray Ionization Mass Spectrometry of Hexanitrohexaazaisowurtzitane (CL-20)." *Analytical Letters* 40(10):1972–1978 (partially funded by this ER-1421, partially by ER-1255).

Szecsody J, J McKinley, A Breshears, and F Crocker. 2008a. "Abiotic/Biotic Degradation and Mineralization of N-Nitrosodimethylamine in Aquifer Sediments." *Remediation* 19(1):109–123.

Szecsody J and J McKinley. 2009. "Abiotic Mineralization of N-Nitrosodimethylamine in Subsurface Sediments and Potential for In Situ Treatment." *Journal of Hazardous Materials* (in preparation).

Conference Paper and Presentation

Szecsody J, J McKinley, J Fruchter, M Williams, V Vermeul, H Fredrickson, and K Thompson. 2006. "In Situ Chemical Reduction of Sediments for TCE, Energetics, and NDMA Remediation. *Remediation of Chlorinated and Recalcitrant Compounds*, Monterey, California.

Szecsody J, J McKinley, A Breshears, R Kukkadapu, and C Burns. 2008b. "Coupled Abiotic/Biotic Degradation of N-Nitrosodimethylamine in Subsurface Sediments. *Remediation of Chlorinated and Recalcitrant Compounds*, Sixth International Conference, Monterey, California.

Book Chapter

Szecsody J, J Fruchter, VR Vermeul, M Williams, and B Devary. 2005. "In Situ Reduction of Aquifer Sediments to Create a Permeable Reactive Barrier to Remediate Chromate: Bench-Scale Tests to Determine Barrier Longevity." Chapter 9, J Jacobs, ed., in *Groundwater Remediation of Chromate*, CRC Press (small portion funded by this project).

Conference Presentation, Invited Speaker

Szecsody J. 2007. "In Situ Chemical Reduction and Resulting Abiotic/Biotic Reactivity, University Consortium for Field-Focused Groundwater Remediation Research." *2007 Focus Meeting on In Situ Chemical Reduction for Source Zones*, Denver, Colorado, October 16–17, 2007.

Conference Abstract

McKinley J, J Szecsody, T Resch, A Fischer, K Thompson, H Fredrickson, C Luce, and S Neville. 2005. "Abiotic and Biotic Processes Controlling Remediation of NDMA in Sediments." *SERDP Annual Meeting*, December 2005, Washington, D.C.

McKinley J, J Szecsody, J Phillips, B Devary, K Thompson, H Fredrickson, and C Luce. 2006. "Abiotic Degradation and Microbial Mineralization of NDMA in Subsurface Sediments." *Annual SERDP Conference*, December 2006, Washington, D.C.

McKinley J, J Szecsody, A Breshears, R Kukkadapu, and B Devary. 2007. "Abiotic Degradation and Microbial Mineralization of NDMA in Subsurface Sediments." *SERDP Annual Conference*, December 2007, Washington, D.C.

Pacific Northwest
NATIONAL LABORATORY

U.S. DEPARTMENT OF
ENERGY

902 Battelle Boulevard
P.O. Box 999
Richland, WA 99352
1-888-375-PNNL (7665)
www.pnl.gov

Table of Contents

Appendix A.1 Task 1.1 NDMA Aqueous Stability

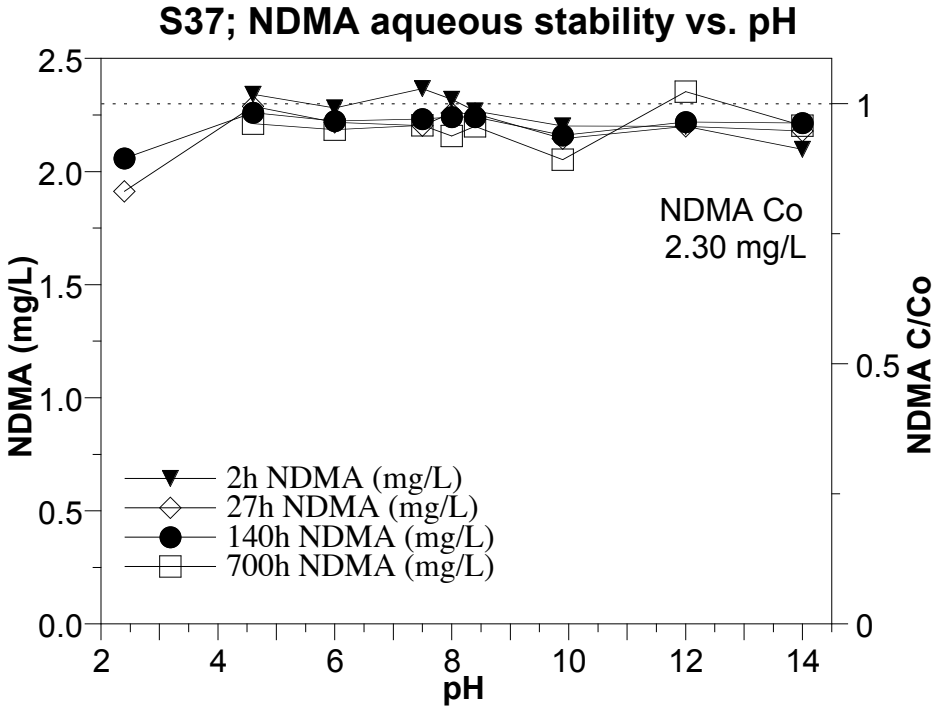

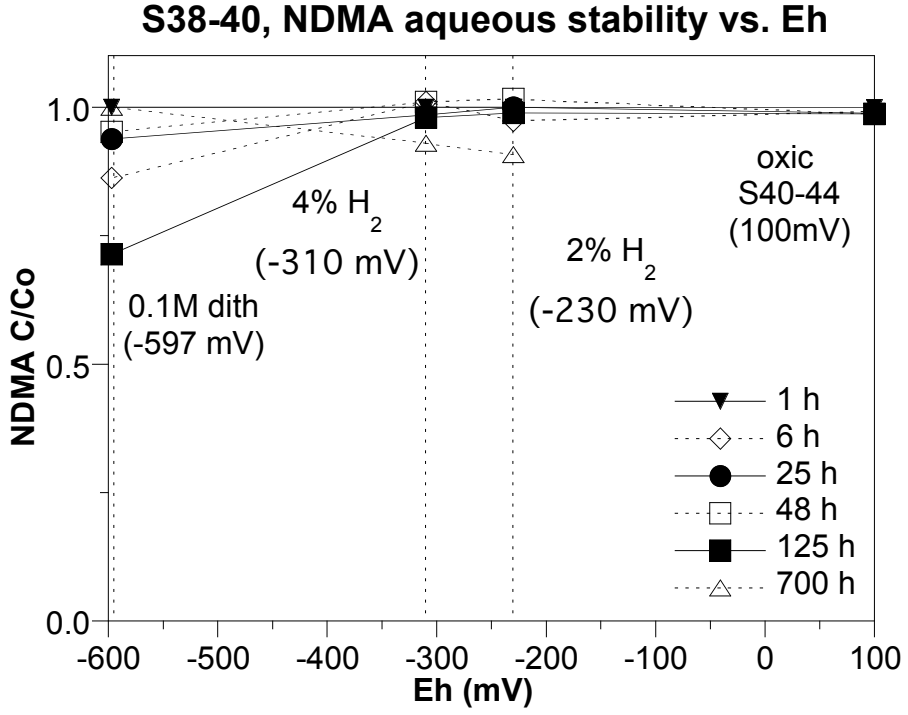

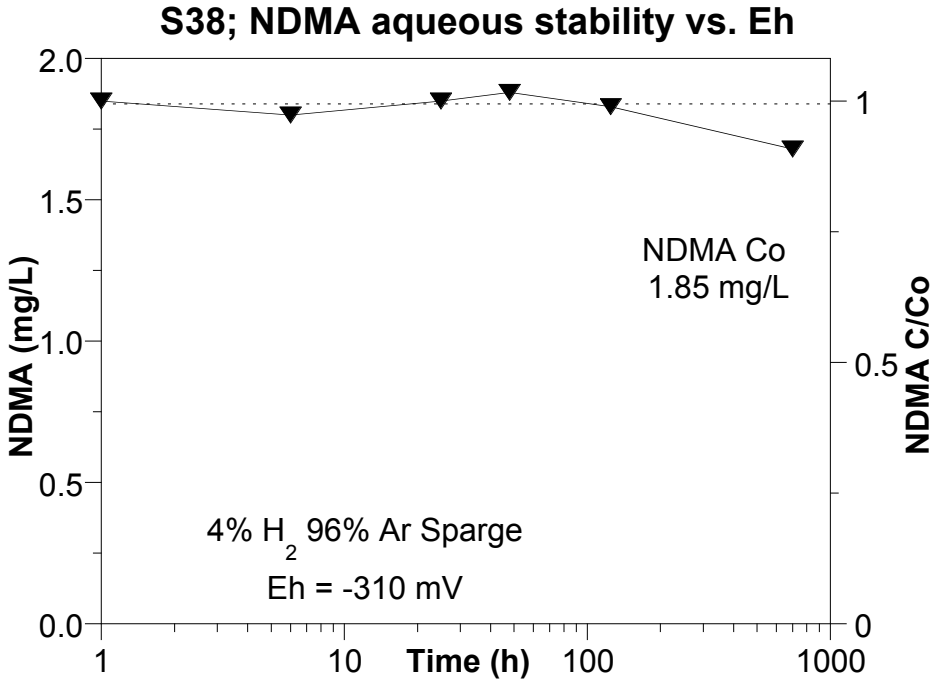
S38; NDMA aqueous stability vs. Eh
NDMA (mg/L)
NDMA C/Co
Time (h)
NDMA Co
1.85 mg/L
4% H2 96% Ar Sparge
Eh = -310 mV
2.0
1.5
1.0
0.5
0.0
1
0.5
0
1
10
100
1000

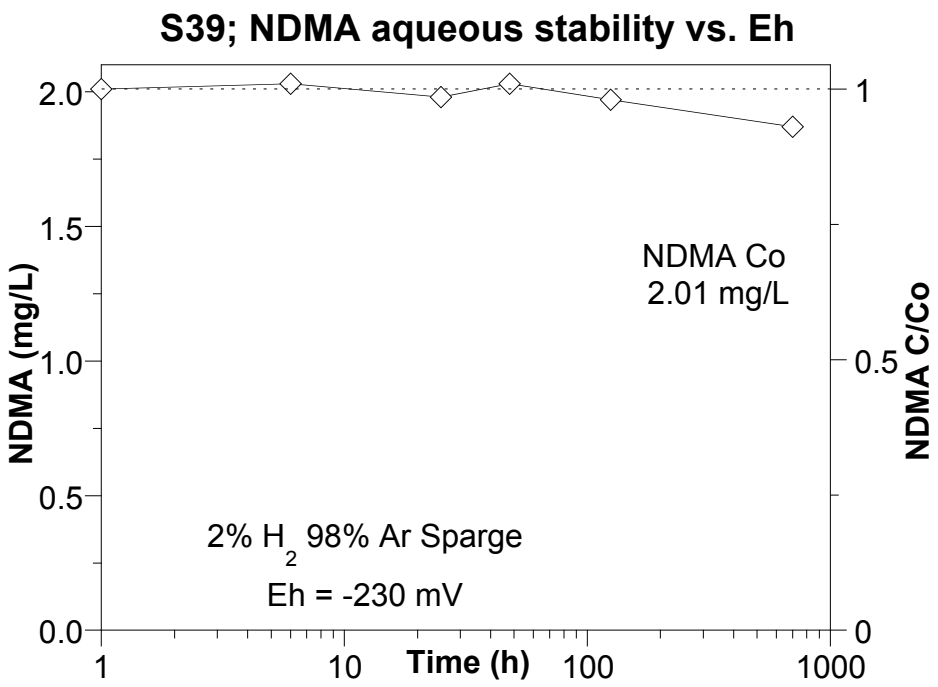
S39; NDMA aqueous stability vs. Eh
NDMA (mg/L)
NDMA C/Co
Time (h)
NDMA Co
2.01 mg/L
2% H2 98% Ar Sparge
Eh = -230 mV
2.0
1.5
1.0
0.5
0.0
1
0.5
0
1
10
100
1000

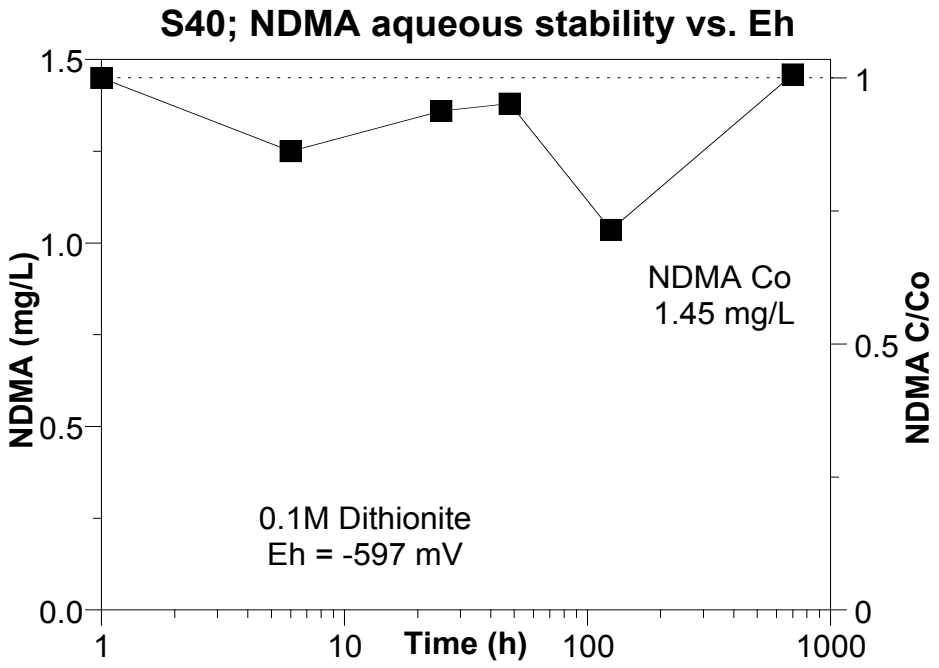
S40; NDMA aqueous stability vs. Eh
1.5
1.0
0.5
0.0
NDMA (mg/L)
1
0.5
0
NDMA C/Co
NDMA Co
1.45 mg/L
0.1M Dithionite
Eh = -597 mV
1
10
Time (h)
100
1000

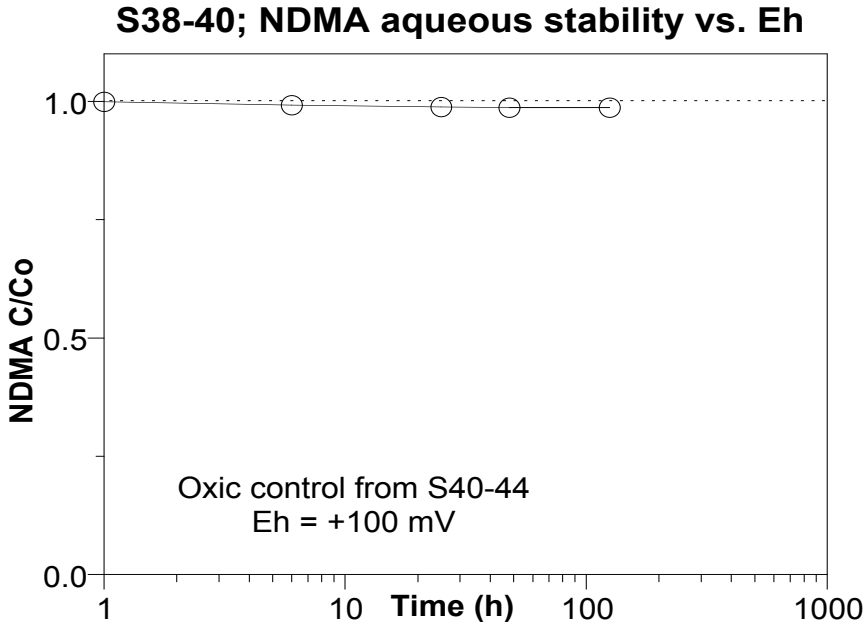
S38-40; NDMA aqueous stability vs. Eh
1.0
0.5
0.0
NDMA C/Co
Oxic control from S40-44
Eh = +100 mV
1
10
Time (h)
100
1000

X95-99: NDMA degradation by aqueous alkaline hydrolysis

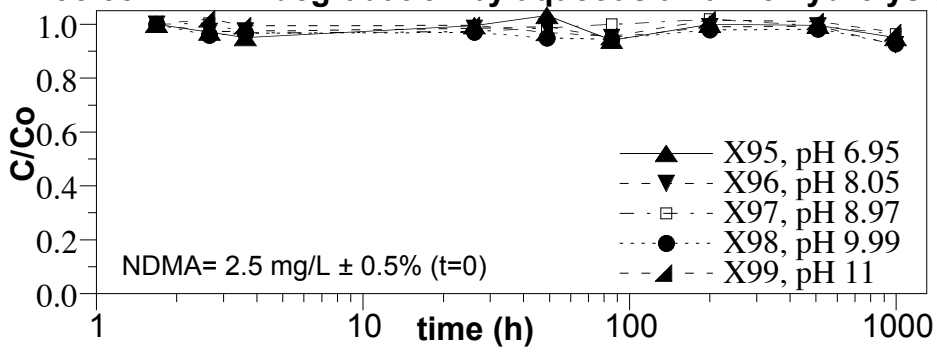

X116-8: NDMA degradation by UV light in aqueous solution

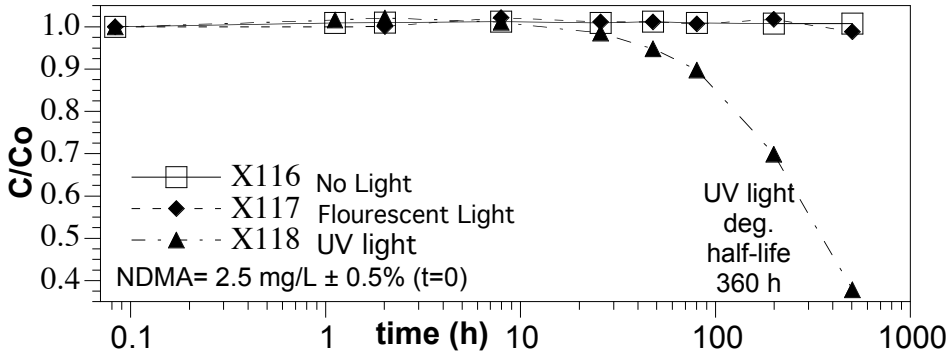

Appendix A.2 Task 1.2 NDMA Degradation by Natural Minerals

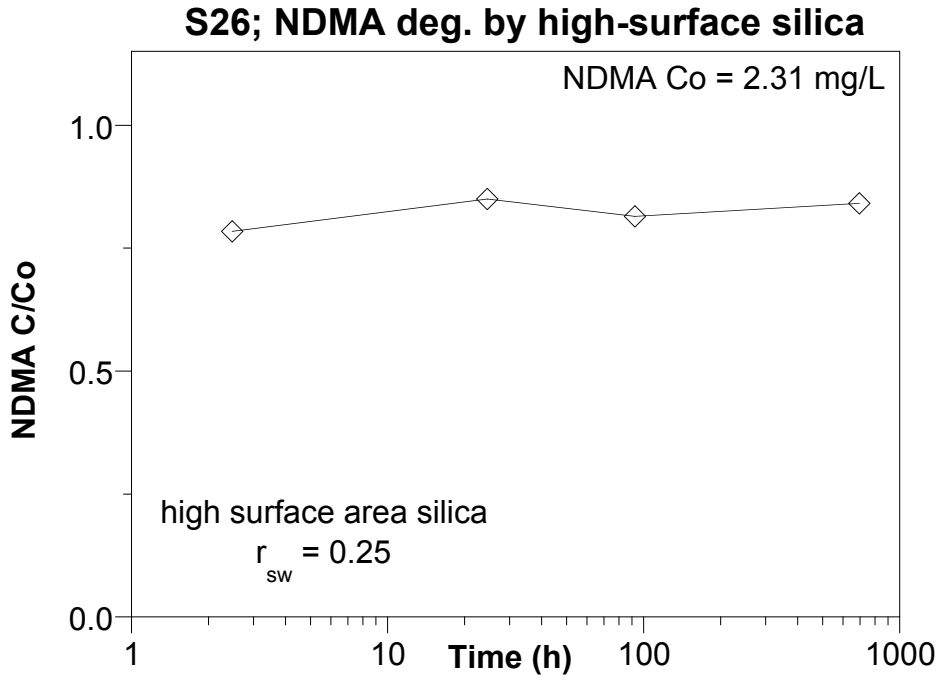

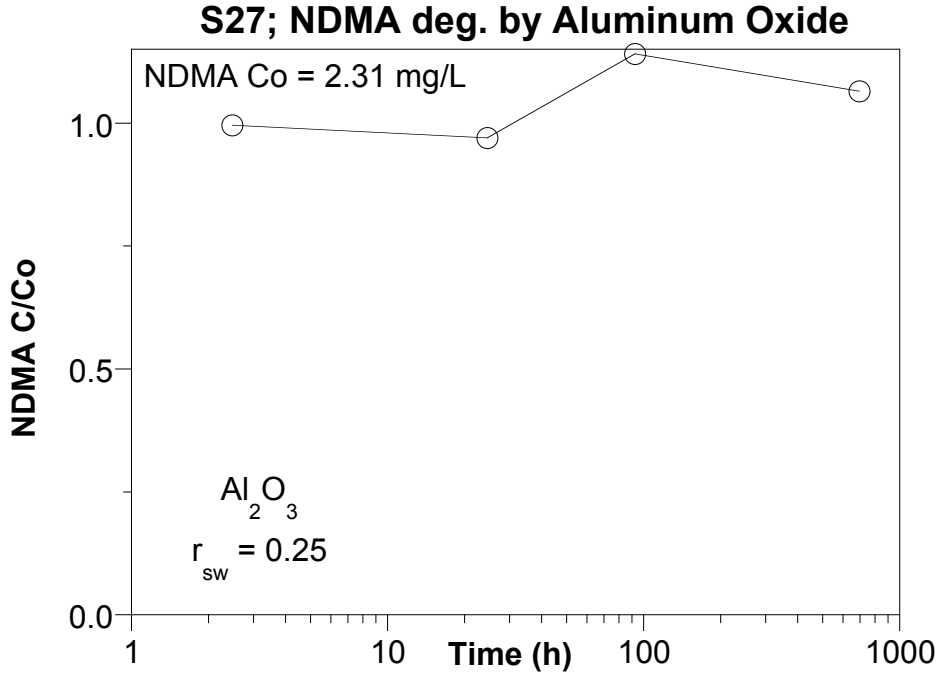

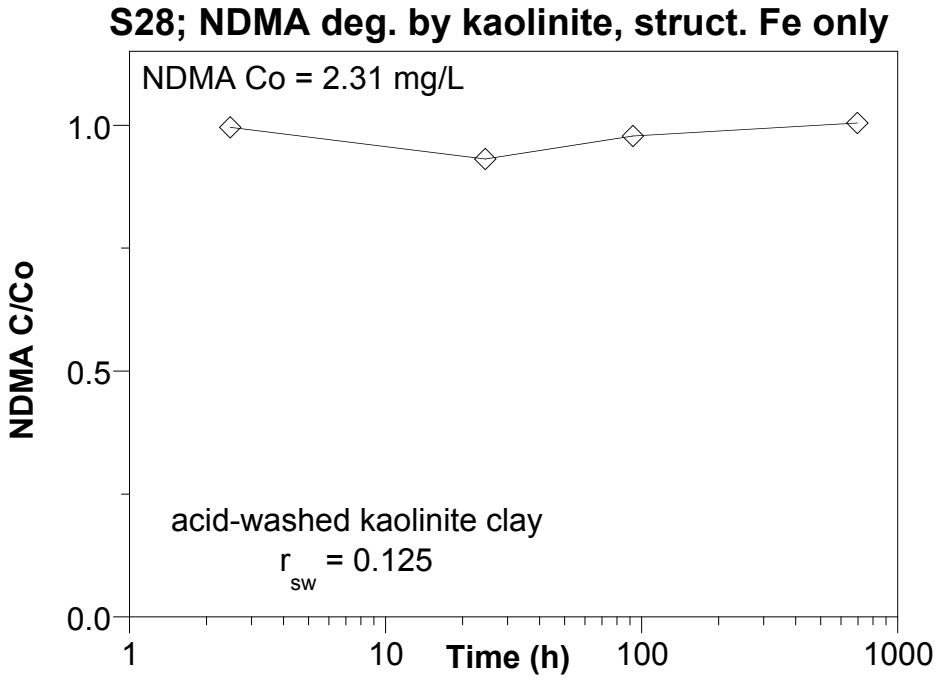
S28; NDMA deg. by kaolinite, struct. Fe only
NDMA Co = 2.31 mg/L
1.0
0.5
0.0
NDMA C/Co
acid-washed kaolinite clay
r sw = 0.125
1
10
Time (h)
100
1000

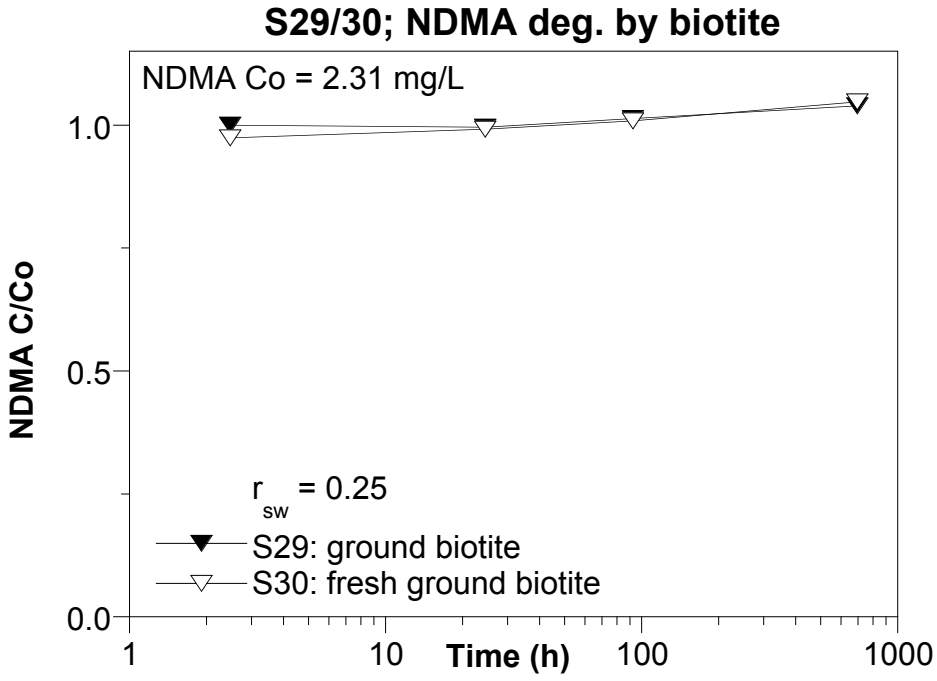
S29/30; NDMA deg. by biotite
NDMA Co = 2.31 mg/L
1.0
0.5
0.0
NDMA C/Co
r sw = 0.25
S29: ground biotite
S30: fresh ground biotite
1
10
Time (h)
100
1000

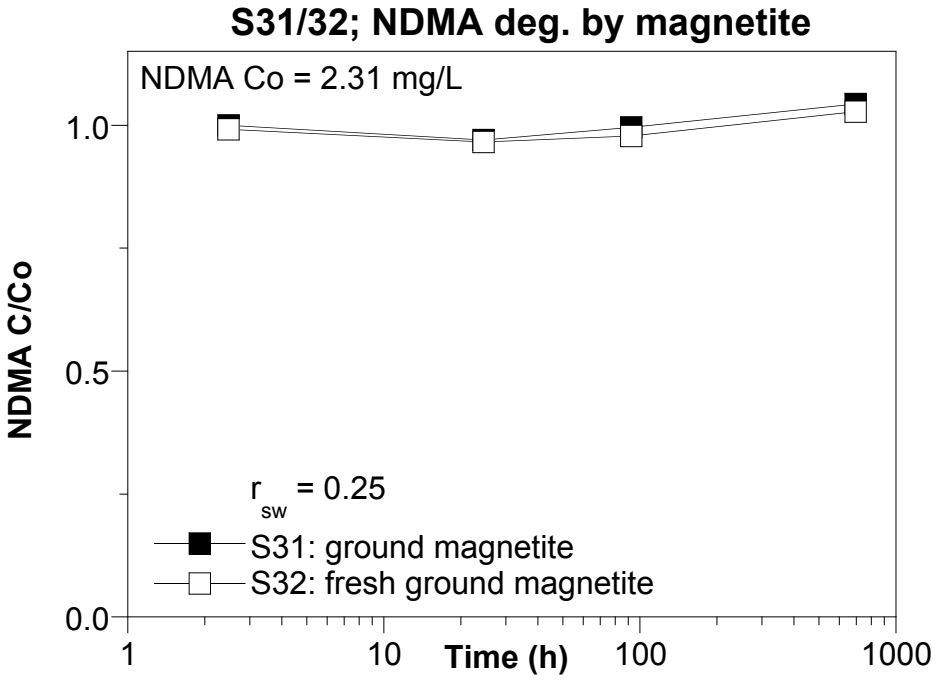
S31/32; NDMA deg. by magnetite
NDMA Co = 2.31 mg/L
1.0
0.5
0.0
NDMA C/Co
r sw = 0.25
S31: ground magnetite
S32: fresh ground magnetite
1
10
100
1000
Time (h)

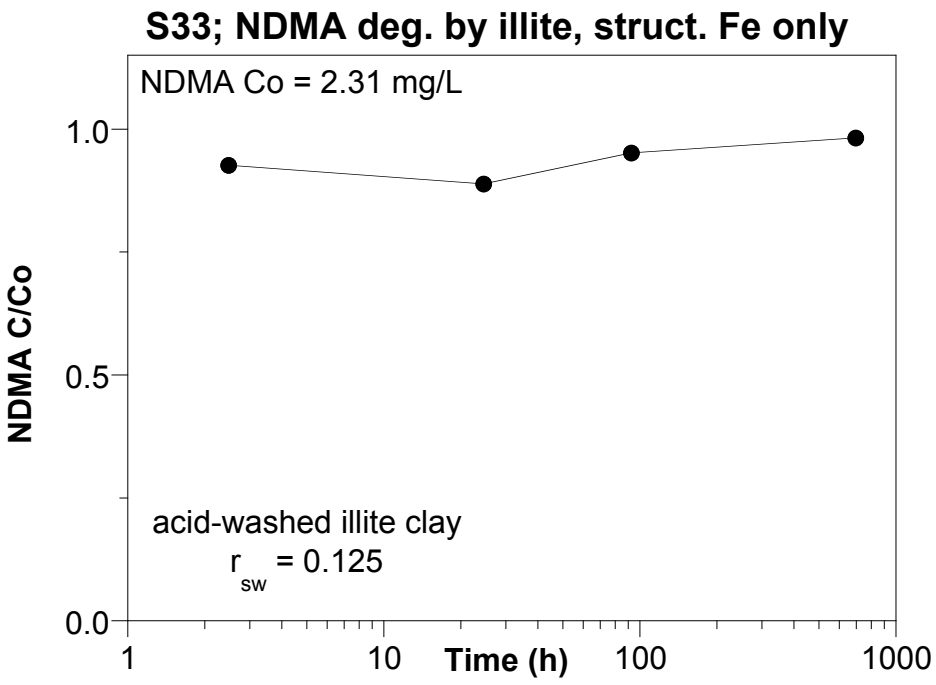
S33; NDMA deg. by illite, struct. Fe only
NDMA Co = 2.31 mg/L
1.0
0.5
0.0
NDMA C/Co
acid-washed illite clay
r sw = 0.125
1
10
100
1000
Time (h)

S34; NDMA deg. by montmorillonite, struct. Fe only

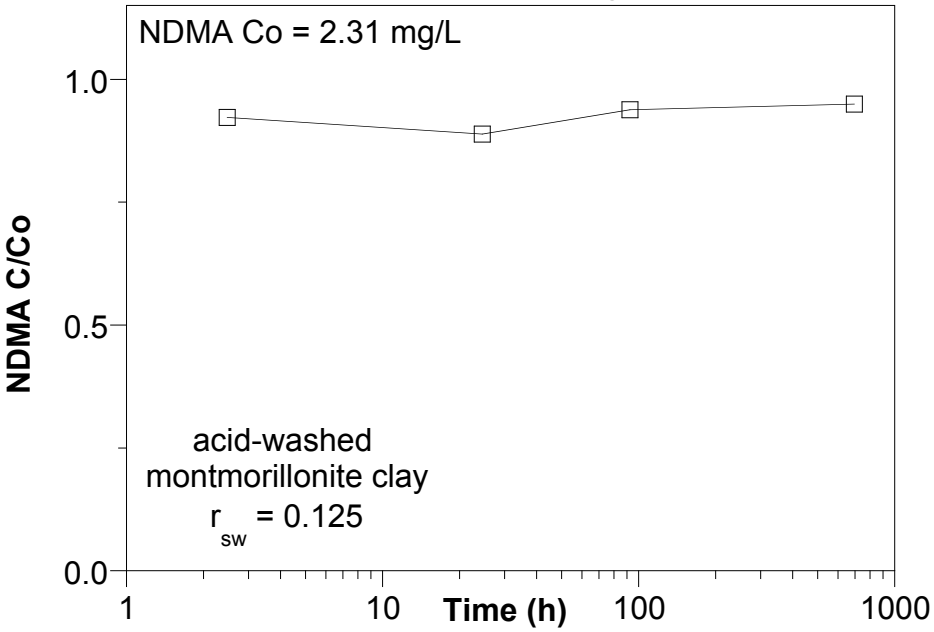

S35; NDMA deg. by nontronite, struct. Fe only

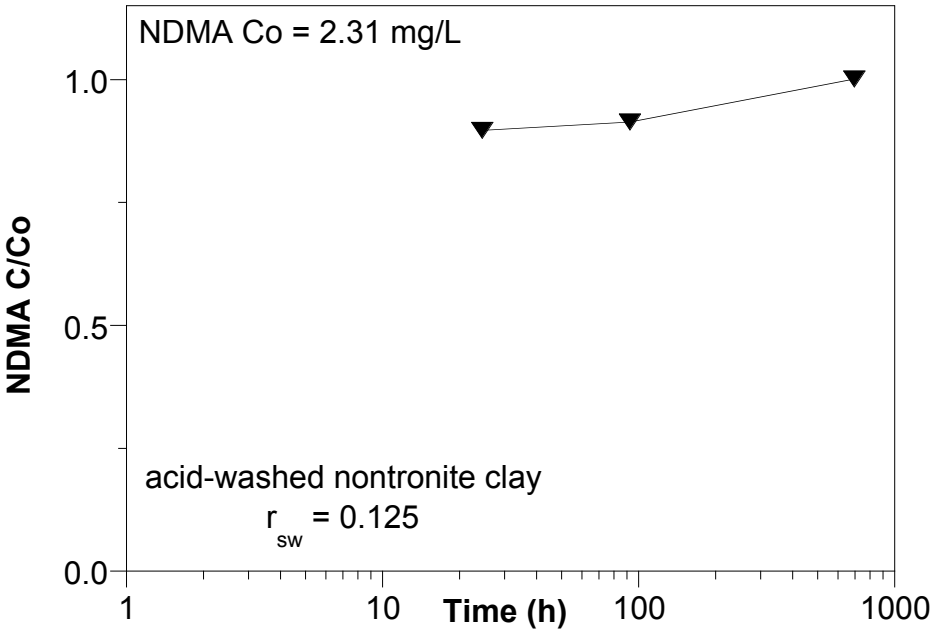

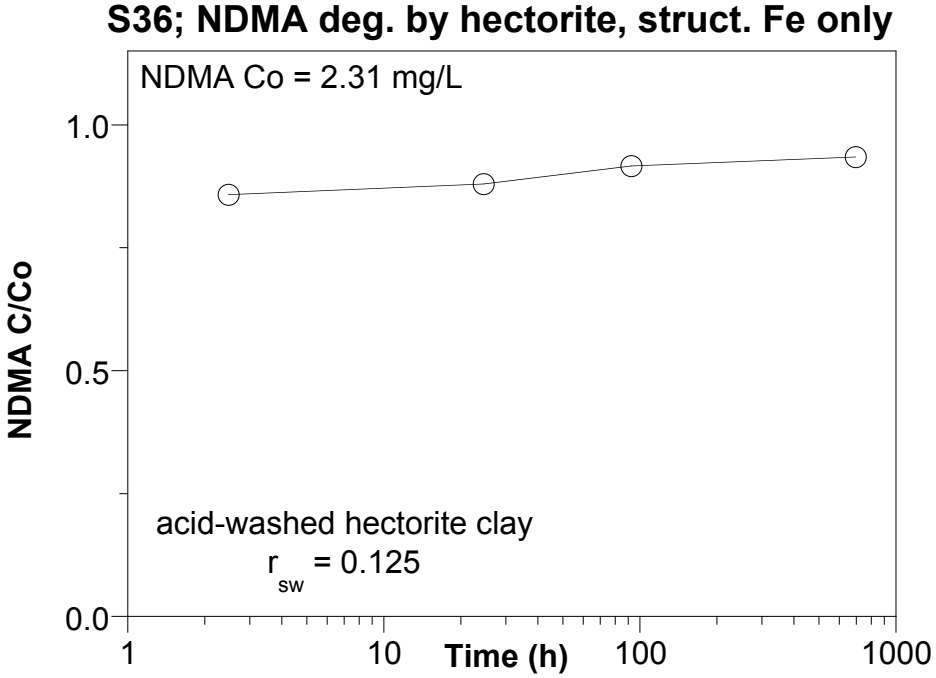
S36; NDMA deg. by hectorite, struct. Fe only
NDMA Co = 2.31 mg/L
1.0
0.5
0.0
NDMA C/Co
acid-washed hectorite clay
r sw = 0.125
1
10
Time (h)
100
1000

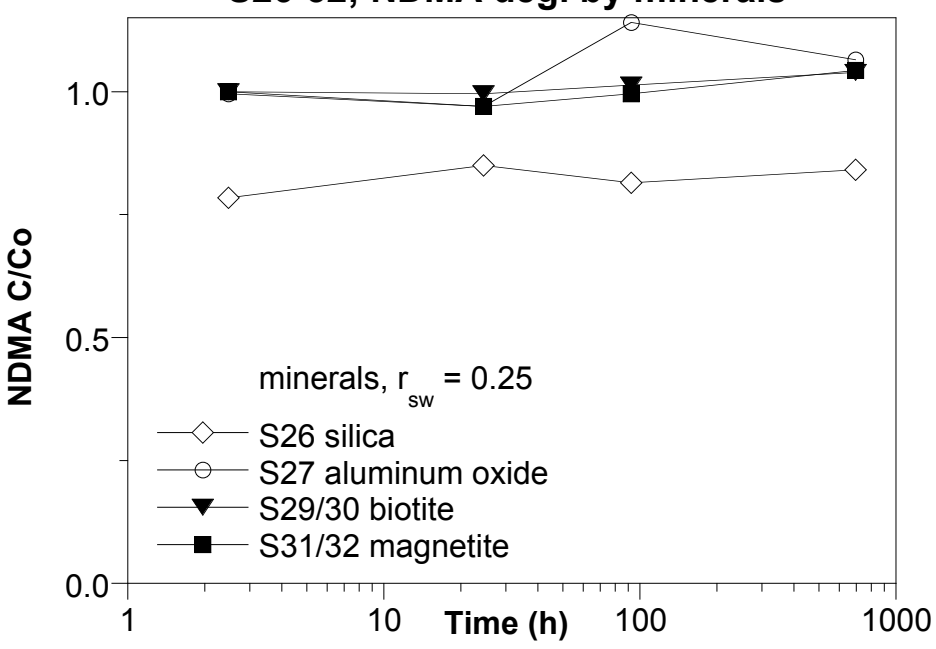
S26-32; NDMA deg. by minerals
1.0
0.5
0.0
NDMA C/Co
minerals, r sw = 0.25
S26 silica
S27 aluminum oxide
S29/30 biotite
S31/32 magnetite
1
10
Time (h)
100
1000

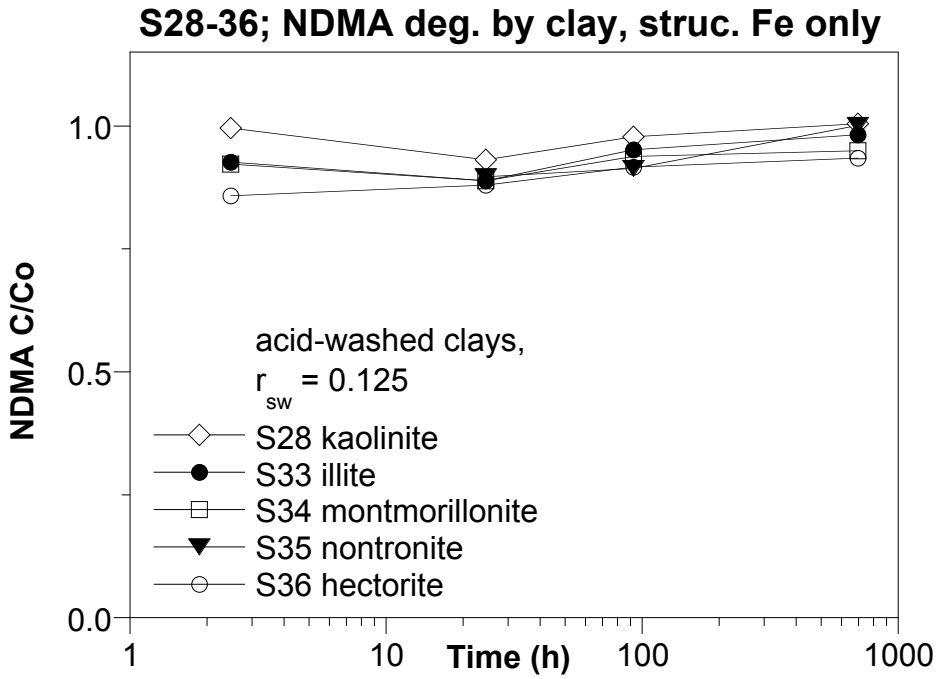
S28-36; NDMA deg. by clay, struc. Fe only
NDMA C/Co
1.0
0.5
0.0
1
10
100
1000
Time (h)
acid-washed clays,
r sw = 0.125
S28 kaolinite
S33 illite
S34 montmorillonite
S35 nontronite
S36 hectorite

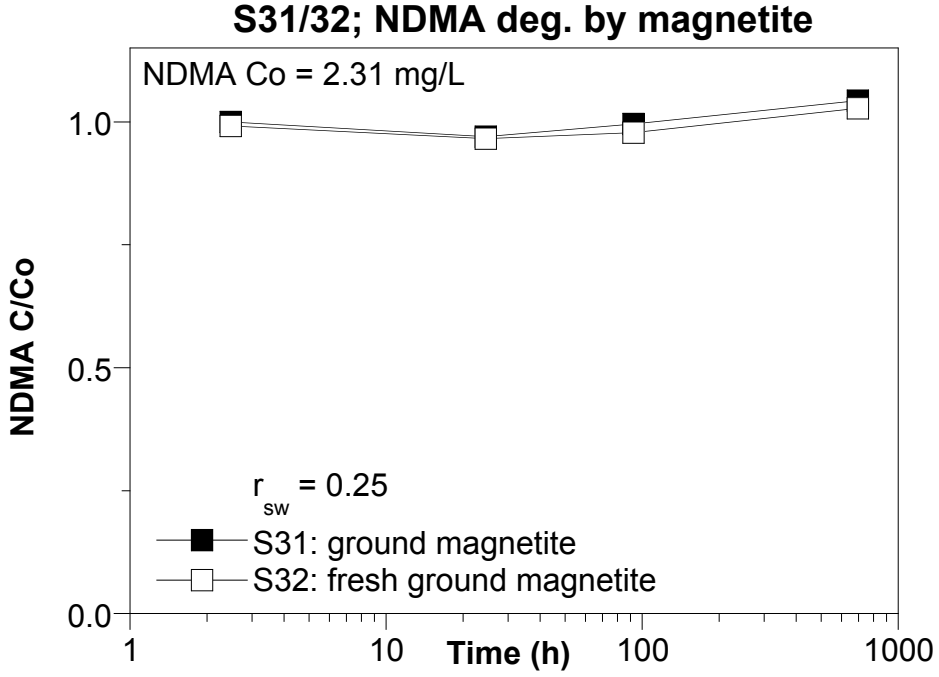
S31/32; NDMA deg. by magnetite
NDMA Co = 2.31 mg/L
NDMA C/Co
1.0
0.5
0.0
1
10
100
1000
Time (h)
r sw = 0.25
S31: ground magnetite
S32: fresh ground magnetite

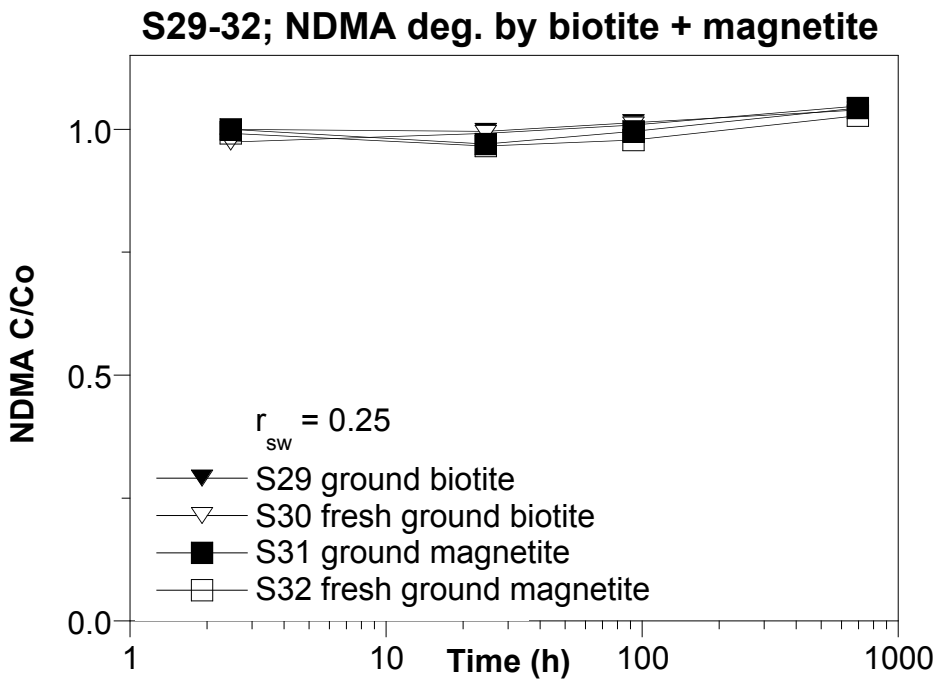
S29-32; NDMA deg. by biotite + magnetite
NDMA C/Co
1.0
0.5
0.0
1
10
100
1000
Time (h)
r sw = 0.25
S29 ground biotite
S30 fresh ground biotite
S31 ground magnetite
S32 fresh ground magnetite

Appendix A.3 Task 1.3 NDMA Degradation by Reduced Sediment (Batch)

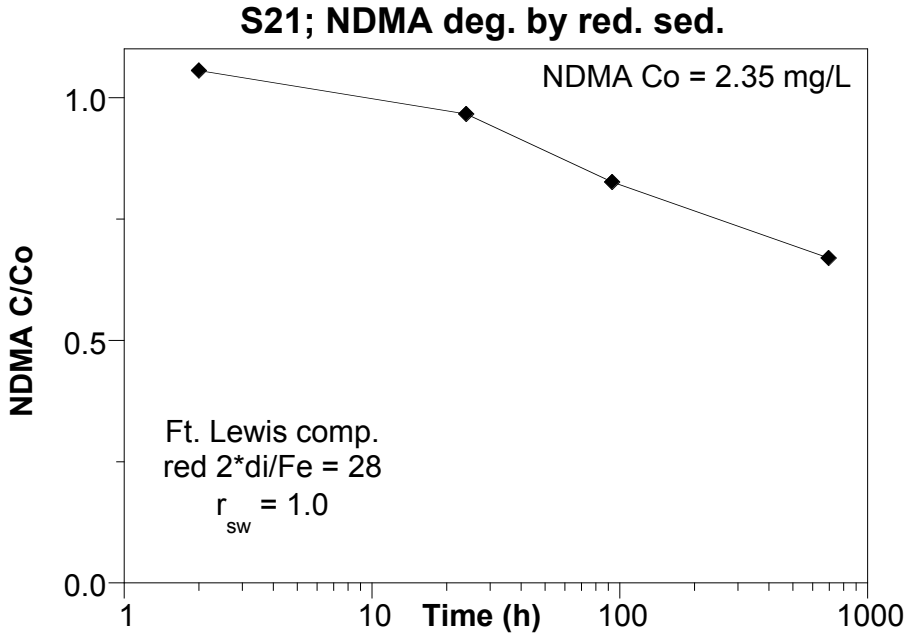

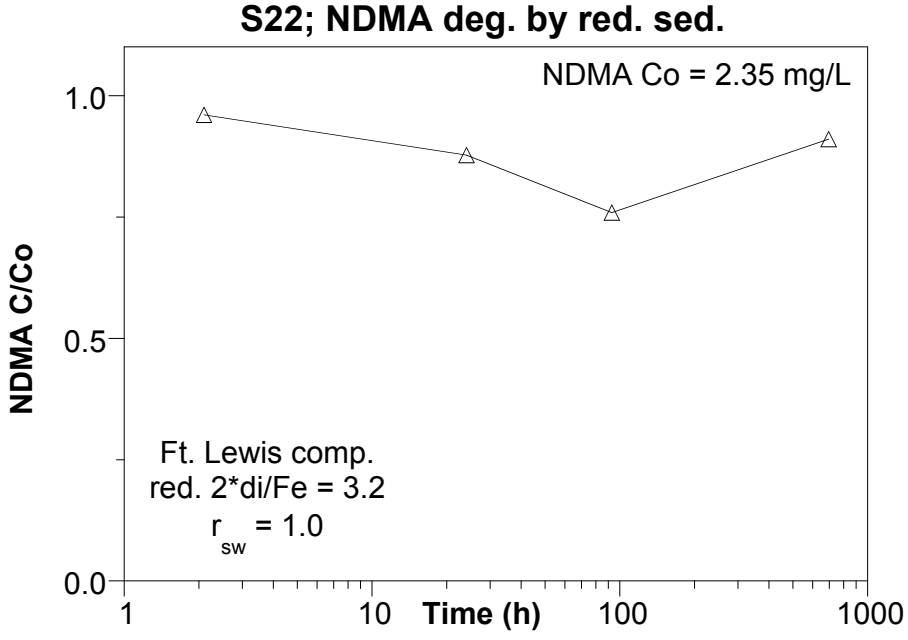

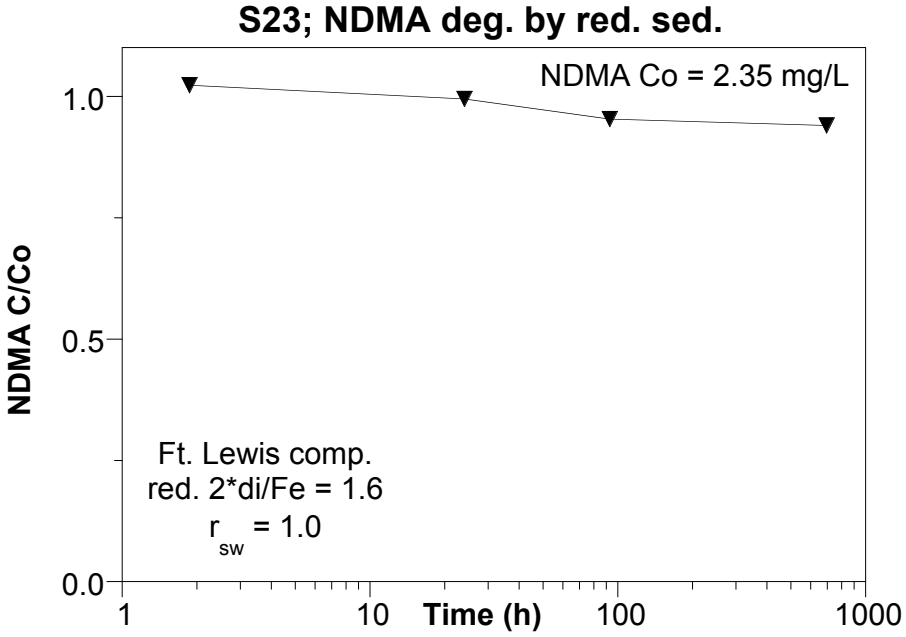
S23; NDMA deg. by red. sed.
NDMA Co = 2.35 mg/L
NDMA C/Co
1.0
0.5
0.0
Ft. Lewis comp.
red. 2*di/Fe = 1.6
r sw = 1.0
1
10
Time (h)
100
1000

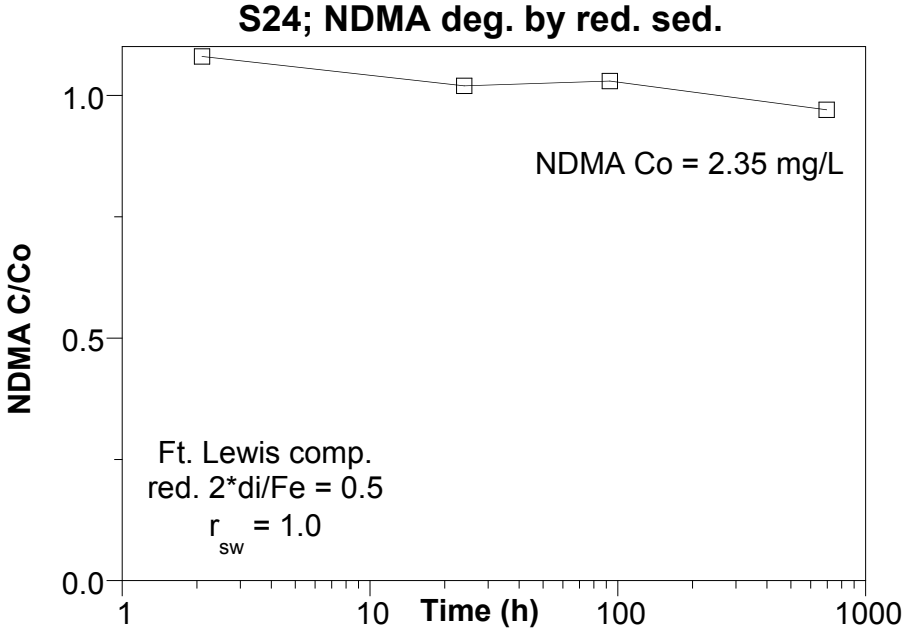
S24; NDMA deg. by red. sed.
NDMA Co = 2.35 mg/L
NDMA C/Co
1.0
0.5
0.0
Ft. Lewis comp.
red. 2*di/Fe = 0.5
r sw = 1.0
1
10
Time (h)
100
1000

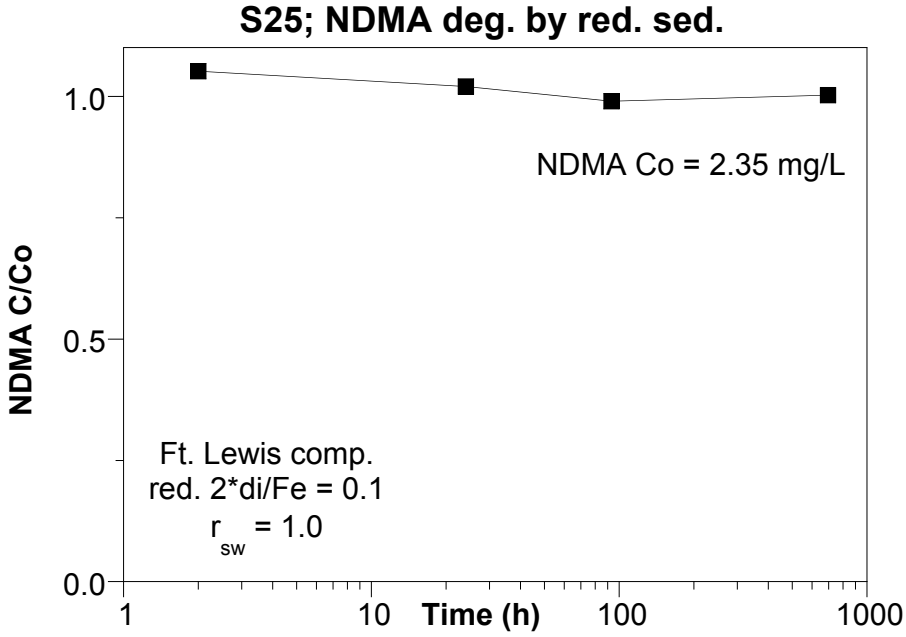
S25; NDMA deg. by red. sed.
NDMA C/Co
1.0
0.5
0.0
NDMA Co = 2.35 mg/L
Ft. Lewis comp.
red. 2*di/Fe = 0.1
r sw = 1.0
1
10
Time (h)
100
1000

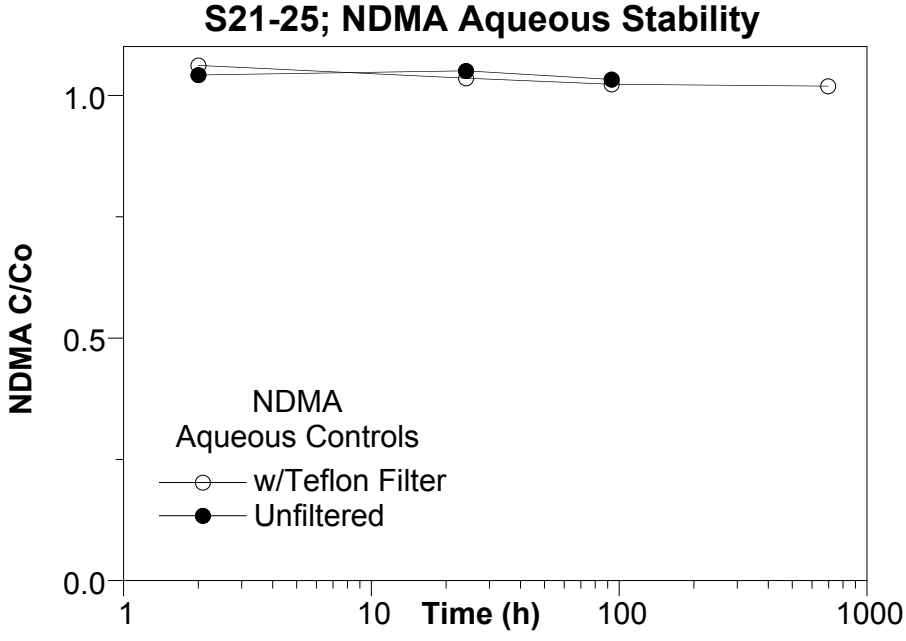
S21-25; NDMA Aqueous Stability
NDMA C/Co
1.0
0.5
0.0
NDMA
Aqueous Controls
w/Teflon Filter
Unfiltered
1
10
Time (h)
100
1000

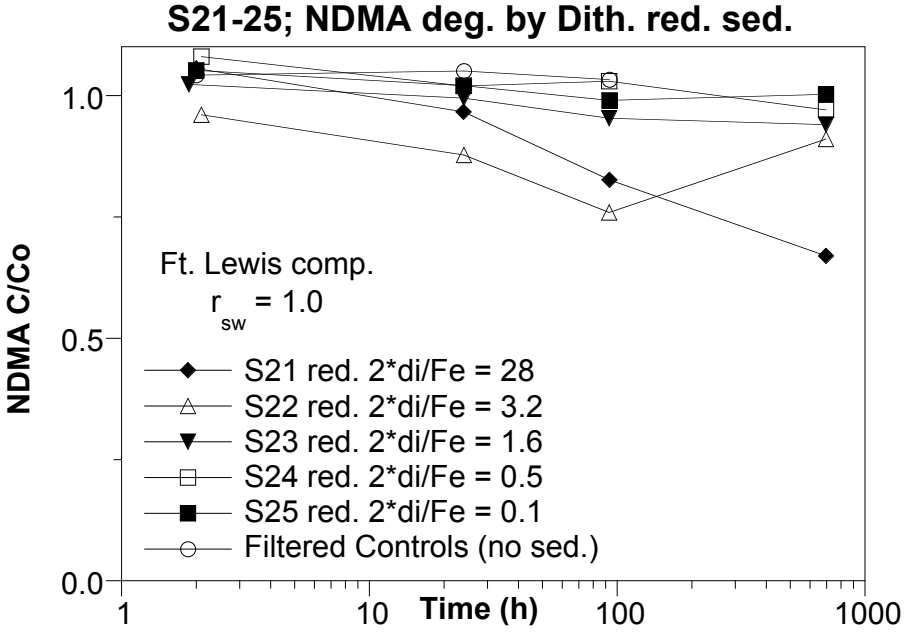
S21-25; NDMA deg. by Dith. red. sed.
NDMA C/Co
1.0
0.5
0.0
Ft. Lewis comp.
r sw = 1.0
S21 red. 2*di/Fe = 28
S22 red. 2*di/Fe = 3.2
S23 red. 2*di/Fe = 1.6
S24 red. 2*di/Fe = 0.5
S25 red. 2*di/Fe = 0.1
Filtered Controls (no sed.)
1
10
Time (h)
100
1000

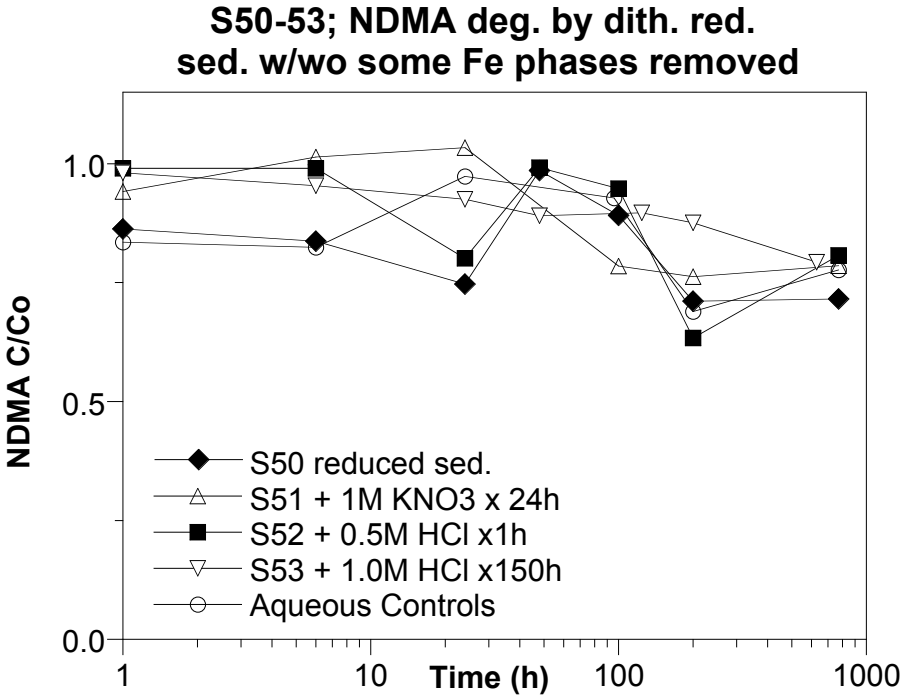
S50-53; NDMA deg. by dith. red.
sed. w/wo some Fe phases removed
NDMA C/Co
1.0
0.5
0.0
S50 reduced sed.
S51 + 1M KNO3 x 24h
S52 + 0.5M HCl x1h
S53 + 1.0M HCl x150h
Aqueous Controls
1
10
Time (h)
100
1000

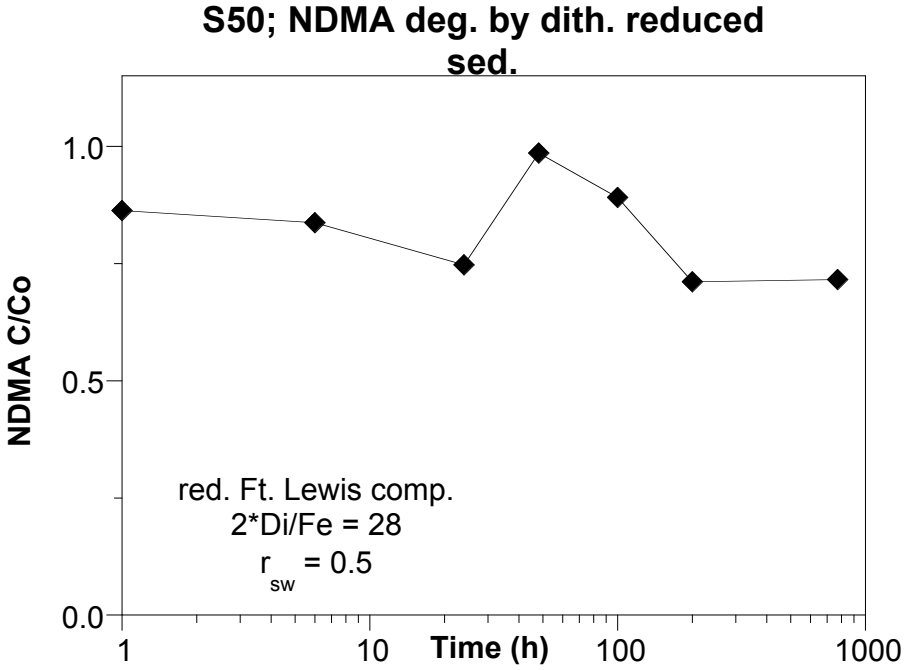
S50; NDMA deg. by dith. reduced sed.
NDMA C/Co
1.0
0.5
0.0
red. Ft. Lewis comp.
2*Di/Fe = 28
r sw = 0.5
1
10
Time (h)
100
1000

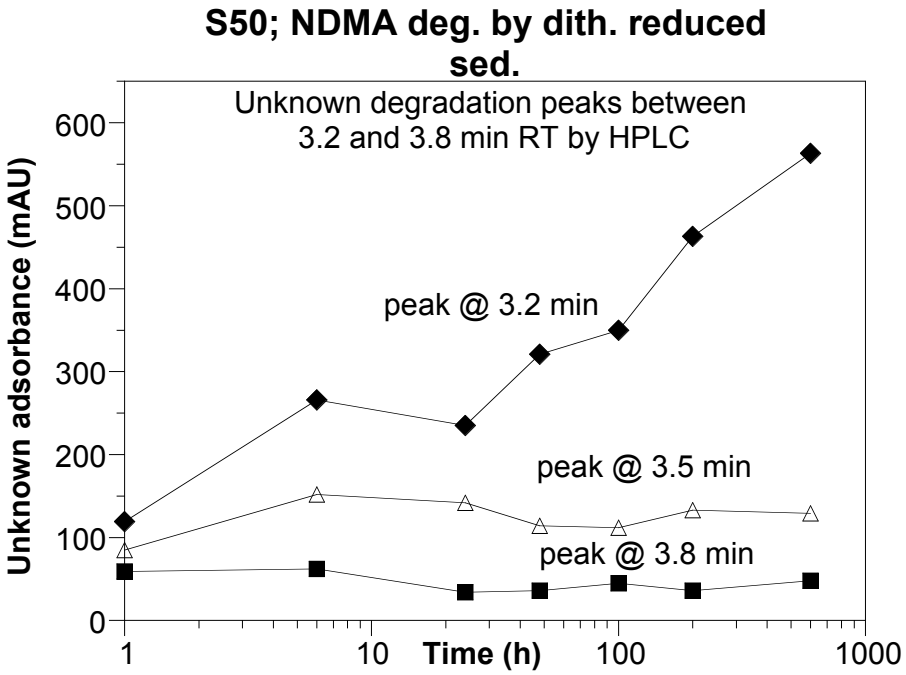
S50; NDMA deg. by dith. reduced sed.
Unknown degradation peaks between 3.2 and 3.8 min RT by HPLC
Unknown adsorbance (mAU)
600
500
400
300
200
100
0
peak @ 3.2 min
peak @ 3.5 min
peak @ 3.8 min
1
10
Time (h)
100
1000

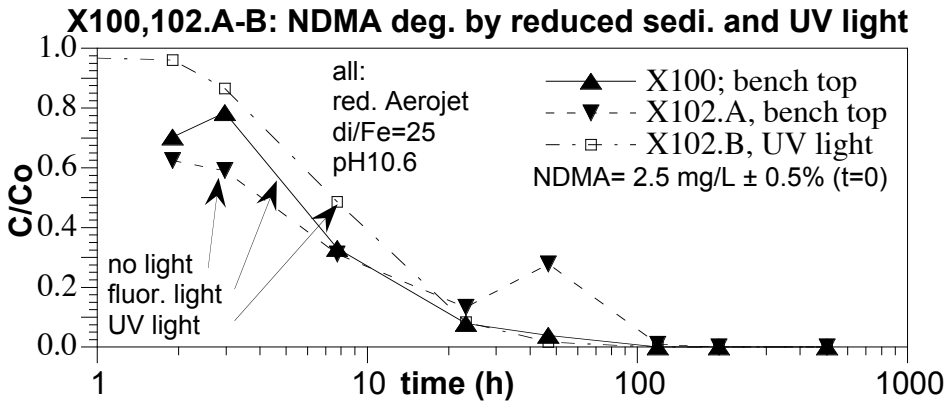
X100,102.A-B: NDMA deg. by reduced sedi. and UV light
C/Co
time (h)
all:
red. Aerojet
di/Fe=25
pH10.6
X100; bench top
X102.A, bench top
X102.B, UV light
NDMA= 2.5 mg/L ± 0.5% (t=0)
no light
fluor. light
UV light

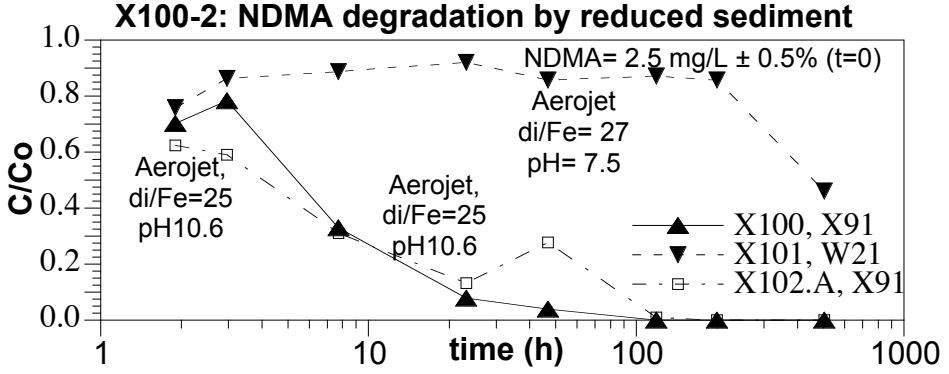
X100-2: NDMA degradation by reduced sediment
C/Co
time (h)
NDMA= 2.5 mg/L ± 0.5% (t=0)
Aerojet
di/Fe= 27
pH= 7.5
Aerojet,
di/Fe=25
pH10.6
Aerojet,
di/Fe=25
pH10.6
X100, X91
X101, W21
X102.A, X91

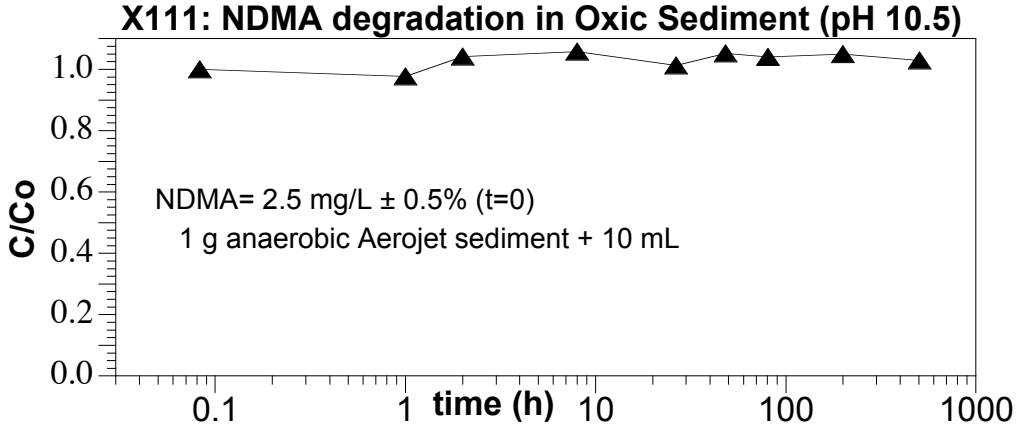
X111: NDMA degradation in Oxic Sediment (pH 10.5)
C/Co
time (h)
NDMA= 2.5 mg/L ± 0.5% (t=0)
1 g anaerobic Aerojet sediment + 10 mL

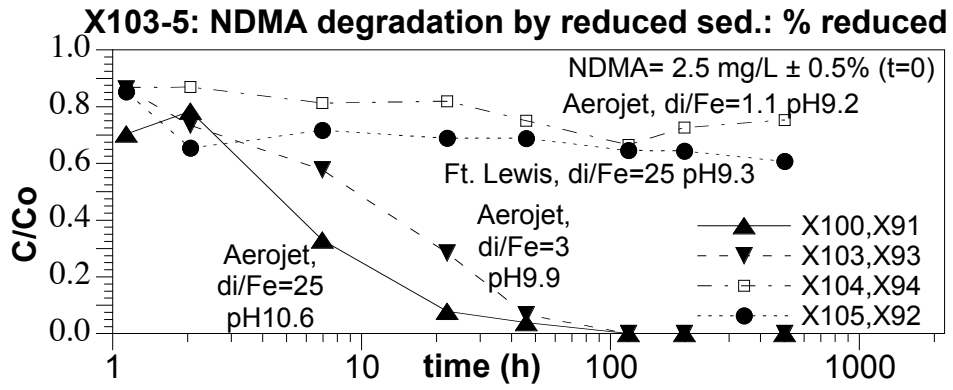
X103-5: NDMA degradation by reduced sed.: % reduced
C/Co
time (h)
NDMA= 2.5 mg/L ± 0.5% (t=0)
Aerojet, di/Fe=1.1 pH9.2
Ft. Lewis, di/Fe=25 pH9.3
Aerojet, di/Fe=3 pH9.9
Aerojet, di/Fe=25 pH10.6
X100,X91
X103,X93
X104,X94
X105,X92

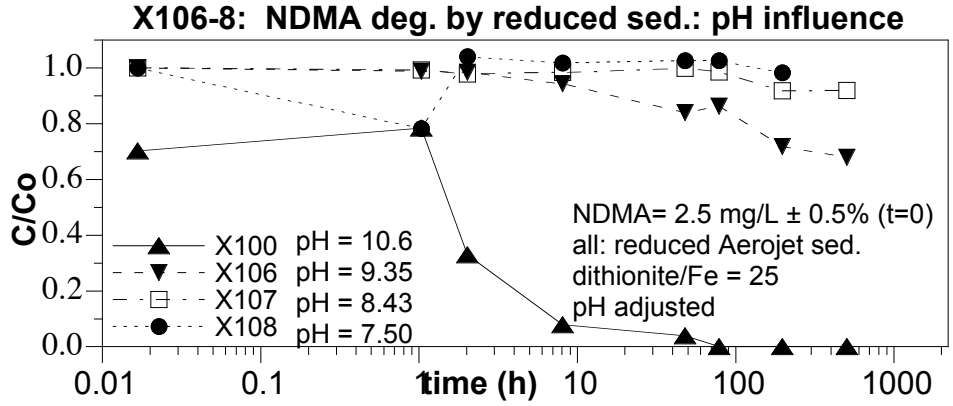
X106-8: NDMA deg. by reduced sed.: pH influence
C/Co
time (h)
X100 pH = 10.6
X106 pH = 9.35
X107 pH = 8.43
X108 pH = 7.50
NDMA= 2.5 mg/L ± 0.5% (t=0)
all: reduced Aerojet sed.
dithionite/Fe = 25
pH adjusted

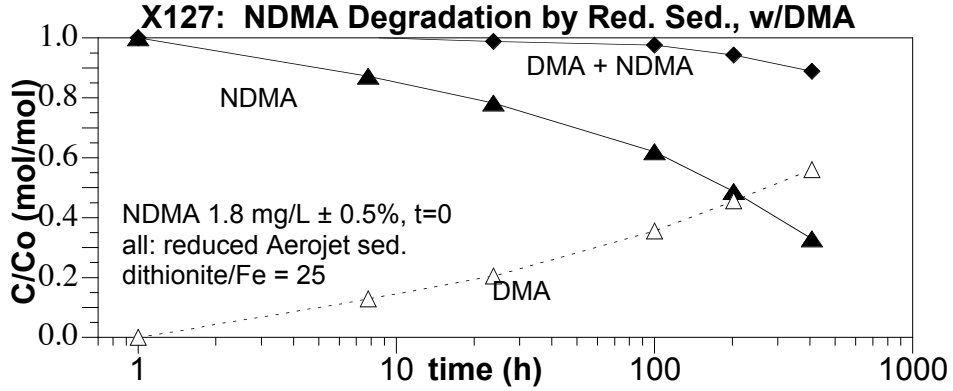
X127: NDMA Degradation by Red. Sed., w/DMA
C/Co (mol/mol)
time (h)
DMA + NDMA
NDMA
NDMA 1.8 mg/L ± 0.5%, t=0
all: reduced Aerojet sed.
dithionite/Fe = 25
DMA

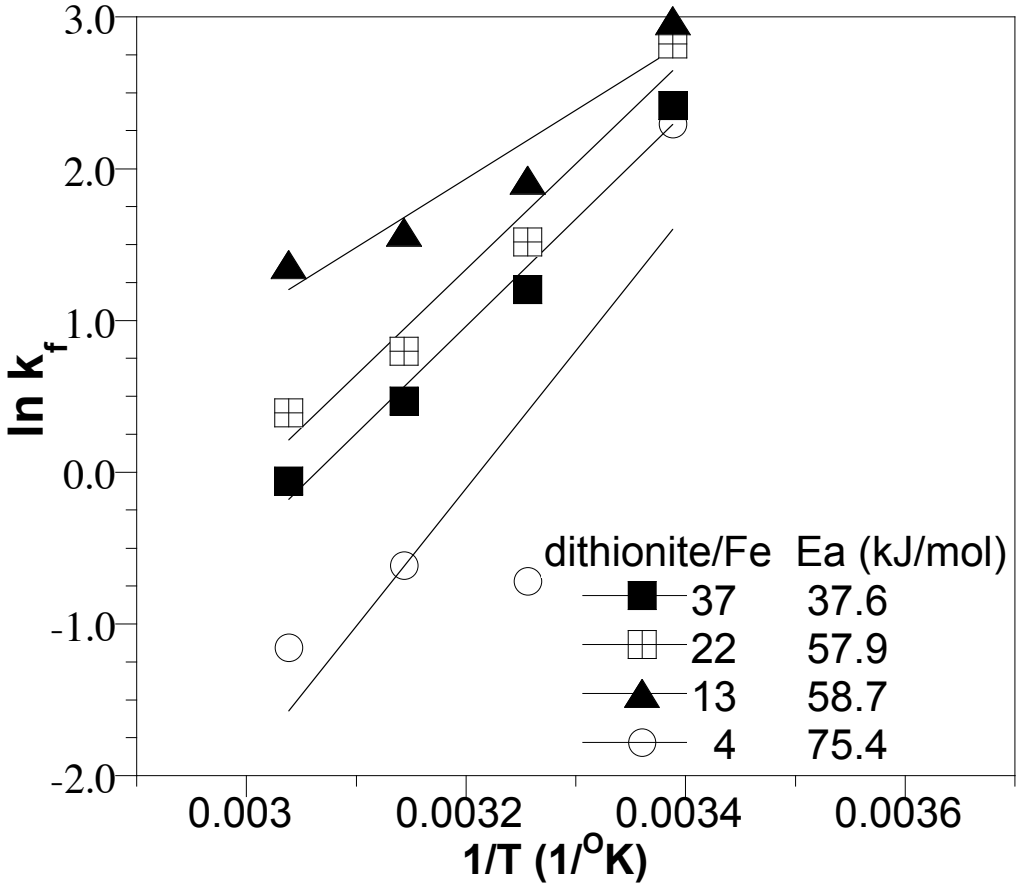

Change in NDMA degradation rate with temperature for different amounts of chemical reduction of Aerojet sediment

Appendix A.4 Task 1.4 NDMA Degradation in Reduced/Chemically Modified Sediment

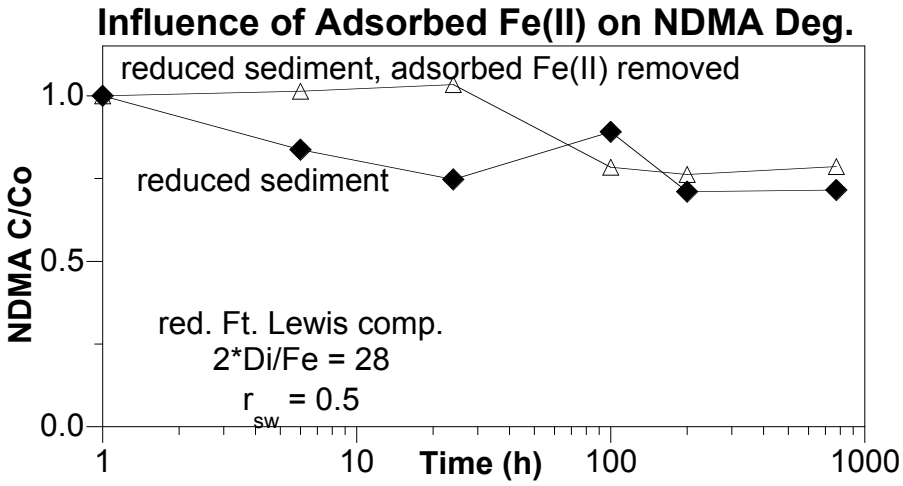

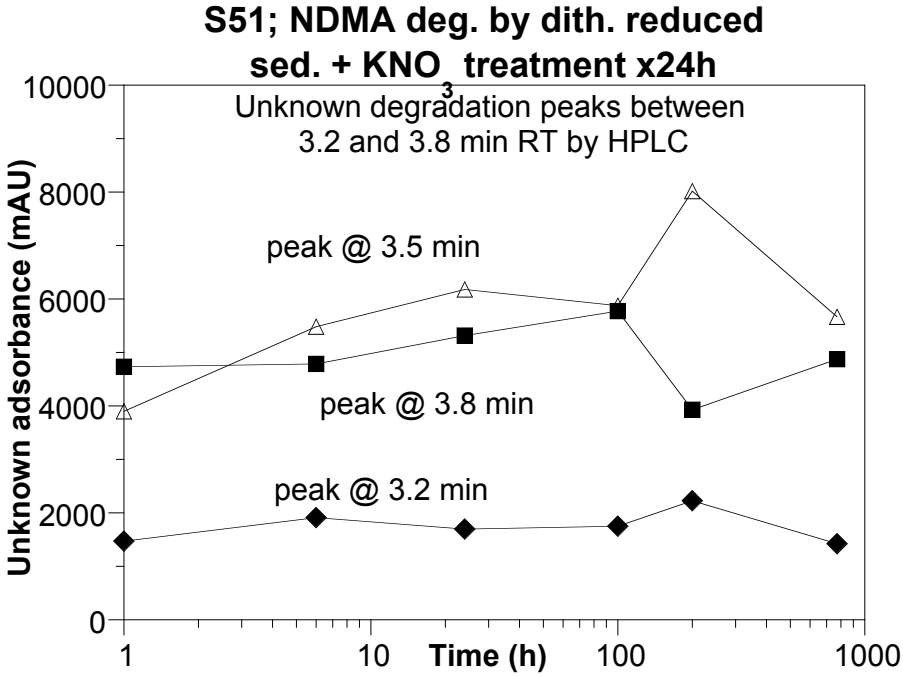

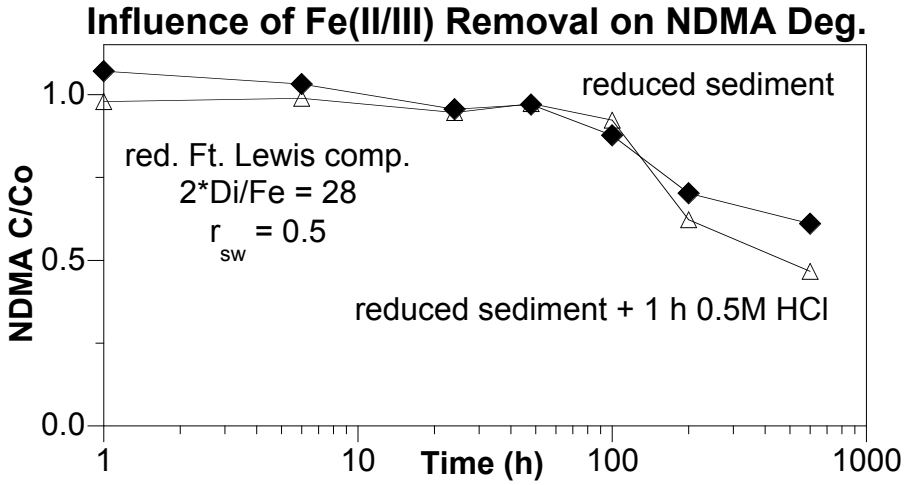
Influence of Fe(II/III) Removal on NDMA Deg.
NDMA C/Co
1.0
0.5
0.0
reduced sediment
red. Ft. Lewis comp.
2*Di/Fe = 28
r sw = 0.5
reduced sediment + 1 h 0.5M HCl
1
10
Time (h)
100
1000

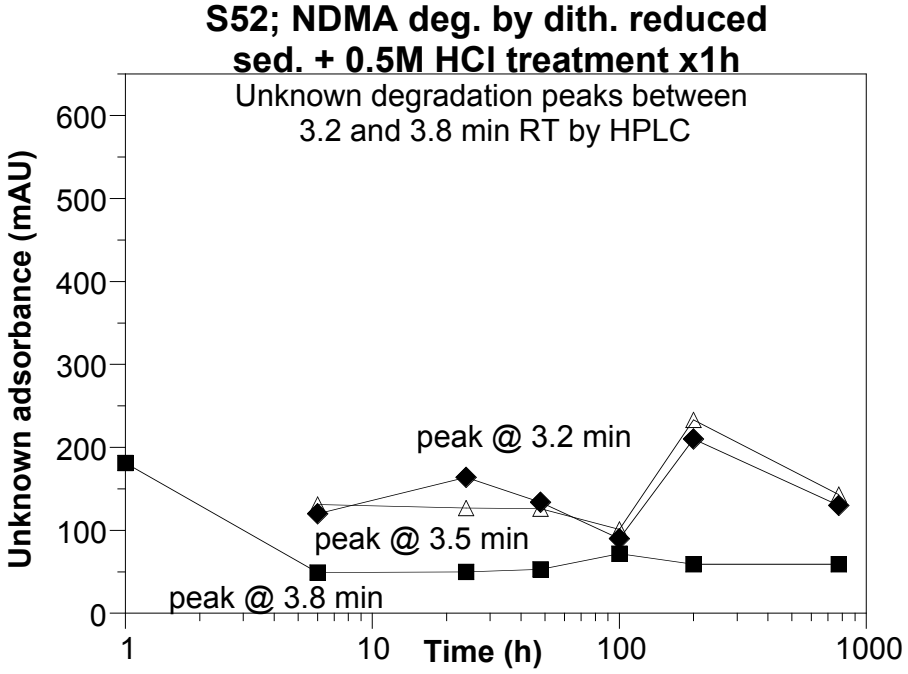
S52; NDMA deg. by dith. reduced sed. + 0.5M HCl treatment x1h
Unknown degradation peaks between 3.2 and 3.8 min RT by HPLC
Unknown adsorbance (mAU)
600
500
400
300
200
100
0
peak @ 3.2 min
peak @ 3.5 min
peak @ 3.8 min
1
10
Time (h)
100
1000

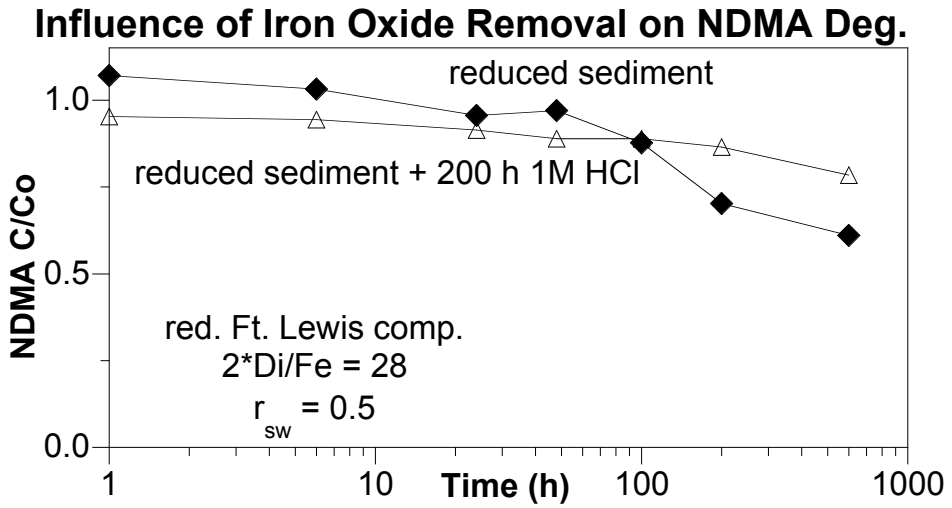
Influence of Iron Oxide Removal on NDMA Deg.
reduced sediment
reduced sediment + 200 h 1M HCl
red. Ft. Lewis comp.
2*Di/Fe = 28
r sw = 0.5
NDMA C/Co
1.0
0.5
0.0
1
10
100
1000
Time (h)

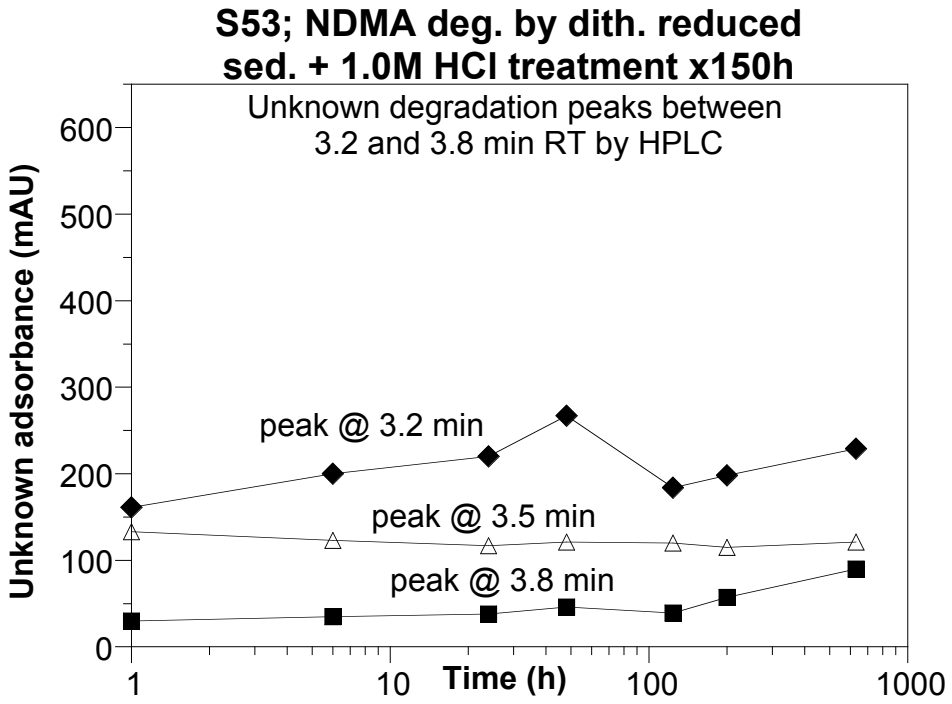
S53; NDMA deg. by dith. reduced sed. + 1.0M HCl treatment x150h
Unknown degradation peaks between 3.2 and 3.8 min RT by HPLC
peak @ 3.2 min
peak @ 3.5 min
peak @ 3.8 min
Unknown adsorbance (mAU)
600
500
400
300
200
100
0
1
10
100
1000
Time (h)

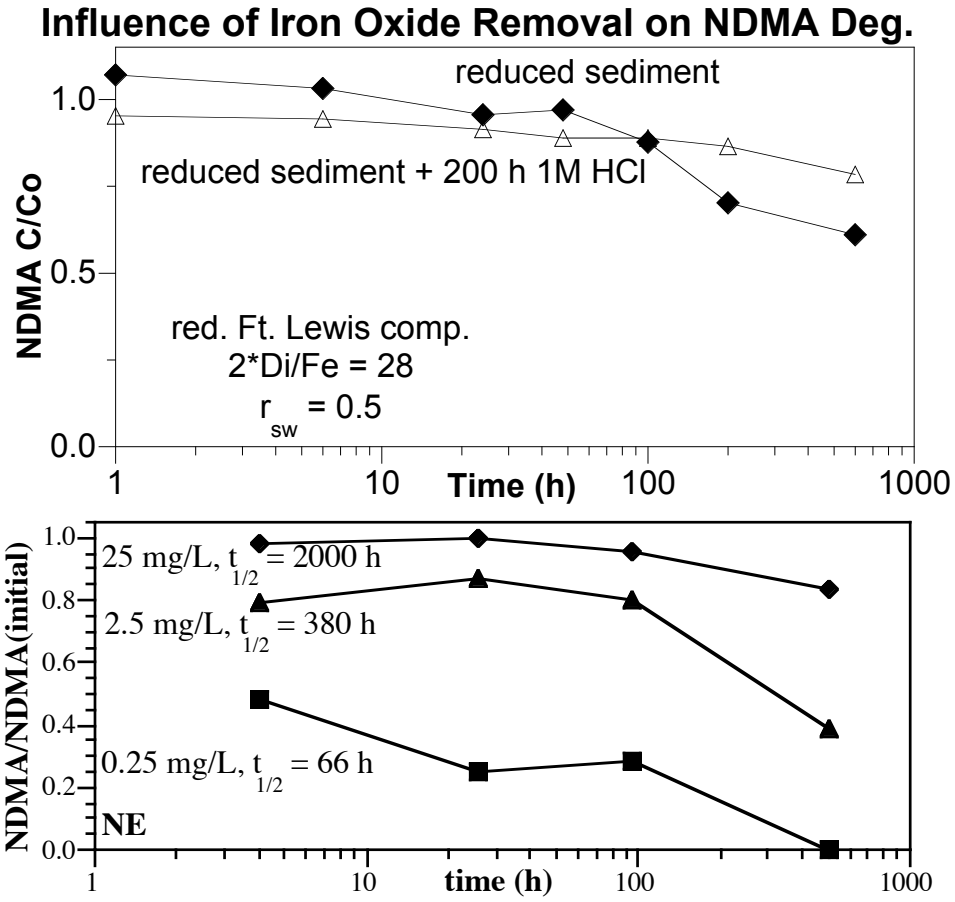
Influence of Iron Oxide Removal on NDMA Deg.
reduced sediment
reduced sediment + 200 h 1M HCl
red. Ft. Lewis comp.
2*Di/Fe = 28
r sw = 0.5
NDMA C/Co
1.0
0.5
0.0
1
10
100
1000
Time (h)
25 mg/L, t 1/2 = 2000 h
2.5 mg/L, t 1/2 = 380 h
0.25 mg/L, t 1/2 = 66 h
NE
NDMA/NDMA(initial)
1.0
0.8
0.6
0.4
0.2
0.0
1
10
100
1000
time (h)

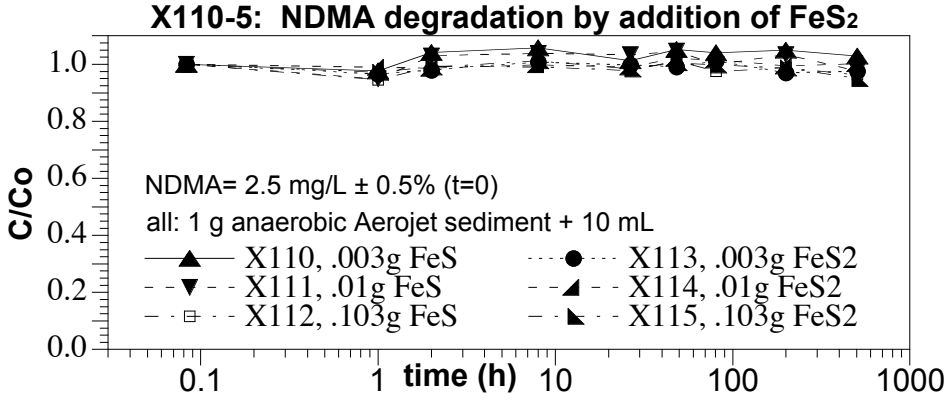
X110-5: NDMA degradation by addition of FeS2
C/Co
time (h)
NDMA= 2.5 mg/L ± 0.5% (t=0)
all: 1 g anaerobic Aerojet sediment + 10 mL
X110, .003g FeS
X111, .01g FeS
X112, .103g FeS
X113, .003g FeS2
X114, .01g FeS2
X115, .103g FeS2

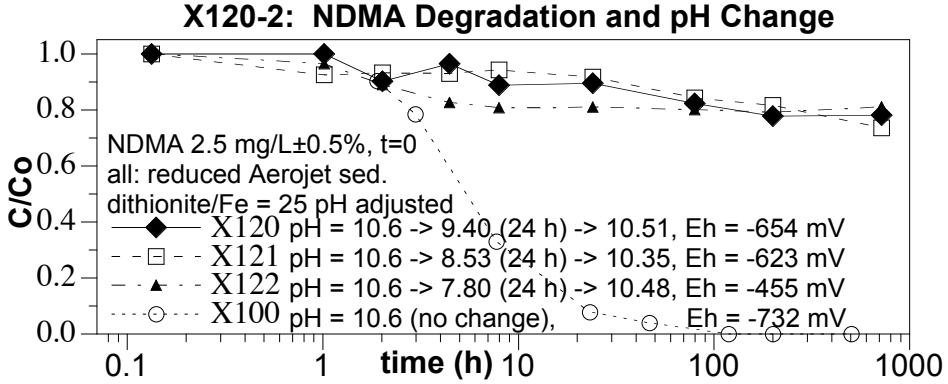
X120-2: NDMA Degradation and pH Change
C/Co
time (h)
NDMA 2.5 mg/L±0.5%, t=0
all: reduced Aerojet sed.
dithionite/Fe = 25 pH adjusted
X120 pH = 10.6 -> 9.40 (24 h) -> 10.51, Eh = -654 mV
X121 pH = 10.6 -> 8.53 (24 h) -> 10.35, Eh = -623 mV
X122 pH = 10.6 -> 7.80 (24 h) -> 10.48, Eh = -455 mV
X100 pH = 10.6 (no change), Eh = -732 mV

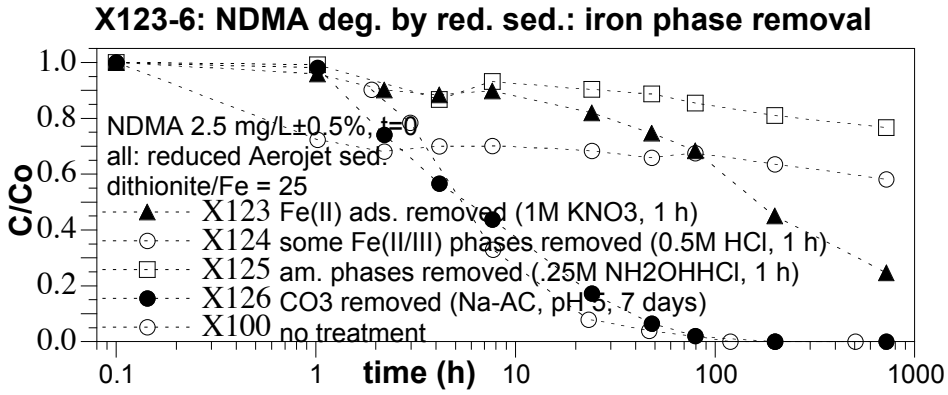
X123-6: NDMA deg. by red. sed.: iron phase removal
C/Co
time (h)
NDMA 2.5 mg/L±0.5%, t=0
all: reduced Aerojet sed.
dithionite/Fe = 25
X123 Fe(II) ads. removed (1M KNO3, 1 h)
X124 some Fe(II/III) phases removed (0.5M HCl, 1 h)
X125 am. phases removed (.25M NH2OHHCl, 1 h)
X126 CO3 removed (Na-AC, pH 5, 7 days)
X100 no treatment

X128-130: NDMA Degradation by Red. Sed., w/o magnetite

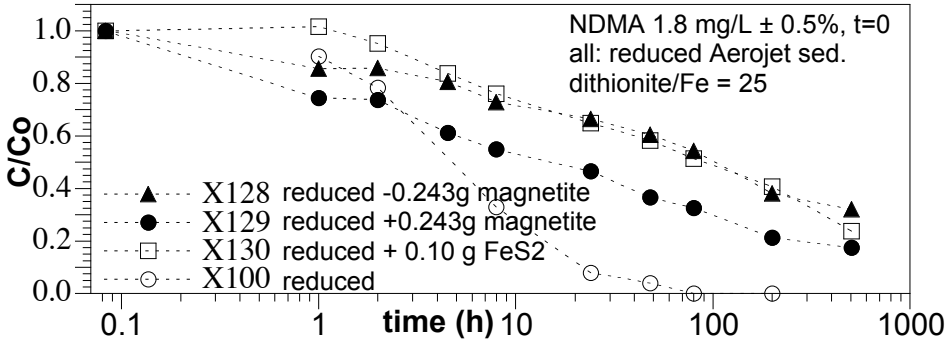

X131: NDMA degradation by aqueous alkaline hydrolysis and with sediment (X131)

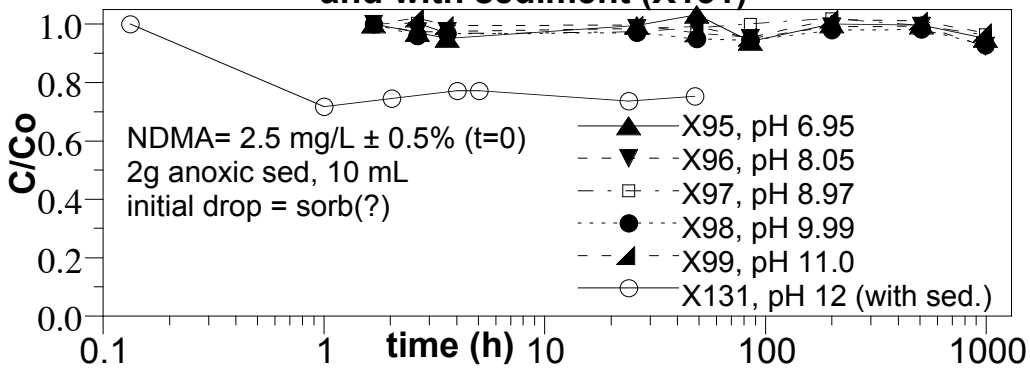

X131,132: NDMA degradation by adsorbed Fe(II) (alkaline sediment)

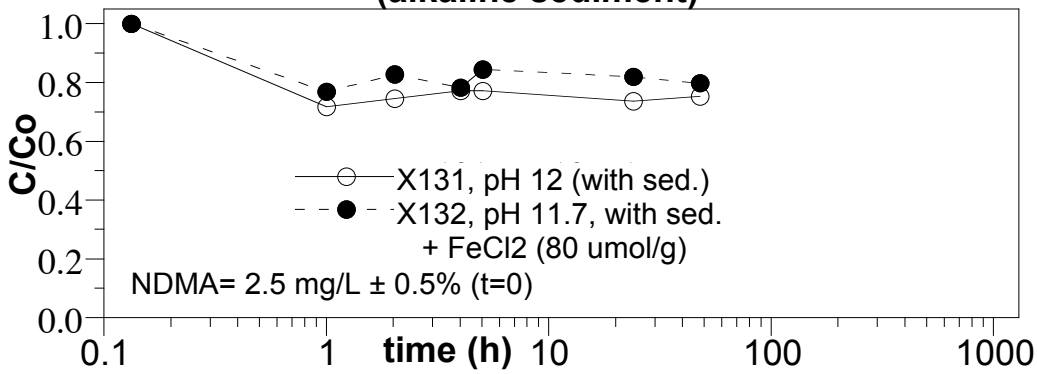

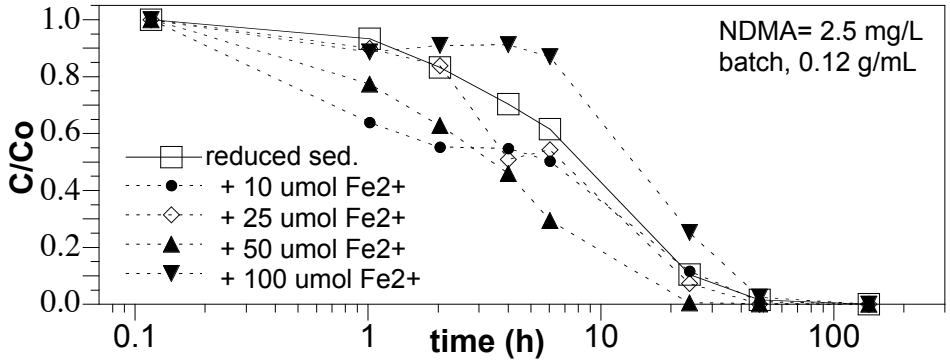
NDMA= 2.5 mg/L
batch, 0.12 g/mL
C/Co
time (h)
reduced sed.
+ 10 umol Fe2+
+ 25 umol Fe2+
+ 50 umol Fe2+
+ 100 umol Fe2+

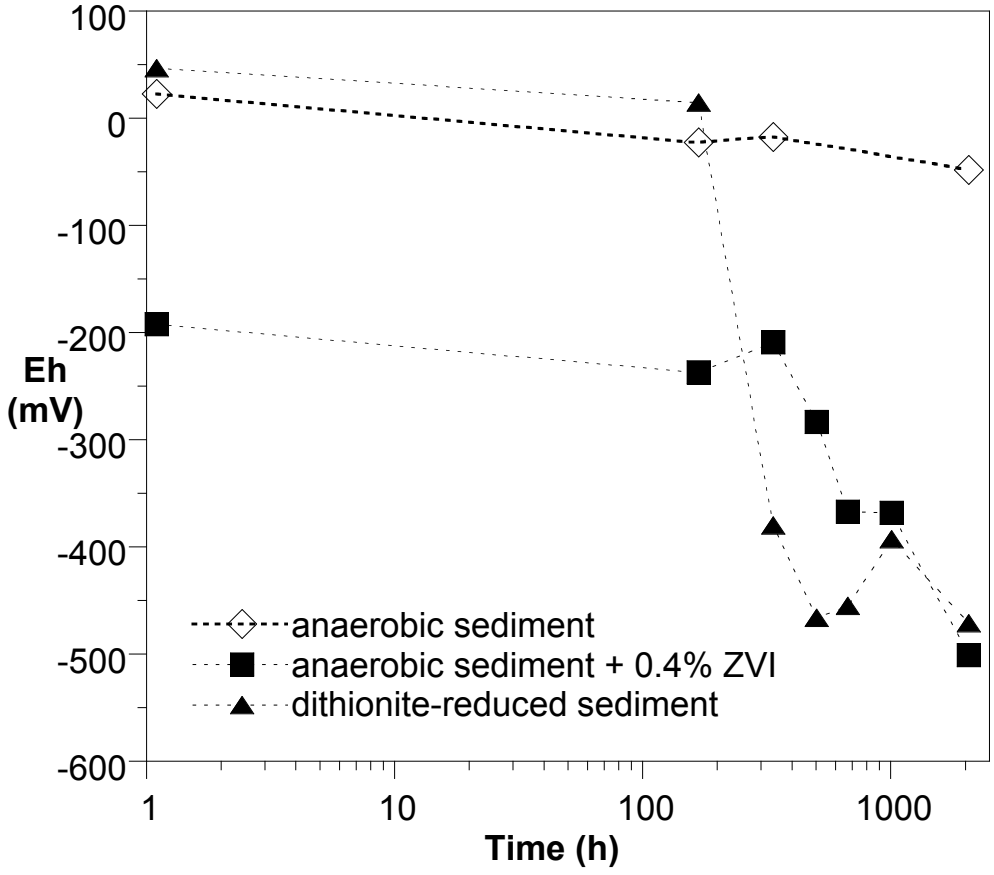
Eh
(mV)
Time (h)
anaerobic sediment
anaerobic sediment + 0.4% ZVI
dithionite-reduced sediment

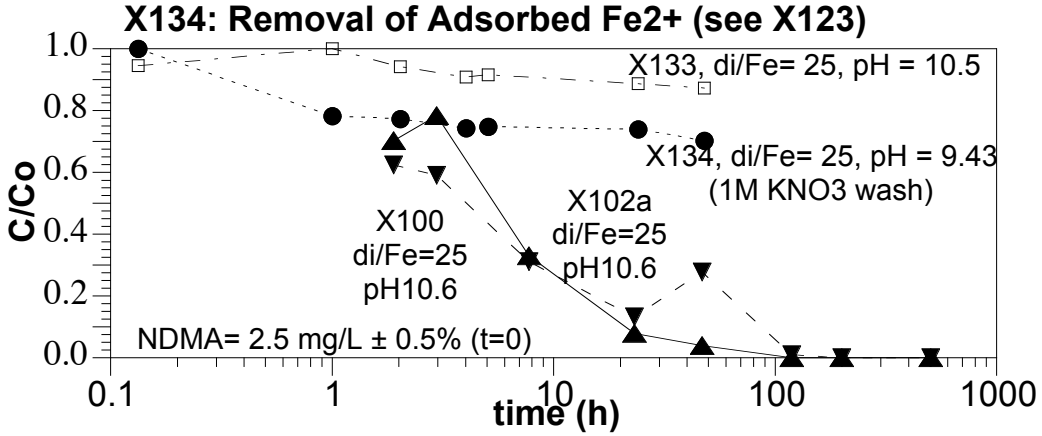
X134: Removal of Adsorbed Fe2+ (see X123)
C/Co
time (h)
X133, di/Fe= 25, pH = 10.5
X134, di/Fe= 25, pH = 9.43
(1M KNO3 wash)
X102a
di/Fe=25
pH10.6
X100
di/Fe=25
pH10.6
NDMA= 2.5 mg/L ± 0.5% (t=0)

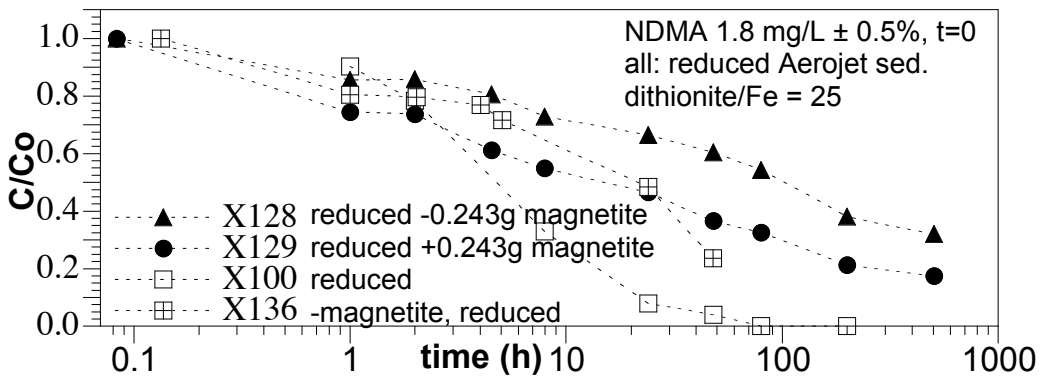
X128-130, 136: NDMA Degradation by Red. Sed., w/o magnetite
C/Co
time (h)
NDMA 1.8 mg/L ± 0.5%, t=0
all: reduced Aerojet sed.
dithionite/Fe = 25
X128 reduced -0.243g magnetite
X129 reduced +0.243g magnetite
X100 reduced
X136 -magnetite, reduced

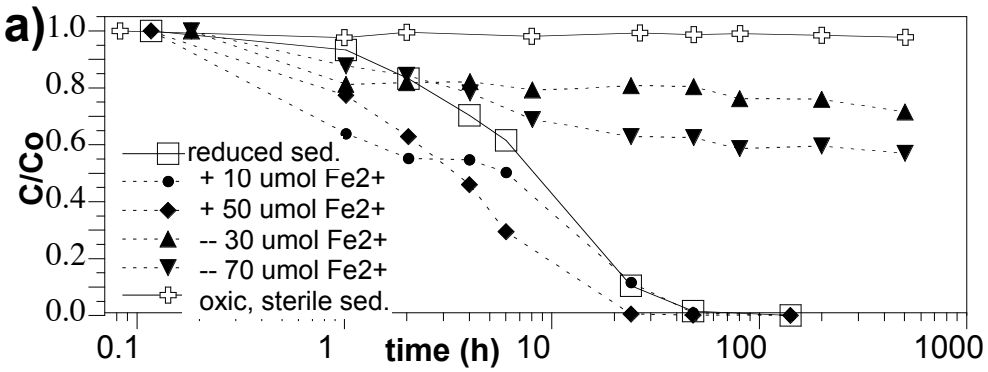
a)
C/Co
time (h)
reduced sed.
+ 10 umol Fe2+
+ 50 umol Fe2+
-- 30 umol Fe2+
-- 70 umol Fe2+
oxic, sterile sed.

Appendix A.5 Task 1.5 NDMA Degradation by Chemically Modified 2:1 Smectite Clays

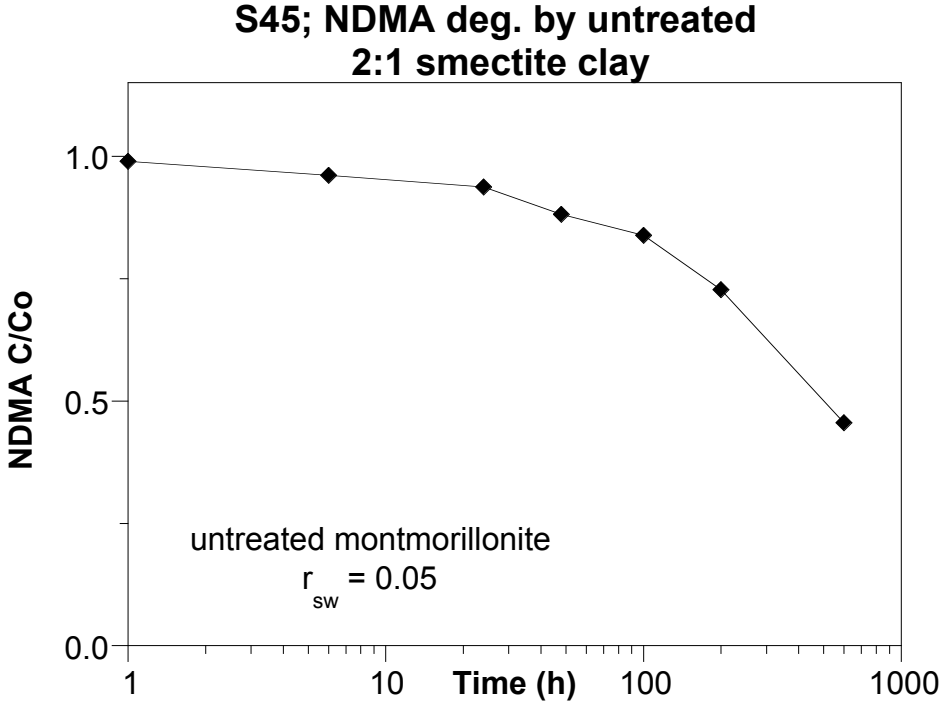

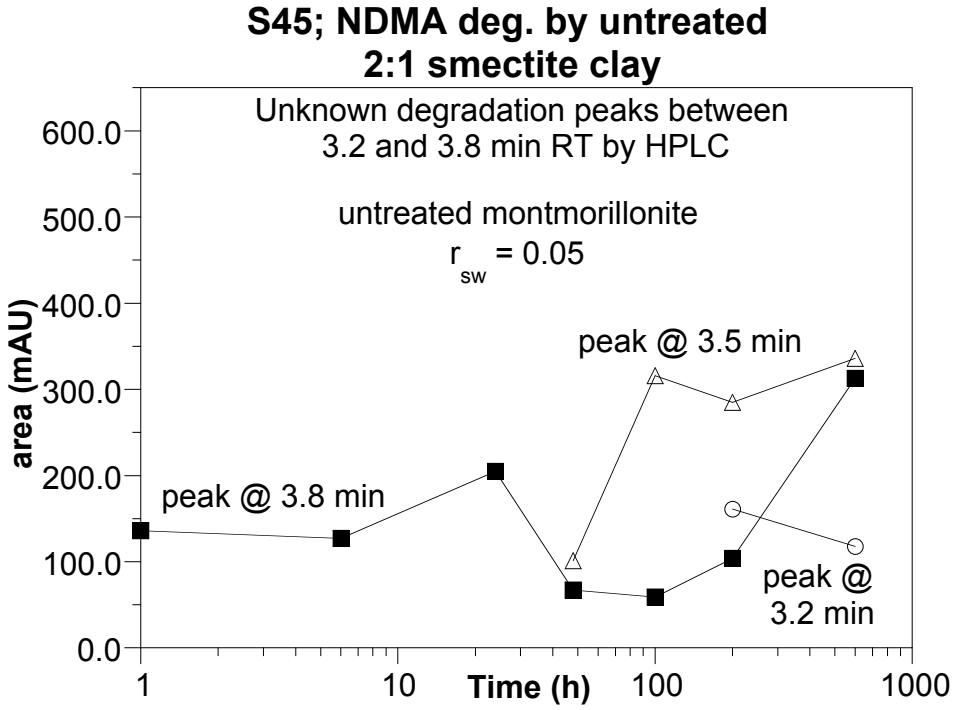

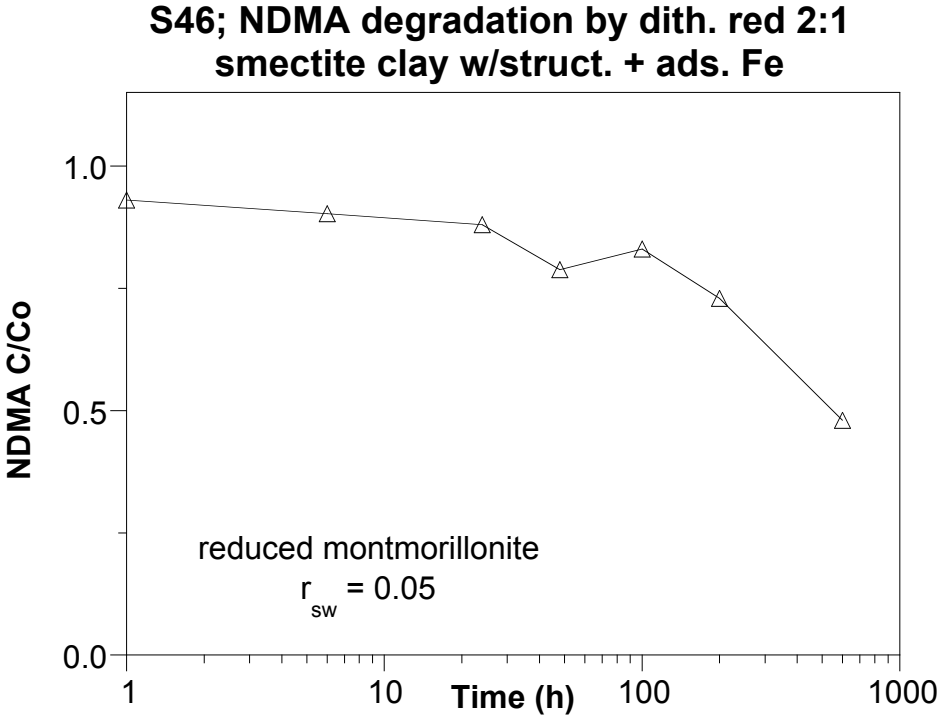
S46; NDMA degradation by dith. red 2:1
smectite clay w/struct. + ads. Fe
NDMA C/Co
1.0
0.5
0.0
reduced montmorillonite
r sw = 0.05
1
10
Time (h)
100
1000

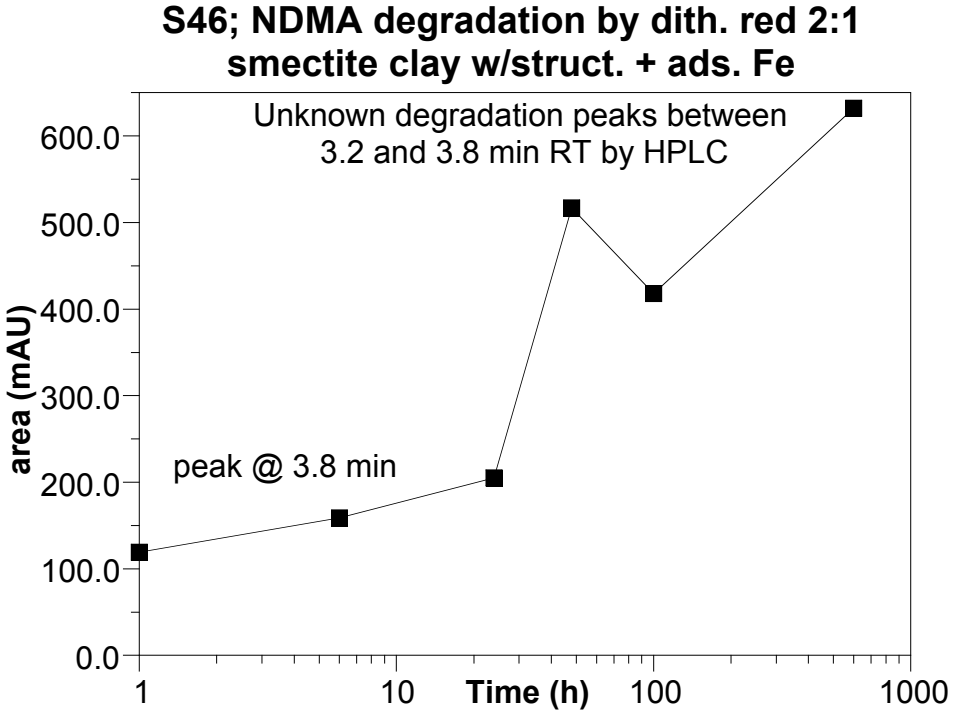
S46; NDMA degradation by dith. red 2:1
smectite clay w/struct. + ads. Fe
Unknown degradation peaks between
3.2 and 3.8 min RT by HPLC
area (mAU)
600.0
500.0
400.0
300.0
200.0
100.0
0.0
peak @ 3.8 min
1
10
Time (h)
100
1000

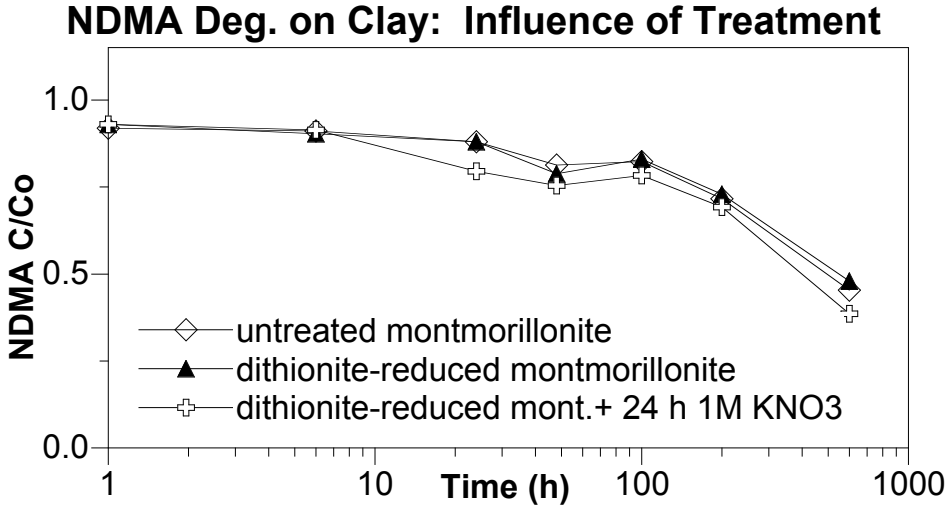
NDMA Deg. on Clay: Influence of Treatment
NDMA C/Co
1.0
0.5
0.0
1
10
100
1000
Time (h)
untreated montmorillonite
dithionite-reduced montmorillonite
dithionite-reduced mont.+ 24 h 1M KNO3

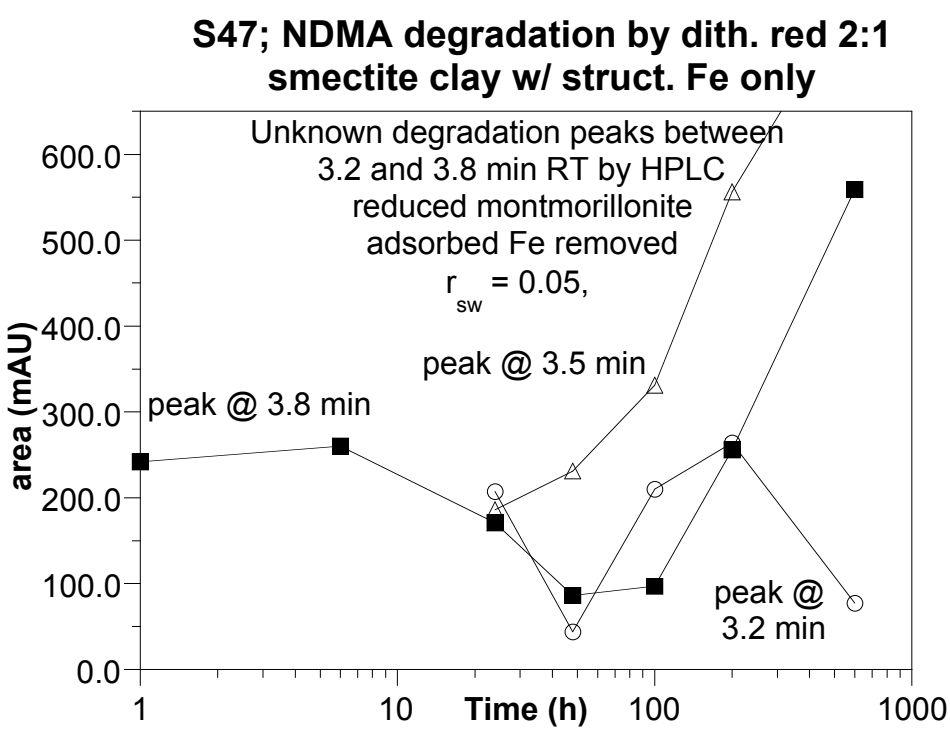
S47; NDMA degradation by dith. red 2:1 smectite clay w/ struct. Fe only
Unknown degradation peaks between 3.2 and 3.8 min RT by HPLC
reduced montmorillonite
adsorbed Fe removed
r sw = 0.05,
peak @ 3.5 min
peak @ 3.8 min
peak @ 3.2 min
area (mAU)
600.0
500.0
400.0
300.0
200.0
100.0
0.0
1
10
100
1000
Time (h)

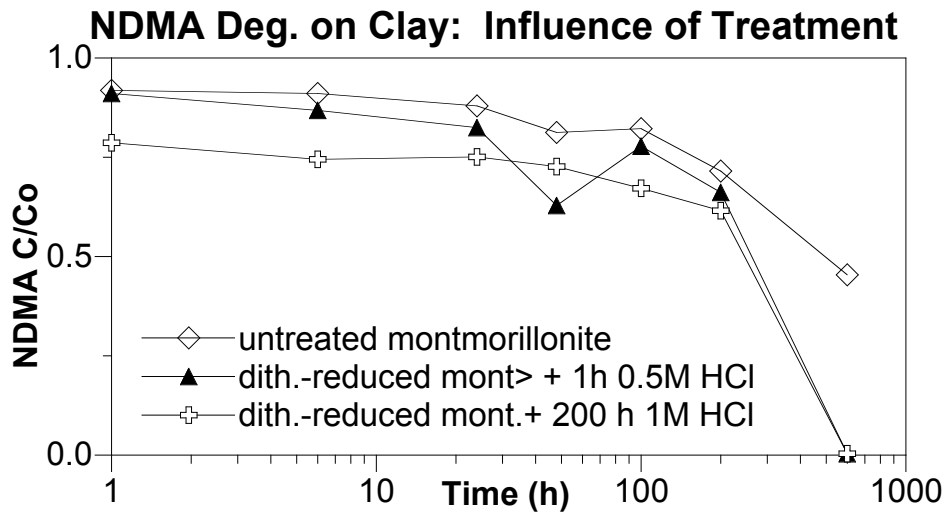
NDMA Deg. on Clay: Influence of Treatment
NDMA C/Co
1.0
0.5
0.0
1
10
100
1000
Time (h)
untreated montmorillonite
dith.-reduced mont> + 1h 0.5M HCl
dith.-reduced mont.+ 200 h 1M HCl

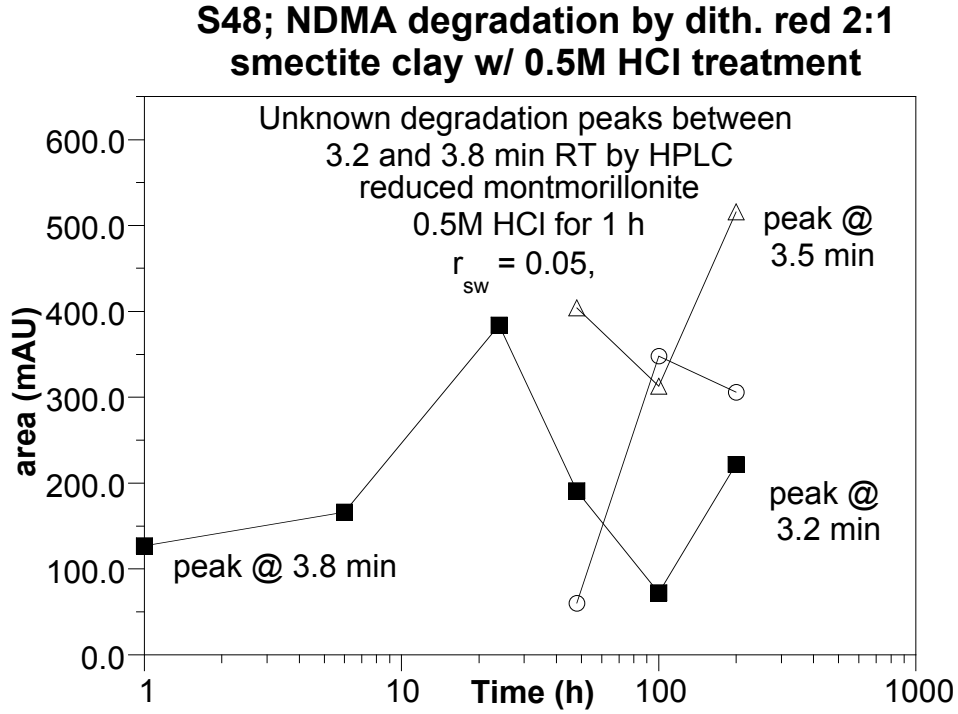
S48; NDMA degradation by dith. red 2:1 smectite clay w/ 0.5M HCl treatment
Unknown degradation peaks between 3.2 and 3.8 min RT by HPLC
reduced montmorillonite
0.5M HCl for 1 h
r sw = 0.05,
peak @ 3.5 min
peak @ 3.2 min
peak @ 3.8 min
area (mAU)
600.0
500.0
400.0
300.0
200.0
100.0
0.0
1
10
100
1000
Time (h)

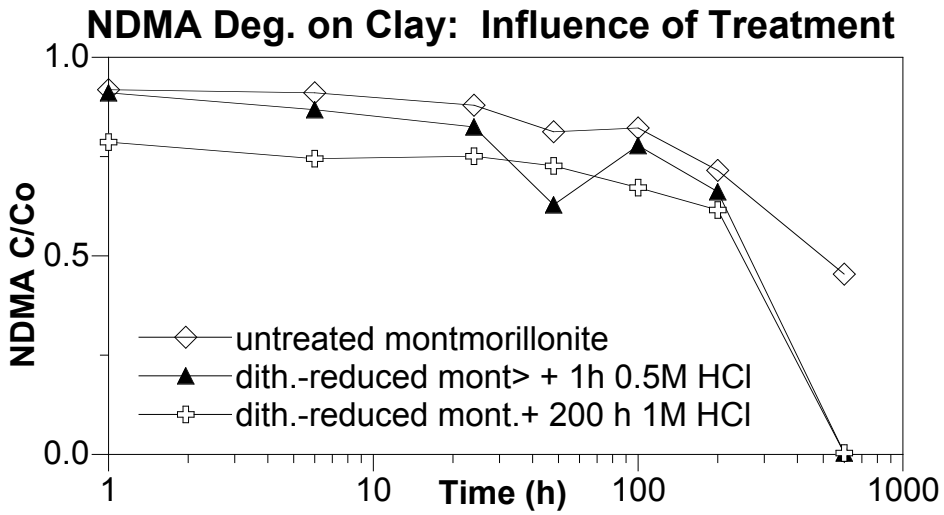
NDMA Deg. on Clay: Influence of Treatment
NDMA C/Co
1.0
0.5
0.0
1
10
100
1000
Time (h)
untreated montmorillonite
dith.-reduced mont> + 1h 0.5M HCl
dith.-reduced mont.+ 200 h 1M HCl

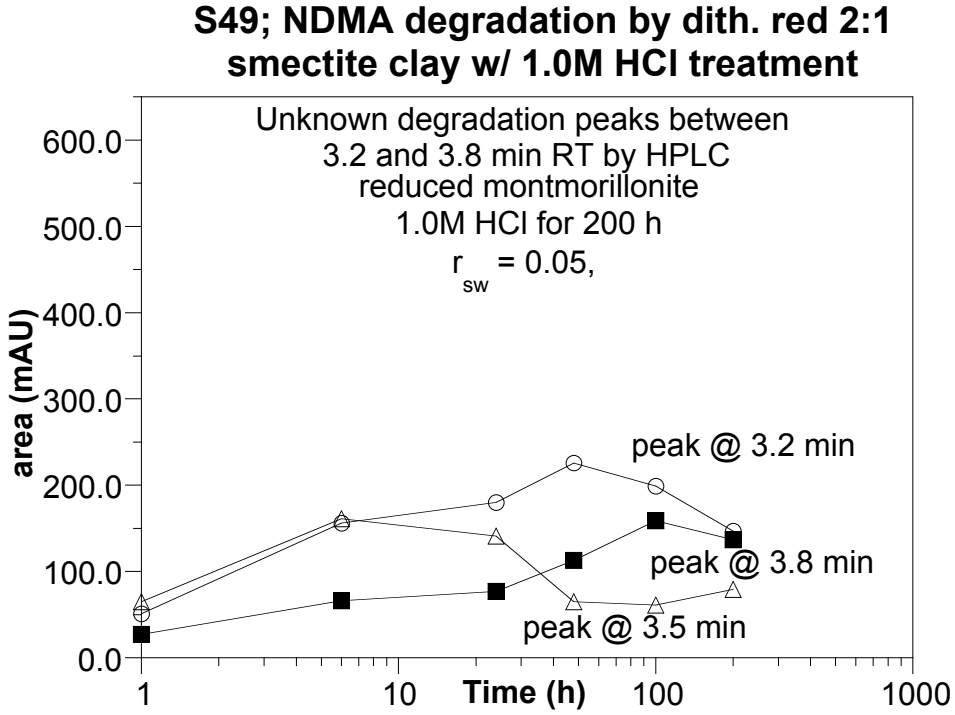
S49; NDMA degradation by dith. red 2:1 smectite clay w/ 1.0M HCl treatment
Unknown degradation peaks between 3.2 and 3.8 min RT by HPLC
reduced montmorillonite
1.0M HCl for 200 h
r sw = 0.05,
area (mAU)
600.0
500.0
400.0
300.0
200.0
100.0
0.0
1
10
100
1000
Time (h)
peak @ 3.2 min
peak @ 3.8 min
peak @ 3.5 min

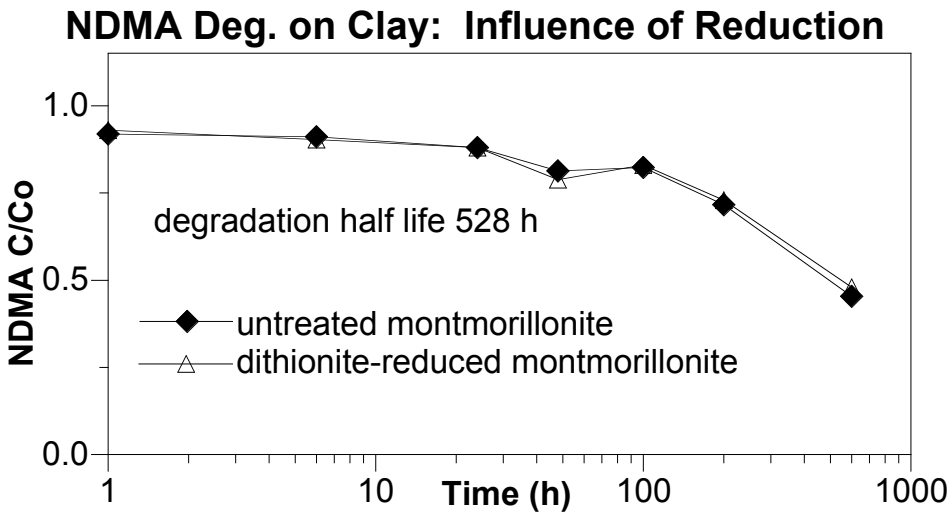
NDMA Deg. on Clay: Influence of Reduction
NDMA C/Co
1.0
0.5
0.0
degradation half life 528 h
untreated montmorillonite
dithionite-reduced montmorillonite
1
10
Time (h)
100
1000

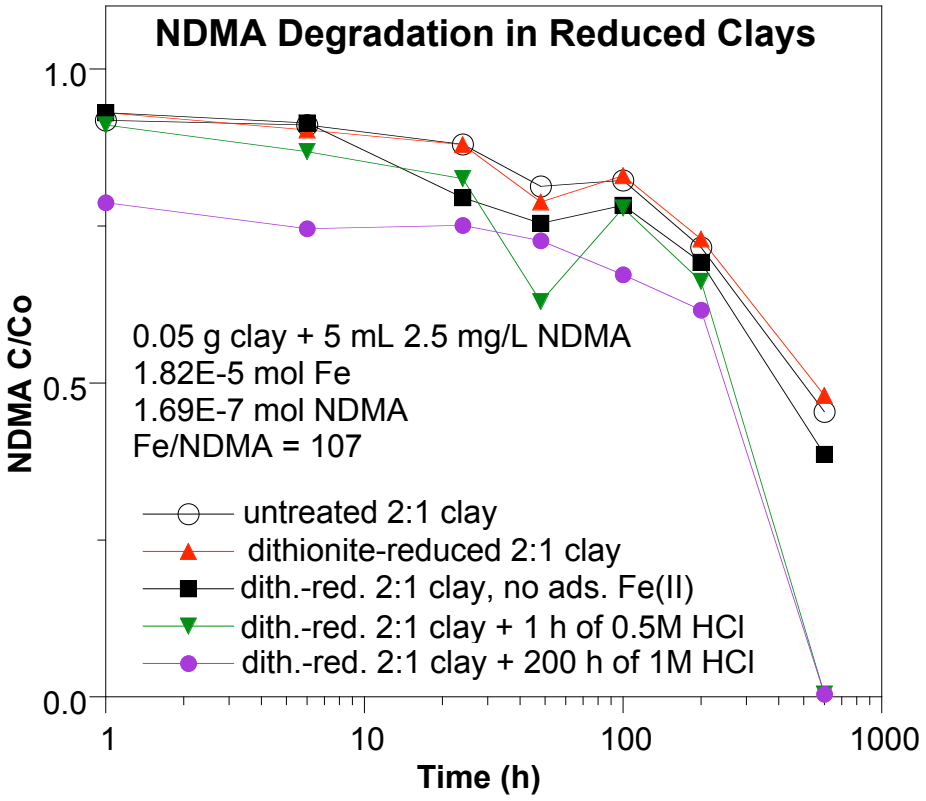
NDMA Degradation in Reduced Clays
NDMA C/Co
1.0
0.5
0.0
0.05 g clay + 5 mL 2.5 mg/L NDMA
1.82E-5 mol Fe
1.69E-7 mol NDMA
Fe/NDMA = 107
untreated 2:1 clay
dithionite-reduced 2:1 clay
dith.-red. 2:1 clay, no ads. Fe(II)
dith.-red. 2:1 clay + 1 h of 0.5M HCl
dith.-red. 2:1 clay + 200 h of 1M HCl
1
10
100
1000
Time (h)

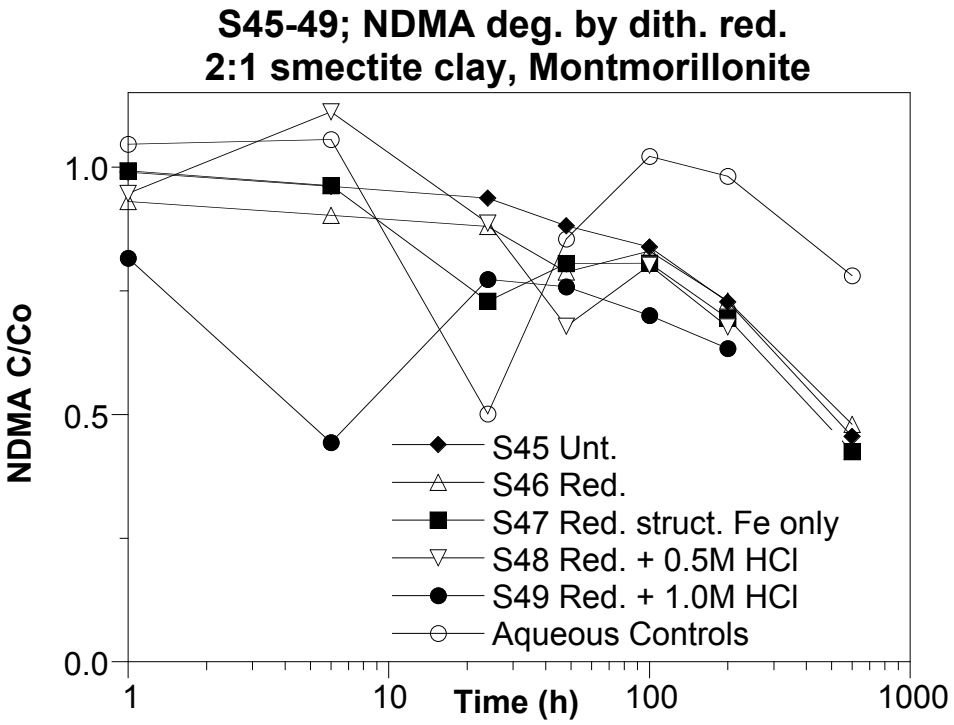
S45-49; NDMA deg. by dith. red.
2:1 smectite clay, Montmorillonite
NDMA C/Co
1.0
0.5
0.0
1
10
100
1000
Time (h)
S45 Unt.
S46 Red.
S47 Red. struct. Fe only
S48 Red. + 0.5M HCl
S49 Red. + 1.0M HCl
Aqueous Controls

Appendix A.6 Task 1.6 NDMA Degradation by Zero Valent Iron

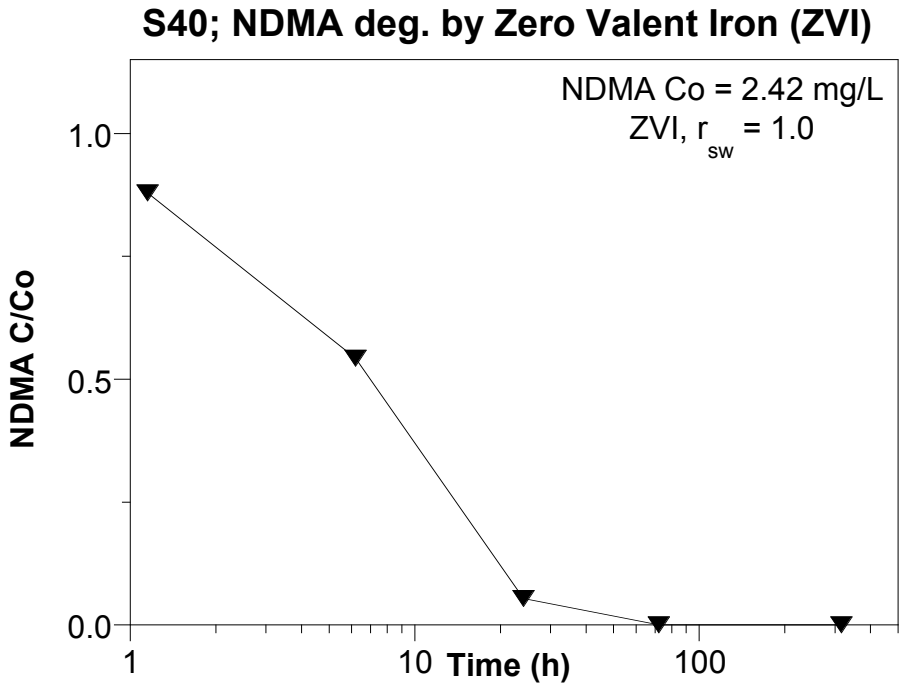

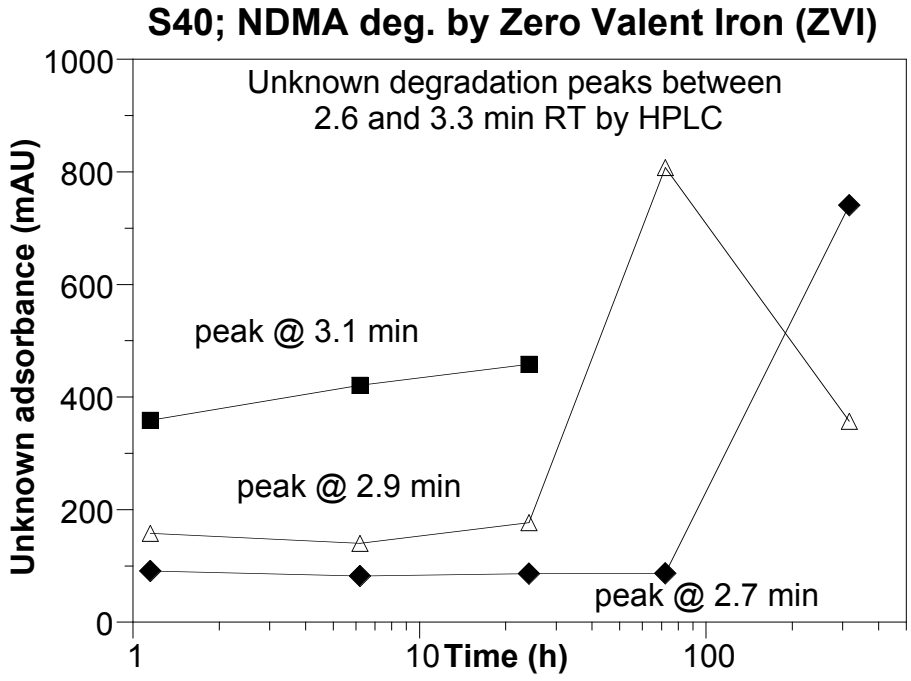

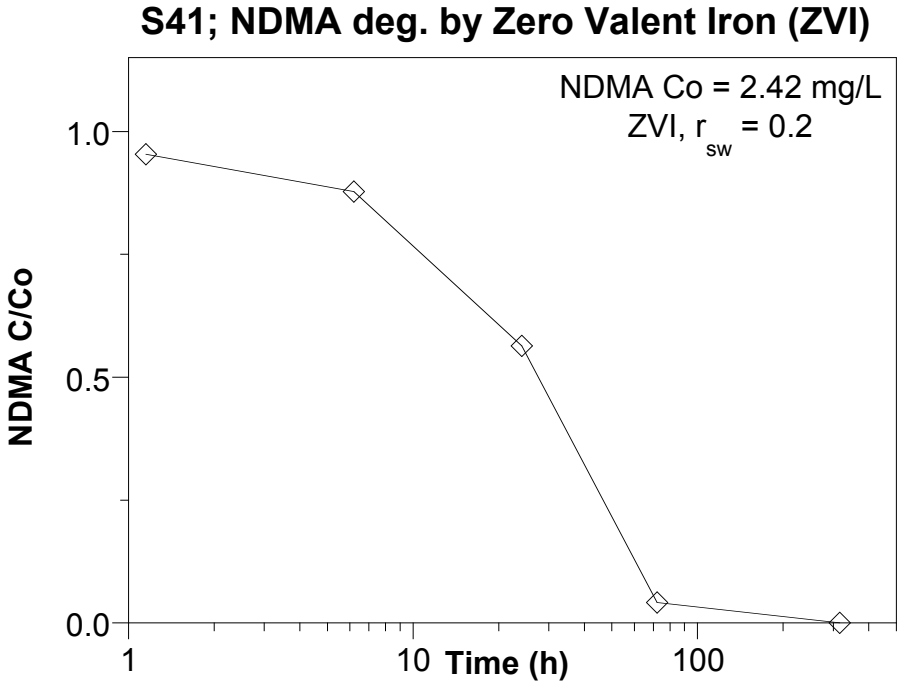
S41; NDMA deg. by Zero Valent Iron (ZVI)
NDMA Co = 2.42 mg/L
ZVI, r sw = 0.2
NDMA C/Co
1.0
0.5
0.0
1
10
100
Time (h)

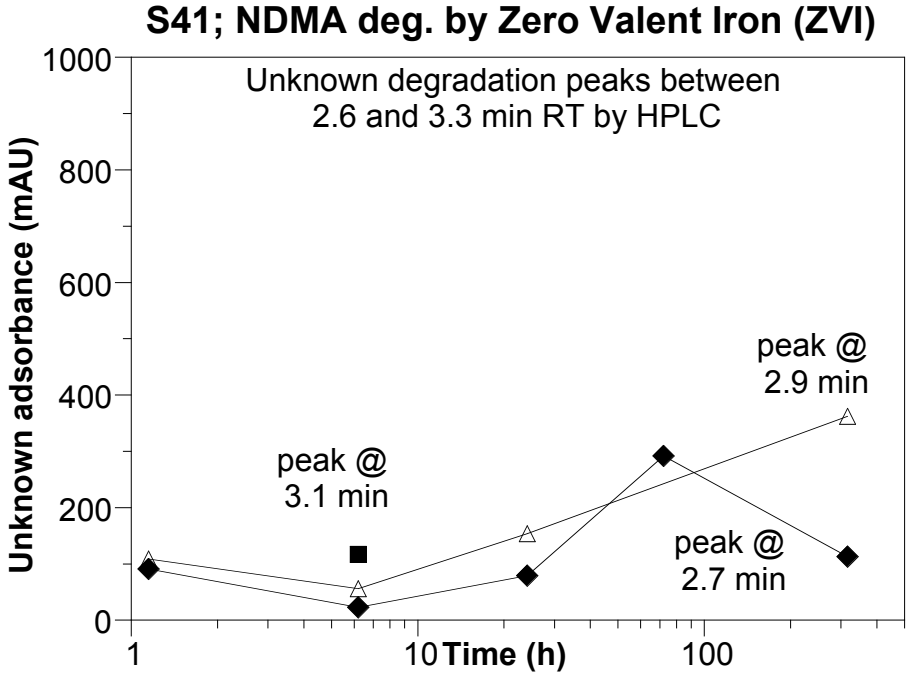
S41; NDMA deg. by Zero Valent Iron (ZVI)
Unknown degradation peaks between
2.6 and 3.3 min RT by HPLC
Unknown adsorbance (mAU)
1000
800
600
400
200
0
peak @
2.9 min
peak @
3.1 min
peak @
2.7 min
1
10
100
Time (h)

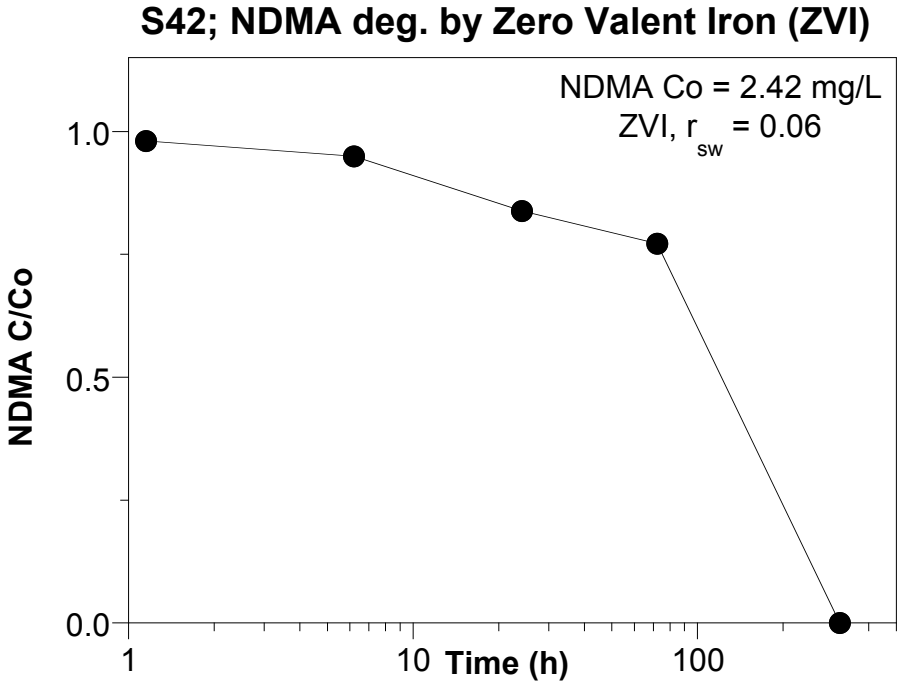
S42; NDMA deg. by Zero Valent Iron (ZVI)
NDMA Co = 2.42 mg/L
ZVI, r sw = 0.06
NDMA C/Co
1.0
0.5
0.0
1
10
100
Time (h)

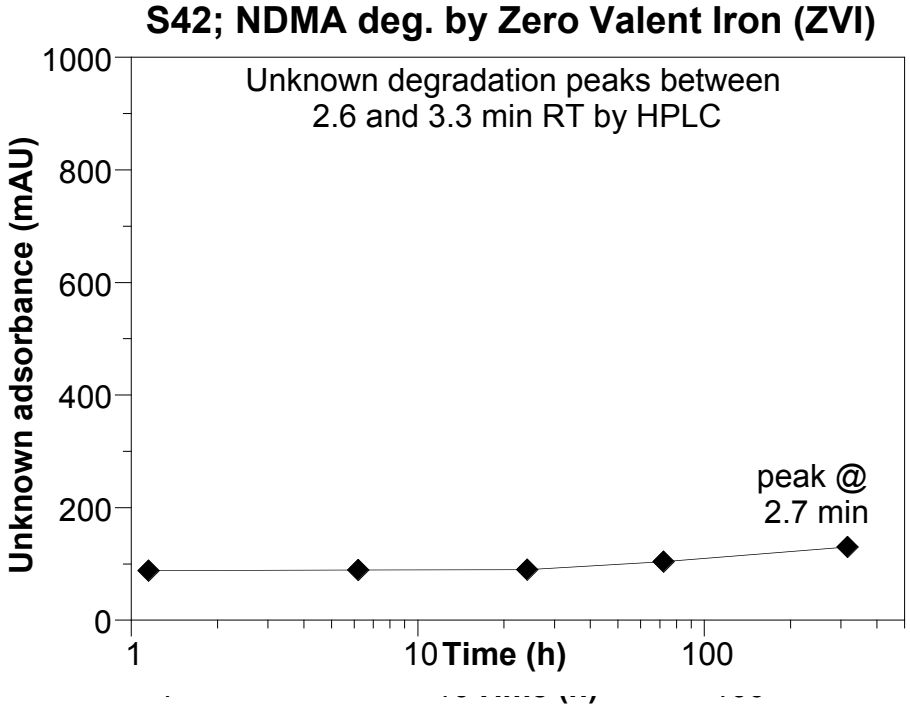
S42; NDMA deg. by Zero Valent Iron (ZVI)
Unknown degradation peaks between
2.6 and 3.3 min RT by HPLC
Unknown adsorbance (mAU)
1000
800
600
400
200
0
peak @
2.7 min
1
10
100
Time (h)

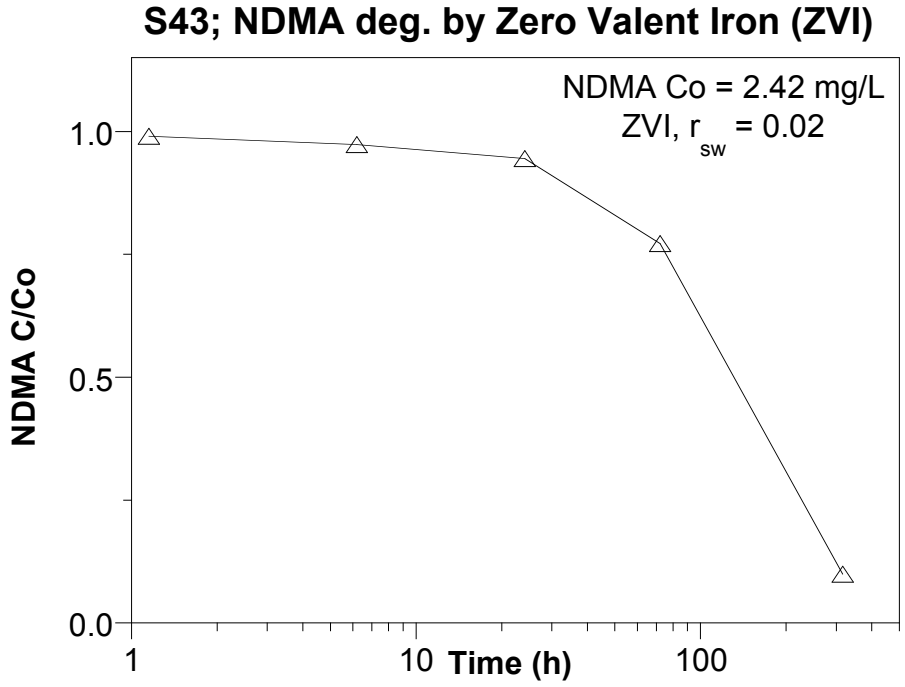
S43; NDMA deg. by Zero Valent Iron (ZVI)
NDMA Co = 2.42 mg/L
ZVI, r sw = 0.02
NDMA C/Co
1.0
0.5
0.0
1
10
100
Time (h)

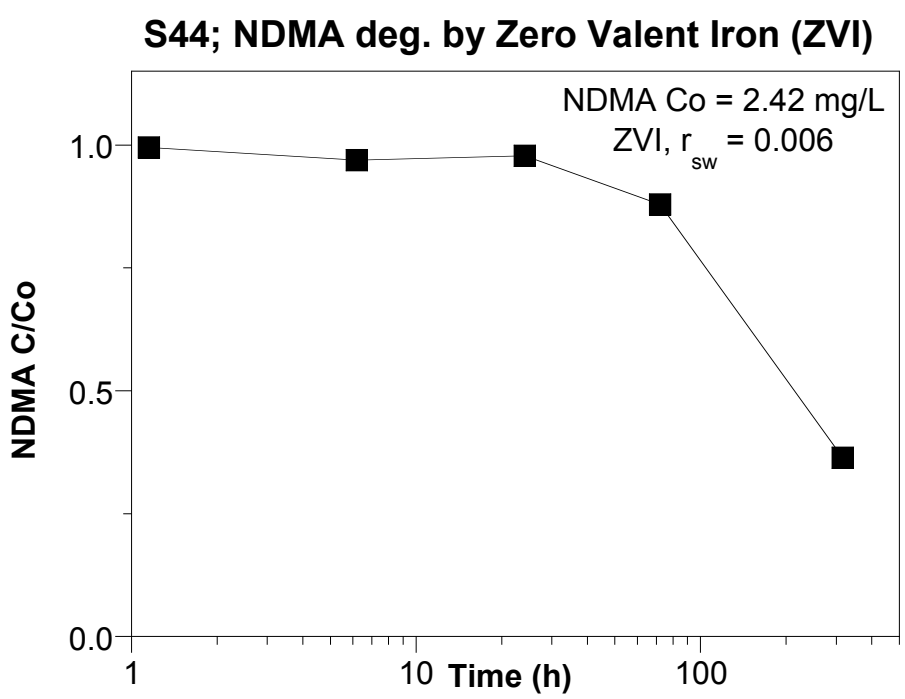
S44; NDMA deg. by Zero Valent Iron (ZVI)
NDMA Co = 2.42 mg/L
ZVI, r sw = 0.006
NDMA C/Co
1.0
0.5
0.0
1
10
100
Time (h)

S40-44; NDMA Aqeuous Stability

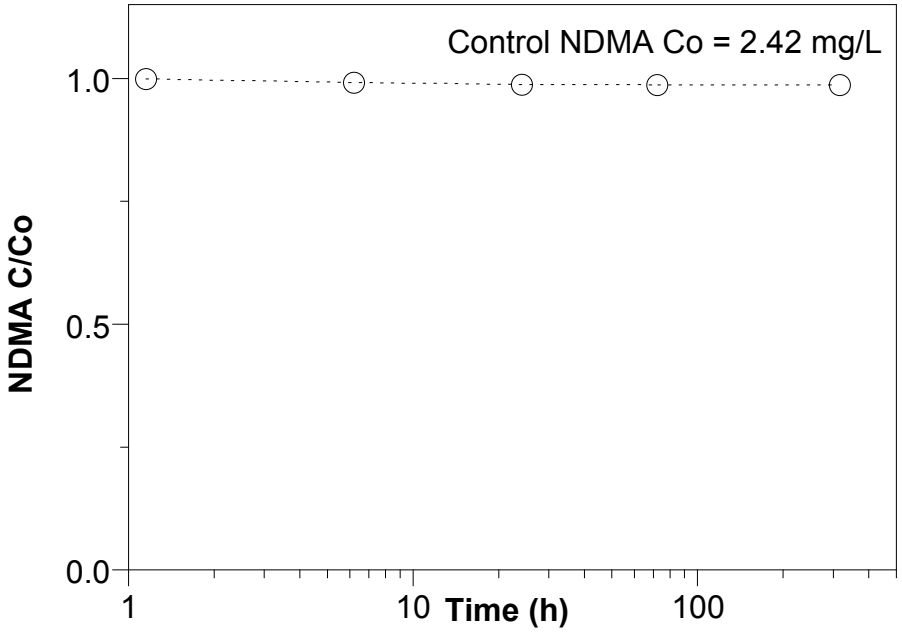

S40-44; NDMA deg. by Zero Valent Iron (ZVI)

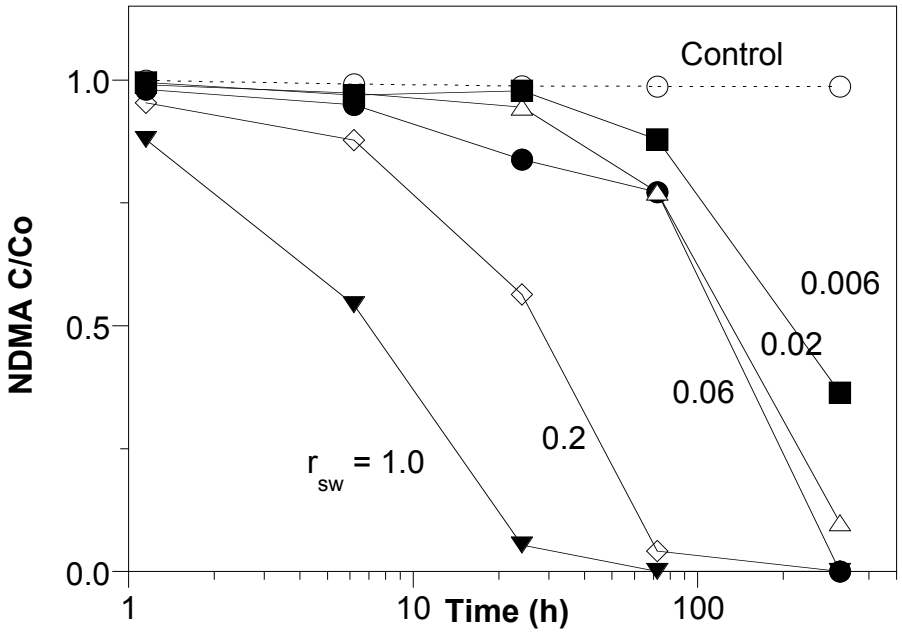

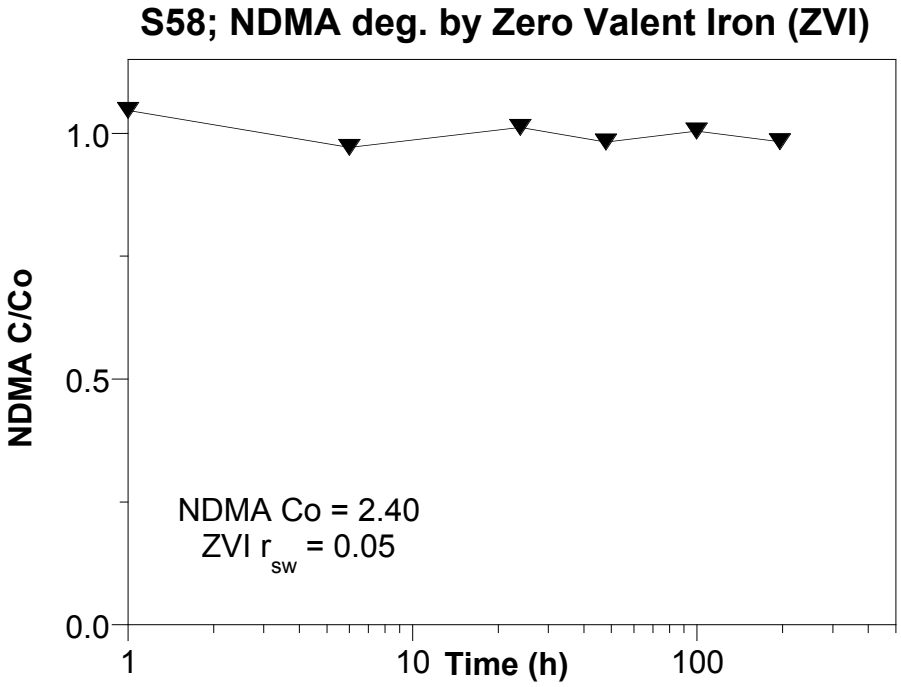
S58; NDMA deg. by Zero Valent Iron (ZVI)
NDMA C/Co
1.0
0.5
0.0
NDMA Co = 2.40
ZVI r sw = 0.05
1
10
Time (h)
100

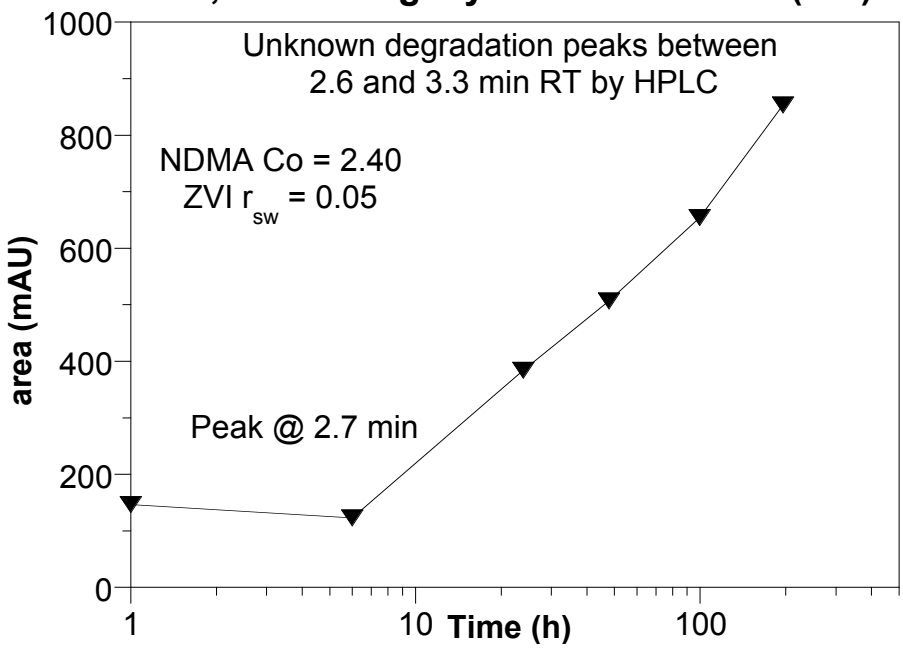
S58; NDMA deg. by Zero Valent Iron (ZVI)
Unknown degradation peaks between
2.6 and 3.3 min RT by HPLC
NDMA Co = 2.40
ZVI r sw = 0.05
Peak @ 2.7 min
area (mAU)
1000
800
600
400
200
0
1
10
Time (h)
100

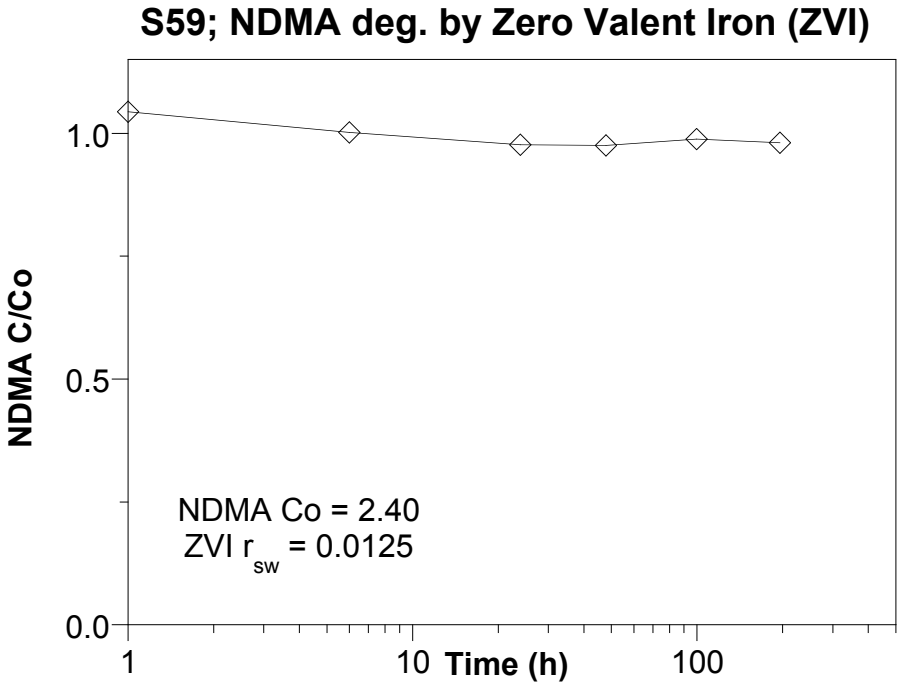
S59; NDMA deg. by Zero Valent Iron (ZVI)
NDMA C/Co
1.0
0.5
0.0
NDMA Co = 2.40
ZVI r sw = 0.0125
1
10
Time (h)
100

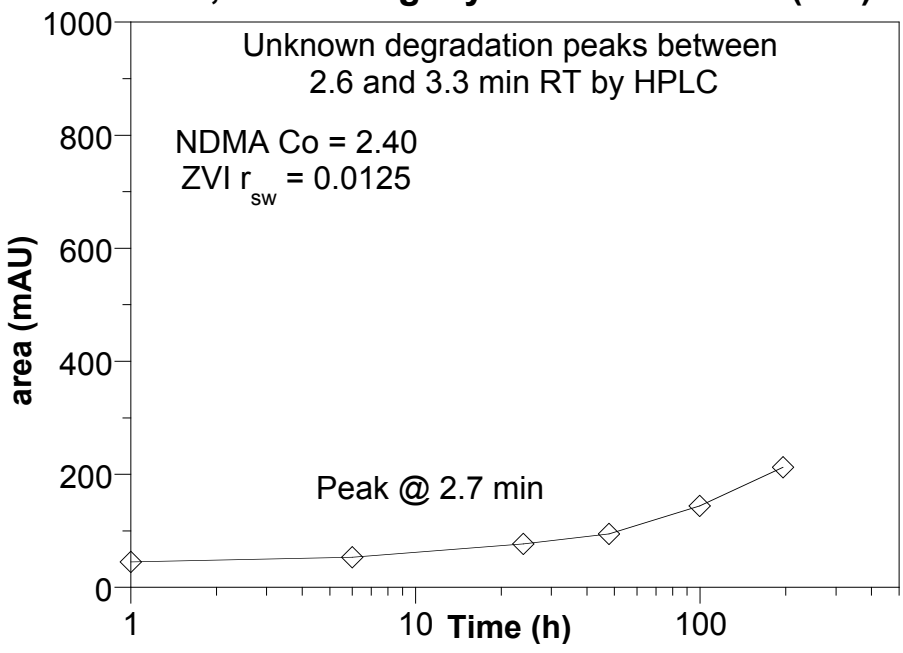
S59; NDMA deg. by Zero Valent Iron (ZVI)
Unknown degradation peaks between
2.6 and 3.3 min RT by HPLC
NDMA Co = 2.40
ZVI r sw = 0.0125
area (mAU)
1000
800
600
400
200
0
Peak @ 2.7 min
1
10
Time (h)
100

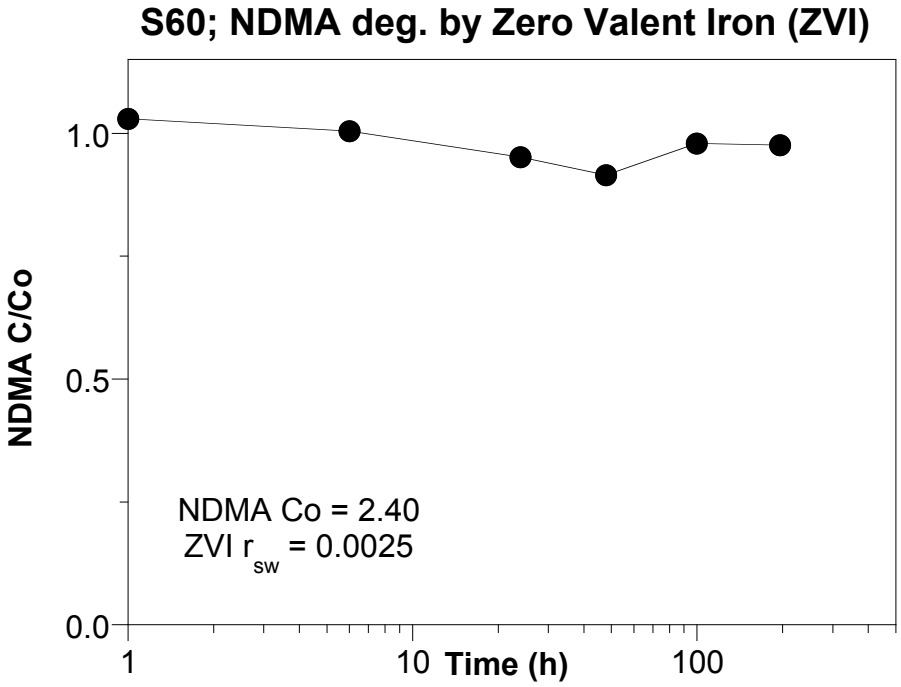
S60; NDMA deg. by Zero Valent Iron (ZVI)
NDMA C/Co
1.0
0.5
0.0
NDMA Co = 2.40
ZVI r sw = 0.0025
1
10
100
Time (h)

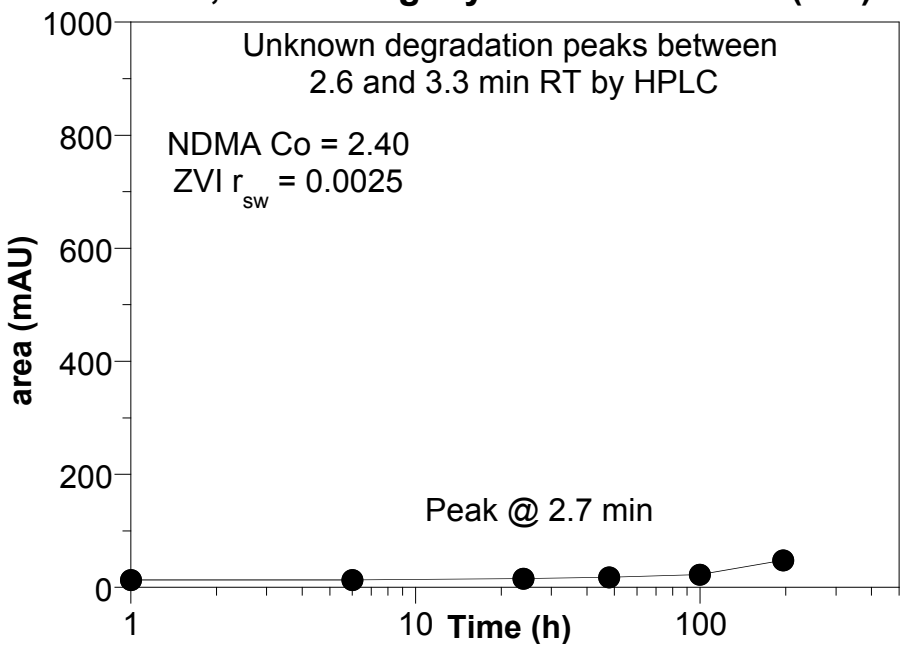
S60; NDMA deg. by Zero Valent Iron (ZVI)
Unknown degradation peaks between
2.6 and 3.3 min RT by HPLC
NDMA Co = 2.40
ZVI r sw = 0.0025
area (mAU)
1000
800
600
400
200
0
Peak @ 2.7 min
1
10
100
Time (h)

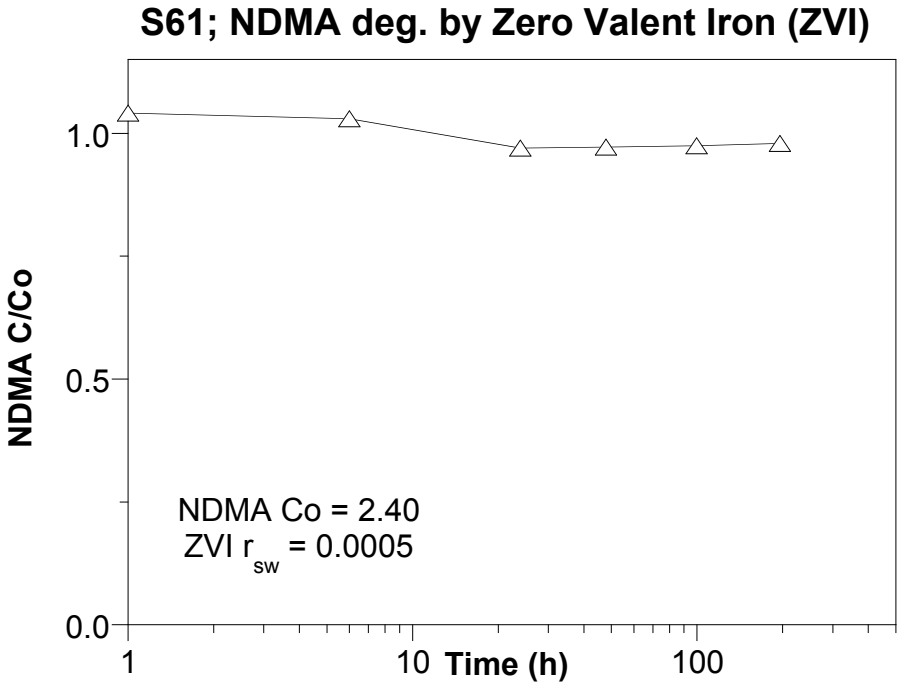
S61; NDMA deg. by Zero Valent Iron (ZVI)
NDMA C/Co
1.0
0.5
0.0
NDMA Co = 2.40
ZVI r sw = 0.0005
1
10
Time (h)
100

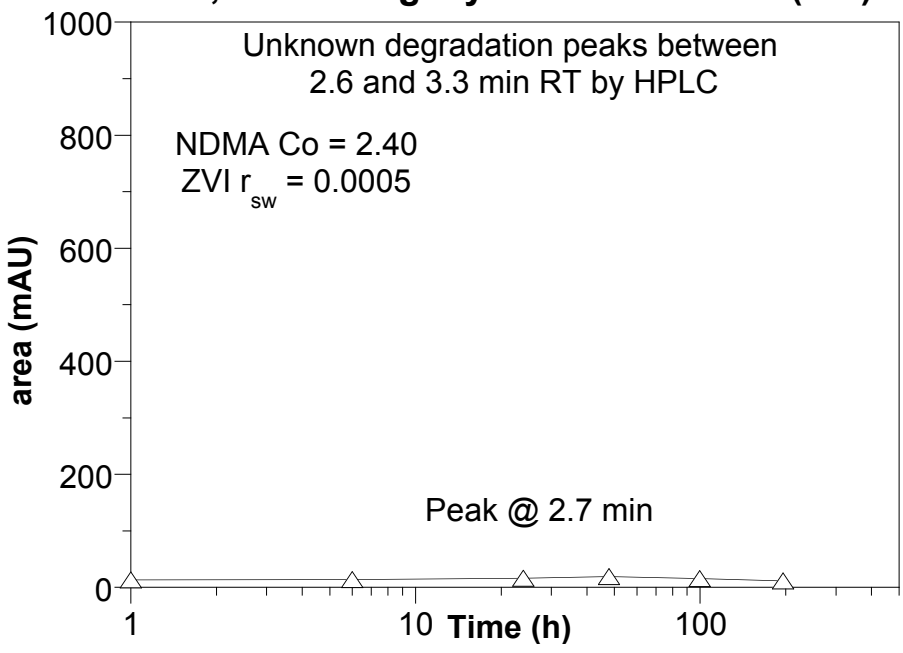
S61; NDMA deg. by Zero Valent Iron (ZVI)
Unknown degradation peaks between
2.6 and 3.3 min RT by HPLC
NDMA Co = 2.40
ZVI r sw = 0.0005
area (mAU)
1000
800
600
400
200
0
Peak @ 2.7 min
1
10
Time (h)
100

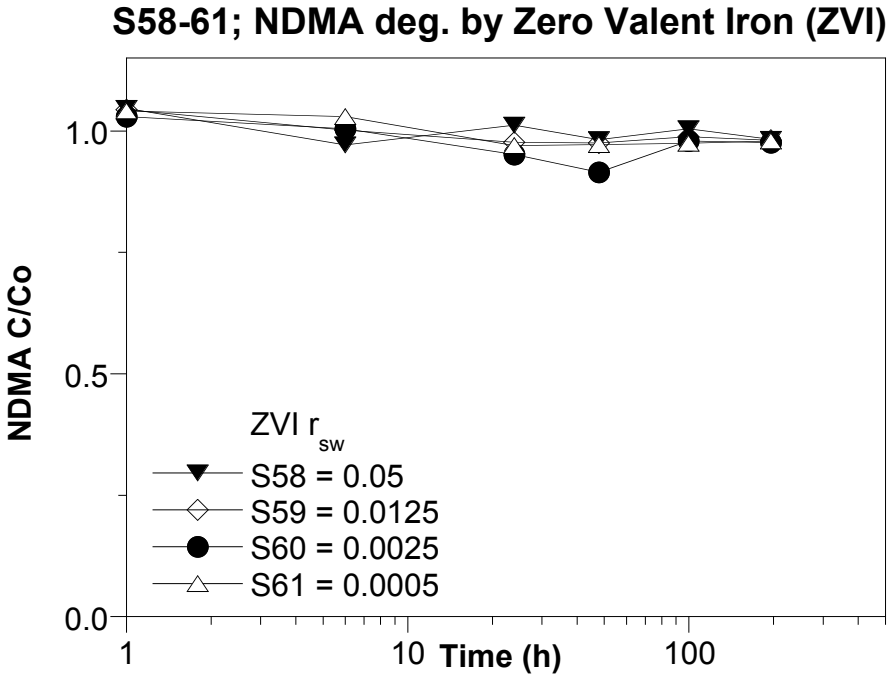
S58-61; NDMA deg. by Zero Valent Iron (ZVI)
NDMA C/Co
1.0
0.5
0.0
ZVI r sw
S58 = 0.05
S59 = 0.0125
S60 = 0.0025
S61 = 0.0005
1
10
100
Time (h)

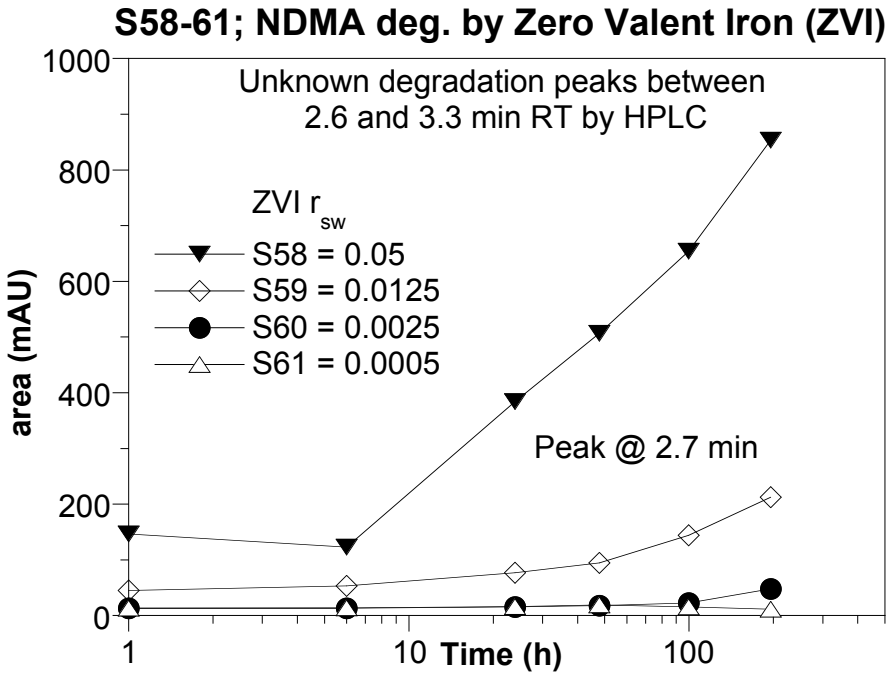
S58-61; NDMA deg. by Zero Valent Iron (ZVI)
Unknown degradation peaks between
2.6 and 3.3 min RT by HPLC
area (mAU)
1000
800
600
400
200
0
ZVI r sw
S58 = 0.05
S59 = 0.0125
S60 = 0.0025
S61 = 0.0005
Peak @ 2.7 min
1
10
100
Time (h)

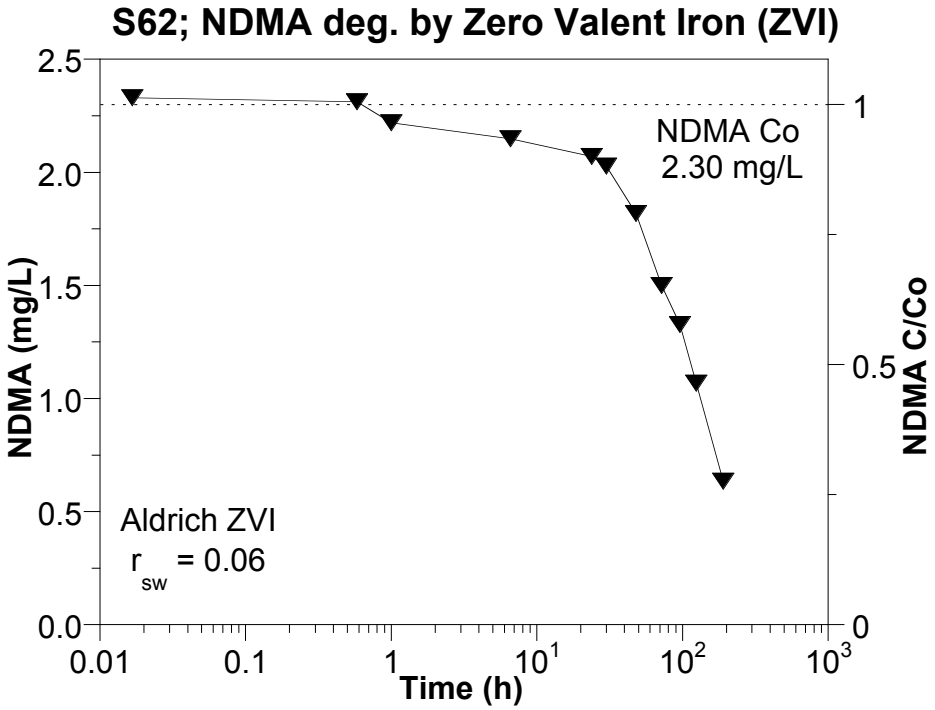
S62; NDMA deg. by Zero Valent Iron (ZVI)
NDMA Co
2.30 mg/L
Aldrich ZVI
r sw = 0.06
NDMA (mg/L)
NDMA C/Co
Time (h)
2.5
2.0
1.5
1.0
0.5
0.0
1
0.5
0
0.01
0.1
1
10^1
10^2
10^3

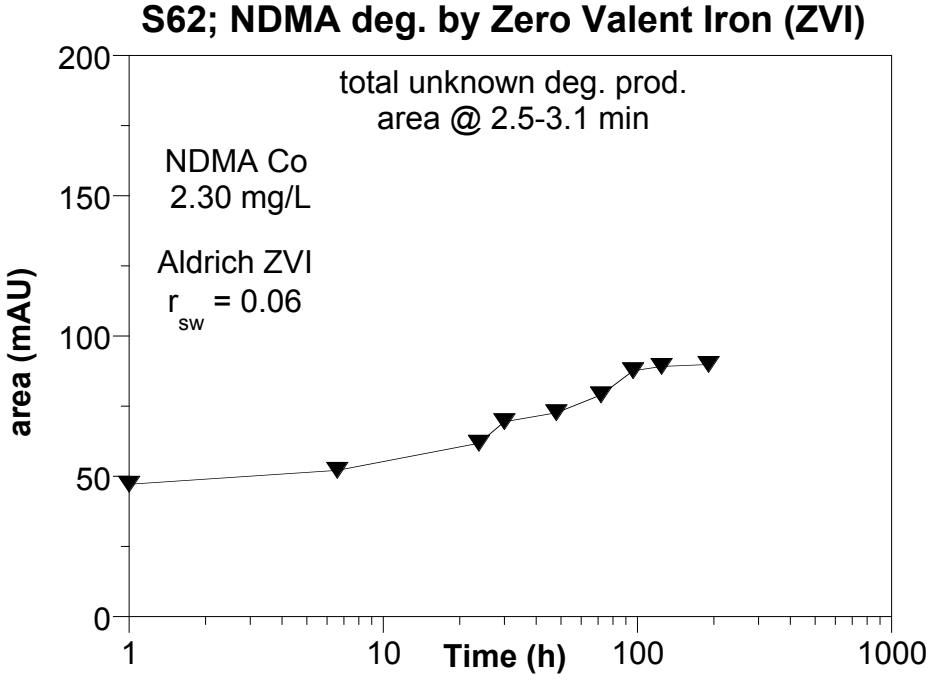
S62; NDMA deg. by Zero Valent Iron (ZVI)
total unknown deg. prod.
area @ 2.5-3.1 min
NDMA Co
2.30 mg/L
Aldrich ZVI
r sw = 0.06
area (mAU)
Time (h)
200
150
100
50
0
1
10
100
1000

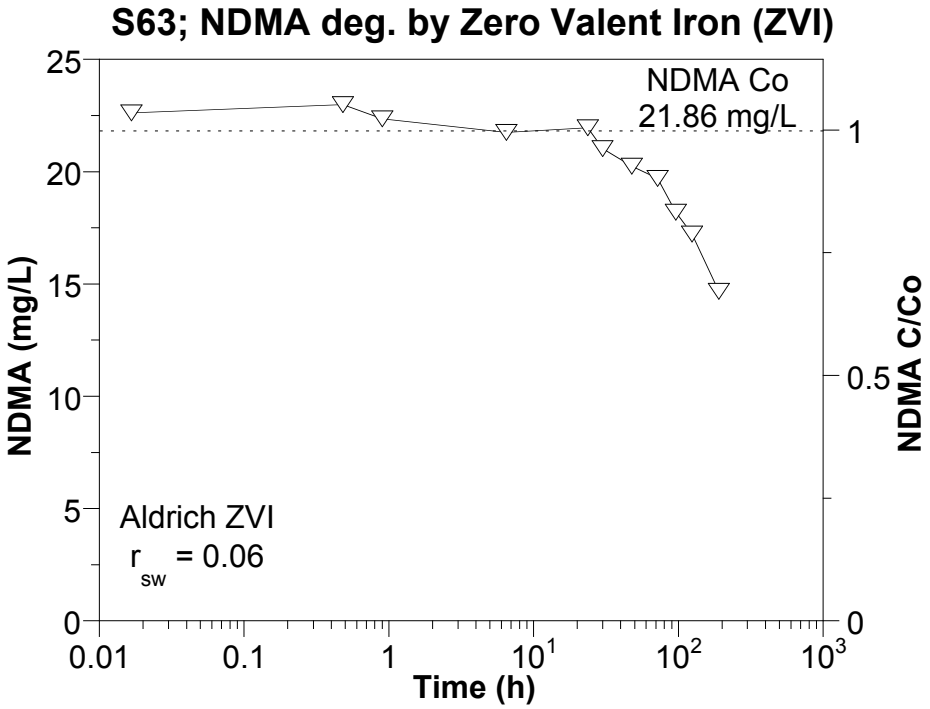
S63; NDMA deg. by Zero Valent Iron (ZVI)
NDMA Co
21.86 mg/L
Aldrich ZVI
r sw = 0.06
NDMA (mg/L)
NDMA C/Co
Time (h)
0
5
10
15
20
25
0.5
1
0.01
0.1
1
10^1
10^2
10^3

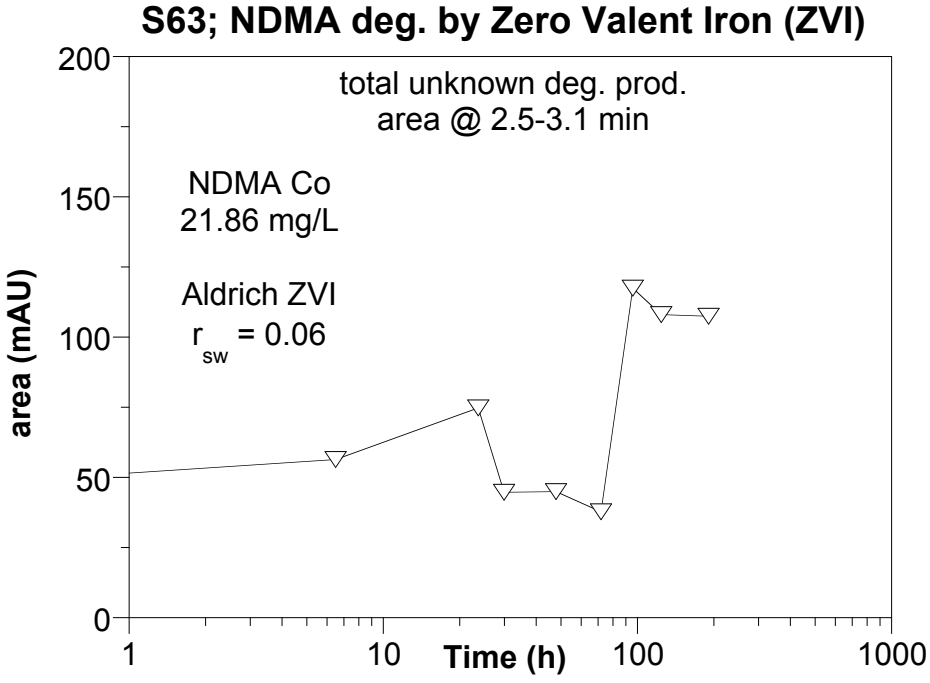
S63; NDMA deg. by Zero Valent Iron (ZVI)
total unknown deg. prod.
area @ 2.5-3.1 min
NDMA Co
21.86 mg/L
Aldrich ZVI
r sw = 0.06
area (mAU)
Time (h)
0
50
100
150
200
1
10
100
1000

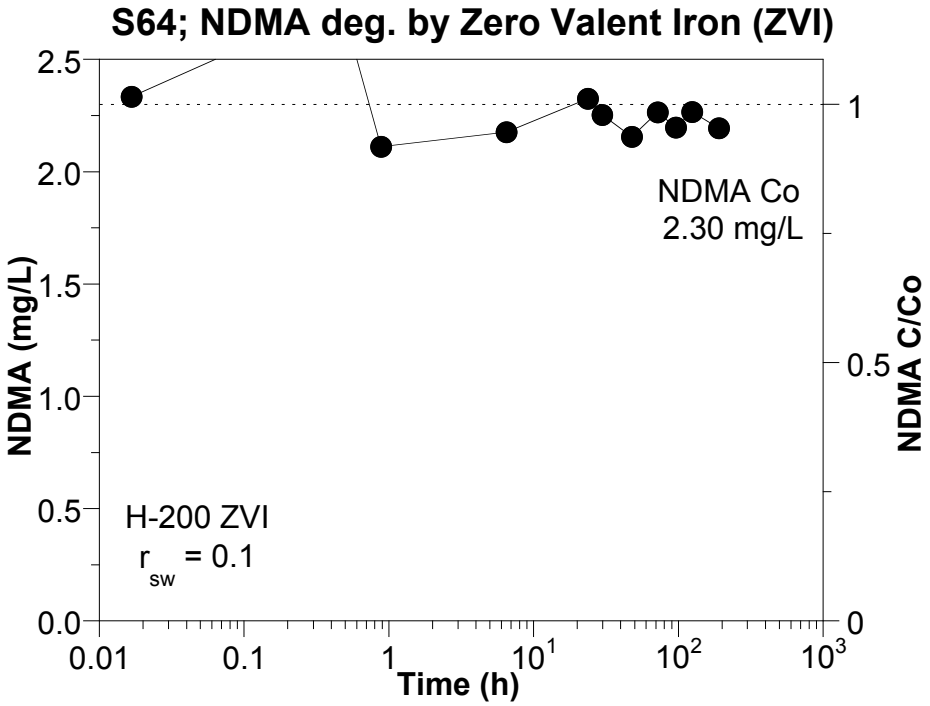
S64; NDMA deg. by Zero Valent Iron (ZVI)
NDMA (mg/L)
NDMA C/Co
Time (h)
NDMA Co
2.30 mg/L
H-200 ZVI
r sw = 0.1
2.5
2.0
1.5
1.0
0.5
0.0
1
0.5
0
0.01
0.1
1
10^1
10^2
10^3

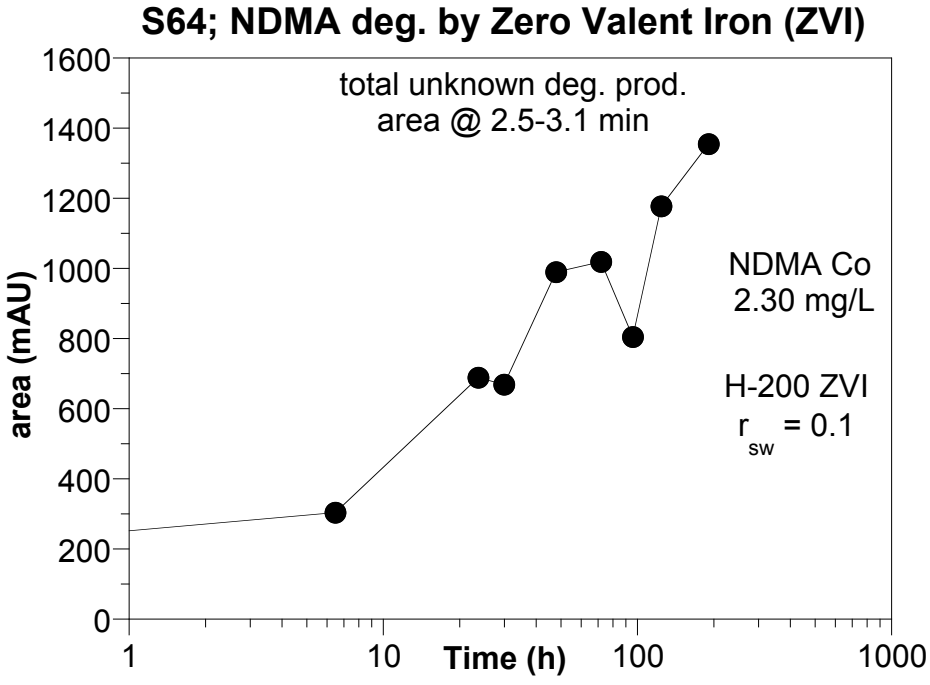
S64; NDMA deg. by Zero Valent Iron (ZVI)
total unknown deg. prod.
area @ 2.5-3.1 min
area (mAU)
Time (h)
NDMA Co
2.30 mg/L
H-200 ZVI
r sw = 0.1
1600
1400
1200
1000
800
600
400
200
0
1
10
100
1000

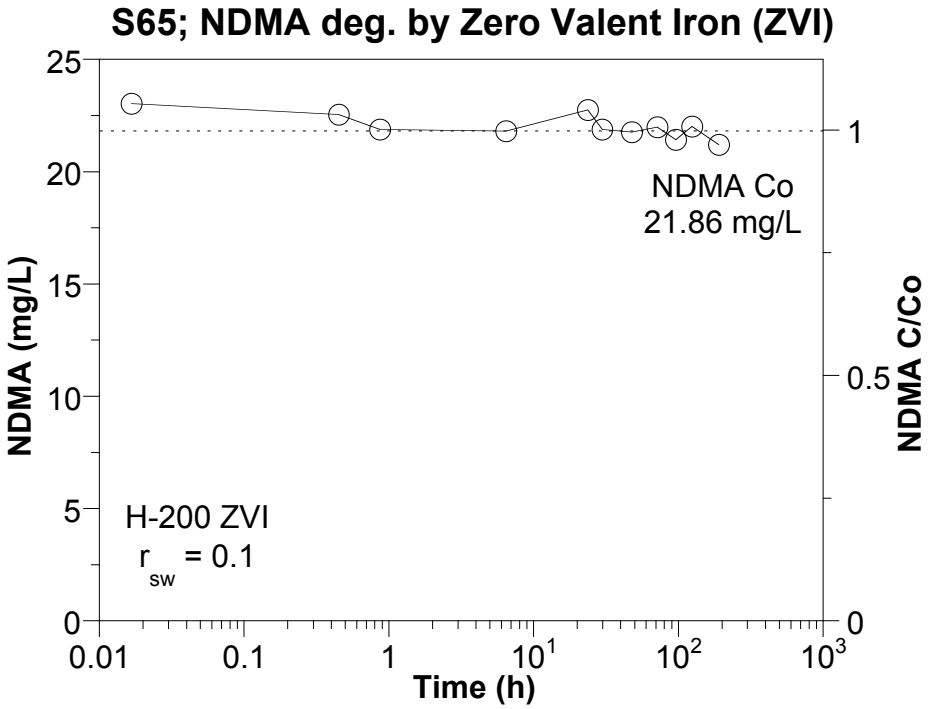
S65; NDMA deg. by Zero Valent Iron (ZVI)
NDMA (mg/L)
NDMA C/Co
Time (h)
NDMA Co
21.86 mg/L
H-200 ZVI
r sw = 0.1
25
20
15
10
5
0
1
0.5
0
0.01
0.1
1
10^1
10^2
10^3

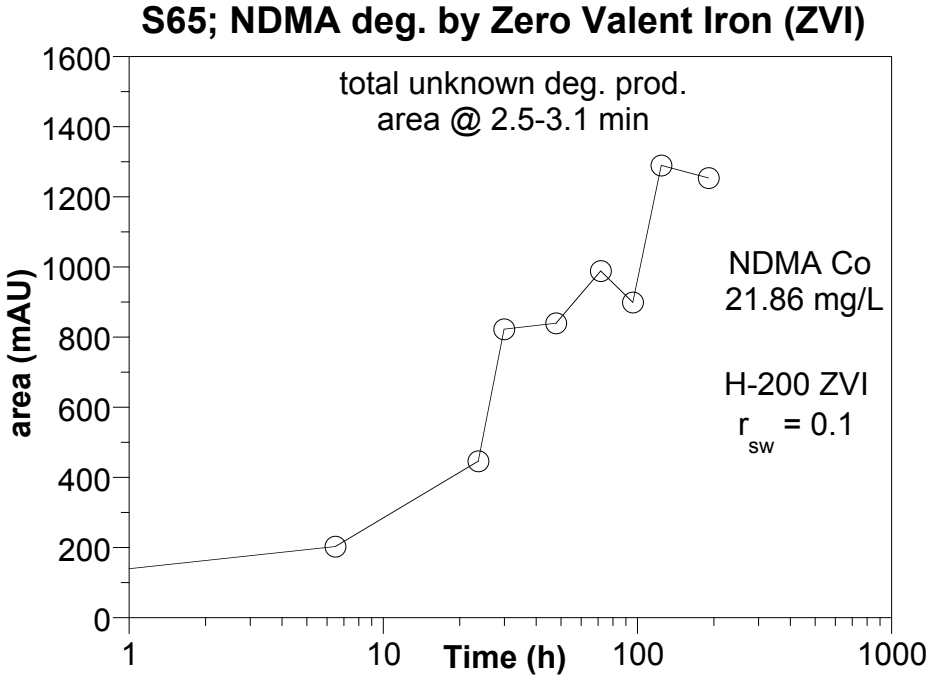
S65; NDMA deg. by Zero Valent Iron (ZVI)
total unknown deg. prod.
area @ 2.5-3.1 min
area (mAU)
Time (h)
NDMA Co
21.86 mg/L
H-200 ZVI
r sw = 0.1
1600
1400
1200
1000
800
600
400
200
0
1
10
100
1000

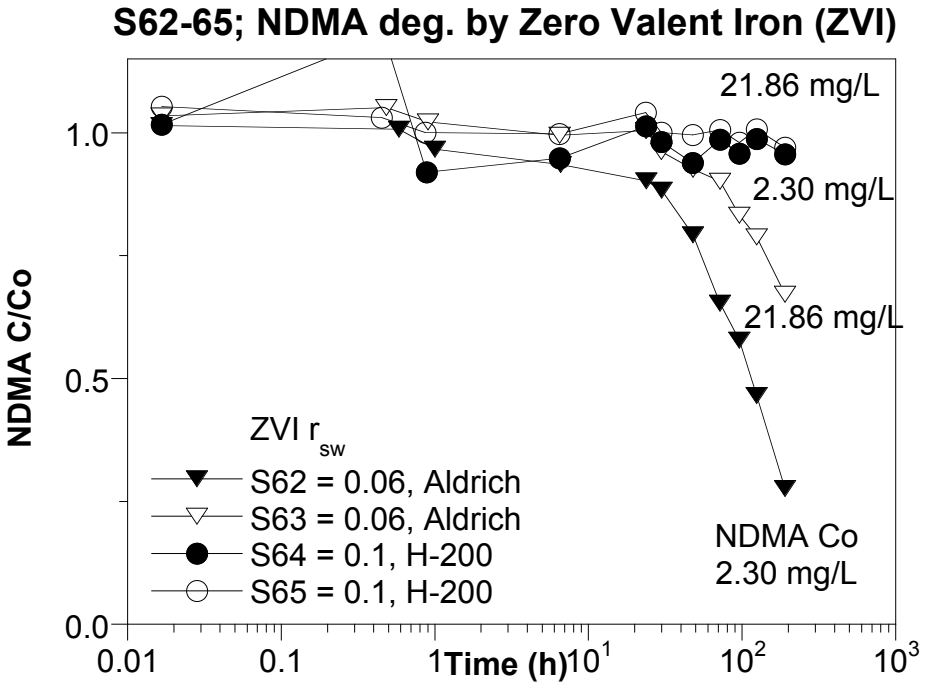
S62-65; NDMA deg. by Zero Valent Iron (ZVI)
21.86 mg/L
2.30 mg/L
21.86 mg/L
NDMA C/Co
1.0
0.5
0.0
ZVI r sw
S62 = 0.06, Aldrich
S63 = 0.06, Aldrich
S64 = 0.1, H-200
S65 = 0.1, H-200
NDMA Co
2.30 mg/L
0.01
0.1
1
Time (h)
10 1
10 2
10 3

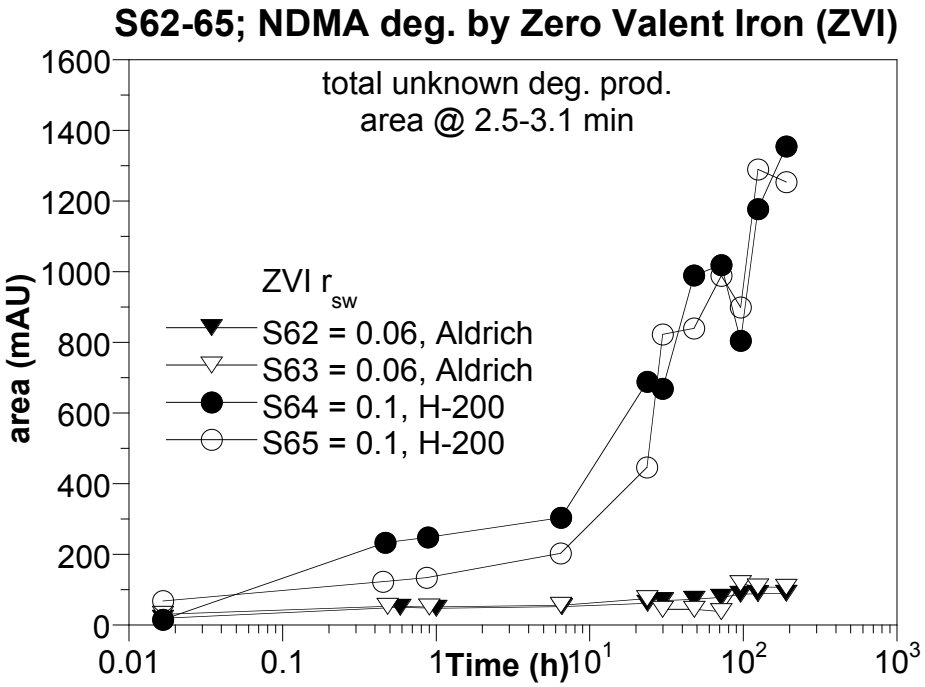
S62-65; NDMA deg. by Zero Valent Iron (ZVI)
total unknown deg. prod.
area @ 2.5-3.1 min
area (mAU)
1600
1400
1200
1000
800
600
400
200
0
ZVI r sw
S62 = 0.06, Aldrich
S63 = 0.06, Aldrich
S64 = 0.1, H-200
S65 = 0.1, H-200
0.01
0.1
1
Time (h)
10 1
10 2
10 3

Appendix A.7 Task 1.7 NDMA Degradation Rate and Fe/NDMA Molar Ratio

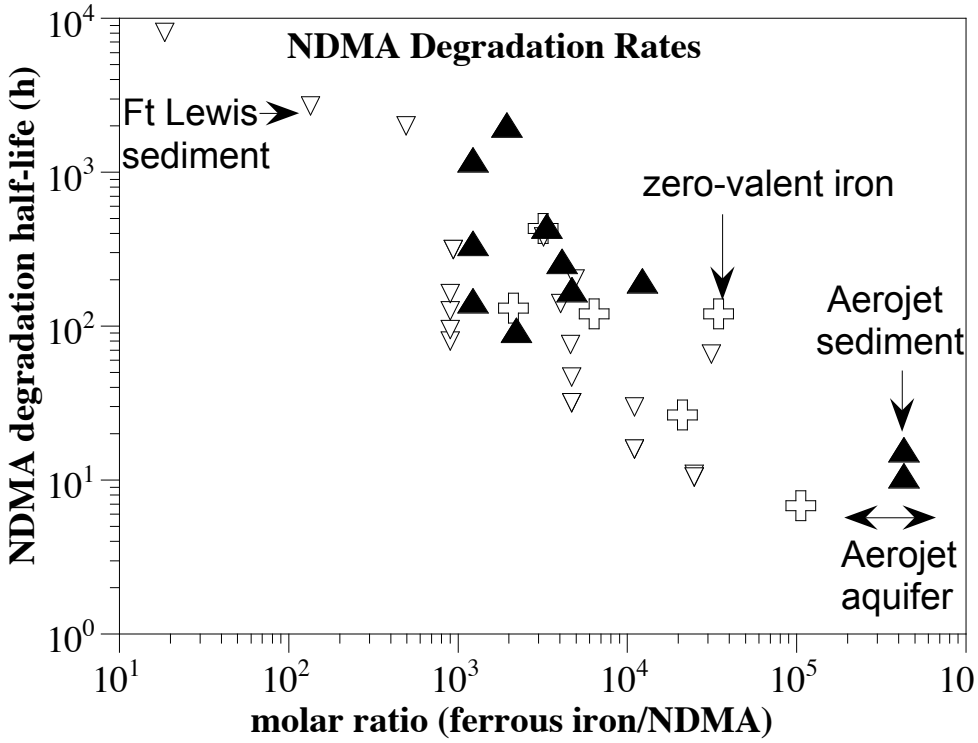

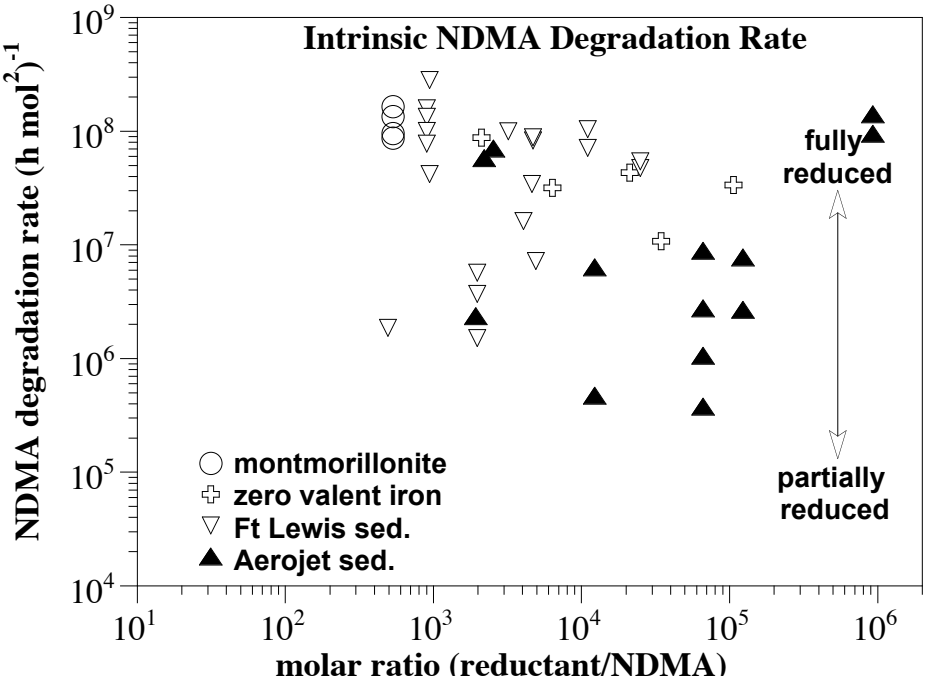

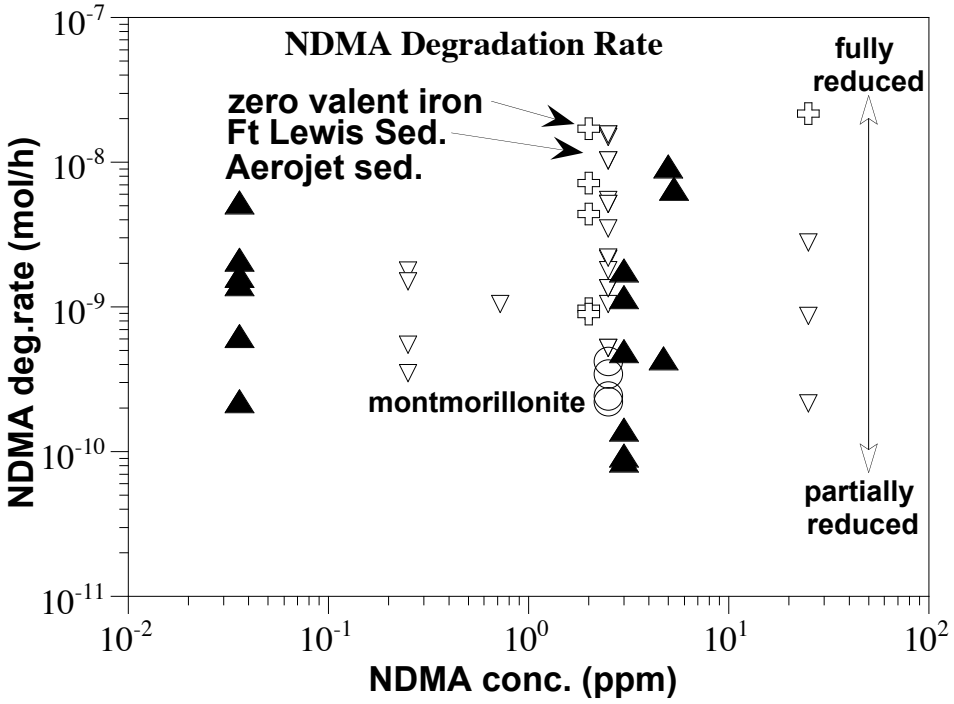
NDMA Degradation Rate
zero valent iron
Ft Lewis Sed.
Aerojet sed.
montmorillonite
fully reduced
partially reduced
NDMA deg.rate (mol/h)
NDMA conc. (ppm)
10-7
10-8
10-9
10-10
10-11
10-2
10-1
100
101
102

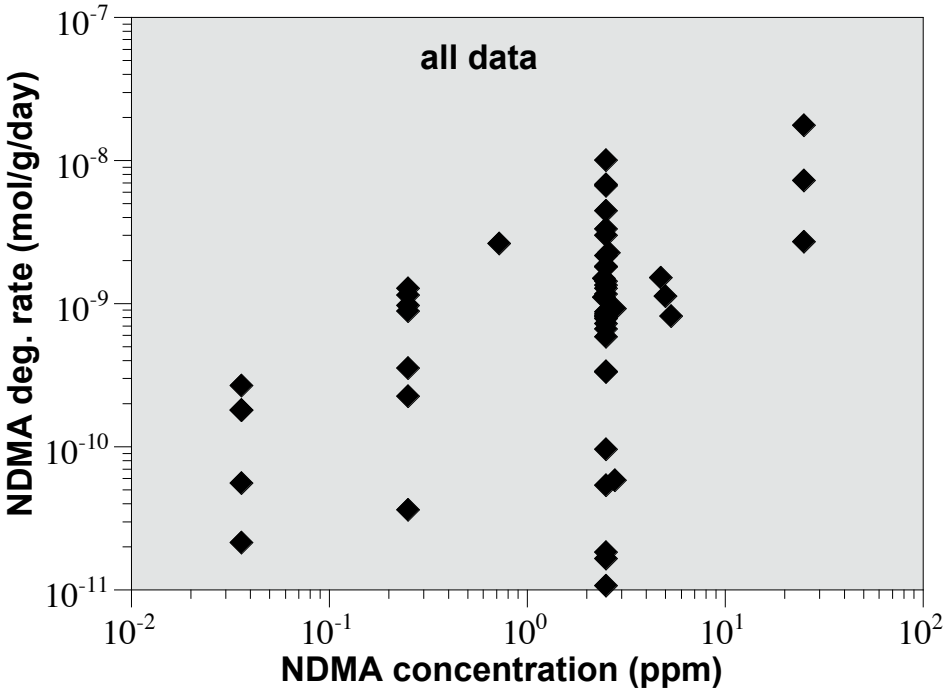
all data
NDMA deg. rate (mol/g/day)
NDMA concentration (ppm)
10^-7
10^-8
10^-9
10^-10
10^-11
10^-2
10^-1
10^0
10^1
10^2

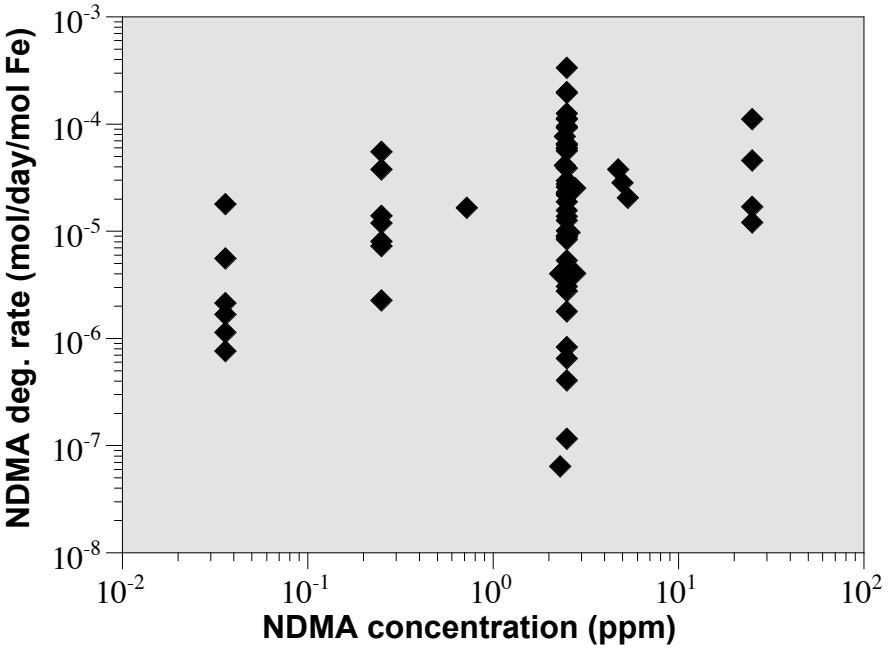
NDMA deg. rate (mol/day/mol Fe)
NDMA concentration (ppm)
10^-3
10^-4
10^-5
10^-6
10^-7
10^-8
10^-2
10^-1
10^0
10^1
10^2

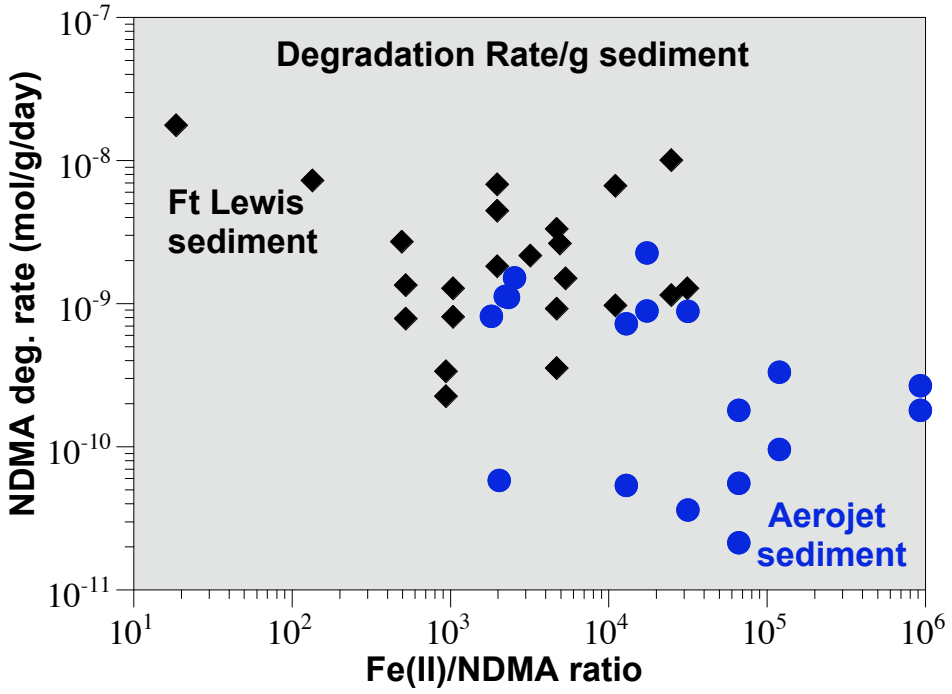
Degradation Rate/g sediment
NDMA deg. rate (mol/g/day)
Fe(II)/NDMA ratio
Ft Lewis sediment
Aerojet sediment
10^{-7}
10^{-8}
10^{-9}
10^{-10}
10^{-11}
10^{1}
10^{2}
10^{3}
10^{4}
10^{5}
10^{6}

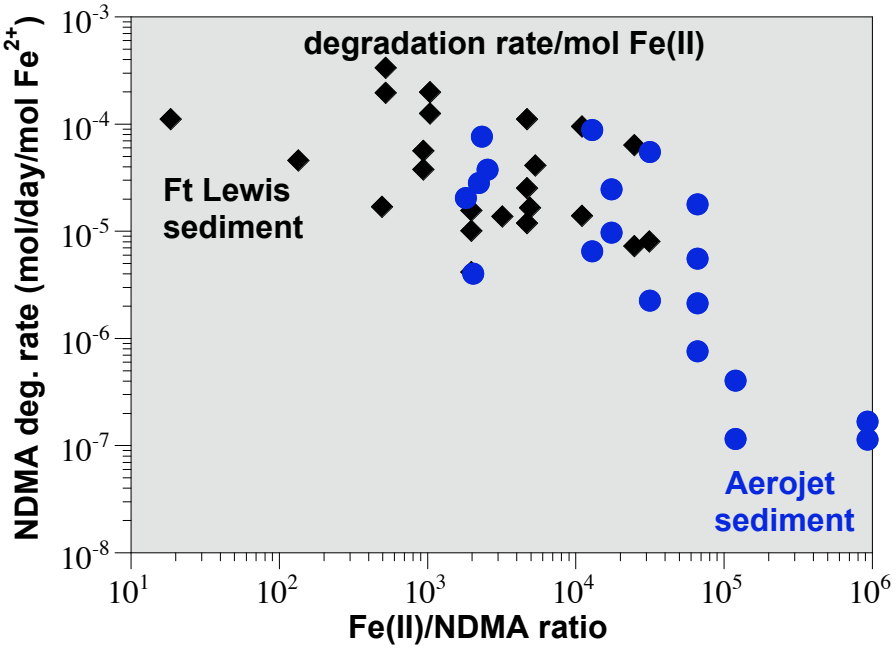
degradation rate/mol Fe(II)
NDMA deg. rate (mol/day/mol Fe^{2+})
Fe(II)/NDMA ratio
Ft Lewis sediment
Aerojet sediment
10^{-3}
10^{-4}
10^{-5}
10^{-6}
10^{-7}
10^{-8}
10^{1}
10^{2}
10^{3}
10^{4}
10^{5}
10^{6}

Appendix A.8 Task 1.8 NDMA Degradation by Reduced Sediment During 1-D Flow

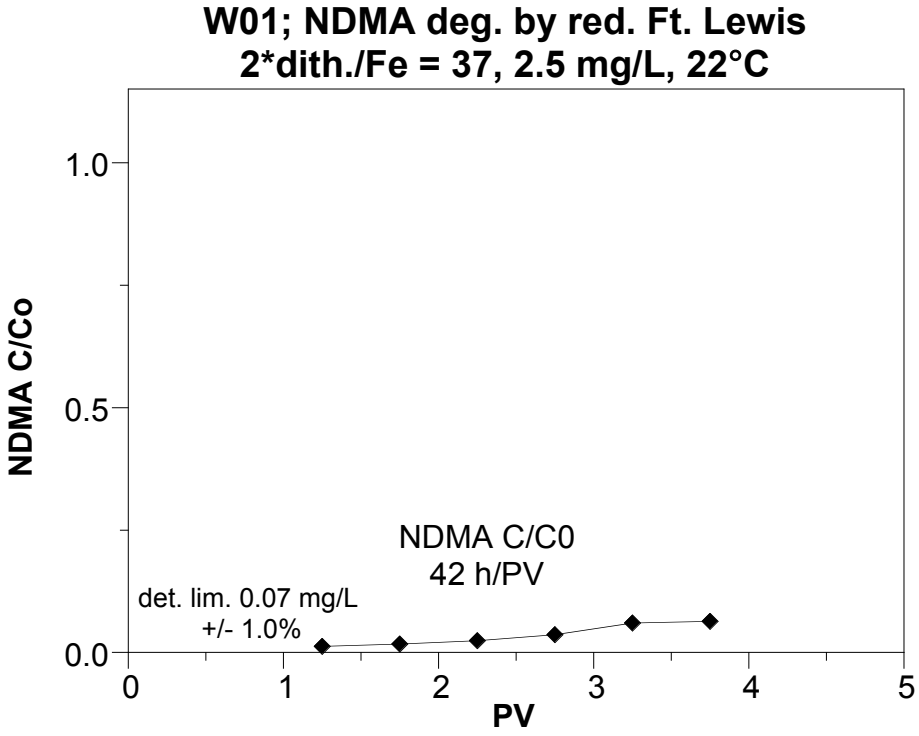

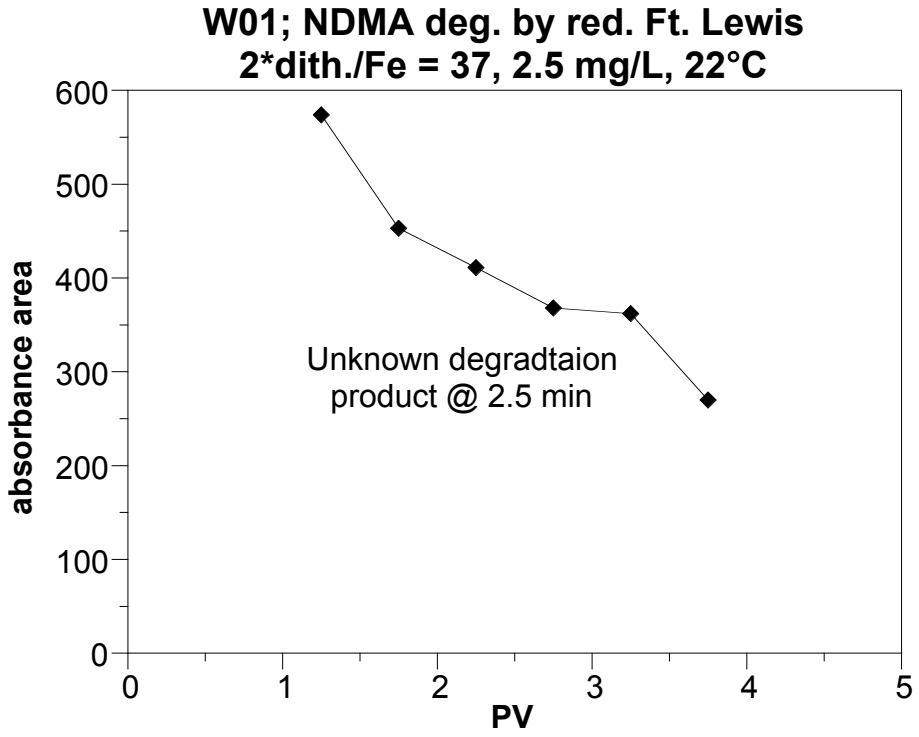

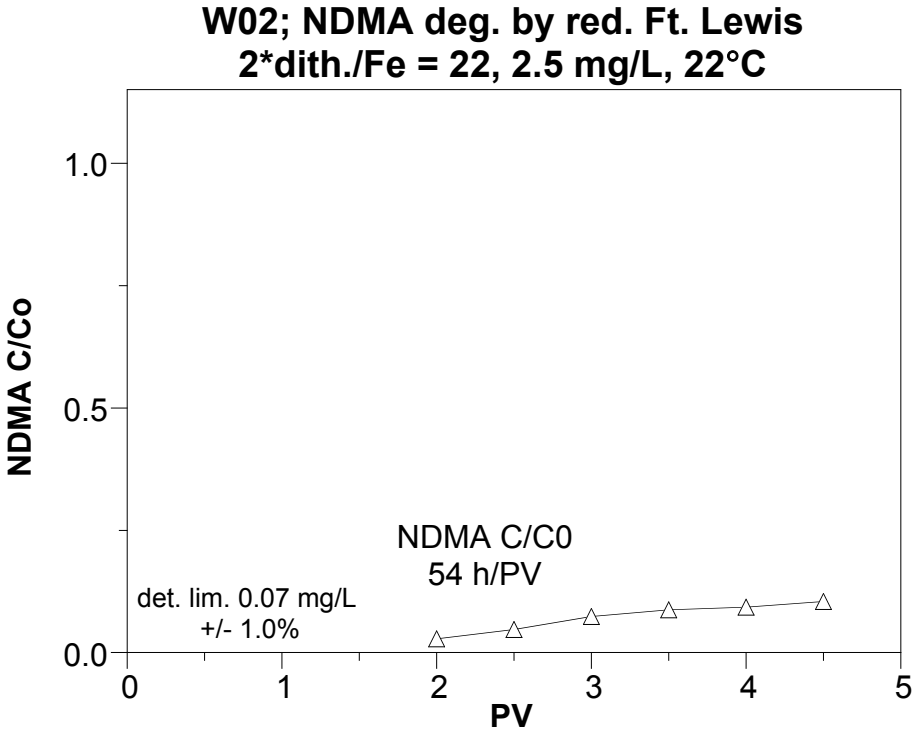
W02; NDMA deg. by red. Ft. Lewis
2*dith./Fe = 22, 2.5 mg/L, 22°C
NDMA C/Co
1.0
0.5
0.0
NDMA C/C0
54 h/PV
det. lim. 0.07 mg/L
+/- 1.0%
0
1
2
3
4
5
PV

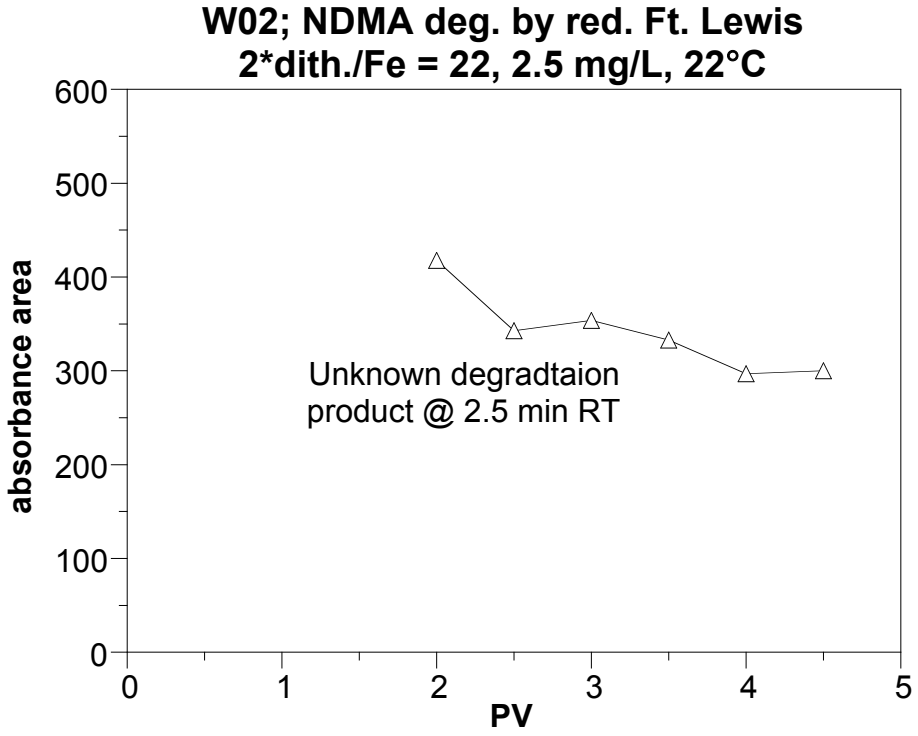
W02; NDMA deg. by red. Ft. Lewis
2*dith./Fe = 22, 2.5 mg/L, 22°C
absorbance area
600
500
400
300
200
100
0
Unknown degradtaion
product @ 2.5 min RT
0
1
2
3
4
5
PV

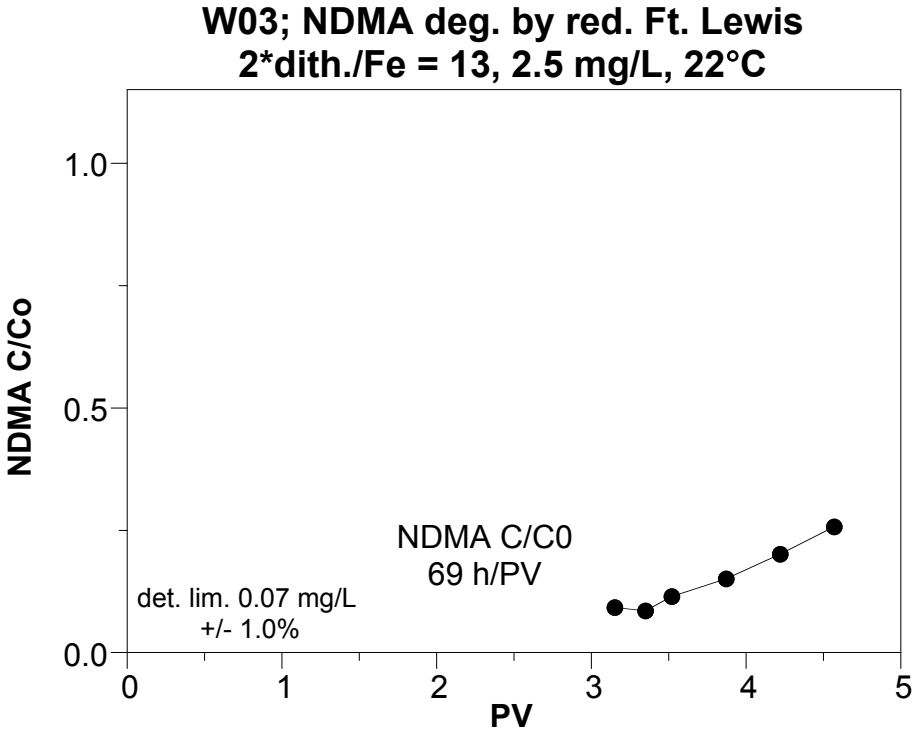
W03; NDMA deg. by red. Ft. Lewis
2*dith./Fe = 13, 2.5 mg/L, 22°C
NDMA C/Co
1.0
0.5
0.0
NDMA C/C0
69 h/PV
det. lim. 0.07 mg/L
+/- 1.0%
0
1
2
3
4
5
PV

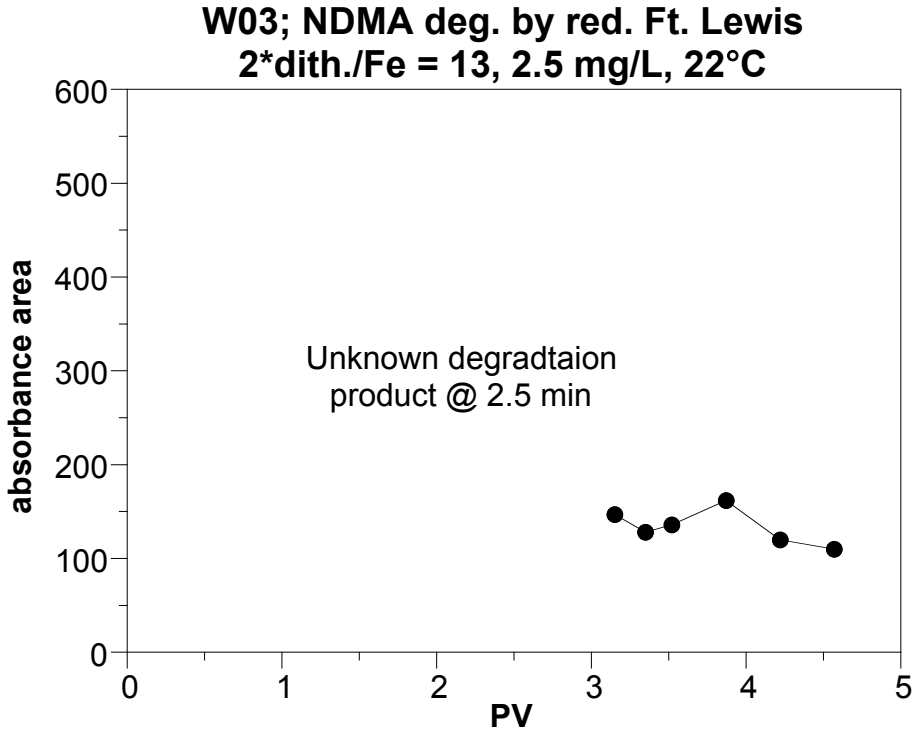
W03; NDMA deg. by red. Ft. Lewis
2*dith./Fe = 13, 2.5 mg/L, 22°C
absorbance area
600
500
400
300
200
100
0
Unknown degradtaion
product @ 2.5 min
0
1
2
3
4
5
PV

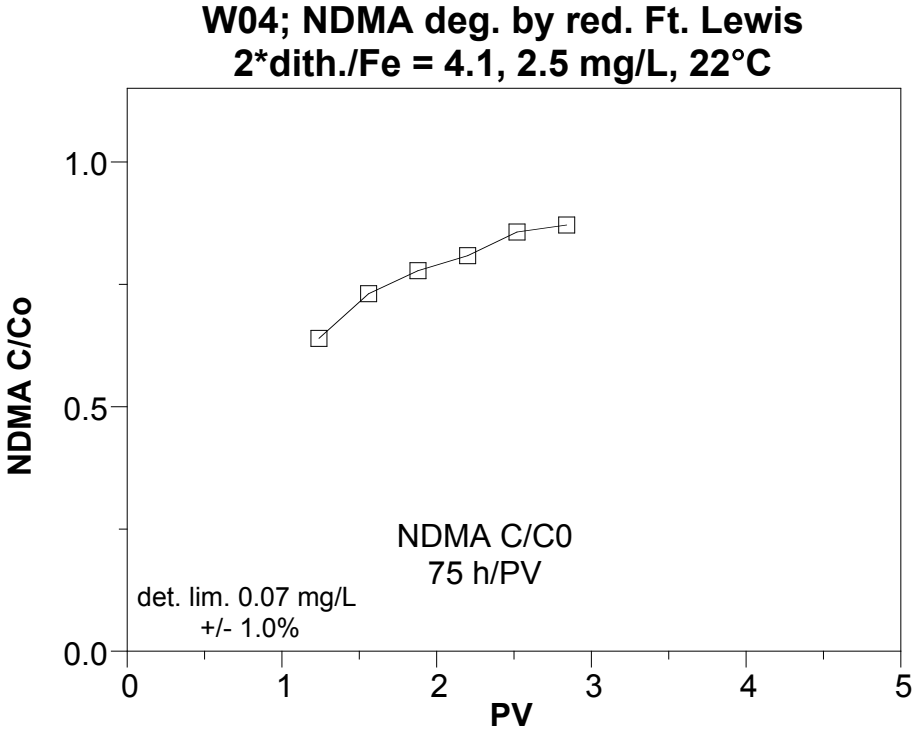
W04; NDMA deg. by red. Ft. Lewis
2*dith./Fe = 4.1, 2.5 mg/L, 22°C
NDMA C/Co
1.0
0.5
0.0
NDMA C/C0
75 h/PV
det. lim. 0.07 mg/L
+/- 1.0%
0
1
2
3
4
5
PV

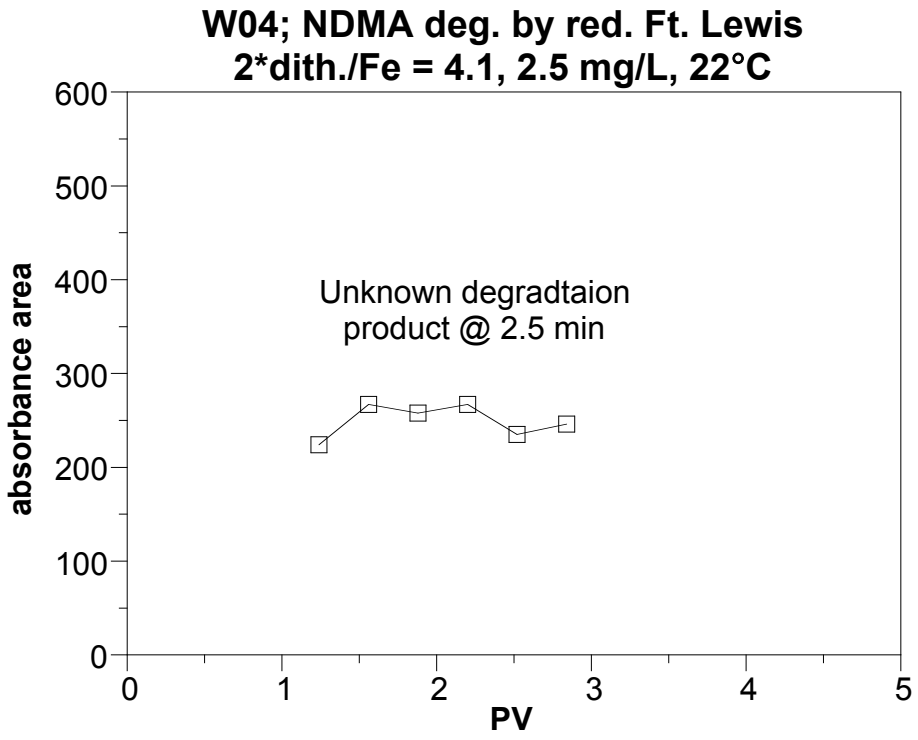
W04; NDMA deg. by red. Ft. Lewis
2*dith./Fe = 4.1, 2.5 mg/L, 22°C
absorbance area
600
500
400
300
200
100
0
Unknown degradtaion
product @ 2.5 min
0
1
2
3
4
5
PV

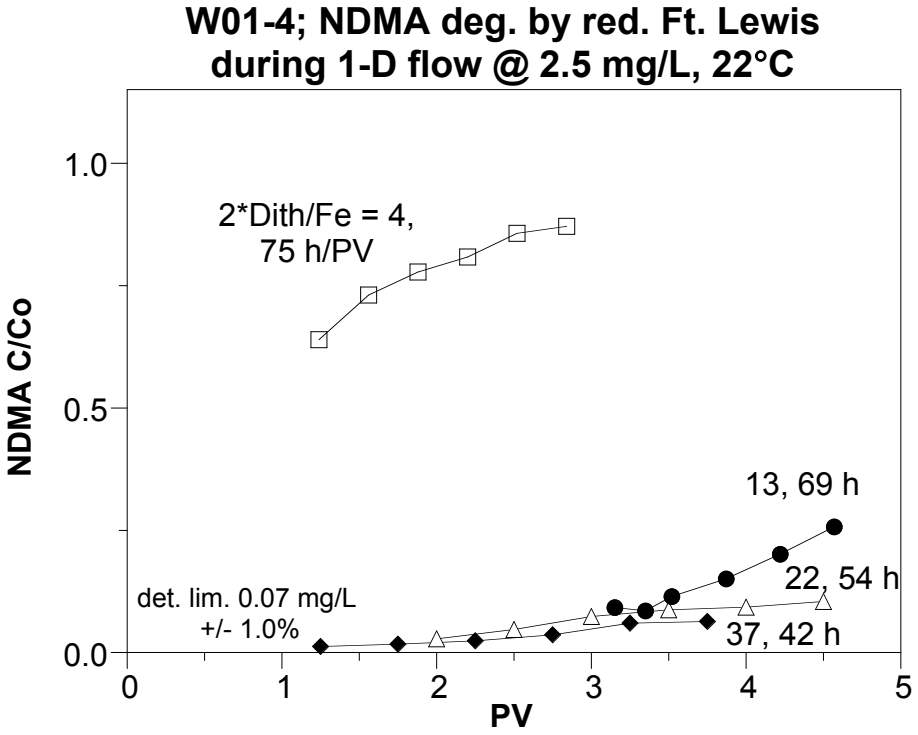
W01-4; NDMA deg. by red. Ft. Lewis
during 1-D flow @ 2.5 mg/L, 22°C
NDMA C/Co
1.0
0.5
0.0
2*Dith/Fe = 4,
75 h/PV
13, 69 h
22, 54 h
det. lim. 0.07 mg/L
+/- 1.0%
37, 42 h
0
1
2
3
4
5
PV

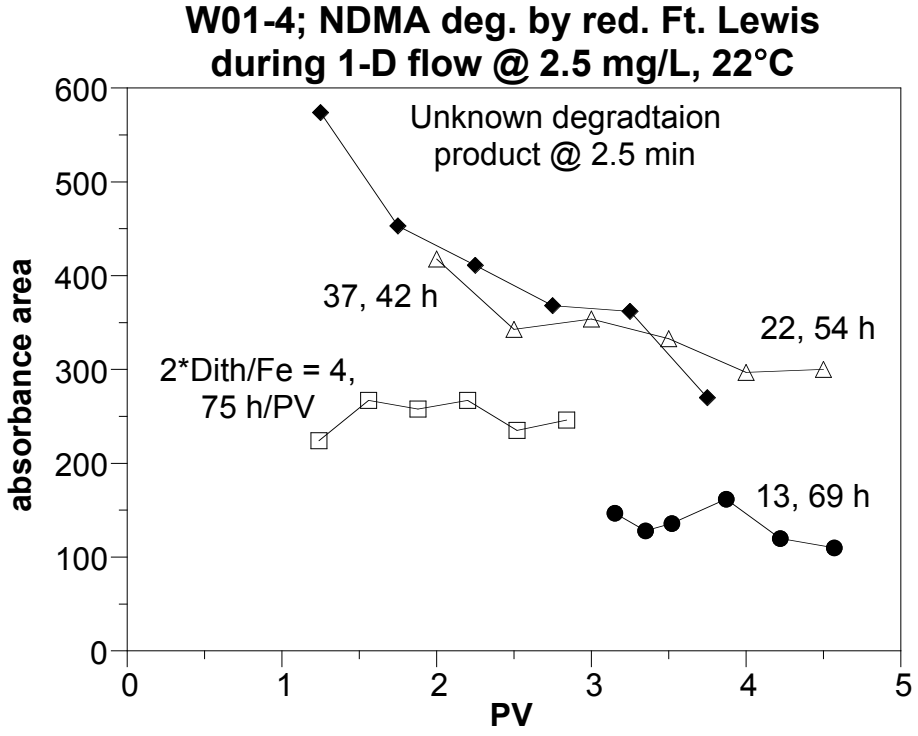
W01-4; NDMA deg. by red. Ft. Lewis
during 1-D flow @ 2.5 mg/L, 22°C
absorbance area
600
500
400
300
200
100
0
Unknown degradtaion
product @ 2.5 min
37, 42 h
22, 54 h
2*Dith/Fe = 4,
75 h/PV
13, 69 h
0
1
2
3
4
5
PV

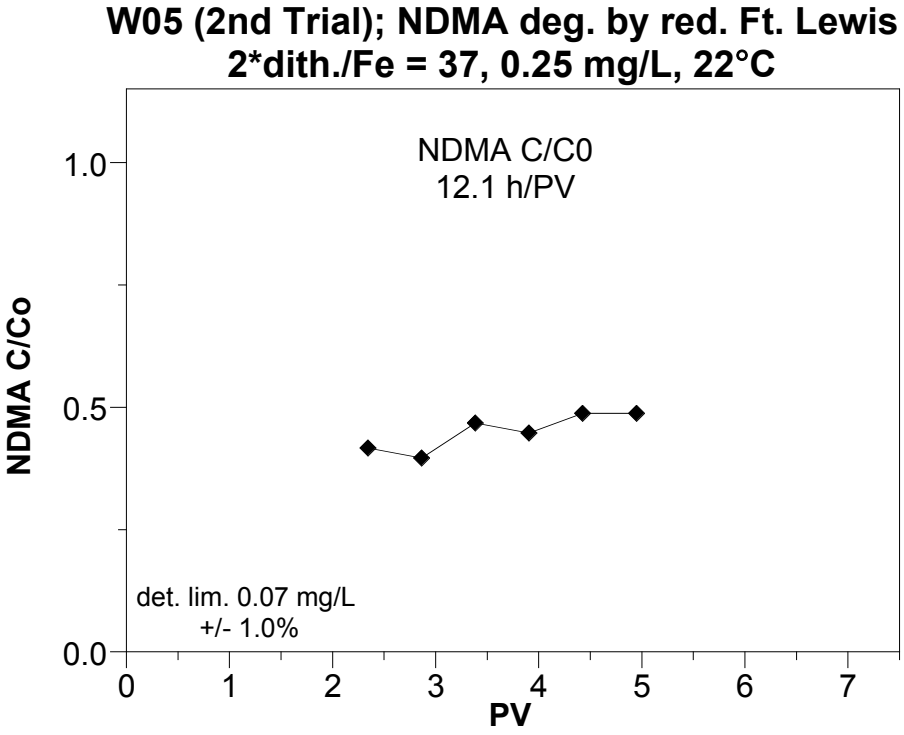
W05 (2nd Trial); NDMA deg. by red. Ft. Lewis
2*dith./Fe = 37, 0.25 mg/L, 22°C
NDMA C/C0
12.1 h/PV
det. lim. 0.07 mg/L
+/- 1.0%
NDMA C/Co
PV
1.0
0.5
0.0
0
1
2
3
4
5
6
7

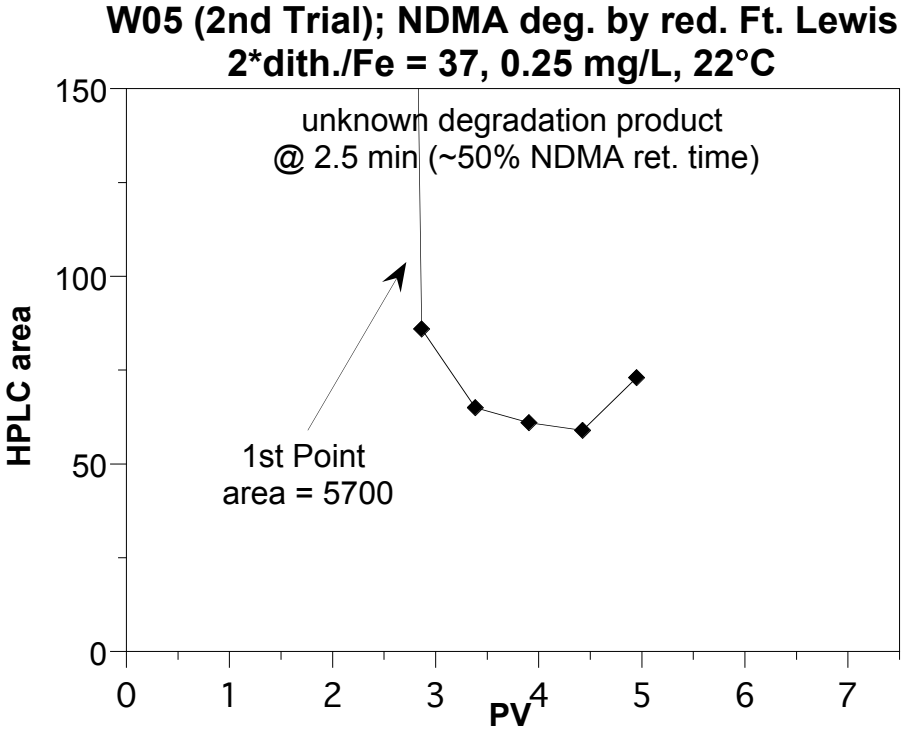
W05 (2nd Trial); NDMA deg. by red. Ft. Lewis
2*dith./Fe = 37, 0.25 mg/L, 22°C
unknown degradation product
@ 2.5 min (~50% NDMA ret. time)
1st Point
area = 5700
HPLC area
PV
150
100
50
0
0
1
2
3
4
5
6
7

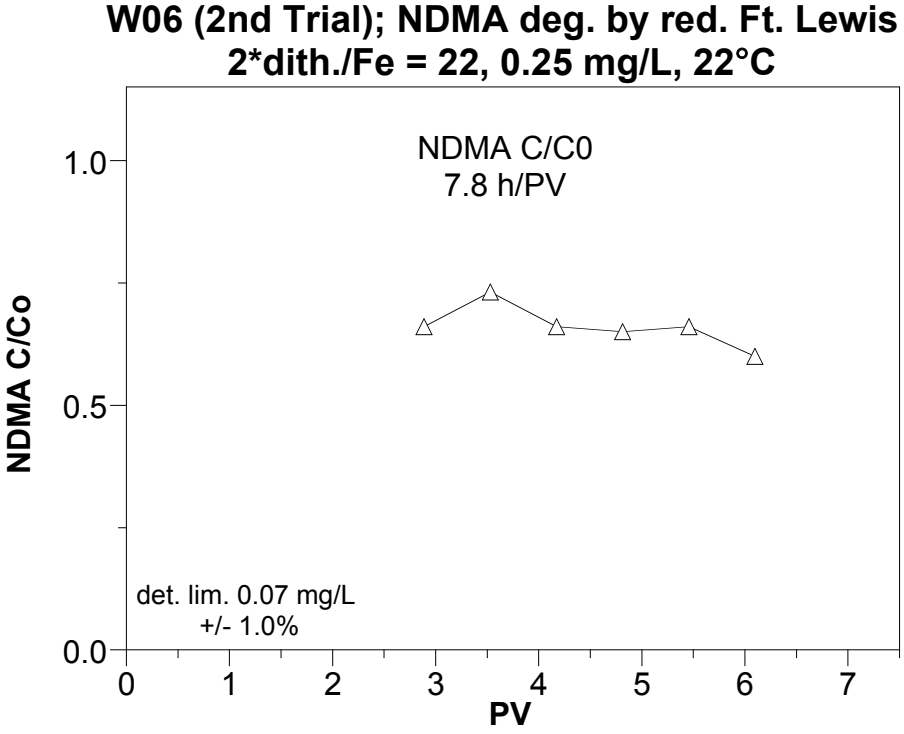
W06 (2nd Trial); NDMA deg. by red. Ft. Lewis
2*dith./Fe = 22, 0.25 mg/L, 22°C
NDMA C/C0
7.8 h/PV
det. lim. 0.07 mg/L
+/- 1.0%
NDMA C/Co
PV
1.0
0.5
0.0
0
1
2
3
4
5
6
7

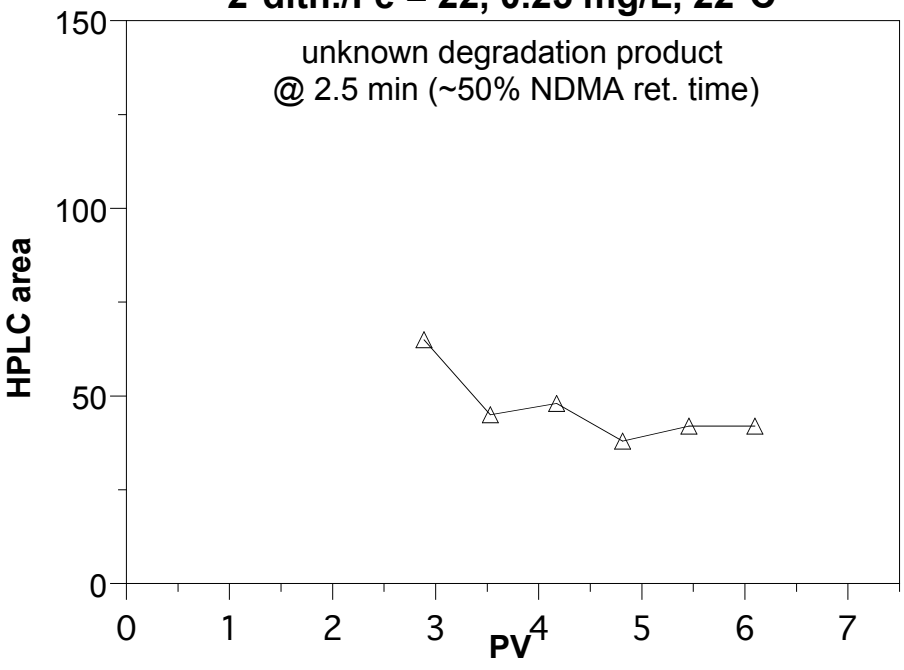
W06 (2nd Trial); NDMA deg. by red. Ft. Lewis
2*dith./Fe = 22, 0.25 mg/L, 22°C
unknown degradation product
@ 2.5 min (~50% NDMA ret. time)
HPLC area
PV
150
100
50
0
0
1
2
3
4
5
6
7

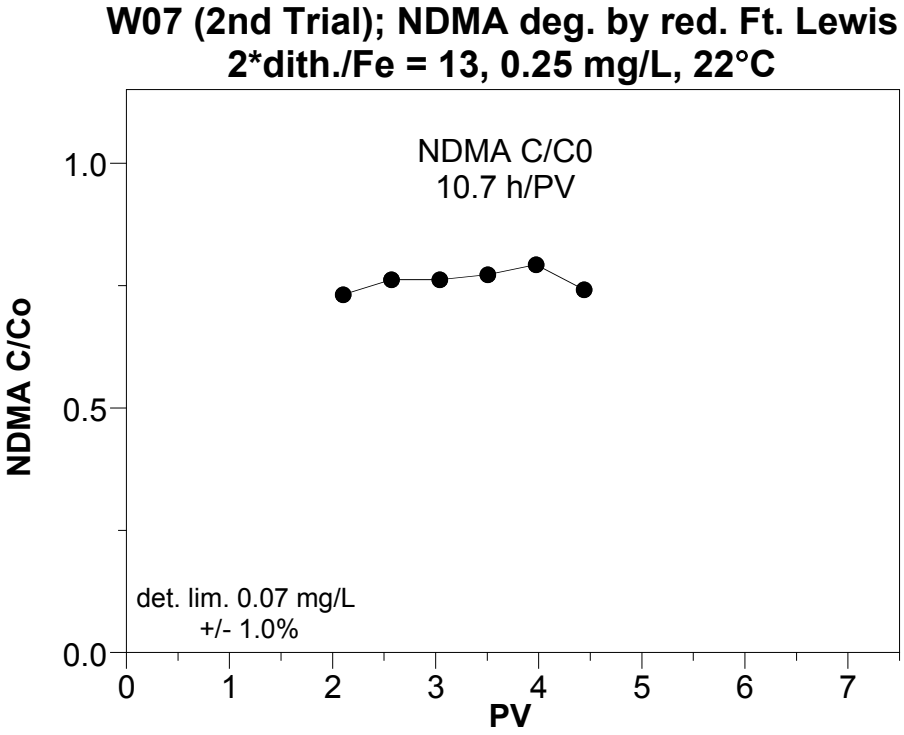
W07 (2nd Trial); NDMA deg. by red. Ft. Lewis
2*dith./Fe = 13, 0.25 mg/L, 22°C
NDMA C/C0
10.7 h/PV
det. lim. 0.07 mg/L
+/- 1.0%
NDMA C/Co
PV
1.0
0.5
0.0
0
1
2
3
4
5
6
7

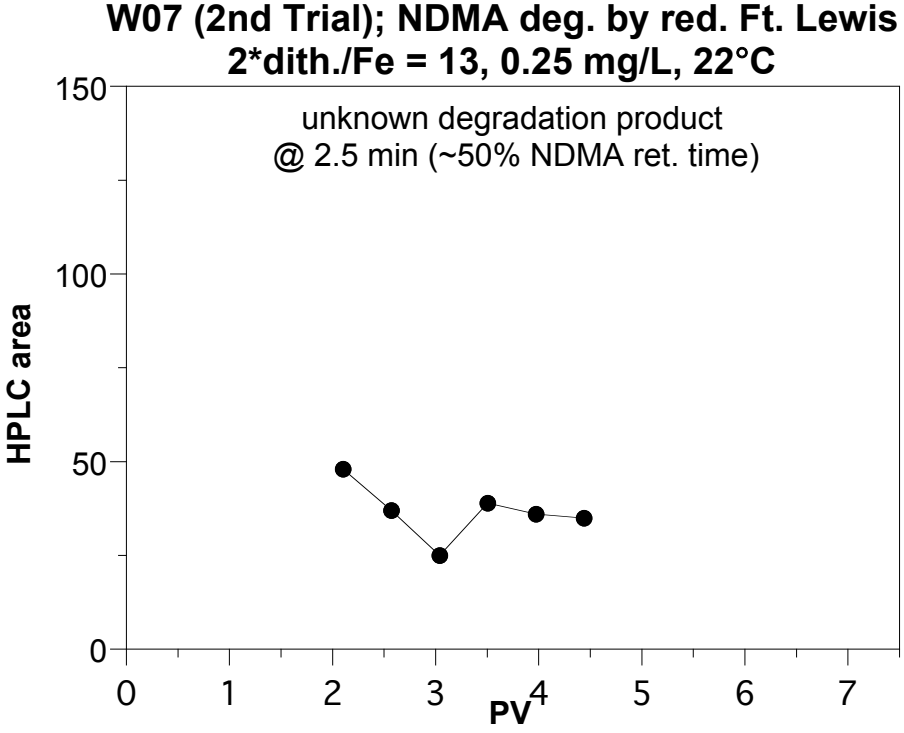
W07 (2nd Trial); NDMA deg. by red. Ft. Lewis
2*dith./Fe = 13, 0.25 mg/L, 22°C
unknown degradation product
@ 2.5 min (~50% NDMA ret. time)
HPLC area
PV
150
100
50
0
0
1
2
3
4
5
6
7

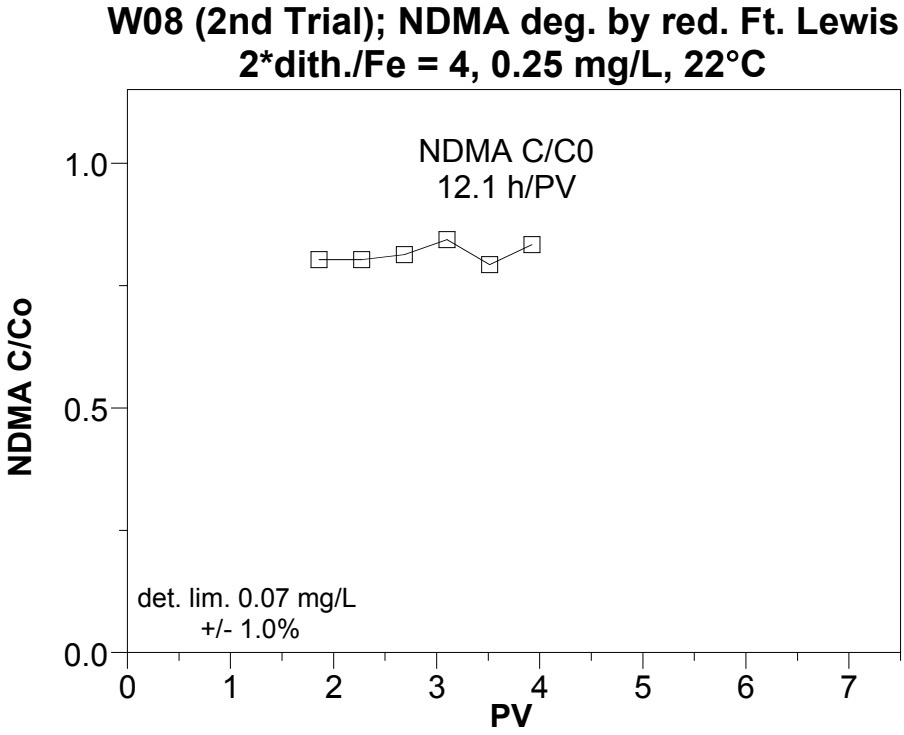
W08 (2nd Trial); NDMA deg. by red. Ft. Lewis
2*dith./Fe = 4, 0.25 mg/L, 22°C
NDMA C/C0
12.1 h/PV
det. lim. 0.07 mg/L
+/- 1.0%
NDMA C/Co
1.0
0.5
0.0
0
1
2
3
4
5
6
7
PV

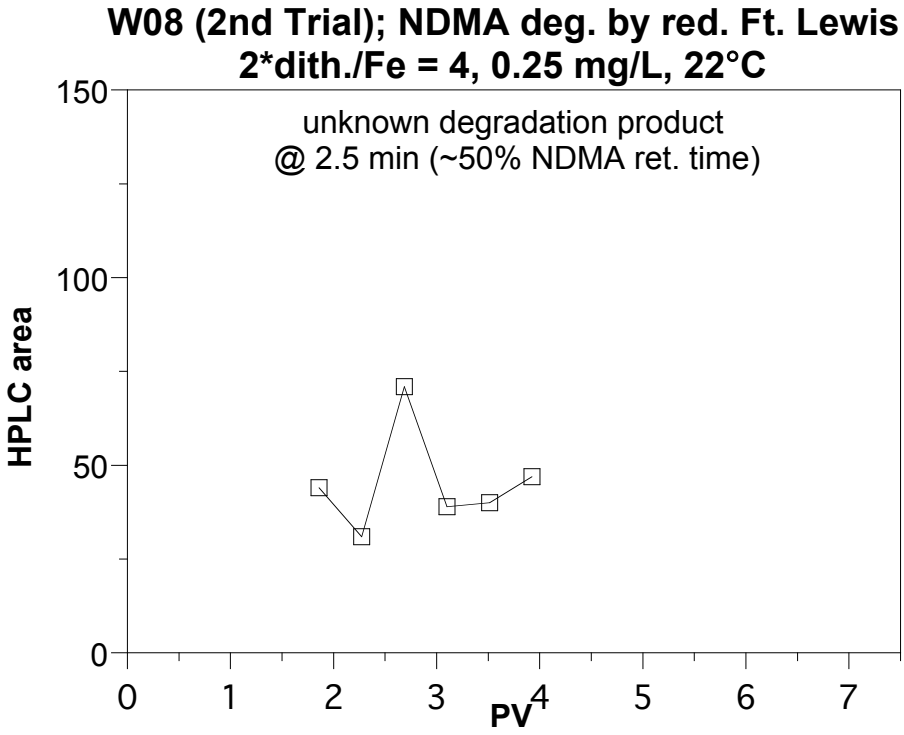
W08 (2nd Trial); NDMA deg. by red. Ft. Lewis
2*dith./Fe = 4, 0.25 mg/L, 22°C
unknown degradation product
@ 2.5 min (~50% NDMA ret. time)
HPLC area
150
100
50
0
0
1
2
3
4
5
6
7
PV

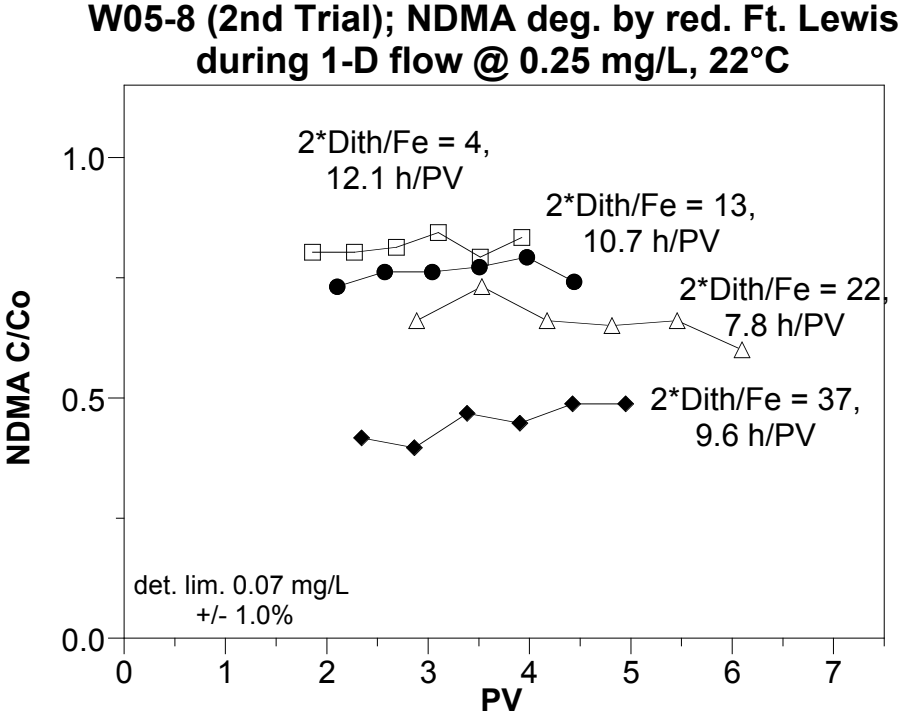
W05-8 (2nd Trial); NDMA deg. by red. Ft. Lewis
during 1-D flow @ 0.25 mg/L, 22°C
2*Dith/Fe = 4,
12.1 h/PV
2*Dith/Fe = 13,
10.7 h/PV
2*Dith/Fe = 22,
7.8 h/PV
2*Dith/Fe = 37,
9.6 h/PV
det. lim. 0.07 mg/L
+/- 1.0%
NDMA C/Co
PV
0.0
0.5
1.0
0
1
2
3
4
5
6
7

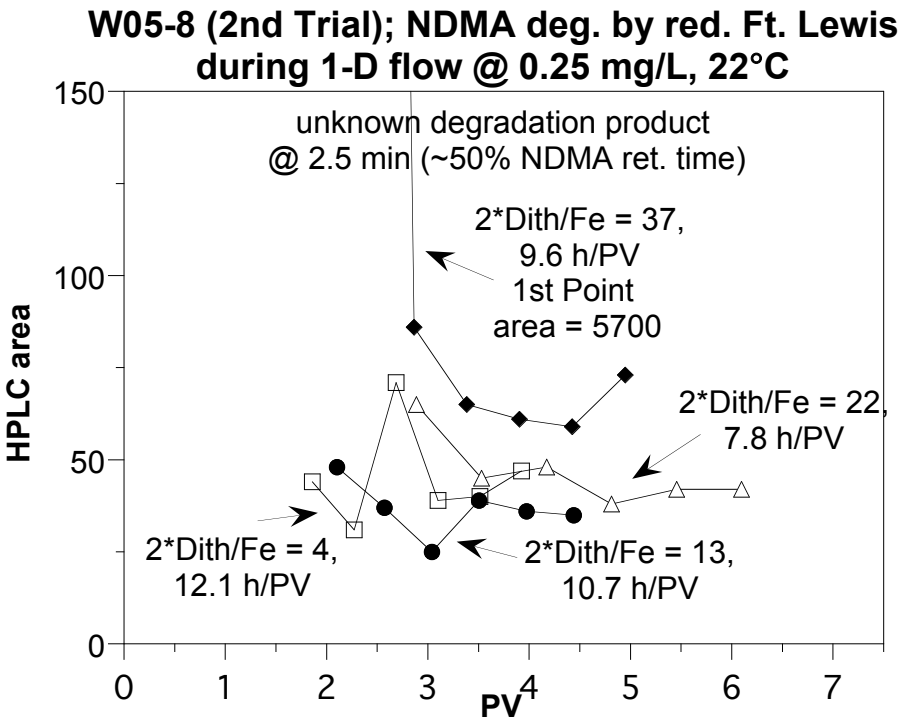
W05-8 (2nd Trial); NDMA deg. by red. Ft. Lewis
during 1-D flow @ 0.25 mg/L, 22°C
unknown degradation product
@ 2.5 min (~50% NDMA ret. time)
2*Dith/Fe = 37,
9.6 h/PV
1st Point
area = 5700
2*Dith/Fe = 22,
7.8 h/PV
2*Dith/Fe = 4,
12.1 h/PV
2*Dith/Fe = 13,
10.7 h/PV
HPLC area
PV
0
50
100
150
0
1
2
3
4
5
6
7

W09; NDMA deg. by red. Ft. Lewis
2*dith./Fe = 37, 2.5 mg/L, 34°C

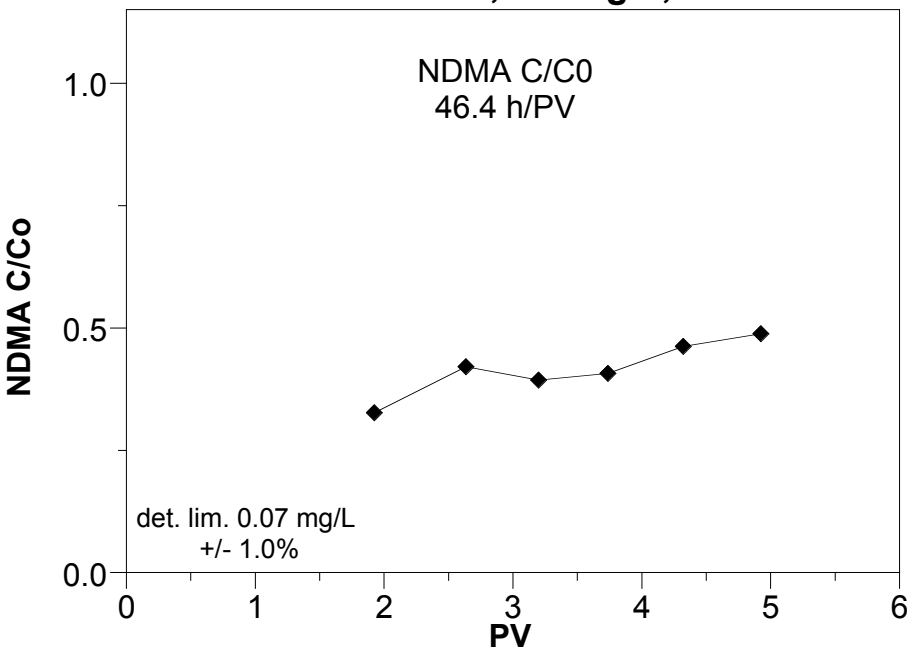

W10; NDMA deg. by red. Ft. Lewis
2*dith./Fe = 22, 2.5 mg/L, 34°C

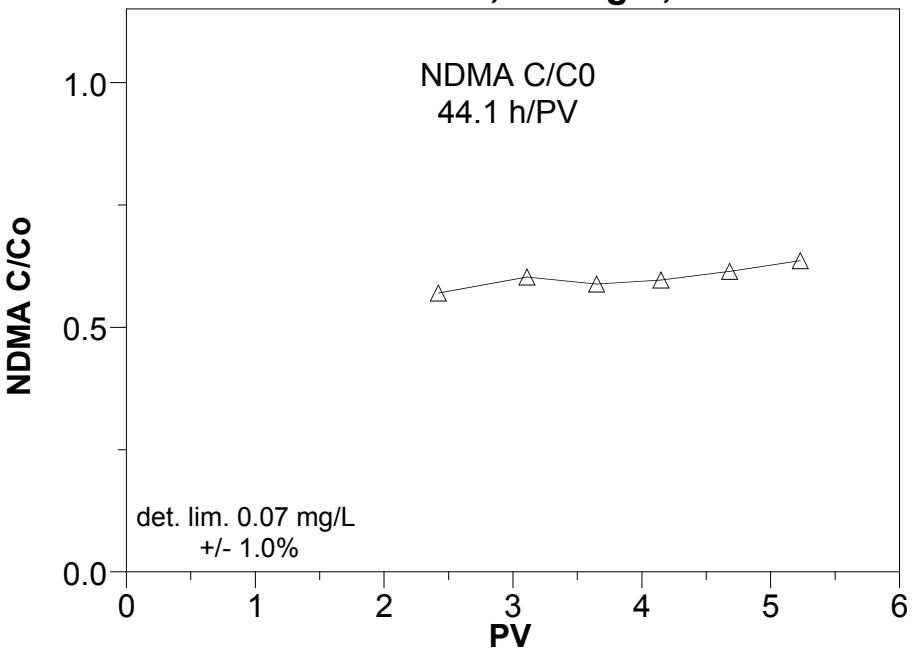

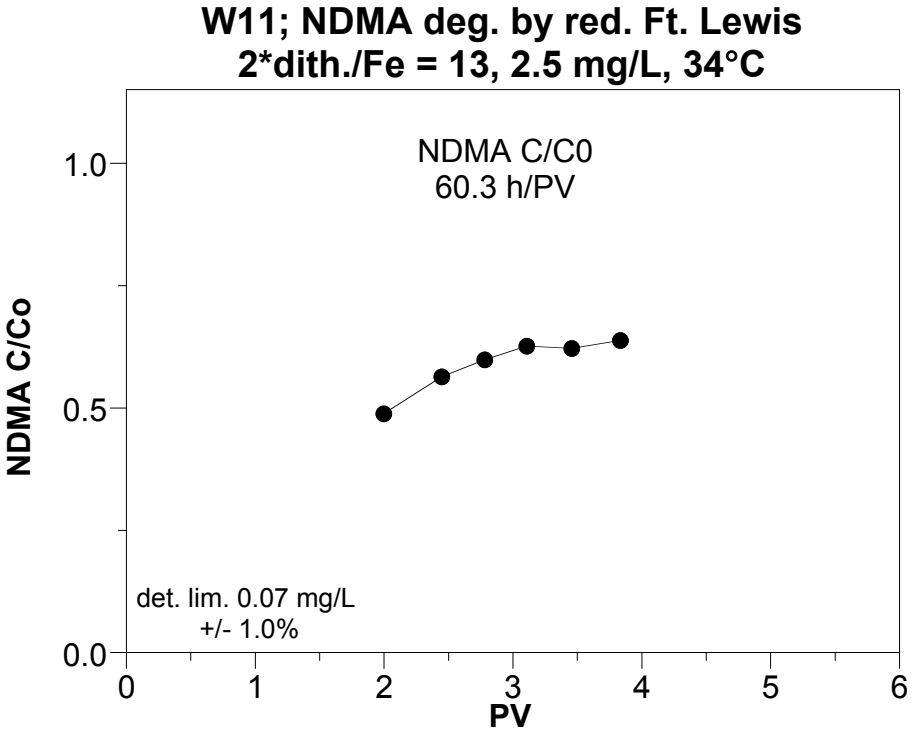
W11; NDMA deg. by red. Ft. Lewis
2*dith./Fe = 13, 2.5 mg/L, 34°C
NDMA C/C0
60.3 h/PV
det. lim. 0.07 mg/L
+/- 1.0%
NDMA C/Co
PV
0.0
0.5
1.0
0
1
2
3
4
5
6

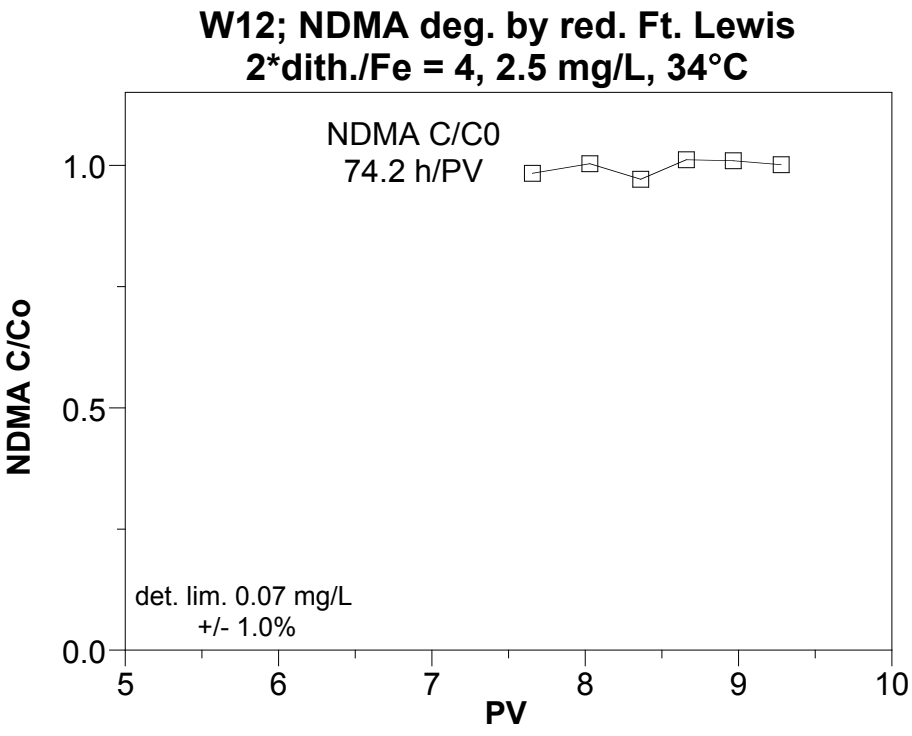
W12; NDMA deg. by red. Ft. Lewis
2*dith./Fe = 4, 2.5 mg/L, 34°C
NDMA C/C0
74.2 h/PV
det. lim. 0.07 mg/L
+/- 1.0%
NDMA C/Co
PV
0.0
0.5
1.0
5
6
7
8
9
10

W09-12; NDMA deg. by red. Ft. Lewis during 1-D flow @ 2.5 mg/L, 34°C

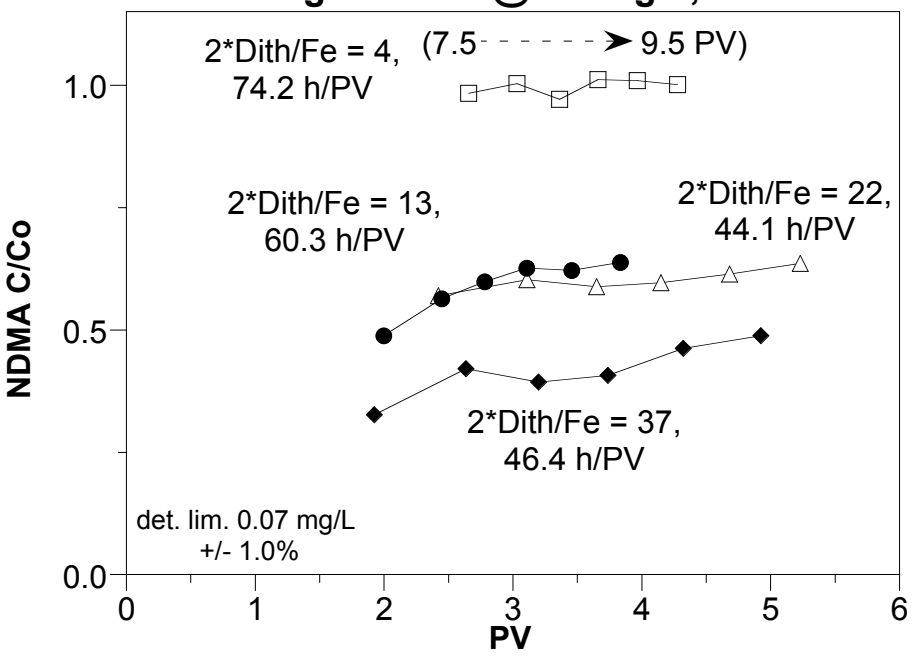

Comments on NDMA deg by 1-D flow @ 34°C

HPLC analysis on previous two column studies at 22°C (room temp) showed a very clean NDMA peak at 5.0 minutes and an inversely proportionate peak at 4.5 minutes.

HPLC analysis on this set at 34°C (using column heater) still shows a very clean NDMA peak, none of the 4.5 minute peak, and a number of new very low and flat peaks, some up to 1.5 minutes wide, between 2 and 4 minutes.

None of the analyzed samples had any peaks breaking through after NDMA.

W13; NDMA deg. by red. Ft. Lewis
2*dith./Fe = 37, 2.5 mg/L, 45°C

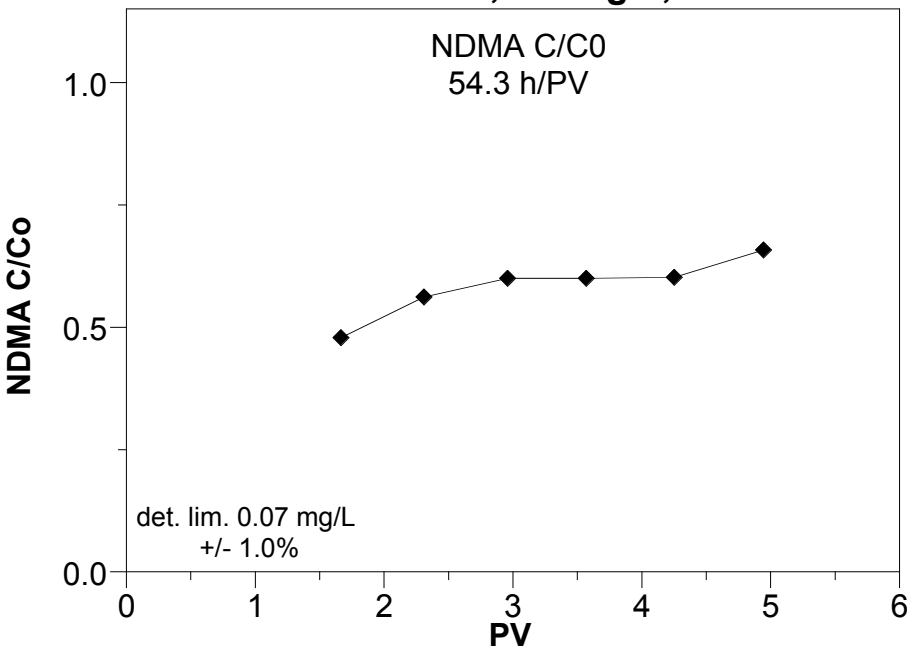

W14; NDMA deg. by red. Ft. Lewis
2*dith./Fe = 22, 2.5 mg/L, 45°C

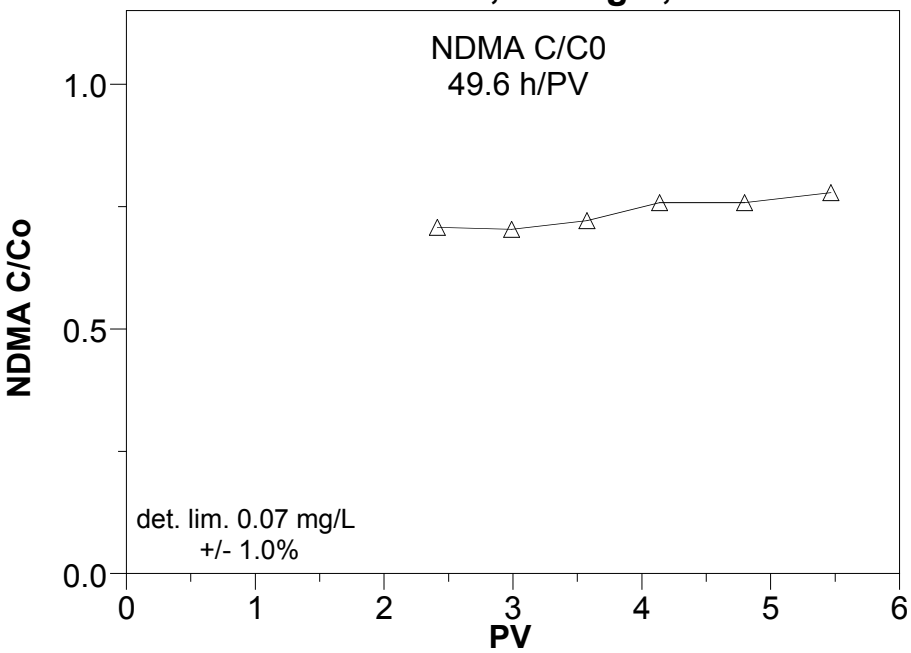

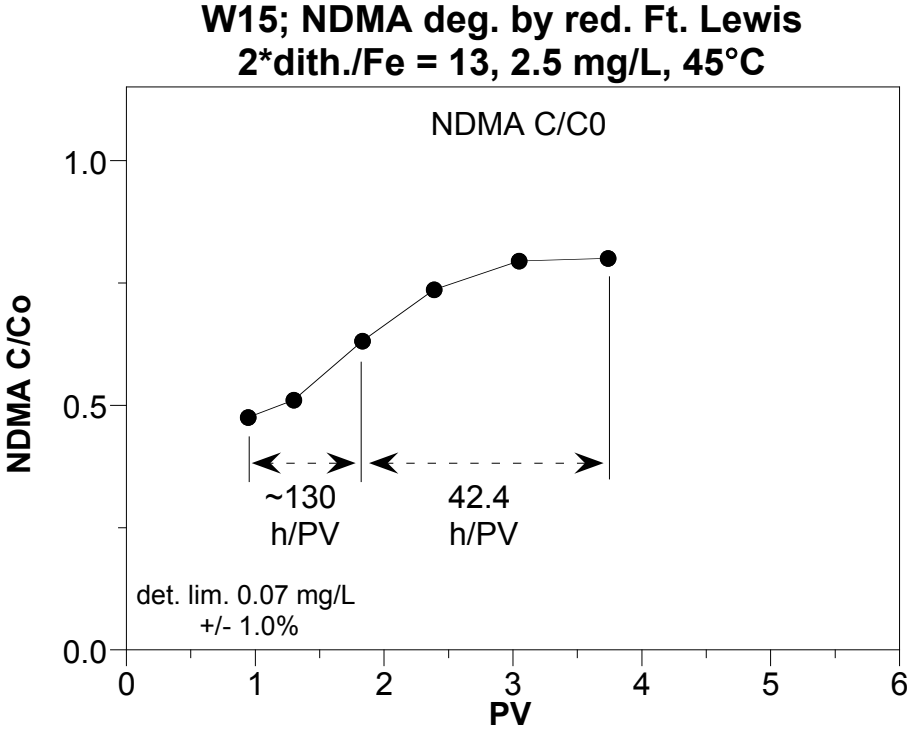
W15; NDMA deg. by red. Ft. Lewis
2*dith./Fe = 13, 2.5 mg/L, 45°C
NDMA C/C0
NDMA C/Co
1.0
0.5
0.0
~130
h/PV
42.4
h/PV
det. lim. 0.07 mg/L
+/- 1.0%
0
1
2
3
4
5
6
PV

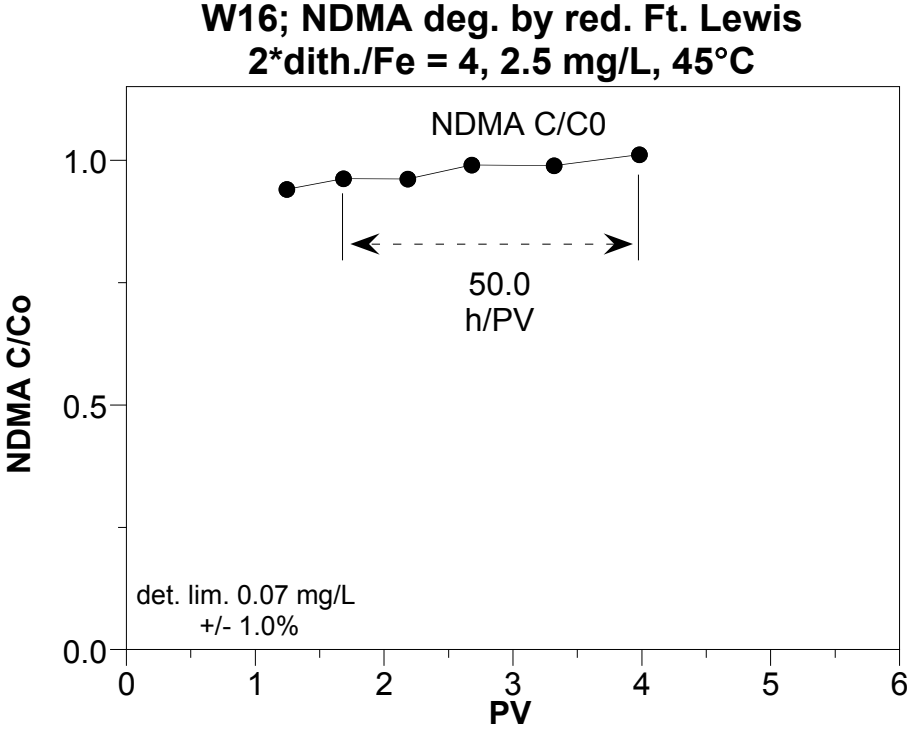
W16; NDMA deg. by red. Ft. Lewis
2*dith./Fe = 4, 2.5 mg/L, 45°C
NDMA C/C0
NDMA C/Co
1.0
0.5
0.0
50.0
h/PV
det. lim. 0.07 mg/L
+/- 1.0%
0
1
2
3
4
5
6
PV

W13-16; NDMA deg. by red. Ft. Lewis during 1-D flow @ 2.5 mg/L, 45°C

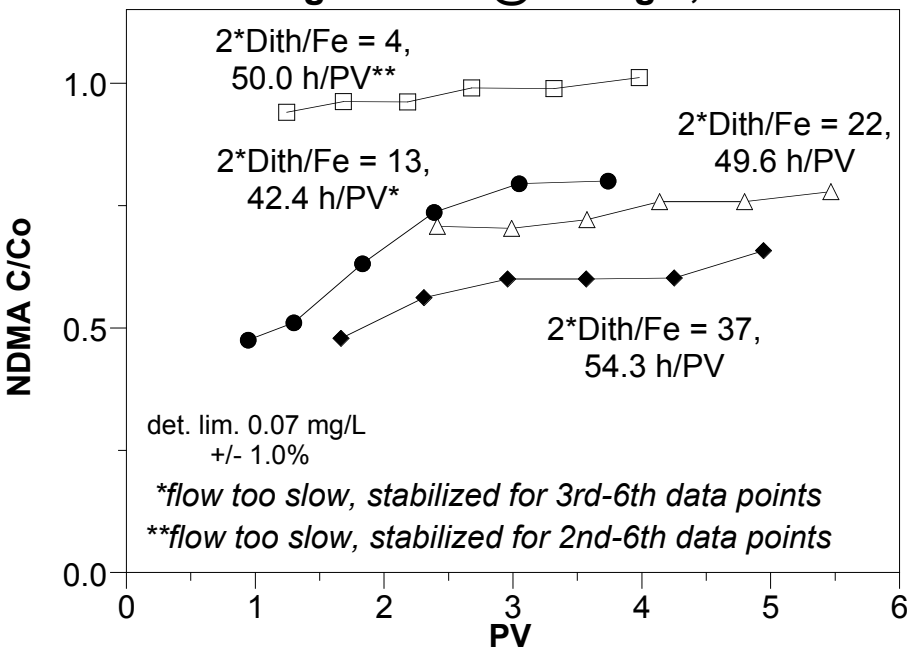

W17; NDMA deg. by red. Ft. Lewis 2*dith./Fe = 37, 2.5 mg/L, 56°C

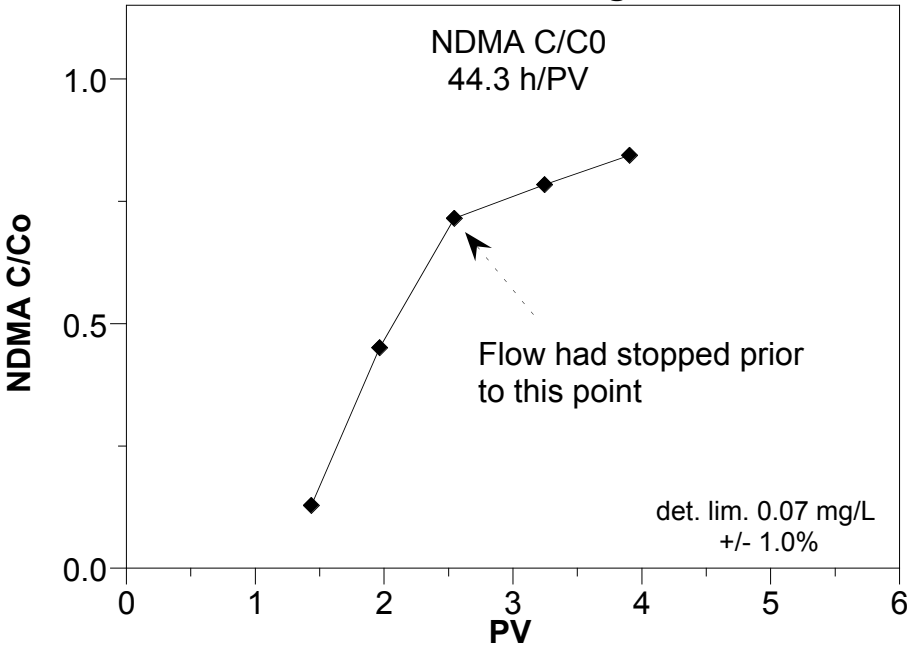

W18; NDMA deg. by red. Ft. Lewis
2*dith./Fe = 22, 2.5 mg/L, 56°C

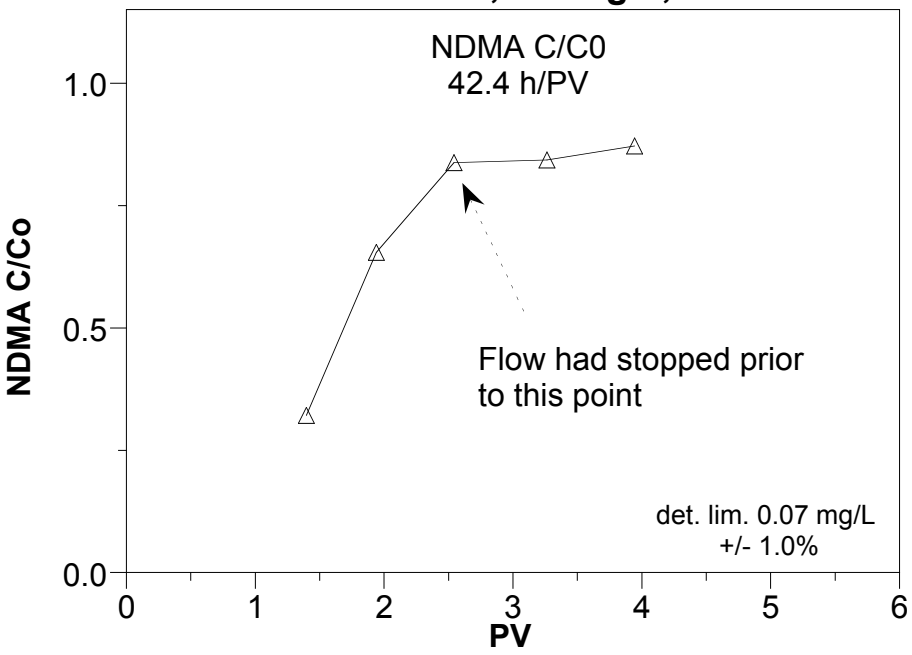

W19; NDMA deg. by red. Ft. Lewis
2*dith./Fe = 13, 2.5 mg/L, 56°C

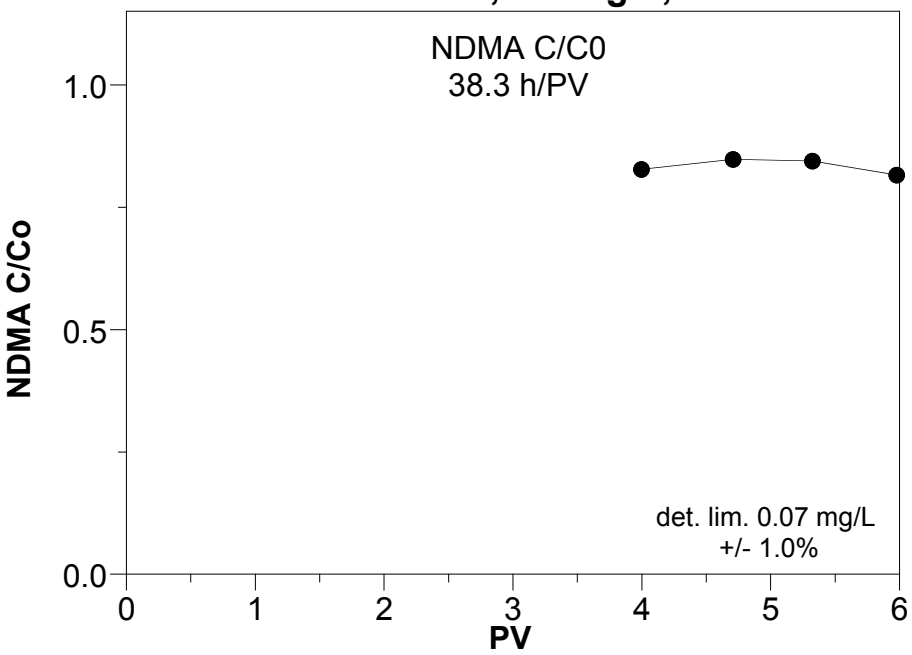

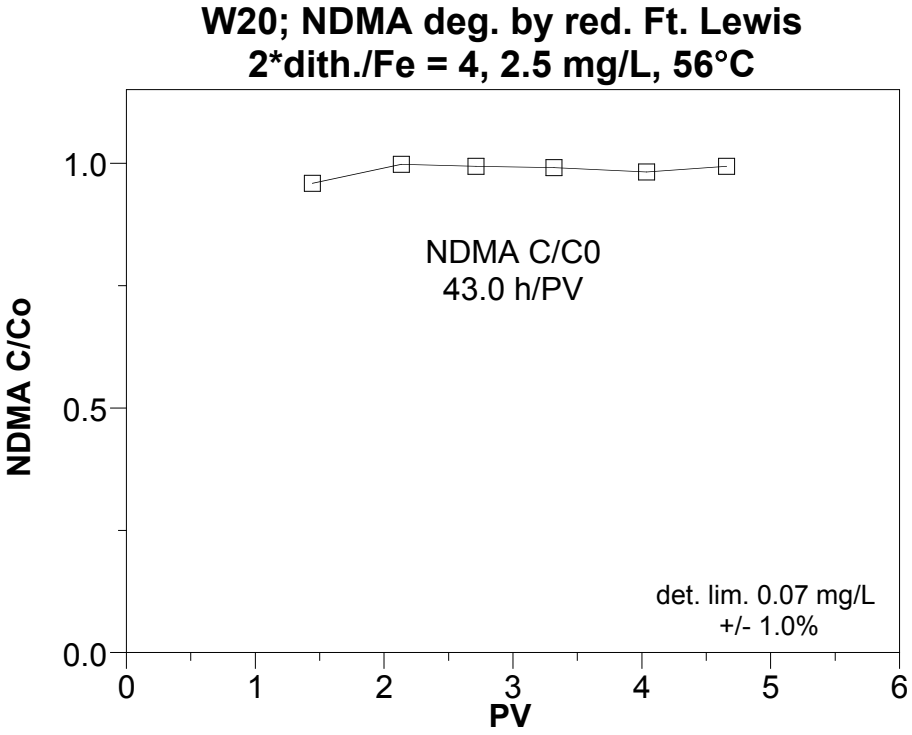
W20; NDMA deg. by red. Ft. Lewis
2*dith./Fe = 4, 2.5 mg/L, 56°C
NDMA C/Co
1.0
0.5
0.0
NDMA C/C0
43.0 h/PV
det. lim. 0.07 mg/L
+/- 1.0%
0
1
2
3
4
5
6
PV

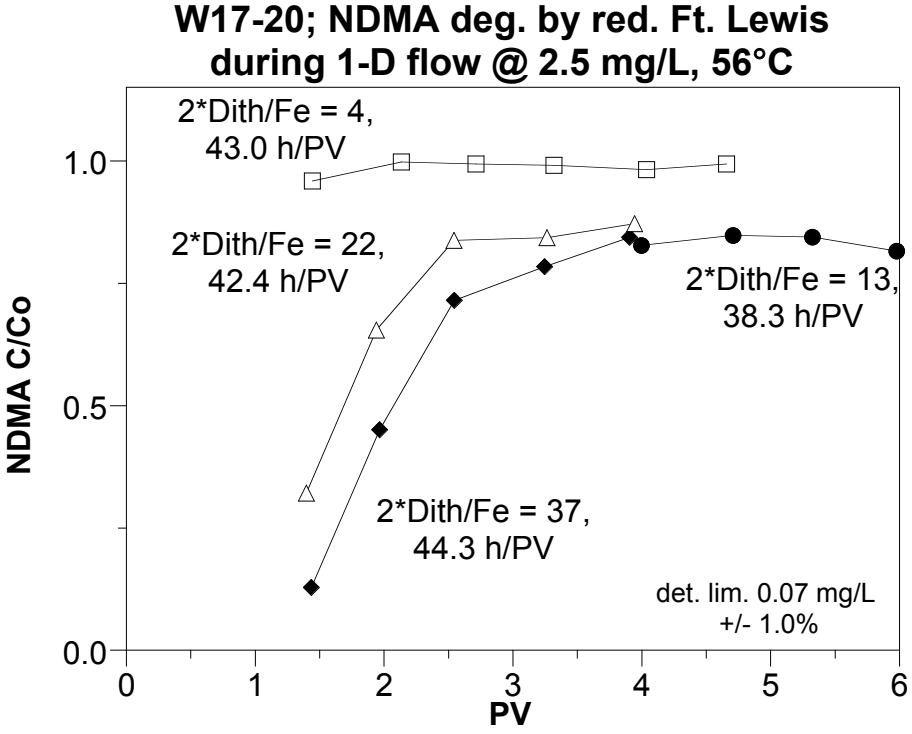
W17-20; NDMA deg. by red. Ft. Lewis
during 1-D flow @ 2.5 mg/L, 56°C
NDMA C/Co
1.0
0.5
0.0
2*Dith/Fe = 4,
43.0 h/PV
2*Dith/Fe = 22,
42.4 h/PV
2*Dith/Fe = 13,
38.3 h/PV
2*Dith/Fe = 37,
44.3 h/PV
det. lim. 0.07 mg/L
+/- 1.0%
0
1
2
3
4
5
6
PV

W1,5,9,13,17; NDMA deg. by red. Ft. Lewis
2*dith/Fe = 37 vs temp

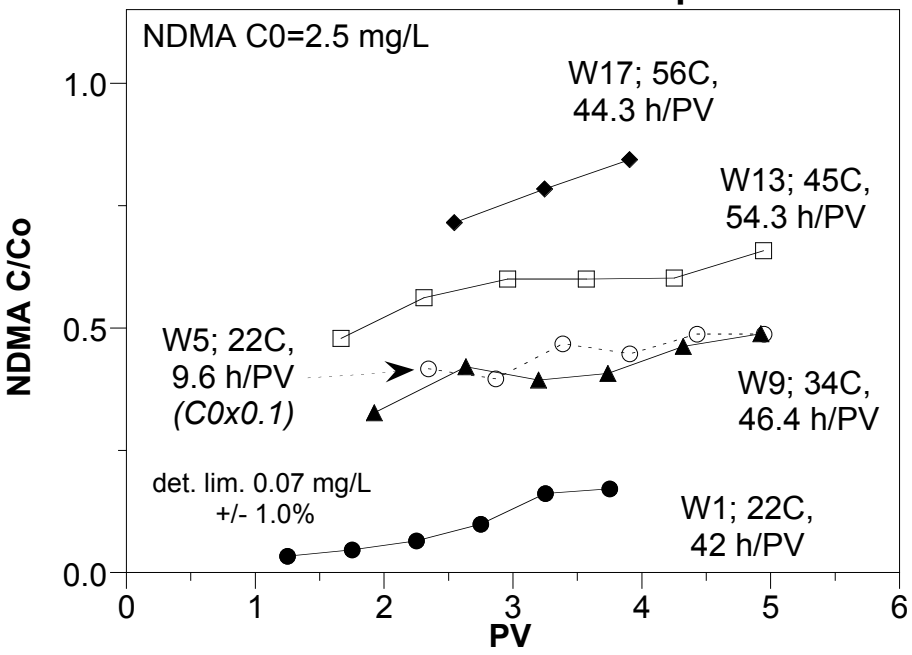

W2,4,10,14,18; NDMA deg. by red. Ft. Lewis
2*dith/Fe = 22 vs temp

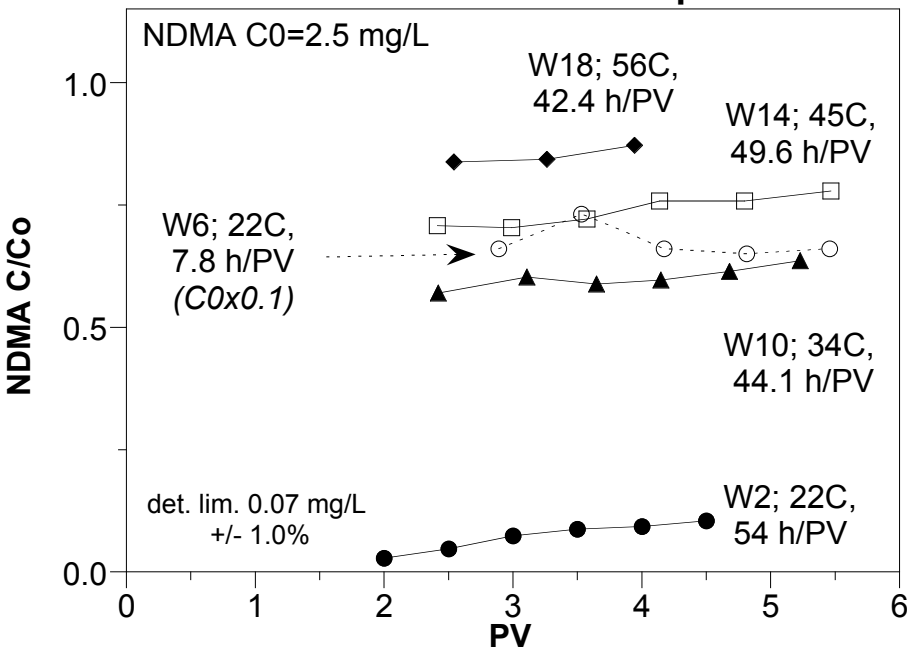

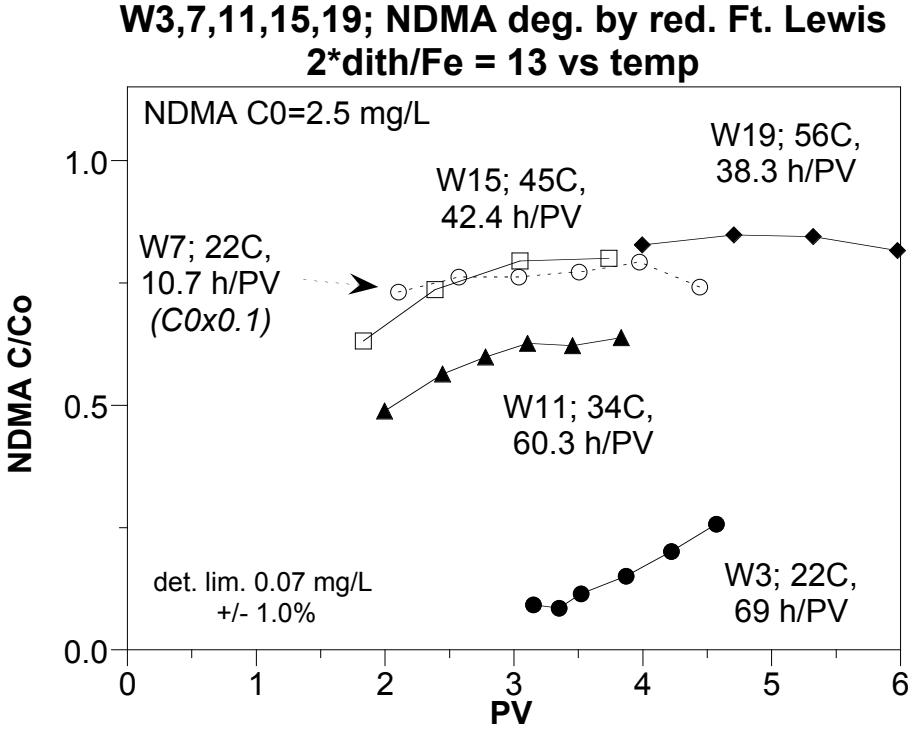
W3,7,11,15,19; NDMA deg. by red. Ft. Lewis
2*dith/Fe = 13 vs temp
NDMA C0=2.5 mg/L
W19; 56C,
38.3 h/PV
W15; 45C,
42.4 h/PV
W7; 22C,
10.7 h/PV
(C0x0.1)
W11; 34C,
60.3 h/PV
W3; 22C,
69 h/PV
det. lim. 0.07 mg/L
+/- 1.0%
NDMA C/Co
PV
0.0
0.5
1.0
0
1
2
3
4
5
6

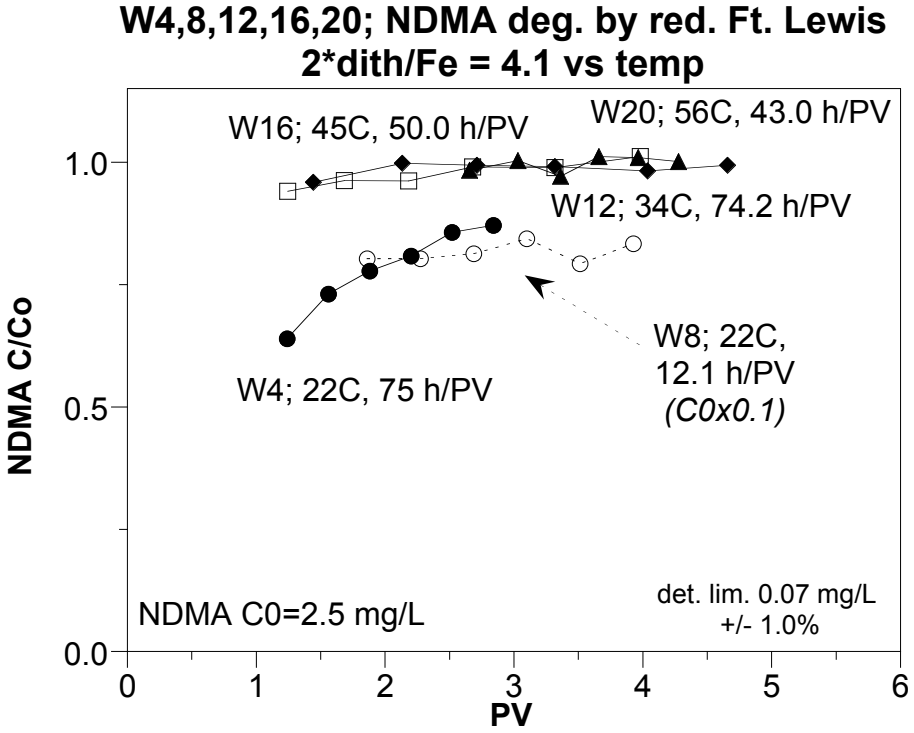
W4,8,12,16,20; NDMA deg. by red. Ft. Lewis
2*dith/Fe = 4.1 vs temp
W16; 45C, 50.0 h/PV
W20; 56C, 43.0 h/PV
W12; 34C, 74.2 h/PV
W8; 22C,
12.1 h/PV
(C0x0.1)
W4; 22C, 75 h/PV
NDMA C0=2.5 mg/L
det. lim. 0.07 mg/L
+/- 1.0%
NDMA C/Co
PV
0.0
0.5
1.0
0
1
2
3
4
5
6

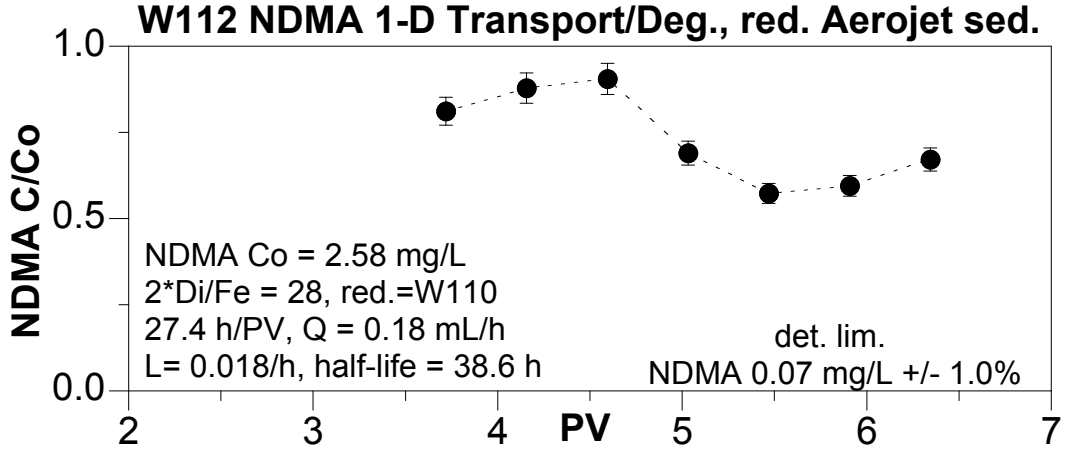
W112 NDMA 1-D Transport/Deg., red. Aerojet sed.
NDMA C/Co
1.0
0.5
0.0
NDMA Co = 2.58 mg/L
2*Di/Fe = 28, red.=W110
27.4 h/PV, Q = 0.18 mL/h
L= 0.018/h, half-life = 38.6 h
det. lim.
NDMA 0.07 mg/L +/- 1.0%
2
3
4
PV
5
6
7

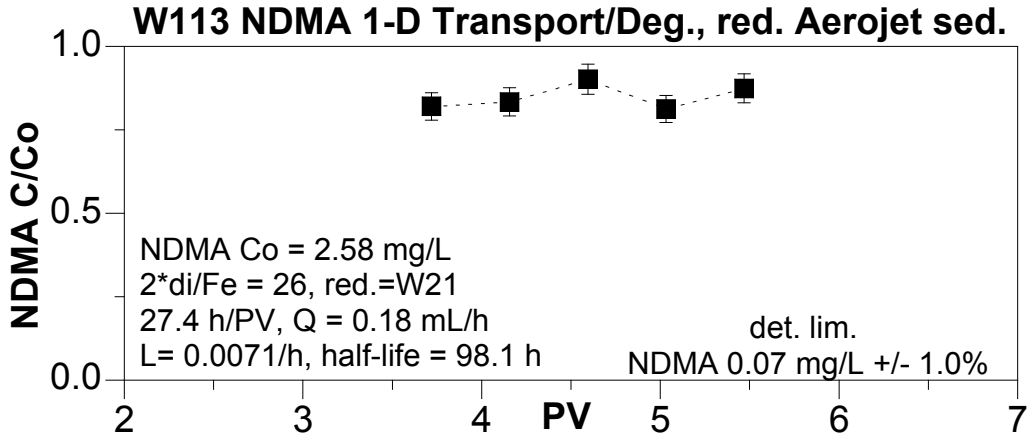
W113 NDMA 1-D Transport/Deg., red. Aerojet sed.
NDMA C/Co
1.0
0.5
0.0
NDMA Co = 2.58 mg/L
2*di/Fe = 26, red.=W21
27.4 h/PV, Q = 0.18 mL/h
L= 0.0071/h, half-life = 98.1 h
det. lim.
NDMA 0.07 mg/L +/- 1.0%
2
3
4
PV
5
6
7

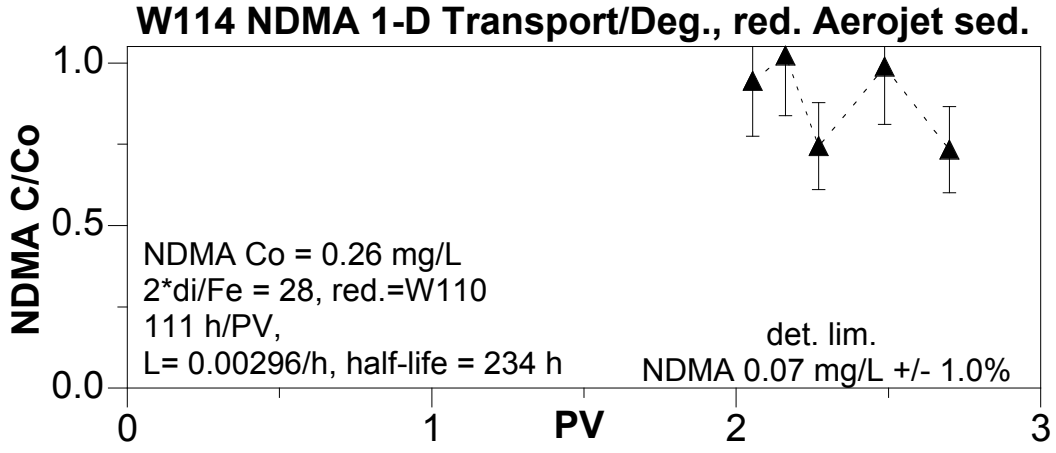
W114 NDMA 1-D Transport/Deg., red. Aerojet sed.
NDMA C/Co
1.0
0.5
0.0
NDMA Co = 0.26 mg/L
2*di/Fe = 28, red.=W110
111 h/PV,
L= 0.00296/h, half-life = 234 h
det. lim.
NDMA 0.07 mg/L +/- 1.0%
0
1
PV
2
3

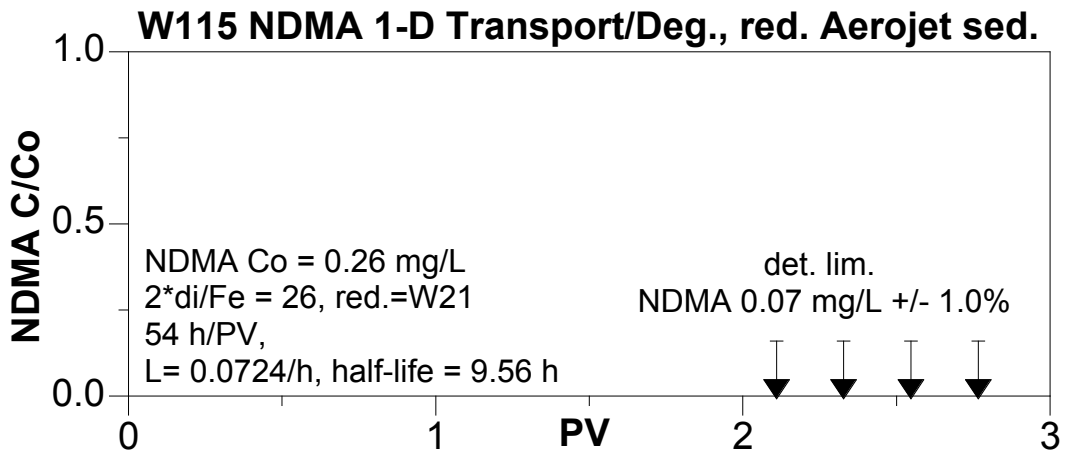
W115 NDMA 1-D Transport/Deg., red. Aerojet sed.
NDMA C/Co
1.0
0.5
0.0
NDMA Co = 0.26 mg/L
2*di/Fe = 26, red.=W21
54 h/PV,
L= 0.0724/h, half-life = 9.56 h
det. lim.
NDMA 0.07 mg/L +/- 1.0%
0
1
PV
2
3

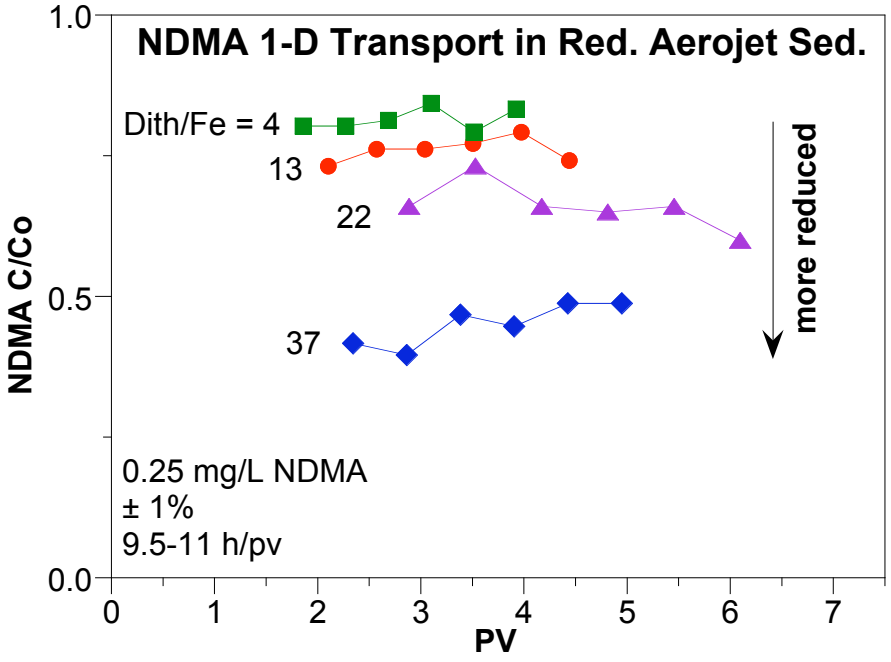
NDMA 1-D Transport in Red. Aerojet Sed.
NDMA C/Co
1.0
0.5
0.0
Dith/Fe = 4
13
22
37
more reduced
0.25 mg/L NDMA
± 1%
9.5-11 h/pv
0
1
2
3
4
5
6
7
PV

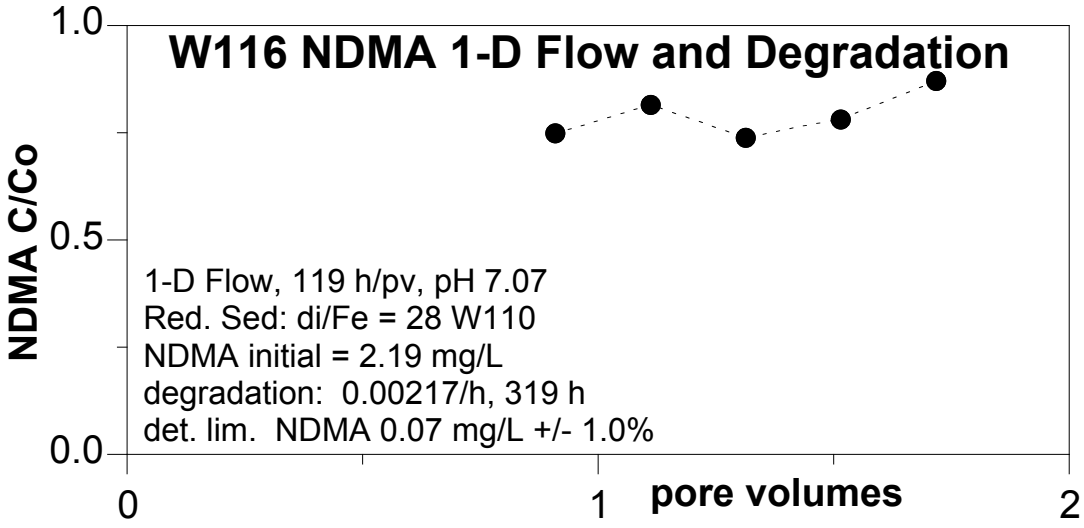
W116 NDMA 1-D Flow and Degradation
NDMA C/Co
1.0
0.5
0.0
1-D Flow, 119 h/pv, pH 7.07
Red. Sed: di/Fe = 28 W110
NDMA initial = 2.19 mg/L
degradation: 0.00217/h, 319 h
det. lim. NDMA 0.07 mg/L +/- 1.0%
0
1
pore volumes
2

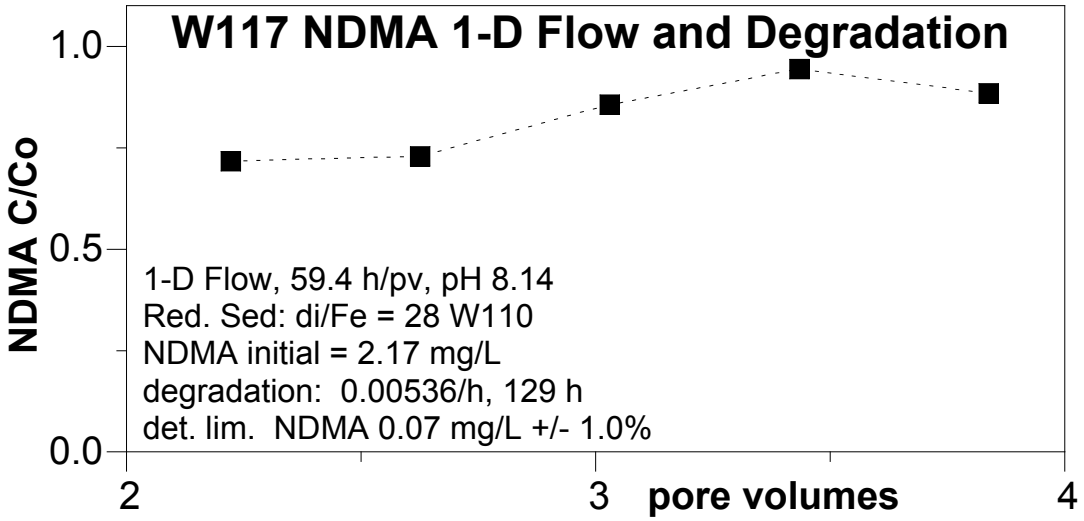
W117 NDMA 1-D Flow and Degradation
NDMA C/Co
1.0
0.5
0.0
1-D Flow, 59.4 h/pv, pH 8.14
Red. Sed: di/Fe = 28 W110
NDMA initial = 2.17 mg/L
degradation: 0.00536/h, 129 h
det. lim. NDMA 0.07 mg/L +/- 1.0%
2
3
pore volumes
4

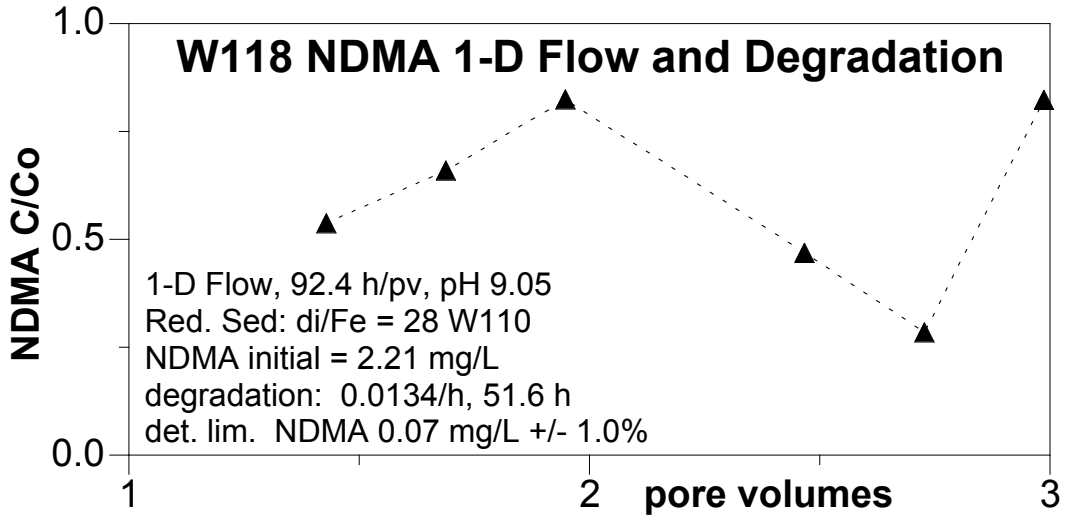
W118 NDMA 1-D Flow and Degradation
NDMA C/Co
1.0
0.5
0.0
1-D Flow, 92.4 h/pv, pH 9.05
Red. Sed: di/Fe = 28 W110
NDMA initial = 2.21 mg/L
degradation: 0.0134/h, 51.6 h
det. lim. NDMA 0.07 mg/L +/- 1.0%
1
2
pore volumes
3

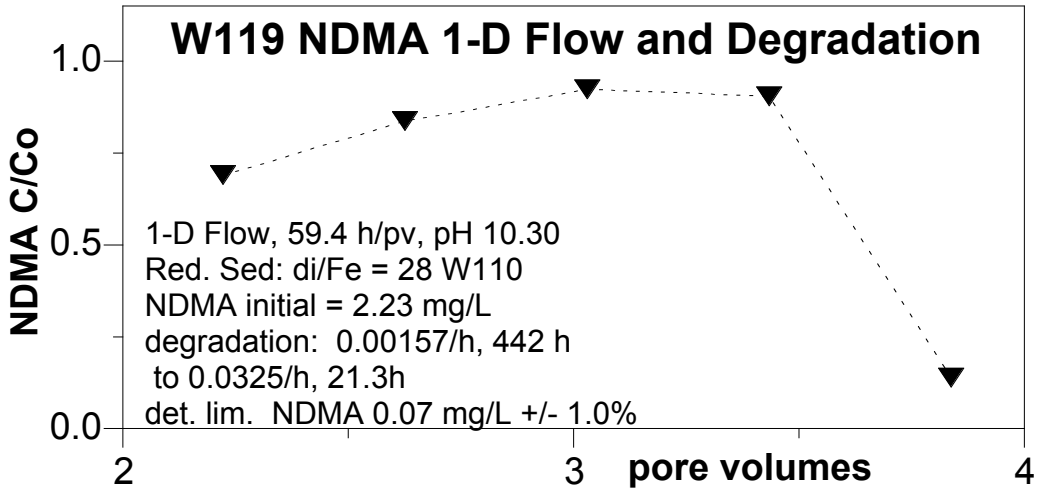
W119 NDMA 1-D Flow and Degradation
NDMA C/Co
1.0
0.5
0.0
1-D Flow, 59.4 h/pv, pH 10.30
Red. Sed: di/Fe = 28 W110
NDMA initial = 2.23 mg/L
degradation: 0.00157/h, 442 h
to 0.0325/h, 21.3h
det. lim. NDMA 0.07 mg/L +/- 1.0%
2
3
pore volumes
4

Stop-flow 1-D Columns

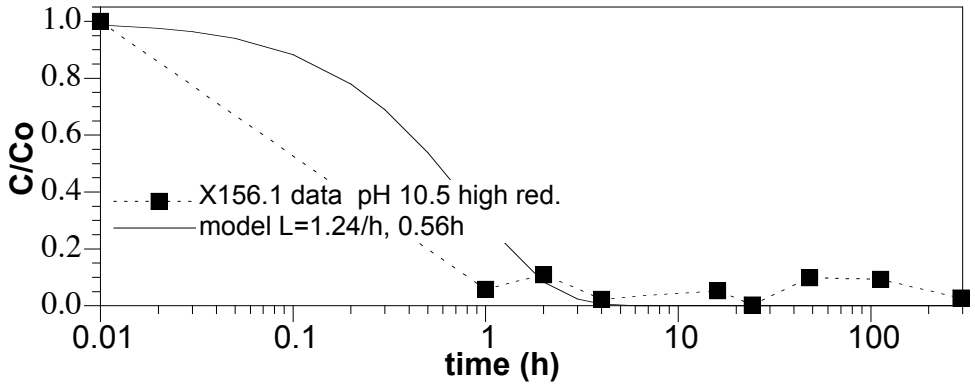

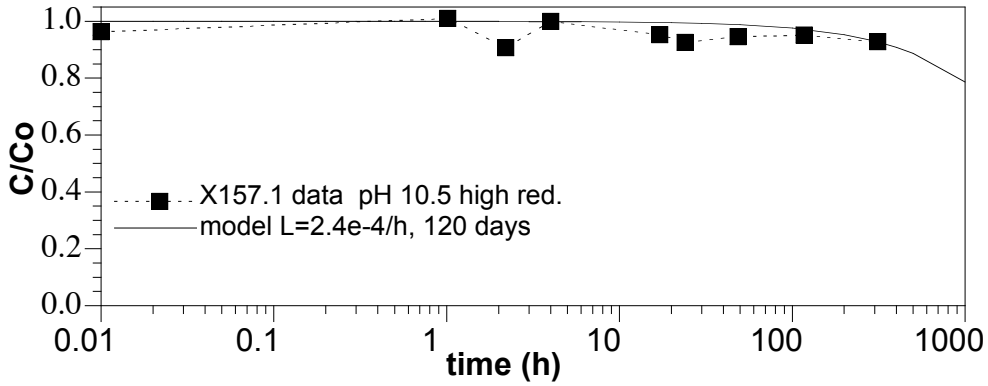

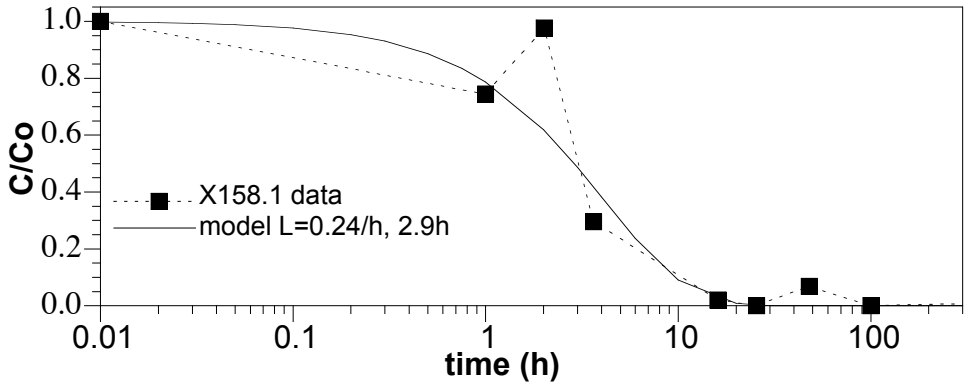

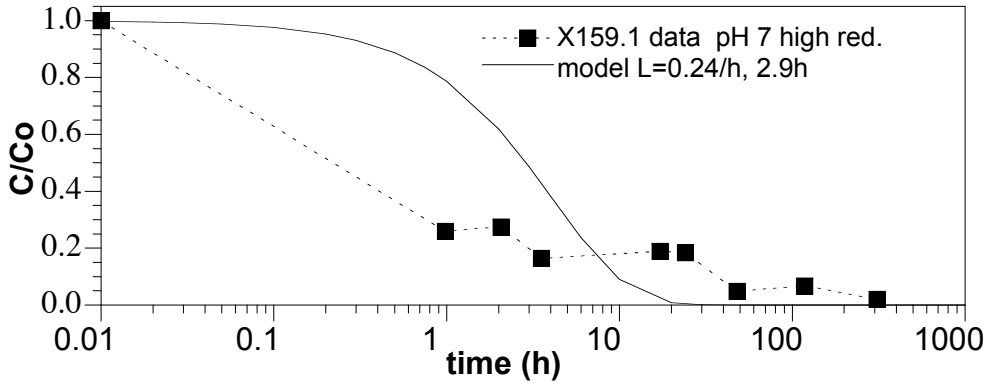

Appendix A.9 Task 1.9 NDMA Degradation in 1-D Columns with DMA Analysis

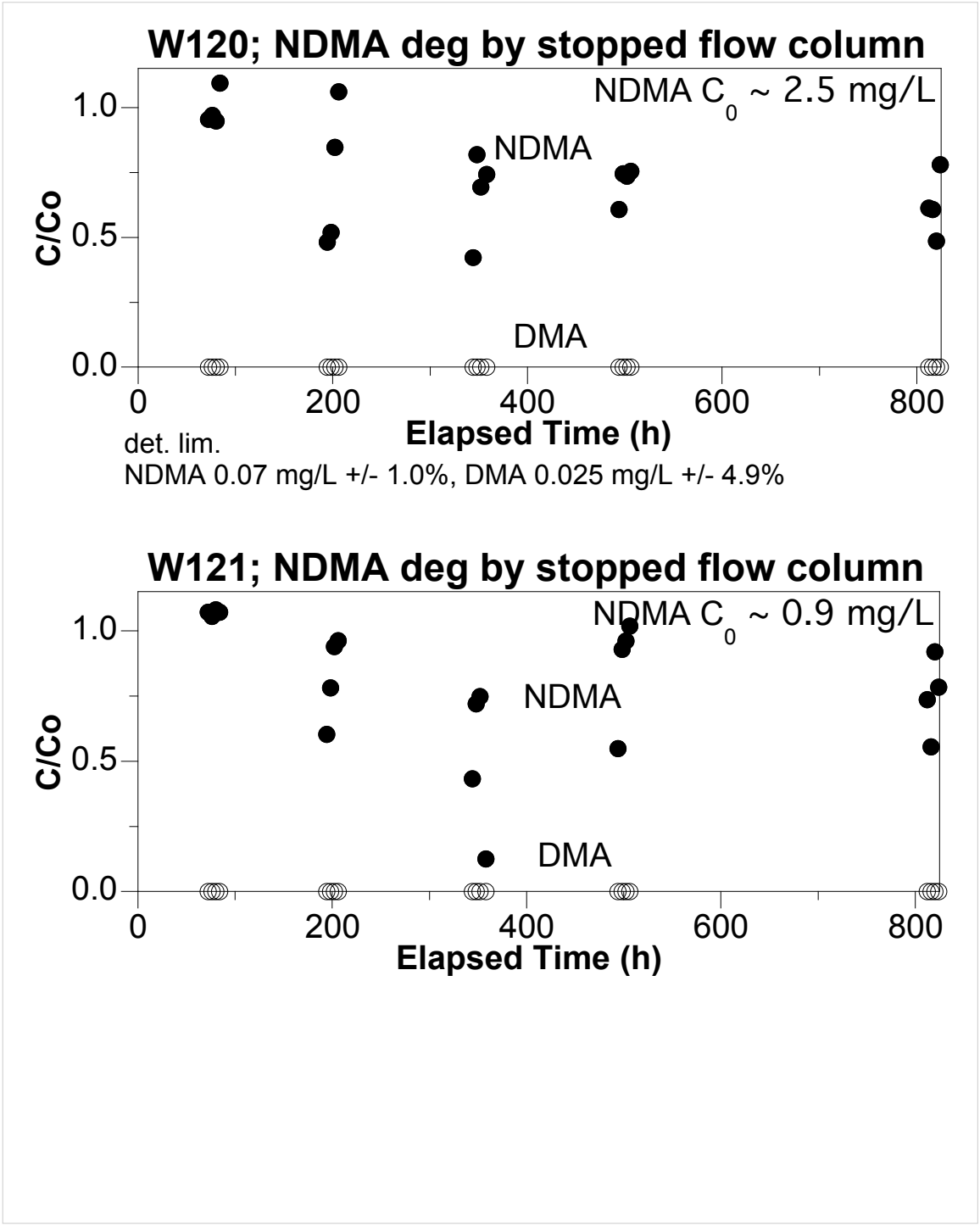

W96; NDMA deg. by red. Ft. Lewis, 13.7 h/PV

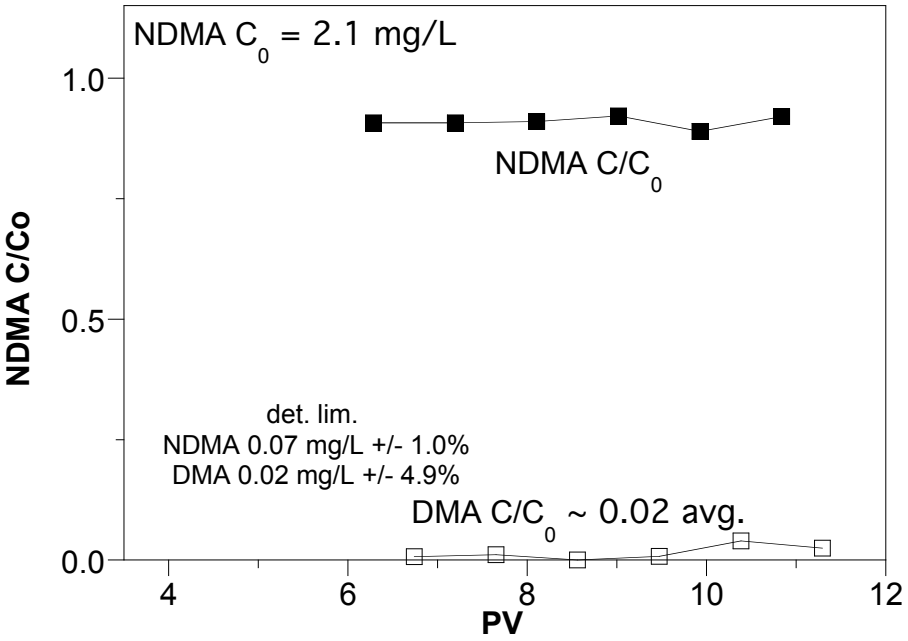

W97; NDMA deg. by red. Ft. Lewis, 33.3 h/PV

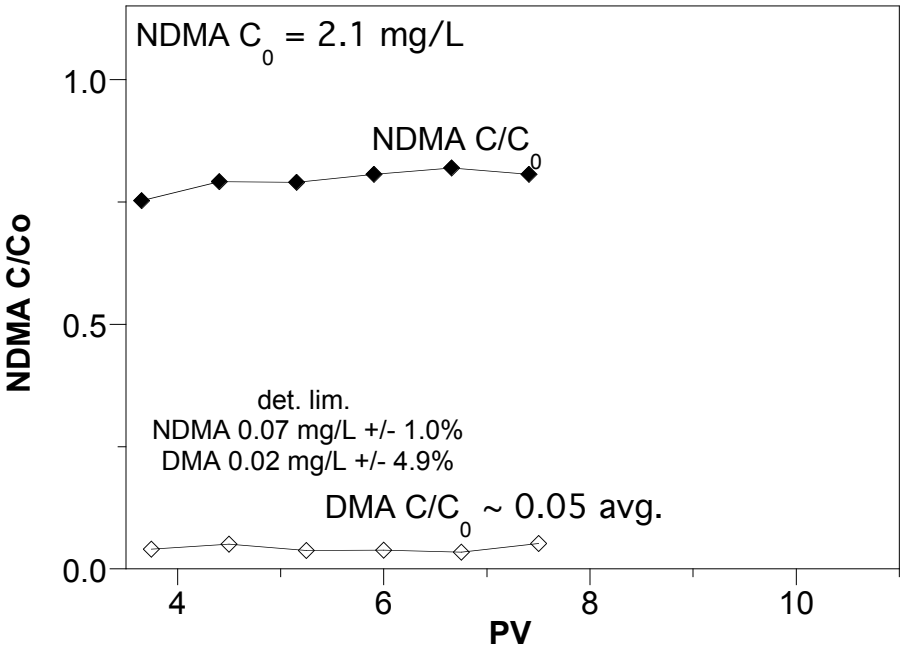

W98; NDMA deg. by red. Ft. Lewis, 67.0 h/PV

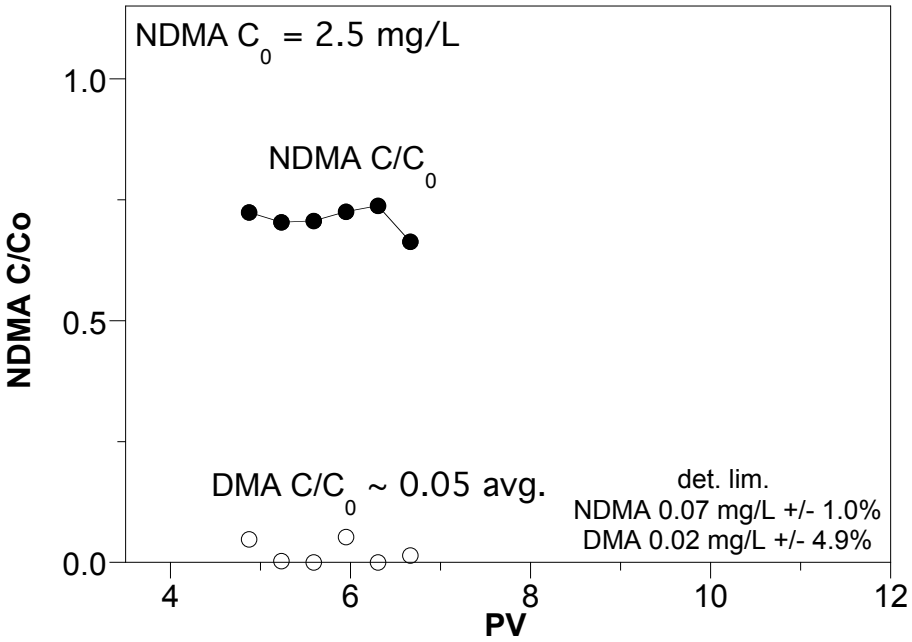

W99; NDMA deg. by red. Ft. Lewis, 147 h/PV

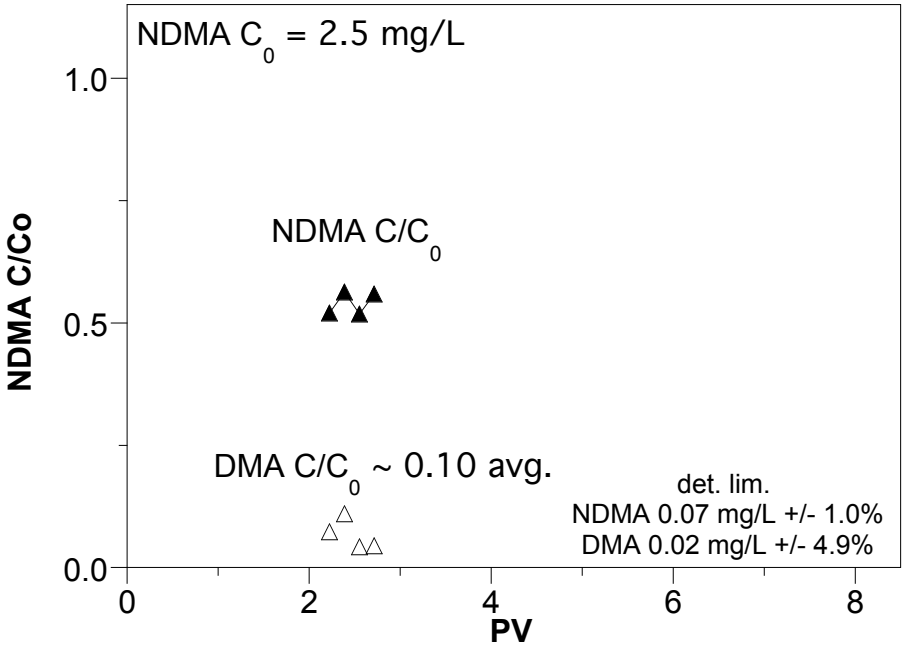

W96-99; NDMA => DMA degradation by Red. Ft. Lewis durring 1-D flow

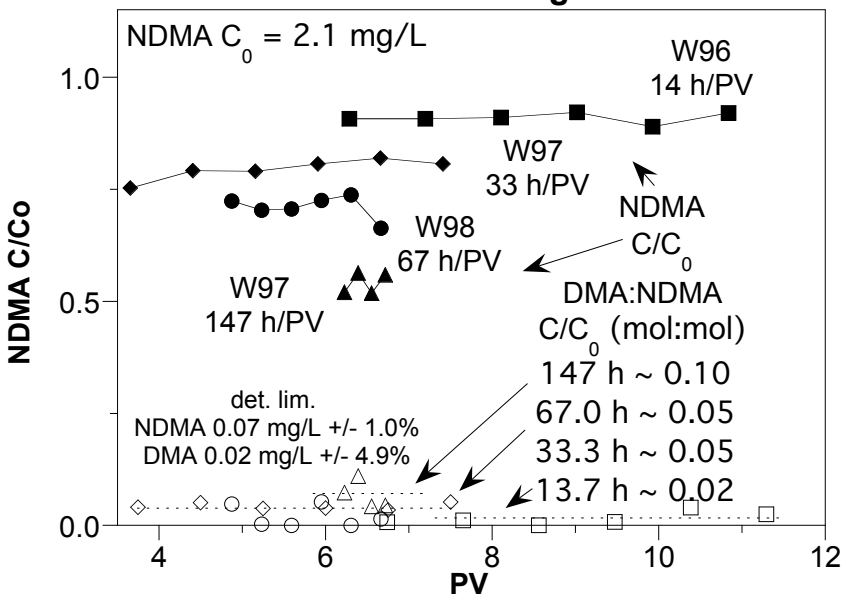

W108: Dissolved O_2 Breakthrough, Probe 2

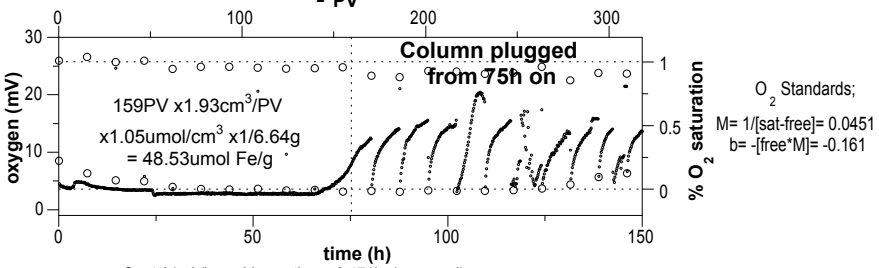

O_2 Standards;
M= 1/[sat-free]= 0.0451
b= -[free*M]= -0.161

Q= 4.01mL/h; residence time= 0.471h (assumed)
column: 0.765 cm dia.x 10.0 cm length

XC = 0.460cm^2 vol = 4.60cm^3

ρ_b = 1.443 g/cm^3,θ= 0.420 cm^3/cm^3

W108-109 were reduced in series from a newly opened and mixed jar of dithionite originally aquired in 2004. W108 was the front-half of the reduction.

W109: Dissolved O_2 Breakthrough, Probe 2

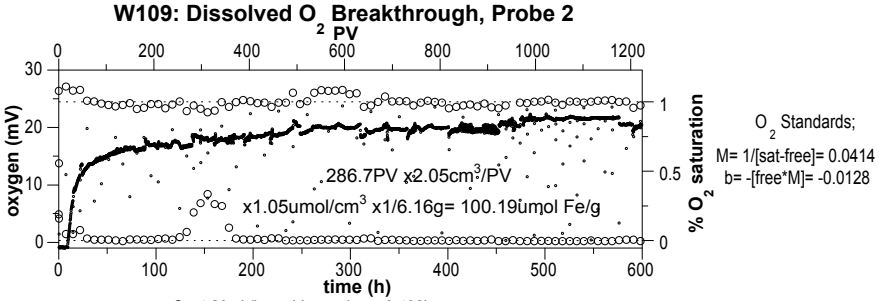

O_2 Standards;
M= 1/[sat-free]= 0.0414
b= -[free*M]= -0.0128

Q= 4.20mL/h; residence time= 0.498h
column: 0.765 cm dia.x 10.0 cm length

XC = 0.460cm^2 vol = 4.60cm^3

ρ_b = 1.339 g/cm^3,θ= 0.446 cm^3/cm^3

W108-109 were reduced in series from a newly opened and mixed jar of dithionite originally aquired in 2004. W109 was the back-half of the reduction.

W100; NDMA deg. by red. Ft. Lewis (2*Di/Fe = 12), 15.0 h/PV

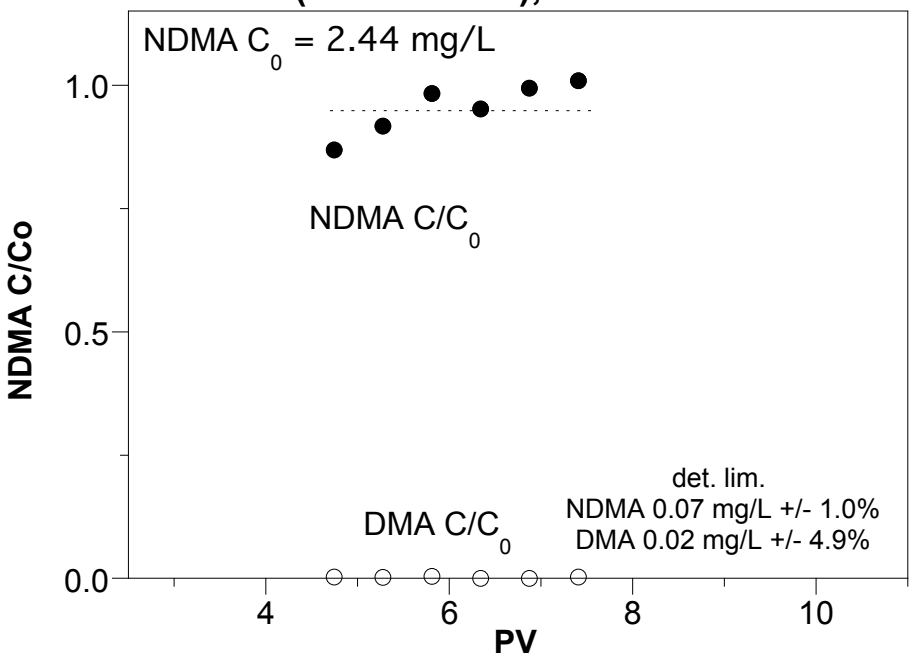

W101; NDMA deg. by red. Ft. Lewis (2*Di/Fe = 12), 66.8 h/PV

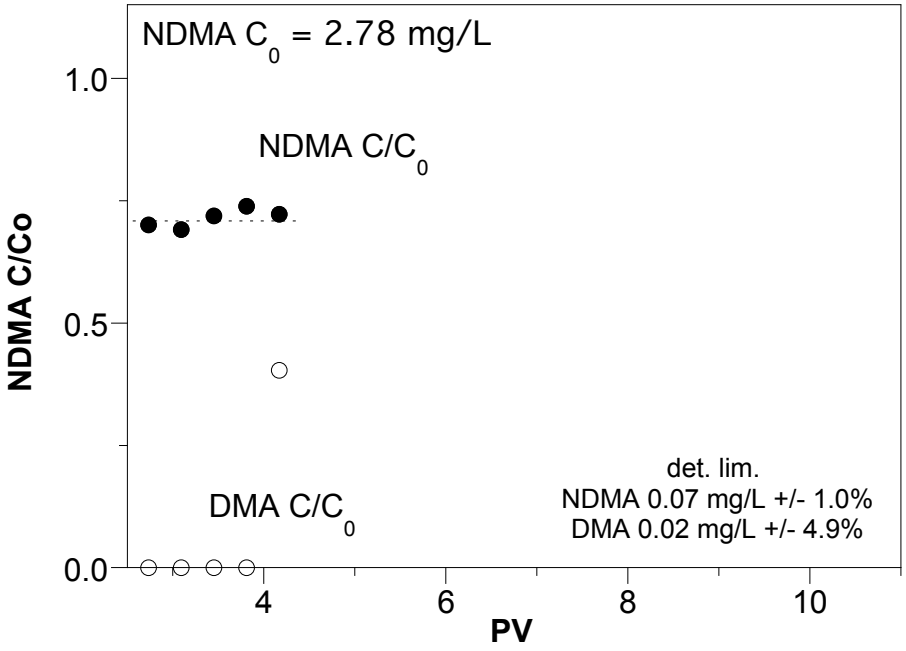

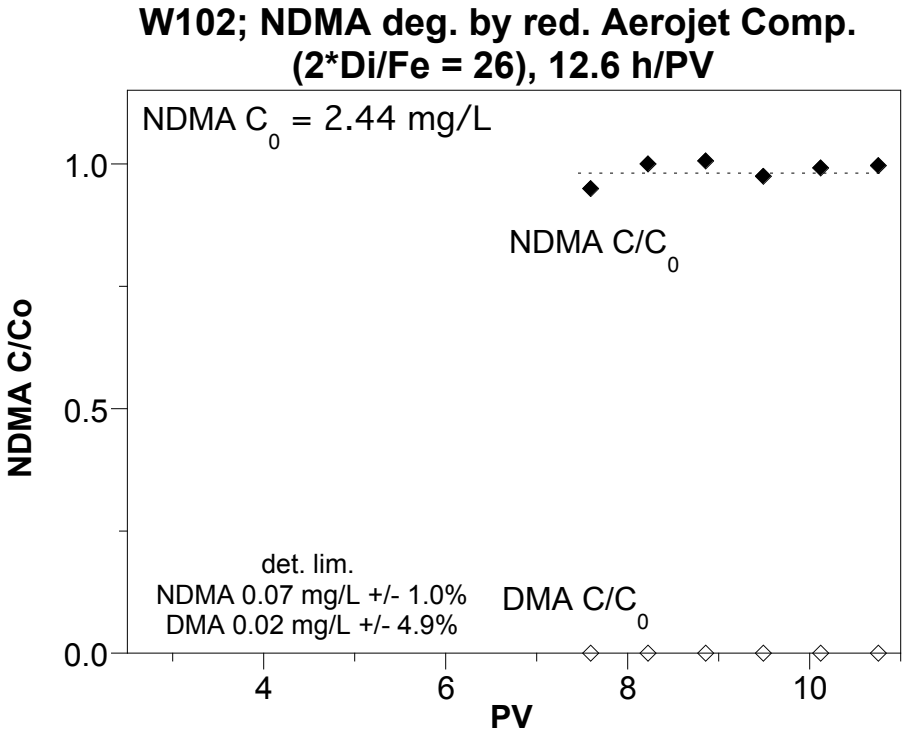
W102; NDMA deg. by red. Aerojet Comp.
(2*Di/Fe = 26), 12.6 h/PV
NDMA C0 = 2.44 mg/L
NDMA C/C0
DMA C/C0
det. lim.
NDMA 0.07 mg/L +/- 1.0%
DMA 0.02 mg/L +/- 4.9%
NDMA C/Co
PV
1.0
0.5
0.0
4
6
8
10

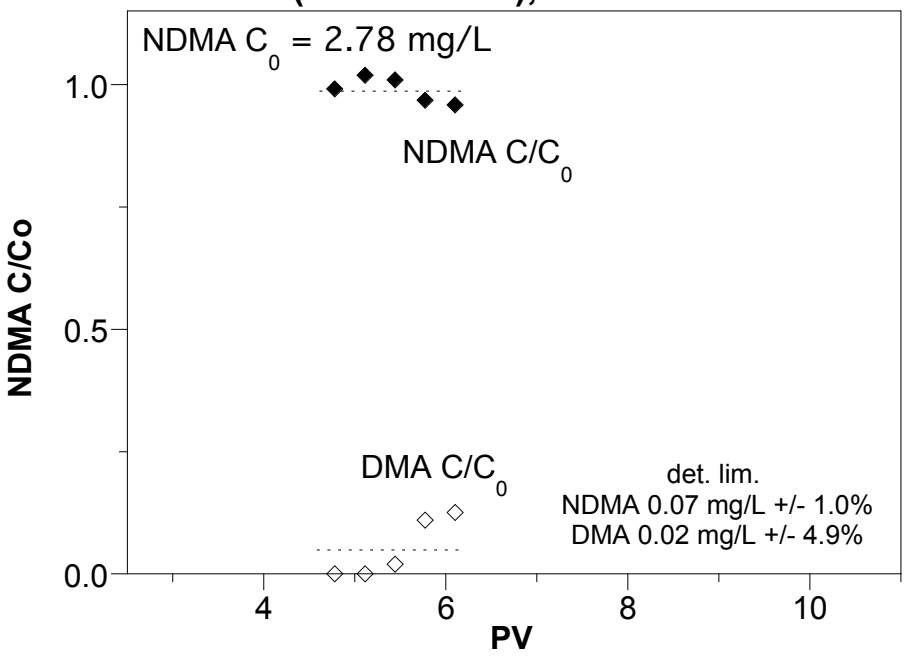
W103; NDMA deg. by red. Aerojet Comp.
(2*Di/Fe = 26), 72.6 h/PV
NDMA C0 = 2.78 mg/L
NDMA C/C0
DMA C/C0
det. lim.
NDMA 0.07 mg/L +/- 1.0%
DMA 0.02 mg/L +/- 4.9%
NDMA C/Co
PV
1.0
0.5
0.0
4
6
8
10

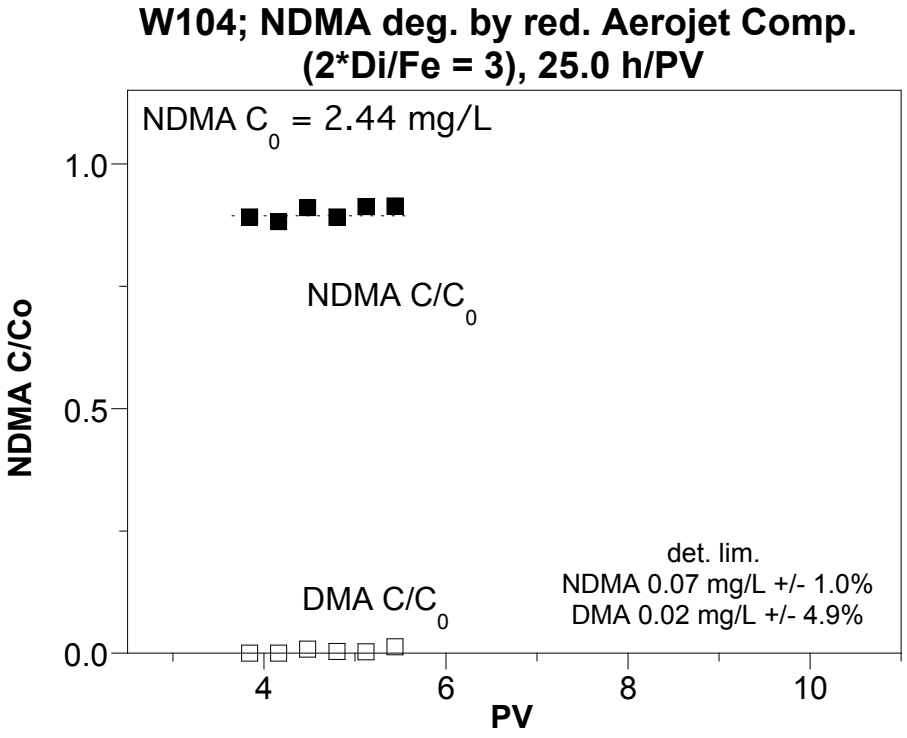
W104; NDMA deg. by red. Aerojet Comp.
(2*Di/Fe = 3), 25.0 h/PV
NDMA C0 = 2.44 mg/L
NDMA C/C0
DMA C/C0
det. lim.
NDMA 0.07 mg/L +/- 1.0%
DMA 0.02 mg/L +/- 4.9%
NDMA C/Co
PV
1.0
0.5
0.0
4
6
8
10

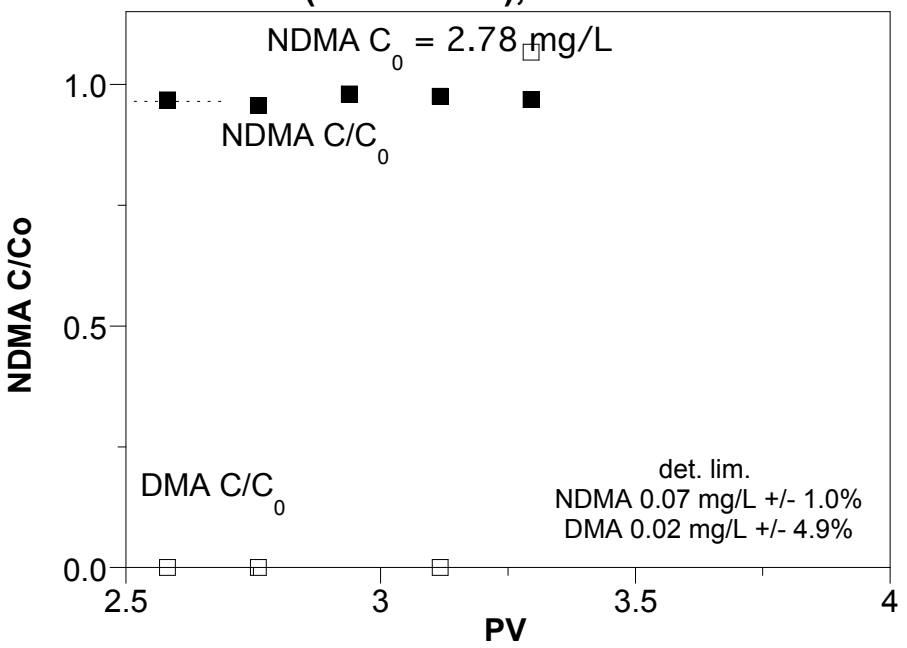
W105; NDMA deg. by red. Aerojet Comp.
(2*Di/Fe = 3), 134 h/PV
NDMA C0 = 2.78 mg/L
NDMA C/C0
DMA C/C0
det. lim.
NDMA 0.07 mg/L +/- 1.0%
DMA 0.02 mg/L +/- 4.9%
NDMA C/Co
PV
1.0
0.5
0.0
2.5
3
3.5
4

W106; NDMA deg. by red. Aerojet Comp. (2*Di/Fe = 0.4), 14.1 h/PV

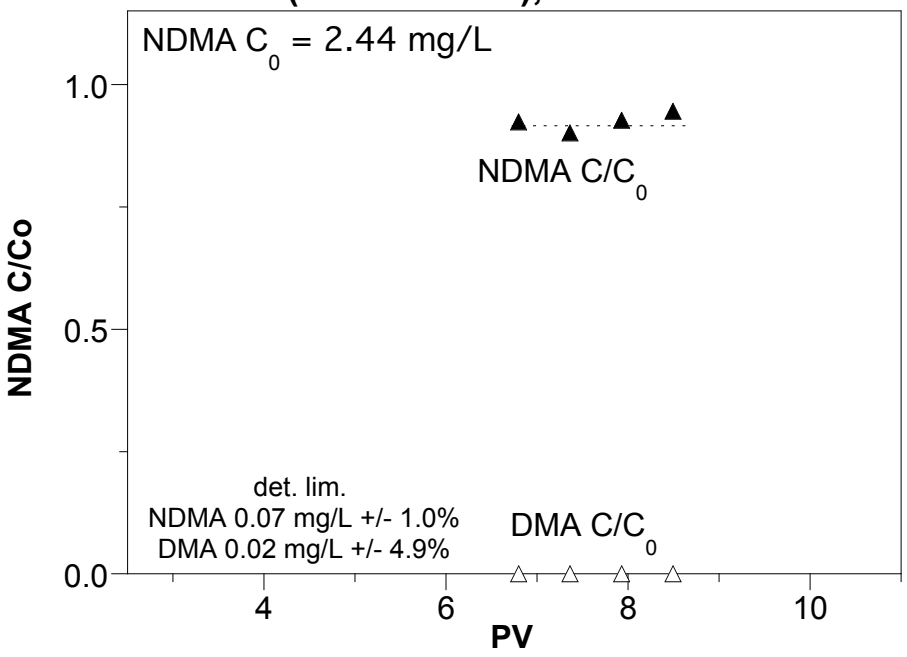

W107; NDMA deg. by red. Aerojet Comp. (2*Di/Fe = 0.4), 73.9 h/PV

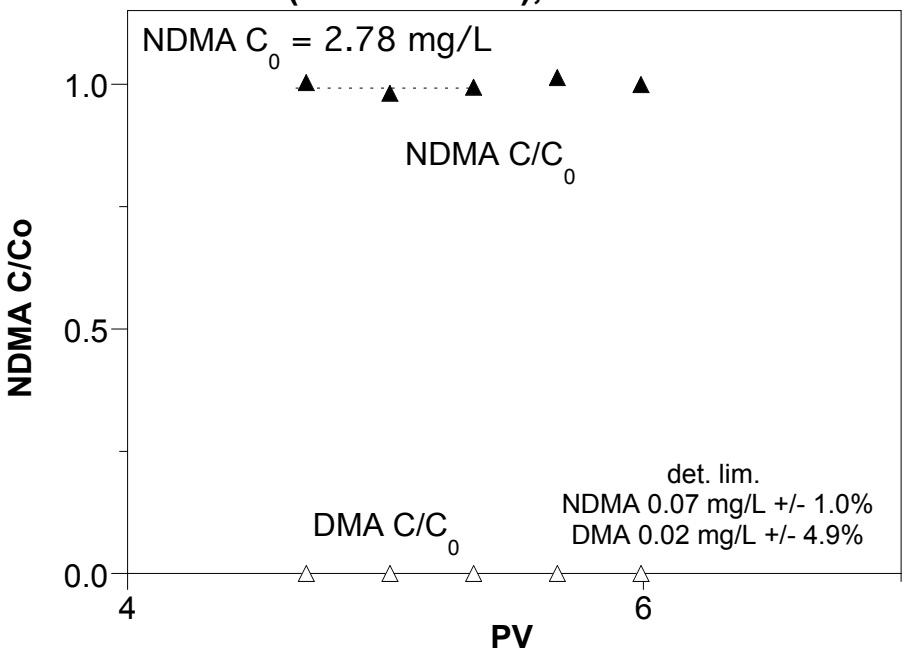

Appendix A.10 Task 1.10 NDMA and DMA HPLC calibrations and detection limits

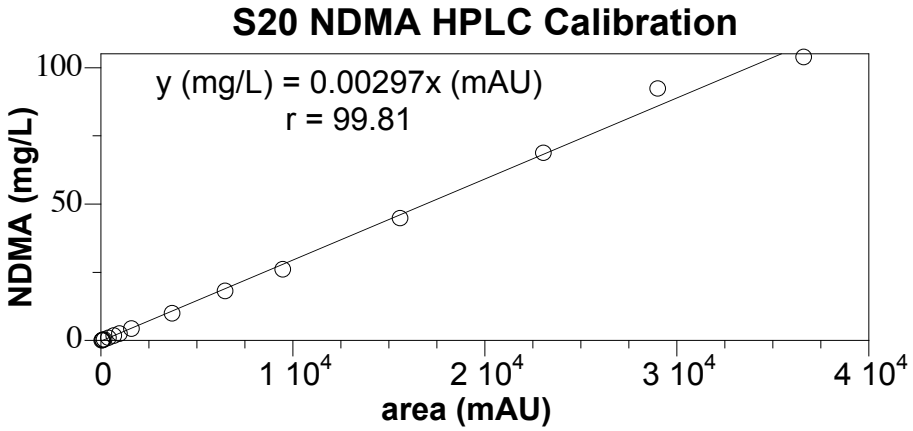

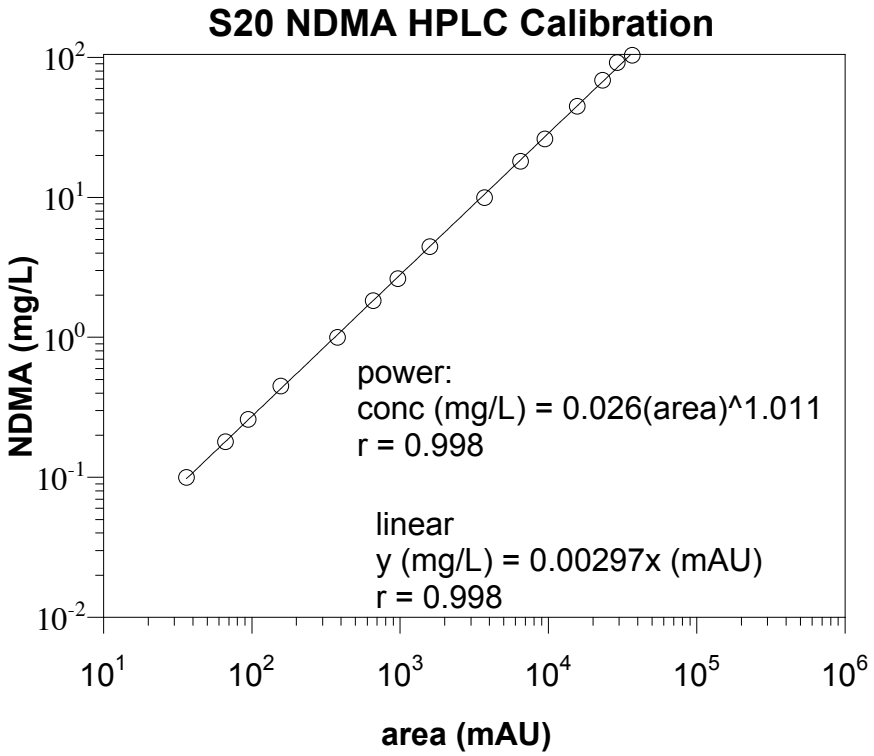

W95; HPLC Cal. for NDMA from stock ampule (5000 mg/L in MeOH)

1.0 mg/L NDMA => 0.6 mg/L DMA (complete deg.)

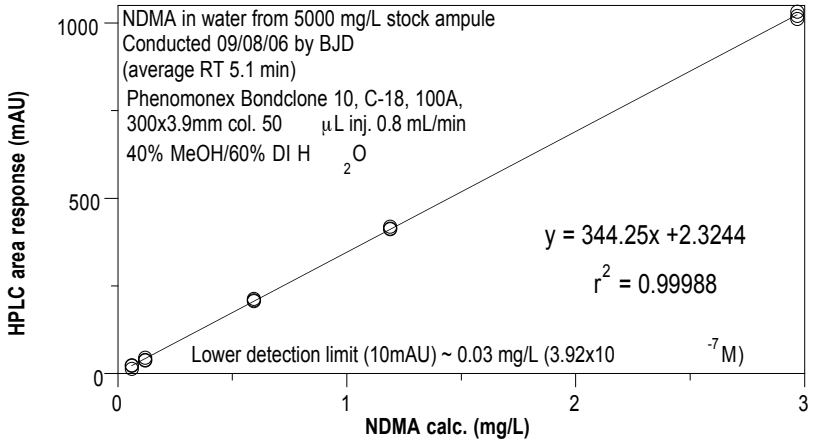

NDMA (mg/L)	HPLC area
2.967	1012
2.967	1033
2.967	1021
1.189	419
1.189	414
1.189	412
0.593	207
0.593	209
0.593	213
0.118	39
0.118	38
0.118	46
0.06	14
0.06	24

W93A; HPLC Cal. for DMA from 2.0M stock (90160 mg/L in water)

not accurate - DNFB peak interfering with DMA peak

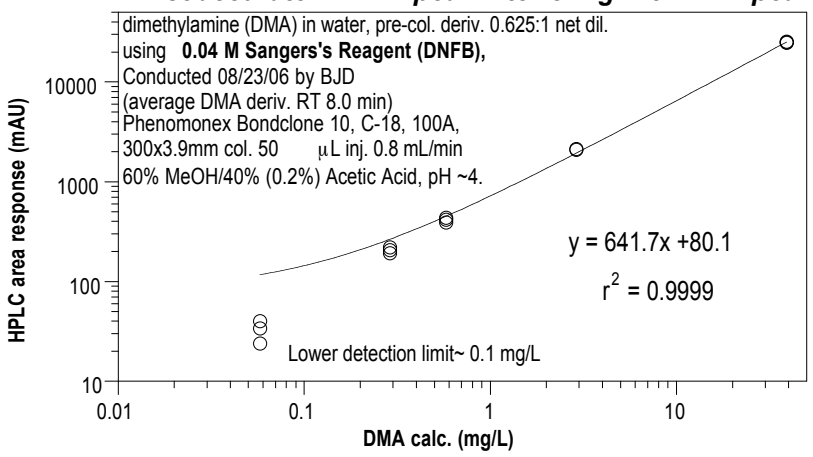

DMA (mg/L)	HPLC area
0.06	24
0.06	34
0.06	40
0.29	207
0.29	193
0.29	220
0.58	418
0.58	392
0.58	437
2.88	2105
2.88	2126
2.88	2134
38.99	24811
38.99	25093
38.99	25365

W94; HPLC Cal. for DMA from 2.0M stock (90160 mg/L in water) 0-2.5 mg/L

DNFB:DMA (mol:mol) >50

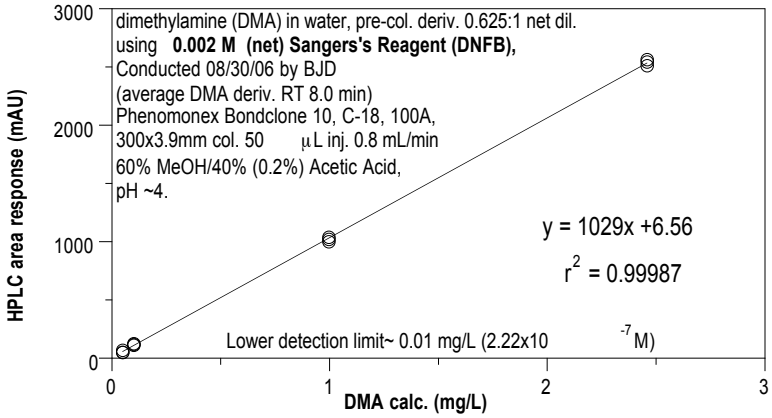

DMA (mg/L)	HPLC area
0.06	51
0.06	68
0.06	50
0.29	111
0.29	119
0.29	124
0.58	1001
0.58	1022
0.58	1040
2.88	2512
2.88	2564
2.88	2543

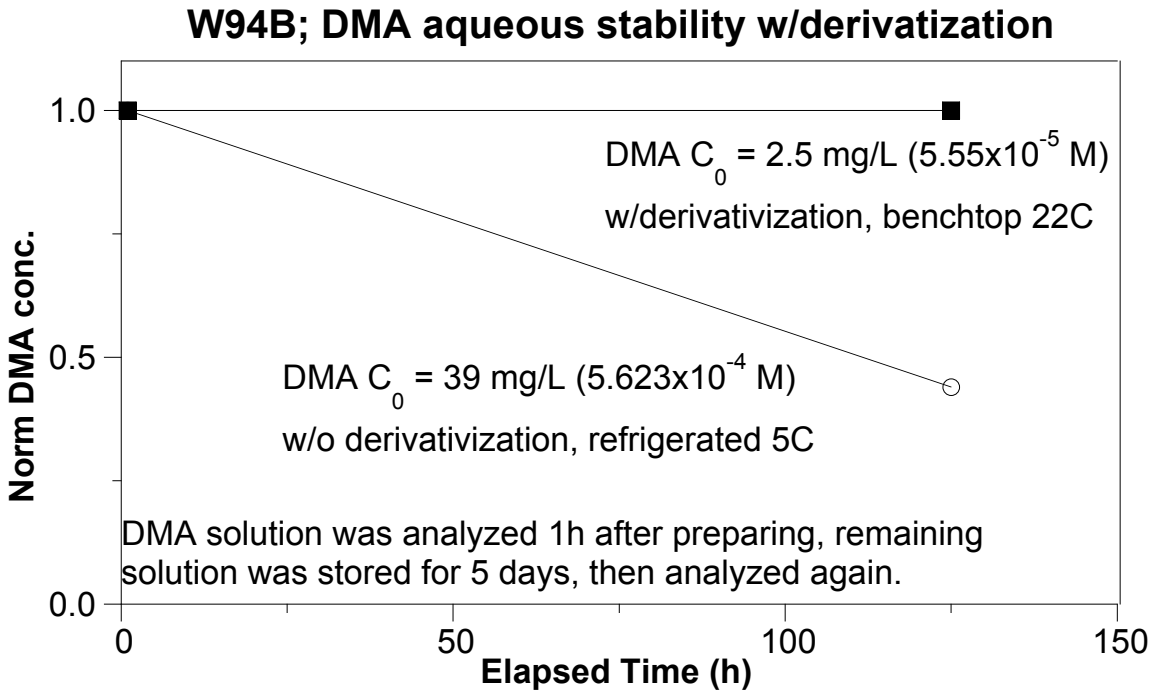
W94B; DMA aqueous stability w/derivatization
Norm DMA conc.
1.0
0.5
0.0
0
50
100
150
Elapsed Time (h)
DMA C0 = 2.5 mg/L (5.55x10-5 M)
w/derivativization, benchtop 22C
DMA C0 = 39 mg/L (5.623x10-4 M)
w/o derivativization, refrigerated 5C
DMA solution was analyzed 1h after preparing, remaining solution was stored for 5 days, then analyzed again.

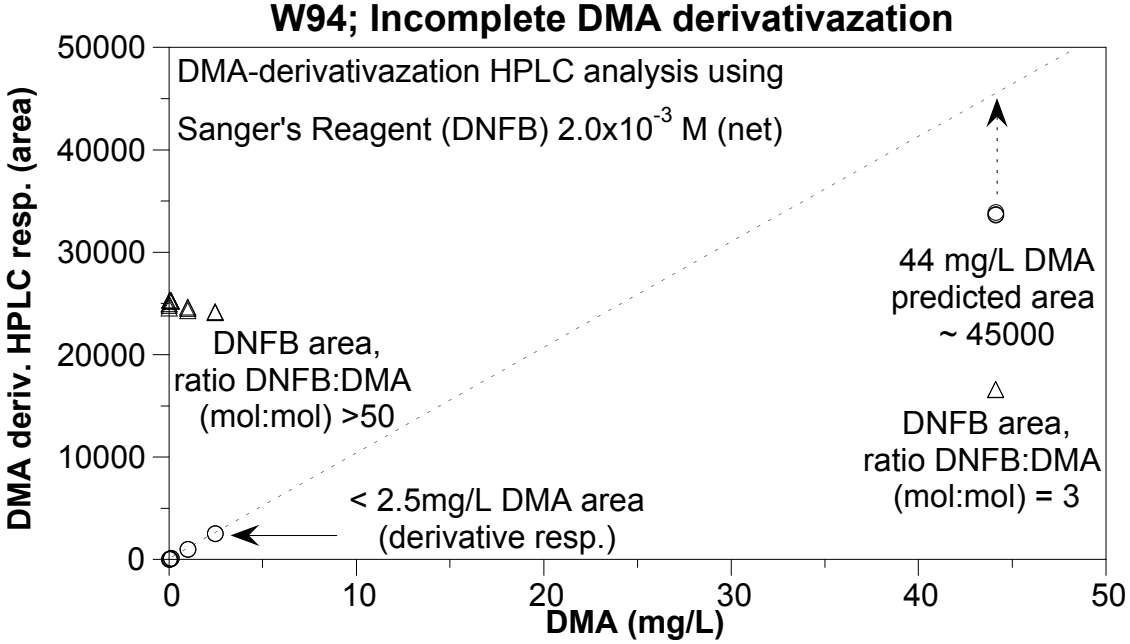
W94; Incomplete DMA derivativazation
DMA deriv. HPLC resp. (area)
50000
40000
30000
20000
10000
0
0
10
20
30
40
50
DMA (mg/L)
DMA-derivativazation HPLC analysis using
Sanger's Reagent (DNFB) 2.0x10-3 M (net)
DNFB area,
ratio DNFB:DMA
(mol:mol) >50
< 2.5mg/L DMA area
(derivative resp.)
44 mg/L DMA
predicted area
~ 45000
DNFB area,
ratio DNFB:DMA
(mol:mol) = 3

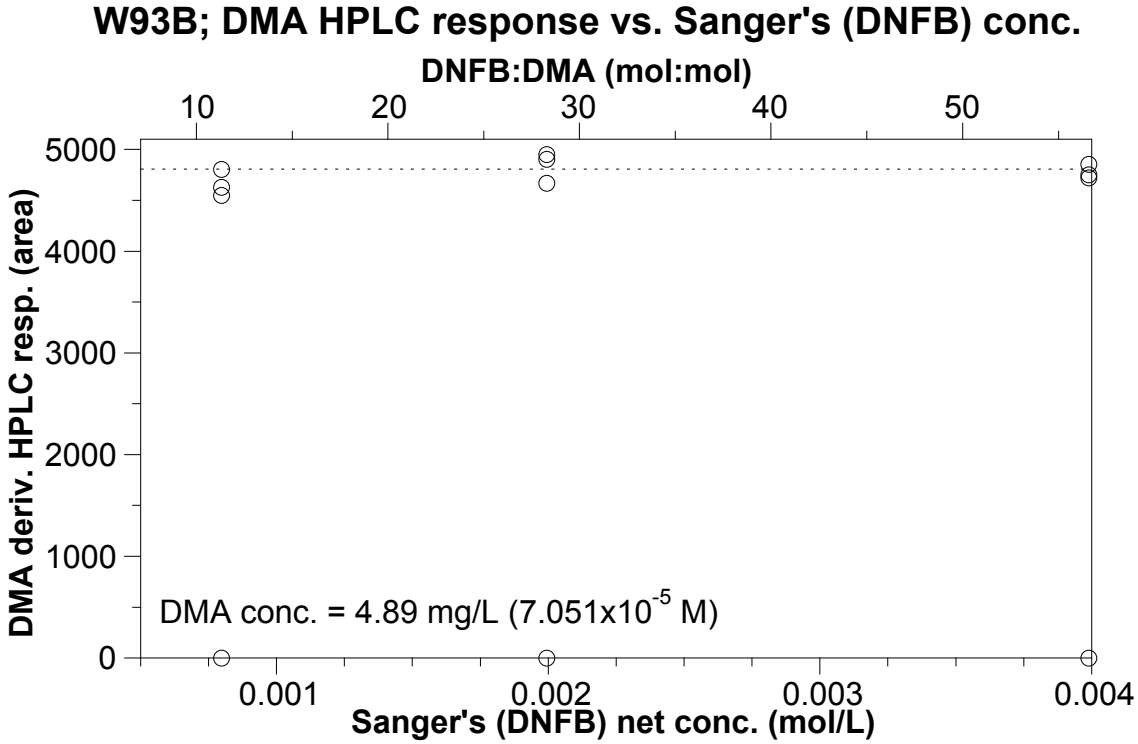
W93B; DMA HPLC response vs. Sanger's (DNFB) conc.
DNFB:DMA (mol:mol)
10
20
30
40
50
5000
4000
3000
2000
1000
0
DMA deriv. HPLC resp. (area)
DMA conc. = 4.89 mg/L (7.051x10-5 M)
0.001
0.002
0.003
0.004
Sanger's (DNFB) net conc. (mol/L)

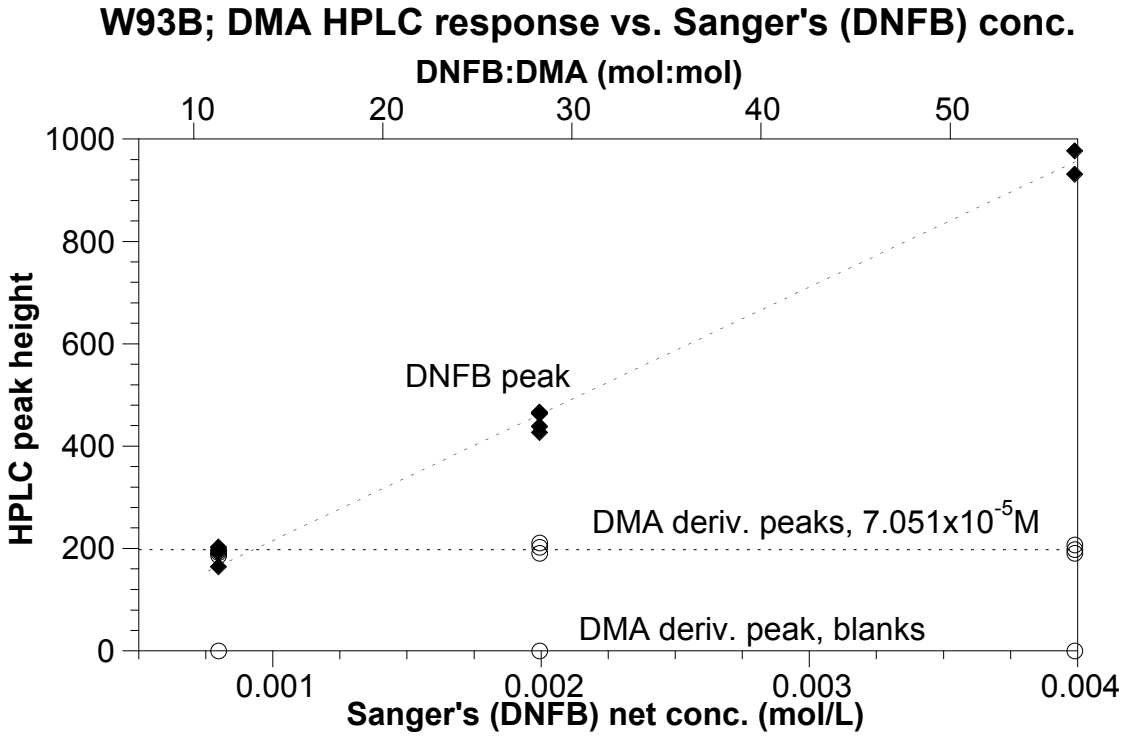
W93B; DMA HPLC response vs. Sanger's (DNFB) conc.
DNFB:DMA (mol:mol)
10
20
30
40
50
1000
800
600
400
200
0
HPLC peak height
DNFB peak
DMA deriv. peaks, 7.051x10-5M
DMA deriv. peak, blanks
0.001
0.002
0.003
0.004
Sanger's (DNFB) net conc. (mol/L)

W93A; HPLC Cal. for DMA from 2.0M stock (90160 mg/L in water)
not accurate - DNFB peak interfering with DMA peak

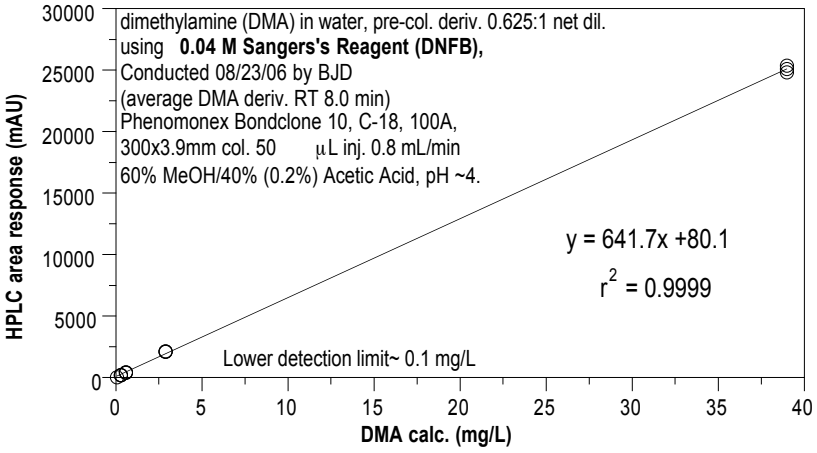

DMA (mg/L)	HPLC area
0.06	24
0.06	34
0.06	40
0.29	207
0.29	193
0.29	220
0.58	418
0.58	392
0.58	437
2.88	2105
2.88	2126
2.88	2134
38.99	24811
38.99	25093
38.99	25365

W93A; HPLC Cal. for DMA from 2.0M stock (90160 mg/L in water)
not accurate - DNFB peak interfering with DMA peak

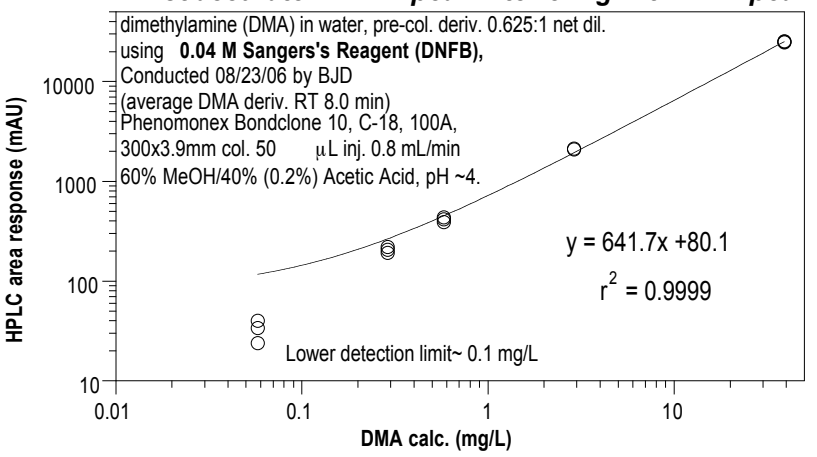

DMA (mg/L)	HPLC area
0.06	24
0.06	34
0.06	40
0.29	207
0.29	193
0.29	220
0.58	418
0.58	392
0.58	437
2.88	2105
2.88	2126
2.88	2134
38.99	24811
38.99	25093
38.99	25365

W93A; DMA vs. Sanger's Reagent (DNFB) relative HPLC response
not accurate - DNFB peak interfering with DMA peak

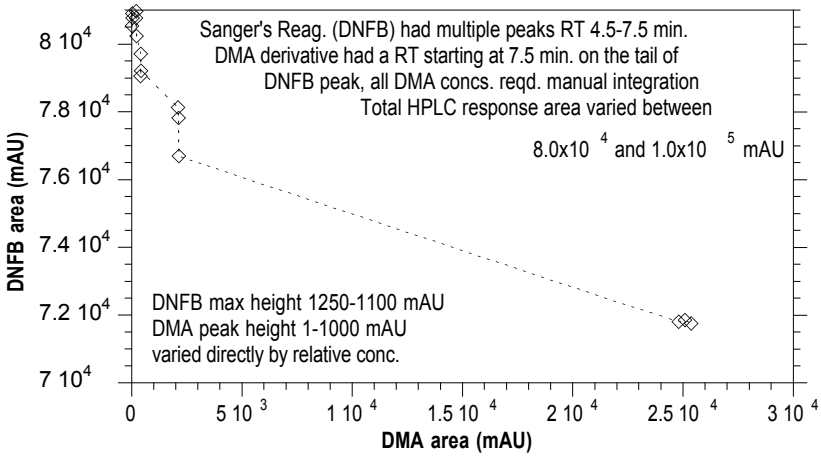

DMA (area)	DNFB (area)
24	80535
34	80903
40	80769
207	80968
193	80764
220	80232
418	79710
392	79052
437	79216
2105	78122
2126	77820
2134	76694
24811	71800
25093	71852
25365	71756

S126: NDMA in 40 mL C18 Column, 25% MeOH

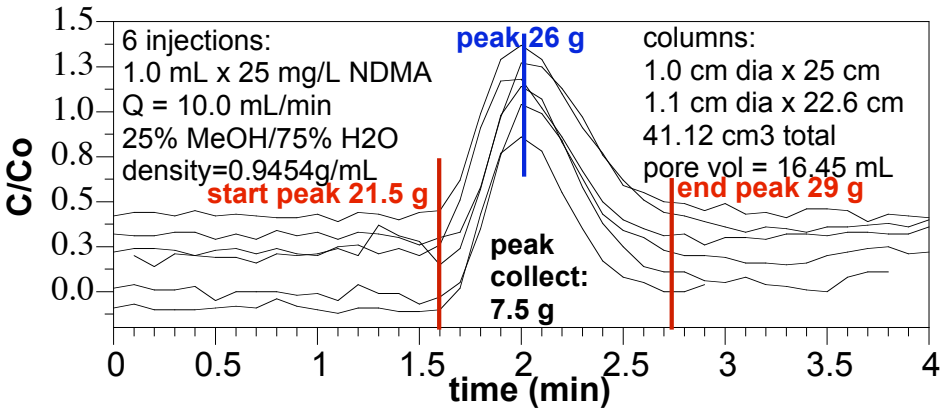

S126: NDMA in 40 mL C18 Column, 12% MeOH

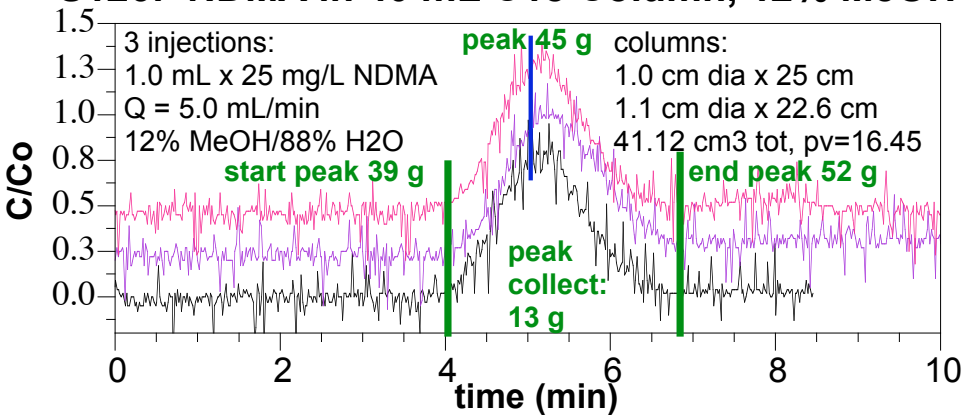

Appendix A.11 Task 2.1 NDMA Mineralization in Oxic/Anoxic Sediment

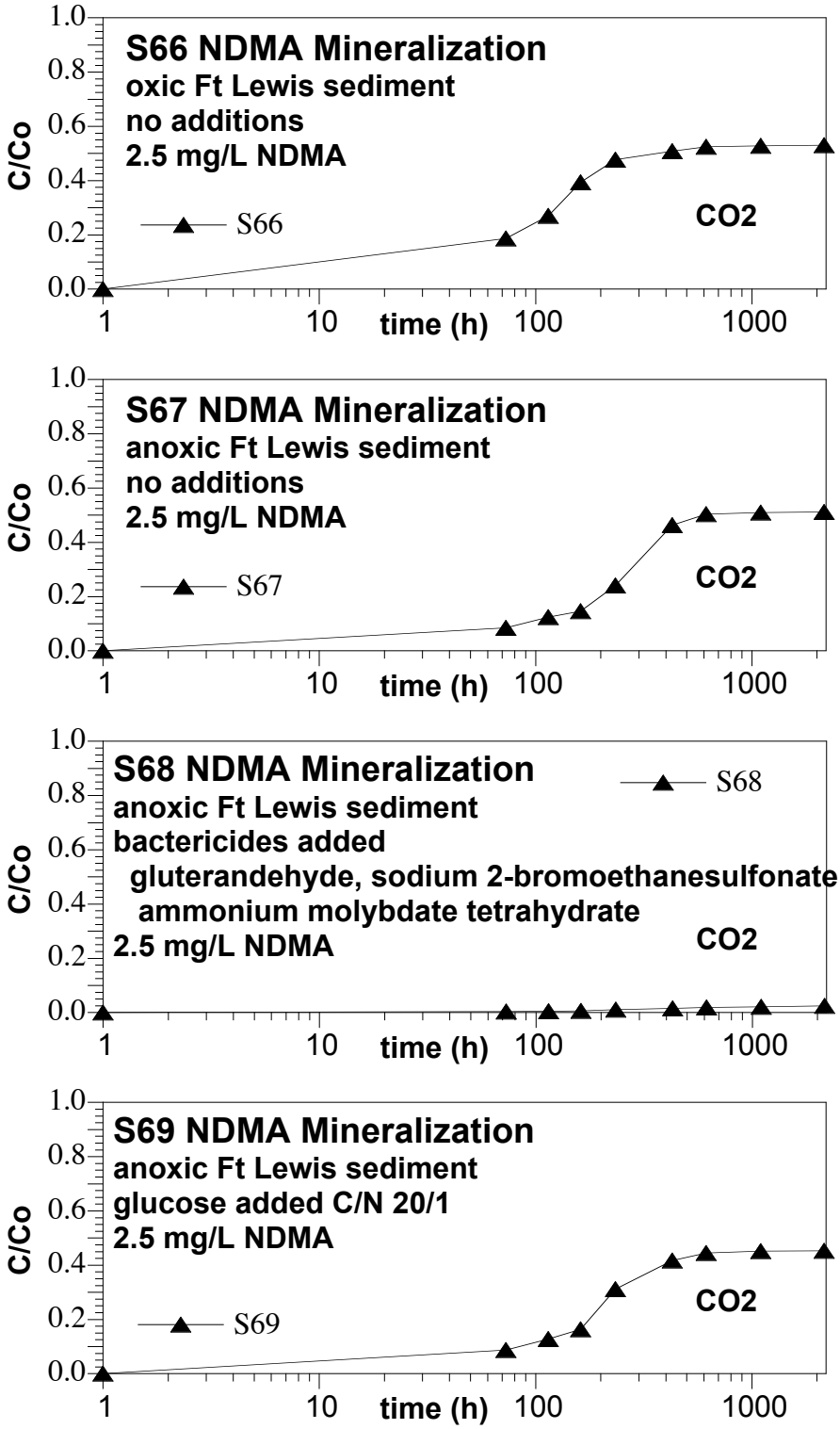

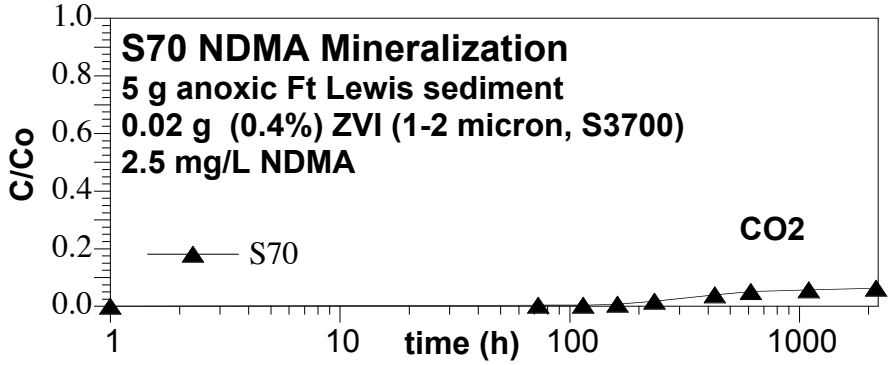
S70 NDMA Mineralization
5 g anoxic Ft Lewis sediment
0.02 g (0.4%) ZVI (1-2 micron, S3700)
2.5 mg/L NDMA
S70
CO2
C/Co
time (h)
1.0
0.8
0.6
0.4
0.2
0.0
1
10
100
1000

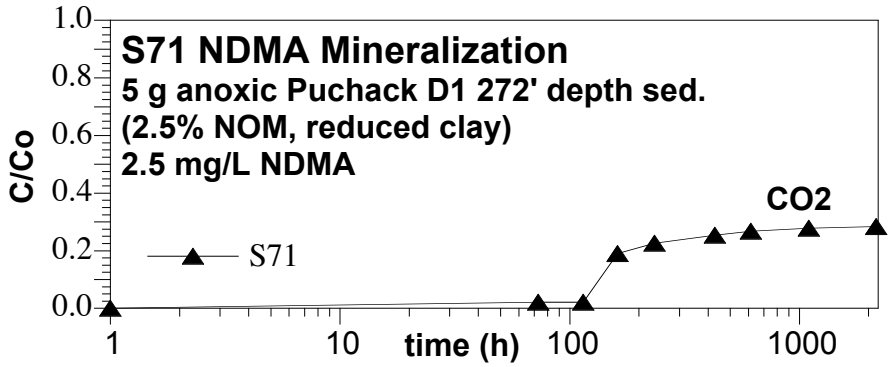
S71 NDMA Mineralization
5 g anoxic Puchack D1 272' depth sed.
(2.5% NOM, reduced clay)
2.5 mg/L NDMA
S71
CO2
C/Co
time (h)
1.0
0.8
0.6
0.4
0.2
0.0
1
10
100
1000

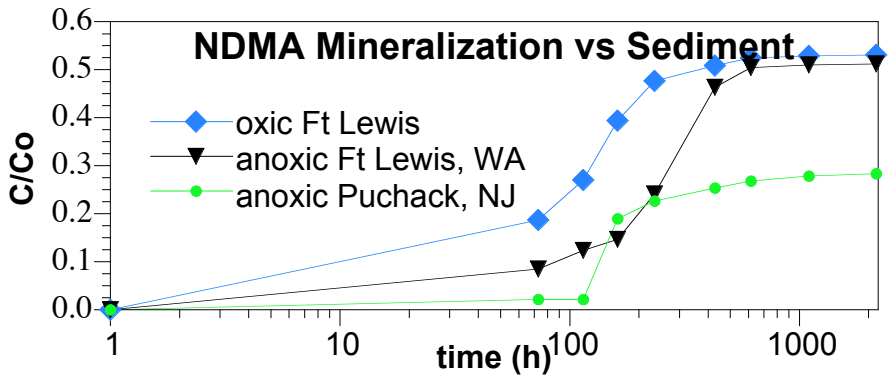
NDMA Mineralization vs Sediment
oxic Ft Lewis
anoxic Ft Lewis, WA
anoxic Puchack, NJ
C/Co
time (h)
0.6
0.5
0.4
0.3
0.2
0.1
0.0
1
10
100
1000

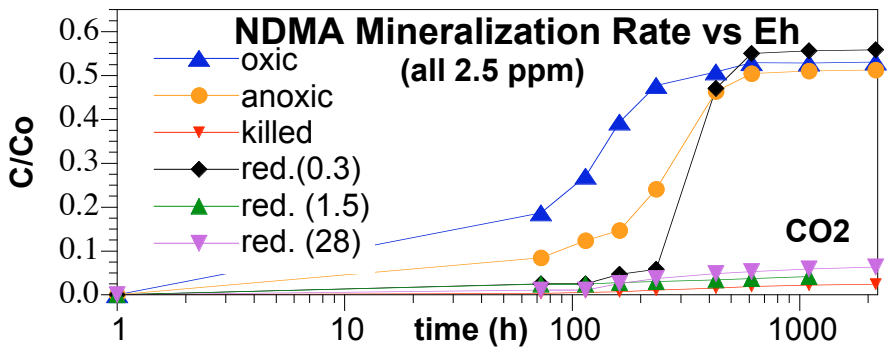
NDMA Mineralization Rate vs Eh
(all 2.5 ppm)
oxic
anoxic
killed
red.(0.3)
red. (1.5)
red. (28)
CO2
C/Co
time (h)
0.6
0.5
0.4
0.3
0.2
0.1
0.0
1
10
100
1000

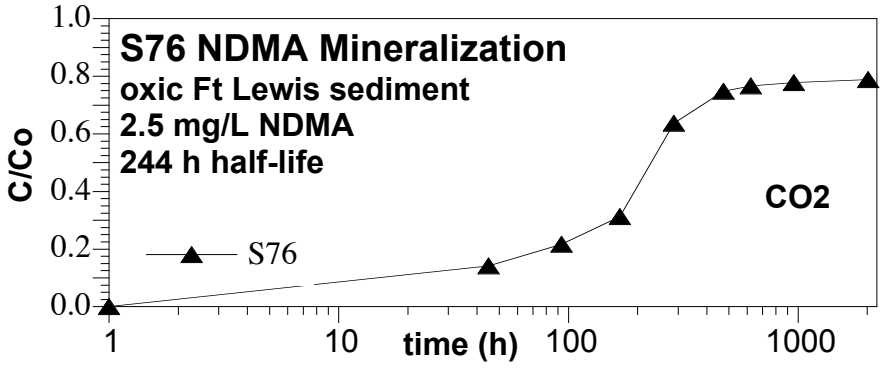
S76 NDMA Mineralization
oxic Ft Lewis sediment
2.5 mg/L NDMA
244 h half-life
CO2
S76
C/Co
time (h)
1.0
0.8
0.6
0.4
0.2
0.0
1
10
100
1000

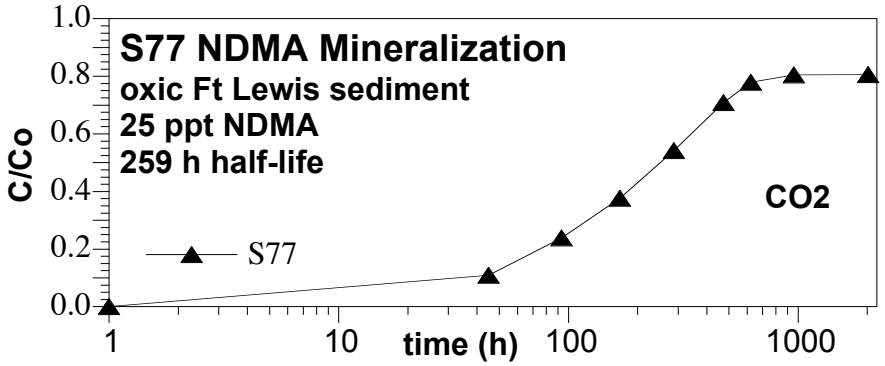
S77 NDMA Mineralization
oxic Ft Lewis sediment
25 ppt NDMA
259 h half-life
CO2
S77
C/Co
time (h)
1.0
0.8
0.6
0.4
0.2
0.0
1
10
100
1000

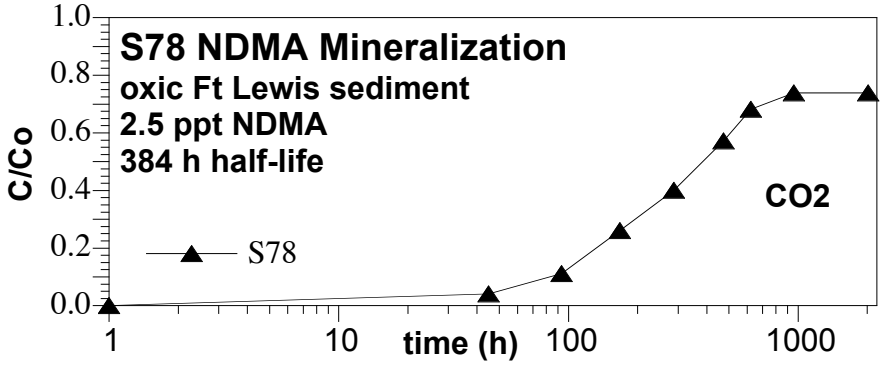
S78 NDMA Mineralization
oxic Ft Lewis sediment
2.5 ppt NDMA
384 h half-life
CO2
S78
C/Co
time (h)
1.0
0.8
0.6
0.4
0.2
0.0
1
10
100
1000

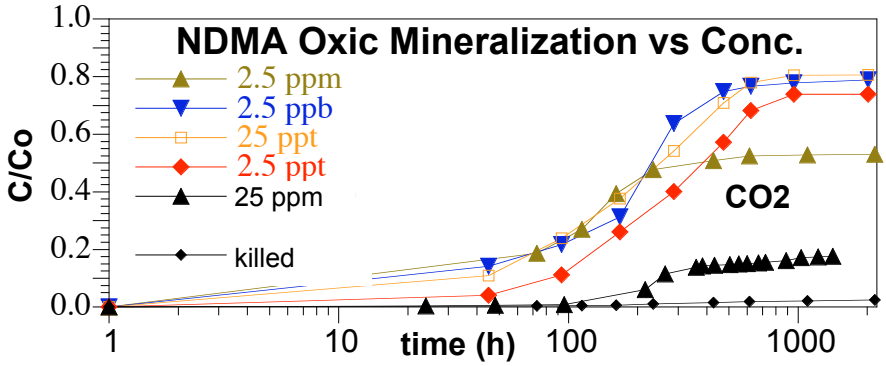
NDMA Oxic Mineralization vs Conc.
2.5 ppm
2.5 ppb
25 ppt
2.5 ppt
25 ppm
killed
CO2
C/Co
time (h)
1.0
0.8
0.6
0.4
0.2
0.0
1
10
100
1000

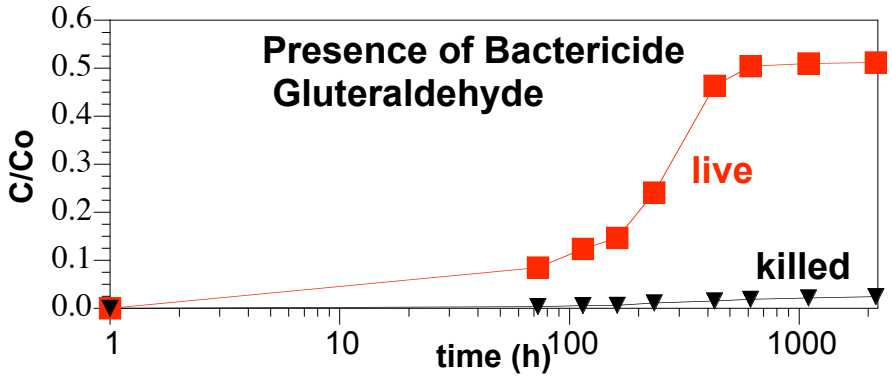
Presence of Bactericide
Gluteraldehyde
live
killed
C/Co
time (h)
0.6
0.5
0.4
0.3
0.2
0.1
0.0
1
10
100
1000

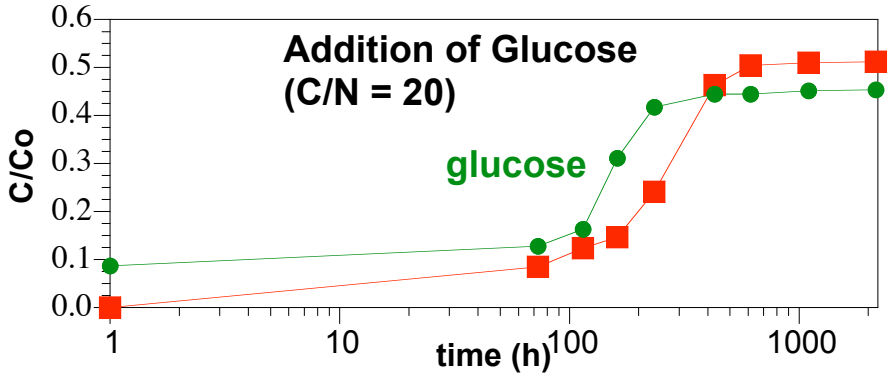
Addition of Glucose
(C/N = 20)
glucose
C/Co
time (h)
0.6
0.5
0.4
0.3
0.2
0.1
0.0
1
10
100
1000

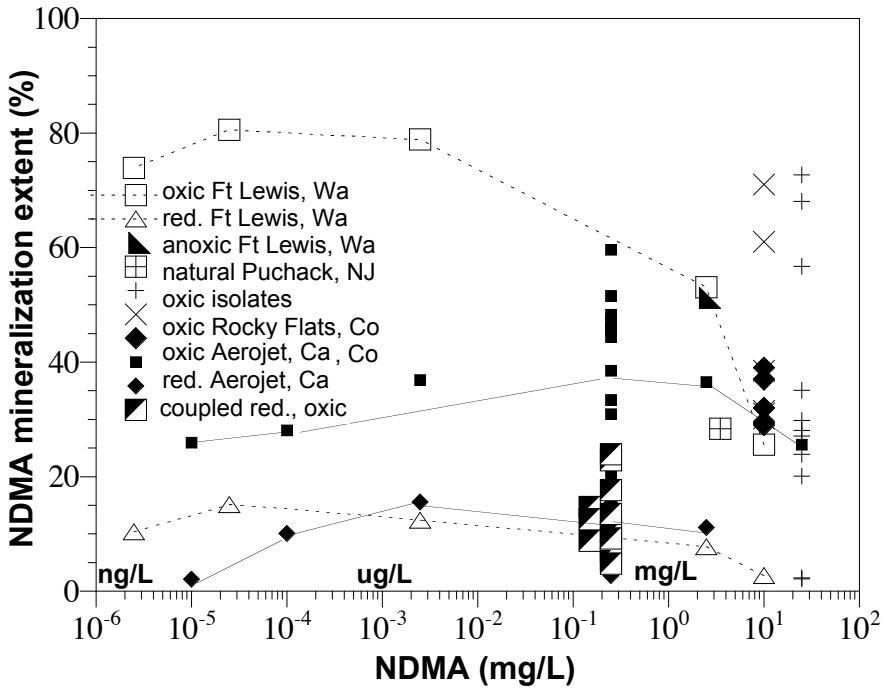
NDMA mineralization extent (%)
NDMA (mg/L)
oxic Ft Lewis, Wa
red. Ft Lewis, Wa
anoxic Ft Lewis, Wa
natural Puchack, NJ
oxic isolates
oxic Rocky Flats, Co
oxic Aerojet, Ca , Co
red. Aerojet, Ca
coupled red., oxic
ng/L
ug/L
mg/L
100
80
60
40
20
0
10^{-6}
10^{-5}
10^{-4}
10^{-3}
10^{-2}
10^{-1}
10^{0}
10^{1}
10^{2}

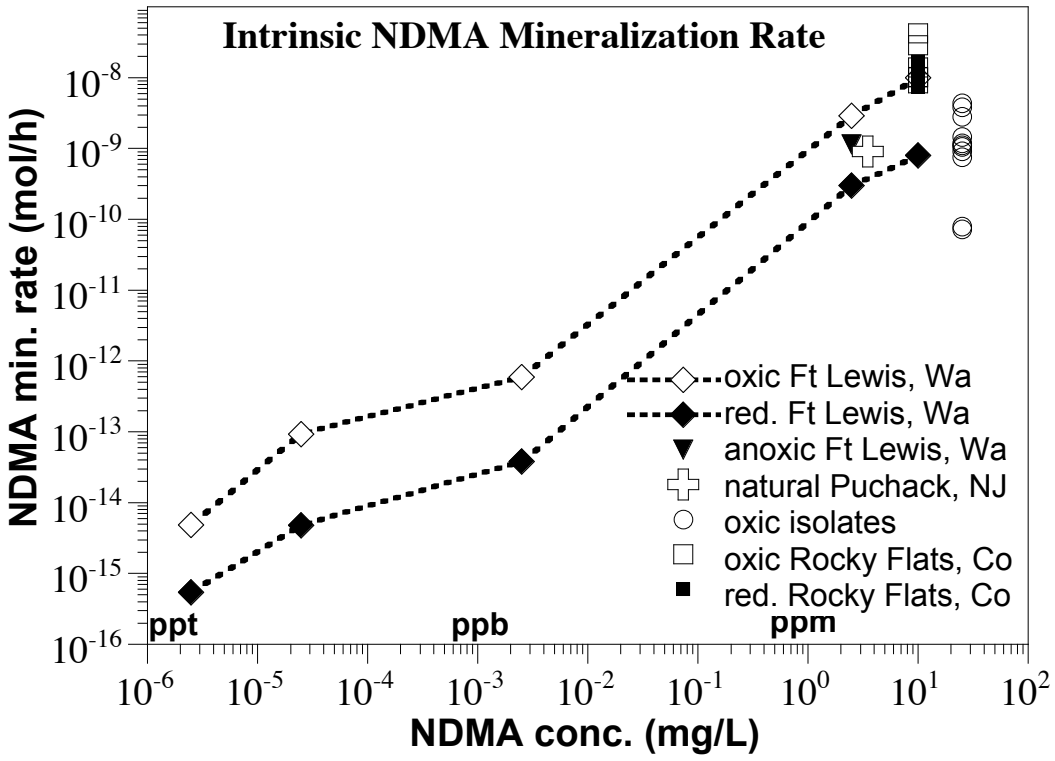
Intrinsic NDMA Mineralization Rate
NDMA min. rate (mol/h)
NDMA conc. (mg/L)
ppt
ppb
ppm
oxic Ft Lewis, Wa
red. Ft Lewis, Wa
anoxic Ft Lewis, Wa
natural Puchack, NJ
oxic isolates
oxic Rocky Flats, Co
red. Rocky Flats, Co

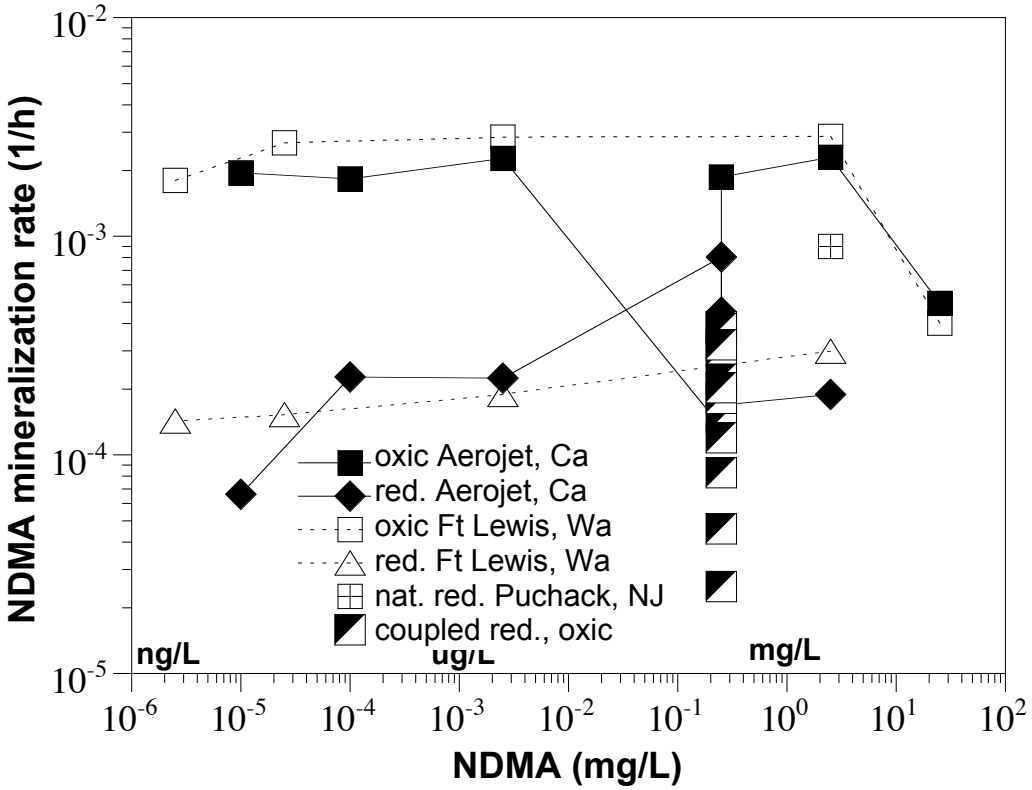
NDMA mineralization rate (1/h)
NDMA (mg/L)
ng/L
ug/L
mg/L
oxic Aerojet, Ca
red. Aerojet, Ca
oxic Ft Lewis, Wa
red. Ft Lewis, Wa
nat. red. Puchack, NJ
coupled red., oxic

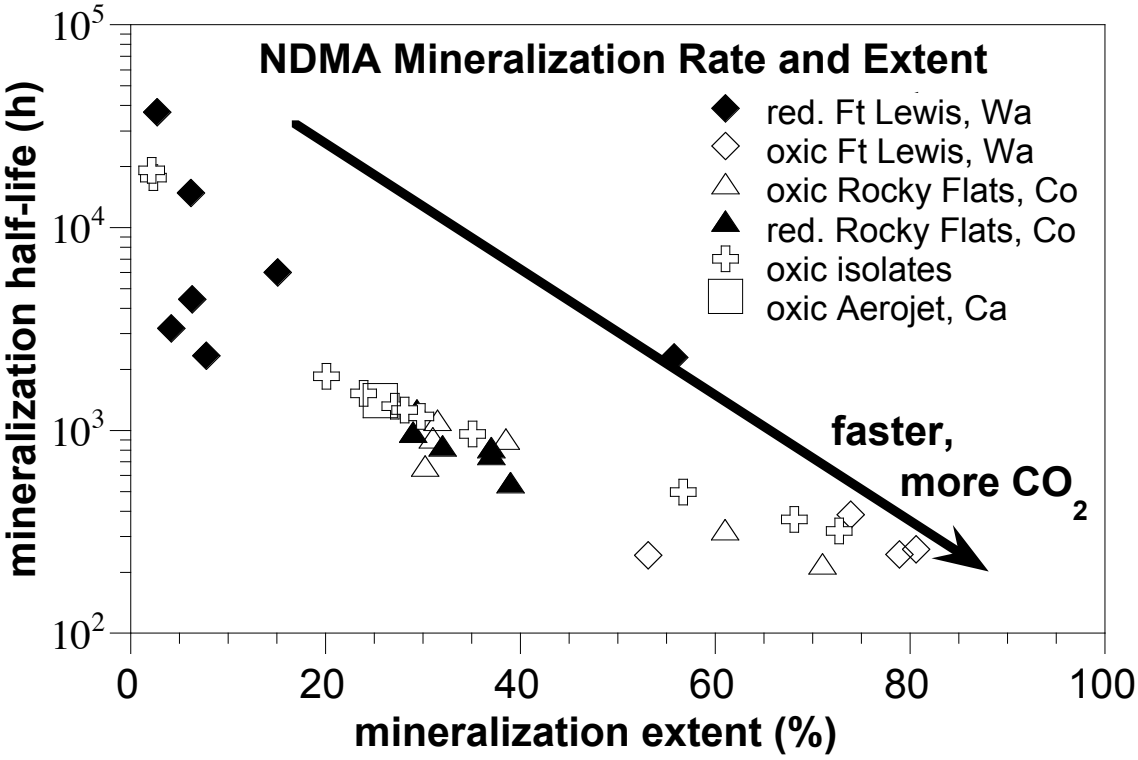
NDMA Mineralization Rate and Extent
red. Ft Lewis, Wa
oxic Ft Lewis, Wa
oxic Rocky Flats, Co
red. Rocky Flats, Co
oxic isolates
oxic Aerojet, Ca
faster,
more CO2
mineralization half-life (h)
mineralization extent (%)
10^5
10^4
10^3
10^2
0
20
40
60
80
100

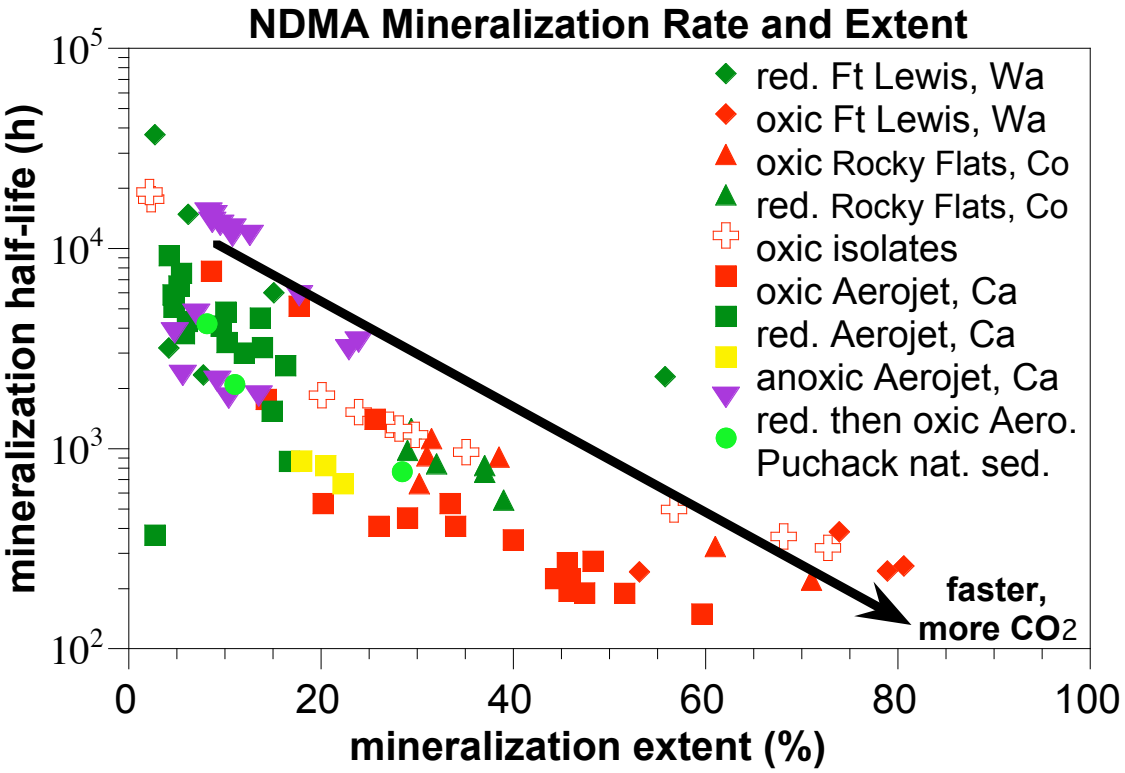
NDMA Mineralization Rate and Extent
red. Ft Lewis, Wa
oxic Ft Lewis, Wa
oxic Rocky Flats, Co
red. Rocky Flats, Co
oxic isolates
oxic Aerojet, Ca
red. Aerojet, Ca
anoxic Aerojet, Ca
red. then oxic Aero.
Puchack nat. sed.
faster,
more CO2
mineralization half-life (h)
mineralization extent (%)
10^5
10^4
10^3
10^2
0
20
40
60
80
100

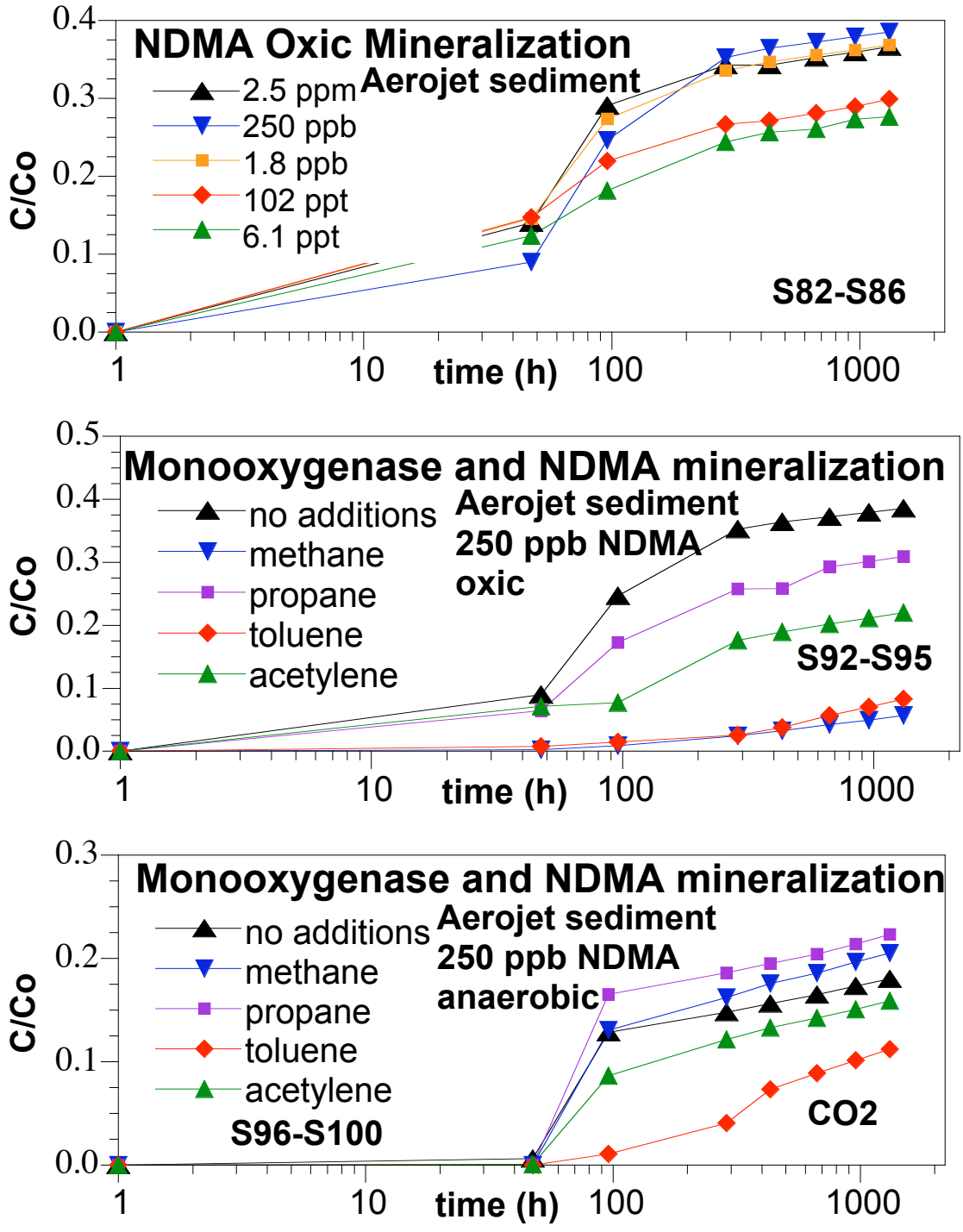
NDMA Oxic Mineralization
Aerojet sediment
2.5 ppm
250 ppb
1.8 ppb
102 ppt
6.1 ppt
S82-S86
C/Co
time (h)
0.0
0.1
0.2
0.3
0.4
1
10
100
1000
Monooxygenase and NDMA mineralization
Aerojet sediment
250 ppb NDMA
oxic
no additions
methane
propane
toluene
acetylene
S92-S95
C/Co
time (h)
0.0
0.1
0.2
0.3
0.4
0.5
1
10
100
1000
Monooxygenase and NDMA mineralization
Aerojet sediment
250 ppb NDMA
anaerobic
no additions
methane
propane
toluene
acetylene
S96-S100
CO2
C/Co
time (h)
0.0
0.1
0.2
0.3
1
10
100
1000

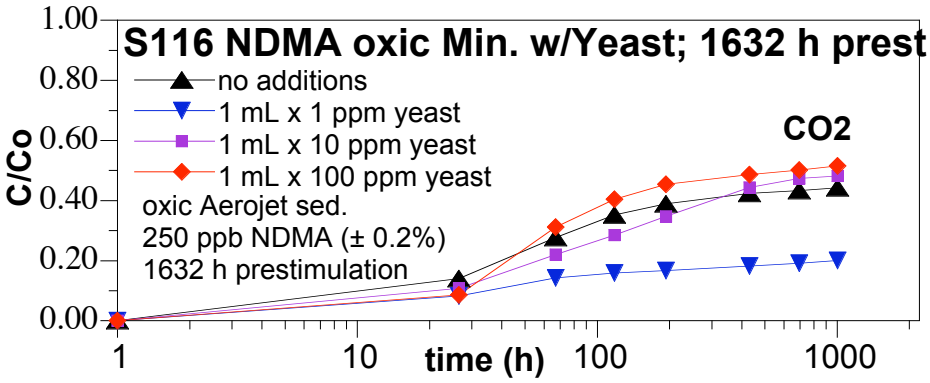
S116 NDMA oxic Min. w/Yeast; 1632 h prest
no additions
1 mL x 1 ppm yeast
1 mL x 10 ppm yeast
1 mL x 100 ppm yeast
oxic Aerojet sed.
250 ppb NDMA (± 0.2%)
1632 h prestimulation
CO2
C/Co
time (h)
1.00
0.80
0.60
0.40
0.20
0.00
1
10
100
1000

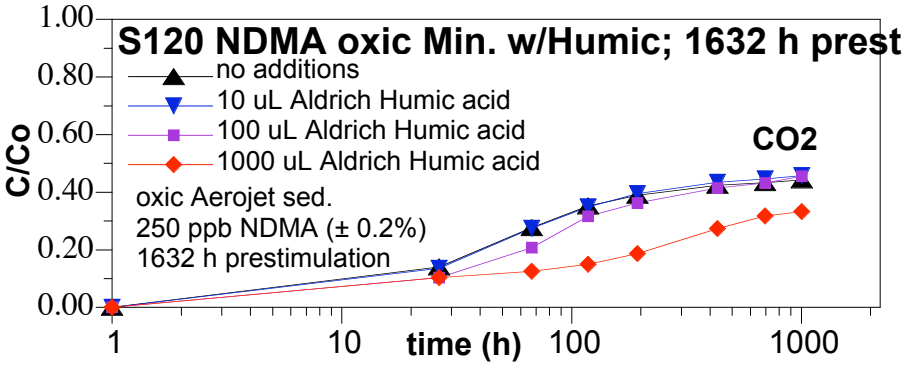
S120 NDMA oxic Min. w/Humic; 1632 h prest
no additions
10 uL Aldrich Humic acid
100 uL Aldrich Humic acid
1000 uL Aldrich Humic acid
oxic Aerojet sed.
250 ppb NDMA (± 0.2%)
1632 h prestimulation
CO2
C/Co
time (h)
1.00
0.80
0.60
0.40
0.20
0.00
1
10
100
1000

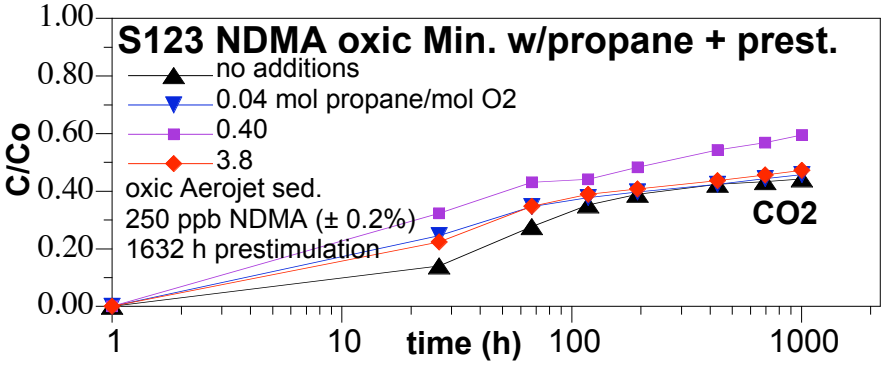
S123 NDMA oxic Min. w/propane + prest.
no additions
0.04 mol propane/mol O2
0.40
3.8
oxic Aerojet sed.
250 ppb NDMA (± 0.2%)
1632 h prestimulation
CO2
C/Co
time (h)
1.00
0.80
0.60
0.40
0.20
0.00
1
10
100
1000

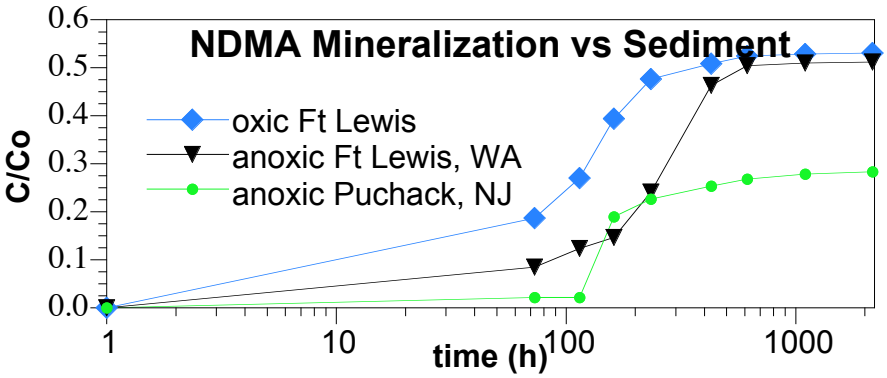
NDMA Mineralization vs Sediment
oxic Ft Lewis
anoxic Ft Lewis, WA
anoxic Puchack, NJ
C/Co
time (h)
0.6
0.5
0.4
0.3
0.2
0.1
0.0
1
10
100
1000

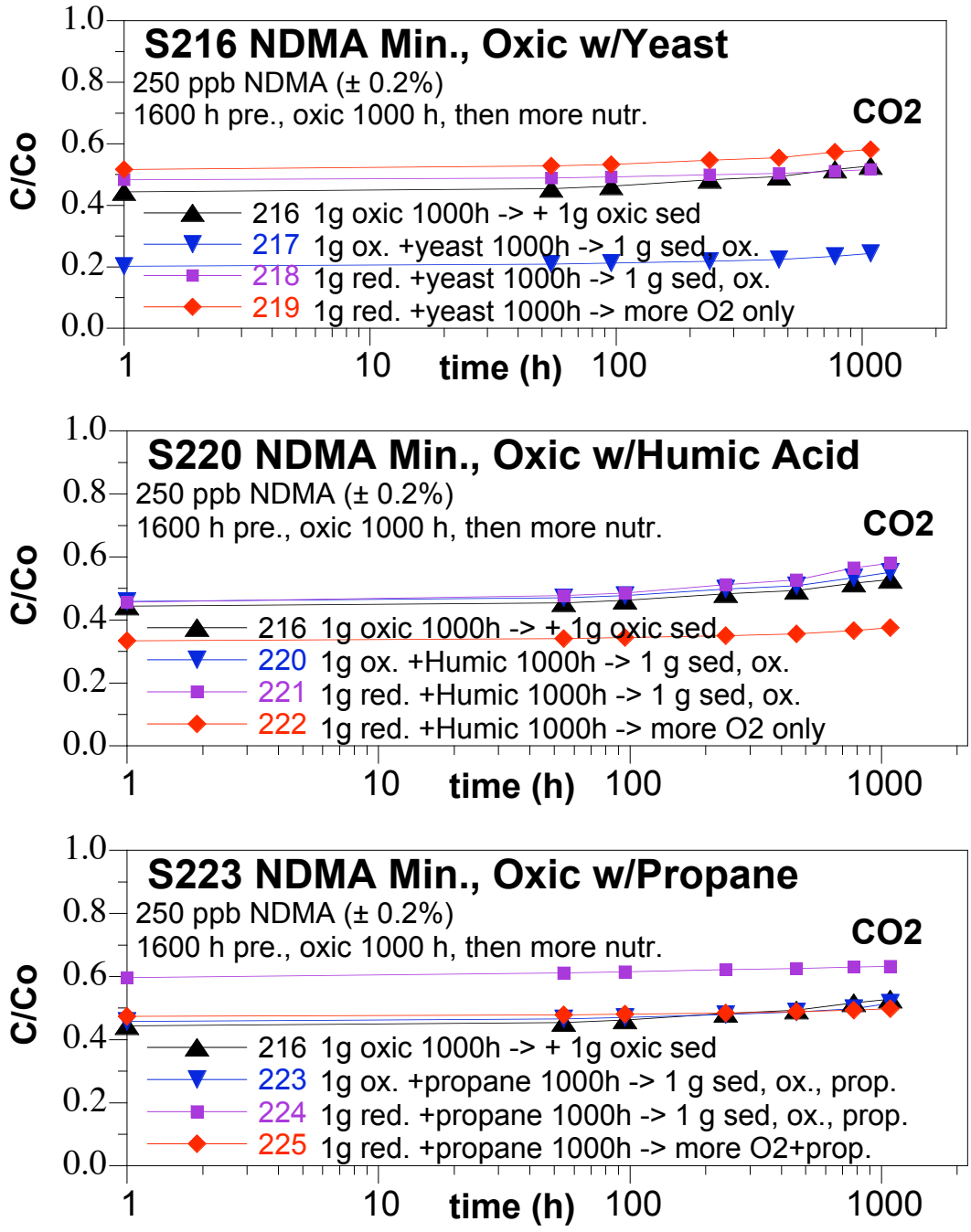
S216 NDMA Min., Oxic w/Yeast
250 ppb NDMA (± 0.2%)
1600 h pre., oxic 1000 h, then more nutr.
CO2
C/Co
time (h)
216 1g oxic 1000h -> + 1g oxic sed
217 1g ox. +yeast 1000h -> 1 g sed, ox.
218 1g red. +yeast 1000h -> 1 g sed, ox.
219 1g red. +yeast 1000h -> more O2 only
S220 NDMA Min., Oxic w/Humic Acid
250 ppb NDMA (± 0.2%)
1600 h pre., oxic 1000 h, then more nutr.
CO2
C/Co
time (h)
216 1g oxic 1000h -> + 1g oxic sed
220 1g ox. +Humic 1000h -> 1 g sed, ox.
221 1g red. +Humic 1000h -> 1 g sed, ox.
222 1g red. +Humic 1000h -> more O2 only
S223 NDMA Min., Oxic w/Propane
250 ppb NDMA (± 0.2%)
1600 h pre., oxic 1000 h, then more nutr.
CO2
C/Co
time (h)
216 1g oxic 1000h -> + 1g oxic sed
223 1g ox. +propane 1000h -> 1 g sed, ox., prop.
224 1g red. +propane 1000h -> 1 g sed, ox., prop.
225 1g red. +propane 1000h -> more O2+prop.

Appendix A.12 Task 2.2 NDMA Mineralization in Reduced Sediment

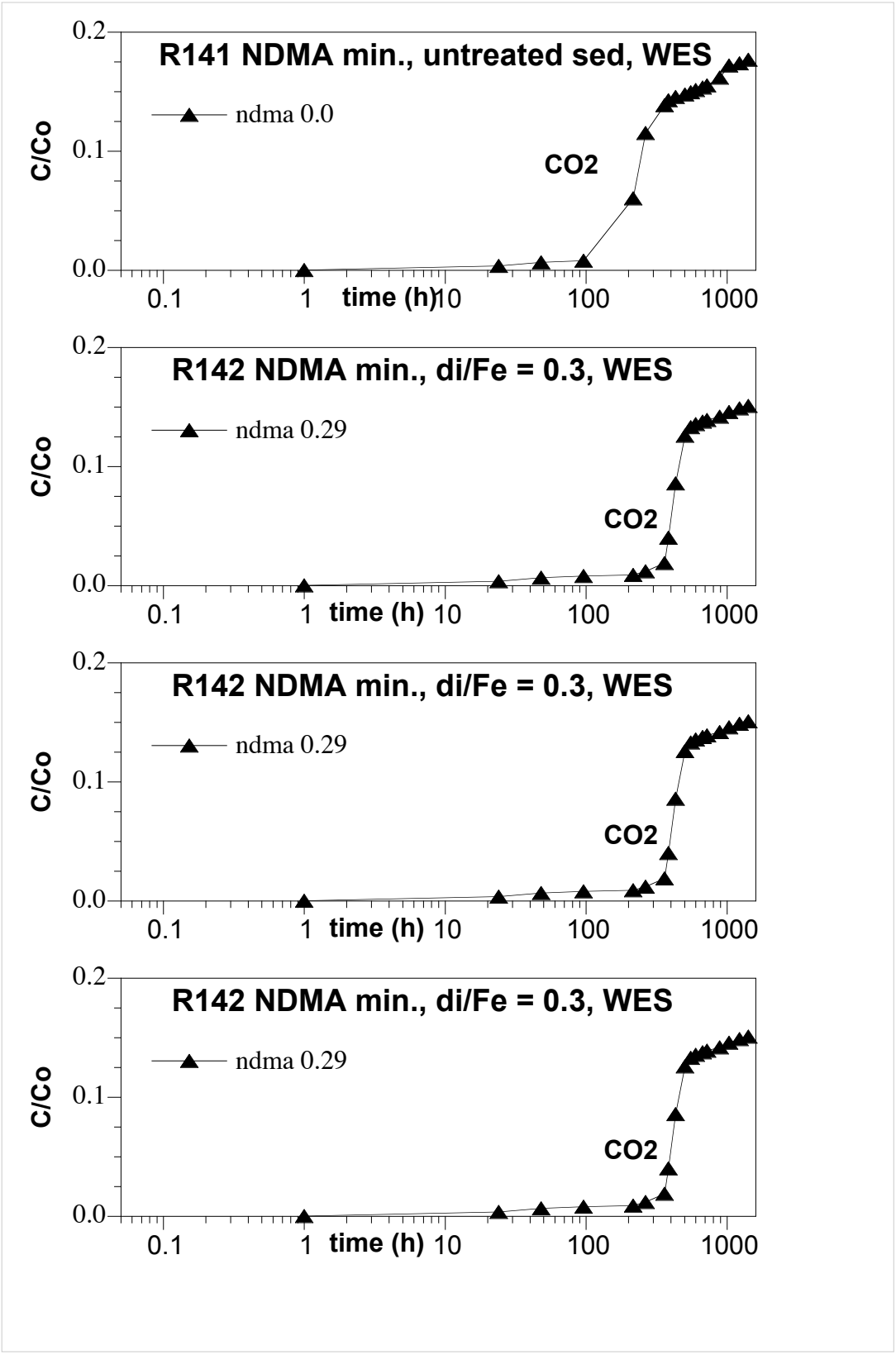

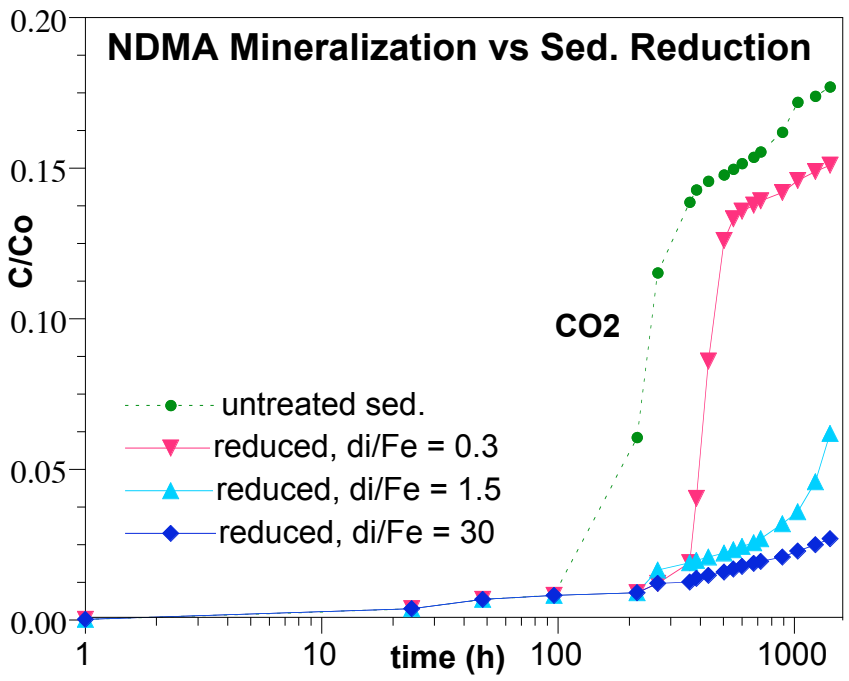
NDMA Mineralization vs Sed. Reduction
0.20
0.15
0.10
0.05
0.00
C/Co
CO2
untreated sed.
reduced, di/Fe = 0.3
reduced, di/Fe = 1.5
reduced, di/Fe = 30
1
10
time (h)
100
1000

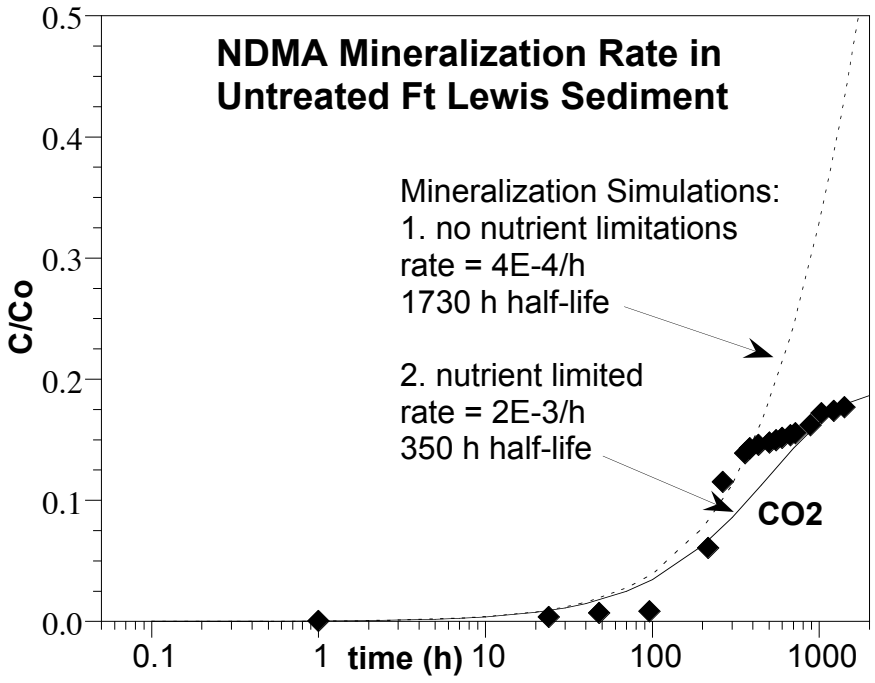
NDMA Mineralization Rate in
Untreated Ft Lewis Sediment
0.5
0.4
0.3
0.2
0.1
0.0
C/Co
Mineralization Simulations:
1. no nutrient limitations
rate = 4E-4/h
1730 h half-life
2. nutrient limited
rate = 2E-3/h
350 h half-life
CO2
0.1
1
time (h)
10
100
1000

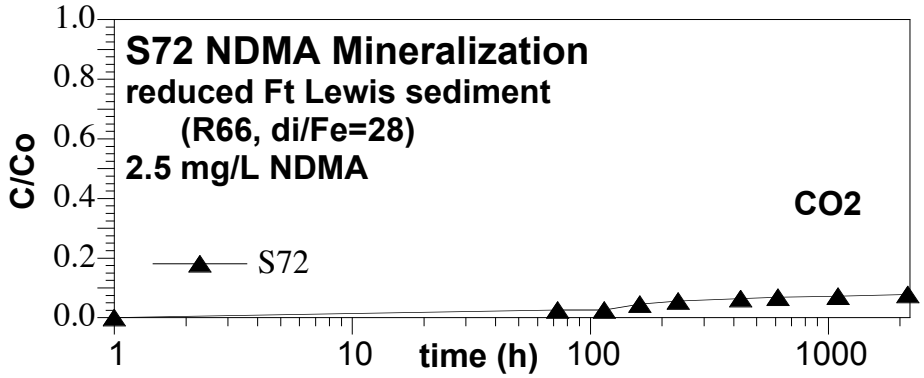
S72 NDMA Mineralization
reduced Ft Lewis sediment
(R66, di/Fe=28)
2.5 mg/L NDMA
CO2
S72
C/Co
time (h)
1.0
0.8
0.6
0.4
0.2
0.0
1
10
100
1000

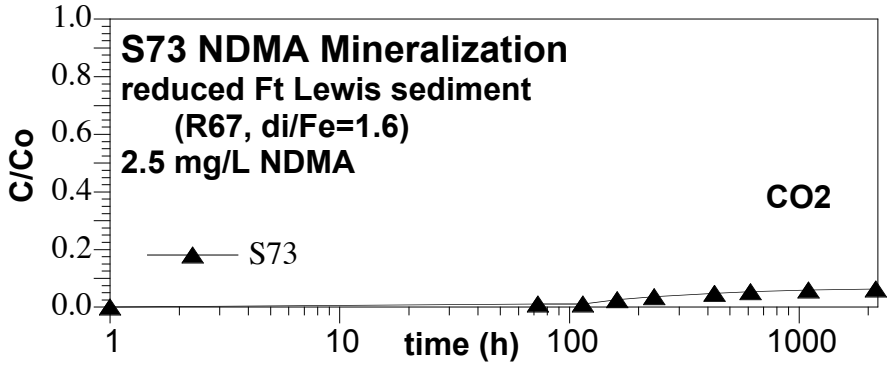
S73 NDMA Mineralization
reduced Ft Lewis sediment
(R67, di/Fe=1.6)
2.5 mg/L NDMA
CO2
S73
C/Co
time (h)
1.0
0.8
0.6
0.4
0.2
0.0
1
10
100
1000

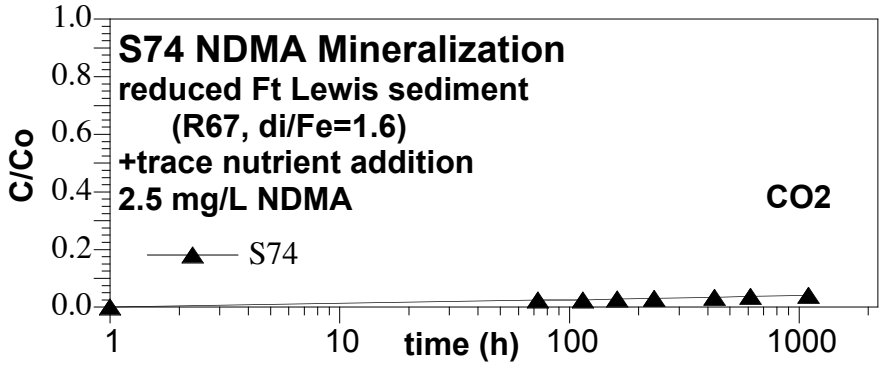
S74 NDMA Mineralization
reduced Ft Lewis sediment
(R67, di/Fe=1.6)
+trace nutrient addition
2.5 mg/L NDMA
CO2
S74
C/Co
time (h)
1.0
0.8
0.6
0.4
0.2
0.0
1
10
100
1000

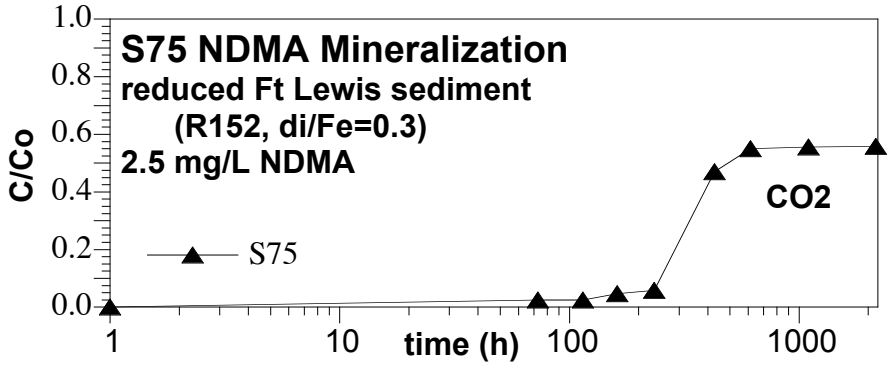
S75 NDMA Mineralization
reduced Ft Lewis sediment
(R152, di/Fe=0.3)
2.5 mg/L NDMA
CO2
S75
C/Co
time (h)
1.0
0.8
0.6
0.4
0.2
0.0
1
10
100
1000

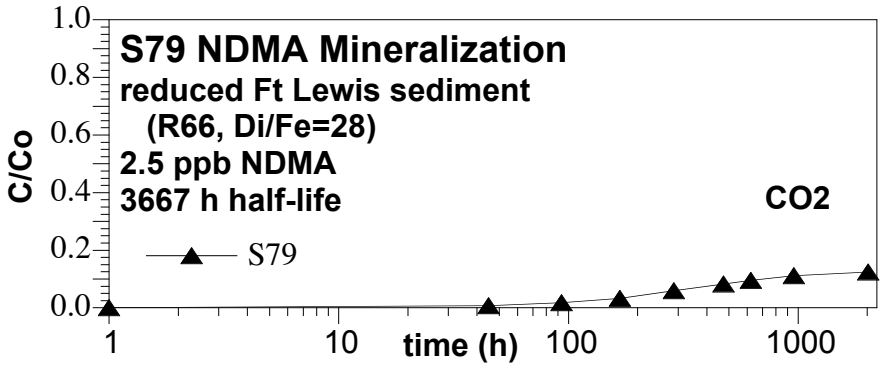
S79 NDMA Mineralization
reduced Ft Lewis sediment
(R66, Di/Fe=28)
2.5 ppb NDMA
3667 h half-life
CO2
S79
C/Co
time (h)
1.0
0.8
0.6
0.4
0.2
0.0
1
10
100
1000

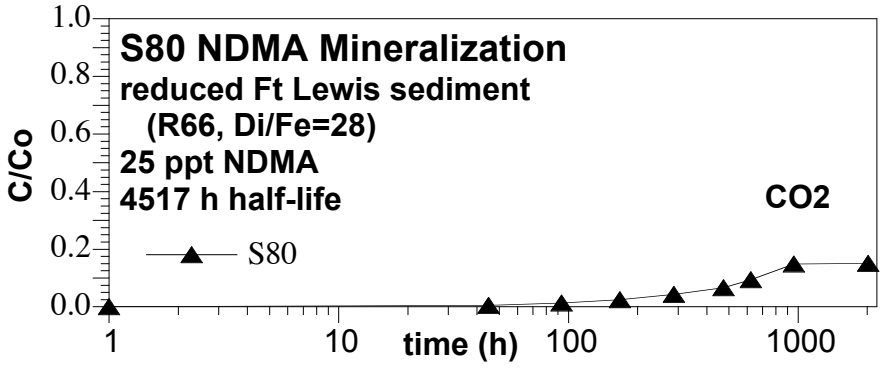
S80 NDMA Mineralization
reduced Ft Lewis sediment
(R66, Di/Fe=28)
25 ppt NDMA
4517 h half-life
CO2
S80
C/Co
time (h)
1.0
0.8
0.6
0.4
0.2
0.0
1
10
100
1000

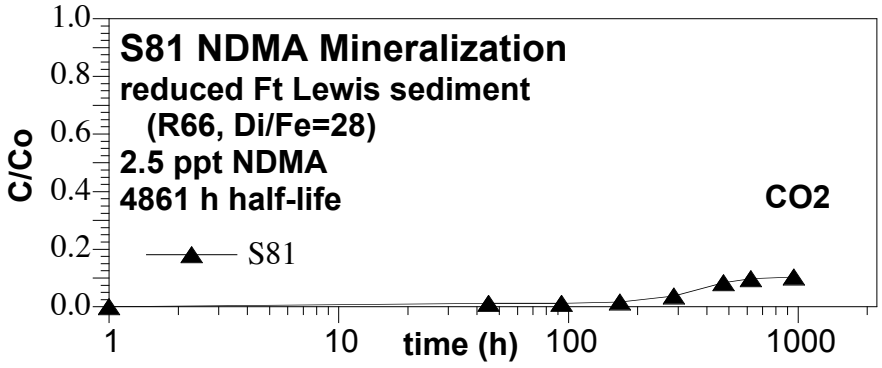
S81 NDMA Mineralization
reduced Ft Lewis sediment
(R66, Di/Fe=28)
2.5 ppt NDMA
4861 h half-life
CO2
S81
C/Co
time (h)
1.0
0.8
0.6
0.4
0.2
0.0
1
10
100
1000

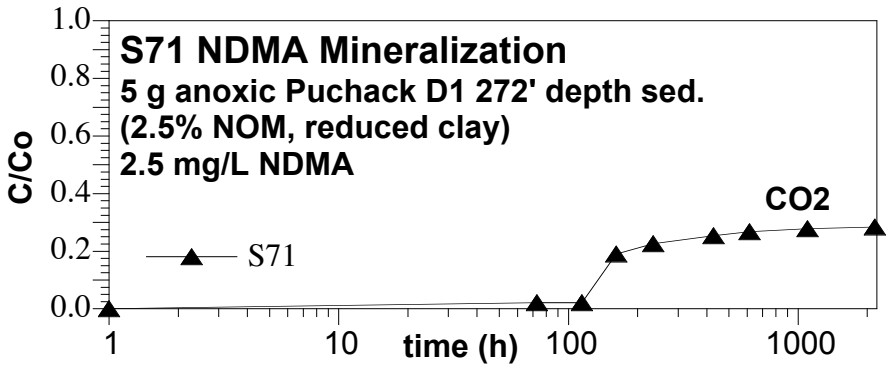
S71 NDMA Mineralization
5 g anoxic Puchack D1 272' depth sed.
(2.5% NOM, reduced clay)
2.5 mg/L NDMA
CO2
S71
C/Co
time (h)
1.0
0.8
0.6
0.4
0.2
0.0
1
10
100
1000

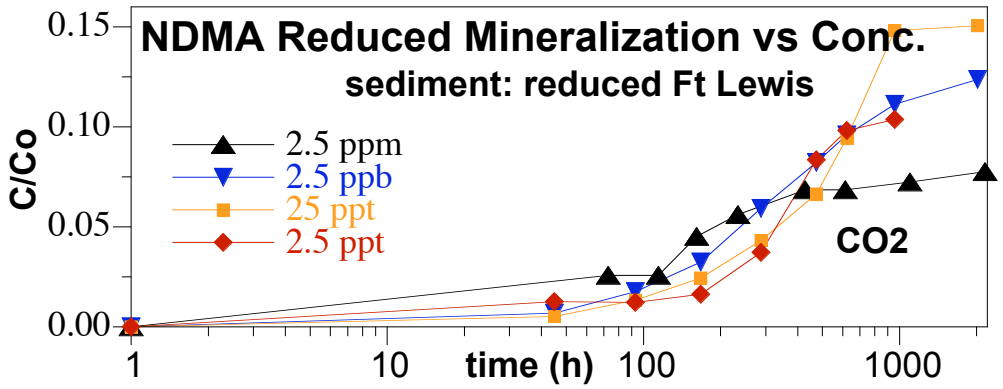
NDMA Reduced Mineralization vs Conc.
sediment: reduced Ft Lewis
2.5 ppm
2.5 ppb
25 ppt
2.5 ppt
CO2
C/Co
time (h)
0.15
0.10
0.05
0.00
1
10
100
1000

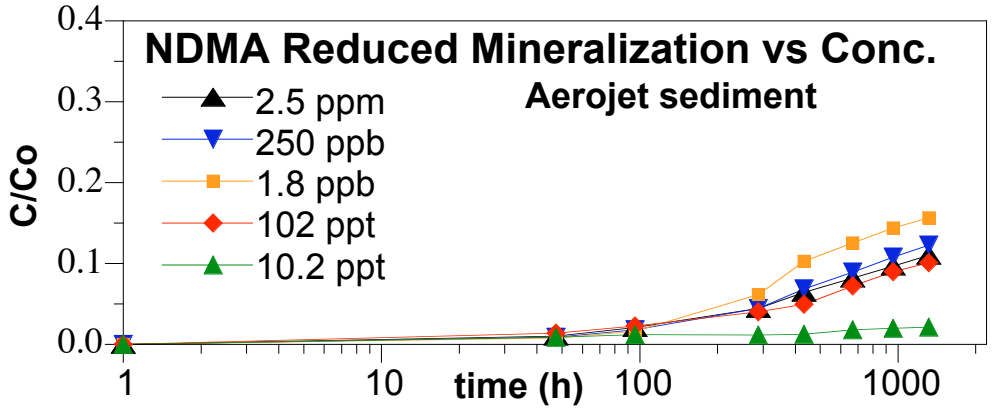
NDMA Reduced Mineralization vs Conc.
Aerojet sediment
2.5 ppm
250 ppb
1.8 ppb
102 ppt
10.2 ppt
C/Co
time (h)
0.4
0.3
0.2
0.1
0.0
1
10
100
1000

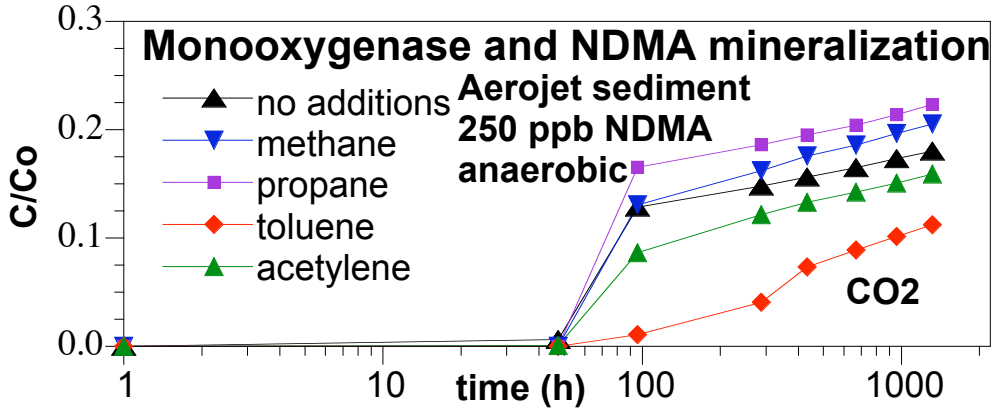
Monooxygenase and NDMA mineralization
Aerojet sediment
250 ppb NDMA
anaerobic
no additions
methane
propane
toluene
acetylene
CO2
C/Co
time (h)
0.3
0.2
0.1
0.0
1
10
100
1000

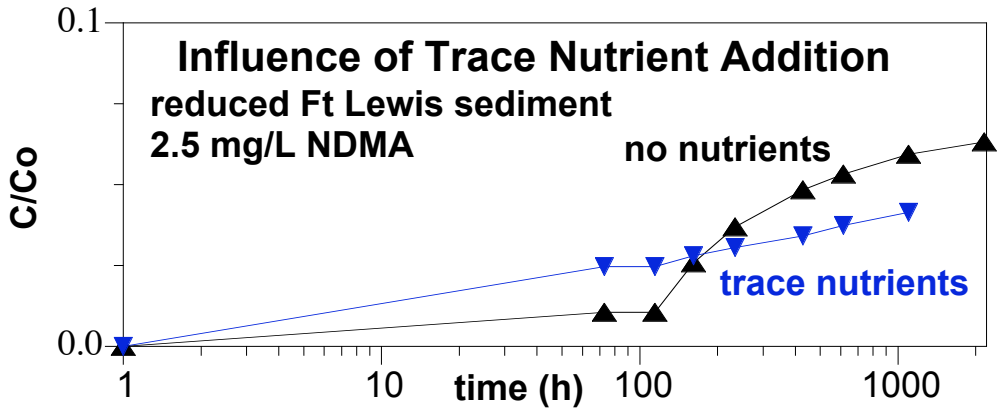
Influence of Trace Nutrient Addition
reduced Ft Lewis sediment
2.5 mg/L NDMA
no nutrients
trace nutrients
C/Co
time (h)
0.1
0.0
1
10
100
1000

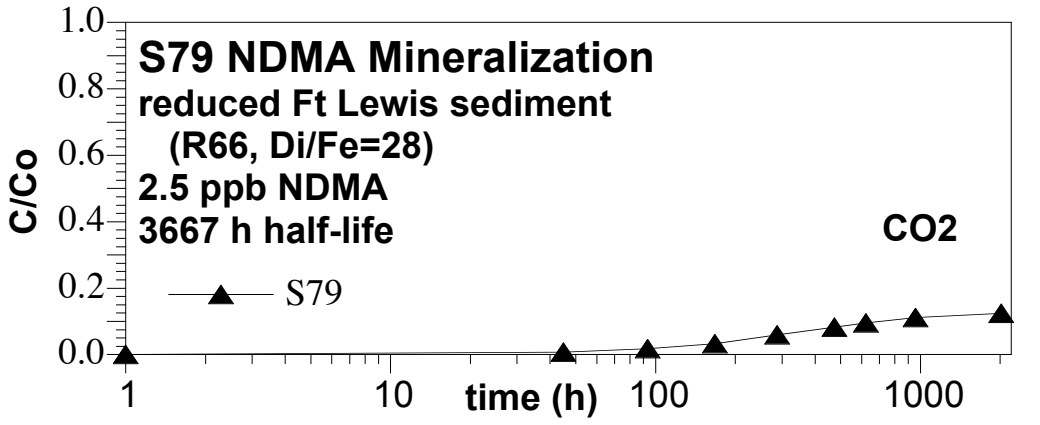
S79 NDMA Mineralization
reduced Ft Lewis sediment
(R66, Di/Fe=28)
2.5 ppb NDMA
3667 h half-life
CO2
S79
C/Co
time (h)
1.0
0.8
0.6
0.4
0.2
0.0
1
10
100
1000

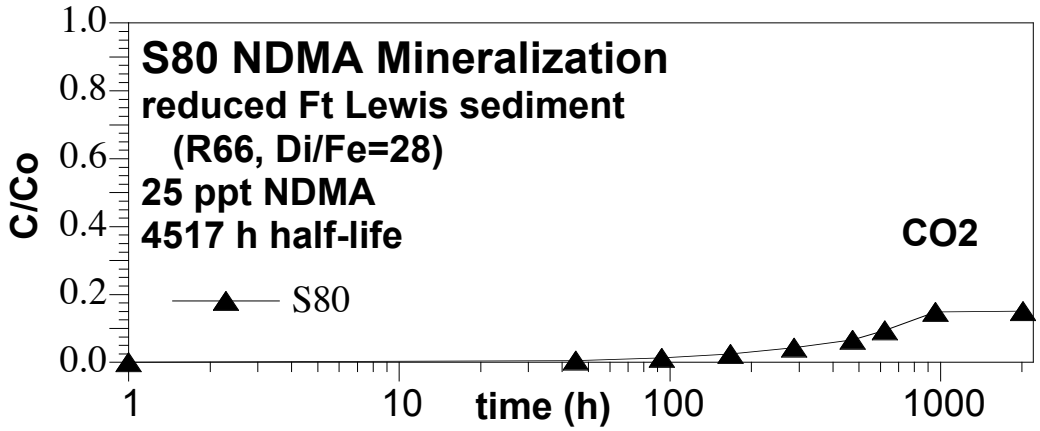
S80 NDMA Mineralization
reduced Ft Lewis sediment
(R66, Di/Fe=28)
25 ppt NDMA
4517 h half-life
CO2
S80
C/Co
time (h)
1.0
0.8
0.6
0.4
0.2
0.0
1
10
100
1000

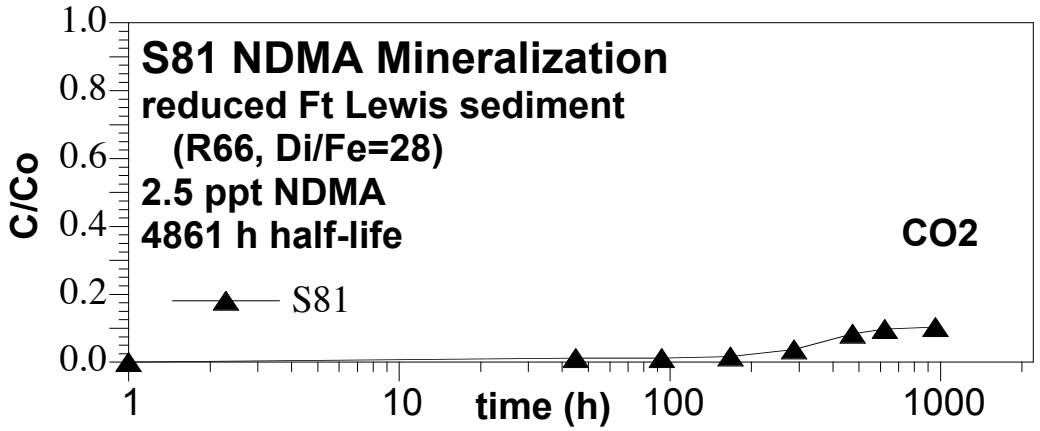
S81 NDMA Mineralization
reduced Ft Lewis sediment
(R66, Di/Fe=28)
2.5 ppt NDMA
4861 h half-life
CO2
S81
C/Co
time (h)
1.0
0.8
0.6
0.4
0.2
0.0
1
10
100
1000

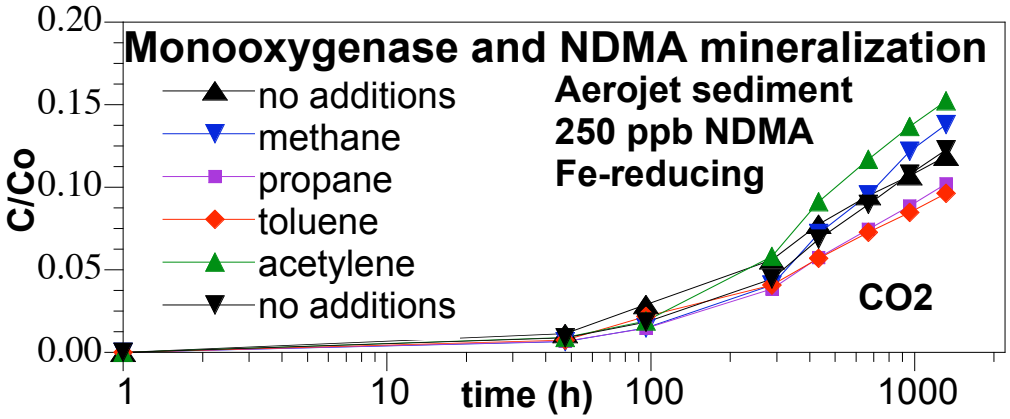
Monooxygenase and NDMA mineralization
Aerojet sediment
250 ppb NDMA
Fe-reducing
no additions
methane
propane
toluene
acetylene
no additions
CO2
C/Co
time (h)
0.20
0.15
0.10
0.05
0.00
1
10
100
1000

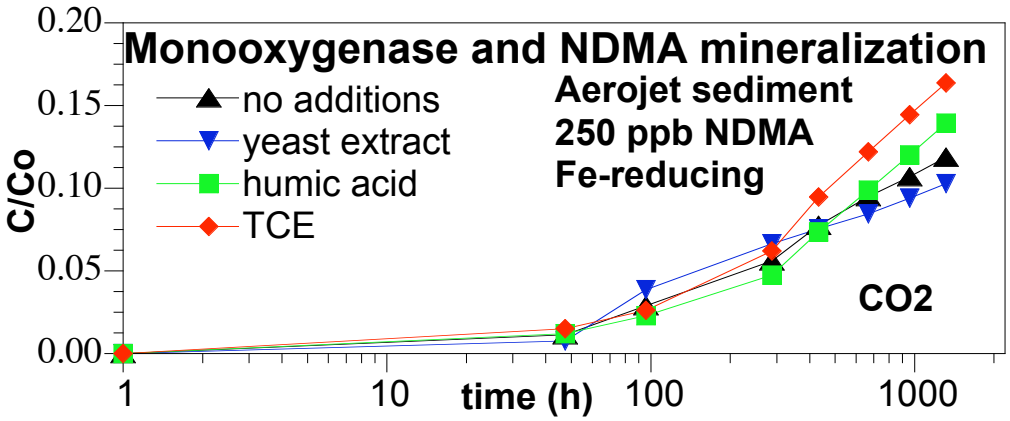
Monooxygenase and NDMA mineralization
Aerojet sediment
250 ppb NDMA
Fe-reducing
no additions
yeast extract
humic acid
TCE
CO2
C/Co
time (h)
0.20
0.15
0.10
0.05
0.00
1
10
100
1000

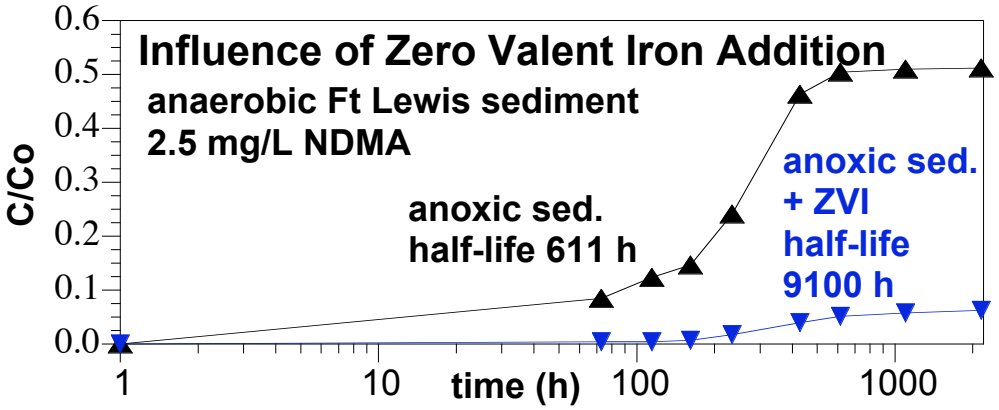
Influence of Zero Valent Iron Addition
anaerobic Ft Lewis sediment
2.5 mg/L NDMA
anoxic sed.
half-life 611 h
anoxic sed.
+ ZVI
half-life
9100 h
C/Co
time (h)
0.6
0.5
0.4
0.3
0.2
0.1
0.0
1
10
100
1000

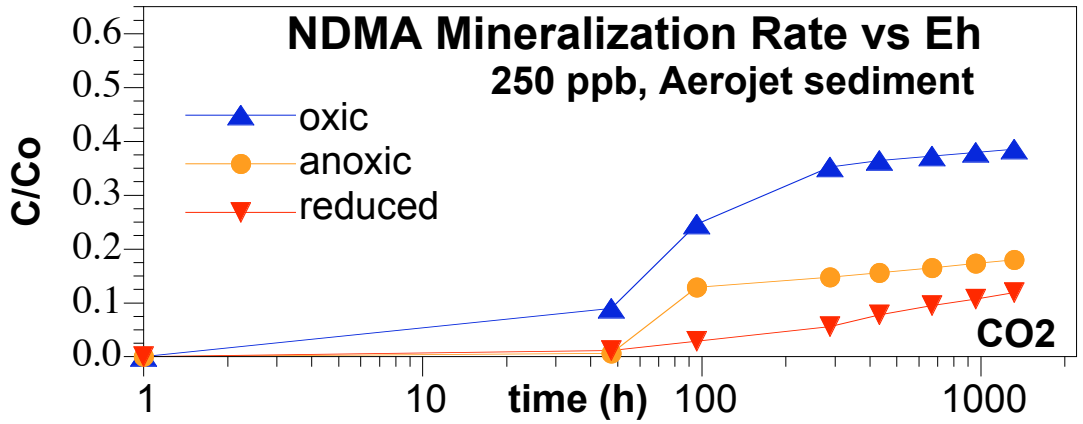
NDMA Mineralization Rate vs Eh
250 ppb, Aerojet sediment
oxic
anoxic
reduced
C/Co
0.6
0.5
0.4
0.3
0.2
0.1
0.0
1
10
time (h)
100
1000
CO2

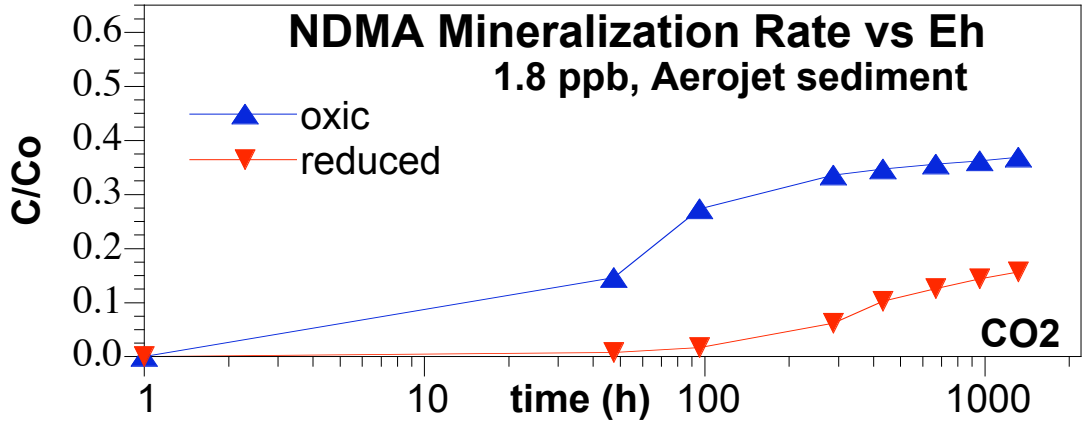
NDMA Mineralization Rate vs Eh
1.8 ppb, Aerojet sediment
oxic
reduced
C/Co
0.6
0.5
0.4
0.3
0.2
0.1
0.0
1
10
time (h)
100
1000
CO2

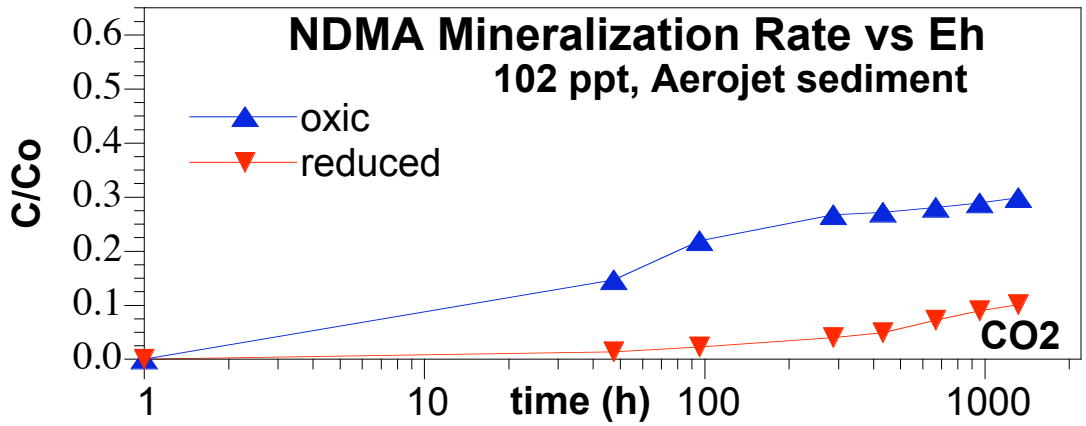
NDMA Mineralization Rate vs Eh
102 ppt, Aerojet sediment
oxic
reduced
C/Co
0.6
0.5
0.4
0.3
0.2
0.1
0.0
1
10
time (h)
100
1000
CO2

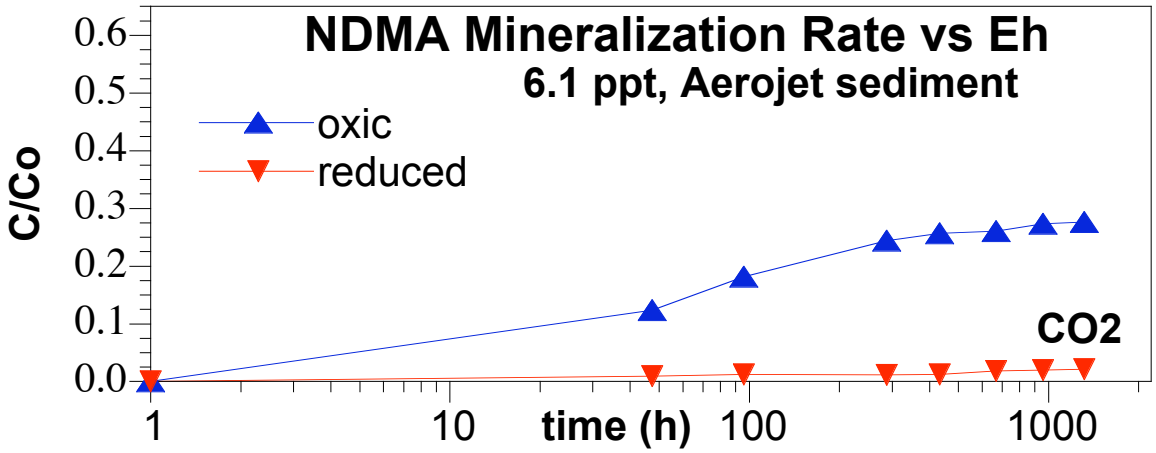
NDMA Mineralization Rate vs Eh
6.1 ppt, Aerojet sediment
oxic
reduced
CO2
C/Co
time (h)
0.0
0.1
0.2
0.3
0.4
0.5
0.6
1
10
100
1000

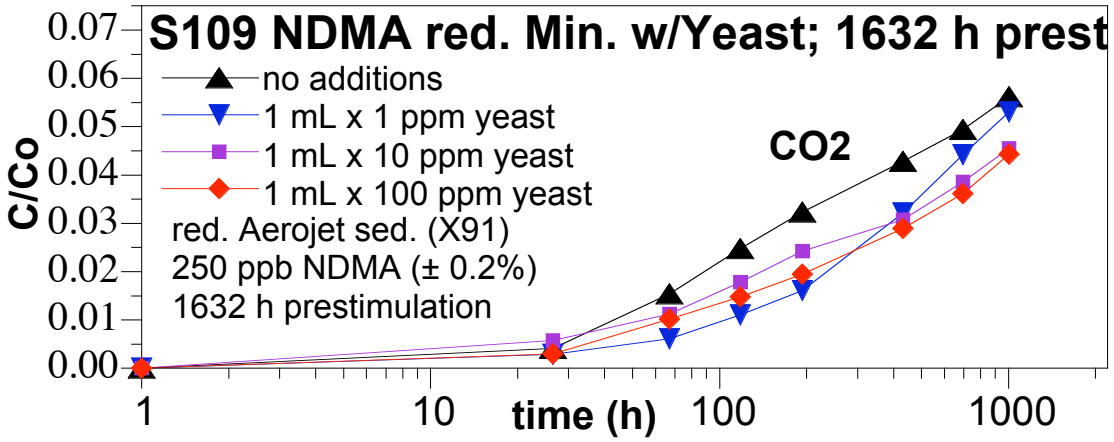
S109 NDMA red. Min. w/Yeast; 1632 h prest
no additions
1 mL x 1 ppm yeast
1 mL x 10 ppm yeast
1 mL x 100 ppm yeast
red. Aerojet sed. (X91)
250 ppb NDMA (± 0.2%)
1632 h prestimulation
CO2
C/Co
time (h)
0.00
0.01
0.02
0.03
0.04
0.05
0.06
0.07
1
10
100
1000

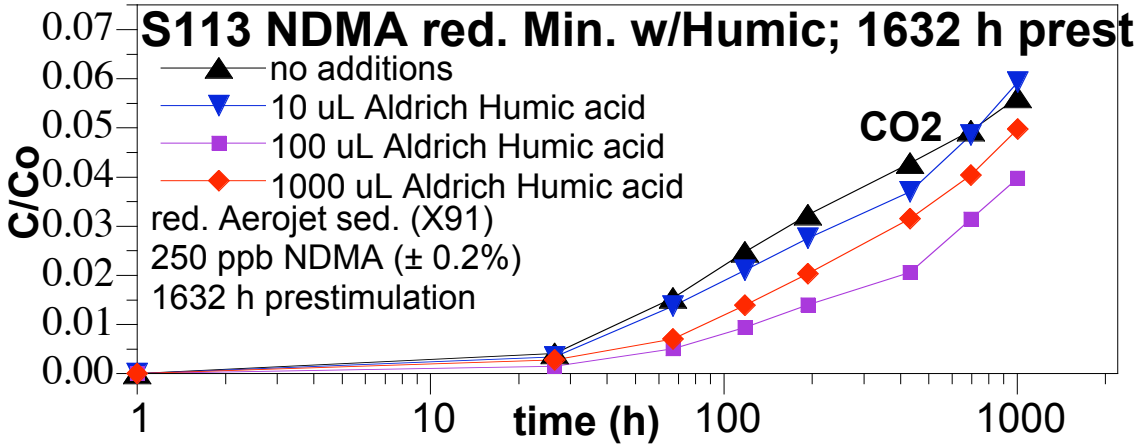
S113 NDMA red. Min. w/Humic; 1632 h prest
no additions
10 uL Aldrich Humic acid
100 uL Aldrich Humic acid
1000 uL Aldrich Humic acid
red. Aerojet sed. (X91)
250 ppb NDMA (± 0.2%)
1632 h prestimulation
CO2
C/Co
time (h)
0.00
0.01
0.02
0.03
0.04
0.05
0.06
0.07
1
10
100
1000

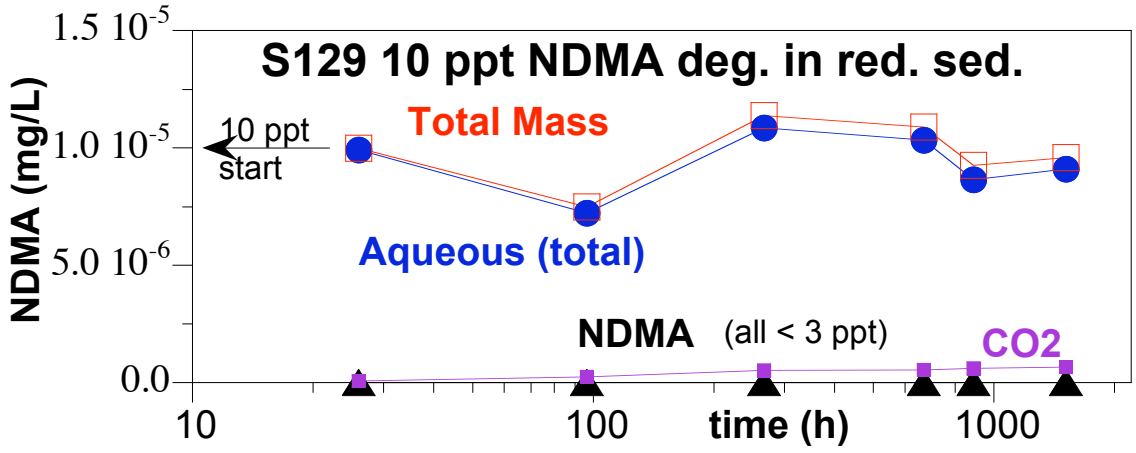
S129 10 ppt NDMA deg. in red. sed.
NDMA (mg/L)
1.5 10-5
1.0 10-5
5.0 10-6
0.0
10 ppt start
Total Mass
Aqueous (total)
NDMA (all < 3 ppt)
CO2
10
100
time (h)
1000

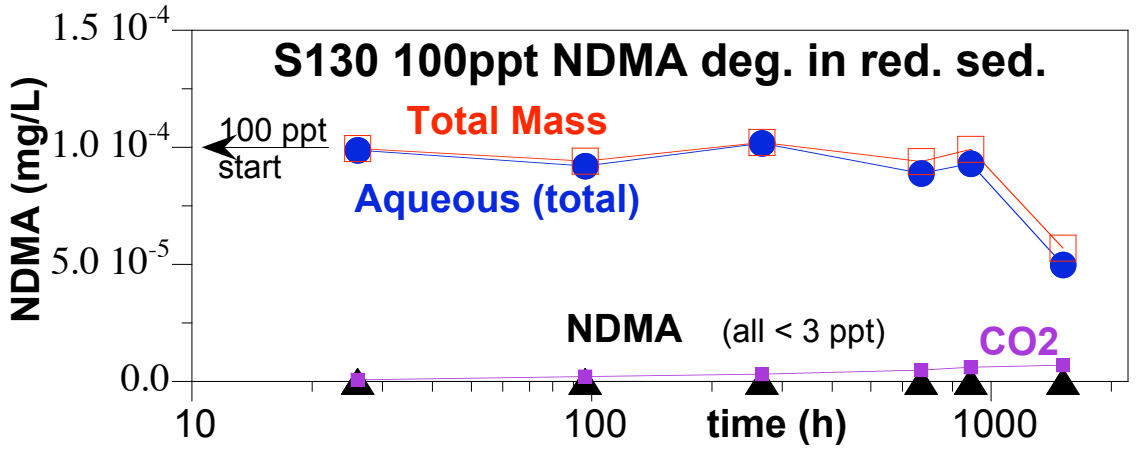
S130 100ppt NDMA deg. in red. sed.
NDMA (mg/L)
1.5 10-4
1.0 10-4
5.0 10-5
0.0
100 ppt start
Total Mass
Aqueous (total)
NDMA (all < 3 ppt)
CO2
10
100
time (h)
1000

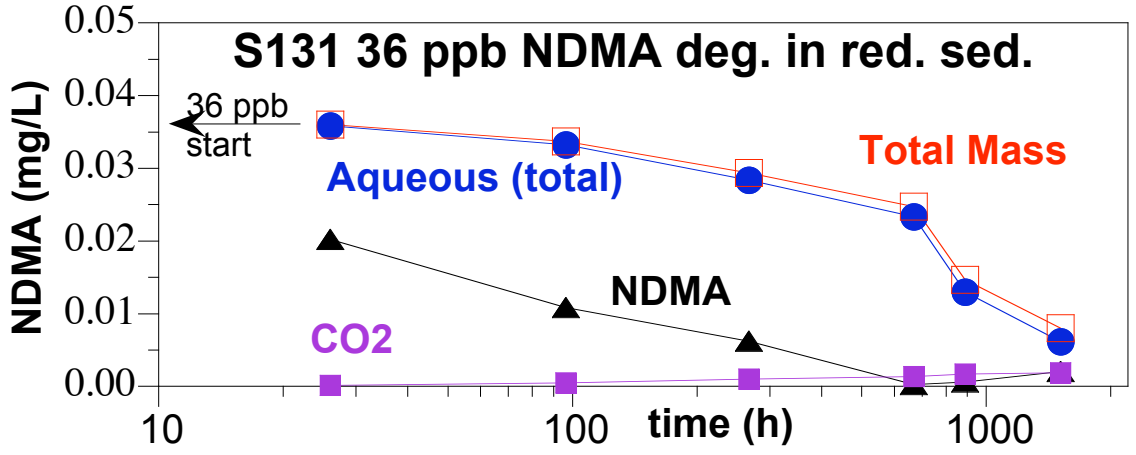
S131 36 ppb NDMA deg. in red. sed.
NDMA (mg/L)
0.05
0.04
0.03
0.02
0.01
0.00
36 ppb start
Aqueous (total)
Total Mass
NDMA
CO2
10
100
time (h)
1000

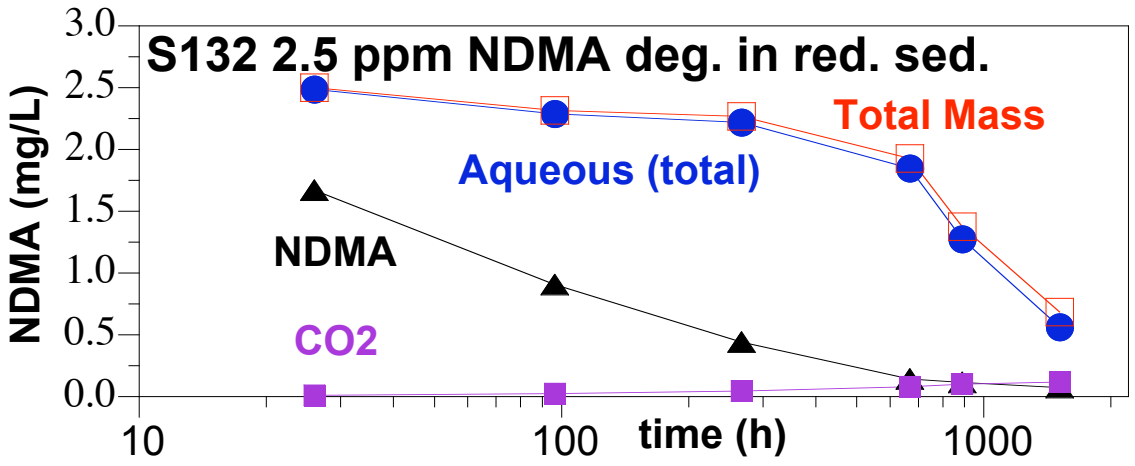
S132 2.5 ppm NDMA deg. in red. sed.
NDMA (mg/L)
3.0
2.5
2.0
1.5
1.0
0.5
0.0
Total Mass
Aqueous (total)
NDMA
CO2
10
100
time (h)
1000

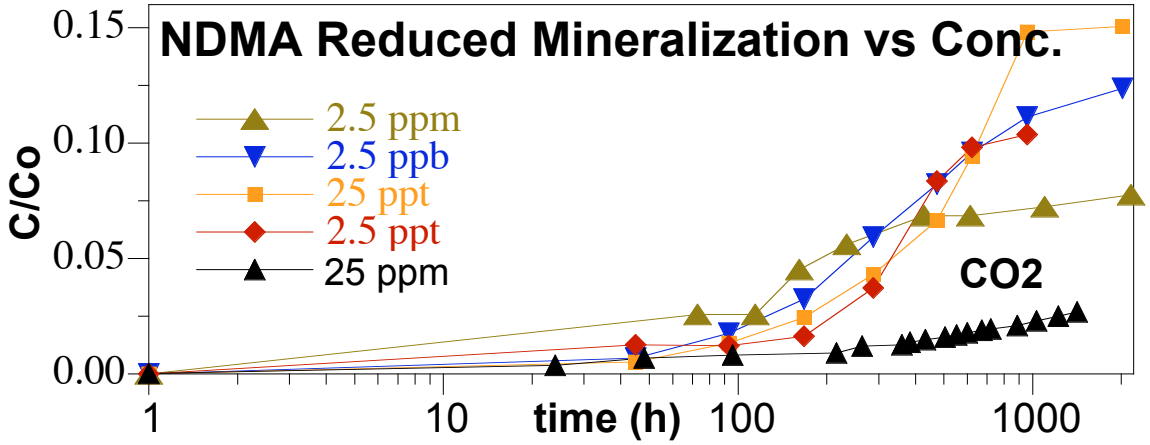
NDMA Reduced Mineralization vs Conc.
C/Co
0.15
0.10
0.05
0.00
2.5 ppm
2.5 ppb
25 ppt
2.5 ppt
25 ppm
CO2
1
10
time (h)
100
1000

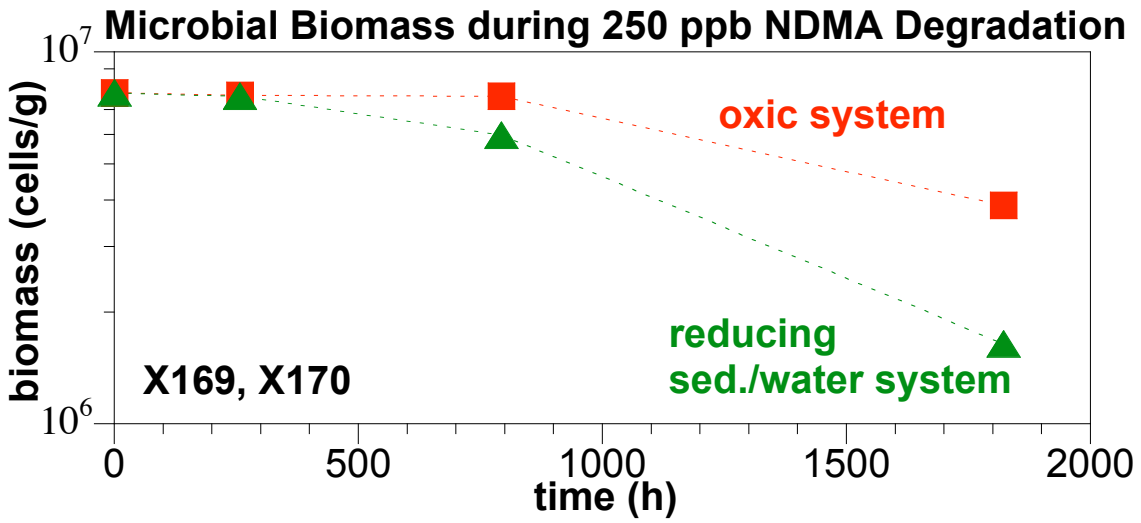
Microbial Biomass during 250 ppb NDMA Degradation
biomass (cells/g)
10^7
10^6
oxic system
reducing
sed./water system
X169, X170
0
500
1000
1500
2000
time (h)

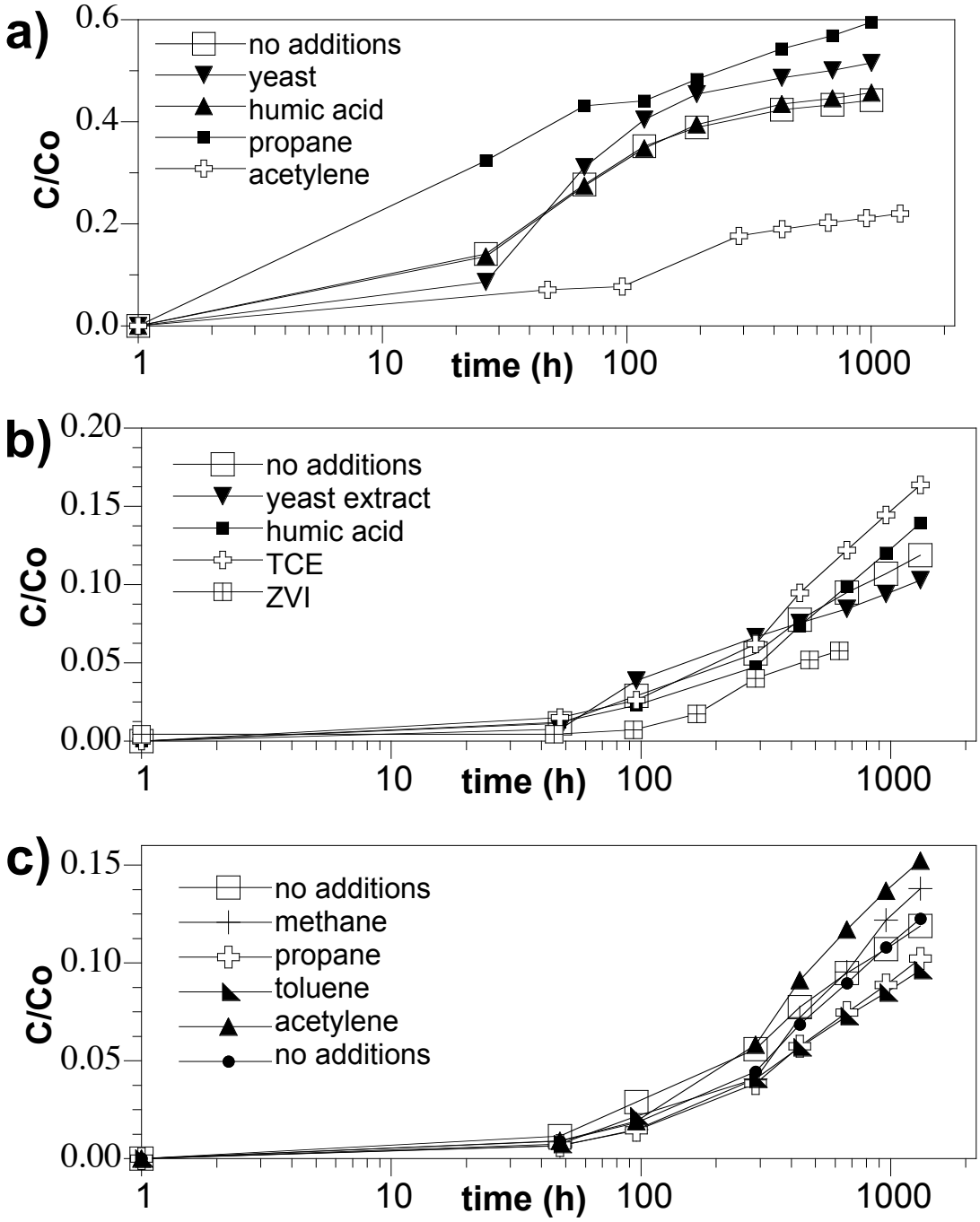
a)
0.6
0.4
0.2
0.0
C/Co
no additions
yeast
humic acid
propane
acetylene
1
10
time (h)
100
1000
b)
0.20
0.15
0.10
0.05
0.00
C/Co
no additions
yeast extract
humic acid
TCE
ZVI
1
10
time (h)
100
1000
c)
0.15
0.10
0.05
0.00
C/Co
no additions
methane
propane
toluene
acetylene
no additions
1
10
time (h)
100
1000

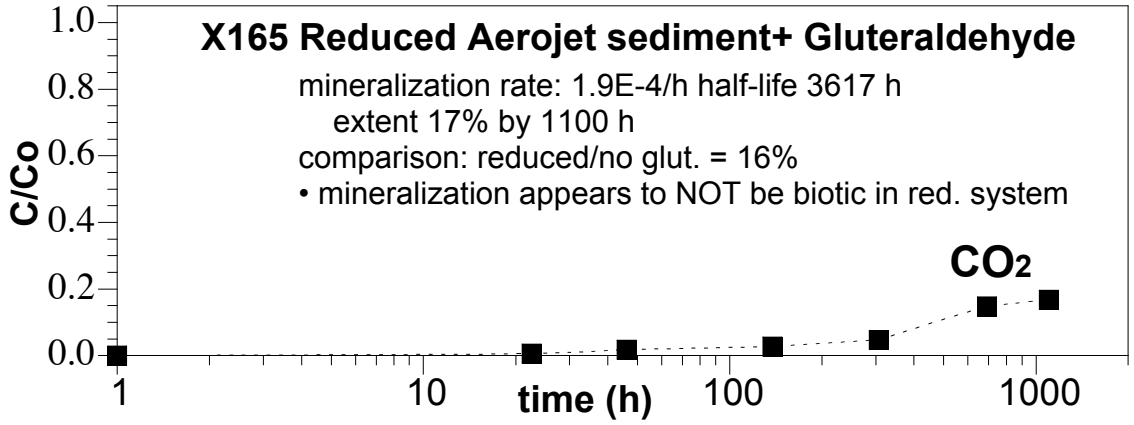
X165 Reduced Aerojet sediment+ Gluteraldehyde
mineralization rate: 1.9E-4/h half-life 3617 h
extent 17% by 1100 h
comparison: reduced/no glut. = 16%
• mineralization appears to NOT be biotic in red. system
CO2
C/Co
time (h)
1.0
0.8
0.6
0.4
0.2
0.0
1
10
100
1000

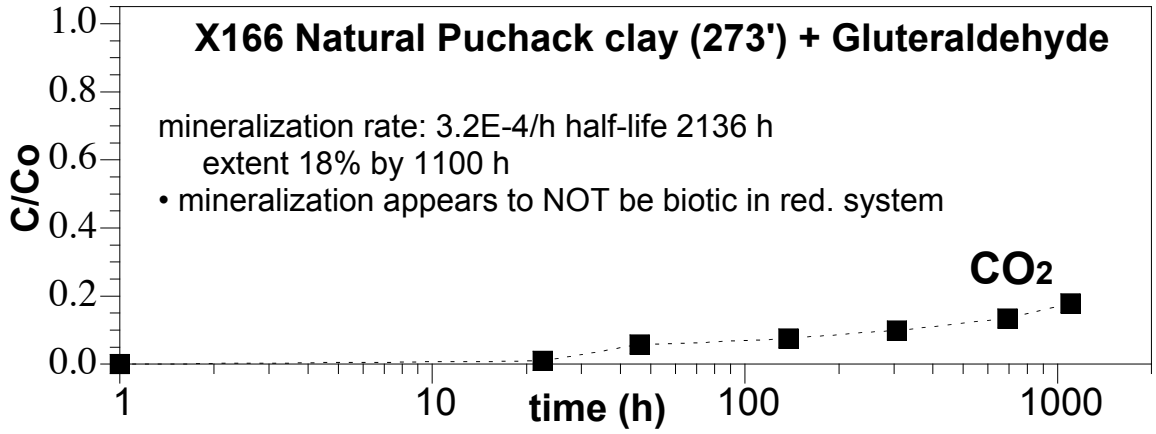
X166 Natural Puchack clay (273') + Gluteraldehyde
mineralization rate: 3.2E-4/h half-life 2136 h
extent 18% by 1100 h
• mineralization appears to NOT be biotic in red. system
CO2
C/Co
time (h)
1.0
0.8
0.6
0.4
0.2
0.0
1
10
100
1000

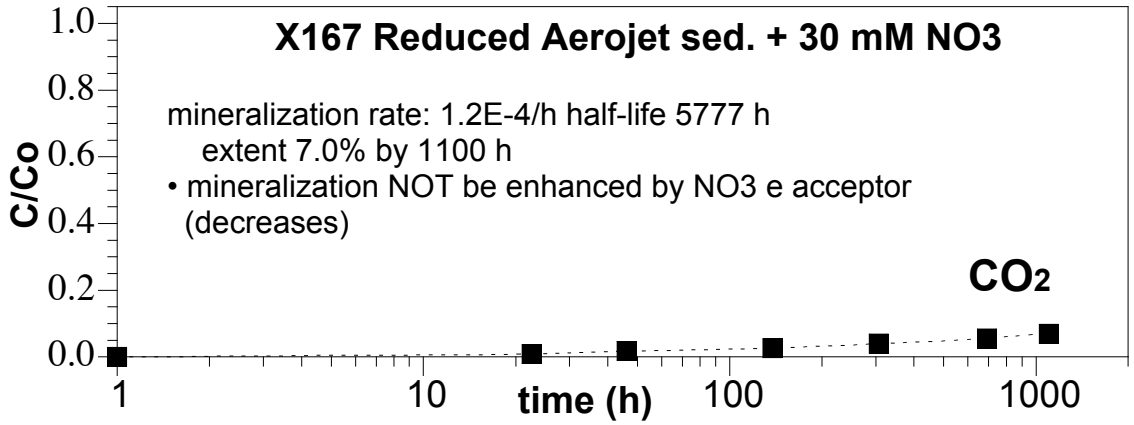
X167 Reduced Aerojet sed. + 30 mM NO3
mineralization rate: 1.2E-4/h half-life 5777 h
extent 7.0% by 1100 h
• mineralization NOT be enhanced by NO3 e acceptor
(decreases)
CO2
C/Co
time (h)
1.0
0.8
0.6
0.4
0.2
0.0
1
10
100
1000

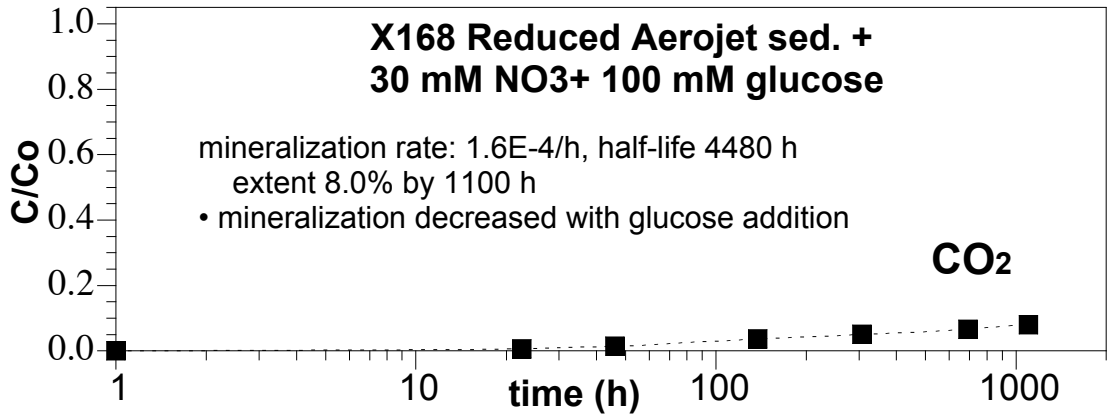
X168 Reduced Aerojet sed. +
30 mM NO3+ 100 mM glucose
mineralization rate: 1.6E-4/h, half-life 4480 h
extent 8.0% by 1100 h
• mineralization decreased with glucose addition
CO2
C/Co
time (h)
1.0
0.8
0.6
0.4
0.2
0.0
1
10
100
1000

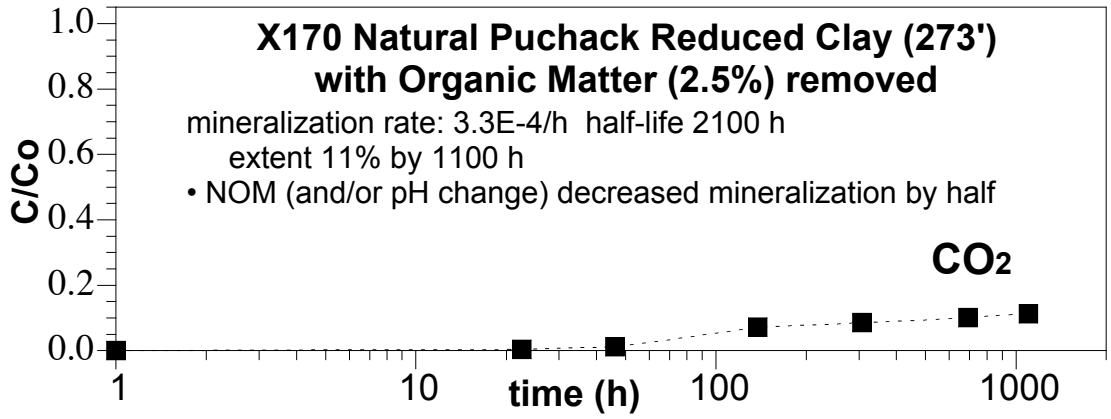
X170 Natural Puchack Reduced Clay (273')
with Organic Matter (2.5%) removed
mineralization rate: 3.3E-4/h half-life 2100 h
extent 11% by 1100 h
• NOM (and/or pH change) decreased mineralization by half
CO2
C/Co
time (h)
1.0
0.8
0.6
0.4
0.2
0.0
1
10
100
1000

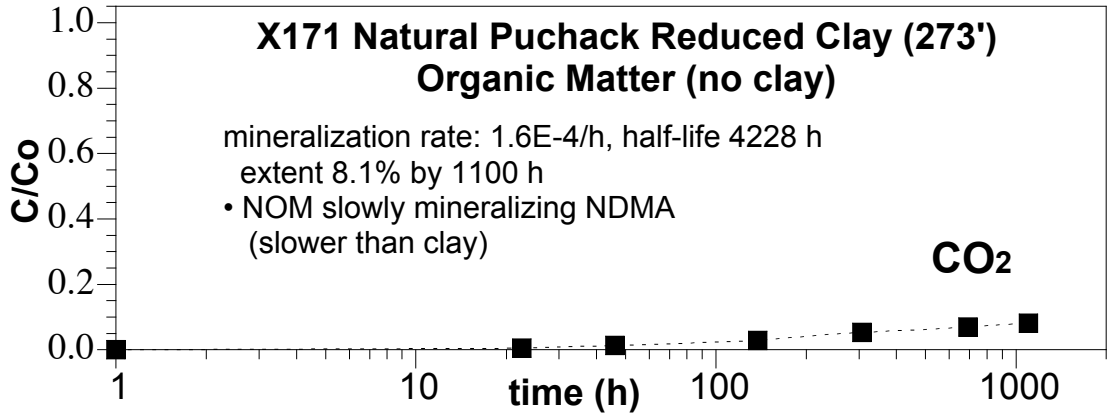
X171 Natural Puchack Reduced Clay (273')
Organic Matter (no clay)
mineralization rate: 1.6E-4/h, half-life 4228 h
extent 8.1% by 1100 h
• NOM slowly mineralizing NDMA
(slower than clay)
CO2
C/Co
time (h)
1.0
0.8
0.6
0.4
0.2
0.0
1
10
100
1000

Appendix A.13 Task 3 Sequential Reduced, Oxic Sediment Mineralization (Batch)

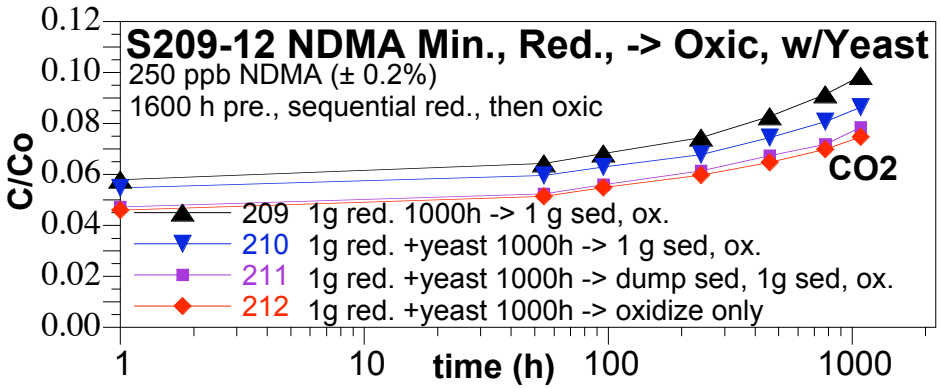

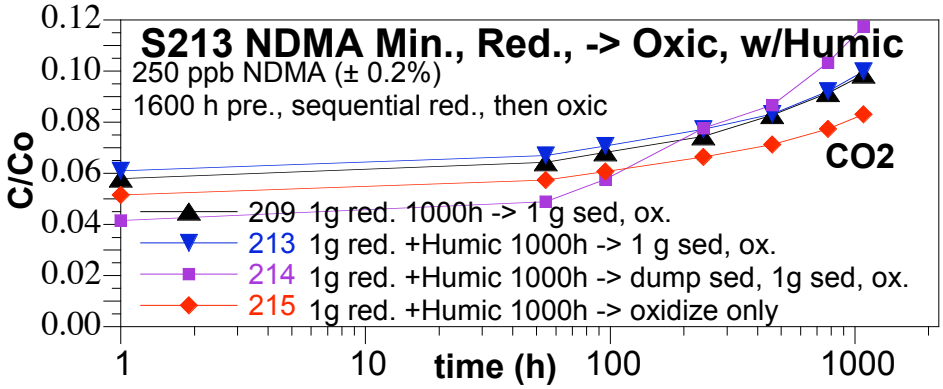

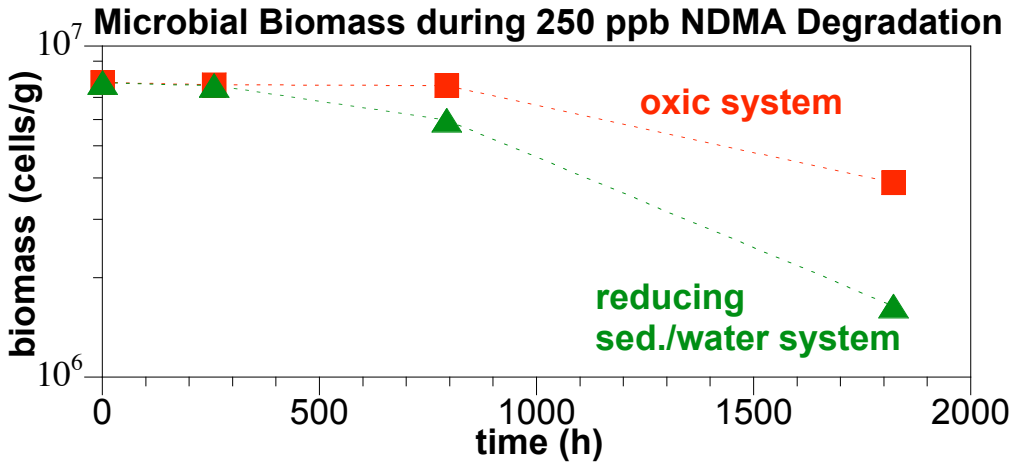

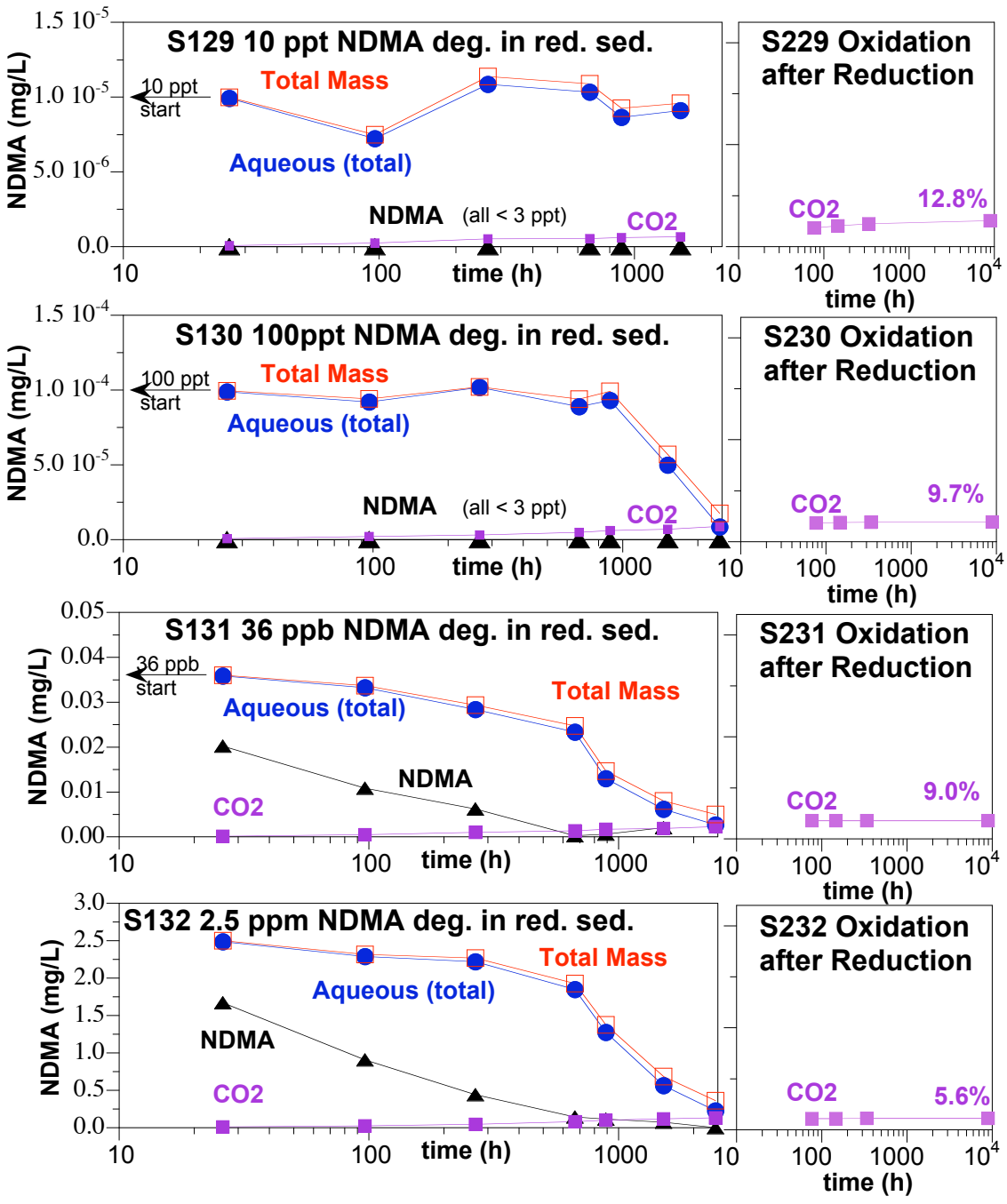
S129 10 ppt NDMA deg. in red. sed.
10 ppt start
Total Mass
Aqueous (total)
NDMA (all < 3 ppt)
CO2
NDMA (mg/L)
time (h)
S229 Oxidation after Reduction
CO2
12.8%
S130 100ppt NDMA deg. in red. sed.
100 ppt start
Total Mass
Aqueous (total)
NDMA (all < 3 ppt)
CO2
NDMA (mg/L)
time (h)
S230 Oxidation after Reduction
CO2
9.7%
S131 36 ppb NDMA deg. in red. sed.
36 ppb start
Aqueous (total)
Total Mass
NDMA
CO2
NDMA (mg/L)
time (h)
S231 Oxidation after Reduction
CO2
9.0%
S132 2.5 ppm NDMA deg. in red. sed.
Total Mass
Aqueous (total)
NDMA
CO2
NDMA (mg/L)
time (h)
S232 Oxidation after Reduction
CO2
5.6%

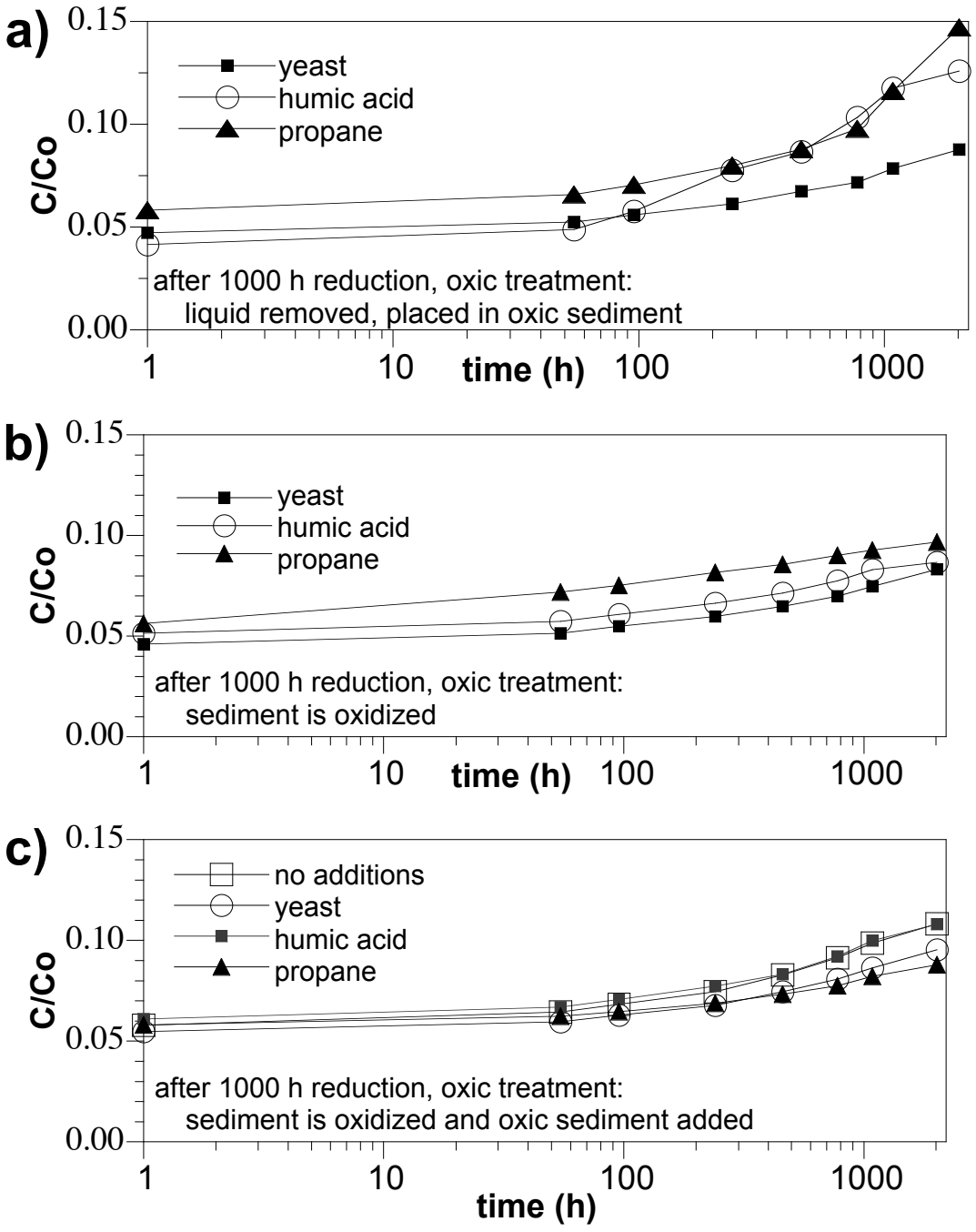
a)
0.15
0.10
0.05
0.00
C/Co
yeast
humic acid
propane
after 1000 h reduction, oxic treatment:
liquid removed, placed in oxic sediment
1
10
time (h)
100
1000
b)
0.15
0.10
0.05
0.00
C/Co
yeast
humic acid
propane
after 1000 h reduction, oxic treatment:
sediment is oxidized
1
10
time (h)
100
1000
c)
0.15
0.10
0.05
0.00
C/Co
no additions
yeast
humic acid
propane
after 1000 h reduction, oxic treatment:
sediment is oxidized and oxic sediment added
1
10
100
1000
time (h)

Appendix A.14 Task 4 Sequential Reduced/Oxic Sediment Mineralization (1-D Columns)

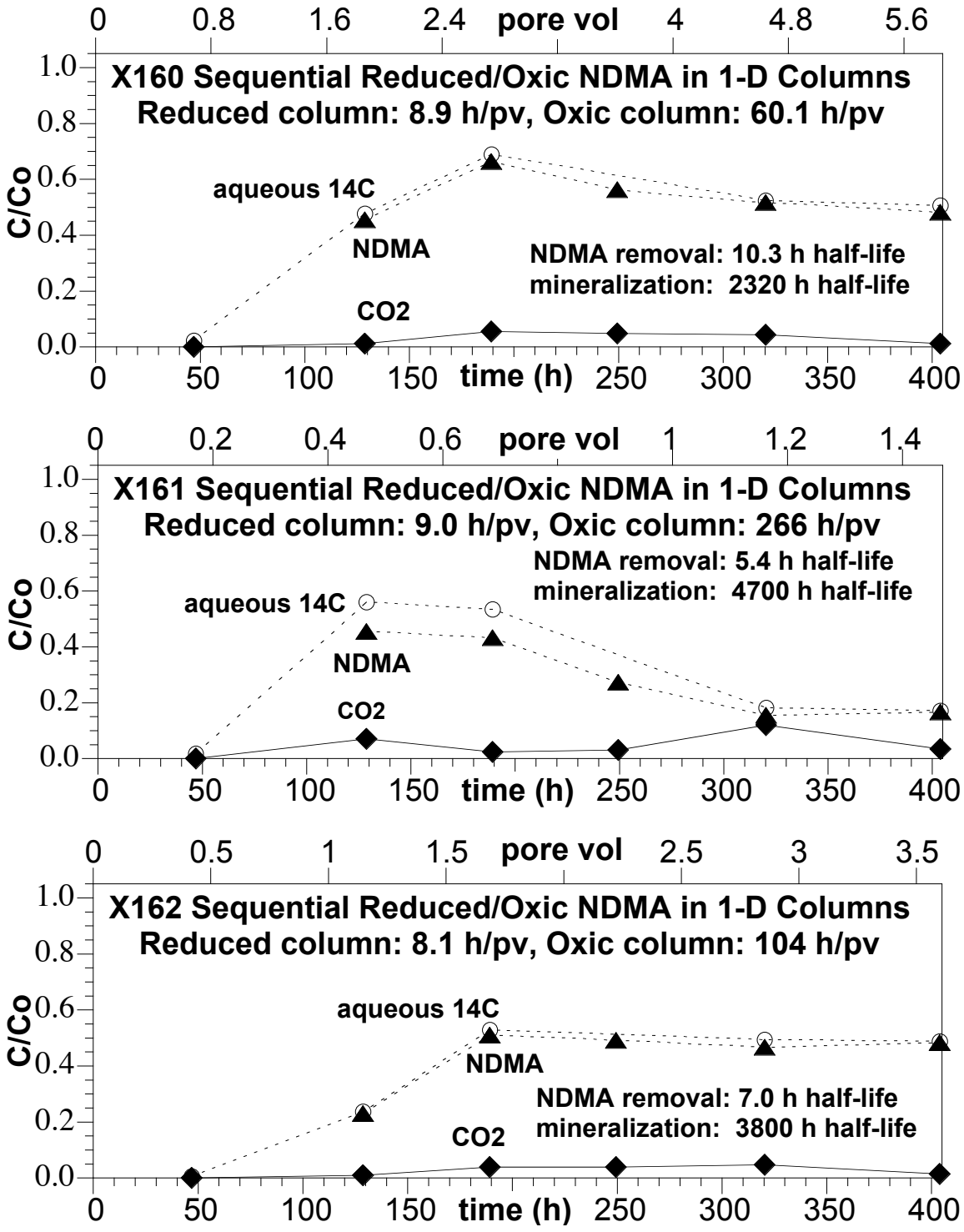

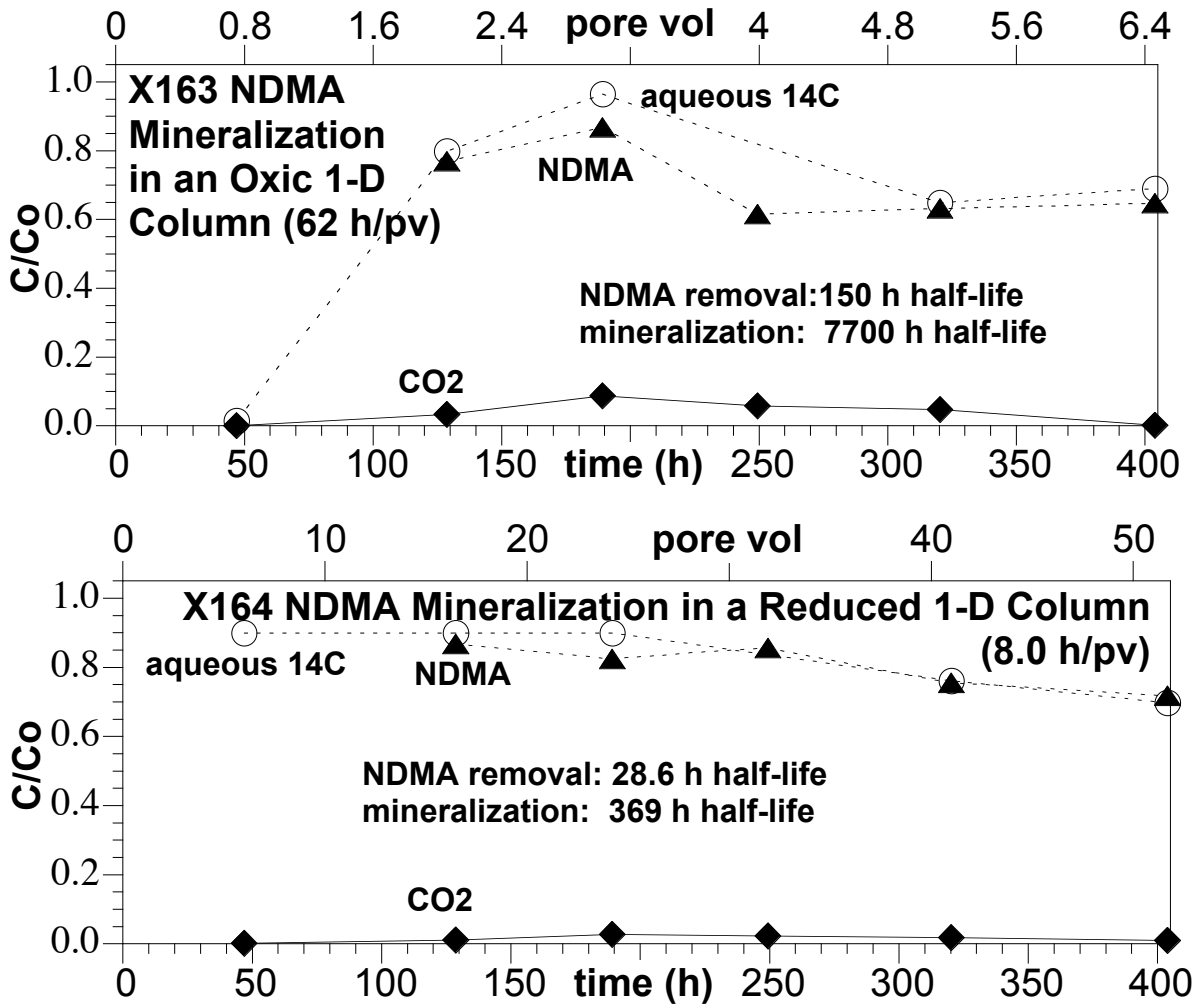
0
0.8
1.6
2.4
pore vol
4
4.8
5.6
6.4
X163 NDMA Mineralization in an Oxic 1-D Column (62 h/pv)
aqueous 14C
NDMA
NDMA removal:150 h half-life
mineralization: 7700 h half-life
CO2
C/Co
1.0
0.8
0.6
0.4
0.2
0.0
0
50
100
150
time (h)
250
300
350
400
0
10
20
pore vol
40
50
X164 NDMA Mineralization in a Reduced 1-D Column (8.0 h/pv)
aqueous 14C
NDMA
NDMA removal: 28.6 h half-life
mineralization: 369 h half-life
CO2
C/Co
1.0
0.8
0.6
0.4
0.2
0.0
0
50
100
150
time (h)
250
300
350
400

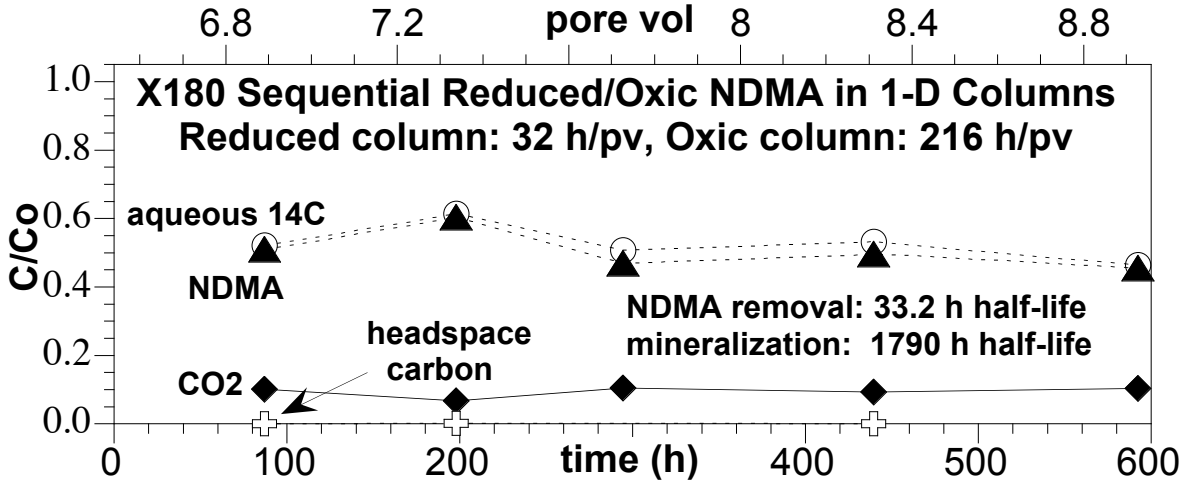
6.8
7.2
pore vol
8
8.4
8.8
X180 Sequential Reduced/Oxic NDMA in 1-D Columns
Reduced column: 32 h/pv, Oxic column: 216 h/pv
aqueous 14C
NDMA
NDMA removal: 33.2 h half-life
mineralization: 1790 h half-life
headspace carbon
CO2
C/Co
1.0
0.8
0.6
0.4
0.2
0.0
0
100
200
time (h)
400
500
600

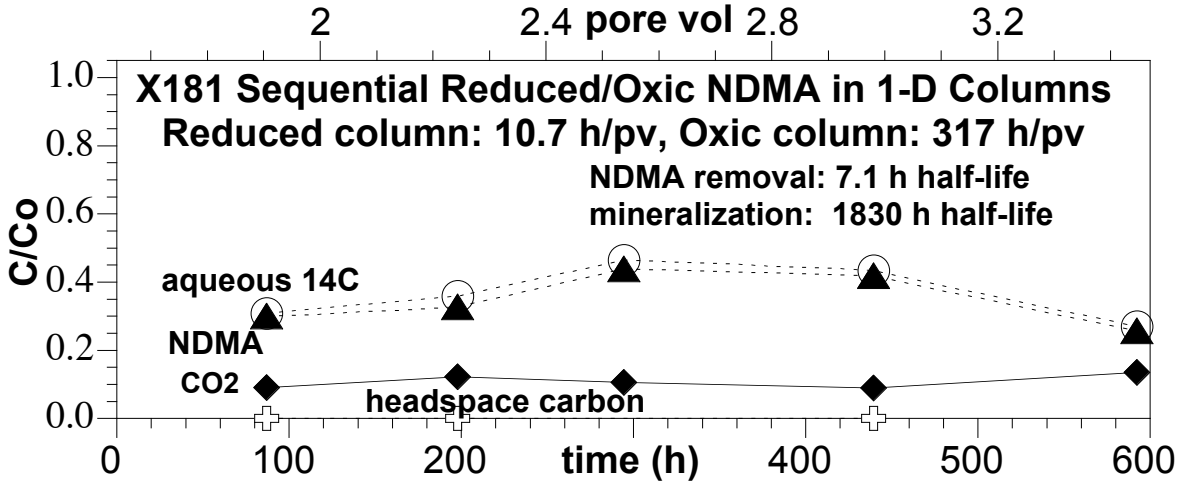
2
2.4
pore vol
2.8
3.2
X181 Sequential Reduced/Oxic NDMA in 1-D Columns
Reduced column: 10.7 h/pv, Oxic column: 317 h/pv
NDMA removal: 7.1 h half-life
mineralization: 1830 h half-life
aqueous 14C
NDMA
CO2
headspace carbon
C/Co
1.0
0.8
0.6
0.4
0.2
0.0
0
100
200
time (h)
400
500
600

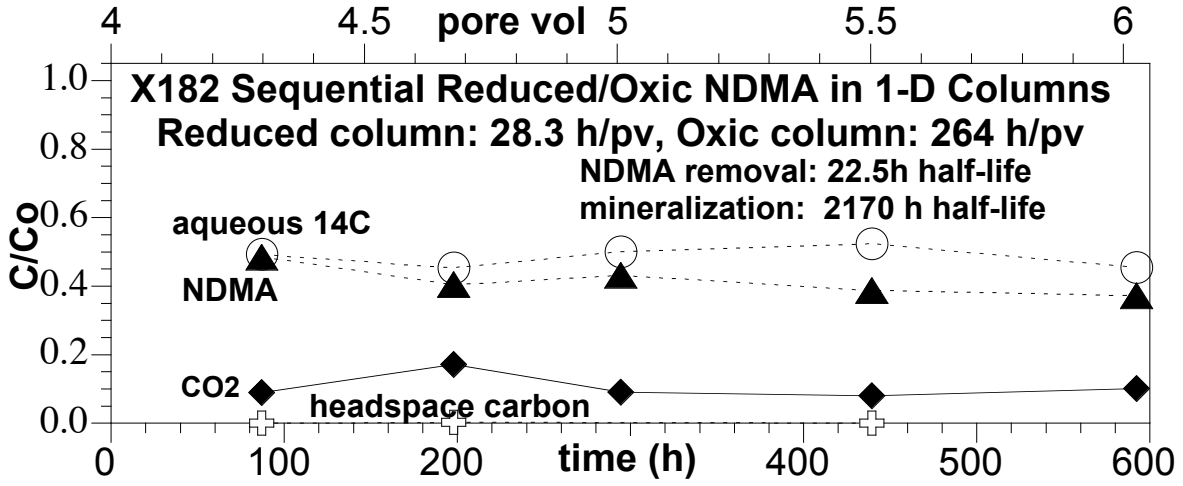
4
4.5
pore vol
5
5.5
6
X182 Sequential Reduced/Oxic NDMA in 1-D Columns
Reduced column: 28.3 h/pv, Oxic column: 264 h/pv
NDMA removal: 22.5h half-life
mineralization: 2170 h half-life
aqueous 14C
NDMA
CO2
headspace carbon
C/Co
1.0
0.8
0.6
0.4
0.2
0.0
0
100
200
time (h)
400
500
600

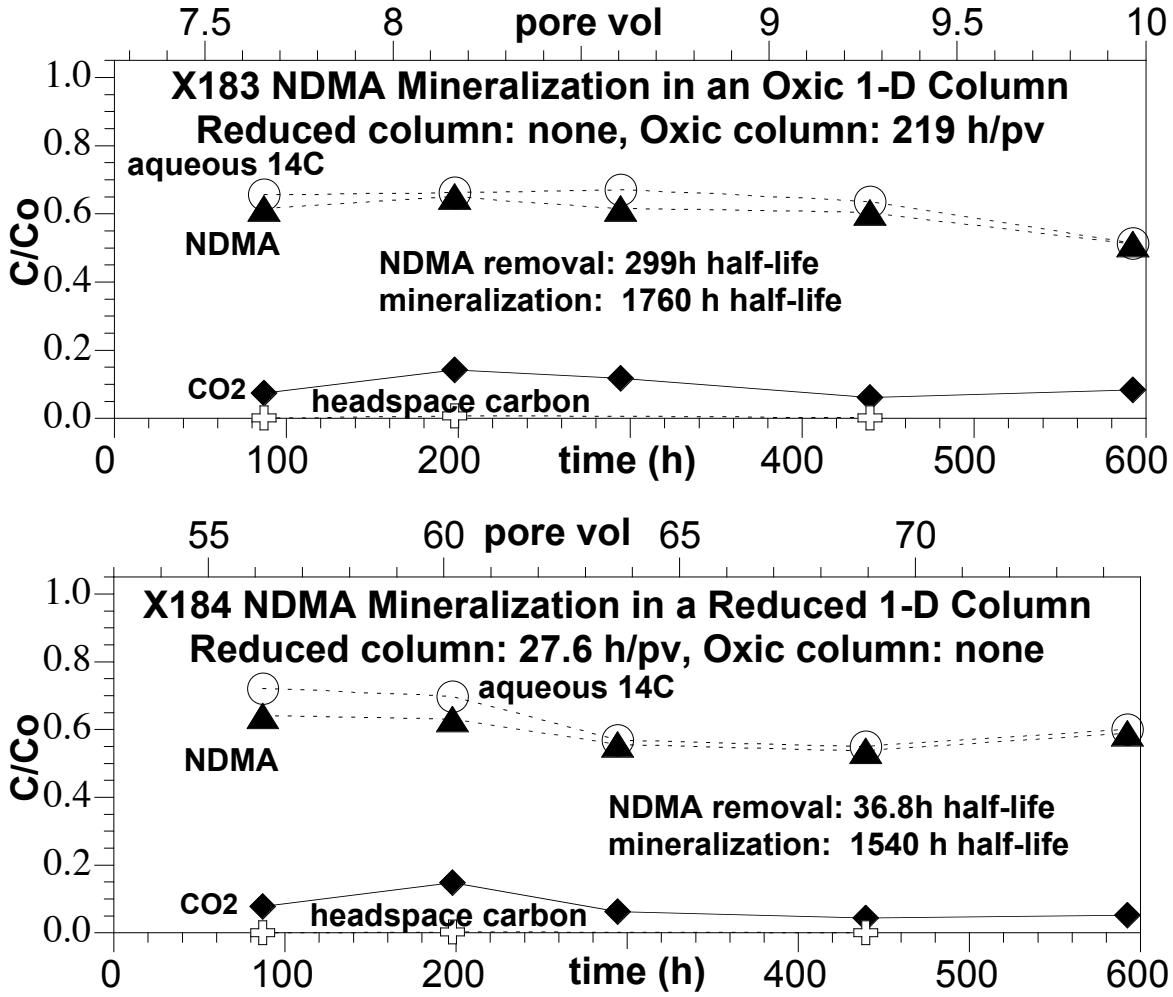
7.5
8
pore vol
9
9.5
10
X183 NDMA Mineralization in an Oxic 1-D Column
Reduced column: none, Oxic column: 219 h/pv
aqueous 14C
NDMA
NDMA removal: 299h half-life
mineralization: 1760 h half-life
CO2
headspace carbon
C/Co
1.0
0.8
0.6
0.4
0.2
0.0
0
100
200
time (h)
400
500
600

55
60
pore vol
65
70
X184 NDMA Mineralization in a Reduced 1-D Column
Reduced column: 27.6 h/pv, Oxic column: none
aqueous 14C
NDMA
NDMA removal: 36.8h half-life
mineralization: 1540 h half-life
CO2
headspace carbon
C/Co
1.0
0.8
0.6
0.4
0.2
0.0
0
100
200
time (h)
400
500
600

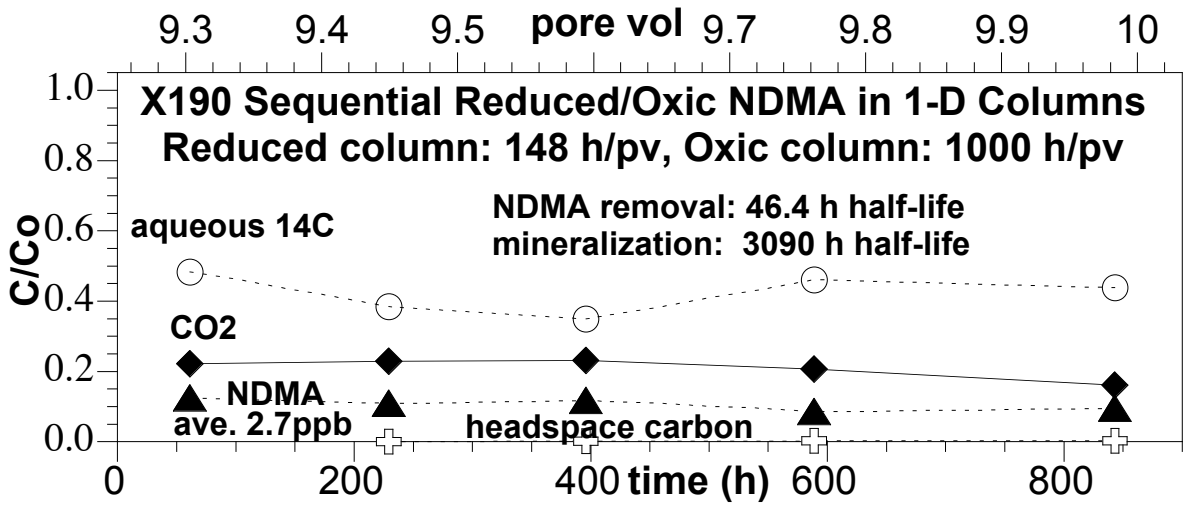
9.3
9.4
9.5
pore vol
9.7
9.8
9.9
10
X190 Sequential Reduced/Oxic NDMA in 1-D Columns
Reduced column: 148 h/pv, Oxic column: 1000 h/pv
NDMA removal: 46.4 h half-life
mineralization: 3090 h half-life
aqueous 14C
CO2
NDMA
ave. 2.7ppb
headspace carbon
C/Co
1.0
0.8
0.6
0.4
0.2
0.0
0
200
400
time (h)
600
800

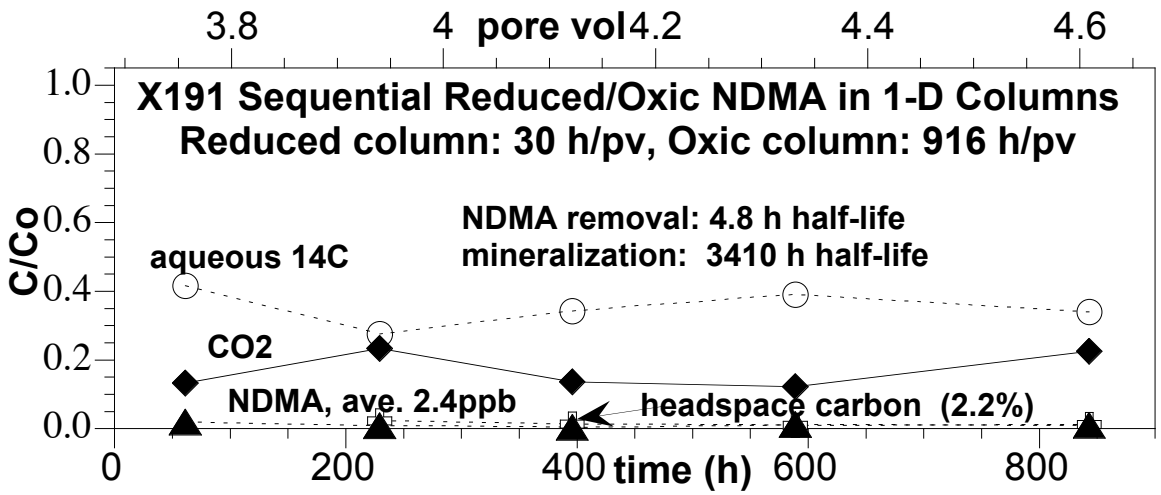
3.8
4
pore vol
4.2
4.4
4.6
X191 Sequential Reduced/Oxic NDMA in 1-D Columns
Reduced column: 30 h/pv, Oxic column: 916 h/pv
NDMA removal: 4.8 h half-life
mineralization: 3410 h half-life
aqueous 14C
CO2
NDMA, ave. 2.4ppb
headspace carbon (2.2%)
C/Co
1.0
0.8
0.6
0.4
0.2
0.0
0
200
400
time (h)
600
800

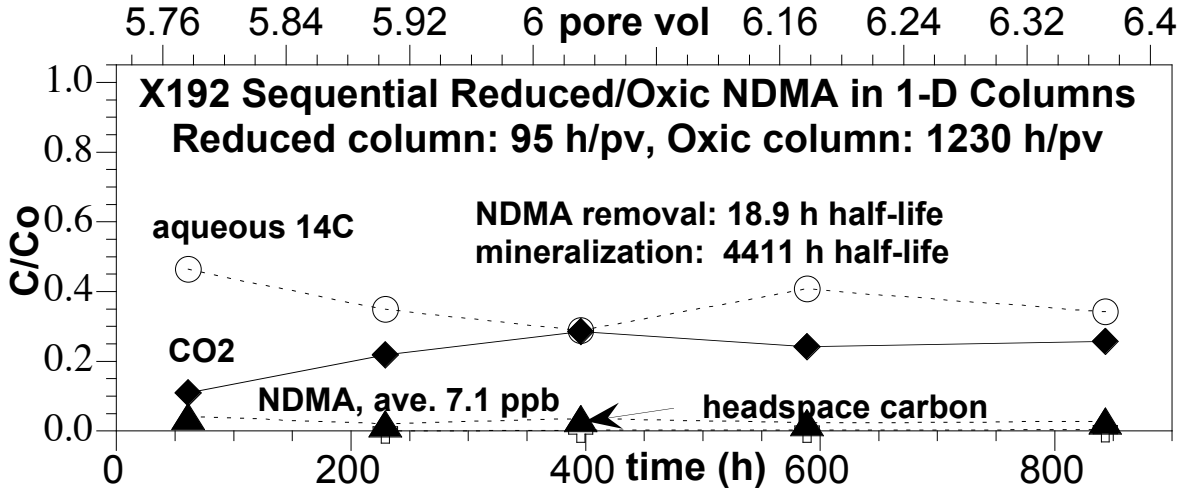
5.76
5.84
5.92
6
pore vol
6.16
6.24
6.32
6.4
X192 Sequential Reduced/Oxic NDMA in 1-D Columns
Reduced column: 95 h/pv, Oxic column: 1230 h/pv
NDMA removal: 18.9 h half-life
mineralization: 4411 h half-life
aqueous 14C
CO2
NDMA, ave. 7.1 ppb
headspace carbon
C/Co
1.0
0.8
0.6
0.4
0.2
0.0
0
200
400
time (h)
600
800

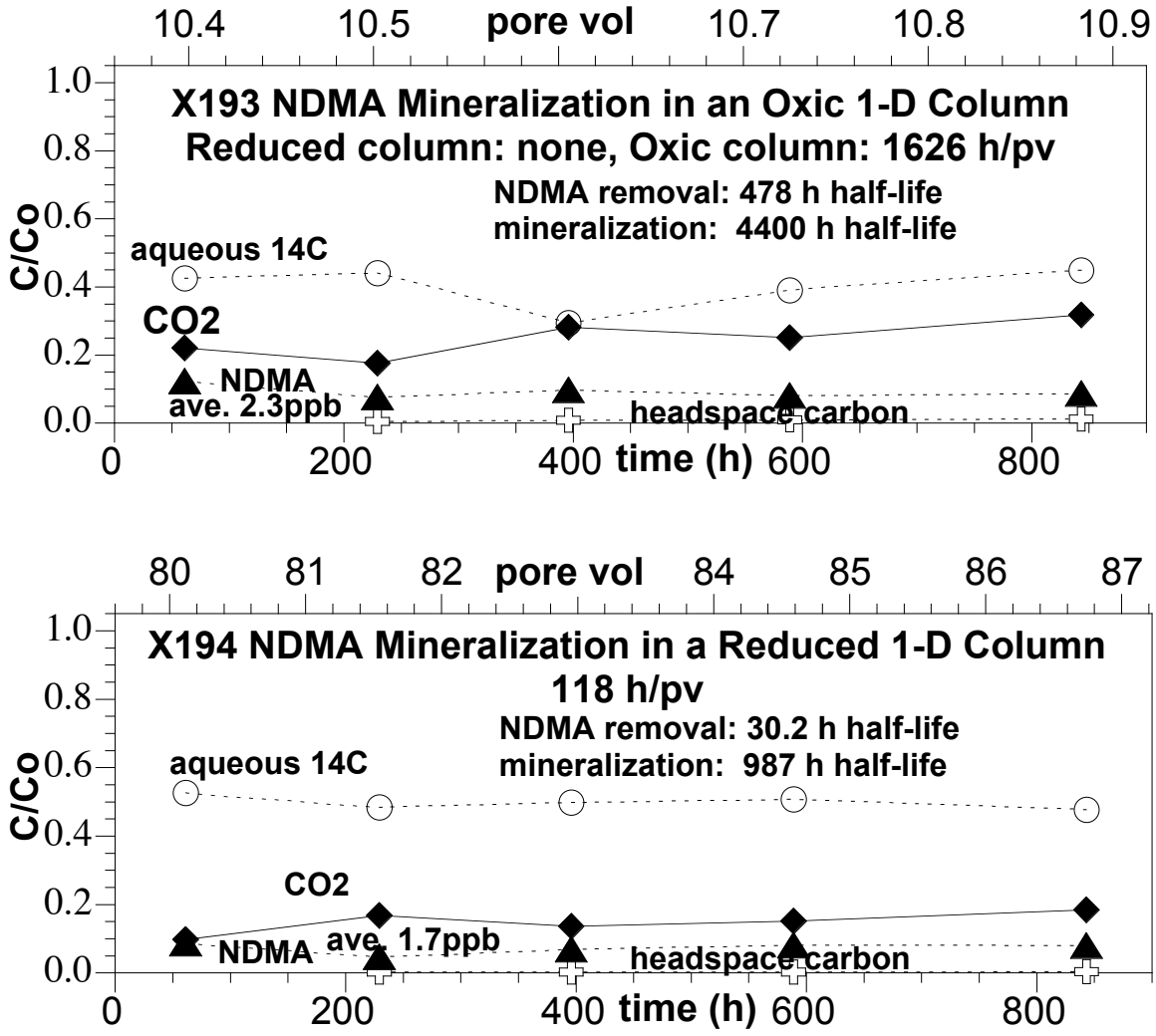
10.4
10.5
pore vol
10.7
10.8
10.9
X193 NDMA Mineralization in an Oxic 1-D Column
Reduced column: none, Oxic column: 1626 h/pv
NDMA removal: 478 h half-life
mineralization: 4400 h half-life
aqueous 14C
CO2
NDMA
ave. 2.3ppb
headspace carbon
C/Co
1.0
0.8
0.6
0.4
0.2
0.0
0
200
400
time (h)
600
800
80
81
82
pore vol
84
85
86
87
X194 NDMA Mineralization in a Reduced 1-D Column
118 h/pv
NDMA removal: 30.2 h half-life
mineralization: 987 h half-life
aqueous 14C
CO2
NDMA
ave. 1.7ppb
headspace carbon
C/Co
1.0
0.8
0.6
0.4
0.2
0.0
0
200
400
time (h)
600
800

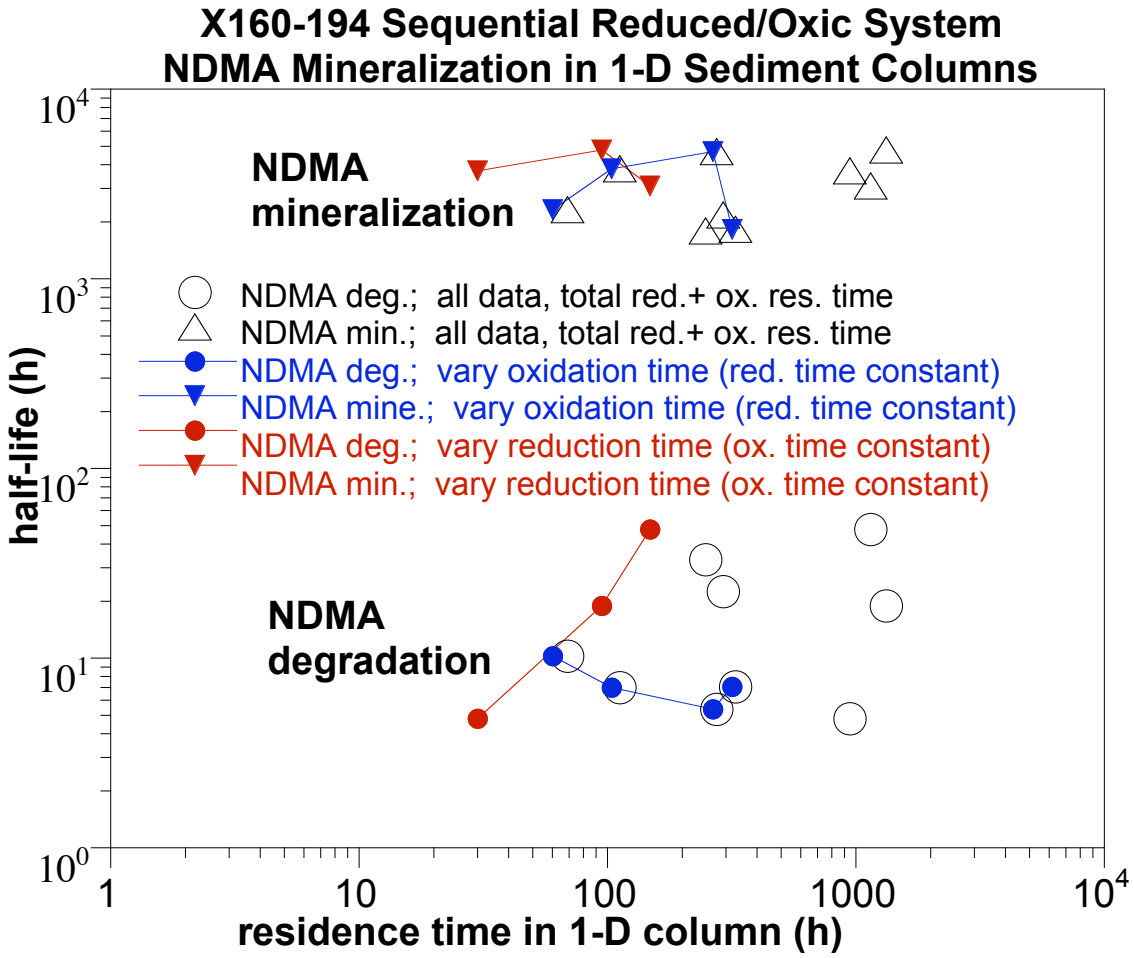
X160-194 Sequential Reduced/Oxic System
NDMA Mineralization in 1-D Sediment Columns
NDMA mineralization
NDMA deg.; all data, total red.+ ox. res. time
NDMA min.; all data, total red.+ ox. res. time
NDMA deg.; vary oxidation time (red. time constant)
NDMA mine.; vary oxidation time (red. time constant)
NDMA deg.; vary reduction time (ox. time constant)
NDMA min.; vary reduction time (ox. time constant)
NDMA degradation
half-life (h)
residence time in 1-D column (h)
10^0
10^1
10^2
10^3
10^4
1
10
100
1000
10^4